

Methods in  
Molecular Biology 1567

Springer Protocols



Dejana Mokranjac  
Fabiana Perocchi *Editors*

# Mitochondria

Practical Protocols

*Second Edition*

 Humana Press

# METHODS IN MOLECULAR BIOLOGY

*Series Editor*  
**John M. Walker**  
School of Life and Medical Sciences  
University of Hertfordshire  
Hatfield, Hertfordshire, AL10 9AB, UK

For further volumes:  
<http://www.springer.com/series/7651>

# Mitochondria

## Practical Protocols

### Second Edition

Edited by

**Dejana Mokranjac**

*Biomedical Center-Physiological Chemistry, LMU Munich, Martinsried, Germany*

**Fabiana Perocchi**

*Gene Center, LMU Munich and Institute for Diabetes and Obesity,  
Helmholtz Zentrum München, Munich, Germany*

*Editors*

Dejana Mokranjac  
Biomedical Center-Physiological Chemistry  
LMU Munich  
Martinsried, Germany

Fabiana Perocchi  
Gene Center, LMU Munich and Institute for  
Diabetes and Obesity  
Helmholtz Zentrum München  
Munich, Germany

ISSN 1064-3745                      ISSN 1940-6029 (electronic)  
Methods in Molecular Biology  
ISBN 978-1-4939-6822-0            ISBN 978-1-4939-6824-4 (eBook)  
DOI 10.1007/978-1-4939-6824-4

Library of Congress Control Number: 2017930957

© Springer Science+Business Media LLC 2017

This work is subject to copyright. All rights are reserved by the Publisher, whether the whole or part of the material is concerned, specifically the rights of translation, reprinting, reuse of illustrations, recitation, broadcasting, reproduction on microfilms or in any other physical way, and transmission or information storage and retrieval, electronic adaptation, computer software, or by similar or dissimilar methodology now known or hereafter developed.

The use of general descriptive names, registered names, trademarks, service marks, etc. in this publication does not imply, even in the absence of a specific statement, that such names are exempt from the relevant protective laws and regulations and therefore free for general use.

The publisher, the authors and the editors are safe to assume that the advice and information in this book are believed to be true and accurate at the date of publication. Neither the publisher nor the authors or the editors give a warranty, express or implied, with respect to the material contained herein or for any errors or omissions that may have been made. The publisher remains neutral with regard to jurisdictional claims in published maps and institutional affiliations.

Cover illustration: mitochondria in mammalian HeLa cells. See *Chapter 17* for details.

Printed on acid-free paper

This Humana Press imprint is published by Springer Nature  
The registered company is Springer Science+Business Media LLC  
The registered company address is: 233 Spring Street, New York, NY 10013, U.S.A.

---

## Preface

It is very hard, if not impossible, to determine who first discovered mitochondria in the second half of the nineteenth century. Carl Benda, a German anatomist and pathologist, was the first, in 1898, to use the name mitochondrion (after Greek *mitos*, a thread, and *chondros*, a grain) to describe peculiar threads of granules he observed in the cytoplasm of cells after staining with crystal violet. For over a century, mitochondria have fascinated generations of scientists who were spellbound by the beauty of their structure or one of their many biochemical activities. And there seems to be no end to this inspiration. On the contrary, the interest in mitochondria seems to be steadily growing, as judged by the yearly number of mitochondria-related publications.

The classical view of mitochondria as an isolated powerhouse has gradually shifted to the one of an organelle that is deeply and dynamically integrated in the physiology of the cell. It has been almost ten years since the first edition of *Mitochondria: Practical Protocols* was published in the *Methods in Molecular Biology* series. During this time, progress in many areas, above all in proteomics, genomics, and bioinformatics, has resulted in an almost complete list of mitochondrial proteins in several species. With this in hand, the major challenge is now to understand their molecular function, both under normal conditions and in a number of human monogenic diseases caused by mutations in mitochondrial proteins. It is also becoming increasingly clear that many cellular processes, traditionally considered to be extramitochondrial, have a mitochondrial angle to it. Likewise, mitochondrial dysfunctions have been associated with common human disorders including cancer, diabetes, Parkinson's, and Alzheimer's diseases. Therefore, mitochondria are today analyzed by an increasing number of specialists, ranging from biochemists and cell and molecular biologists, over structural biologists, biophysicists, and bioinformaticians, to pharmacologists and medical doctors. When preparing this second edition, our intention was to reflect this multidisciplinary approach needed to study mitochondria. We attempted to compile a broad range of step-by-step protocols, complementary to the ones published in the first edition of this book, to study various aspects of mitochondrial structure and function in different model organisms, both in vitro and in vivo. Therefore, we hope that this second edition of the book will be useful for beginners as well as for experienced researchers in the field.

In the end, we would like to express our gratitude to the series editor, John Walker, for his constant support during the preparation of this book. But above all, we would like to thank all the authors for their contributions—without you, there would not be this book! Thank you for the time you took to share your knowledge and experience. We have learned a lot while reading the chapters and hope that you, dear readers, will do the same.

*Martinsried, Germany*  
*Munich, Germany*

*Dejana Mokranjac*  
*Fabiana Perocchi*

---

# Contents

<i>Preface</i> . . . . .	<i>v</i>
<i>Contributors</i> . . . . .	<i>ix</i>
1 A Guide to Computational Methods for Predicting Mitochondrial Localization . . . . . <i>Su Sun and Bianca H. Habermann</i>	1
2 Isolation of Functional Mitochondria from Cultured Cells and Mouse Tissues . . . . . <i>Jennifer Wettmarshausen and Fabiana Perocchi</i>	15
3 Isolation of Mitochondria from <i>Saccharomyces cerevisiae</i> . . . . . <i>Toshiaki Izawa and Ann-Katrin Unger</i>	33
4 Isolation of Contact Sites Between Inner and Outer Mitochondrial Membranes . . . . . <i>Max Harner</i>	43
5 Isolation of Mitochondria-Associated Membranes (MAM) from Mouse Brain Tissue . . . . . <i>Bernadette Schreiner and Maria Ankarcrona</i>	53
6 Label-Free Quantitative Analysis of Mitochondrial Proteomes Using the Multienzyme Digestion-Filter Aided Sample Preparation (MED-FASP) and “Total Protein Approach” . . . . . <i>Jacek R. Wiśniewski</i>	69
7 Quantitative Analysis of Glycerophospholipids in Mitochondria by Mass Spectrometry . . . . . <i>Takashi Tatsuta</i>	79
8 Detection of Cysteine Redox States in Mitochondrial Proteins in Intact Mammalian Cells . . . . . <i>Markus Habich and Jan Riemer</i>	105
9 Chemical Crosslinking in Intact Mitochondria . . . . . <i>Rupa Banerjee, Umut Günzel, and Dejana Mokranjac</i>	139
10 Reconstitution of Mitochondrial Membrane Proteins into Nanodiscs by Cell-Free Expression . . . . . <i>Ketan Malhotra and Nathan N. Alder</i>	155
11 Detection of Dual Targeting and Dual Function of Mitochondrial Proteins in Yeast . . . . . <i>Reut Ben-Menachem and Ophry Pines</i>	179
12 Localizing mRNAs Encoding Mitochondrial Proteins in Yeast by Fluorescence Microscopy and Subcellular Fractionation . . . . . <i>Dmitry Zabezhinsky, Hannah Sperber, and Jeffrey E. Gerst</i>	197

13	Assessing Mitochondrial Bioenergetics in Isolated Mitochondria from Various Mouse Tissues Using Seahorse XF96 Analyzer . . . . .	217
	<i>Arcangela Iuso, Birgit Repp, Caroline Biagosch, Caterina Terrile, and Holger Prokisch</i>	
14	Application of FRET-Based Biosensor “ATeam” for Visualization of ATP Levels in the Mitochondrial Matrix of Living Mammalian Cells . . . . .	231
	<i>Tomoki Yoshida, Soaad Alfaqaan, Norio Sasaoka, and Hiromi Imamura</i>	
15	A Microplate-Based Bioluminescence Assay of Mitochondrial Calcium Uptake . . . . .	245
	<i>María Teresa Alonso, Paloma Navas-Navarro, and Javier García-Sancho</i>	
16	New Imaging Tools to Analyze Mitochondrial Morphology in <i>Caenorhabditis elegans</i> . . . . .	255
	<i>Saroj G. Regmi and Stéphane G. Rolland</i>	
17	Single Molecule Tracking and Localization of Mitochondrial Protein Complexes in Live Cells . . . . .	273
	<i>Timo Appelhans and Karin Busch</i>	
18	Analysis of Yeast Mitochondria by Electron Microscopy. . . . .	293
	<i>Ann-Katrin Unger, Stefan Geimer, Max Harner, Walter Neupert, and Benedikt Westermann</i>	
19	Analysis of Mitochondrial Membrane Protein Complexes by Electron Cryo-tomography . . . . .	315
	<i>Vicki A.M. Gold, Tobias Brandt, Laetitia Cavellini, Mickael M. Cohen, Raffaele Ieva, and Martin van der Laan</i>	
20	Assays for Mitophagy in Yeast . . . . .	337
	<i>Akinori Eiyama and Koji Okamoto</i>	
21	Assessing Mitochondrial Selective Autophagy in the Nematode <i>Caenorhabditis elegans</i> . . . . .	349
	<i>Konstantinos Palikaras and Nektarios Tavernarakis</i>	
22	Assessing Mitochondrial Unfolded Protein Response in Mammalian Cells . . . . .	363
	<i>Fiona Durand and Nicholas Hoogenraad</i>	
23	Analysis of Mitochondrial RNA-Processing Defects in Patient-Derived Tissues by qRT-PCR and RNAseq. . . . .	379
	<i>Robert Kopajtich, Johannes A. Mayr, and Holger Prokisch</i>	
24	Identification of Disease-Causing Mutations by Functional Complementation of Patient-Derived Fibroblast Cell Lines . . . . .	391
	<i>Laura S. Kremer and Holger Prokisch</i>	
	<i>Index</i> . . . . .	407

---

## Contributors

- NATHAN N. ALDER • *Department of Molecular and Cell Biology, University of Connecticut, Storrs, CT, USA*
- SOAAD ALFAQAAN • *Department of Functional Biology, Graduate School of Biostudies, Kyoto University, Kyoto, Japan*
- MARÍA TERESA ALONSO • *Instituto de Biología y Genética Molecular (IBGM), Universidad de Valladolid y Consejo Superior de Investigaciones Científicas (CSIC), Valladolid, Spain*
- MARIA ANKARCORONA • *Center for Alzheimer Research, Division of Neurogeriatrics, Department of Neurobiology, Care Sciences and Society, Karolinska Institutet, Huddinge, Sweden*
- TIMO APPELHANS • *Mitochondrial Dynamics Group, School of Biology, University of Osnabrück, Osnabrück, Germany*
- RUPA BANERJEE • *Biomedical Center-Physiological Chemistry, LMU Munich, Martinsried, Germany*
- REUT BEN-MENACHEM • *Department of Microbiology and Molecular Genetics, IMRIC, Faculty of Medicine, Hebrew University, Jerusalem, Israel*
- CAROLINE BIAGOSCH • *Institute of Human Genetics, Helmholtz Zentrum München, German Research Center for Environmental Health, Neuherberg, Germany; Institute of Human Genetics, Technische Universität München, Munich, Germany*
- TOBIAS BRANDT • *Department of Structural Biology, Max-Planck-Institute of Biophysics, Frankfurt am Main, Germany*
- KARIN BUSCH • *Mitochondrial Dynamics Group, School of Biology, University of Osnabrück, Osnabrück, Germany; Department of Biology, Institute of Molecular Cell Biology, Westphalian Wilhelms-University Münster, Münster, Germany*
- LAETITIA CAVELLINI • *Laboratoire de Biologie Moléculaire et Cellulaire des Eucaryotes, Institut de Biologie Physico-Chimique, Sorbonne Universités, CNRS, Paris, France*
- MICKAEL M. COHEN • *Laboratoire de Biologie Moléculaire et Cellulaire des Eucaryotes, Institut de Biologie Physico-Chimique, Sorbonne Universités, CNRS, Paris, France*
- FIONA DURAND • *Department of Biochemistry and Genetics, La Trobe Institute for Molecular Science, La Trobe University, Melbourne, VIC, Australia*
- AKINORI EIYAMA • *Graduate School of Frontier Biosciences, Osaka University, Suita, Osaka, Japan*
- JAVIER GARCÍA-SANCHO • *Instituto de Biología y Genética Molecular (IBGM), Universidad de Valladolid y Consejo Superior de Investigaciones Científicas (CSIC), Valladolid, Spain*
- STEFAN GEIMER • *Institut für Zellbiologie, Universität Bayreuth, Bayreuth, Germany*
- JEFFREY E. GERST • *Department of Molecular Genetics, Weizmann Institute of Science, Rehovot, Israel*
- VICKI A.M. GOLD • *Department of Structural Biology, Max-Planck-Institute of Biophysics, Frankfurt am Main, Germany; Living Systems Institute, University of Exeter, Exeter, UK*
- UMUT GÜNSEL • *Biomedical Center-Physiological Chemistry, LMU Munich, Martinsried, Germany*

- BIANCA H. HABERMANN • *Computational Biology Group, Max Planck Institute of Biochemistry, Martinsried, Germany; Aix Marseille Université, CNRS, IBDM, UMR, Marseille, France*
- MARKUS HABICH • *Institute for Biochemistry, University of Cologne, Cologne, Germany*
- MAX HARNER • *Institute of Cardiovascular Physiology and Pathophysiology, Ludwig-Maximilians University Munich, Munich, Germany*
- NICHOLAS HOOGENRAAD • *Department of Biochemistry and Genetics, La Trobe Institute for Molecular Science, La Trobe University, Melbourne, VIC, Australia*
- RAFFAELE IEVA • *Institute of Biochemistry and Molecular Biology, ZBMZ, Faculty of Medicine, University of Freiburg, Freiburg, Germany; Laboratoire de Microbiologie et Génétique Moléculaire (LMGM), Centre de Biologie Intégrative (CBI), Université de Toulouse, CNRS, UPS, Toulouse, France*
- HIROMI IMAMURA • *Department of Functional Biology, Graduate School of Biostudies, Kyoto University, Kyoto, Japan*
- ARCANGELA IUSO • *Institute of Human Genetics, Helmholtz Zentrum München, German Research Center for Environmental Health, Neuherberg, Germany; Institute of Human Genetics, Technische Universität München, Munich, Germany*
- TOSHIAKI IZAWA • *Max Planck Institute of Biochemistry, Martinsried, Germany*
- ROBERT KOPAJTICH • *Institute of Human Genetics, Helmholtz Zentrum München, German Research Center for Environmental Health, Neuherberg, Germany; Institute of Human Genetics, Technische Universität München, Munich, Germany*
- LAURA S. KREMER • *Institute of Human Genetics, Helmholtz Zentrum München, Neuherberg, Germany; Institute of Human Genetics, Technische Universität München, Munich, Germany*
- MARTIN VAN DER LAAN • *Institute of Biochemistry and Molecular Biology, ZBMZ, Faculty of Medicine, University of Freiburg, Freiburg, Germany; BIOSS Centre for Biological Signalling Studies, University of Freiburg, Freiburg, Germany; Medical Biochemistry and Molecular Biology, Saarland University, Homburg, Germany*
- KETAN MALHOTRA • *Department of Molecular and Cell Biology, University of Connecticut, Storrs, CT, USA; Department of Pharmacology, Yale University School of Medicine, New Haven, CT, USA*
- JOHANNES A. MAYR • *Department of Pediatrics, Paracelsus Medical University Salzburg, Salzburg, Austria*
- DEJANA MOKRANJAC • *Biomedical Center-Physiological Chemistry, LMU Munich, Martinsried, Germany*
- PALOMA NAVAS-NAVARRO • *Instituto de Biología y Genética Molecular (IBGM), Universidad de Valladolid y Consejo Superior de Investigaciones Científicas (CSIC), Valladolid, Spain*
- WALTER NEUPERT • *Max Planck Institute for Biochemistry, Martinsried, Germany*
- KOJI OKAMOTO • *Graduate School of Frontier Biosciences, Osaka University, Suita, Osaka, Japan*
- KONSTANTINOS PALIKARAS • *Institute of Molecular Biology and Biotechnology, Foundation for Research and Technology Hellas, Heraklion, Crete, Greece*
- FABIANA PEROCCHI • *Gene Center, LMU Munich and Institute for Diabetes and Obesity, Helmholtz Zentrum München, Munich, Germany*
- OPHRY PINES • *Department of Microbiology and Molecular Genetics, IMRIC, Faculty of Medicine, Hebrew University, Jerusalem, Israel*

- HOLGER PROKISCH • *Institute of Human Genetics, Helmholtz Zentrum München, German Research Center for Environmental Health, Neuherberg, Germany; Institute of Human Genetics, Technische Universität München, Munich, Germany*
- SAROJ G. REGMI • *LMU Biocenter, Department of Biology II, Ludwig-Maximilians University Munich, Martinsried, Germany; Department of Genetics, Geisel School of Medicine at Dartmouth, Hanover, NH, USA; National Institute of Child Health and Human Development, NIH, Bethesda, MD, USA*
- BIRGIT REPP • *Institute of Human Genetics, Technische Universität München, Munich, Germany*
- JAN RIEMER • *Institute for Biochemistry, University of Cologne, Cologne, Germany*
- STÉPHANE G. ROLLAND • *LMU Biocenter, Department of Biology II, Ludwig-Maximilians University Munich, Martinsried, Germany*
- NORIO SASAOKA • *Department of Functional Biology, Graduate School of Biostudies, Kyoto University, Kyoto, Japan*
- BERNADETTE SCHREINER • *Center for Alzheimer Research, Division of Neurogeriatrics, Department of Neurobiology, Care Sciences and Society, Karolinska Institutet, Huddinge, Sweden*
- HANNAH SPERBER • *Department of Molecular Genetics, Weizmann Institute of Science, Rehovot, Israel*
- SU SUN • *Computational Biology Group, Max Planck Institute of Biochemistry, Munich, Germany*
- TAKASHI TATSUTA • *Institute for Genetics, Cologne Excellence Cluster on Cellular Stress Responses in Aging-Associated Diseases (CECAD), University of Cologne, Cologne, Germany*
- NEKTARIOS TAVERNARAKIS • *Institute of Molecular Biology and Biotechnology, Foundation for Research and Technology Hellas, Heraklion, Crete, Greece; Faculty of Medicine, Department of Basic Sciences, University of Crete, Heraklion, Crete, Greece*
- CATERINA TERRILE • *Institute of Human Genetics, Helmholtz Zentrum München, German Research Center for Environmental Health, Neuherberg, Germany*
- ANN-KATRIN UNGER • *Cell Biology and Electron Microscopy, Institut für Zellbiologie, Universität Bayreuth, Bayreuth, Germany*
- BENEDIKT WESTERMANN • *Institut für Zellbiologie, Universität Bayreuth, Bayreuth, Germany*
- JENNIFER WETTMARSHAUSEN • *Genzentrum, Department of Biochemistry, Ludwig-Maximilians University, Munich, Germany; Institute for Diabetes and Obesity, Helmholtz Zentrum München, Neuherberg, Germany*
- JACEK R. WIŚNIEWSKI • *Biochemical Proteomics Group, Department of Proteomics and Signal Transduction, Max-Planck Institute for Biochemistry, Martinsried, Germany*
- TOMOKI YOSHIDA • *Department of Functional Biology, Graduate School of Biostudies, Kyoto University, Kyoto, Japan*
- DMITRY ZABEZHINSKY • *Department of Molecular Genetics, Weizmann Institute of Science, Rehovot, Israel*

# Chapter 1

## A Guide to Computational Methods for Predicting Mitochondrial Localization

Su Sun and Bianca H. Habermann

### Abstract

Predicting mitochondrial localization of proteins remains challenging for two main reasons: (1) Not only one but several mitochondrial localization signals exist, which primarily dictate the final destination of a protein in this organelle. However, most localization prediction algorithms rely on the presence of a so-called presequence (or N-terminal mitochondrial targeting peptide, mTP), which occurs in only ~70% of mitochondrial proteins. (2) The presequence is highly divergent on sequence level and therefore difficult to identify on the computer.

In this chapter, we review a number of protein localization prediction programs and propose a strategy to predict mitochondrial localization. Finally, we give some helpful suggestions for bench scientists when working with mitochondrial protein candidates *in silico*.

**Key words** Mitochondrial targeting peptide, Mitochondrial protein localization, *In silico*, Prediction methods, Protein localization algorithms

---

## 1 Introduction

Mitochondria are essential organelles of most eukaryotic cells. They are necessary for the survival under aerobic conditions and fulfill a multitude of functions including the production of energy, calcium homeostasis, heme and steroid synthesis, hormonal signaling, regulation of membrane potential and cellular metabolism, and apoptosis [1]. Most mitochondrial proteins are encoded in the nucleus and need to be actively imported into mitochondria. Consequently, the proper localization of mitochondrial proteins is a necessary prerequisite for mitochondrial function; strikingly, mislocalization or loss of function of mitochondrial proteins is causative for more than 100 human diseases [2, 3] (*see also* <http://neuromuscular.wustl.edu/mitosyn.html>).

Accurately predicting mitochondrial proteins is an essential step for elucidating their functions, as well as for understanding why their loss of function can trigger diseases. However, separating

and defining the mitochondrial proteome is challenging due to the size and content differences of the mitochondrial inventory in different tissues, cell types, and developmental stages [4]. High-throughput analysis and computational prediction can however assist in the proper recognition of mitochondrial proteins.

Neither a common transport signal nor a similar peptide shared by all mitochondrial proteins has been discovered. The final localization and consequently the import route of a protein into the mitochondrion rather seem to determine which signal is required (Fig. 1): (1) the presequence (also called N-terminal mitochondrial targeting peptide or signal (mTP)) is the only known motif targeting proteins to the mitochondrial matrix. The presequence is cleaved off by the mitochondrial processing peptidase (MPP), resulting in the mature peptide within the mitochondrial matrix [5]; (2) a presequence in combination with an additional non-cleavable hydrophobic anchor and a presequence-like internal signal or multiple internal signals as found in metabolite carrier are targeted to the inner membrane; (3) targeting to the intermembrane space requires either a bipartite presequence or a cysteine-containing signal; (4) outer membrane proteins are either of the

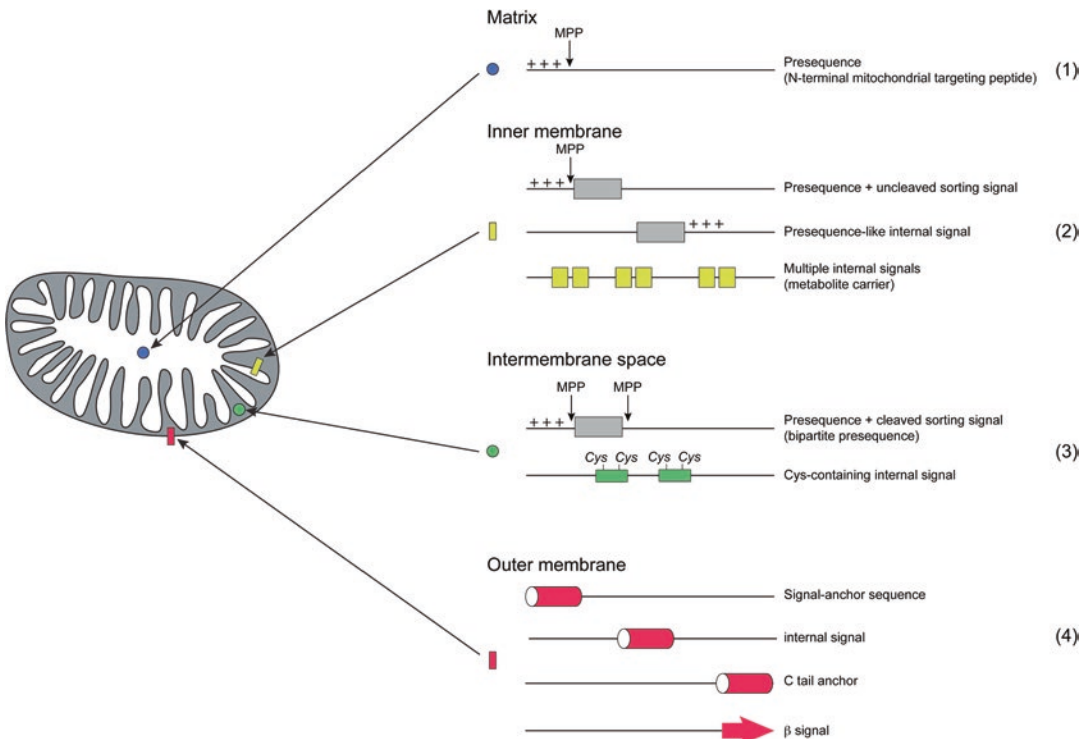


**Fig. 1** Overview of mitochondrial localization signals. There are four different localizations in mitochondria: (1) the matrix, (2) the inner membrane, (3) the intermembrane space, and (4) the outer membrane. Depending on its mitochondrial targeting signal, the protein will be localized to a different part of the mitochondrion

type  $\beta$ -barrel with a C-terminal  $\beta$ -signal or  $\alpha$ -helical, with a signal-anchor sequence, an internal signal, or a C-tail signal.

Given the high diversity of mitochondrial targeting signals, nearly all computational prediction methods employ machine-learning algorithms trained to detect certain sequence features in proteins, e.g., their amino acid composition. In the last two decades, dozens of programs for predicting mitochondrial protein localization were developed. A comprehensive review in 2009 by Daniel Gaston and colleagues [6] reviewed 13 methods in detail and divided them into four broad classes (Table 1): (a) homology-based methods detecting orthologs of well-characterized mitochondrial proteomes, such as CBOrg [6], (b) methods predicting N-terminal targeting peptides, such as Predotar [7], MitoProt [8], TargetP [9], and PProwler [10]; (c) a method predicting sequence features of full-length sequences, called CELLO [11]; and (d) “mixed” methods, which unite both feature-based classifiers and N-terminal targeting peptide predictors, such as WoLF PSORT [12], iPSORT [13] and PSORT II [14], PA-SUB [15], and SherLoc [16]. The meta-analysis program YimLOC [17] finally combines results of several localization predictors, providing a consensus for a query sequence. Meanwhile, the webservers of several of the abovementioned tools are no longer supported and have new releases or updated webserver addresses.

Based on the review by Gaston in 2009 [6], we here briefly describe a number of web-based prediction methods with respect to their usability; we provide the up-to-date version and webserver addresses of useable mitochondrial localization prediction tools; we review several new methods developed after 2009. Finally, we give advice on optimizing prediction strategies for mitochondrial protein localization for bench scientists.

---

## 2 Materials

### 2.1 Data Formats

#### 2.1.1 FASTA Format

Almost all subcellular localization prediction methods require the query in FASTA format.

The FASTA format consists of at least two lines: the first line starts with the symbol “>” and contains information on the sequence, typically including an accession number, the database, as well as a name or description of the sequence.

An example for a FASTA-formatted file:

```
>ref.|NP_001291415.1| Tim9 isoform a [Homo sapiens].  
MAAQIPESDQIKQFKFELGTYNKLTETCFLDCVKDFTTREV  
KPEETTCSEHCLQKYLKMTQRISMRFQEY.  
HIQQNEALAAKAGLLGQPR.
```

**Table 1**  
**List of available prediction methods for subcellular localization**

Program	Prediction category	Class	Algorithm	Only mTP	N-terminal signal detection	Cleavage site prediction	Tested
CBorg	Homology based	a	BLAST				
Predator	Presequence	b	Neural network		✓		✓
MitoProt/ MitoProt II	Presequence	b	PCA <sup>a</sup> and LDF <sup>b</sup>	✓	✓	✓	✓
TargetP	Presequence	b	Feed-forward neural network		✓	✓	✓
PProwler	Presequence	b	Recurrent neural network		✓		✓
PredAlgo	Presequence	b	Neural network		✓	✓	✓
CELLO	Specific mitochondrial features	c	Support vector machine				✓
PSORT/ PSORT II/ WoLF PSORT	Presequence + feature based	d	K-nearest neighbors				
iPSORT	Presequence + feature based	d	Decision list		✓		✓
PA-SUB	Presequence + feature based	d	Naïve Bayes classifier				
SherLOC/ SherLoc2	Presequence + feature based	d	Support vector machine				
TPpred2	Presequence + feature based	d	GRHCRF <sup>c</sup>	✓	✓	✓	✓
MitoFates	Presequence + feature based	d	Support vector machine	✓	✓	✓	✓
YimLOC	Presequence + feature based	Meta	Decision tree				

<sup>a</sup>Principal component analysis

<sup>b</sup>Linear discriminant function

<sup>c</sup>Grammatical-restrained hidden conditional random fields

### 2.1.2 GenBank

Some tools such as Predotar also accept the GenBank format as an input. This format stores the sequence plus some associated information, including a numbering of the sequence. A GenBank file must start with the term LOCUS, containing information such as the accession number, has numbered sequence lines split into blocks of ten and stops with two slashes.

An example for a GenBank file:

```
LOCUS           NP_001291415           89 aa
linear         PRI 13-MAY-2015
ORIGIN
1  maaqipesdq ikqfkeflgt ynkltetcf1
31 dcvkdfttre vkpeettcse hclqkylkmt
61 grismrfqey hiqqnealaa kagllgqpr
//
```

---

## 3 Methods

Prediction methods for mitochondrial localization can generally be separated in two groups: (1) Predictors trained to recognize targeting peptide-containing proteins. These programs try to find and discriminate the three types of presequences of mitochondria, chloroplasts, and the secretory pathway; some are exclusive for predicting mitochondrial proteins. (2) General localization prediction methods, which aim to predict the localization of proteins for all compartments, including mitochondria.

### 3.1 Prediction Methods Specific for Targeting Peptide Recognition

#### 3.1.1 MitoProt II

MitoProt [8] predicts mitochondrial localization based on the presence or absence of an mTP and attempts to predict the cleavage site. MitoProt uses discriminant analysis with 47 parameters to distinguish mTPs in proteins. The algorithm was trained on a set of mitochondrial proteins annotated in SwissProt, which possess a targeting peptide, are encoded in the nuclear genome, and are not localized to the chloroplast. Meanwhile, MitoProt II has been released and is available at <https://ihg.helmholtz-muenchen.de/ihg/mitoprot.html>. Only one query sequence is accepted at a time in text format (not FASTA, the protein sequence must start with a methionine). MitoProt II can be downloaded as a stand-alone version from the following website <ftp://ftp.biologie.ens.fr/pub/molbio>.

#### 3.1.2 TargetP

TargetP [9] searches for an N-terminal targeting peptide and predicts four potential destinations for proteins: mitochondria (mTP), chloroplasts (cTP), the secretory pathway (SP), and other (O). TargetP is neural network based and trained to also predict the cleavage site. Proteins with annotated localizations from the SwissProt database were taken for training the network. Cleavage

site prediction was trained with sequences annotated to have an arginine at position  $-2$ ,  $-3$ , or  $-10$  relative to the experimentally determined cleavage site. Only the first 100 amino acids are considered for presequence prediction. The developers of TargetP claimed superiority in discriminating between mitochondrial and chloroplast localization of query proteins to previously published methods (MitoProt and PSORT) [9].

TargetP offers a webserver (<http://www.cbs.dtu.dk/services/TargetP/>), where users can submit at most 2000 FASTA-formatted sequences with a maximum of 200,000 amino acids. Single FASTA-formatted sequences can also be submitted. Cleavage site prediction is optional and has to be actively selected. The user has to choose between plant and non-plant sequences for optimizing prediction of localization and can choose different cutoff settings to tailor the search for a specific purpose. Besides location of cleavage site and presequence length, TargetP returns a score in the form of a reliability class (RC) level. This score ranges from 1 to 5, with lower values having higher confidence. A local version of TargetP is available for download at the following site: [http://www.cbs.dtu.dk/cgi-bin/nph-sw\\_request?targetp](http://www.cbs.dtu.dk/cgi-bin/nph-sw_request?targetp).

### 3.1.3 *Predotar*

Similar to TargetP, Predotar [7] is a neural network-based method predicting protein N-terminal targeting peptides for cellular destinations (mitochondria, plastids, the ER targeting peptide, or no targeting peptide). Predotar was however optimized for large-scale predictions of entire proteomes, reducing the number of false-positive predictions. Compared to TargetP, it was trained on a much larger dataset; instead of chloroplast, Predotar took into account all plastid proteins, which were annotated to possess a targeting peptide. The server does not predict the cleavage site.

Predotar offers a web interface (<https://urgi.versailles.inra.fr/Tools/Predotar>) with no theoretical limitation to the number of input queries. The input format should be FASTA or GenBank. Sequences lacking the starting methionine are not accepted. As a result, the probability for a query containing a mitochondrial, plastid or ER targeting peptide, or no targeting peptide is returned.

### 3.1.4 *PProwler*

PProwler [10] introduced the recurrent network model to targeting peptide prediction, taking into account the states of neighboring amino acids when calculating the state of a residue as being part of a presequence or not. The same dataset was used as with TargetP, and likewise, it detects the occurrence of SP, mTP, and cTP or returns “Other” when no N-terminal targeting peptide is found. By making use of recurrent networks, PProwler increased the accuracy by 6 and 5% for non-plant and plant proteins, respectively.

PProwler is available for online analysis at [http://bioinf.scmb.uq.edu.au:8080/pprowler\\_webapp\\_1-2/index.jsp](http://bioinf.scmb.uq.edu.au:8080/pprowler_webapp_1-2/index.jsp). A maximum of 100 FASTA-formatted sequences is accepted per request.

### 3.1.5 iPSORT

iPSORT [13] is a predictor specific for detecting presequences. It predicts the occurrence of a signal peptide, a chloroplast transit peptide, or a mitochondrial targeting peptide. iPSORT makes a set of decisions based on simple rules such as the *amino acid index* and an *alphabet indexing + approximate pattern*. The aim of the method was to simplify the algorithm for predicting presequences, while achieving a similarly high accuracy as TargetP. The model was trained on the TargetP dataset. A putative cleavage site is predicted, and the program outputs the type of presequence, as well as the position of the cleavage site.

iPSORT can be accessed via its webserver <http://ipsort.hgc.jp/index.html>. Any text string can be submitted, and characters that are not recognized as amino acids will be automatically removed. The user needs to specify, if the query is a plant or non-plant protein. A command-line version of iPSORT can be found here <http://ipsort.hgc.jp/caml-iPSORT/>.

iPSORT is part of the PSORT family, which can generally be used to predict the subcellular localization of a protein sequence. PSORT [14], PSORT II, and WoLF PSORT [12] can recognize signal sequences, transmembrane segments, nuclear proteins, mitochondrial proteins, and others. Depending on the input organism, three to ten subcellular localizations can be classified. According to the PSORT server, PSORT II is recommended for animal or yeast proteins. PSORT-B [18] is specific for bacterial proteins and is the newest member of the PSORT family.

### 3.1.6 TPpred2

TPpred [19] and its improved version TPpred2 [20] were designed to identify mitochondrial and plastid targeting signals using Grammatical-Restrained Hidden Conditional Random Fields. It labels the queried protein with “t” (targeting signal detected) or “n” (no targeting signal detected). It predicts the position of the cleavage site; TPpred was trained on 202 proteins from mitochondria and 95 from plastids, whose cleavage sites were experimentally determined. TPpred claimed to have higher specificity as compared to other tools. Though, as the algorithm has been trained using both mTPs and cTPs, it will most likely be less suitable to distinguish mitochondrial from plastid proteins.

The TPpred2 web interface is available at <http://tppred2.biocomp.unibo.it/>. Only a single FASTA-formatted sequence is accepted by the webserver. Prediction results can be retrieved within 30 days using the individual job identifiers. For searching multiple sequences, a stand-alone version is available at <http://tppred2.biocomp.unibo.it/tppred2/default/software>. As the server is often unresponsive, the local installation of the software is

recommended. Recently, a new version of TPpred, TPpred 3.0, was released (<http://tppred3.biocomp.unibo.it/tppred3>).

### 3.1.7 MitoFates

MitoFates [21] is a software for specifically predicting mitochondrial targeting peptides and their cleavage sites. MitoFates uses a support vector machine. Next to standard features, specific features for mitochondrial presequences, like positively charged amphiphilicity, presequence motifs, as well as available evolutionary information on cleavage sites, are implemented. The model was trained on classical eukaryotic proteins possessing mitochondrial presequences (as used in TargetP and Predotar), as well as on presequences identified in large-scale studies of the proteomes of *S. cerevisiae* [22], *A. thaliana*, and *O. sativa* [23]. With three separate learning models (yeast, plant, metazoan), four physicochemical features, and a simple MPP-cleavage site set (with arginine at position -2), MitoFates claims to achieve more accurate predictions of presequences, as well as cleavage sites. Cleavage sites of the mitochondrial peptidases Oct1 and Icp55 are also returned as a result, based on a local sequence model (position weight matrix) centered on the amino acid sequence surrounding the cleavage site.

MitoFates can be accessed through its webserver at <http://mitf.cbrc.jp/MitoFates/cgi-bin/top.cgi>. The user can paste or upload a single FASTA sequence or a file containing multiple FASTA-formatted sequences. A maximum of 2000 sequences can be submitted at a time. As the classifier has been trained separately for yeast, metazoans, and plants, the user has to specify the species model. MitoFates returns the probability of the query containing a presequence, the positions of MPP, Oct1 and Icp55 cleavage sites, as well as predicted presequence motifs. A standalone version is available at <http://mitf.cbrc.jp/MitoFates/program.html>.

### 3.1.8 PredAlgo

PredAlgo [24] was developed to assign proteins from algae to three intracellular compartments: mitochondria, chloroplasts, and the secretory pathway. PredAlgo was trained on a carefully assembled set of N-terminal signals of proteins from *Chlamydomonas reinhardtii*. Next to returning the localization of the query, the probable cleavage site is also predicted. PredAlgo was shown to have higher accuracy for proteins from *C. reinhardtii* and related green algae species, including Chlorophyceae and Trebouxiophyceae.

PredAlgo is available as a web service at <https://giavap-genomes.ibpc.fr/cgi-bin/predalgotdb.perl?page=main>; for a set of less than 100 queries, the user can directly retrieve prediction results. For a larger dataset, one can receive the results by submitting a user-defined email address. PredAlgo predicts proteins as being M, C, SP, or O which refer to mitochondrion, chloroplast, secretory pathway, and others, respectively. Furthermore, the cleavage sites are suggested with mTPlength, cTPlength, and spTPlength.

## 3.2 General Prediction Methods of Protein Localization

### 3.2.1 PA-SUB

PA-SUB [15] is a subcellular localization predictor developed as part of the proteome analyst web service (latest server version: PA3). It was constructed with five classifiers for localization of proteins from animal, plants, fungi, gram-negative bacteria, and gram-positive bacteria to a broad range of compartments. The prediction is based on searching homologous sequences in the SwissProt database. Hence, a prediction is only possible, if the query has homologs in this database. Neither mitochondrial targeting peptides nor cleavage sites are predicted.

The webserver of PA-SUB has been replaced by the “Proteome Processor” in the latest version of the Proteome Analyst server at <http://pa.wishartlab.com/pa/pa/user/tools/proteomeProcessor.html>. A user needs to create an account (free for academics) and log-in for running predictions; a classifier has to be chosen from the five available models. Only a FASTA-formatted sequence is accepted; multiple FASTA sequences can be submitted at once. Note that the queuing time for one submission might be extremely long.

### 3.2.2 SherLoc and SherLoc2

SherLoc [16] and SherLoc2 [25] are support vector machine (SVM)-based classifiers and integrate a number of sequence-based as well as text-based features to predict all major subcellular localizations for proteins in eukaryotic cells. N-terminal targeting peptides are used to generate the classifiers SVMTarget and SVMSA. SherLoc2 is an advancement of SherLoc in that it uses different feature sources and was shown to have significantly improved performance over SherLoc. The webserver of SherLoc2 is available at <http://abi.inf.uni-tuebingen.de/Services/SherLoc2>, where a maximum of 20 FASTA-formatted sequences can be submitted at once. The high frequency of error message during the prediction is in need of improvement. A standalone version of SherLoc2 is available at [http://abi.inf.uni-tuebingen.de/Services/SherLoc2/sherloc2\\_download](http://abi.inf.uni-tuebingen.de/Services/SherLoc2/sherloc2_download).

### 3.2.3 CELLO

CELLO [11] is a two-level SVM, combining sequence-based feature vectors (first level) with a jury machine calculating a probability distribution of decisions for possible localizations (second level). It was designed to predict subcellular localizations in bacteria, as well as eukaryotes, covering a broad range of destinations. Mitochondrial cleavage sites are not predicted.

CELLO is available as a web service <http://cello.life.nctu.edu.tw/>; no stand-alone version exists. The user can paste or upload a single or multiple sequences in FASTA format. A version of CELLO is CELLO2GO (<http://cello.life.nctu.edu.tw/cello2go/>), a webserver for protein classification based on the CELLO server, as well as BLAST homology searching [26].

### **3.3 Overall Evaluation of Mitochondrial Prediction Methods**

We systematically tested nine of the described localization prediction methods (*see* Table 1; Sun and Habermann, unpublished). None of the selected localization predictors returned error-free predictions for mitochondrial proteins. Most methods had the least problems with presequence-containing proteins, as well as non-mitochondrial proteins. Most of them, however, performed poorly with mitochondrial targeting signals other than the presequence (*see* **Notes 1 and 3**). Opposing to this, CELLO worked reasonably well for other mitochondrial targeting signals, however performed poorly for presequence-containing mitochondrial proteins.

Predicting the cleavage site accurately is a difficult challenge for all methods; it appears to be rather by chance that the correct site is identified (*see* **Note 2**). Given the high variance of the cleavage site, this is not an unexpected finding. This however implies that a user should not rely on cleavage site prediction by any of the tested programs.

Ranking the programs according to their performance in identifying mitochondrial proteins is challenging, given the mixed performance of most of them. For mTP containing proteins, all except for CELLO and PredAlgo can be used. More than one algorithm should generally be used to find a potential mTP. CELLO, on the other hand, can be used for mitochondrial proteins with other types of mitochondrial targeting signals: if a first screen for presequence-like signals fails, use CELLO to identify potential other mitochondrial targeting domains (*see* **Note 3**). It can be stated that the community is in desperate need of more methods taking into account all mitochondrial targeting signals.

### **3.4 A Strategy to Mitochondrial Localization Prediction**

How can one proceed in predicting mitochondrial localization of a query protein? We have depicted a potential workflow in Fig. 2.

We advise on relying foremost on any experimental evidence available for a query protein: has it been described to localize to mitochondria? Experimentally determined mitochondrial localization of an ortholog of the query is also a good indicator that the query itself is in fact a mitochondrial protein (Fig. 2, section A). Make sure, however, that a true ortholog of the query protein has confirmed mitochondrial localization (*see* **Note 2**). Sources for orthology information are, for instance, HomoloGene [27], OrthoMCL [28], Berkeley PHOG [29], Inparanoid [30], PhylomeDB [31], TreeFam [32], or EnsembleCompara [33]. Orthology based on reciprocal best hits can also be established using reciprocal BLAST searches [34]. For large-scale prediction of mitochondrial localization based on orthology, CBOrg [6] can be installed and used locally.

If mitochondrial localization of the query has been predicted by orthology, we recommend verifying it experimentally (*see* **Notes 4 and 9**); though unlikely, it cannot be excluded entirely that an ortholog of a mitochondrial protein in a more distantly related species has a function that is not related to mitochondria (*see* **Note 5**). To determine the type of localization signal, one can then

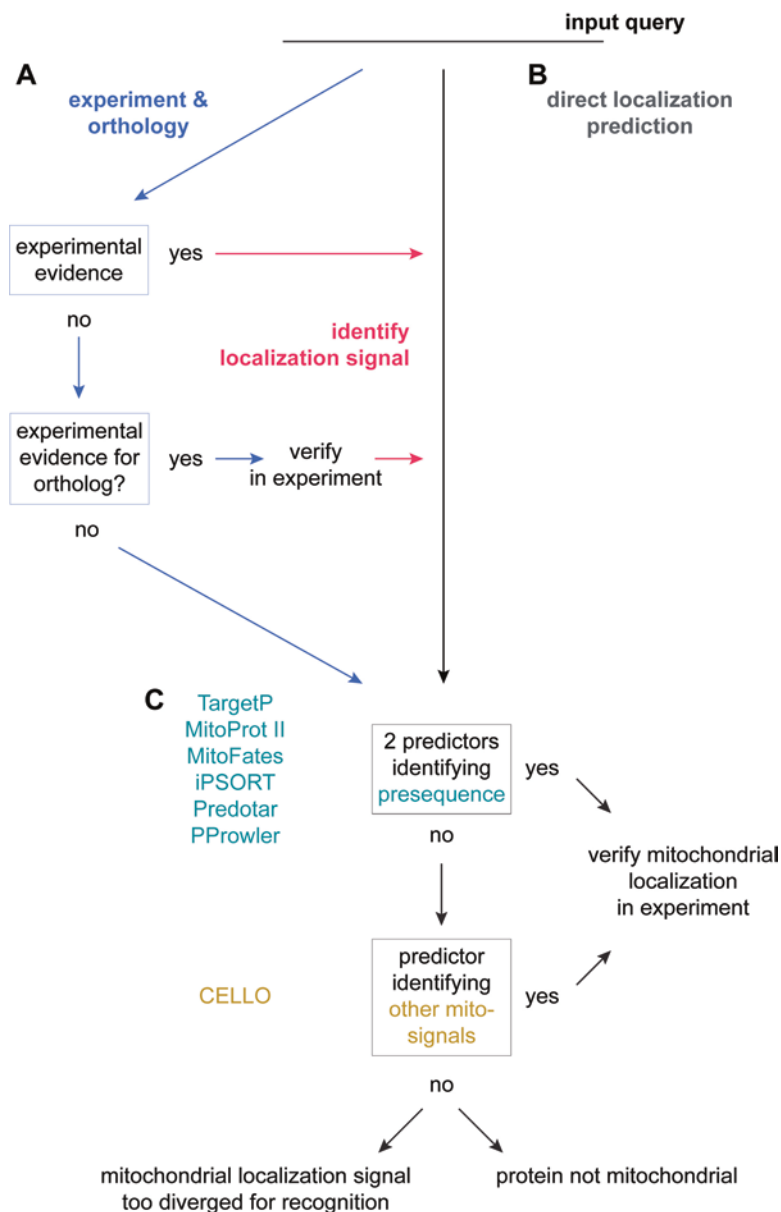


**Fig. 2** A strategy to predict mitochondrial localization of a protein query. (a) Rely on available experimental information and orthology to predict mitochondrial localization of a protein sequence. (b) Directly perform in silico prediction of mitochondrial localization (as detailed in C). (c) In silico strategy for predicting mitochondrial localization of a protein sequence. For a detailed description, see main text

proceed to predicting the targeting signal using a combination of localization predictors (Fig. 2c).

If no experimental information on the protein query or its orthologs is available, the query should be directly submitted to a localization prediction program (Fig. 2b). One can also chose this

path directly. We recommend a two-step strategy (Fig. 2c): first, use a prediction method that identifies N-terminal mitochondrial targeting peptides (*see* **Notes 6–8**). Ideally, two algorithms should be chosen, which rely on a different algorithm and have been trained with a different dataset. This could, for instance, be TargetP (feed-forward neural network) together with MitoFates (support vector machine) or MitoProt II (PCA and LDF based). If two programs predict mitochondrial localization of the query, as well as the presence of a presequence, one can directly continue to verify this hypothesis experimentally. If, however, no presequence is detected, we recommend to use a method like CELLO to identify potential other localization signals. A positive prediction of mitochondrial localization should again be verified experimentally.

If none of the methods predict mitochondrial localization—and no experimental evidence for mitochondrial localization of the query or its orthologs exists—the protein in question might simply not be a mitochondrial protein. However, please note also that some proteins may not be correctly recognized as mitochondrial proteins by any of the programs (*see* **Note 9**).

---

## 4 Notes

1. Identification of N-terminal, mitochondrial targeting peptides is not trivial. The programs will perform differently for different protein families. Use at least two prediction engines, if in doubt.
2. Cleavage sites are not reliably predicted by any of the methods. Therefore, do not rely on predicted cleavage sites.
3. Not all mitochondrial proteins possess an mTP, but only around 70%. If a localization predictor is based on detecting an mTP, it will produce a false-negative result for those proteins that lack this classical presequence. Suggestion: use a method like CELLO as a second step for localization prediction, if no presequence is found.
4. A multitude of mitoproteomes is meanwhile published (*see* MitoMiner [35], <http://mitominer.mrc-mbu.cam.ac.uk/release-3.1/begin.do>). Typically, large-scale proteomics studies are performed to characterize the mitoproteome of a tissue or an organism. Though these methods also yield a number of false-positive and false-negative assignments, such studies are nevertheless a valuable resource to mine for mitochondrial localization prediction based on orthology.
5. The presequence shows high divergence even among orthologs. Consequently, it can happen that localization prediction results for orthologs are different. One would assume that orthologs of proteins from such a fundamental cellular compartment as the

mitochondrion would not localize somewhere else in the cell, even though this cannot be excluded. If the function of a mitochondrial protein is well characterized in one species, all its orthologs most likely also localize to mitochondria. Orthology detection methods or resources can thus be useful to predict mitochondrial localization of a protein.

6. Carefully read the original manuscript, help pages, as well as pages on data interpretation of the programs you are using. Predotar, for instance, offers information on interpreting prediction results and points out some important facts on the software itself (<https://urgi.versailles.inra.fr/predotar/interpretation.html>).
7. Pay attention to required input formats for the query (like FASTA). A wrong input format will in most cases trigger an error message. iPSORT, for instance, requires plain text and cannot deal with FASTA headers. Letters that do not code for an amino acid will be removed and prediction starts with part of the FASTA header. The prediction will therefore return false results.
8. Some tools remove nonstandard letters, which do not code for an amino acid, some do not. If a program returns an error message like “invalid line,” although the format of your submission is correct, check whether there is a “U” or “X” in the query protein.
9. As a localization prediction is only a prediction and, thus, only provides a hypothesis, experimental verification of the protein under study is necessary.

## References

1. Nunnari J, Suomalainen A (2012) Mitochondria: in sickness and in health. *Cell* 148:1145–1159
2. Schmidt O, Pfanner N, Meisinger C (2010) Mitochondrial protein import: from proteomics to functional mechanisms. *Nat Rev Mol Cell Biol* 11:655–667
3. Wallace DC, Fan W (2009) The pathophysiology of mitochondrial disease as modeled in the mouse. *Genes Dev* 23:1714–1736
4. Calvo SE, Mootha VK (2010) The mitochondrial proteome and human disease. *Annu Rev Genomics Hum Genet* 11:25–44
5. Omura T (1998) Mitochondria-targeting sequence, a multi-role sorting sequence recognized at all steps of protein import into mitochondria. *J Biochem* 123:1010–1016
6. Gaston D, Tsaousis AD, Roger AJ (2009) Predicting proteomes of mitochondria and related organelles from genomic and expressed sequence tag data. *Methods Enzymol* 457:21–47
7. Small I, Peeters N, Legeai F et al (2004) Predotar: A tool for rapidly screening proteomes for N-terminal targeting sequences. *Proteomics* 4:1581–1590
8. Claros MG, Vincens P (1996) Computational method to predict mitochondrially imported proteins and their targeting sequences. *Eur J Biochem* 241:779–786
9. Emanuelsson O, Nielsen H, Brunak S et al (2000) Predicting subcellular localization of proteins based on their N-terminal amino acid sequence. *J Mol Biol* 300:1005–1016
10. Bodén M, Hawkins J (2005) Prediction of subcellular localization using sequence-biased recurrent networks. *Bioinformatics* 21:2279–2286
11. Yu C-S, Chen Y-C, Lu C-H et al (2006) Prediction of protein subcellular localization. *Proteins* 64:643–651

12. Horton P, Park K-J, Obayashi T et al (2007) WoLF PSORT: protein localization predictor. *Nucleic Acids Res* 35:W585–W587
13. Bannai H, Tamada Y, Maruyama O et al (2002) Extensive feature detection of N-terminal protein sorting signals. *Bioinformatics* 18: 298–305
14. Nakai K, Horton P (1999) PSORT: a program for detecting sorting signals in proteins and predicting their subcellular localization. *Trends Biochem Sci* 24:34–36
15. Lu Z, Szafron D, Greiner R et al (2004) Predicting subcellular localization of proteins using machine-learned classifiers. *Bioinformatics* 20:547–556
16. Shatkay H, Höglund A, Brady S et al (2007) SherLoc: high-accuracy prediction of protein subcellular localization by integrating text and protein sequence data. *Bioinformatics* 23:1410–1417
17. Shen YQ, Burger G (2007) “Unite and conquer”: enhanced prediction of protein subcellular localization by integrating multiple specialized tools. *BMC Bioinformatics* 8:420
18. Gardy JL, Spencer C, Wang K et al (2003) PSORT-B: Improving protein subcellular localization prediction for Gram-negative bacteria. *Nucleic Acids Res* 31:3613–3617
19. Indio V, Martelli PL, Savojardo C et al (2013) The prediction of organelle-targeting peptides in eukaryotic proteins with grammatical-restrained hidden conditional random fields. *Bioinformatics* 29:981–988
20. Savojardo C, Martelli PL, Fariselli P et al (2014) TPpred2: improving the prediction of mitochondrial targeting peptide cleavage sites by exploiting sequence motifs. *Bioinformatics* 30:2973–2974
21. Fukasawa Y, Tsuji J, Fu S-C et al (2015) MitoFates: improved prediction of mitochondrial targeting sequences and their cleavage sites. *Mol Cell Proteomics* 14:1113–1126
22. Vögtle F-N, Wortelkamp S, Zahedi RP et al (2009) Global analysis of the mitochondrial N-proteome identifies a processing peptidase critical for protein stability. *Cell* 139:428–439
23. Huang S, Taylor NL, Whelan J et al (2009) Refining the definition of plant mitochondrial presequences through analysis of sorting signals, N-terminal modifications, and cleavage motifs. *Plant Physiol* 150:1272–1285
24. Tardif M, Atteia A, Specht M et al (2012) PredAlgo: a new subcellular localization prediction tool dedicated to green algae. *Mol Biol Evol* 29:3625–3639
25. Briesemeister S, Blum T, Brady S et al (2009) SherLoc2: a high-accuracy hybrid method for predicting subcellular localization of proteins. *J Proteome Res* 8:5363–5366
26. Yu C-S, Cheng C-W, Su W-C et al (2014) CELLO2GO: a web server for protein subcellular LOCALization prediction with functional gene ontology annotation. *PLoS One* 9:e99368
27. Resource Coordinators NCBI (2014) Database resources of the National Center for Biotechnology Information. *Nucleic Acids Res* 42:D7–17
28. Li L, Stoeckert CJ Jr, Roos DS (2003) OrthoMCL: identification of ortholog groups for eukaryotic genomes. *Genome Res* 13(9): 2178–2189
29. Datta RS, Meacham C, Samad B et al (2009) Berkeley PHOG: phylofacts orthology group prediction web server. *Nucleic Acids Res* 37:W84–W89
30. Sonnhammer ELL, Östlund G (2015) InParanoid 8: orthology analysis between 273 proteomes, mostly eukaryotic. *Nucleic Acids Res* 43:D234–D239
31. Huerta-Cepas J, Bueno A, Dopazo J et al (2007) PhylomeDB: a database for genome-wide collections of gene phylogenies. *Nucleic Acids Res* 36:D491–D496
32. Schreiber F, Patricio M, Muffato M et al (2014) TreeFam v9: a new website, more species and orthology-on-the-fly. *Nucleic Acids Res* 42:D922–D925
33. Vilella AJ, Severin J, Ureta-Vidal A et al (2009) EnsemblCompara GeneTrees: complete, duplication-aware phylogenetic trees in vertebrates. *Genome Res* 19:327–335
34. Altschul SF, Madden TL, Schäffer AA et al (1997) Gapped BLAST and PSI-BLAST: a new generation of protein database search programs. *Nucleic Acids Res* 25:3389–3402
35. Smith AC, Blackshaw JA, Robinson AJ (2012) MitoMiner: a data warehouse for mitochondrial proteomics data. *Nucleic Acids Res* 40:D1160–D1167

## Isolation of Functional Mitochondria from Cultured Cells and Mouse Tissues

Jennifer Wettmarshausen and Fabiana Perocchi

### Abstract

Mitochondria serve as the center stage for a number of cellular processes, including energy production, apoptosis, ion homeostasis, iron and copper processing, steroid metabolism, de novo pyrimidine, and heme biosynthesis. The study of mitochondrial function often requires the purification of intact and respiratory-competent organelles. Here, we provide detailed protocols to isolate functional mitochondria from various types of mammalian cells and mouse tissues, in both crude and pure forms. We introduce the use of nitrogen cavitation for the disruption of plasma membrane and the reproducible isolation of mitochondria-enriched fractions of high yield. Mitochondria that are isolated by these procedures are intact and coupled and can directly be used for several downstream analyses, such as measurements of oxygen consumption and calcium buffering capacity.

**Key words** Crude mitochondria, Pure mitochondria, Mitochondrial integrity, Organelle isolation, Nitrogen cavitation

---

### 1 Introduction

Mitochondria are double membrane organelles found in virtually all of eukaryotic cells. The organelle hosts several cellular processes, including but not limited to ATP synthesis. Over 200 metabolic reactions take place inside mitochondria, supporting numerous anabolic and catabolic pathways such as biosynthesis of iron-sulfur clusters and phospholipids and degradation of fatty acids and amino acids [1]. Besides, mitochondria are equipped with macromolecular machineries for the import of proteins and the exchange of inorganic ions and solutes. Given the central role of the organelle in cell biology, its dysfunction underlies a large set of common and rare human diseases [2].

Numerous mitochondrial processes, for example, the oxidative phosphorylation [3], the import of proteins [4], and the replication of mitochondrial DNA [5], have been elucidated at the sub-cellular level, using mitochondria-enriched fractions as starting

material. This still remains the method of choice to investigate the effect of genetic, chemical, or pathological perturbations on mitochondrial-specific functions. Likewise, isolated mitochondria are instrumental to establish a direct and causal involvement of the organelle in a cellular phenotype. Finally, relatively pure preparations of mitochondria isolated from cells and tissues are often used for proteomics analyses that aim at studying composition, abundance, and modifications of the mitochondrial proteome under different conditions.

The most commonly used protocols for the isolation of mitochondria from cells and tissues include three main steps: (1) the selective disruption of plasma membrane to release intracellular organelles without compromising their integrity, (2) a differential centrifugation at low speed to remove cellular debris and large organelles such as nuclei, and (3) a high-speed centrifugation step of the supernatant to pellet lighter intracellular structures including mitochondria. However, available protocols may differ in the methods used to permeabilize the plasma membrane and in the speed of the differential centrifugation steps. While the latter should not compromise the quality and yield of the preparation, the first step is key to obtain intact mitochondria with high yields. On the one hand, an incomplete homogenization of the tissue may substantially decrease yields. On the other hand, the abrupt disruption of the cell membrane may compromise mitochondrial integrity and functions.

Mechanical homogenization procedures (e.g., mortar-pestle, bead beater, French press, cold shock) are often employed to generate cell and tissue lysates. The main drawback is that, by creating friction during sample tearing and ripping, these approaches generate extensive heat and shearing stress which can damage the organelles. Moreover, if performed manually by the user, tissue grinding can result in highly variable samples. The latter could be minimized by motorization of pestles.

In contrast, cell disruption by nitrogen cavitation, although less commonly used, has been shown to be an effective technique to extract intact and enzymatically active mitochondria from different sources [6–8]. This is achieved by a rapid decompression of the cell suspension placed in a cavitation chamber and subjected to high pressure in presence of nitrogen gas. Nitrogen, initially dissolved in the cell suspension under high pressure, comes out of solution when the pressure is released. As a result, bubbles are formed that will expand and rupture pressure-sensitive cellular structures such as plasma and nuclear membranes, while keeping smaller organelles intact. Afterwards, mitochondria are enriched by differential centrifugation. Cell lysis by nitrogen cavitation offers several advantages: (1) It is more reproducible than conventional homogenization methods because it is conducted under controlled and constant thermodynamic parameters (temperature and pressure).

(2) It minimizes shearing stress, thus increasing the yield of functionally active mitochondria. (3) It enables the enrichment of mitochondria from small organs like the cortex, spinal cord, and other brain regions as it can be easily applied to very small volumes of cell suspension. Moreover, it can efficiently extract mitochondria from synaptic membranes which form during tissue grinding.

In this chapter, we provide in-depth protocols for isolating functional crude and pure mitochondria in high yield from cultured cells (e.g., HeLa, HEK293, mouse embryonic fibroblasts (MEF), human primary fibroblasts, and lung epithelial cells), as well as from soft (e.g., brain, spinal cord, liver, and kidney) and hard rodent tissues (skeletal muscle and heart) (Fig. 1). These protocols will allow the user to purify mitochondria with high yields that can be used for downstream functional assays such as respiration, swelling and calcium buffering, as well as for proteomics profiling studies. Finally, we also provide a protocol to measure mitochondrial  $\text{Ca}^{2+}$  uptake kinetics, as a fast and simple method to test integrity of isolated mitochondria.

---

## 2 Materials

### 2.1 Equipment

1. Cell disruption vessel 45 ml (Parr Instruments).
2. Commercial nitrogen cylinder.
3. Ultracentrifuge up to  $45,000 \times g$  (Beckman Coulter).
4. Ultracentrifuge rotor for 3 ml tubes (Beckman Coulter, SW 55 Ti).
5. Refrigerated superspeed centrifuge (Sorvall, Evolution RC).
6. Centrifuge rotor, fixed angle (Sorvall, SS-34).
7. Centrifuge tubes 30 ml, glass.
8. Rubber adapter sleeves for ultracentrifuge tubes.
9. Dounce tissue grinder, all glass, 2 ml.
10. Mouse dissection and surgical tools.
11. Tissue grinder, PTFE pestle and glass tube, 45 ml.
12. Tissue grinder stirrer (IKA Eurostar digital).
13. Cell strainer for falcon tubes, pore size  $70 \mu\text{m}$ .
14. Stericup-GP sterile vacuum filtration system, pore size  $0.22 \mu\text{m}$ .
15. Glass rods.
16. 96-well fluorescence plate reader suitable for fast kinetic measurements with injection (BMG LABTECH, Clario star).
17. 96-well plate, black.

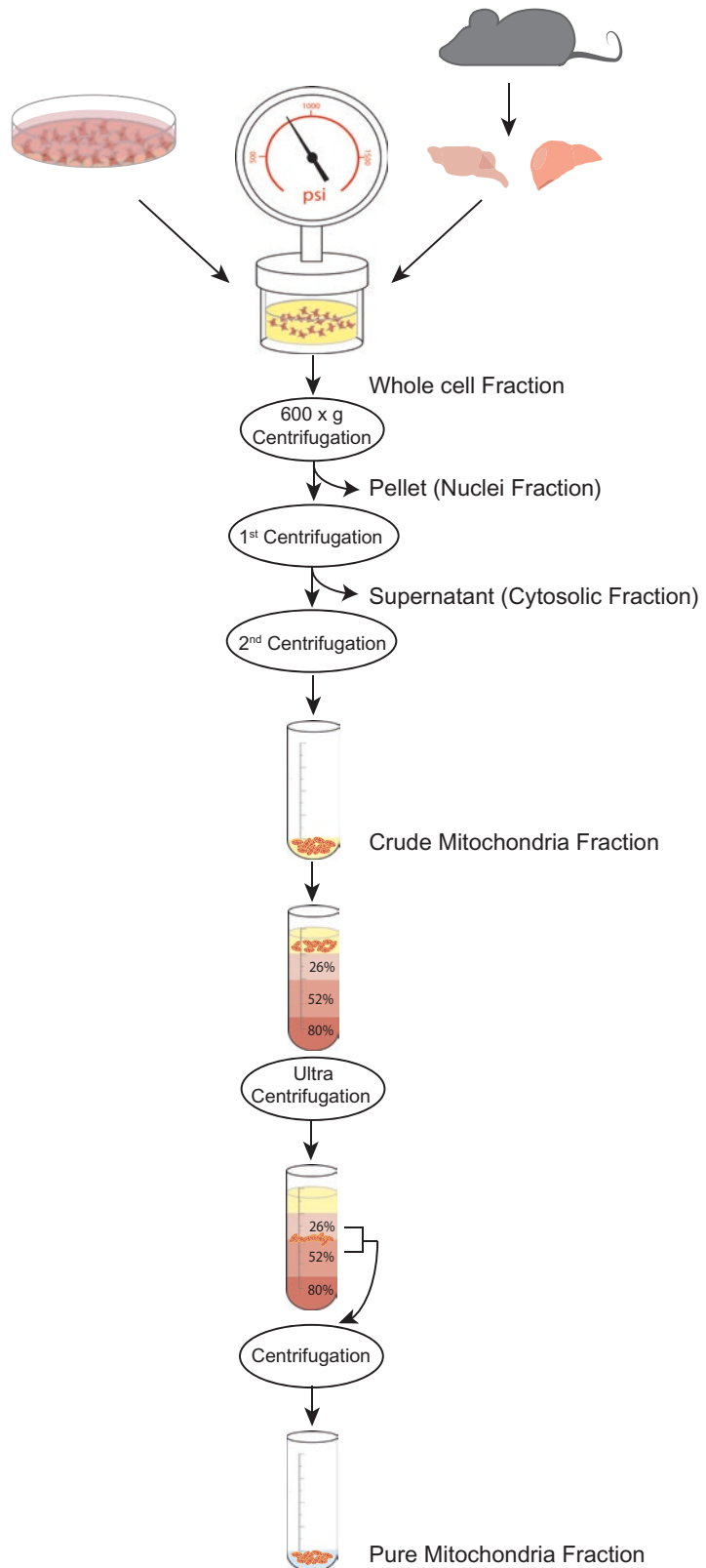


**Fig. 1** Experimental approach to isolate crude and pure mitochondrial fractions. A crude mitochondrial fraction can be isolated by differential centrifugation and if required it can be loaded on a discontinuous Percoll density gradient to obtain pure mitochondria

## 2.2 Reagents

1. 0.1 M ATP: dissolve 551.14 mg of adenosine 5'-triphosphate disodium salt hydrate (ATP) powder in 8 ml of distilled water. Adjust pH to 7.4 using KOH. Bring the solution to 10 ml with water, aliquot in 500  $\mu$ l samples, and store at  $-20^{\circ}\text{C}$ .
2. 0.5 M EDTA-KOH: dissolve 18.61 g of ethylenediaminetetraacetic acid (EDTA) disodium salt dihydrate in 80 ml of distilled water, and adjust pH to 7.4 using KOH (*see Note 1*). Bring the solution to 100 ml with water and store at room temperature.
3. 0.5 M EGTA-KOH: dissolve 19.02 g of ethylene glycol-bis(2-aminoethylether) (EGTA) in 80 ml of distilled water and adjust pH to 7.4 using KOH (*see Note 1*). Bring the solution to 100 ml with water and store at room temperature.
4. 1 M HEPES-KOH: dissolve 119.15 g of HEPES in 400 ml of distilled water and adjust pH to 7.4 using KOH. Bring the solution to 500 ml with water and store at room temperature.
5. 1 M KCl: dissolve 37.28 g of KCl in 400 ml of distilled water. Bring the solution to 500 ml with water and store at room temperature.
6. 1 M Tris-HCl: dissolve 60.57 g of Tris in 400 ml of distilled water. Adjust the pH to 7.4 using HCl. Bring the solution to 500 ml with water and store at room temperature.
7. 1 M  $\text{MgCl}_2$ : dissolve 50.8 g of magnesium chloride hexahydrate ( $\text{MgCl}_2$ ) in 200 ml of distilled water. Bring the solution to 250 ml with water and store at room temperature.
8. Isolation buffer (IB): 220 mM d-mannitol, 70 mM d-sucrose, 5 mM HEPES-KOH pH 7.4, 1 mM EGTA-KOH pH 7.4. Dissolve 40.08 g of d-mannitol and 23.96 g of d-sucrose in 900 ml of distilled water. Add 5 ml of 0.5 M HEPES-KOH and 2 ml of 0.5 M EGTA-KOH. Adjust with KOH pH to 7.4 at  $4^{\circ}\text{C}$ . Bring the solution to 1 L with water. Sterilize the solution using sterile vacuum filter units with a pore size of 0.22  $\mu\text{m}$ . Sterile IB solution can be stored at  $4^{\circ}\text{C}$  for several months.
9. 5 $\times$  isolation buffer (5 $\times$  IB): 1.1 M D-mannitol, 350 mM d-sucrose, 25 mM HEPES-KOH pH 7.4, 5 mM EGTA-KOH pH 7.4. Dissolve 200.32 g of d-mannitol and 119.84 g of d-sucrose in 900 ml of distilled water. Add 25 ml of 1 M HEPES-KOH and 10 ml of 0.5 M EGTA-KOH. Adjust with KOH pH to 7.4 at  $4^{\circ}\text{C}$ . Bring the solution to 1 L with water. Sterilize the solution using sterile vacuum filter units with a pore size of 0.22  $\mu\text{m}$ . Sterile 5 $\times$  IB solution can be stored at  $4^{\circ}\text{C}$  for several months.
10. Isolation buffer 1 muscle ( $\text{IB1}_M$ ): 100 mM KCl, 50 mM Tris-HCl pH 7.4, 2 mM EDTA-KOH pH 7.4. Mix 100 ml of 1 M KCl, 50 ml of 1 M Tris-HCl pH 7.4, and 4 ml of 0.5 M

EDTA-KOH with 800 ml of distilled water. Adjust with KOH pH to 7.4 at 4 °C and bring the solution to 1 L. Sterilize the solution using sterile vacuum filter units with a pore size of 0.22 µm. Sterile IB<sub>1M</sub> solution can be stored at 4 °C for several months.

11. 5× isolation buffer 1 muscle (5× IB<sub>1M</sub>): 500 mM KCl, 250 mM Tris-HCl pH 7.4, 10 mM EDTA-KOH pH 7.4. Mix 500 ml of 1 M KCl, 250 ml of 1 M Tris-HCl, and 20 ml of 0.5 M EDTA-KOH. Adjust with KOH pH to 7.4 at 4 °C and bring the solution to 1 L with distilled water. Sterilize the solution using sterile vacuum filter units with a pore size of 0.22 µm. Sterile 5× IB<sub>1M</sub> solution can be stored at 4 °C for several months.
12. 2× isolation buffer 2 muscle (2× IB<sub>2M</sub>): 200 mM KCl, 100 mM Tris-HCl pH 7.4, 4 mM EDTA-KOH pH 7.4, 10 mM MgCl<sub>2</sub>. Mix 50 ml of 1 M KCl, 25 ml of 1 M Tris-HCl, 2 ml of 1 M EDTA-KOH, and 2.5 ml 1 M MgCl<sub>2</sub> with 150 ml of distilled water. Adjust with KOH pH to 7.4 at 4 °C and bring the solution to 250 ml. Sterilize the solution using sterile vacuum filter units with a pore size of 0.22 µm. Sterile IB<sub>2M</sub> solution can be stored at 4 °C for several months.
13. 0.5 M succinate: dissolve 2.95 g of succinic acid in 40 ml of distilled water. Adjust pH with KOH to 7.4 at RT and bring the solution to 50 ml with water. Aliquot the solution in 0.5 ml aliquots and store at -20 °C. Do not freeze and thaw.
14. 0.5 M malate: dissolve 3.35 g of L-(-)-malic acid in 40 ml of distilled water. Adjust pH with KOH to 7.4 at RT and bring the solution to 50 ml with water. Aliquot the solution in 0.5 ml aliquots and store at -20 °C. Do not freeze and thaw.
15. 0.5 M glutamate: dissolve 3.68 g of l-glutamic acid in 40 ml of distilled water. Adjust pH with KOH to 7.4 at RT and bring the solution to 50 ml with water. Aliquot the solution in 0.5 ml aliquots and store at -20 °C. Do not freeze and thaw.
16. 1 M KH<sub>2</sub>PO<sub>4</sub>: dissolve 6.80 g of KH<sub>2</sub>PO<sub>4</sub> in 40 ml distilled water and adjust pH with KOH to 7.4 at RT and bring the solution to 50 ml with water. Sterilize the solution using filter with a pore size of 0.22 µm pore size. Sterile solution is stable for several months.
17. 2× respiration buffer (2× RB): 274 mM KCl, 20 mM HEPES-KOH pH 7.4, 5 mM MgCl<sub>2</sub>, 6 mM KH<sub>2</sub>PO<sub>4</sub>-KOH pH 7.4, 50 µM EDTA. Combine 68.5 ml of 1 M KCl, 5 ml of 1 M HEPES-KOH, 1.25 ml of 1 M MgCl<sub>2</sub>, 1.5 ml KH<sub>2</sub>PO<sub>4</sub>-KOH, and 25 µl of 0.5 M EDTA-KOH with 150 ml distilled water, and adjust pH to 7.4 at RT using KOH. Bring solution to 250 ml, and sterilize the solution using sterile vacuum filter units with a pore size of 22 µM. Sterile 2× RB solution can be stored at RT for several months.

18. Bicinchoninic acid assay (BCA) kit.
19. 100% Percoll solution (pH 8.5–9.5).
20. 420  $\mu$ M Calcium Green-5 N Stock solution: Dissolve 0.5 mg Calcium Green-5 N powder with 1 ml distilled water. Aliquot solution to 15  $\mu$ l aliquots and store at  $-20^{\circ}\text{C}$  protected from light. Do not freeze and thaw.
21. 1 mM Ru360 stock solution: dissolve 0.5 mg Ru360 with 909  $\mu$ l distilled water to obtain 1 mM Ru360 stock solution. Aliquot solution to 15  $\mu$ l aliquots and store at  $-20^{\circ}\text{C}$ .
22. 1 $\times$  PBS (phosphate-buffered saline), commercially available.
23. Fatty acid-free bovine serum albumin (BSA).
24. EDTA-free protease inhibitor cocktail tablets for 50 ml medium.
25. Heparin.

### 2.3 Working Solutions

Working solutions should be prepared fresh on the day of the experiment and should be kept on ice the whole time, unless indicated otherwise.

1. IB(++) buffer: add 500 mg of fatty acid-free BSA (0.5%) (*see Note 2*) and two tablets of protease inhibitor cocktail to 100 ml of IB. 100 ml of IB(++) are sufficient for the isolation of mitochondria from one mouse liver ( $\sim 2$  g tissue).
2. IB<sub>M</sub>(+) buffer: add 500 mg of fatty acid-free BSA to 100 ml of IB<sub>M</sub>. 80 ml of IB<sub>M</sub>(+) are sufficient for the isolation of mitochondria from  $\sim 2$  g of skeletal muscle tissue.
3. IB<sub>M</sub>(++) buffer: add 500 mg of fatty acid-free BSA and two tablets of EDTA-free protease inhibitor cocktail to 100 ml of IB<sub>M</sub>. 80 ml of IB<sub>M</sub>(++) are sufficient for the isolation of mitochondria from  $\sim 2$  g of hind limb muscle tissue.
4. IB<sub>2M</sub>(++) buffer: mix 25 ml of 2 $\times$  IB<sub>2M</sub> with 500  $\mu$ l 100 mM ATP and 122.85 U of protease from *Bacillus licheniformis* and fill up to 50 ml with distilled water. If necessary, adjust the pH to 7.4 with KOH at  $4^{\circ}\text{C}$ . 30 ml of IB<sub>2M</sub>(++) are sufficient for the isolation of mitochondria from  $\sim 2$  g of hind limb muscle tissue.
5. Heparin/PBS solution: Prepare 20 U heparin/ml PBS solution using heparin sodium salt from porcine intestinal mucosa ( $\geq 150$  U/mg, dry basis). Depending on the perfusion system used, between 10 and 50 ml of heparin/PBS solution are required for the perfusion of a whole mouse.
6. 80% Percoll solution: mix 4 ml of 5 $\times$  IB buffer with 16 ml of 100% Percoll solution.
7. 52% Percoll solution: mix 6.5 ml of 80% Percoll solution with 3.5 ml of 1 $\times$  IB(++) buffer.

8. 26% Percoll solution: mix 3.25 ml of 80% Percoll solution with 6.75 ml of IB(++) buffer.
9. Respiration buffer (RB++): For 50 ml RB++, add 0.5 ml of each 0.5 M succinate, 0.5 M glutamate, and 0.5 M malate to 25 ml 2× RB. Add 11.9  $\mu$ l of 420  $\mu$ M Calcium Green-5 N and fill up to 50 ml with distilled water. Keep the solution at RT protected from light.
10. Ca<sup>2+</sup> injection solution: add 8  $\mu$ l of 0.5 M CaCl<sub>2</sub> stock solution to 10 ml of RB++. Keep the solution at RT and protected from light until use.

### 3 Methods

#### 3.1 Isolation of Crude Mitochondria from Cultured Cells

The isolation of crude mitochondria from cells by nitrogen cavitation requires approximately 40 min. Working solutions as well as tissue grinder and cell disruption vessel should be kept ice-cold during the whole procedure.

1. Seed cells 2–3 days before the experiment. The number of cells that is required to isolate more than 1 mg of crude mitochondria may vary between cell types, and it usually reflects cell size and mitochondrial content. The typical yields for commonly used cell types are listed in Table 1 (*see Note 3*).
2. Remove the medium from the cells and wash once with 5–10 ml of room temperature PBS.
3. Remove PBS and detach the cells using a cell scraper. Collect the cells in a pre-weighted falcon tube. If needed, use few ml PBS to collect the remaining cells from the plate. Keep the sample on ice at all time.
4. Centrifuge cells at 600  $\times g$  for 5 min at 4 °C.
5. Discard the supernatant and weight out the cell pellet (*see Note 4*).
6. Resuspend the cells using 1 ml IB(++) per 10 mg of cells.

**Table 1**  
Yield of mitochondria isolated from commonly used cell line

Cell line	Culture surface (cm <sup>2</sup> )	Mitochondrial yield (mg)
HEK-293	450	~1.5
HeLa	450	~2.25
MEF	450	~1.8
Human fibroblast	450	~0.4

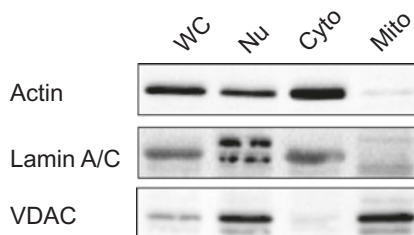


**Fig. 2** Isolation of intact mitochondria from mouse liver. The enrichment of intact mitochondria from cell lysate is confirmed by immunoblot analysis of whole cell (WC) lysate, cytosolic (Cyto), nuclear, and crude mitochondrial (Mito) fractions, using antibodies against actin (actin, cytosolic marker), laminin A/C (nuclear marker), and VDAC (mitochondrial marker)

7. Transfer the solution into a prechilled cell disruption vessel, add the magnetic stirrer bar into the vessel, and place it on a magnetic stirrer in a cold room. Close the vessel and attach the filling connection to a commercial nitrogen cylinder as in the instructions manual. To pressurize the vessel, open first the nitrogen cylinder to release nitrogen into the flexible nylon pressure hose. Then open carefully the valve on the head of the cylinder and adjust the pressure to 800 *psi* (*see Note 5*). Leave the sample in the vessel at 800 *psi* for 10 min.
8. Hold a 50 ml falcon tube at the lower valve of the vessel while depressurizing to collect the sample (*see Note 6*).
9. If the quality of mitochondria isolation is to be tested, save ~100  $\mu$ l of sample for quality analysis (Fig. 2). This represents the whole cell (WC) fraction (*see Note 7*).
10. Centrifuge the whole cell sample at  $600 \times g$  for 10 min at 4 °C.
11. Carefully transfer the supernatant to a prechilled glass centrifuge tube without touching the pellet.
12. If the quality of mitochondria isolation is to be tested, save the pellet for quality analysis (Fig. 2). This represents the nuclei fraction (*see Note 7*).
13. Centrifuge the supernatant at  $8000 \times g$  for 10 min at 4 °C.
14. If the quality of mitochondria isolation is to be tested, save after centrifugation 500  $\mu$ l for quality analysis. This represents the cytosolic (Cyto) fraction (*see Note 7*), while the pellet contains the mitochondrial fraction.
15. Discard the supernatant, and remove any loose or light-colored material surrounding the pellet, preferably by aspiration with a glass micropipette (*see Note 8*).

16. Carefully dislodge the pellet using a glass rod.
17. Resuspend the pellet in a small volume of IB(++) by slowly pipetting up and down first with a cut 200  $\mu$ l pipette tip to minimize shearing forces and afterwards with an intact 200  $\mu$ l pipette tip to obtain a homogeneous sample. The volume for resuspension depends on the pellet size and should be as small as possible (50–100  $\mu$ l for mitochondria isolated from cells). Avoid the formation of bubbles during resuspension.
18. Quantify the concentration of crude mitochondria by BCA method (*see Note 9*).

### 3.2 Isolation of Crude Mitochondria from Soft Mouse Tissues

Timing for the isolation of crude mitochondria from soft mouse tissues depends on the number of processed tissues and animals. Approximately 1.5 h are necessary to isolate crude mitochondria from one mouse liver. The typical yields for several soft tissues are listed in Table 2 and refer to one mouse per tissue.

Working solutions as well as tissue grinder and cell disruption vessel should be kept ice-cold during the whole procedure.

1. Sacrifice the mouse by cervical dislocation and rapidly explant the organs of interest (*see Note 10*).
2. Weight out the organ and place it in a beaker on ice.
3. Add 1 ml IB(++)/0.1 g of tissue (*see Note 11*).
4. Mince the tissue in small pieces (2–4 mm) using scissors and wash several times with IB(++) to remove any contaminating blood (*see Note 12*).
5. Transfer the tissue pieces to a prechilled tissue grinder and homogenize with one stroke at 300 rpm (*see Notes 13–15*).

**Table 2**  
**Yield of mitochondria isolated from mouse tissues**

Tissue	Weight (mg)	Mitochondrial yield (mg)
Liver	~1500	~15
Kidney	~350	~1.9
Spinal cord	~60	~0.4
Cerebellum	~75	~2.7
Cortex	~125	~4
Ventral midbrain	~40	~0.5
Striatum	~40	~0.5
Skeletal muscle	~1800	~25
Heart	~160	~2

6. Transfer the homogenate into a prechilled cell disruption vessel, add the magnetic stirrer bar into the vessel, and place it on a magnetic stirrer in a cold room (*see* **Notes 14** and **15**). Close the vessel and attach the filling connection to a commercial nitrogen cylinder as in the instructions manual. To pressurize the vessel, open first the nitrogen cylinder to release nitrogen into the flexible nylon pressure hose. Then open carefully the valve on the head of the cylinder and adjust the pressure to 800 psi (*see* **Note 5**). Leave the sample in the vessel at 800 psi for 10 min.
7. Hold a 50 ml falcon tube at the lower valve of the vessel while depressurizing to collect the sample (*see* **Note 6**).
8. If the quality of mitochondria isolation is to be tested, save a 100  $\mu$ l of sample for quality analysis. This represents the whole cell (WC) fraction (*see* **Note 7**).
9. Centrifuge at  $600 \times g$  for 10 min at 4 °C.
10. Transfer the supernatant to a prechilled glass centrifuge tube. Be careful to prevent contaminations from the cell pellet. If the quality of mitochondria isolation is to be tested, keep the pellet for quality analysis (*see* **Note 7**). This represents the nuclei fraction (Nu).
11. Centrifuge the supernatant at “centrifuge speed 1” as in Table 3 for 10 min at 4 °C (*see* **Note 16**).
12. If the quality of mitochondria isolation is to be tested, save after centrifugation 500  $\mu$ l for quality analysis. This represents the cytosolic (Cyto) fraction (*see* **Note 7**), while the pellet contains the mitochondrial fraction.
13. Discard the supernatant and carefully dislodge the pellet using a glass rod.
14. Resuspend the pellet with a pipette in the initial volume of IB(++), (*see* **step 3**). Avoid the formation of bubbles during resuspension.

**Table 3**  
**Centrifugation speeds for isolation of mitochondria from mouse tissues**

Tissue	Centrifugation speed 1	Centrifugation speed 2
Kidney	10 min $8000 \times g$	2 min $2000 \times g$ followed by 8 min $4000 \times g$
Liver	10 min $8000 \times g$	2 min $2000 \times g$ followed by 8 min $4000 \times g$
Spinal cord	10 min $12,000 \times g$	10 min $12,000 \times g$
Brain	10 min $12,000 \times g$	10 min $12,000 \times g$

15. Centrifuge the sample at “centrifugation speed 2” as in Table 3 for 10 min at 4 °C (*see Note 16*).
16. Discard the supernatant and resuspend the pellet with a small volume of IB(++) by slowly pipetting up and down first with a cut 200  $\mu$ l pipette tip to minimize shearing forces and afterward with an intact 200  $\mu$ l pipette tip to obtain a homogeneous sample. The volume for resuspension depends on the pellet size and should be as small as possible (e.g., 100–200  $\mu$ l for the liver and ~50  $\mu$ l for the brain tissues or spinal cord). Avoid the formation of bubbles during resuspension.
17. Quantify the concentration of the crude mitochondrial fraction by BCA method (*see Note 9*).

### **3.3 Isolation of Crude Mitochondria from Mouse Skeletal Muscle and Heart**

Timing for the isolation of crude mitochondria from skeletal muscle or heart depends on the number of processed tissues and animals. Approximately 2 h are necessary to isolate crude mitochondria from one mouse heart. Working solutions as well as tissue grinder and cell disruption vessel should be kept ice-cold during the whole procedure. Skeletal muscle and heart are fibrous tissues, which cannot be easily homogenized without previous enzymatic digestion. To avoid that an uneven homogenization of the tissue clogs the cavitation vessel, we employ for mitochondrial isolation from muscle and heart tissue the following protocol:

1. Sacrifice the mouse by cervical dislocation and rapidly explant the organs of interest (*see Note 10*).
2. Weight out the organ and place it in a beaker on ice (*see Note 11*).
3. Mince the tissue in small pieces (2–4 mm) using scissors and wash it several times with IB1<sub>M</sub>(+) to remove any contaminating blood.
4. Decant any IB1<sub>M</sub>(+) and add 1 ml IB2<sub>M</sub>(+)/0.1 g of tissue.
5. Incubate for 3 min while stirring on ice.
6. Transfer the tissue pieces to a prechilled tissue grinder and homogenize with three strokes at 500 rpm. Use motorized system to ensure efficient homogenization and minimize variations between samples.
7. Transfer the homogenate into a falcon tube, and centrifuge at  $600 \times g$  for 10 min at 4 °C to remove plasma membrane and nuclei and not homogenized tissue.
8. Collect the supernatant which contains mitochondria, and filter it through a cell strainer of 70  $\mu$ m pore size that is placed on a prechilled glass centrifuge tube.
9. Immediately centrifuge the sample at  $10,400 \times g$  for 10 min at 4 °C.

10. Discard the supernatant and dislodge the pellet using a glass rod. Resuspend the pellet with 300–500  $\mu\text{l}$  volume of  $\text{IB1}_{\text{M}(++)}$  by slowly pipetting up and down first with a cut 200  $\mu\text{l}$  pipette tip to minimize shearing forces and afterward with an intact 200  $\mu\text{l}$  pipette tip to obtain a homogeneous sample. Avoid the formation of bubbles during resuspension.
11. Dilute the sample with  $\text{IB1}_{\text{M}(++)}$  at 1 ml/0.1 g of tissue.
12. Repeat **steps 9–11** once to thoroughly wash out the remaining proteinases.
13. Centrifuge at  $4000 \times g$  for 10 min at 4 °C.
14. Discard the supernatant and dislodge the pellet using a glass rod. Resuspend the pellet with  $\sim 100 \mu\text{l}$  volume of  $\text{IB1}_{\text{M}(++)}$  by slowly pipetting up and down first with a cut 200  $\mu\text{l}$  pipette tip to minimize shearing forces and afterward with an intact 200  $\mu\text{l}$  pipette tip to obtain a homogeneous sample. The volume for resuspension depends on the pellet size and should be as small as possible. Avoid the formation of bubbles during resuspension.
15. Quantify the concentration of crude mitochondria by BCA method (*see Note 9*).

### **3.4 Isolation of Pure Mitochondria by Discontinuous Percoll Gradient**

Preparations of crude mitochondrial fractions usually contain other cellular structures as well. Lysosomes and endoplasmic reticulum are common contaminants which either co-sediment with mitochondria during differential centrifugation or are physically associated with them. To increase mitochondrial purity, the differential centrifugation step can be combined with a discontinuous Percoll density gradient. The advantage of a discontinuous gradient, over a continuous one, is that mitochondria concentrate as a sharp band at the interface between two Percoll steps, which facilitates their collection. Here, we provide a fast protocol which can be performed after obtaining a crude mitochondrial fraction. As an example, we apply this protocol to purify intact organelles from crude skeletal muscle mitochondria.

1. Transfer 1 ml of 80% Percoll solution into the ultracentrifuge tube. Mark the level of the solution (*see Note 17*).
2. Add 1.5 ml of 52% Percoll solution drop wise on top of the 80% Percoll solution. Hold the tube in a 45° angle to prevent mixing of the two solutions. Mark the level of the second solution.
3. Add 500  $\mu\text{l}$  of 26% Percoll solution drop wise on top of the 52% Percoll solution. Hold the tube in a 45° angle to prevent mixing of solutions.
4. Dilute the freshly isolated, crude mitochondrial fraction with 500  $\mu\text{l}$  of the corresponding IB solution supplemented with fatty acid-free BSA and protease inhibitors ( $\text{IB}(++)$  or  $\text{IB1}_{\text{M}(++)}$  depending on the tissue of origin).

5. Place the diluted sample on top of the Percoll gradient. Balance the rotor carefully. In case of unequal sample number, use a balance tube (tube with the same weight as the sample tube).
6. Centrifuge at  $44,000 \times g$  for 45 min at 4 °C.
7. Collect pure mitochondria at the interface between 26% and 52% Percoll gradient (Fig. 1) (*see Note 18*).
8. Dilute the sample at least tenfold with the corresponding IB solution (IB(++) or IB<sub>1M</sub>), and transfer it to a glass centrifuge tube.
9. Centrifuge at  $8000 \times g$  for 10 min at 4 °C.
10. Decanted the supernatant. The pellet contains pure mitochondria.
11. Dislodge the pellet using a small glass rod. Resuspend the pellet with a small volume of IB solution (IB(++) or IB<sub>1M</sub>) by slowly pipetting up and down first with a cut 200 µl pipette tip to minimize shearing forces and afterward with a 200 µl pipette tip to obtain a homogeneous sample. Avoid formation of bubbles during resuspension.
12. Measure the concentration of the pure mitochondrial fraction by BCA method (*see Note 9*).

### 3.5 Measuring Mitochondrial Calcium (Ca<sup>2+</sup>) Buffering Capacity

Measuring mitochondrial Ca<sup>2+</sup> buffering capacity is a fast and efficient method to assess the integrity of isolated mitochondria. The organelle takes up Ca<sup>2+</sup> via an inner membrane channel called the mitochondrial calcium uniporter (MCU) [9–11]. Ca<sup>2+</sup> uptake is driven by the mitochondrial membrane potential, which is generated by the oxidative phosphorylation system through pumping of protons across the inner mitochondrial membrane. Therefore, the integrity and coupling of isolated mitochondria will be reflected by their ability to buffer exogenously added Ca<sup>2+</sup> to the respiration medium.

First, mitochondria are diluted in a buffer containing a non-permeable Ca<sup>2+</sup> indicator such as Calcium Green-5 N ( $K_d$  of 14 µM in the absence of magnesium). If the indicator binds Ca<sup>2+</sup>, it exhibits an increase in fluorescence emission intensity with little shift in wavelength. By taking up Ca<sup>2+</sup>, mitochondria compete with the dye, and as a result the intensity of the emitted light decreases.

1. Use a fluorescence microplate reader with the following settings: Ex/Em of 503/536 nm, kinetic reading mode and short time interval (e.g., reading of 24 wells with a 2 s interval).
2. Prime the injector with 400 µM Ca<sup>2+</sup> injection solution.
3. Dilute an appropriate amount of freshly isolated crude or pure mitochondria in RB++ to 1 mg/ml. This amount should be sufficient to test all of the conditions of interest in at least technical triplicates (*see Note 19*).
4. Pipette 90 µl of the mitochondria-containing solution per well into a black 96-well plate. As a positive control for mitochondrial Ca<sup>2+</sup> uptake, include 10 µM Ru360, a known MCU

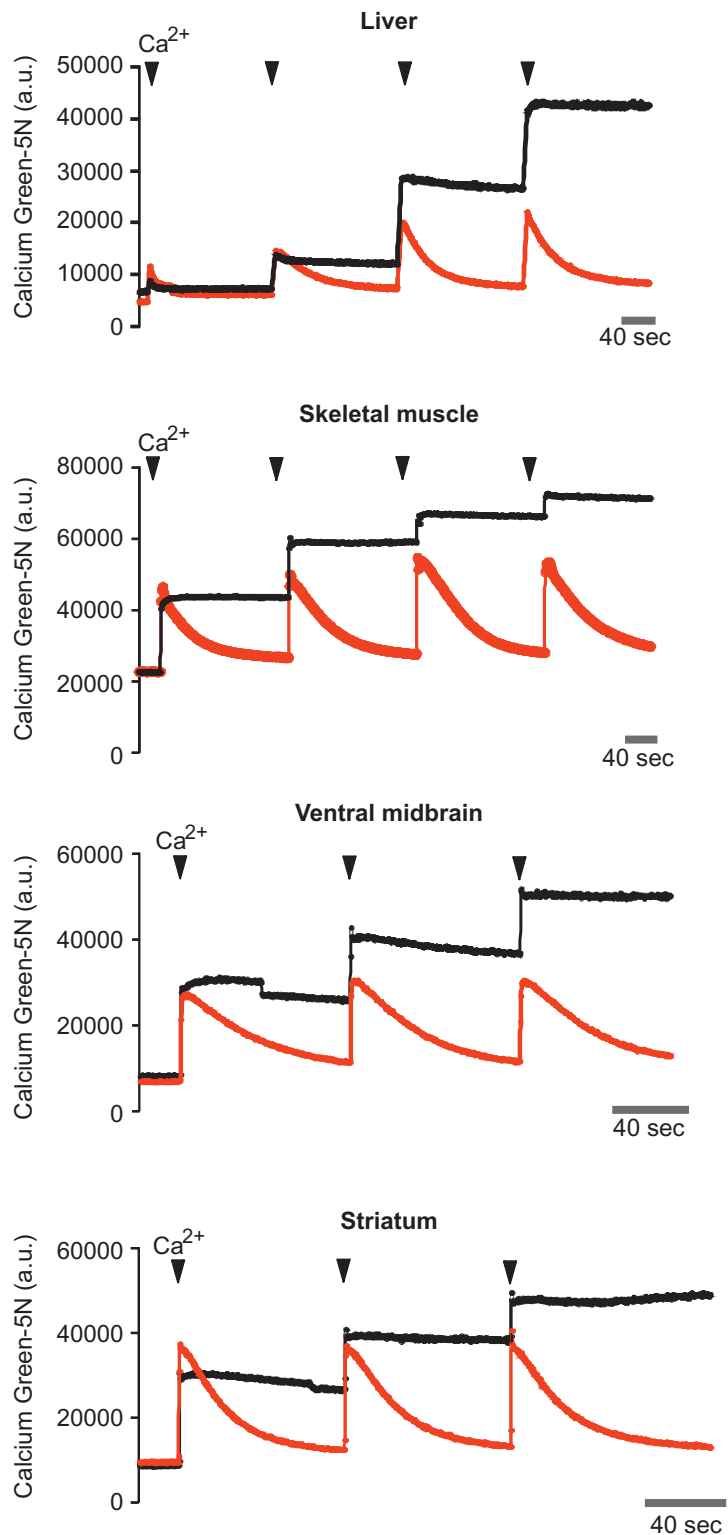


**Fig. 3** Ca<sup>2+</sup> uptake kinetics in purified mitochondria from different mouse tissues. Intact and coupled mitochondria are isolated from mouse organs using nitrogen cavitation. MCU-dependent Ca<sup>2+</sup> uptake kinetics are measured in 96-well plates with Calcium Green-5N following consecutive injections of 40 μM Ca<sup>2+</sup> (red traces). Ca<sup>2+</sup> uptake can be inhibited by the addition of 10 μM Ru360 (black traces)

inhibitor. If possible, use a multichannel pipette to minimize pipetting error.

5. Mix well and incubate for 5 min at RT.
6. Place the plate inside the plate reader.
7. Start the assay and monitor basal fluorescence, followed by a repetitive injection of 10  $\mu\text{l}$  from the 400  $\mu\text{M}$   $\text{Ca}^{2+}$  solution. Figure 3 shows typical  $\text{Ca}^{2+}$  uptake kinetics of crude mitochondria isolated from different mouse tissues.

---

## 4 Notes

1. EDTA and EGTA solutions are very acidic and dissolve poorly in water. Add KOH tablets till reaching a pH of  $\sim 7$ , and then continue adjusting the pH with a 5 M KOH solution.
2. BSA binds fatty acids. Those are released from the cells during the permeabilization process and can disrupt the integrity of mitochondrial membranes. Therefore, the addition of fatty acid-free BSA is critical for preserving mitochondrial integrity. It is recommended to wash out the BSA for proteomics.
3. The metabolic state of cells is influenced by the number of culturing passages and cell density. In order to minimize variation between samples, all cell lines to be processed should be cultured in parallel and have a similar passage number and a cell density corresponding to approximately 80% of the culture dish surface.
4. To weight out the cell pellet, balance the empty Falcon before use.
5. A pressure of 800 psi selectively permeabilizes the plasma membrane but not the mitochondrial membranes. Large sample volumes can absorb significant amounts of nitrogen leading to a drop of the pressure after several seconds. If necessary, readjust the pressure.
6. The permeabilization by nitrogen cavitation occurs at the decompression step. It is recommended to become completely familiar with the sample collection step before performing the experiment.
7. The enrichment of mitochondria from whole cells can be tested by Western blot analyses of whole cell (WC), nuclear (Nu), cytosolic (Cyto), and mitochondrial (Mito) fractions (Fig. 2). This step is particularly useful when testing an isolation protocol or the isolation from a specific tissue for the first time.

Equal protein amounts of those fractions are decorated with antibodies that recognize bona fide cytosolic (e.g., actin), nuclear (e.g., lamine A/C), and mitochondrial proteins (e.g., OXPHOS subunits and porin). The integrity of the mitochondrial fraction can also be tested by protein immunoblot. To

this goal, loss of soluble matrix and intermembrane space proteins, such as cyclophilin D and cytochrome c, respectively, should be quantified.

8. Removing of loose or lighter-colored material surrounding the pellet can increase purity of the mitochondrial fraction but can also increase variation between samples. We recommend to skip this step if the sample is used in sensitive analysis such as mass spectrometry. In this case, the whole pellet should be carefully resuspended in the same volume of IB (without BSA and protease inhibitors). The sample should be centrifuged again at  $8000 \times g$  for 10 min at 4 °C, and the resulting pellet should be resuspended in a small volume of IB (50–100  $\mu$ l).
9. Other protein quantification methods can also be used (e.g., Bradford protein assay). It is recommended to test several dilution factors (25 $\times$ , 50 $\times$  and 100 $\times$ ) to obtain an accurate sample concentration. For reproducible results, ensure to use the same quantification method for all samples and the same standard for the calibration curve.
10. During the isolation procedure, blood cells are ruptured and release hemoglobin which sediments with the mitochondrial pellet and can compromise the functionality of mitochondria. When isolating mitochondria from organs that are well supplied by blood, such as the liver, it is recommended to euthanize the mice with CO<sub>2</sub> and to perform a whole body perfusion with heparin/PBS [12].
11. If necessary, organs can be kept for up to 2 h in ice-cold PBS before proceeding with the isolation protocol.
12. When isolating mitochondria from larger and compact tissue like the liver or kidney, a motorized homogenizer improves dislodging and minimizes variation between samples. When isolating mitochondria from small organs such as spinal cord or brain regions, it is not necessary to mince the tissue. Instead, use a small, prechilled glass tissue grinder with a loose pestle to dislodge the tissue and transfer the sample directly to the nitrogen cavitation vessel.
13. This step is performed with the aim of dislodging the tissue and not of permeabilizing the cells. The latter occurs during nitrogen cavitation.
14. Remove any large tissue pieces that remain after homogenization as they can clog the valve of the nitrogen cavitation vessel.
15. When working with small volumes of homogenate (less than 3 ml) place the sample in a test tube or a small beaker that can be placed inside the vessel cylinder. As a general rule, the test tube should be twice the size of the sample volume.
16. Sedimentation speed varies for mitochondria of different tissues.

17. During the centrifugation, mitochondria will sediment at the interface between 26 and 54% Percoll density. Demarking the interface will facilitate the identification of the right density band.
18. To collect mitochondria either aspirate with a long glass micro-pipette or remove layer by layer till reaching the mitochondria-containing band.
19. Mitochondria isolation buffer contains EDTA or EGTA which influence the calcium kinetics. Therefore, it is beneficial to work with highly concentrated mitochondria (25–50 mg/ml).

## References

1. Smith AC, Robinson AJ (2011) A metabolic model of the mitochondrion and its use in modelling diseases of the tricarboxylic acid cycle. *BMC Syst Biol* 5:102. doi:[10.1186/1752-0509-5-102](https://doi.org/10.1186/1752-0509-5-102)
2. Labbe K, Murley A, Nunnari J (2014) Determinants and functions of mitochondrial behavior. *Annu Rev Cell Dev Biol* 30:357–391. doi:[10.1146/annurev-cellbio-101011-155756](https://doi.org/10.1146/annurev-cellbio-101011-155756)
3. Mitchell P, Moyle J (1967) Chemiosmotic hypothesis of oxidative phosphorylation. *Nature* 213(5072):137–139
4. Hallermayer G, Zimmermann R, Neupert W (1977) Kinetic studies on the transport of cytoplasmically synthesized proteins into the mitochondria in intact cells of *Neurospora crassa*. *Eur J Biochem* 81(3):523–532
5. Schatz G, Haslbrunner E, Tuppy H (1964) Deoxyribonucleic acid associated with yeast mitochondria. *Biochem Biophys Res Commun* 15(2):127–132
6. Hunter MJ, Commerford SL (1961) Pressure homogenization of mammalian tissues. *Biochim Biophys Acta* 47:580–586
7. Krippner A, Matsuno-Yagi A, Gottlieb RA, Babior BM (1996) Loss of function of cytochrome c in Jurkat cells undergoing fas-mediated apoptosis. *J Biol Chem* 271(35):21629–21636
8. Gottlieb RA, Adachi S (2000) Nitrogen cavitation for cell disruption to obtain mitochondria from cultured cells. *Methods Enzymol* 322:213–221
9. Perocchi F, Gohil VM, Girgis HS, Bao XR, McCombs JE, Palmer AE, Mootha VK (2010) MICU1 encodes a mitochondrial EF hand protein required for Ca<sup>2+</sup> uptake. *Nature* 467(7313):291–296. doi:[10.1038/nature09358](https://doi.org/10.1038/nature09358)
10. Baughman JM, Perocchi F, Girgis HS, Plovanich M, Belcher-Timme CA, Sancak Y, Bao XR, Strittmatter L, Goldberger O, Bogorad RL, Kotliansky V, Mootha VK (2011) Integrative genomics identifies MCU as an essential component of the mitochondrial calcium uniporter. *Nature* 476(7360):341–345. doi:<http://www.nature.com/nature/journal/v476/n7360/abs/nature10234.html#supplementary-information>
11. De Stefani D, Raffaello A, Teardo E, Szabo I, Rizzuto R (2011) A forty-kilodalton protein of the inner membrane is the mitochondrial calcium uniporter. *Nature* 476(7360):336–340. doi:[10.1038/nature10230](https://doi.org/10.1038/nature10230)
12. Gage GJ, Kipke DR, Shain W (2012) Whole animal perfusion fixation for rodents. *J Vis Exp* 65. doi:[10.3791/3564](https://doi.org/10.3791/3564)

## Isolation of Mitochondria from *Saccharomyces cerevisiae*

Toshiaki Izawa and Ann-Katrin Unger

### Abstract

The budding yeast *Saccharomyces cerevisiae* is an important model organism to study cellular structure and function. Due to its excellent accessibility to genetics and biochemical and microscopic analyses, studies with yeast have provided fundamental insights into mitochondrial biology. Yeast offers additional advantages because it can grow under fermenting conditions when oxidative phosphorylation is not obligatory and because the majority of mitochondrial structure and function are largely conserved during evolution. Isolation of mitochondria is an important technique for mitochondrial studies. This chapter focuses on procedures for the isolation and purification of intact yeast mitochondria that can be used for numerous functional assays as well as for analyses of mitochondrial ultrastructure.

**Key words** Yeast culture media, Spheroplasts, Homogenization, Cellular fractionation, Isolation and purification of mitochondria

---

### 1 Introduction

Mitochondria are essential organelles of eukaryotic cells. They exert a multitude of important metabolic functions including energy transduction by the citrate cycle and oxidative phosphorylation, metabolism of amino acids and fatty acids, and synthesis of FeS clusters, heme, quinones, and phospholipids. They are involved in apoptosis and developmental processes such as aging and play an important role in many important human disorders, including diabetes, cancer, and neurodegenerative disorders, such as the Alzheimer, Parkinson, and Huntington diseases.

The budding yeast *Saccharomyces cerevisiae* is a powerful model organism to study mitochondrial function and architecture. Since protein composition, function, and architecture of mitochondria are highly conserved among eukaryotes, studies of yeast mitochondria are instructive for understanding the molecular biology of mitochondria also of mammalian cells. In addition, since *Saccharomyces cerevisiae* can satisfy its energy requirement by fermentation, a number of viable knockout mutants for the genes required for respiration can be constructed. This makes it much

easier to analyze the function of mitochondrial proteins essential for respiration. Furthermore, *Saccharomyces cerevisiae* offers excellent accessibility to genetic manipulation and biochemical and macroscopic analyses. Indeed, a large number of conserved proteins and complexes required for mitochondrial function and architecture were first discovered using yeast cells.

*Saccharomyces cerevisiae* can utilize both fermentable and nonfermentable carbon sources. Depending on carbon source availability, the cells regulate the quantity and architecture of mitochondria [1–3]. Glucose is a routinely used fermentable carbon source. On glucose-containing medium, most of ATP is produced in the cytosol by fermentation. Under these conditions the expression of a number of mitochondrial proteins including enzymes of the citrate cycle and oxidative phosphorylation are strongly repressed, as well as is the formation of a highly branched mitochondrial network. Galactose is another fermentable carbon source; however, it does not repress induction of mitochondrial proteins. In contrast, on nonfermentable carbon source such as glycerol or lactate, the cells produce ATP for growth exclusively in the mitochondria by oxidative phosphorylation. Under these conditions, expression of mitochondrial proteins is highly induced, and mitochondria form an extensive, highly branched network.

Isolation of mitochondria is a fundamental and important technique for mitochondrial research. Isolated mitochondria can be used for many purposes, e.g., isolation and characterization of mitochondrial proteins, analysis of the topology and modification of mitochondrial proteins, and in vitro protein import [4–7]. Critical steps during the isolation process are the homogenization of cells and their separation from other organelles by cell fractionation [8]. The following quality criteria must be taken into consideration: yield, purity, and intactness of mitochondria. Many downstream procedures require substantial amounts of mitochondria. In our laboratory, mitochondria are typically isolated from the cells grown in 500–2000 ml of liquid medium when OD<sub>600</sub> is around 1. The choice of carbon source is also important. Higher yields of mitochondria can be obtained when the cells are grown on nonfermentable carbon sources such as glycerol or lactate. The purity of the isolated mitochondria is particularly important when clear separation of mitochondria from other organellar membranes is required. This further step is usually performed by density gradient centrifugation [9]. Several measures to maintain the functional intactness of yeast mitochondria are described.

---

## 2 Materials

### 2.1 Growth Media

1. YP medium: Dissolve 10 g Bacto yeast extract and 20 g Bacto Peptone in 800 ml of water. Adjust pH to 5.5 with potassium hydroxide and fill up to 900 ml. Sterilize by autoclaving.

2. Synthetic minimum (S) medium: Dissolve 6.7 g of yeast nitrogen base without amino acids in 800 ml water. Adjust pH to 5.5 with potassium hydroxide and fill up to 900 ml. Sterilize by autoclaving.
3. Dropout mix: Mix the following: alanine, arginine, asparagine, aspartic acid, cysteine, glutamine, glutamic acid, glycine, methionine, isoleucine, phenylalanine, proline, serine, threonine, tyrosine, valine, myoinositol (2 g each), and p-aminobenzoic acid (0.2 g). For storage, homogenize the mixture using a mortar and pestle.
4. Synthetic complete (SC) medium: Dissolve 6.7 g of yeast nitrogen base without amino acids and 1.3 g of dropout mix in 800 ml water. Adjust pH to 5.5 with potassium hydroxide and fill up to 900 ml. Sterilize by autoclaving.
5. 50× auxotrophic markers: Dissolve 112 mg of uracil, 1095 mg of leucine, 410 mg of tryptophan, 314 mg of histidine, 203 mg of adenine, and 900 mg of lysine in 90 ml of water, and fill up to 100 ml (*see Note 1*). Sterilize by filtration. Omit the auxotrophic marker(s) used for selection of transformants.
6. 10× carbon sources: Glucose, galactose, glycerol, or lactate can be used as a carbon source. To make 20% (w/v) glucose, dissolve 20 g of glucose in 80 ml of water and fill up to 100 ml. To make 30% (w/v) galactose, dissolve 30 g of galactose in 70 ml of water and fill up to 100 ml. To make 30% (v/v) glycerol, fill up 30 ml of glycerol to 100 ml with water. To make 20% (v/v) lactate, dilute 20 ml of lactic acid with 30 ml of water, adjust pH to 5.5 with potassium hydroxide, and fill up to 100 ml. Sterilize all solutions by autoclaving.
7. Growth media: Mix 900 ml of YP, S, or SC medium and 100 ml of 10× carbon source. For S and SC media, add 20 ml of 50× auxotrophic markers.

## **2.2 Isolation of Mitochondria**

1. Alkaline solution: 100 mM Tris-SO<sub>4</sub> pH 9.4, 10 mM DTT (*see Note 2*).
2. Spheroplast buffer: 20 mM Tris-HCl pH 7.4, 1 mM EDTA, 1.2 M sorbitol.
3. 20 × zymolyase buffer: 20 mg/ml of zymolyase 20 T, 20 mM Tris-HCl pH 7.4, 1 mM EDTA, 1.2 M sorbitol (*see Note 3*).
4. Lysis buffer: 20 mM MOPS-KOH pH 7.2, 1 mM EDTA, 0.6 M sorbitol, 0.2% (w/v) BSA, 1 mM PMSF (*see Note 4*).
5. SEM buffer: 20 mM MOPS-KOH pH 7.2, 1 mM EDTA, 0.6 M sorbitol.

## **2.3 Purification of Mitochondria by Sucrose Gradient Centrifugation**

1. SEM buffer: 20 mM MOPS-KOH pH 7.2, 1 mM EDTA, 0.6 M sorbitol.
2. 60% sucrose buffer: 60% sucrose (w/v), 20 mM MOPS-KOH pH 7.2, 1 mM EDTA.

3. 32% sucrose buffer: 32% sucrose (w/v), 20 mM MOPS-KOH pH 7.2, 1 mM EDTA.
4. 23% sucrose buffer: 23% sucrose (w/v), 20 mM MOPS-KOH pH 7.2, 1 mM EDTA.
5. 15% sucrose buffer: 15% sucrose (w/v), 20 mM MOPS-KOH pH 7.2, 1 mM EDTA.

---

## 3 Methods

### 3.1 Growth of Yeast Cells

YP is a rich medium, routinely used for yeast growth. S and SC media are used for selection of yeast transformants for auxotrophic markers. S medium is the synthetic minimum medium composed of salts, trace elements, vitamins, and nitrogen source. Addition of dropout mix (mixture of amino acids) to S medium can improve yeast growth [10]. For selection of yeast transformants, uracil, leucine, tryptophan, histidine, adenine, and lysine are typically used as auxotrophic markers. In this protocol, these amino acids are omitted from dropout mix. Depending on auxotrophic marker used for transformant selection, appropriate amino acids should be added.

Budding yeast can utilize a variety of carbon sources. Glucose and galactose are fermentable carbon sources, and glycerol and lactate are nonfermentable carbon sources. Glucose, but not other carbon sources, represses the expression of a number of mitochondrial proteins as well as the formation of a highly branched mitochondrial network [1–3]. Selection of the suitable carbon source depends on the scientific question asked. In this section, the regular procedure for cultivation of wild-type yeast cells in 500 ml of YP glycerol medium is described.

1. Inoculate yeast colony with the size of 2–3 mm in diameter from an agarose plate medium in 20 ml of YP glycerol medium and cultivate for 2–3 days at 30 °C with shaking. The cells are in the stationary phase when OD<sub>600</sub> reaches around 6–7 (*see Notes 5 and 6*).
2. Dilute yeast pre-culture in 500 ml of YP glycerol medium and cultivate cells at 30 °C with shaking until OD<sub>600</sub> reaches 1 (*see Notes 7 and 8*).
3. Harvest cells by centrifugation at 2000 × *g* for 5 min at room temperature for isolation of mitochondria (*see Note 9*).

### 3.2 Isolation of Crude Mitochondria

The procedure consists of three steps: (1) preparation of spheroplasts, (2) homogenization of spheroplasts, and (3) isolation of mitochondria by differential centrifugation. Two different procedures for homogenization of spheroplasts are described. In the classical method, the spheroplasts are homogenized using a Dounce homogenizer [8]. In the alternative method, instead, the spheroplasts are

homogenized by repeated pipetting without using homogenizer [11]. This alternative method may reduce the yield of mitochondria but significantly improves intactness of mitochondria, which is crucial for analysis of mitochondrial ultrastructure.

### 3.2.1 Preparation of Spheroplasts

Yeast cells have cell walls mainly composed of  $\beta$ -1,3-d-glucan,  $\beta$ -1,6-d-glucan, chitin, and mannoproteins [12]. For efficient homogenization, yeast cells need to be converted into spheroplasts by digestion of cell walls. To this end, zymolyase is typically used. Zymolyase is produced from *Arthrobacter luteus* and contains an essential enzyme,  $\beta$ -1,3-glucan laminaripentaohydrolase, for lysis of yeast cell walls [13, 14]. Because cell wall lysis can lead to the break of plasma membranes that is triggered by the high internal turgor pressure, the buffer contains sorbitol to protect cells from osmotic stress.

1. Resuspend the harvested cells with 20 ml water.
2. Harvest the cells by centrifugation at  $2000 \times g$  for 5 min at room temperature.
3. Measure the wet weight (g) of the cells (*see Note 10*).
4. Resuspend the cells in 10 ml alkaline solution (*see Note 11*).
5. Incubate the cells at 30 °C for 10 min with gentle shaking.
6. Harvest the cells by centrifugation at  $2000 \times g$  for 5 min at room temperature.
7. Resuspend the cells with 10 ml spheroplast buffer per gram wet weight of cells.
8. Add 500  $\mu$ l 20 $\times$  zymolyase buffer per gram wet weight of cells.
9. Incubate cells at 30 °C for 20–40 min with gentle shaking (*see Note 12*).
10. Harvest the spheroplasts by centrifugation at  $2000 \times g$  for 5 min at 4 °C. All further steps should be done at 4 °C.
11. Wash the spheroplasts briefly with 30 ml ice-cold lysis buffer. It is not necessary to pipet to homogeneity. Just invert the centrifuge bottle several times.
12. Harvest the spheroplasts by centrifugation at  $2000 \times g$  for 5 min.
13. Repeat **steps 11 and 12**.
14. Go to Subheading **3.2.2**. for the classical homogenization method using Dounce homogenizer or go to Subheading **3.2.3**. for the gentle homogenization method by pipetting.

### 3.2.2 Homogenization of the Spheroplasts with Dounce Homogenizer

All steps should be performed at 4 °C using precooled buffers and glassware and plastic ware. It is also important to precool all rotors and centrifuges used.

1. Resuspend the pellet of spheroplasts in 20 ml ice-cold lysis buffer and transfer it to a 50-ml Dounce homogenizer.
2. Homogenize the spheroplasts with 15 strokes.
3. Centrifuge the homogenate at  $2000 \times g$  for 5 min and transfer the supernatant to a new tube.
4. Repeat **steps 1–3** with the pellet from the **step 3**.
5. Combine the supernatants to a tube and centrifuge at  $12,000 \times g$  for 10 min. Remove the supernatant.
6. Resuspend the pellet containing mitochondria in 1 ml ice-cold SEM buffer by gentle pipetting using a P1000 tip with 1 cm cutoff, and fill up to 30 ml with ice-cold SEM buffer.
7. Centrifuge again at  $12,000 \times g$  for 10 min. Remove the supernatant.
8. Resuspend the pellet in 500  $\mu$ l ice-cold SEM buffer by gentle pipetting using a P1000 tip with 1 cm cutoff.
9. Take an aliquot to determine protein concentration.
10. Make single-use aliquots (typically 30–50  $\mu$ l) and freeze them in liquid nitrogen. Store at  $-80^\circ\text{C}$  (*see Note 14*).

### 3.2.3 Homogenization of the Spheroplasts by Pipetting

All steps should be performed at  $4^\circ\text{C}$  using precooled buffers and glassware and plastic ware. It is also important to precool all rotors and centrifuges used.

1. Add 10 ml ice-cold lysis buffer to the harvested spheroplasts.
2. Resuspend the spheroplasts by repeated pipetting using a P5000 tip with 1 cm cutoff. Pipet gently 40 times.
3. Centrifuge at  $2000 \times g$  for 5 min and collect the supernatant to a new tube.
4. Add 10 ml ice-cold lysis buffer to the pellet.
5. Repeat **steps 2 and 3**.
6. Combine the supernatants to a tube, and centrifuge at  $2000 \times g$  for 5 min to remove remaining cell debris. Collect the supernatant to a new tube.
7. Centrifuge the supernatant at  $12,000 \times g$  for 5 min. Remove the supernatant.
8. Wash the pellet containing mitochondria in 20 ml ice-cold SEM buffer by gentle pipetting using a P5000 tip with 1 cm cutoff.
9. Centrifuge at  $12,000 \times g$  for 5 min. Remove the supernatant.
10. Resuspend the mitochondrial pellet in 500  $\mu$ l ice-cold SEM buffer by gentle pipetting using a P1000 tip with 1 cm cutoff.
11. Take an aliquot to determine protein concentration (*see Note 13*).

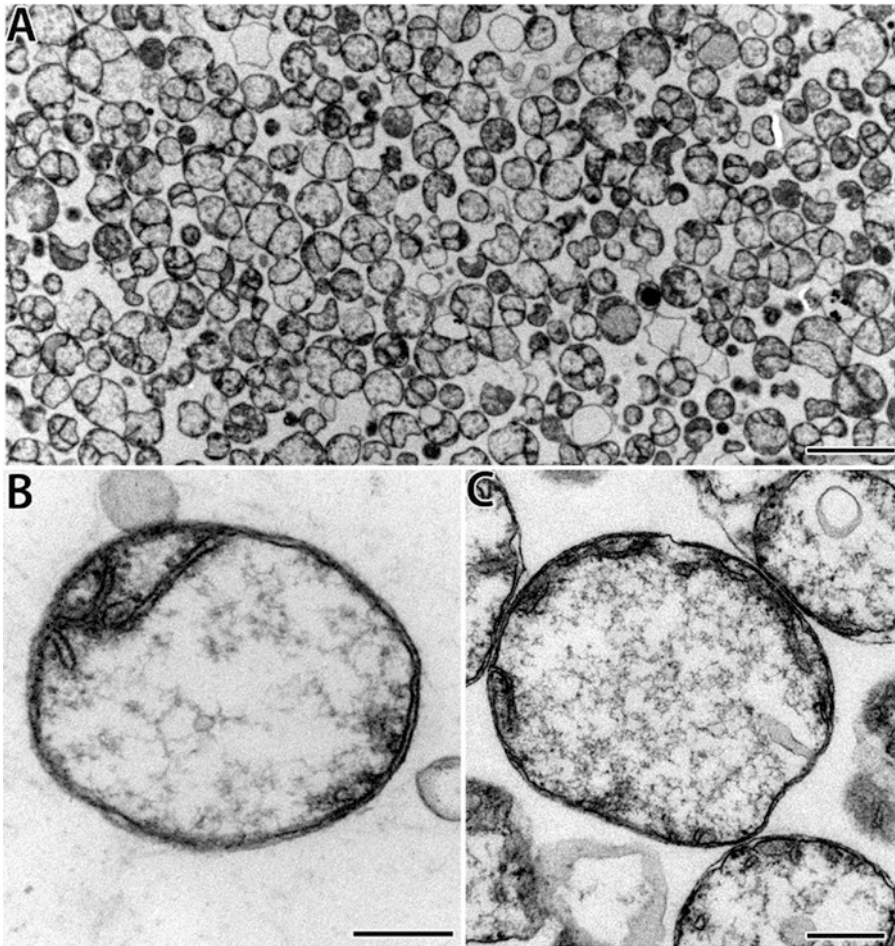


**Fig. 1** Electron microscopic analysis of isolated mitochondria of *S. cerevisiae* (YPH499). (a) Overview (magnification 7000-fold). (b and c) Ultrastructure of single mitochondria. Scale bars: 0.2  $\mu\text{m}$

12. Make single-use aliquots (typically 30–50  $\mu\text{l}$ ) and freeze them in liquid nitrogen. Store at  $-80\text{ }^{\circ}\text{C}$  (*see Note 14*).

Electron microscopy images of the mitochondria isolated by homogenization of spheroplasts by pipetting are shown in Fig. 1.

### **3.3 Purification of Mitochondria by Sucrose Gradient Centrifugation**

All steps should be performed at  $4\text{ }^{\circ}\text{C}$  using precooled buffers and glassware and plastic ware. It is also important to precool all rotors and centrifuges used.

Isolation of crude mitochondria as described above can provide sufficient quality of mitochondria, e.g., for the topological analysis of mitochondrial proteins and *in vitro* protein import analysis. However, the crude mitochondria contain significant amounts of non-mitochondrial membranes such as ER and vacuolar membranes. Several applications may need the separation of mitochondria from ER and vacuolar membranes. In the following, a method,

based on a previously published procedure [9], for the purification of mitochondria using sucrose density gradient is described.

1. Homogenize the crude mitochondrial fraction (5 mg/ml in SEM) by 10 strokes in a glass-Teflon potter.
2. Prepare a four-step sucrose gradient in a SW41 rotor tube. For this, pipet 1.5 ml 60% sucrose buffer to a tube, carefully overlay it with 4 ml 32%, then 1.5 ml 23%, and finally 1.5 ml 15% sucrose buffer.
3. Load the crude mitochondrial fraction onto the sucrose gradient.
4. Centrifuge at  $134,000 \times g$  in a Beckman SW41 Ti rotor for 1 h at 4 °C.
5. Collect the purified mitochondrial fraction from the 60/32% interface.
6. Dilute the recovered mitochondrial fraction with 2 volumes of SEM and centrifuge at  $10,000 \times g$  for 15 min at 4 °C.
7. Resuspend the pellet in ice-cold SEM buffer by gentle pipetting using a P1000 tip with 1 cm cutoff.
8. Take an aliquot to determine protein concentration.
9. Make aliquots of 30–50  $\mu$ l and freeze them in liquid nitrogen. Store at –80 °C.

---

## 4 Notes

1. The amino acids can be dissolved in water at 50 °C.
2. DTT should be added in the buffer just before use. 1 M DTT stock solution can be stored at –20 °C.
3. Zymolyase 20 T should be dissolved in the buffer just before use.
4. PMSF and BSA should be added in the buffer just before use. Prepare a stock of 100 mM PMSF in isopropanol and store it at –20 °C. PMSF is not soluble in water at high concentration.
5. Wild-type cells can be stored on YP glucose, galactose, or glycerol agarose plate at least for 1 month at 4 °C.
6. High mitochondria yields can be obtained by cultivating yeast cells in YP medium with glycerol, lactate, or galactose. Cultivation of yeast cells in YP medium with glucose represses mitochondrial gene expression and therefore reduces mitochondrial yield. If the mutant strain is defective in respiratory function or lacking mitochondrial DNA but is viable in fermentable carbon sources, galactose or glucose medium can be used as a carbon source. If the mutant strain shows temperature-sensitive phenotype, the cells can be cultivated at 23 °C instead of 30 °C.

7. The growth rate of the cells is different dependent on the yeast strain used. To estimate when OD<sub>600</sub> will reach 1, a preliminary experiment for the growth rate is recommended.
8. In our laboratory, the pre-culture in the stationary phase is diluted with fresh medium to OD<sub>600</sub> less than 0.2 to allow cells to grow more than two generations.
9. For isolation of mitochondria, freshly harvested cells should be used.
10. Approximately 0.5 g of the cells is obtained from 500 ml culture. The easiest way to determine the wet weight of cells is to weigh an empty centrifuge tube, use it to harvest the cells, and then determine the weight of the same tube with cell pellet after centrifugation. The wet weight of the cells represents the difference between two measurements.
11. The cells are resuspended in 10 ml of alkaline solution irrespective of the wet weight of the cells.
12. To control spheroplast formation, add 10 µl of the resuspended cells in 1 ml of water before and after zymolyase treatment. When the cells are converted into spheroplasts sufficiently, OD<sub>600</sub> is decreased to approximately 5–10% of that before the addition of zymolyase. Do not increase the incubation time with zymolyase to longer than 1 h.
13. Usually the concentration of crude mitochondria is 5–10 µg/µl. The concentration of mitochondria can be adjusted by adding SEM buffer.
14. Frozen mitochondria can be used for many applications such as in vitro protein import assay. However, some applications require freshly isolated mitochondria. Sub-fractionation of the mitochondria is one such example [4].

## References

1. Gancedo JM (1998) Yeast carbon catabolite repression. *Microbiol Mol Biol Rev* 62(2): 334–361
2. Egner A, Jakobs S, Hell SW (2002) Fast 100-nm resolution three-dimensional microscope reveals structural plasticity of mitochondria in live yeast. *Proc Natl Acad Sci U S A* 99(6):3370–3375
3. Visser W, van Spronsen EA, Nanninga N, Pronk JT, Gijs Kuenen J, van Dijken JP (1995) Effects of growth conditions on mitochondrial morphology in *Saccharomyces cerevisiae*. *Antonie Van Leeuwenhoek* 67(3):243–253
4. Harner M, Körner C, Walther D, Mokranjac D, Kaesmacher J, Welsch U, Griffith J, Mann M, Reggiori F, Neupert W (2011) The mitochondrial contact site complex, a determinant of mitochondrial architecture. *EMBO J* 30(21):4356–4370
5. Yamamoto H, Esaki M, Kanamori T, Tamura Y, Nishikawa S, Endo T (2002) Tim50 Is a subunit of the TIM23 complex that links protein translocation across the outer and inner mitochondrial membranes. *Cell* 111(4):519–528
6. Mokranjac D, Mokranjac D, Paschen SA, Kozany C, Prokisch H, Hoppins SC, Nargang FE, Neupert W, Hell K (2003) Tim50, a novel component of the TIM23 preprotein translocase of mitochondria. *EMBO J* 22(4):816–825
7. Geissler A, Chacinska A, Truscott KN, Wiedemann N, Brandner K, Sickmann A, Meyer HE, Meisinger C, Pfanner N, Rehling P (2002) Mitochondrial presequence translo-

case: an essential role of Tim50 in directing preproteins to the import channel. *Cell* 111(4):507–518

8. Daum G, Böhni PC, Schatzg G (1982) Import of proteins into mitochondria. Cytochrome b2 and cytochrome c peroxidase are located in the intermembrane space of yeast mitochondria. *J Biol Chem* 257(21):13034–13041
9. Meisinger C, Sommer T, Pfanner N (2000) Purification of *saccharomyces cerevisiae* mitochondria devoid of microsomal and cytosolic contaminations. *Anal Biochem* 287(2):339–342
10. Altmann K, Dürr M, Westermann B (2007) *Saccharomyces cerevisiae* as a model organism to study mitochondrial biology: general considerations and basic procedures. *Methods Mol Biol* 372:81–90
11. Lee AC, Xu X, Blachly-Dyson E, Forte M, Colonbini M (1998) The role of yeast VDAC genes on the permeability of the mitochondrial outer membrane. *J Membr Biol* 161(2):173–181
12. Cabib E, Roberts R, Bowers B (1982) Synthesis of the yeast cell wall and its regulation. *Annu Rev Biochem* 51:763–793
13. Kitamura K, Kaneko T, Yamamoto Y (1971) Lysis of viable yeast cells by enzymes of *arhrobacfer luteus*. *Arch Biochem Biophys* 145(1):402–404
14. Kitamura K (1982) Re-examination of zymolyase purification. *Agric Biol Chem* 46(4):963–969

## Isolation of Contact Sites Between Inner and Outer Mitochondrial Membranes

Max Harner

### Abstract

Mitochondria are essential organelles of all eukaryotic cells. They perform a plethora of important metabolic functions and have a highly complex architecture that differs drastically between different cells and tissues. Mitochondria are delimited from the cytosol by the mitochondrial envelope that consists of the outer membrane and the inner membrane. The inner membrane is subdivided into the inner boundary membrane that runs parallel to the outer membrane and the crista membrane. Both sections of the inner membrane are linked by crista junctions. A further important architectural element of mitochondria are the contact sites between outer membrane and inner membrane. These sites were observed a long time ago by classical electron microscopy, but their molecular structure was identified only recently when it was recognized that proteins of crista junctions and proteins of the outer membrane are responsible for these strong contacts. Mitochondrial function is severely affected when contact sites are disturbed. This underlines the notion that mitochondrial architecture and function are intimately connected. In the following a method is described to generate and to isolate membrane vesicles from isolated yeast mitochondria that contain these contact sites.

**Key words** Contact sites, Membrane vesicles, Protein purification, Mitochondria, MICOS, Mitochondrial subfractionation, Sonication

---

### 1 Introduction

Mitochondria perform a multitude of important functions such as energy transduction to generate a proton gradient and ATP, synthesis of iron sulfur clusters, as well as protein and lipid synthesis. They are involved in processes such as programmed cell death and mitophagy. Additionally they play intricate roles in numerous inherited and acquired diseases. Mitochondria are conspicuous because of their highly complex architecture. They are made up by two membranes — the outer membrane (OM) and the inner membrane (IM). The IM consists of the inner boundary membrane (IBM) that runs in close proximity to the OM and the crista membrane (CM). Cristae are invaginations of the IM into the interior, the matrix of mitochondria. IBM and CM are linked by crista

junctions (CJ). OM and IBM are connected by proteinaceous contact sites. The existence of such structural elements has been known for a long time [1–4], but their molecular nature remained largely unknown.

Different kinds of contact sites have been described, both permanent and transient ones. The apparently most stable and best characterized ones are mediated by the MICOS complex. MICOS is an essential building element of the CJ. It interacts physically with the TOB/SAM complex and the Fzo1/mitofusin-Ugo1 complex of the OM [5–10]. Other contacts between OM and IBM are likely transient, such as those between the protein import complexes of OM and IM and the TOM and TIM complexes. Furthermore, contacts have been reported that facilitate export and import of solutes such as ATP/ADP [11–19].

To isolate contact sites between the inner and the outer mitochondrial membrane, one can make use of the different physical properties of these membranes. The two membranes differ strongly in their protein-to-lipid ratio. The IM has a much higher protein content as compared to the OM and therefore has a higher specific density [20–23]. Submitochondrial membrane vesicles can be generated by sonication of mitochondria after subjecting them to hyperosmotic shrinking. Vesicles formed in this way consist of OM and IM fragments [24–26]. From sites where IBM and OM are connected, vesicles are formed that are comprised of both kinds of membranes [27]. Such vesicles exhibit a density that is between those of OM and IM vesicles and therefore can be separated by sucrose buoyant density gradient centrifugation. The light OM vesicles move to the top of the gradient; the protein rich IM vesicles stay at the bottom. The contact sites containing vesicles are enriched in fractions in the middle of the gradient (Fig. 1).

For the confirmation of a successful fractionation and a precise localization of contact site containing vesicles in the gradient, a marker is indispensable. A protein that accumulates at contact sites can serve as a proteinaceous marker of contact sites. For this purpose, I made use of a fusion protein consisting of green fluorescent protein (GFP) fused to the N-terminus of Tim23. Tim23 is integrated into the IBM with its C-terminal part that contains four transmembrane helices. Interestingly, this essential core component of the TIM23 translocase exposes its N-terminus to the cytosol in an import activity-dependent manner [28, 29]. Therefore, Tim23 transiently spans both mitochondrial membranes. Since the GFP part folds in the cytosol before crossing the pore of the TOM complex in the OM, this double membrane-spanning topology can be stabilized [30]. Upon osmotic treatment of isolated mitochondria, the matrix space condenses, and the IBM detaches from the OM. At contact sites this is prevented. Due to the osmotic retraction of the IBM, contact site forming proteins will accumulate by lateral movement. Thus, GFP-Tim23 becomes a marker for

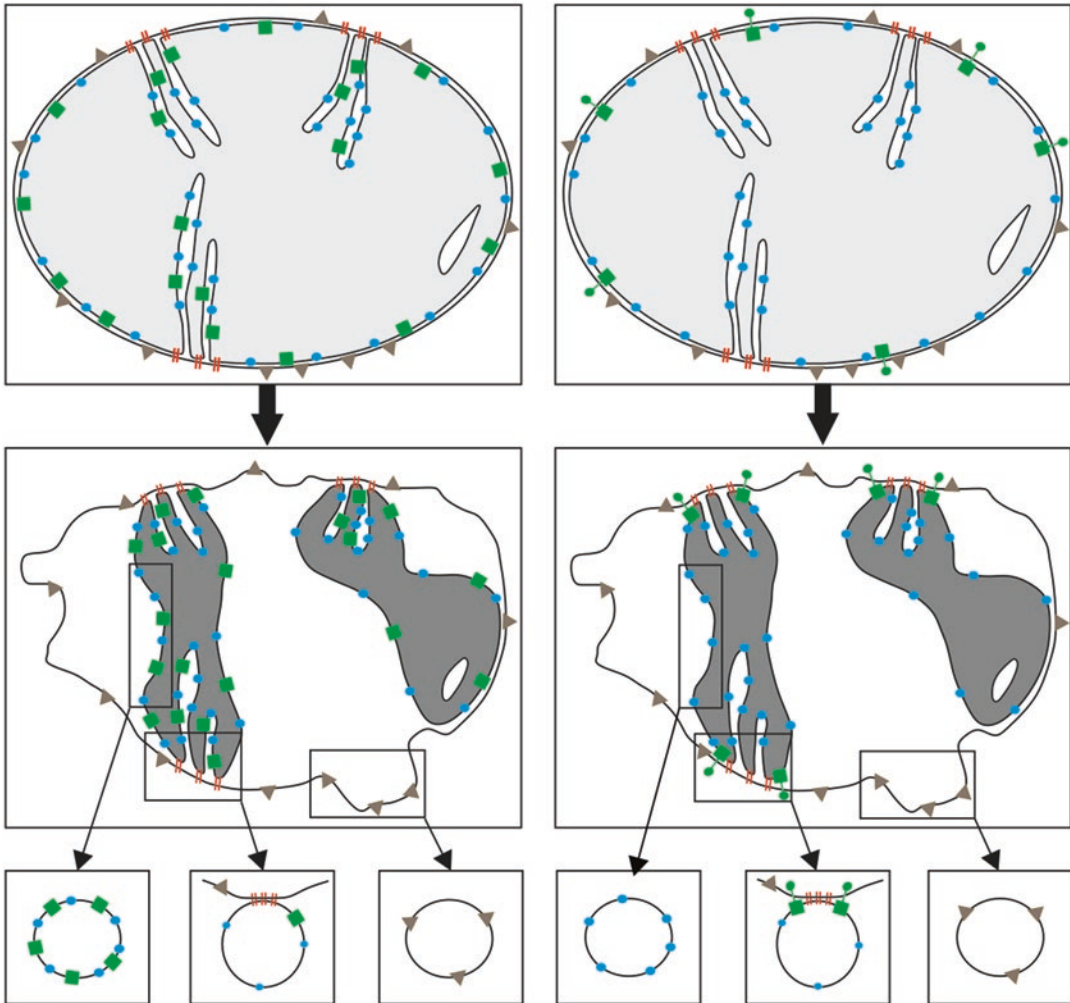


**Fig. 1** Rationale for the generation and analysis of contact sites containing vesicles. *Left panels:* mitochondria and submitochondrial vesicles derived from wild-type cells expressing Tim23. *Right panels:* mitochondria and submitochondrial vesicles derived from cells expressing GFP-Tim23. *Upper panels:* distribution of mitochondrial membrane proteins including Tim23 or GFP-Tim23 and putative contact site proteins of mitochondria in the “orthodox state”. *Middle panels:* distribution of mitochondrial membrane proteins including Tim23 or GFP-Tim23 and putative contact site proteins of mitochondria in the “condensed”, hyperosmotically shrunken state. *Lower panels:* generated vesicles and their protein composition. *Red bars* putative contact site proteins, *blue circles* inner membrane proteins, *green squares* Tim23, *green dumbbells* GFP-Tim23, *gray triangles* OM proteins (taken from Harner et al., 2011 with permission [5])

contact sites. Importantly, this fusion protein is fully functional like the wild-type form of Tim23 [30]. Though GFP-Tim23 was originally used as a marker for isolation of contact sites, subsequent proteomic analysis of contact sites containing vesicles revealed the existence of an endogenous protein complex, the MICOS complex, that behaves exactly like GFP-Tim23 (Fig. 2) [5]. Therefore, one of the MICOS subunits, now called Mic10, Mic12, Mic19, Mic26,

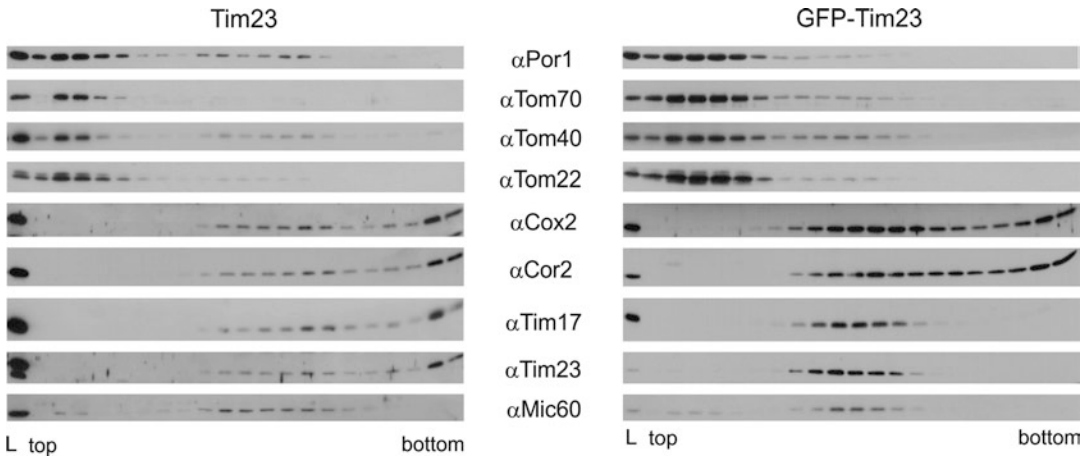


**Fig. 2** Separation of submitochondrial vesicles of mitochondria generated from wild-type Tim23 and GFP-Tim23 expressing cells. Submitochondrial vesicles were generated by swelling, shrinking, and sonication. The vesicles were separated by a floatation equilibrium density gradient centrifugation. Proteins in the various fractions were subjected to TCA precipitation and were analyzed by SDS-PAGE and immunoblotting using the indicated antibodies. *L* load fraction, *top* and *bottom* indicate first and last fraction of the gradient (taken from Harner et al., 2011 with permission [5]). Marker proteins for the OM: Por1, Tom70, Tom40, Tom22. Marker proteins for the IM: Cox2, Cor2, Tim17, Tim23. Marker for contact sites: GFP-Tim23

Mic27, and Mic60 [31], can be used as a marker protein for contact sites in wild-type mitochondria obviating the use of GFP-Tim23.

## 2 Materials

1. 10 mg of freshly isolated yeast mitochondria. Adjust protein concentration to 5 mg/ml with ice-cold isotonic buffer like SM buffer (*see Note 1*).
2. SM buffer: 20 mM MOPS-KOH, pH 7.4, 0.6 M sorbitol. Store at  $-20^{\circ}\text{C}$ .
3. Swelling buffer: 20 mM MOPS-KOH, pH 7.4, 0.5 mM EDTA. Store at  $4^{\circ}\text{C}$ . Shortly before use, add 1 mM PMSF and  $1\times$  Roche protease inhibitor cocktail.
4. PMSF: 0.2 M solution of phenylmethylsulfonyl fluoride in ethanol. Store at  $-20^{\circ}\text{C}$ .
5. Sucrose: 2.5 M solution in water. Store at room temperature (*see Note 2*).
6. Sonifier with a tapered microtip (tip diameter, 3 mm) (*see Note 3*).
7. Rosette cell for sonication. Size  $\approx 25$  ml (*see Note 4*).
8. 2 ml potter homogenizer of Teflon/glass type (*see Note 5*).
9. Refractometer.

10. Sucrose gradient buffer 1: 20 mM MOPS-KOH, pH 7.4, 0.5 mM EDTA, 0.8 M sucrose. Store at  $-20^{\circ}\text{C}$ .
11. Sucrose gradient buffer 2: 20 mM MOPS-KOH, pH 7.4, 0.5 mM EDTA, 1.25 M sucrose. Store at  $-20^{\circ}\text{C}$ .
12. 120 mm needle.
13. Ultracentrifuge and swinging bucket rotor fitting ca. 15 ml tubes (comparable to SW41 rotor from Beckman Coulter).
14. TCA solution: 72% (w/v) solution in water. Store at  $4^{\circ}\text{C}$ .

---

### 3 Methods

#### 3.1 Generation of Submitochondrial Membrane Vesicles

1. Add dropwise 20 ml of swelling buffer to 2 ml of mitochondrial suspension (5 mg/ml, 10 mg in total) under continuous stirring on ice (*see Note 6*).
2. Leave the suspension for 30 min on ice. During this step, the mitochondrial outer membrane is disrupted by exposure to a hypotonic solution (this process is referred to as swelling of mitochondria).
3. Add dropwise 5 ml of 2.5 M sucrose to adjust the sucrose concentration to 0.5 M and incubate for 15 min on ice under continuous stirring. During this step, mitochondria are shrunken, and the IBM retracts from the OM. The two membranes remain in a close proximity only at the contact sites.
4. Transfer the suspension to a precooled rosette cell and sonicate three times for 30 s with 30 s breaks in between. In this step the different kinds of vesicles are formed, consisting of pure OM, of pure IM, or, at contact sites, of both OM and IM.

Use the following settings on the sonifier: output control = 0 and duty cycle = 60%.

Ensure efficient cooling of the suspension during sonication by putting the rosette cell in a beaker containing a water-ice mixture (*see Note 7*).
5. Remove intact mitochondria by centrifugation for 20 min at  $20,000 \times g$  and  $4^{\circ}\text{C}$ .
6. Transfer the supernatant to an ultracentrifugation tube and then layer 0.3 ml of 2.5 M sucrose under it. Therefore, you should use a syringe with a 120 mm needle (*see Note 8*).
7. Harvest the generated membrane vesicles by centrifugation for 100 min at  $118,000 \times g$  and  $4^{\circ}\text{C}$ . Use a swinging bucket rotor fitting ca. 15 ml tubes.
8. Discard the supernatant and resuspend the vesicles in the 2.5 M sucrose cushion by pipetting.

9. Transfer the vesicles to a precooled Potter homogenizer, and homogenize the vesicles by ten strokes with the Teflon pestle to achieve complete resuspension of the vesicle (*see Note 9*).
10. Measure the sucrose concentration with a refractometer and adjust it to 1.3 M (*see Note 10*).

### **3.2 Separation of Submitochondrial Membrane Vesicles**

1. Prepare a continuous 13 ml sucrose gradient (0.8–1.25 M sucrose) (*see Note 11*).
2. Load the vesicle suspension under the sucrose gradient using a 2 ml syringe with a 120 mm needle. You should be able to load 1 ml of vesicle suspension with a concentration of ca. 1 mg/ml under the gradient.
3. Float the membrane vesicles by centrifugation for 24 h at  $200,000 \times g$  and 4 °C. During this step, vesicles are separated from each other based on different densities (*see Note 12*).
4. Harvest the gradient by fractionation into 0.6 ml fractions (*see Note 13*).
5. Analyze the fractions by SDS-PAGE and immunodecoration or quantitative mass spectrometry. Two examples of such experiments are shown in Fig. 2 (*see Note 14*).

---

## **4 Notes**

1. For this method, the culture conditions of the yeast cells used for isolation of mitochondria have to be kept constant, especially in terms of growth temperature and medium. Changes in growth conditions can lead to changes in the lipid composition and therefore altered behavior of mitochondria and their membranes.

I routinely used SM buffer to dilute mitochondria. However, addition of EDTA or use of other buffers like HEPES should be possible as well.

2. It is not absolutely necessary to autoclave the solution because of the high sucrose concentration. Though, fungal contamination cannot be completely excluded.
3. In this case a Branson Sonifier 250 was used, but, since even for the different sonifiers of the same model, conditions of sonication have to be experimentally determined so other sonifiers can be used as well.
4. I recommend to use a rosette cell for sonication. This is elevating the efficiency of sonication.
5. For resuspension of the membrane vesicles, I recommend using a Teflon-/glass-type homogenizer to avoid sticking of vesicles to the surface.

6. The mitochondria used for generation of submitochondrial vesicles should be freshly isolated. Freezing of mitochondria harms the integrity of mitochondrial membranes and therefore disturbs the entire procedure. For the same reason, the isolation of mitochondria should be as gentle as possible. A gradient purification of mitochondria is not recommended in order to keep the mechanical stress as low as possible. The easiest way to add the buffer dropwise is using a glass pipette. For continuous stirring use a magnetic stirrer. To keep the mitochondrial suspension cool, perform the mixing and stirring in an Erlenmeyer flask. This should be put in a small Styrofoam box filled with ice.

7. The conditions of sonication have to be determined for each individual sonifier. When the desired conditions are found, it is advisable not to remove or change the tip, otherwise the conditions will likely have to be optimized again. Ideally use the sonifier only for the purpose of generating vesicles.

To define the exact sonication conditions, use an artificial double membrane-spanning protein such as GFP-Tim23 as a marker protein. Alternatively a subunit of the MICOS complex can be used.

The sonication must not be too harsh. This will lead to massive mixing of OM and IM. You will see this easily after the Ponceau S staining of your Western blot membrane. Almost everything will be present in fractions of intermediate density, but you will not see any protein in top and bottom fractions.

8. I recommend to transfer the supernatant into an ultracentrifuge tube and then layer the 2.5 M sucrose cushion under it as in this way dilution of the sucrose solution is prevented. The sucrose cushion is necessary as otherwise the vesicles will stick to the centrifuge tube and it will not be possible to resuspend the vesicles in the pellet. The volume of the sucrose cushion is optimized for a Beckman Coulter SW41 tube. If you use a similar rotor of another company, add as much sucrose to compensate the curvature at the tip of the tube to get a planar tube ending.

9. Thorough homogenization of the vesicle suspension is absolutely necessary. If not thoroughly homogenized, the vesicles will stick together, and it will not be possible to separate them by gradient density centrifugation.

10. The use of refractometer is highly recommended. There are variations in the amount of discarded supernatant volume. This makes it almost impossible to calculate the actual sucrose concentration. However, this has got a not negligible influence on the gradient.

11. In order to obtain reproducible results, the generation of the gradient should be standardized. A pump system or an automated gradient mixer should be used to generate gradients. Depending on the chosen growth conditions, the vesicles generated can differ in their density. Therefore, it might be necessary to adjust the sucrose concentrations in the gradient. Determine in the first experiments the sonication conditions to obtain pure OM and IM vesicles and find out at which sucrose concentration these vesicles are enriched by using a higher range of sucrose concentration. You might start with a gradient ranging from 0.6 M to 1.5 M sucrose. It is important to obtain empty fraction at the top and the bottom of the gradient to be sure where these vesicles are actual exactly enriched. In the next step, keep the sonication conditions constant and optimize the resolution of the gradient.

Measuring the sucrose concentration is not absolutely necessary but strongly recommended. Changes in the gradient will have dramatic effects of the resolution of vesicle separation.

12. Using a floatation gradient prevents artifacts. Soluble and aggregated proteins will stay at the very bottom and will not enter the gradient, in contrast to a sedimentation gradient. To reach the equilibrium, shorter centrifugation times are not sufficient.
13. Like the generation of the gradient, the fractionation procedure should be standardized and automated. The use of a pump system or a gradient fractionater in combination with a fraction collector is advisable.
14. For detailed analysis I recommend using SDS-PAGE and immunodecoration. Therefore, you have to subject the proteins to TCA precipitation. This precipitation has to be done twice. After the first round, a high amount of the sucrose will be left. Since these are fractions of a sucrose gradient, this amount will increase from fraction to fraction. The remaining sucrose would increase the volume of the samples to different extents.

For immunodecoration you should use marker for the OM (like proteins of the TOM complex), for the IM (like proteins of the TIM23 complex or the respiratory chain) and for contact sites (such as MICOS complex subunits).

## References

1. Hackenbrock CR (1968) Ultrastructural bases for metabolically linked mechanical activity in mitochondria. II. Electron transport-linked ultrastructural transformations in mitochondria. *J Cell Biol* 37(2):345–369
2. Hackenbrock CR (1966) Ultrastructural bases for metabolically linked mechanical activity in mitochondria. I. Reversible ultrastructural changes with change in metabolic steady state in isolated liver mitochondria. *J Cell Biol* 30(2):269–297
3. Perkins GA et al (1997) Electron tomography of large, multicomponent biological structures. *J Struct Biol* 120(3):219–227

4. Perkins GA et al (1998) Electron tomography of mitochondria from brown adipocytes reveals crista junctions. *J Bioenerg Biomembr* 30(5):431–442
5. Harner M et al (2011) The mitochondrial contact site complex, a determinant of mitochondrial architecture. *EMBO J* 30(21):4356–4370
6. Korner C et al (2012) The C-terminal domain of Fcjl is required for formation of crista junctions and interacts with the TOB/SAM complex in mitochondria. *Mol Biol Cell* 23(11):2143–2155
7. Xie J et al (2007) The mitochondrial inner membrane protein mitofilin exists as a complex with SAM50, metaxins 1 and 2, coiled-coil-helix coiled-coil-helix domain-containing protein 3 and 6 and DnaJC11. *FEBS Lett* 581(18):3545–3549
8. Zerbes RM et al (2012) Role of MINOS in mitochondrial membrane architecture: cristae morphology and outer membrane interactions differentially depend on mitofilin domains. *J Mol Biol* 422(2):183–191
9. Darshi M et al (2011) ChChd3, an inner mitochondrial membrane protein, is essential for maintaining crista integrity and mitochondrial function. *J Biol Chem* 286(4):2918–2932
10. Bohnert M et al (2012) Role of mitochondrial inner membrane organizing system in protein biogenesis of the mitochondrial outer membrane. *Mol Biol Cell* 23(20):3948–3956
11. Schleyer M, Neupert W (1985) Transport of proteins into mitochondria: translocational intermediates spanning contact sites between outer and inner membranes. *Cell* 43(1):339–350
12. Schwaiger M, Herzog V, Neupert W (1987) Characterization of translocation contact sites involved in the import of mitochondrial proteins. *J Cell Biol* 105(1):235–246
13. Brdiczka DG, Zorov DB, Sheu SS (2006) Mitochondrial contact sites: their role in energy metabolism and apoptosis. *Biochim Biophys Acta* 1762(2):148–163
14. Bucheler K, Adams V, Brdiczka D (1991) Localization of the ATP/ADP translocator in the inner membrane and regulation of contact sites between mitochondrial envelope membranes by ADP. A study on freeze-fractured isolated liver mitochondria. *Biochim Biophys Acta* 1056(3):233–242
15. Speer O et al (2005) Octameric mitochondrial creatine kinase induces and stabilizes contact sites between the inner and outer membrane. *Biochem J* 385(Pt 2):445–450
16. Chacinska A et al (2003) Mitochondrial translocation contact sites: separation of dynamic and stabilizing elements in formation of a TOM-TIM-preprotein supercomplex. *EMBO J* 22(20):5370–5381
17. Rojo M et al (1991) Mitochondrial creatine kinase mediates contact formation between mitochondrial membranes. *J Biol Chem* 266:20290–29295
18. Neupert W (2015) A perspective on transport of proteins into mitochondria: a myriad of open questions. *J Mol Biol* 427(6 Pt A):1135–1158
19. Waegemann K et al (2015) Cooperation of TOM and TIM23 complexes during translocation of proteins into mitochondria. *J Mol Biol* 427(5):1075–1084
20. Daum G (1985) Lipids of mitochondria. *Biochim Biophys Acta* 822(1):1–42
21. Hovius R et al (1990) Improved methods to isolate and subfractionate rat liver mitochondria. Lipid composition of the inner and outer membrane. *Biochim Biophys Acta* 1021:217–226
22. Hallermayer G, Neupert W (1974) Lipid composition of mitochondrial outer and inner membranes of *Neurospora crassa*. *Hoppe Seylers Z Physiol Chem* 355(3):279–288
23. Werner S, Neupert W (1972) Functional and biogenetical heterogeneity of the inner membrane of rat-liver mitochondria. *Eur J Biochem* 25(2):379–396
24. Riezman H et al (1983) The outer membrane of yeast mitochondria: isolation of outside-out sealed vesicles. *EMBO J* 2(7):1105–1111
25. Ohlendieck K et al (1986) Enrichment and biochemical characterization of boundary membrane contact sites from rat-liver mitochondria. *Biochim Biophys Acta* 860(3):672–689
26. Sottocasa GL et al (1967) An electron-transport system associated with the outer membrane of liver mitochondria. A biochemical and morphological study. *J Cell Biol* 32(2):415–438
27. Pon L et al (1989) Protein import into mitochondria: ATP-dependent protein translocation activity in a submitochondrial fraction enriched in membrane contact sites and specific proteins. *J Cell Biol* 109(6 Pt 1):2603–2616
28. Donzeau M et al (2000) Tim23 links the inner and outer mitochondrial membranes. *Cell* 101(4):401–412
29. Popov-Celeketic D et al (2008) Active remodelling of the TIM23 complex during translocation of preproteins into mitochondria. *EMBO J* 27(10):1469–1480
30. Harner M, Neupert W, Deponte M (2011) Lateral release of proteins from the TOM complex into the outer membrane of mitochondria. *EMBO J* 30(16):3232–3241
31. Pfanner N et al (2014) Uniform nomenclature for the mitochondrial contact site and cristae organizing system. *J Cell Biol* 204(7):1083–1086

## Isolation of Mitochondria-Associated Membranes (MAM) from Mouse Brain Tissue

Bernadette Schreiner and Maria Ankarcrona

### Abstract

During the last decades, increasing evidence indicated that subcellular organelles do not exist as autarkic units but instead communicate constantly and extensively with each other in various ways. Some communication, for example, the exchange of small molecules, requires the marked convergence of two distinct organelles for a certain period of time. The cross talk between endoplasmic reticulum (ER) and mitochondria, two subcellular organelles of utmost importance for cellular bioenergetics and protein homeostasis, has been increasingly investigated under the last years. This development was significantly driven by the establishment of optimized subcellular fractionation techniques. In this chapter, we will describe and critically discuss the currently used protocol for the isolation of the membrane fraction containing mitochondria-associated membranes (MAM).

**Key words** Mitochondria, ER, MAM, Contact sites, Subcellular fractionation, Mouse brain

---

### 1 Introduction

Already since the 1960s, electron microscopists have observed a close juxtaposition of the ER and mitochondria [1, 2]. Advanced imaging approaches revealed that up to 20% of the mitochondrial surface is in contact with the ER [3, 4]. However, only upon the development of improved biochemical methods for the isolation of subcellular fractions, this interorganellar contact site obtained substantial attention [5–7]. Initially, Jean E. Vance referred to the membrane fraction co-sedimenting with mitochondria as “fraction X” [8]. The subsequently imprinted term “mitochondria-associated ER membranes” (MAM) for this fraction is a technical term, based on the currently employed subcellular fractionation process for its isolation.

It should be noted that the term MAM has to be used with caution. The close physical interaction between proteins of the ER and the outer mitochondrial membrane (OMM) at the contact sites entails that the commonly used subcellular fractionation technique

for “MAM isolation” yields a fraction containing ER-side and mitochondria-side components of the contact site [9–15].

Analysis of enzymatic activities and protein content of this fraction showed many but not all characteristics of the ER [8], and the lipid composition of MAM is similar to that of lipid rafts [16]. MAM is thus thought to comprise a lipid raft-like subcompartment of the ER that co-sediments with mitochondria due to its tethering to the OMM [14, 17]. Enhanced electron microscopy techniques showed that the distance between ER and mitochondria at these contact sites is between 9 and 30 nm [18–20]. This distance is in line with the idea of a proteinaceous tether bridging the two membranes [21].

In yeast, the proteins forming the ER-mitochondria tethering complex (ERMES) have been identified and investigated in detail [22–26].

Mammalian ER-mitochondria contact sites constitute highly dynamic structures that vary both from tissue to tissue and over time in composition and extension. An ERMES-like tethering complex has not been identified, and it proves impossible to determine universal characteristics, including issues to define bona fide “MAM-associated marker proteins” [14, 27].

In mammalian cells, the mitochondrial fusion protein, mitofusin 2 (Mfn2), residing in MAM, is thought to form homo- and heterotypic tethers with Mfn2 and mitofusin1 (Mfn1) in the OMM, respectively. However, the knockdown of Mfn2 impairs ER-mitochondrial contacts only by 40%, speaking for the existence of further structural tethers [28]. In liver tissue, the first tissue used to isolate the “MAM” fraction and several enzymes of the phospholipid synthesis pathway, such as acyl-CoA/cholesterol acyltransferase (ACAT1) and diacylglycerol acyltransferase (DGAT), are constantly detected [29–31]. The ER-resident inositol 1,4,5-trisphosphate receptors (IP3Rs) and the OMM protein voltage-dependent anion channel 1 (VDAC1), constituting an ER-to-mitochondria calcium ( $\text{Ca}^{2+}$ ) bridge, have been found to form a functional tether between both organelles [10, 18, 32]. Although all of these proteins are enriched in ER-mitochondria contact sites, they are not exclusively found in this fraction. IP3 receptors, for example, reside also in non-MAM areas of the ER membrane, and VDAC1 is found in OMM regions exterior of the contact site. This highly variable protein composition of ER-mitochondria contact sites in mammalian cells explains why different approaches to identify their proteome overlap only in part [33, 34].

Interestingly, a multitude of essential cellular functions are located at or governed by ER-mitochondria cross talk at the contact sites. Among those crucial functions are the regulation of intracellular  $\text{Ca}^{2+}$  signaling (reviewed in [35]) including  $\text{Ca}^{2+}$ -induced apoptosis (reviewed in [36]) and  $\text{Ca}^{2+}$ -dependent activation of the mitochondrial energy metabolism (reviewed in [14]),

phospholipid synthesis and transport, (reviewed in [27, 37]), cholesterol ester synthesis (reviewed in [38]), the regulation of mitochondrial dynamics, and, only recently unraveled, the formation of autophagosomes (reviewed in [27, 39]).

### **1.1 Intracellular $Ca^{2+}$ Signaling and Apoptosis Regulation**

ER and mitochondria represent important sites of subcellular  $Ca^{2+}$  storage [18, 40–42], and  $Ca^{2+}$  transfer between ER and mitochondria is important for the regulation of mitochondrial bioenergetics according to the cellular state [43–45].  $Ca^{2+}$  is released from the ER by IP3 receptors and taken up into mitochondria by the VDACL1 channel of the OMM [10, 18]. IP3 receptors and VDACL1 are physically linked by the OMM heat shock protein Grp75/mortalin, thus forming an ER-mitochondria tether [10]. The close apposition of ER and mitochondria at contact sites is crucial to generate a  $Ca^{2+}$  hot spot providing sufficiently high  $Ca^{2+}$  concentrations to activate gating of MCU, the  $Ca^{2+}$  channel of the inner mitochondrial membrane (IMM) [46, 47]. In addition, the high concentration of  $Ca^{2+}$ -binding enzymes throughout the cytosol results in the trapping of  $Ca^{2+}$  shortly after its release from IP3 receptors.  $Ca^{2+}$ -responsive organelles, such as mitochondria, thus have to be in close proximity to the sites of ER  $Ca^{2+}$  release [48]. This is achieved by the adjustment of mitochondrial positioning according to  $Ca^{2+}$  signals. Several enzymes of the mitochondrially localized TCA cycle and of the electron transport chain are activated by ER-to-mitochondria  $Ca^{2+}$  transfer [49–51]. In line with this, disruption of the contact sites leads to reduced mitochondrial ATP production [52].

Short-term increased ER-to-mitochondria  $Ca^{2+}$  signaling can arise as a consequence of acute ER stress and leads to an activation of mitochondrial bioenergetics increasing the production of ATP. This mechanism aims to boost the ER unfolded protein response (UPR) [53, 54]. On the other hand, chronically increased ER-to-mitochondria  $Ca^{2+}$  signaling leads to  $Ca^{2+}$  overload of the mitochondria. This in turn leads to the opening of the mitochondrial permeability transition pore. The release of pro-apoptotic mitochondrial proteins such as cytochrome c induces the endogenous pathway of apoptosis [18, 32, 36]. The MAM-associated multifunctional sorting protein PACS2 has been suggested to control ER-mitochondria communication under pathological conditions and thereby the onset of apoptosis [9]. The increased ER-mitochondria  $Ca^{2+}$  communication upon ER stress can be visualized as enhanced fluorescence overlap upon staining with probes tracking ER and mitochondria [19, 55].

### **1.2 Phospholipid and Cholesterol Metabolism**

The subcellular site of phospholipid synthesis and trafficking is the ER, and most of the corresponding enzymes reside in the ER membrane. The generation of phosphatidylserine (PS) is accomplished by PS synthases 1 and 2 in the ER [56]. Phosphatidylethanolamine

(PE) synthesis, however, requires trafficking of phospholipids between ER and mitochondria. At ER-mitochondria contact sites, PS is shuttled from the ER to the inner mitochondrial membrane (IMM) by a non-vesicular mechanism [57, 58]. PS is then converted to PE by PS decarboxylase (PSD1) [59–61]. PE either stays in the IMM or it is shuttled back to the ER [57, 62]. Mainly in liver cells, PE is further converted to phosphatidylcholine by the MAM-resident enzyme PE N-methyltransferase (PMET) [63, 64].

The enzymes for cholesterol synthesis are mainly localized in the ER membrane, whereas further enzymatic conversion of newly synthesized cholesterol to steroid hormones occurs in the mitochondrial matrix. This implies the transport of cholesterol from ER membranes to mitochondria. ER-mitochondria contact sites appear to be a valid candidate for the regulation of this process [27]. Notably, it had been shown that ER stress increases mitochondrial cholesterol trafficking at ER-mitochondria contact sites under neuropathological conditions [65]. A proportion of newly synthesized cholesterol is converted to cholesterol esters. As mentioned above, the responsible enzyme ACAT1 has been shown to be enriched in the MAM area of the ER and is often used as a “MAM marker protein” [29].

Likewise, fatty acid CoA ligase 4 (FACL4) that is involved in triacylglycerol synthesis concentrates in the MAM region of the ER and is nowadays accepted to be one of the most reliable “MAM markers” [3, 66].

### **1.3 Autophagosome Formation**

Only recently, a novel interesting role has been ascribed to ER-mitochondria contact sites, i.e., in providing a platform for the formation of autophagosomes. During the last decade, autophagy gained increasing attention with regards to its role in cell survival by governing cellular nutrient supply as well as quality control [67]. During autophagy, terminally damaged proteins or whole organelles are engulfed by phagosomal membranes and degraded upon fusion of the autophagosome with lysosomes [68, 69]. However, some basic characteristics of autophagy, such as the source of autophagic membranes, are still a matter of debate. In fact, not only the ER [70, 71] but also the plasma membrane [72] and the mitochondrial outer membrane [73] have been suggested as source of autophagic membranes.

Interestingly, a recent study of the Yoshimori Laboratory suggested that ER-mitochondria contact sites could serve as a platform for autophagosome formation [74, 75]. In line with this, the group showed that two autophagosomal marker proteins, ATG5 and ATG14, re-localize to ER-mitochondria contact sites upon starvation-induced autophagy [74]. And finally, this hypothesis is supported by the observation that depletion of Mfn2 impairs the formation of autophagosomes significantly [73].

#### **1.4 Mitochondrial Dynamics**

Mitochondria are highly dynamic organelles, changing their shape according to cellular needs by the processes of fusion and fission. Mitochondrial membrane fission and fusion are regulated by the GTPases dynamin-related protein 1 (Drp1), mitochondrial fission protein (Mff), Mfn2, and Mfn1 [76]. Interestingly, all of these proteins have been detected at ER-mitochondria contact sites.

Mitochondrial fission is not abolished upon knockout of the two fission proteins Drp1 and Mff [77] suggesting that further promoters of the fission process exist. Interestingly, live cell and electron microscopy showed that mitochondrial fission events occurred preferentially at ER-mitochondria contact sites [78]. This observation points toward a role of ER-mitochondria contact sites in mitochondrial fission, whereas a role of the contact sites in mitochondrial fusion remains unknown [25].

#### **1.5 ER-Mitochondria Contact Sites and Disease**

During the last decades, the importance of the integrity of ER-mitochondria contact sites for overall cellular function and survival has been unraveled. Researchers from diverse basic and clinical scientific areas recognized that disturbances in the structure and function of ER-mitochondria contact sites underlie the pathogenesis of a multitude of human diseases. Such alterations have, for example, been suggested to be involved in the development of obesity and diabetes [79–81], heart and brain ischemia [82, 83], as well as cancer [84–86].

Importantly, the integrity of ER-mitochondria contact sites seems also to hold a central role in the pathogenesis of a variety of neurodegenerative disorders including Alzheimer's disease (AD), Parkinson's disease (PD), Charcot-Marie-Tooth disease, and dominant optic atrophy [27].

Neuronal cells have large energy requirements which are mainly served by ATP produced during mitochondrial oxidative phosphorylation [25]. As described before, the functional integrity of mitochondrial bioenergetics is closely connected with the integrity of ER-mitochondria contact sites. These considerations explain why alterations in the integrity of ER-mitochondria contact sites have such profound impact on cells of the central nervous system (CNS) [14, 27]. Mutations in proteins associated with ER-mitochondria contact sites have been shown to underlie neurodegeneration. For example, alterations in the presenilin 1 and 2 (PS1, PS2) and Drp1 have been linked to AD [31, 87, 88], whereas mutations in synuclein and Mfn2 are causative for PD [89, 90]. Hence, in-depth investigation of ER-mitochondria contact sites under physiologic and pathologic conditions will prepare the basis for a broader understanding of the associated diseases and open the possibility for novel treatment strategies. The initial protocol for the isolation of MAM from mouse liver tissue was developed by Jean E. Vance [8]. Until today, the outline of this protocol remained the same with minor changes. In our lab, the procedure was optimized

for the usage of fresh mouse brain tissue and is nowadays performed routinely [91, 92]. In the following section, the isolation of MAM from mouse brain tissue will be described and discussed in detail. The preparation of further subcellular fractions containing plasma membrane (PM), ER, and pure mitochondria is included. In case divergent tissues or cell lines shall be used as starting material, buffer volumes and homogenization steps have to be adjusted.

---

## 2 Materials

1. Five brains from 3- to 4-month-old female C57BL6/J mice (corresponding to 2–2.5 g starting material).
2. Teflon pestle homogenizer with motor (1500 rpm: 10rcf).
3. Small laboratory utensils: 15 cm glass petri dish, filter paper, bent blunt forceps, scissors, 15 and 50 ml screw cap centrifugation tubes, 5 ml tips, Pasteur pipettes, soft painting brush (approx. size 6, synthetic fibers).
4. The described protocol is established for usage of the following Beckman Coulter equipment: Avant J-20P centrifuge with JA-18 rotor, Optima MAX ultracentrifuge with TLA-55 rotor and 1.5 ml ultracentrifugation tubes #357448, Optima L-90K ultracentrifuge with SW40 rotor and 14 ml ultracentrifugation tubes #331374. Equipment with corresponding specifications of other suppliers can be used.
5. Brain fractionation buffer 1 (BFB1): 225 mM mannitol, 75 mM sucrose, 0.5 mM EGTA, 0.5% bovine serum albumin, 30 mM Tris-HCl, pH 7.4. Prepare 1 day before the experiment using bi-distilled water.
6. Brain fractionation buffer 2 (BFB2): 225 mM mannitol, 75 mM sucrose, 0.5% (w/v) bovine serum albumin, 30 mM Tris-HCl, pH 7.4. Prepare 1 day before the experiment using bi-distilled water.
7. Brain fractionation buffer 3 (BFB3): 225 mM mannitol, 75 mM sucrose, 30 mM Tris-HCl, pH 7.4. Prepare 1 day before the experiment using bi-distilled water.
8. Brain fractionation (BFB4): 250 mM mannitol, 0.5 mM EGTA, 5 mM HEPES/KOH, pH 7.4. Prepare 1 day before the experiment using bi-distilled water.
9. Percoll dilution buffer: 225 mM mannitol, 1 mM EGTA, 25 mM HEPES/KOH, pH 7.4. Prepare 1 day before the experiment using bi-distilled water.
10. Percoll pH 8.5–9.5: the protocol is established for usage of Sigma-Aldrich product #P1644. Similar Percoll solutions of other suppliers can be used.

### 3 Methods

The subcellular fractionation of mouse brain tissue, outlined in Fig. 1, is performed by an adjusted and optimized protocol based on the method by the Pinton Laboratory [93]. A typical separation that can be achieved using this method is shown in Fig. 2.

1. Sacrifice five mice by neck dislocation (*see* **Notes 1–4**).
2. Open the skull with scissors, eviscerate the brain, and transfer into a 50 ml screw cap centrifugation tube containing 20 ml ice-cold BFB1 (*see* **Notes 5 and 6**).
3. Transfer the brain onto a BFB1-soaked filter paper on an upside-down 15 cm glass petri dish on ice.
4. Cut the brain into small pieces
5. Rinse away blood by dropping 15–20 ml ice-cold BFB3 onto the brain pieces and moving the brain pieces in the buffer.
6. Transfer the brain pieces of 2.5 brains to a glass Teflon homogenizer with 4 ml ice-cold BFB1.
7. Homogenize by 12 slow strokes at 1500 rpm on ice using a glass Teflon homogenizer (*see* **Notes 7 and 8**), and pool the homogenates.
8. Spin down unbroken material by centrifugation at  $800 \times g$  for 5 min at 4 °C.
9. Transfer the supernatant with a cut 5 ml tip into a fresh tube, and spin down further unbroken material by centrifugation at  $800 \times g$  for 5 min at 4 °C (*see* **Note 9**).
10. Transfer the supernatant with a cut 5 ml tip into a fresh tube, and centrifuge at  $9000 \times g$  for 10 min at 4 °C (*see* **Note 9**).
11. Optional: Collect the supernatant for the separation of the fraction containing plasma membrane (PM) from that containing ER. Centrifuge the supernatant at  $20,000 \times g$  for 20 min at 4 °C. The pellet will contain PM and lysosomes while the supernatant will contain ER. Transfer the supernatant into a fresh tube and pellet the ER fraction by centrifugation at  $100,000 \times g$  for 1 h at 4 °C.
12. Resuspend the crude mitochondrial pellet from **step 9** gently in 12 ml ice-cold BFB2 using a soft brush (*see* **Note 10**).
13. Spin down the crude mitochondrial suspension by centrifugation at  $10,000 \times g$  for 10 min at 4 °C.
14. Discard the supernatant and resuspend the crude mitochondrial pellet in 12 ml ice-cold BFB3 using a soft brush (*see* **Note 10**).
15. Spin down the crude mitochondrial suspension by centrifugation at  $10,000 \times g$  for 10 min at 4 °C.

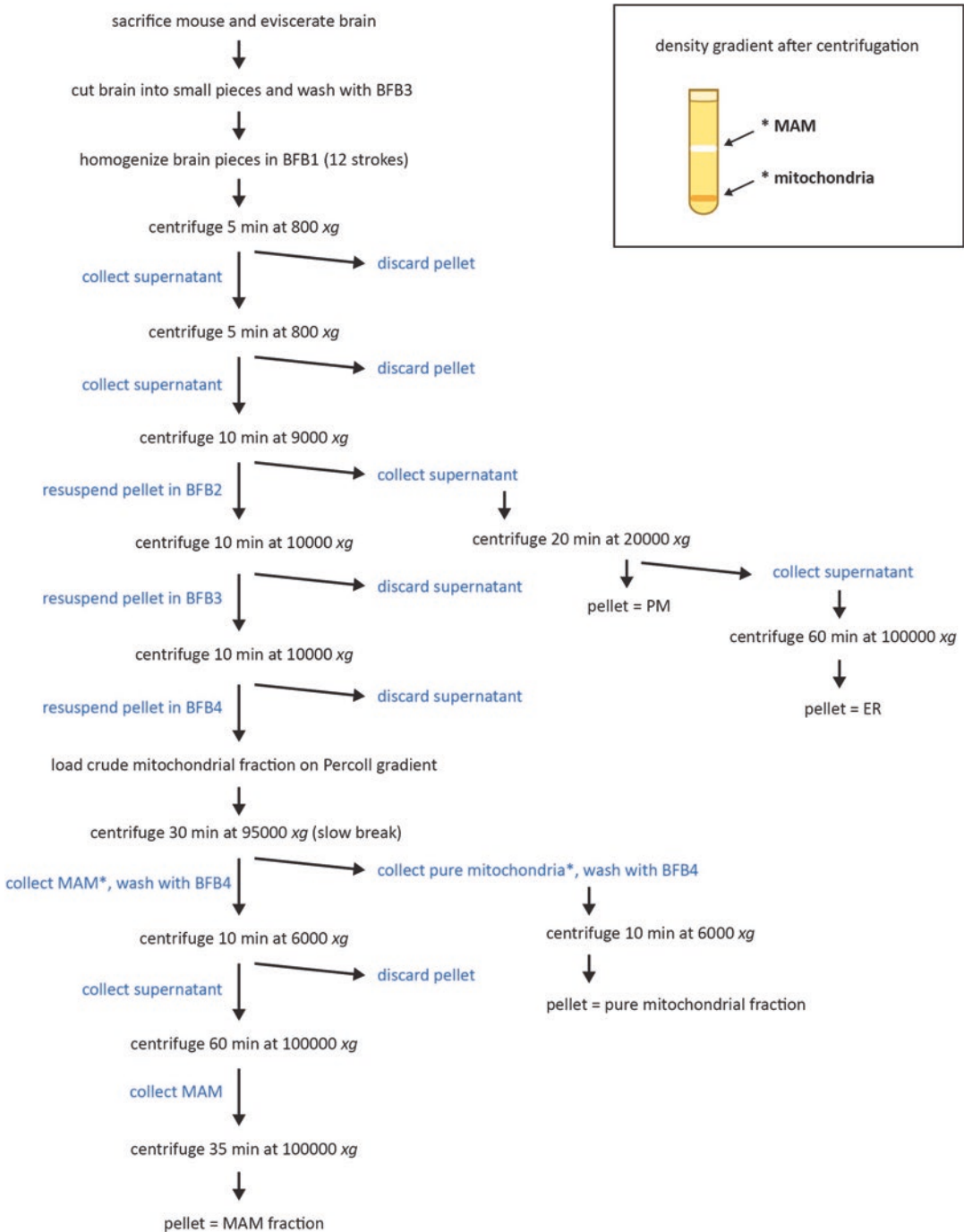


**Fig. 1.** Chronological overview of sequential steps during MAM isolation. The inserted box shows a schematic view of the density gradient after centrifugation with the approximate location of MAM and mitochondrial fraction

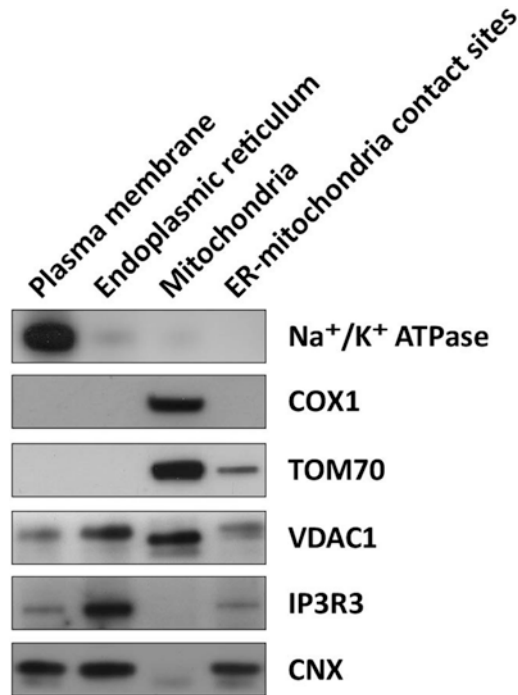


**Fig. 2** Distribution of proteins in subcellular fractions. The distribution of sodium potassium ATPase (Na<sup>+</sup>/K<sup>+</sup> ATPase), IP3R3 (inositol 1,4,5-trisphosphate receptor type 3), CNX (calnexin), mitochondrial import receptor subunit TOM70 (TOM70), voltage-dependent anion-selective channel protein 1 (VDAC1), and cytochrome c oxidase subunit 1 (COX1) in the isolated subcellular fractions was analyzed by immunoblotting using respective antibodies

16. Meanwhile; prepare 20 ml of 30% Percoll gradient premix by dilution of 6 ml Percoll colloidal suspension in 14 ml Percoll dilution buffer.
17. Discard the supernatant and resuspend the crude mitochondrial pellet gently in 2 ml ice-cold BFB4 using a soft brush (*see Note 10*).
18. Add 9 ml of 30% Percoll gradient premix to a 14 ml ultracentrifugation tube (*see Note 11*).
19. Layer the crude mitochondrial suspension slowly (*see Note 12*) with a cut tip (*see Note 9*) onto the Percoll gradient.
20. Layer ca. 1 ml BFB4 slowly (*see Note 12*) on top of the crude mitochondrial suspension up to 2 mm below the upper rim of the tube (*see Note 13*).
21. Prepare a similar 14 ml ultracentrifugation tube with 30% Percoll gradient premix and BFB4 as tare weight (*see Note 13*).
22. Ultracentrifuge the gradient in a swing-out rotor at 95,000 × *g* for 30 min at 4 °C and employ the “slow brake” mode.

23. After this centrifugation step, the “MAM fraction” is visible as a white cloudy band in the middle of the gradient. The pure mitochondrial fraction is visible as a yellow band close to the bottom of the gradient.
24. Collect the “MAM fraction” with a thin Pasteur pipette and transfer to a fresh centrifugation tube.
25. Optional: Collect pure mitochondria with a thin Pasteur pipette and transfer to a fresh centrifugation tube. To remove the remaining Percoll, add ice-cold BFB4 up to 13 ml, mix, and centrifuge at  $6000 \times g$  for 10 min at 4 °C. The pellet represents the pure mitochondrial fraction.
26. To remove the remaining Percoll and contaminating non-MAM membranes, add ice-cold BFB4 up to 13 ml to the collected MAM fraction from **step 24** and mix (*see Note 13*).
27. Ultracentrifuge in a swing-out rotor at  $100,000 \times g$  for 1 h at 4 °C employing “fast break” mode.
28. The fraction containing “pure MAM” is visible as a white diffuse band at the bottom of tube.
29. Collect pure MAM with a thin Pasteur pipette into a 1.5 ml ultracentrifugation tube and pellet by centrifugation at  $100,000 \times g$  for 35 min at 4 °C (optional centrifugation step: *see Note 14*).

---

## 4 Notes

1. **Step 1:** Approximately 200 µg MAM fraction can be isolated from five brains from 3- to 4-month-old female C57BL6/J mice.
2. **Step 1:** To minimize biological variance, mice of same genotype, gender, and approximately same age should be taken at approximately the same time of day.
3. In **step 1**, it is important to use fresh brain. Upon freezing the separation of MAM from mitochondria is no longer possible.
4. **Step 1:** In order to exclude side effects, mice should not be anesthetized before sacrifice.
5. All steps: Indicated volumes apply to subcellular fractionation of five mouse brains and have to be adjusted according to the input amount and type of tissue or cell line.
6. All steps: It is important to work swiftly through the complete protocol in order to minimize the time for unwanted proteolysis.
7. In **step 7**, it is important to move the glass homogenizer slowly and smoothly up and down to avoid the generation of air bubbles. The pestle has to be thoroughly centered all times in

order to assure equal distance between the Teflon pestle and the glass homogenizer along the whole perimeter. Changing the angle of the pestle will reduce the width of the diameter at some places which can cause rupture of mitochondria.

8. **Step 7:** The count of strokes must be adjusted to the respective tissue/cell type. Successful homogenization should be monitored microscopically. In our hands, for example, up to 200 strokes are needed for the homogenization of HeLa or MEF cells. If applicable, existing cell-/tissue-specific protocols should be followed and, if necessary, optimized (e.g., [15, 93, 94]).
9. **Steps 9, 10, and 19:** In order to avoid disruption of the OMM while transferring the crude mitochondrial suspension between reaction tubes, pipette tips must be clipped off to enlarge the diameter of the opening.
10. **Steps 12, 14, and 17:** In order to avoid disruption of the mitochondrial outer membrane, all resuspension steps of the crude mitochondrial pellet must be performed by gentle, turning movements with a soft brush or a polished glass rod but *not* with a pipette tip.
11. In **step 18**, no traces of Percoll premix should remain at the wall of the ultracentrifuge tube above the gradient.
12. **Step 19 and 20:** It is critical to layer the crude mitochondrial suspension and BFB4 very slowly on top of the Percoll gradient. Loading too fast will lead to damage of the gradient.
13. **Step 20 and 21:** It must be made sure that the ultracentrifuge tube is filled up to 2 mm below the upper rim, otherwise the tube will collapse due to the vacuum.
14. **Step 29:** Care must be taken that all traces of residual Percoll gradient are completely removed. A second centrifugation step may be needed to achieve that.

## References

1. Copeland DE, Dalton AJ (1959) An association between mitochondria and the endoplasmic reticulum in cells of the pseudobranch gland of a teleost. *J Biophys Biochem Cytol* 5(3):393–396
2. Morre DJ, Merritt WD, Lembi CA (1971) Connections between mitochondria and endoplasmic reticulum in rat liver and onion stem. *Protoplasma* 73(1):43–49
3. Pickett CB, Montisano D, Eisner D, Cascarano J (1980) The physical association between rat liver mitochondria and rough endoplasmic reticulum. I. Isolation, electron microscopic examination and sedimentation equilibrium centrifugation analyses of rough endoplasmic reticulum-mitochondrial complexes. *Exp Cell Res* 128(2):343–352
4. Montisano DF, Cascarano J, Pickett CB, James TW (1982) Association between mitochondria and rough endoplasmic reticulum in rat liver. *Anat Rec* 203(4):441–450. doi:10.1002/ar.1092030403
5. Lewis JA, Tata JR (1973) A rapidly sedimenting fraction of rat liver endoplasmic reticulum. *J Cell Sci* 13(2):447–459
6. Shore GC, Tata JR (1977) Two fractions of rough endoplasmic reticulum from rat liver. I Recovery of rapidly sedimenting endoplasmic

- reticulum in association with mitochondria. *J Cell Biol* 72(3):714–725
7. Meier PJ, Spycher MA, Meyer UA (1981) Isolation and characterization of rough endoplasmic reticulum associated with mitochondria from normal rat liver. *Biochim Biophys Acta* 646(2):283–297
  8. Vance JE (1990) Phospholipid synthesis in a membrane fraction associated with mitochondria. *J Biol Chem* 265(13):7248–7256
  9. Simmen T, Aslan JE, Blagoveshchenskaya AD, Thomas L, Wan L, Xiang Y, Feliciangeli SF, Hung CH, Crump CM, Thomas G (2005) PACS-2 controls endoplasmic reticulum-mitochondria communication and Bid-mediated apoptosis. *EMBO J* 24(4):717–729. doi:[10.1038/sj.emboj.7600559](https://doi.org/10.1038/sj.emboj.7600559)
  10. Szabadkai G, Bianchi K, Varnai P, De Stefani D, Wieckowski MR, Cavagna D, Nagy AI, Balla T, Rizzuto R (2006) Chaperone-mediated coupling of endoplasmic reticulum and mitochondrial Ca<sup>2+</sup> channels. *J Cell Biol* 175(6):901–911. doi:[10.1083/jcb.200608073](https://doi.org/10.1083/jcb.200608073)
  11. Iwasawa R, Mahul-Mellier AL, Datler C, Pazarentzos E, Grimm S (2011) Fis1 and Bap31 bridge the mitochondria-ER interface to establish a platform for apoptosis induction. *EMBO J* 30(3):556–568. doi:[10.1038/emboj.2010.346](https://doi.org/10.1038/emboj.2010.346)
  12. De Vos KJ, Morotz GM, Stoica R, Tudor EL, Lau KF, Ackerley S, Warley A, Shaw CE, Miller CC (2012) VAPB interacts with the mitochondrial protein PTPIP51 to regulate calcium homeostasis. *Hum Mol Genet* 21(6):1299–1311. doi:[10.1093/hmg/ddr559](https://doi.org/10.1093/hmg/ddr559)
  13. Betz C, Stracka D, Prescianotto-Baschong C, Frieden M, Demaurex N, Hall MN (2013) Feature article: mTOR complex 2-Akt signaling at mitochondria-associated endoplasmic reticulum membranes (MAM) regulates mitochondrial physiology. *Proc Natl Acad Sci U S A* 110(31):12526–12534. doi:[10.1073/pnas.1302455110](https://doi.org/10.1073/pnas.1302455110)
  14. Raturi A, Simmen T (2013) Where the endoplasmic reticulum and the mitochondrion tie the knot: the mitochondria-associated membrane (MAM). *Biochim Biophys Acta* 1833(1):213–224. doi:[10.1016/j.bbamcr.2012.04.013](https://doi.org/10.1016/j.bbamcr.2012.04.013)
  15. Area-Gomez E (2014) Assessing the function of mitochondria-associated ER membranes. *Methods Enzymol* 547:181–197. doi:[10.1016/B978-0-12-801415-8.00011-4](https://doi.org/10.1016/B978-0-12-801415-8.00011-4)
  16. Hayashi T, Fujimoto M (2010) Detergent-resistant microdomains determine the localization of sigma-1 receptors to the endoplasmic reticulum-mitochondria junction. *Mol Pharmacol* 77(4):517–528. doi:[10.1124/mol.109.062539](https://doi.org/10.1124/mol.109.062539)
  17. Fujimoto M, Hayashi T, Su TP (2012) The role of cholesterol in the association of endoplasmic reticulum membranes with mitochondria. *Biochem Biophys Res Commun* 417(1):635–639. doi:[10.1016/j.bbrc.2011.12.022](https://doi.org/10.1016/j.bbrc.2011.12.022)
  18. Rizzuto R, Pinton P, Carrington W, Fay FS, Fogarty KE, Lifshitz LM, Tuft RA, Pozzan T (1998) Close contacts with the endoplasmic reticulum as determinants of mitochondrial Ca<sup>2+</sup> responses. *Science* 280(5370):1763–1766
  19. Csordas G, Renken C, Varnai P, Walter L, Weaver D, Buttler KF, Balla T, Mannella CA, Hajnoczky G (2006) Structural and functional features and significance of the physical linkage between ER and mitochondria. *J Cell Biol* 174(7):915–921. doi:[10.1083/jcb.200604016](https://doi.org/10.1083/jcb.200604016)
  20. Goetz JG, Nabi IR (2006) Interaction of the smooth endoplasmic reticulum and mitochondria. *Biochem Soc Trans* 34(Pt 3):370–373. doi:[10.1042/BST0340370](https://doi.org/10.1042/BST0340370)
  21. Perkins G, Renken C, Martone ME, Young SJ, Ellisman M, Frey T (1997) Electron tomography of neuronal mitochondria: three-dimensional structure and organization of cristae and membrane contacts. *J Struct Biol* 119(3):260–272. doi:[10.1006/jsbi.1997.3885](https://doi.org/10.1006/jsbi.1997.3885)
  22. Kornmann B, Currie E, Collins SR, Schuldiner M, Nunnari J, Weissman JS, Walter P (2009) An ER-mitochondria tethering complex revealed by a synthetic biology screen. *Science* 325(5939):477–481
  23. Kornmann B, Osman C, Walter P (2011) The conserved GTPase Gem1 regulates endoplasmic reticulum-mitochondria connections. *Proc Natl Acad Sci U S A* 108(34):14151–14156. doi:[10.1073/pnas.1111314108](https://doi.org/10.1073/pnas.1111314108)
  24. Michel AH, Kornmann B (2012) The ERMES complex and ER-mitochondria connections. *Biochem Soc Trans* 40(2):445–450. doi:[10.1042/BST20110758](https://doi.org/10.1042/BST20110758)
  25. Helle SC, Kanfer G, Kolar K, Lang A, Michel AH, Kornmann B (2013) Organization and function of membrane contact sites. *Biochim Biophys Acta* 1833(11):2526–2541. doi:[10.1016/j.bbamcr.2013.01.028](https://doi.org/10.1016/j.bbamcr.2013.01.028)
  26. Mishra P, Chan DC (2014) Mitochondrial dynamics and inheritance during cell division, development and disease. *Nat Rev Mol Cell Biol* 15(10):634–646. doi:[10.1038/nrm3877](https://doi.org/10.1038/nrm3877)
  27. Vance JE (2013) MAM (mitochondria-associated membranes) in mammalian cells: lipids and beyond. *Biochim Biophys Acta*. doi:[10.1016/j.bbailip.2013.11.014](https://doi.org/10.1016/j.bbailip.2013.11.014)
  28. de Brito OM, Scorrano L (2008) Mitofusin 2 tethers endoplasmic reticulum to mitochondria. *Nature* 456(7222):605–610. doi:[10.1038/nature07534](https://doi.org/10.1038/nature07534)

29. Rusinol AE, Cui Z, Chen MH, Vance JE (1994) A unique mitochondria-associated membrane fraction from rat liver has a high capacity for lipid synthesis and contains pre-Golgi secretory proteins including nascent lipoproteins. *J Biol Chem* 269(44):27494–27502
30. Stone SJ, Levin MC, Zhou P, Han J, Walther TC, Farese RV Jr (2009) The endoplasmic reticulum enzyme DGAT2 is found in mitochondria-associated membranes and has a mitochondrial targeting signal that promotes its association with mitochondria. *J Biol Chem* 284(8):5352–5361. doi:10.1074/jbc.M805768200
31. Area-Gomez E, Del Carmen Lara Castillo M, MD T, Guardia-Laguarta C, AJ d G, Madra M, Ikenouchi J, Umeda M, TD B, SL S, EA S (2012) Upregulated function of mitochondria-associated ER membranes in Alzheimer disease. *EMBO J* 31(21):4106–4123. doi:10.1038/emboj.2012.202
32. Rizzuto R, Brini M, Murgia M, Pozzan T (1993) Microdomains with high  $Ca^{2+}$  close to IP<sub>3</sub>-sensitive channels that are sensed by neighboring mitochondria. *Science* 262(5134):744–747
33. Zhang A, Williamson CD, Wong DS, Bullough MD, Brown KJ, Hathout Y, Colberg-Poley AM (2011) Quantitative proteomic analyses of human cytomegalovirus-induced restructuring of endoplasmic reticulum-mitochondrial contacts at late times of infection. *Mol Cell Proteomics* 10(10):M111 009936. doi:10.1074/mcp.M111.009936
34. Poston CN, Krishnan SC, Bazemore-Walker CR (2013) In-depth proteomic analysis of mammalian mitochondria-associated membranes (MAM). *J Proteomics* 79:219–230. doi:10.1016/j.jprot.2012.12.018
35. Patergnani S, Suski JM, Agnoletto C, Bononi A, Bonora M, De Marchi E, Giorgi C, Marchi S, Missiroli S, Poletti F, Rimessi A, Duszynski J, Wieckowski MR, Pinton P (2011) Calcium signaling around mitochondria associated membranes (MAMs). *Cell Commun Signal* 9:19. doi:10.1186/1478-811X-9-19
36. Pinton P, Giorgi C, Siviero R, Zecchini E, Rizzuto R (2008) Calcium and apoptosis: ER-mitochondria  $Ca^{2+}$  transfer in the control of apoptosis. *Oncogene* 27(50):6407–6418. doi:10.1038/onc.2008.308
37. Vance JE (2015) Phospholipid synthesis and transport in mammalian cells. *Traffic* 16(1):1–18. doi:10.1111/tra.12230
38. Schon EA, Area-Gomez E (2013) Mitochondria-associated ER membranes in Alzheimer disease. *Mol Cell Neurosci* 55:26–36. doi:10.1016/j.mcn.2012.07.011
39. van Vliet AR, Verfaillie T, Agostinis P (2014) New functions of mitochondria associated membranes in cellular signaling. *Biochim Biophys Acta* 1843(10):2253–2262. doi:10.1016/j.bbamcr.2014.03.009
40. Rizzuto R, Bastianutto C, Brini M, Murgia M, Pozzan T (1994) Mitochondrial  $Ca^{2+}$  homeostasis in intact cells. *J Cell Biol* 126(5):1183–1194
41. Szabadkai G, Simoni AM, Bianchi K, De Stefani D, Leo S, Wieckowski MR, Rizzuto R (2006) Mitochondrial dynamics and  $Ca^{2+}$  signaling. *Biochim Biophys Acta* 1763(5–6):442–449. doi:10.1016/j.bbamcr.2006.04.002
42. Pizzo P, Drago I, Filadi R, Pozzan T (2012) Mitochondrial  $Ca(2)(+)$  homeostasis: mechanism, role, and tissue specificities. *Pflugers Arch* 464(1):3–17. doi:10.1007/s00424-012-1122-y
43. Somlyo AP (1984) Cell physiology: cellular site of calcium regulation. *Nature* 309(5968):516–517
44. Somlyo AP, Bond M, Somlyo AV (1985) Calcium content of mitochondria and endoplasmic reticulum in liver frozen rapidly in vivo. *Nature* 314(6012):622–625
45. Cardenas C, Miller RA, Smith I, Bui T, Molgo J, Muller M, Vais H, Cheung KH, Yang J, Parker I, Thompson CB, Birnbaum MJ, Hallows KR, Foscett JK (2010) Essential regulation of cell bioenergetics by constitutive InsP<sub>3</sub> receptor  $Ca^{2+}$  transfer to mitochondria. *Cell* 142(2):270–283. doi:10.1016/j.cell.2010.06.007
46. Baughman JM, Perocchi F, Girgis HS, Plovanich M, Belcher-Timme CA, Sancak Y, Bao XR, Strittmatter L, Goldberger O, Bogorad RL, Koteliensky V, Mootha VK (2011) Integrative genomics identifies MCU as an essential component of the mitochondrial calcium uniporter. *Nature* 476(7360):341–345. doi:10.1038/nature10234
47. De Stefani D, Raffaello A, Teardo E, Szabo I, Rizzuto R (2011) A forty-kilodalton protein of the inner membrane is the mitochondrial calcium uniporter. *Nature* 476(7360):336–340. doi:10.1038/nature10230
48. Allbritton NL, Meyer T, Stryer L (1992) Range of messenger action of calcium ion and inositol 1,4,5-trisphosphate. *Science* 258(5089):1812–1815
49. Jouaville LS, Pinton P, Bastianutto C, Rutter GA, Rizzuto R (1999) Regulation of mitochondrial ATP synthesis by calcium: evidence for a long-term metabolic priming. *Proc Natl Acad Sci U S A* 96(24):13807–13812
50. Szabadkai G, Duchen MR (2008) Mitochondria: the hub of cellular  $Ca^{2+}$  signaling. *Physiology (Bethesda)* 23:84–94. doi:10.1152/physiol.00046.2007

51. Gellerich FN, Gizatullina Z, Trumbeckaite S, Nguyen HP, Pallas T, Arandarcikaite O, Vielhaber S, Seppet E, Striggow F (2010) The regulation of OXPHOS by extramitochondrial calcium. *Biochim Biophys Acta* 1797(6-7):1018-1027. doi:[10.1016/j.bbabi.2010.02.005](https://doi.org/10.1016/j.bbabi.2010.02.005)
52. Rowland AA, Voeltz GK (2012) Endoplasmic reticulum-mitochondria contacts: function of the junction. *Nat Rev Mol Cell Biol* 13(10):607-625. doi:[10.1038/nrm3440](https://doi.org/10.1038/nrm3440)
53. Schroder M (2006) The unfolded protein response. *Mol Biotechnol* 34(2):279-290. doi:[10.1385/MB.34.2.279](https://doi.org/10.1385/MB.34.2.279)
54. Costa RO, Ferreira E, Oliveira CR, Pereira CM (2013) Inhibition of mitochondrial cytochrome c oxidase potentiates abeta-induced ER stress and cell death in cortical neurons. *Mol Cell Neurosci* 52:1-8. doi:[10.1016/j.mcn.2012.09.005](https://doi.org/10.1016/j.mcn.2012.09.005)
55. Bravo R, Vicencio JM, Parra V, Troncoso R, Munoz JP, Bui M, Quiroga C, Rodriguez AE, Verdejo HE, Ferreira J, Iglewski M, Chiong M, Simmen T, Zorzano A, Hill JA, Rothermel BA, Szabadkai G, Lavandero S (2011) Increased ER-mitochondrial coupling promotes mitochondrial respiration and bioenergetics during early phases of ER stress. *J Cell Sci* 124(Pt 13):2143-2152. doi:[10.1242/jcs.080762](https://doi.org/10.1242/jcs.080762)
56. Stone SJ, Vance JE (2000) Phosphatidylserine synthase-1 and -2 are localized to mitochondria-associated membranes. *J Biol Chem* 275(44):34534-34540. doi:[10.1074/jbc.M002865200](https://doi.org/10.1074/jbc.M002865200)
57. Vance JE (1991) Newly made phosphatidylserine and phosphatidylethanolamine are preferentially translocated between rat liver mitochondria and endoplasmic reticulum. *J Biol Chem* 266(1):89-97
58. Shiao YJ, Lupo G, Vance JE (1995) Evidence that phosphatidylserine is imported into mitochondria via a mitochondria-associated membrane and that the majority of mitochondrial phosphatidylethanolamine is derived from decarboxylation of phosphatidylserine. *J Biol Chem* 270(19):11190-11198
59. Percy AK, Moore JF, Carson MA, Waechter CJ (1983) Characterization of brain phosphatidylserine decarboxylase: localization in the mitochondrial inner membrane. *Arch Biochem Biophys* 223(2):484-494
60. Vance JE, Vance DE (2004) Phospholipid biosynthesis in mammalian cells. *Biochem Cell Biol* 82(1):113-128. doi:[10.1139/o03-073](https://doi.org/10.1139/o03-073)
61. Choi JY, Wu WI, Voelker DR (2005) Phosphatidylserine decarboxylases as genetic and biochemical tools for studying phospholipid traffic. *Anal Biochem* 347(2):165-175. doi:[10.1016/j.ab.2005.03.017](https://doi.org/10.1016/j.ab.2005.03.017)
62. Vance JE, Aasman EJ, Szarka R (1991) Brefeldin A does not inhibit the movement of phosphatidylethanolamine from its sites for synthesis to the cell surface. *J Biol Chem* 266(13):8241-8247
63. Cuif MH, Porteu A, Kahn A, Vaulont S (1993) Exploration of a liver-specific, glucose/insulin-responsive promoter in transgenic mice. *J Biol Chem* 268(19):13769-13772
64. Vance JE, Stone SJ, Faust JR (1997) Abnormalities in mitochondria-associated membranes and phospholipid biosynthetic enzymes in the mnd/mnd mouse model of neuronal ceroid lipofuscinosis. *Biochim Biophys Acta* 1344(3):286-299
65. Barbero-Camps E, Fernandez A, Baulies A, Martinez L, Fernandez-Checa JC, Colell A (2014) Endoplasmic reticulum stress mediates amyloid beta neurotoxicity via mitochondrial cholesterol trafficking. *Am J Pathol* 184(7):2066-2081. doi:[10.1016/j.ajpath.2014.03.014](https://doi.org/10.1016/j.ajpath.2014.03.014)
66. Lewin TM, Kim JH, Granger DA, Vance JE, Coleman RA (2001) Acyl-CoA synthetase isoforms 1, 4, and 5 are present in different subcellular membranes in rat liver and can be inhibited independently. *J Biol Chem* 276(27):24674-24679. doi:[10.1074/jbc.M102036200](https://doi.org/10.1074/jbc.M102036200)
67. Arias E, Cuervo AM (2011) Chaperone-mediated autophagy in protein quality control. *Curr Opin Cell Biol* 23(2):184-189. doi:[10.1016/j.ceb.2010.10.009](https://doi.org/10.1016/j.ceb.2010.10.009)
68. Eskelinen EL, Saftig P (2009) Autophagy: a lysosomal degradation pathway with a central role in health and disease. *Biochim Biophys Acta* 1793(4):664-673. doi:[10.1016/j.bbamcr.2008.07.014](https://doi.org/10.1016/j.bbamcr.2008.07.014)
69. Cuervo AM, Wong E (2014) Chaperone-mediated autophagy: roles in disease and aging. *Cell Res* 24(1):92-104. doi:[10.1038/cr.2013.153](https://doi.org/10.1038/cr.2013.153)
70. Axe EL, Walker SA, Manifava M, Chandra P, Roderick HL, Habermann A, Griffiths G, Ktistakis NT (2008) Autophagosome formation from membrane compartments enriched in phosphatidylinositol 3-phosphate and dynamically connected to the endoplasmic reticulum. *J Cell Biol* 182(4):685-701. doi:[10.1083/jcb.200803137](https://doi.org/10.1083/jcb.200803137)
71. Hayashi-Nishino M, Fujita N, Noda T, Yamaguchi A, Yoshimori T, Yamamoto A (2009) A subdomain of the endoplasmic reticulum forms a cradle for autophagosome formation. *Nat Cell Biol* 11(12):1433-1437. doi:[10.1038/ncb1991](https://doi.org/10.1038/ncb1991)

72. Cuervo AM (2010) The plasma membrane brings autophagosomes to life. *Nat Cell Biol* 12(8):735–737. doi:[10.1038/ncb0810-735](https://doi.org/10.1038/ncb0810-735)
73. Hailey DW, Rambold AS, Satpute-Krishnan P, Mitra K, Sougrat R, Kim PK, Lippincott-Schwartz J (2010) Mitochondria supply membranes for autophagosome biogenesis during starvation. *Cell* 141(4):656–667. doi:[10.1016/j.cell.2010.04.009](https://doi.org/10.1016/j.cell.2010.04.009)
74. Hamasaki M, Furuta N, Matsuda A, Nezu A, Yamamoto A, Fujita N, Oomori H, Noda T, Haraguchi T, Hiraoka Y, Amano A, Yoshimori T (2013) Autophagosomes form at ER-mitochondria contact sites. *Nature* 495(7441):389–393. doi:[10.1038/nature11910](https://doi.org/10.1038/nature11910)
75. Hamasaki M, Shibutani ST, Yoshimori T (2013) Up-to-date membrane biogenesis in the autophagosome formation. *Curr Opin Cell Biol* 25(4):455–460. doi:[10.1016/j.ceb.2013.03.004](https://doi.org/10.1016/j.ceb.2013.03.004)
76. Zhao J, Lendahl U, Nister M (2013) Regulation of mitochondrial dynamics: convergences and divergences between yeast and vertebrates. *Cell Mol Life Sci* 70(6):951–976. doi:[10.1007/s00018-012-1066-6](https://doi.org/10.1007/s00018-012-1066-6)
77. Otera H, Wang C, Cleland MM, Setoguchi K, Yokota S, Youle RJ, Mihara K (2010) Mff is an essential factor for mitochondrial recruitment of Drp1 during mitochondrial fission in mammalian cells. *J Cell Biol* 191(6):1141–1158. doi:[10.1083/jcb.201007152](https://doi.org/10.1083/jcb.201007152)
78. Friedman JR, Lackner LL, West M, DiBenedetto JR, Nunnari J, Voeltz GK (2011) ER tubules mark sites of mitochondrial division. *Science* 334(6054):358–362. doi:[10.1126/science.1207385](https://doi.org/10.1126/science.1207385)
79. Zorzano A, Liesa M, Palacin M (2009) Role of mitochondrial dynamics proteins in the pathophysiology of obesity and type 2 diabetes. *Int J Biochem Cell Biol* 41(10):1846–1854. doi:[10.1016/j.biocel.2009.02.004](https://doi.org/10.1016/j.biocel.2009.02.004)
80. Arruda AP, Pers BM, Parlakgul G, Guney E, Inouye K, Hotamisligil GS (2014) Chronic enrichment of hepatic endoplasmic reticulum-mitochondria contact leads to mitochondrial dysfunction in obesity. *Nat Med* 20(12):1427–1435. doi:[10.1038/nm.3735](https://doi.org/10.1038/nm.3735)
81. Tubbs E, Theurey P, Vial G, Bendridi N, Bravard A, Chauvin MA, Ji-Cao J, Zoulim F, Bartosch B, Ovize M, Vidal H, Rieusset J (2014) Mitochondria-associated endoplasmic reticulum membrane (MAM) integrity is required for insulin signaling and is implicated in hepatic insulin resistance. *Diabetes* 63(10):3279–3294. doi:[10.2337/db13-1751](https://doi.org/10.2337/db13-1751)
82. Paillard M, Tubbs E, Thiebaut PA, Gomez L, Fauconnier J, Da Silva CC, Teixeira G, Mewton N, Belaidi E, Durand A, Abrial M, Lacampagne A, Rieusset J, Ovize M (2013) Depressing mitochondria-reticulum interactions protects cardiomyocytes from lethal hypoxia-reoxygenation injury. *Circulation* 128(14):1555–1565. doi:[10.1161/CIRCULATIONAHA.113.001225](https://doi.org/10.1161/CIRCULATIONAHA.113.001225)
83. Ouyang YB, Giffard RG (2012) ER-mitochondria crosstalk during cerebral ischemia: molecular chaperones and ER-mitochondrial calcium transfer. *Int J Cell Biol* 2012:493934. doi:[10.1155/2012/493934](https://doi.org/10.1155/2012/493934)
84. Pinton P, Giorgi C, Pandolfi PP (2011) The role of PML in the control of apoptotic cell fate: a new key player at ER-mitochondria sites. *Cell Death Differ* 18(9):1450–1456. doi:[10.1038/cdd.2011.31](https://doi.org/10.1038/cdd.2011.31)
85. Bononi A, Pinton P (2014) Study of PTEN subcellular localization. *Methods*. doi:[10.1016/j.ymeth.2014.10.002](https://doi.org/10.1016/j.ymeth.2014.10.002)
86. Akl H, Vervloessem T, Kiviluoto S, Bittremieux M, Parys JB, De Smedt H, Bultynck G (2014) A dual role for the anti-apoptotic Bcl-2 protein in cancer: mitochondria versus endoplasmic reticulum. *Biochim Biophys Acta* 1843(10):2240–2252. doi:[10.1016/j.bbamcr.2014.04.017](https://doi.org/10.1016/j.bbamcr.2014.04.017)
87. Area-Gomez E, de Groof AJ, Boldogh I, Bird TD, Gibson GE, Koehler CM, Yu WH, Duff KE, Yaffe MP, Pon LA, Schon EA (2009) Presenilins are enriched in endoplasmic reticulum membranes associated with mitochondria. *Am J Pathol* 175(5):1810–1816. doi:[10.2353/ajpath.2009.090219](https://doi.org/10.2353/ajpath.2009.090219)
88. Wang S, Polo-Parada L, Landmesser LT (2009) Characterization of rhythmic Ca<sup>2+</sup> transients in early embryonic chick motoneurons: Ca<sup>2+</sup> sources and effects of altered activation of transmitter receptors. *J Neurosci* 29(48):15232–15244. doi:[10.1523/JNEUROSCI.3809-09.2009](https://doi.org/10.1523/JNEUROSCI.3809-09.2009)
89. Pham AH, Meng S, Chu QN, Chan DC (2012) Loss of Mfn2 results in progressive, retrograde degeneration of dopaminergic neurons in the nigrostriatal circuit. *Hum Mol Genet* 21(22):4817–4826. doi:[10.1093/hmg/dd3311](https://doi.org/10.1093/hmg/dd3311)
90. Cali T, Ottolini D, Negro A, Brini M (2012) Alpha-Synuclein controls mitochondrial calcium homeostasis by enhancing endoplasmic reticulum-mitochondria interactions. *J Biol Chem* 287(22):17914–17929. doi:[10.1074/jbc.M111.302794](https://doi.org/10.1074/jbc.M111.302794)
91. Hedskog L, Pinho CM, Filadi R, Ronnback A, Hertwig L, Wichager B, Larssen P, Gellhaar S, Sandebring A, Westerlund M, Graff C, Winblad B, Galter D, Behbahani H, Pizzo P, Glaser E, Ankarcrona M (2013) Modulation of the endoplasmic reticulum-mitochondria interface in Alzheimer's disease and related models. *Proc*

- Natl Acad Sci U S A 110(19):7916–7921. doi:[10.1073/pnas.1300677110](https://doi.org/10.1073/pnas.1300677110)
92. Schreiner B, Hedskog L, Wiehager B, Ankarcona M (2015) Amyloid-beta peptides are generated in mitochondria-associated endoplasmic reticulum membranes. *J Alzheimers Disease* 43(2):369–374. doi:[10.3233/JAD-132543](https://doi.org/10.3233/JAD-132543)
93. Wieckowski MR, Giorgi C, Lebiedzinska M, Duszynski J, Pinton P (2009) Isolation of mitochondria-associated membranes and mitochondria from animal tissues and cells. *Nat Protoc* 4(11):1582–1590. doi:[10.1038/nprot.2009.151](https://doi.org/10.1038/nprot.2009.151)
94. Annunziata I, Patterson A, d'Azzo A (2015) Isolation of mitochondria-associated ER membranes (MAMs) and glycosphingolipid-enriched microdomains (GEMs) from brain tissues and neuronal cells. *Methods Mol Biol* 1264:25–33. doi:[10.1007/978-1-4939-2257-4\\_3](https://doi.org/10.1007/978-1-4939-2257-4_3)

## Label-Free Quantitative Analysis of Mitochondrial Proteomes Using the Multienzyme Digestion-Filter Aided Sample Preparation (MED-FASP) and “Total Protein Approach”

Jacek R. Wiśniewski

### Abstract

Determination of proteome composition and measuring of changes in protein titers provide important information with a substantial value for studying mitochondria.

This chapter describes a workflow for the quantitative analysis of mitochondrial proteome with a focus on sample preparation and quantitative analysis of the data. The workflow involves the multienzyme digestion-filter aided sample preparation (MED-FASP) protocol enabling efficient extraction of proteins and high rate of protein-to-peptide conversion. Consecutive protein digestion with Lys C and trypsin enables generation of peptide fractions with minimal overlap, largely increases the number of identified proteins, and extends their sequence coverage. Abundances of proteins identified by multiple peptides can be assessed by the “Total Protein Approach.”

**Key words** Proteomic sample preparation, Multienzyme Digestion-Filter Aided Sample Preparation (MED-FASP), “Total Protein Approach”, Absolute protein quantitation, WF-assay

---

### 1 Introduction

Respectively to cell type, mitochondria constitute from a few to 30% of total cellular protein and therefore they can be considered abundant organelles [1]. They include about 1000 proteins that allow covering of the entire mitochondrial proteome in analyses with uncomplicated protein or peptide fractionation strategies. Single shot liquid chromatography tandem mass spectrometry (LC/MS/MS) analyses of purified mitochondria have the potential to map their entire proteome [2]. Irrespectively of the type of instrumentation, the quality of LC-MS/MS, and as a consequence, the whole proteomic analysis depends on the quality of the sample, which should contain well-digested peptides and be free from other substances, such as lipids, partially digested proteins, or

nucleic acids. Generation of samples fulfilling this condition seems trivial, but in fact, it has been a topic of many publications. The key difficulty in sample preparation consists of combining different conditions required for efficient protein extraction and cleavage. Whereas protein extraction requires the use of strong denaturants, most of the proteases, including trypsin, are becoming inefficient in the presence of these reagents. For this reason sample preparation protocols often compromise between these conditions and lead to an incomplete protein extraction and low peptide yield. Confronted with these problems we have developed the filter aided sample preparation (FASP) method that allows processing of protein lysates obtained by the aid of sodium dodecyl sulfate (SDS) or other detergents [2].

In the FASP method centrifugal ultrafiltration concentrators, commonly used for concentrating protein and nucleic acid solutions, are repurposed to reactor units. In the reactor, the ultrafiltration membrane allows depletion of detergent and isolation of pure peptides. In the first step of the procedure the lysate is depleted from the detergent using concentrated urea (Fig. 1). At high urea concentrations, denatured proteins are kept in solution whereas the detergent micelles decrease and dissociate, which is the prerequisite for efficient exclusion of detergents [3]. Once the detergent is removed cysteine thiols are carboamidomethylated with iodoacetamide and after the completion of the reaction, the excess of the reagent can be removed quickly, before digestion of protein begins (Fig. 1). Protein cleavage can be performed in the presence or absence of urea. While using the denaturant attention should be paid to the fact that many proteases lose enzymatic activity and specificity under denaturing conditions. Digestion in the absence of urea abrogates these limitations and allows using of many different proteases. However, among several proteases, cleavage with trypsin, and endoproteases LysC and ArgC results in the highest peptide identification rates during the LC-MS/MS analysis [2, 4].

Next, peptides released from protein digestion are collected by ultrafiltration. This allows retaining of undigested protein fragments and other genuine macromolecules present in the lysate, such as nucleic acids and oligosaccharides. Removal of these substances improves the chromatography of peptides and reduces the deterioration of the LC-column and mass spectrometer contamination.

In a standard FASP protocol, proteins are digested with a single protease. In the multi enzyme digestion FASP (MED-FASP) proteins are consecutively cleaved with various proteinases and the released peptides are collected after each digestion step. This approach generates peptide fractions with only a few percent of peptides present in more than one fraction. Compared to the standard FASP procedure, separate LC-MS/MS analyses of the fractions significantly improve the total number of protein identifications and result in higher sequence coverage [4].

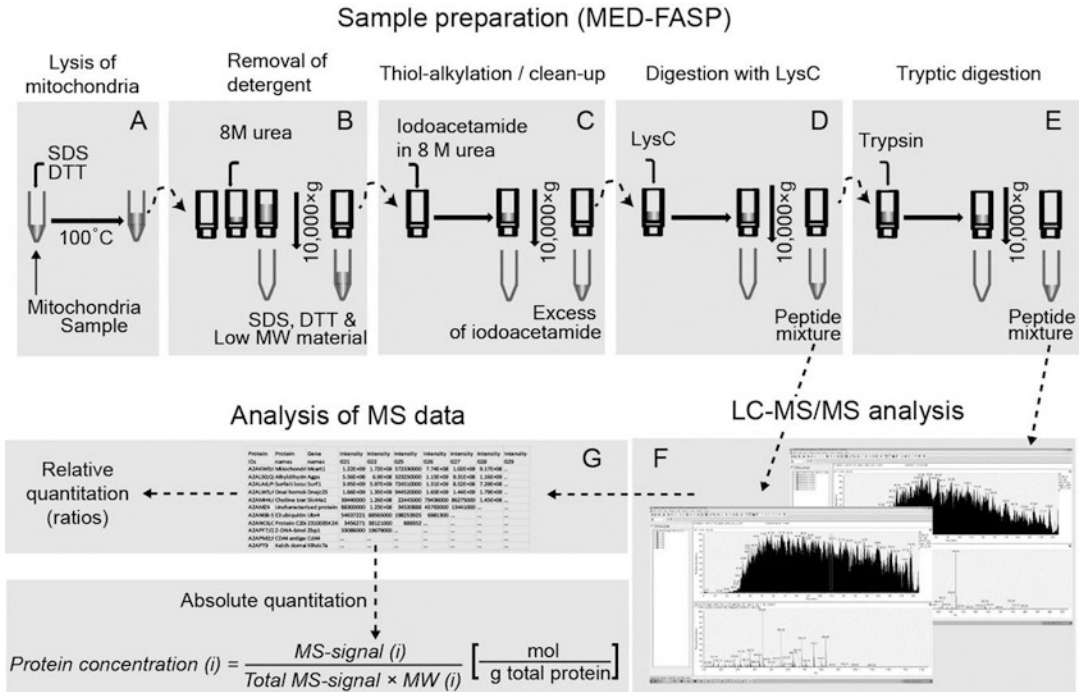


**Fig. 1.** Workflow for the analysis of mitochondrial proteomes by mass-spectrometry. Fractions enriched in mitochondria are lysed in SDS and DTT containing buffer (a) and processed by Multienzyme Digestion—Filter aided sample preparation method (b–e). The resulting LysC and tryptic peptides are analyzed in separate LC-MS/MS runs (f). Mass spectrometry data are processed to generate quantitative data (g)

Beside protein identification and mapping of posttranslational modifications, quantification of proteins remains the major task of proteomics analysis. There are two major types of protein quantification in mass spectrometry-based proteomics: the “relative” and “absolute.” In both cases, ion abundances observed in the mass spectra are related to peptide quantities present in the analyte. The averaged or summed quantities of peptides matching a given protein sequence are used to calculate protein titers. Whereas “relative” quantification provides only protein ratios reflecting differences between analyzed samples, the “absolute” quantification allows determination of protein titers expressed in concentrations or protein copies per a countable biological unit such as a cell or an organelle. Among different experimental approaches the “Total Protein Approach” [5–7] allows uncomplicated calculations of protein titers on the basis of an in-depth proteomic analysis. For mitochondria, such data can be obtained using the MED-FASP sample preparation protocol followed by two separate LC-MS/MS runs with LyC and tryptic peptides. Notably, this strategy does not require labeling of the samples or labeled standards.

In this chapter, the proteomic workflow for proteomic analysis of mitochondria is described (Fig. 1). The initial step of the entire procedure, the MED-FASP sample preparation is described in detail whereas only a brief description of the LC-MS/MS and data processing is provided, because these parts of the workflow can be performed using various chromatography systems and mass spectrometers, and the spectra can be processed by different software packages.

---

## 2 Materials

### 2.1 *Lysates of Mitochondria*

1. Pellet of isolated mitochondria (fresh or frozen).
2. Boiling water bath (*see Note 1*).
3. Bench-top centrifuge.
4. Lysis buffer: 0.05 M Tris-HCl, pH 7.6, 2% (v/w) SDS, 0.05 M DTT (prepare fresh).

### 2.2 *Total Protein Determination by WF Assay*

1. Assay buffer: 8 M urea, 10 mM Tris-HCl pH 7.5.
2. Microtiter plate reader with fluorescence detection.
3. Corning Costar 96-well black flat-bottomed polystyrene plates (Sigma-Aldrich, CLS3915).
4. Tryptophan standard: 0.1 mg tryptophan/mL water (*see Note 2*).

### 2.3 *MED-FASP*

1. Ultrafiltration—unit: Microcon-30 kDa Centrifugal Filter Unit with Ultracel-30 membrane (Previously sold as Microcon YM-30 and Forensic 30 k) (Merck-Millipore, Cat. No. MRCF0R030) (*see Note 3*).
2. Bench-top centrifuge.
3. Humid chamber (box) with a rack for Eppendorf-type disposal tubes.
4. Thermo-mixer.
5. UA: 8 M urea in 0.1 M Tris-HCl, pH 8.5. Prepare 1 mL per 1 sample.
6. IAA solution: 0.05 M iodoacetamide in UA. Prepare 0.1 mL per 1 sample (*see Note 4*).
7. Trypsin, Stock 0.4  $\mu\text{g}/\mu\text{L}$  (V5280, Promega, Madison, WI).
8. Endoproteinase LysC.
9. Digestion buffer (DB): 0.05 M Tris-HCl, pH 8.5. Prepare 0.5 mL per 1 sample.
10. Spectrophotometer.

### 2.4 Peptide Desalting and Sample Storage

1. Buffer A: 1% (v/v) CH<sub>3</sub>COOH in deionized water.
2. Buffer B: 60% (v/v) CH<sub>3</sub>CN, 1% (v/v) CH<sub>3</sub>COOH in deionized water.
3. StageTips: 3 layers of Empore-C<sub>18</sub> (Catalog Number 2215, 3 M Company, St. Paul MN) stacked in a 0.2 mL pipette tip.
4. Methanol.
5. SpeedVac.

### 2.5 LC-MS/MS Analysis

1. Mass spectrometer.
2. Nano-liquid chromatography system.
3. Analytical reverse phase C<sub>18</sub> column.
4. Software for data processing.

### 2.6 Relative and Absolute Protein Quantitation

Table calculation software such as Microsoft Excel.

---

## 3 Methods

### 3.1 Preparation of Mitochondrial Lysates

The major advantage of FASP over many other proteomic digestion protocols is its applicability to the proteomic sample processing of SDS-containing lysates.

1. Mix the pellet of isolated mitochondria with about fivefold excess (volume) of lysis buffer (*see Note 5*).
2. Place the tubes with the homogenate in a bath with boiling water and incubate them for 3 min. Cool the sample to room temperature.
3. Centrifuge the lysate at 10,000 × *g* for 5 min (*see Note 6*).

### 3.2 Determination of Total Protein in Lysates by WF Assay Using Fluorescence Microtiter Plate Reader (See Note 7)

1. Mix 2 μL of the sample with 0.200 mL assay buffer per well.
2. Mix 1 μL of the tryptophan standard with 0.200 mL assay buffer per well.
3. Set the excitation wavelength to 295 nm with a 5 nm bandwidth and the emission to 350 nm with a 20 nm bandwidth. Individual measurements should consist of at least 10 reads each with 50 μs integration time. Set the temperature to 25 °C.
4. Read the fluorescence.
5. Calculate the protein concentration:  
$$C = 8.56 \frac{[\text{sample fluorescence}]}{[\text{tryptophan fluorescence}]}$$
(mg/mL).

### 3.3 MED-FASP Protocol

1. Mix up to 30  $\mu\text{L}$  of protein extract with 200  $\mu\text{L}$  of UA in the filter unit and centrifuge at  $14,000 \times g$  until less than 10  $\mu\text{L}$  of sample remains above the filter. The total protein content in the loaded extract should not exceed 200  $\mu\text{g}$ . This usually requires centrifugation time of 10–15 min. This applies to all further centrifugation steps (*see Note 8*).
2. Add 200  $\mu\text{L}$  of UA to the filter unit and repeat the centrifugation.
3. Discard the flow-through from the collection tube.
4. Add 100  $\mu\text{L}$  IAA solution to the concentrated sample and mix at 600 rpm in a thermo-mixer at room temperature for 1 min.
5. Centrifuge the filter units at  $14,000 \times g$  for 10 min.
6. Add 100  $\mu\text{L}$  of UA to the filter unit and centrifuge at  $14,000 \times g$  for 15 min. Repeat this step twice.
7. Add 100  $\mu\text{L}$  of DB to the filter unit and centrifuge at  $14,000 \times g$  for 10 min. Repeat this step twice.
8. Add 40  $\mu\text{L}$  DB with endoproteinase LysC (enzyme to protein ratio 1:100) and mix at 600 rpm in thermo-mixer at room temperature for 1 min.
9. Incubate the units in a humid chamber at 37 °C overnight.
10. Transfer the filter units to new collection tubes.
11. Centrifuge the filter units at  $14,000 \times g$  until the solution completely passed the filter membrane (about 5 min).
12. Add 100  $\mu\text{L}$  of DB and centrifuge the filter unit at  $14,000 \times g$  until the solution completely passed the filter membrane (about 5 min). The flow-through contains peptides obtained by LysC digestion.
13. Transfer the filter unit to a new tube.
14. Add 40  $\mu\text{L}$  DB with trypsin (enzyme to protein ratio 1:100) and mix at 600 rpm in thermo-mixer at room temperature for 1 min.
15. Incubate the units in a humid chamber at 37 °C for 4 h.
16. Centrifuge the filter units at  $14,000 \times g$  until the solution entirely passed the filter membrane (about 5 min).
17. Add 100  $\mu\text{L}$  of DB and centrifuge the filter units at  $14,000 \times g$  until the solution entirely passed the filter membrane (about 5 min). The flow-through contains peptides obtained by trypsin digestion.
18. Determine concentrations of the Lys C and tryptic peptides by  $A_{280}$  measurement in a spectrophotometer (*see Note 9*) or by the fluorometric WF-assay [8] as described in Subheading 3.2 using DB buffer instead of the urea assay buffer.

### 3.4 Peptide Desalting and Sample Storage

1. Wash and equilibrate the C18-“StageTips” with 0.05 mL of methanol, followed by 0.05 mL of Buffer B and 0.05 mL of Buffer A using a benchtop centrifuge (*see Note 10*).
2. Pipet aliquots containing 10 µg of LysC or tryptic peptides onto the “StageTips.”
3. Wash the C<sub>18</sub>-“StageTips” with 0.05 mL of Buffer A.
4. Elute fractions with 0.05 mL of Buffer B into vials used directly for injection of the samples into LC system assembled with a mass spectrometer.
5. Concentrate the eluate to ca. 5 µL using a centrifugal vacuum concentrator (SpeedVac).
6. The samples can be stored frozen at –20 °C for at least 1 month or –80 °C for several months.

### 3.5 LC-MS/MS, Spectra Analysis, and Protein Quantitation

1. Separate the mixtures of the LysC and tryptic peptides over C<sub>18</sub> reverse phase column and analyze them by a tandem mass spectrometer (*see Note 11*).
2. Analyze the recorded mass spectrometric data using a software such as MaxQuant to obtain summed spectral MS spectral intensities of all peptides related to individual proteins.
3. Calculate titers of proteins by the “Total Protein Approach” (*see Note 12*):

$$\text{Total protein } (i): \quad TP(i) = \frac{MS - \text{signal}(i)}{\text{Total } MS - \text{signal}} \quad \text{or}$$

$$\text{Protein concentration } (i): \quad C(i) = \frac{TP(i)}{MW(i)} \left[ \frac{\text{mol}}{g \text{ total protein}} \right]$$

---

## 4 Notes

1. Lysis in boiling water assures 100 °C temperature that is often difficult to achieve and control in thermomixers. Due to high thermal capacity of water the lysis is faster than in thermomixers.
2. Initially, prepare a 10 mg/mL tryptophan stock solution in 50% methanol and then dilute with water to the final concentration of 0.1 mg/mL.
3. Improper use of ultrafiltration devices can result in failure in the sample preparation. Be sure that the units were correctly stored and centrifuged at maximally 10,000 × *g*. Check the integrity of the membrane by passing aliquots of water before commence FASP sample preparation. Note that denatured

proteins are more bulky than native folded ones and therefore small proteins such as histones do not pass the membrane with 30,000 MW cut off [3]. Filtration units with lower MW cut-offs require several fold longer centrifugation times and therefore they are not practicable.

4. UA and IAA solutions must be freshly prepared and used within a day.
5. To achieve the best results of lysis, it is important to use a sufficient excess of the lysis buffer over the sample. Typically, a fivefold excess is recommended. However, protein concentrations of the lysates below 1 mg/mL should be avoided as too large amounts of the detergent require additional detergent depletion steps in the FASP procedure. The lysis buffer should be stored at above 15 °C to avoid precipitation of SDS.
6. Potassium and other cations form insoluble salts with SDS. They can appear as a film over the clarified lysate or crystal-like pellets, but they do not affect the FASP procedure and the total protein assay.
7. Determination of total protein content in lysates containing high concentrations of SDS and DTT using Bradford or BCA assay is unreliable. In contrast, tryptophan fluorescence-based WF-assay is an easy method allowing total protein measurement in the presence of high concentrations of detergents and disulfide-reducing reagents [8].
8. The centrifugation step has to continue until less than 5% of the initial solution remains above the filter. The time needed to achieve this varies between the filter types, lysate properties, and the total protein concentration.
9. Concentration of the peptides can be estimated by UV spectrometer, assuming that 0.1% solution of vertebrate proteins has at 280 nm an extinction of 1.1 units (1 mg/mL solution has an  $A_{280}$  of 1.1). Always record a spectrum from 240 to 340 nm. A distinct peak should be observed at 270–280 nm and the extinction at 320 nm should be 0. Measurements of peptide concentrations are reliable when the absorbance value at  $A_{280}$  is above 0.1 in a cuvette with a 10 mm path. Extinction values below 0.1 can be used only for rough protein estimation due to increasing contribution of light scattering.
10. “StageTips” [9] are convenient and low-expensive tools for desalting of peptide solutions. The sequential passage of solvents is enforced by low-speed centrifugation at 1000–3000  $\times g$ . The stage tips can be assembled in Eppendorf-type tubes using adaptors or just by piercing the tube lid [10, 11].
11. Various LC-MS/MS systems can be used. The author used 3 h LC gradients for analysis of LysC and tryptic peptides while spectra were acquired by the QExactive HF instruments

(Thermo Instruments, CA). This allowed identification of 15,000–25,000 peptides in enriched mitochondrial lysates per sample.

12. Accuracy of the calculated protein concentration depends on the number of identified and quantified peptides. Usually, concentrations of proteins with at least five matching peptides are close to concentrations assessed by targeted proteomics (Manuscript in preparation). However, for proteins with less peptides the calculated values are often good concentration estimates [5].

---

## Acknowledgments

This work was supported by the Max-Planck Society for the Advancement of Science.

## References

1. Wisniewski JR, Koepsell H, Gizak A, Rakus D (2015) Absolute protein quantification allows differentiation of cell-specific metabolic routes and functions. *Proteomics* 15(7):1316–1325. doi:10.1002/pmic.201400456
2. Wisniewski JR, Zougman A, Nagaraj N, Mann M (2009) Universal sample preparation method for proteome analysis. *Nat Methods* 6(5):359–362. doi:10.1038/nmeth.1322
3. Wisniewski JR, Zielinska DF, Mann M (2011) Comparison of ultrafiltration units for proteomic and N-glycoproteomic analysis by the filter-aided sample preparation method. *Anal Biochem* 410(2):307–309. doi:10.1016/j.ab.2010.12.004
4. Wisniewski JR, Mann M (2012) Consecutive proteolytic digestion in an enzyme reactor increases depth of proteomic and phosphoproteomic analysis. *Anal Chem* 84(6):2631–2637. doi:10.1021/ac300006b
5. Wisniewski JR, Rakus D (2014) Multi-enzyme digestion FASP and the 'Total Protein Approach'-based absolute quantification of the *Escherichia coli* proteome. *J Proteomics* 109:322–331. doi:10.1016/j.jpro.2014.07.012
6. Wisniewski JR, Ostasiewicz P, Dus K, Zielinska DF, Gnad F, Mann M (2012) Extensive quantitative remodeling of the proteome between normal colon tissue and adenocarcinoma. *Mol Syst Biol* 8:611. doi:10.1038/msb.2012.44
7. Wisniewski JR, Hein MY, Cox J, Mann M (2014) A “proteomic ruler” for protein copy number and concentration estimation without spike-in standards. *Mol Cell Proteomics* 13(12):3497–3506. doi:10.1074/mcp.M113.037309
8. Wisniewski JR, Gaugaz FZ (2015) Fast and sensitive total protein and Peptide assays for proteomic analysis. *Anal Chem* 87(8):4110–4116. doi:10.1021/ac504689z
9. Rappsilber J, Ishihama Y, Mann M (2003) Stop and go extraction tips for matrix-assisted laser desorption/ionization, nanoelectrospray, and LC/MS sample pretreatment in proteomics. *Anal Chem* 75(3):663–670
10. Wisniewski JR, Zougman A, Mann M (2009) Combination of FASP and StageTip-based fractionation allows in-depth analysis of the hippocampal membrane proteome. *J Proteome Res* 8(12):5674–5678. doi:10.1021/pr900748n
11. Wisniewski JR (2013) Proteomic sample preparation from formalin fixed and paraffin embedded tissue. *J Vis Exp* 79. doi:10.3791/50589

## Quantitative Analysis of Glycerophospholipids in Mitochondria by Mass Spectrometry

Takashi Tatsuta

### Abstract

Lipids draw increasing attention of cell biologists because of the wide variety of functions beyond their role as building blocks of cellular membranes. Mitochondrial membranes possess characteristic lipid compositions that are intimately associated with mitochondrial architecture and activities. Therefore, quantitative assessment of lipids in isolated mitochondria is of importance for mitochondrial research. Here, I describe our workflow for quantitative analysis of glycerophospholipids in mitochondria with a focus on purification of pure mitochondrial fractions from yeast and cultured mammalian cells as well as improved settings for the analysis of cardiolipin by nano-electrospray ionization mass spectrometry.

**Key words** Lipidomics, Nano-electrospray ionization mass spectrometry, Mitochondria, Glycerophospholipids, Cardiolipin

---

### 1 Introduction

Mitochondria are surrounded by two membranes—the inner and outer mitochondrial membranes. Mitochondrial membranes have characteristic lipid compositions distinct from other cellular membranes. Especially, the mitochondrial inner membrane contains high level of cardiolipin (CL), a class of diphosphatidylglycerols that exists almost exclusively in mitochondrial membranes of eukaryotic cells [1]. Recent studies have revealed that lipids have multiple functions beyond their role as building blocks of mitochondrial membranes [2–4]. Activities of mitochondria are dependent on the lipid environment within their membranes, and vice versa, cells control the lipid composition of mitochondrial membranes to tune the activities of mitochondria. Not surprisingly, many neurodegenerative and myocardial diseases caused by mitochondrial defects are associated with an altered lipid composition of mitochondrial membranes [5–7].

Therefore, quantitative lipid analysis of mitochondria is gaining importance, not only for lipid researchers but also for cell biologists

working on a wide range of mitochondrial processes. Fortunately, novel methods are emerging, and many tools are becoming available along with the rapid advance of the mass spectrometric analysis of lipids (“lipidomics”) [8]. Most lipid classes show a characteristic fragmentation pattern upon collision-induced dissociation (CID; *see* Fig. 3a as an example) that enables the selective determination and quantification of a single lipid class within a complex lipid extract by direct infusion into triple quadrupole instruments. This approach of direct infusion without pre-separation of the lipid extract by chromatographic techniques is called “shotgun lipidomics” and is now allowing high-throughput and simultaneous determination of hundreds of different lipid species in a complex sample [9, 10]. On the other hand, the advance opens up a possibility for “non-lipid specialists” to do simple lipidomics of their samples—as a service provided by core technical facilities in many institutions.

Mitochondrial membranes are mainly composed of glycerophospholipids, and thus accurate determination of the amounts of the major glycerophospholipid classes—phosphatidylcholine (PC), phosphatidylethanolamine (PE), phosphatidylinositol (PI), phosphatidylserine (PS), phosphatidic acid (PA), phosphatidylglycerol (PG), and CL—is the first and most important step to study the lipid environment in mitochondria [2, 3]. In this chapter, I will describe our protocols for the determination of the glycerophospholipid composition in mitochondria. The protocol can be divided into two parts. The first part is the procedure to isolate pure mitochondria largely devoid of membranes from other organelles. Methods to obtain a pure mitochondrial fraction via gradient centrifugation from yeast and human HEK293 cells and to assess the purity of mitochondria will be described. The second part is the procedure for the mass spectrometric (MS) determination of glycerophospholipids. Our MS methods are based on nano-electrospray ionization mass spectrometry (nano-ESI-MS) by direct infusion [11, 12]. For more comprehensive information on nano-ESI-MS, please refer to recent publications [8, 9, 13]. Special attention will be given to the determination of CL species, for which procedures are still not standardized. I will introduce our approach to improve sensitivity and accuracy of CL detection in whole-cell lipid extract by scanning for diacylglycerol (DAG) fragments in the precursor ion scanning mode [14] combined with nano-ESI.

---

## 2 Materials

### 2.1 Purification of Mitochondria from Yeast Cells

1. Stock solutions: 40% (w/v) glucose; 30% (w/v) galactose; 1 M Tris base (pH is not adjusted); 1 M Tris-HCl, pH 7.4; 1 M potassium phosphate buffer, pH 7.4; 0.5 M MES-KOH, pH 6.0; 2.4 M sorbitol; 0.5 M EDTA, pH 8.0 (EDTA will be dissolved upon adjustment of pH). Sterilize them by autoclaving. Store at room temperature (RT).

2. 0.1 M phenyl methyl sulfonyl fluoride (PMSF) in ethanol. Store at  $-20^{\circ}\text{C}$ .
3. YP medium supplemented with glucose (YPD) or galactose (YP-gal): 2% (w/v) Bacto-peptone, 1% (w/v) yeast extract, 2% (w/v) glucose or galactose. Dissolve Bacto-peptone and yeast extract in deionized water, and adjust the pH of the media to 5.5 with HCl. Sterilize it by autoclaving. Carbon sources should be added to media after autoclaving from the 40% glucose or 30% galactose stock.
4. 5 $\times$  SEM buffer: 1.25 M sucrose, 5 mM EDTA, 50 mM MOPS-KOH, pH 7.2, sterile autoclaved.
5. Tris-DTT buffer: 100 mM Tris base, 10 mM dithiothreitol (DTT). Prepare freshly from 1 M Tris base stock and DTT.
6. 1.2 M sorbitol. Diluted freshly from the 2.4 M stock solution.
7. Sorbitol phosphate buffer: 20 mM potassium phosphate buffer, pH 7.4, 1.2 M sorbitol. Prepare freshly from stock solutions.
8. Homogenization buffer: 10 mM Tris-HCl, pH 7.4, 1 mM EDTA, 0.2% (w/v) bovine serum albumin (BSA, fatty acid free), 1 mM PMSF, 0.6 M sorbitol. Prepare freshly from 1 M Tris-HCl, pH 7.4, 0.5 mM EDTA, 2.4 M sorbitol stock solutions, and BSA. Prepare 0.1 M PMSF solution in EtOH and put it into the buffer just before use.
9. Lyticase (*see Note 1*).
10. Buffer A: 5 mM MES-KOH, pH 6.0, 0.6 M sorbitol. Prepare freshly from 0.5 M MES-KOH, pH 6.0, and 2.4 M sorbitol stock solutions, and keep it on ice. Check pH and adjust if necessary.
11. Buffer B: 10 mM Tris-HCl, pH 7.4, 0.6 M sorbitol. Prepare freshly from 1 M Tris-HCl, pH 7.4, and 2.4 M sorbitol stock solutions, and keep it on ice.
12. 20 and 50% sucrose solutions in buffer A: dissolve 10 or 25 g sucrose in 25 mL of buffer A, respectively, and adjust the final volume to 50 mL. Prepare freshly and keep them on ice.
13. 1 $\times$  SEM: prepare 1 $\times$  SEM freshly by mixing one part of 5 $\times$  SEM stock with four parts of Milli-Q water.
14. Ultracentrifuge, a swing rotor and tubes (*see Note 2*).
15. Gradient mixer (Gradient master 108, BIOCAMP or an equivalent gradient maker).
16. Glass hand homogenizer, Sartorius (30 and 5 ml) (*see Note 3*).
17. Yeast colonies, freshly growing on an appropriate solid media plate.

## 2.2 Purification of Mitochondria from Mammalian Cells

1. Stock solutions: 1 M mannitol (dissolve 45.5 g mannitol in 250 mL Milli-Q water, store aliquots in sterile 50 ml Falcon-type tubes at  $-20^{\circ}\text{C}$ ); 1 M sucrose (sterilized by filtration); 0.5 M HEPES-KOH pH 7.4 (sterilized by autoclaving); 0.5 M EGTA-KOH pH 7.4 (EGTA will be dissolved upon adjustment of pH). Store them at RT.
2.  $2\times$  Buffer M: 440 mM Mannitol, 140 mM sucrose, 10 mM HEPES-KOH pH 7.4, 2 mM EGTA-KOH. Prepare freshly from stock solutions and keep it on ice.
3.  $1\times$  Buffer M: mix 1 part of  $2\times$  buffer M and 1 part of sterile Milli-Q water. Keep it on ice.
4. Complete protease inhibitor EDTA-free (Roche) shall be added to buffers prior to use.
5. DPBS (PBS, Gibco), store in a refrigerator.
6. Percoll (GE Healthcare), store in a refrigerator. Although the Percoll solution from GE contains only 23% of colloidal Percoll, the solution will be treated as “100% Percoll solution” in this protocol.
7. HEK293 cells,  $\sim 90\%$  confluency from  $3 \times 15$  cm dishes ( $\sim 4 \times 10^7$  cells) (*see Note 4*).
8. Ultracentrifuge, a swing rotor and tubes (*see Note 2*).
9. Glass-Teflon homogenizer with motor-driven rod (Sartorius/B. Braun) (*see Note 3*).

## 2.3 Extraction of Lipids

All solvents and chemicals shall be obtained in a “mass spectrometry-certified” grade if possible. If MS grade is not available for a solvent or substance, test a production lot of a HPLC or a gas chromatography (GC) grade.

The cleanness of all tubes, bottles, and pipettes should be checked (*see Note 5*), especially those in contact with organic solvents. If available, take materials made of borosilicate glass or Teflon. Avoid silicone (especially on the back of bottle lids) or grease. In general, use of Eppendorf-type tubes or Pipetman tips made of a plastic material should be minimized (*see Note 6*).

### 2.3.1 One-Step Lipid Extraction

1. Starting materials: gradient-purified yeast or mammalian mitochondria, prepared as described in Subheadings 3.1 and 3.2, respectively, or yeast culture in logarithmically growing phase in an appropriate medium.
2. Chemicals and solvents: chloroform, methanol, highly pure water, 25% HCl (w/v, 7.75 N), ammonium acetate (*see Note 7*).
3. Internal standard lipids for quantification: PC 17:0/20:4, PE 17:0/20:4, PI 17:0/20:4, PS 17:0/20:4, PG 17:0/20:4, PA 17:0/20:4, PC 17:0/14:1, PE 17:0/14:1, PI 17:0/14:1, PS 17:0/14:1, PA 17:0/14:1, PG 17:0/14:1, CDP-DAG 17:0/18:1, and CL standard mix (CL 57:4/CL 61:1/CL 80:4 /CL 86:4) (*see Table 1*).

4. SBD: mix chloroform/methanol/25% HCl = 40:80:1 (v/v/v). Store in a glass bottle at RT.
5. Tabletop mixer for 10 ml glass tubes (VIBRAX mixing platform from IKA or an equivalent).
6. Pasteur pipettes, glass tubes with a lid with a Teflon back (10 mL, equivalent to Corning 99502-10 and 9998-15), and glass vials with screw caps (1.5 and 4 mL).
7. Glass beads (0.4–0.6 mm).
8. Gas-tight Hamilton syringes (10, 25, and 100  $\mu$ L).
9. Heating block equipped with gas nozzles (equivalent to Evaporator from Liebig Labortechnik) connected to inert gas line/bottle (nitrogen or argon).

### 2.3.2 Neutral-Acidic Lipid Extraction

1. Starting materials: HEK293 cells ( $10^6$  cells).
2. Chemicals and solvents: chloroform, methanol, highly pure water, 25% HCl (w/v, 7.75 N), ammonium carbonate, and ammonium acetate (*see Note 7*).
3. Internal standard lipids for quantification: PC 17:0/20:4, PE 17:0/20:4, PI 17:0/20:4, PS 17:0/20:4, PG 17:0/20:4, PA

**Table 1**  
**Amount of internal standard (IS) infused (in pmol)**

Mammalian			Yeast		
IS	Whole cell	Pure mitochondria	IS	Whole cell	Pure mitochondria
PC 17:0/20:4	200	150	PC 17:0/14:1	130	100
PE 17:0/20:4	100	100	PE 17:0/14:1	70	70
PI 17:0/20:4	70	100	PI 17:0/14:1	70	40
PS 17:0/20:4	70	50	PS 17:0/14:1	40	40
PG 17:0/20:4	15	20	PA 17:0/14:1	20	20
PA 17:0/20:4	40	30	PG 17:0/14:1	15	15
CL 57:4 <sup>a</sup>	20	50	CDP-DAG 17:0/18:1	10	10
CL 61:1 <sup>a</sup>	20	50	CL 57:4 <sup>a</sup>	20	50
CL 80:4 <sup>a</sup>	20	50	CL 61:1 <sup>a</sup>	20	50
CL 86:4 <sup>a</sup>	20	50	CL 80:4 <sup>a</sup>	20	50
			CL 86:4 <sup>a</sup>	20	50

Lipid standards except the CDP-DAG are Quantitative LIPID MAPS MS STANDARDS from Avanti Polar Lipids. CDP-DAG is only available in qualitative grade

<sup>a</sup>From CL mix I. The amount of individual CL will vary among production lots (the exact concentrations of each CL in the mix are provided by the supplier)

17:0/20:4, and CL standard mix (CL 57:4/CL 61:1/CL 80:4 /CL 86:4) (*see* Table 1).

4. Chloroform/methanol 17:1 (v/v): store in a glass bottle at RT.
5. SBD: mix chloroform/methanol/25% HCl = 40:80:1 (v/v/v). Store in a glass bottle at RT.
6. 2N HCl: mix 1 ml 25% HCl and 2.875 mL pure water. Store in a glass vial at RT.
7. 155 mM ammonium carbonate in water: dissolve 3.72 g in 247 mL pure water. Store in a glass bottle at RT.
8. Reinforced tubes and 1.4 mm ceramic balls for bead mill cell disruptor.
9. Bead mill cell disruptor (Precellys 24 from Bertin Technologies or an equivalent).
10. Tabletop mixer for 10 ml glass tubes (VIBRAX mixing platform from IKA or an equivalent).
11. Pasteur pipettes, glass tubes with a lid with a Teflon back (10 mL), and glass vials with screw caps (1.5 and 4 mL).
12. Gas-tight Hamilton syringes (10, 25, and 100  $\mu$ L).
13. Heating block equipped with gas nozzles (equivalent to Evaporator from Liebig Labortechnik) connected to inert gas line/bottle (nitrogen or argon).

#### **2.4 Nano-electrospray Ionization Mass Spectrometry**

1. Glass vials with lipid films prepared according to Subheading 3.2 or 3.3.
2. TriVersa NanoMate (Advion).
3. ESI-Chip type "A" (HD-A-384, Advion).
4. 96-well plate (*see* Note 7).
5. Sealing foil for 96-well plate (*see* Note 7).
6. 10 mM ammonium acetate in methanol: dissolve 154 mg in 200 mL methanol, and store in a glass bottle.
7. Ultrasonic bath.
8. QTRAP 6500, SCIEX.
9. Analyst software version 1.6.2, SCIEX.
10. LipidView software version 1.2, SCIEX.

---

### **3 Methods**

Current quantitative mass spectrometric methods offer accurate and targeted quantification of lipids in complex extract by using internal standards (ISs) corresponding to the different lipid classes. These ISs are added to each sample in known and constant amounts

prior to the lipid extraction. For the analysis of the major glycerophospholipid classes, a set of ISs carrying an acyl chain with an odd number of carbon atoms (which do not exist in mammalian and yeast samples) is commercially available (*see* Table 1). Recovery during the extraction steps as well as fragmentation behavior and ionization efficiency is largely dependent on the nature of the head group; therefore, the intensity of the IS peak can be used to normalize the values of the endogenous lipids within the same class. Of note, in the case of glycerophospholipid analyses in isolated mitochondria, accuracy is largely dependent on the purity of the mitochondria preparation, especially when analyzing a glycerophospholipid species whose concentration is different between mitochondria and other organelles. For example, CL exists almost exclusively in mitochondria. Therefore only half of the amount of CL species (in comparison to their content in pure mitochondria) will be detected if the purity of the mitochondria preparation is only 50%.

Lipid profiles in cellular membranes are varied by the metabolic status of the cell. Especially, overgrowing imposes metabolic shift and mitochondrial stress to the cell thus should be avoided. When lipid profiles are compared between two conditions (e.g., between control cells and mutant cells), both cells shall be grown in parallel and be harvested at the same growth phase and then be subjected to organelle isolation or lipid extraction simultaneously.

To isolate pure mitochondria, cell-type-dependent optimization in homogenization and density gradient steps is necessary. Mitochondria physically interact with a fraction of the ER (*mitochondria-associated membranes of the ER, MAM* [15]), but the fraction of ER-associated mitochondria often has lower density than the fraction of “pure” mitochondria (*see* Fig. 1). Therefore, pure mitochondria largely devoid of ER membrane can be isolated as a higher density fraction upon density gradient centrifugation. Standard protocols for the isolation of mitochondria from yeast and HEK293 cells and an assessment of purity of mitochondria by immunoblotting analysis will be shown as examples (Subheadings 3.1 and 3.2) (*see* Fig. 1 and **Note 4**).

Extraction of glycerophospholipids from pure mitochondria or whole yeast cells can be achieved by a one-step extraction protocol according to Bligh and Dyer ([16], Subheading 3.3.1). However, different extraction methods will be used in the following cases: (1) to analyze CL in whole mammalian cells, neutral and acidic lipids should be extracted according to Gray et al. and be analyzed separately ([17], Subheading 3.3.2). This reduces the complexity of the lipid extract and eases the detection of minor CL species. (2) To analyze highly polar/charged minor intermediate lipids (phosphatidylglycerolphosphate (PGP) and cytidine diphosphate diacylglycerol (CDP-DAG), we do a one-step extraction of acidic lipids without wash and evaporation steps (*see* **Note 12**).

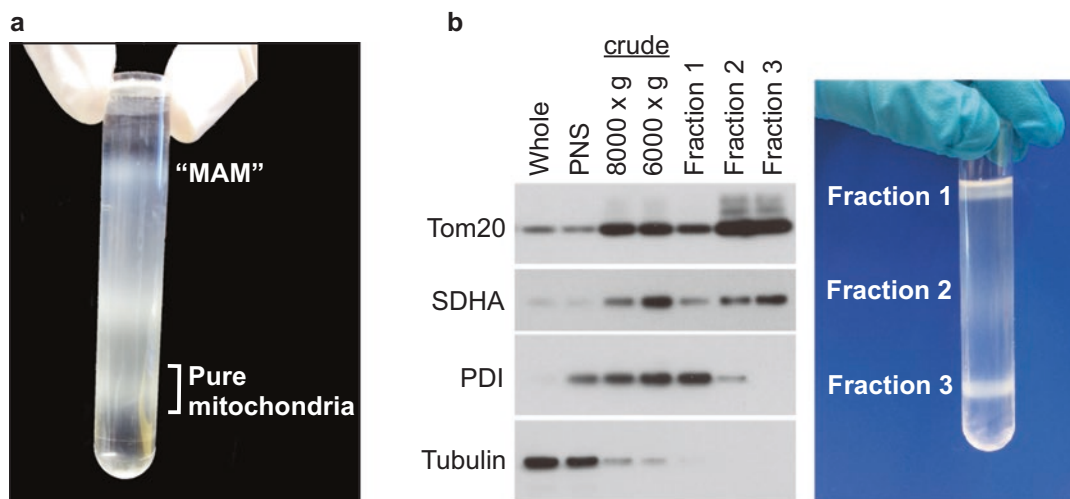


**Fig. 1** Representative result from purification of mitochondria by gradient centrifugation from (a) yeast or (b) HEK293 cells. In the case of HEK293 cells, the assessment of purity of mitochondria by immunodetection of mitochondrial marker proteins (Tom20 and SDHA), an ER marker protein (PDI), and a cytosolic marker protein (Tubulin) is shown (*left panel*)

After extraction, lipid samples are analyzed by nano-ESI-MS (Subheading 3.4). The MS methods for the analysis of the major glycerophospholipid classes are adopted from those developed in the laboratory of B. Brügger [12] with some optimization for the new-generation triple quadrupole instrument (QTRAP 6500). The MS analysis of CLs is challenging because of their large size, their tendency to form doubly charged ions, and their high symmetry in structure. To increase the sensitivity of CL detection, we adopted the detection procedure developed for LC-MS/MS analysis of CL [14] to nano-ESI-MS (*see* Table 4). Processing of MS data including correction of isotopic overlap in CL spectra will be explained (Subheading 3.4.2).

### 3.1 Purification of Mitochondria from Yeast *S. cerevisiae*

1. Inoculate yeast cells from freshly growing colonies on a plate in 20 ml of YPD (*see* Note 8). Incubate the culture at appropriate temperature (usually 30 °C) for overnight.
2. Dilute the overnight culture in 200 ml YPD to OD<sub>600</sub> ~0.1. Incubate the culture until the OD<sub>600</sub> reaches to ~2, and then dilute it in pre-warmed YP-gal (up to 10 liters, starting OD of the culture should be adjusted for each strain). Incubate the culture overnight to OD<sub>600</sub> ~1.5 (*see* Note 9).
3. Isolate cells by centrifugation (3000 × *g*, 5 min, RT) and resuspend cell pellets in water (500 ml). Reisolate cells again (3000 × *g*, 5 min, RT) and measure the weight of the cell pellet.

4. Resuspend the cell pellet in Tris-DTT buffer (2 ml per g pellet), and incubate the suspension at 30 °C for 10 min with shaking. Start preparation of homogenization buffer and cool it on ice.
5. Isolate cells by centrifugation (2000 × *g*, 5 min, RT). Resuspend the cell pellet in 1.2 M sorbitol (2 ml per g pellet), and re-isolate cells by centrifugation (2000 × *g*, 5 min, RT). Cool the centrifuge to 4 °C after this centrifugation step.
6. Spheroplast formation. Resuspend the cell pellet in sorbitol phosphate buffer (6.7 ml per g pellet), and add lyticase powder (~2 mg per g pellet; *see Note 1*). Incubate it at 30 °C for 30 min with shaking. To check for the formation of spheroplast, measure the OD600 of (A) 50 μl suspension + 2 ml water and (B) 50 μl suspension + 2 ml 1.2 M sorbitol. The value of (A) should be 10–20% of (B).
7. Keep solutions on ice in all subsequent steps. Cool centrifuge tubes and the glass homogenizers (30 and 5 ml) on ice.
8. Isolate cells by centrifugation (1200 × *g*, 5 min, 4 °C). The pellet will be very soft and sticky. Resuspend the soft cell pellet carefully in ice-cold homogenization buffer by gentle pipetting (6.7 ml per g pellet).
9. Homogenize the cell suspension by twelve strokes in the large (30 ml) glass homogenizer (*see Note 3*). Rinse the homogenizer with homogenization buffer to recover the remaining material.
10. Precipitate unbroken cells by centrifugation (2000 × *g*, 5 min, 4 °C). Now mitochondria are in the supernatant. Recover supernatant to new centrifuge tube and discard pellet. After an additional centrifugation (2000 × *g*, 5 min, 4 °C), transfer the supernatant to new centrifuge tube.
11. Isolate mitochondrial fraction by centrifugation (17,500 × *g*, 12 min, 4 °C).
12. Discard the supernatant. Resuspend the crude mitochondrial pellet gently by pipetting in 2 mL buffer A, and then homogenize the suspension in the small (5 ml) glass homogenizer (five times). Determine protein concentration of the mitochondrial solution by a Bradford assay. Dilute the solution to 5 mg/ml with buffer A.
13. Prepare 10 mL sucrose gradient in an ultracentrifuge tube for a swing rotor (*see Note 2*) by a gradient mixer (50 to 20% in buffer A).
14. Load 2 ml mitochondrial suspension (containing 10 mg mitochondrial protein) on the top of the gradient (*see Note 10*). If you have odd numbers of samples, setup a blank sample (10 ml gradient + 2 ml buffer A) as a balance. Run sedimentation centrifugation (100,000 × *g*, 1 h, 4 °C).

15. Mitochondria are concentrated at the 1/4–1/3 position from the bottom (Fig. 1a). Remove the top half of the gradient (this fraction contains “MAM”; *see Note 11*). Collect the mitochondrial layer carefully by a glass pipette and transfer it in a centrifuge tube.
16. Add 5× volume of buffer A and mix it gently by pipetting.
17. Harvest mitochondria by centrifugation ( $17,500 \times g$ , 12 min, 4 °C).
18. Carefully resuspend the pellet in 10 mL buffer B by gentle pipetting.
19. Harvest mitochondria by centrifugation ( $17,500 \times g$ , 12 min, 4 °C).
20. Carefully resuspend the pellet in 500  $\mu$ L 1× SEM by gentle pipetting using a tip with wide opening (or a tip whose top is chopped off), and measure the protein concentration by Bradford assay.
21. Dilute mitochondria to 10 mg protein/ml with 1× SEM. Divide mitochondria into small aliquots (50  $\mu$ g protein/tube), and freeze them in liquid nitrogen and store them at –80 °C.

### **3.2 Purification of Mitochondria from Mammalian Cells**

1. Rinse HEK293 cells on plates with 10 mL cold PBS carefully, and then scrape cells with 10 mL cold PBS. Transfer cell suspension to a Falcon tube. Do NOT treat cells by trypsin.
2. Harvest cells by centrifugation ( $500 \times g$ , 5 min, 4 °C).
3. Resuspend the cell pellet in 4 ml cold 1× M buffer (~1 ml per  $10^7$  cells), and transfer it to a precooled small glass homogenizer (5 mL) on ice (*see Note 3*).
4. Treat cells by 15 strokes with motor-driven glass-Teflon homogenizer (1000 rpm). Refrain from creating vacuum with upstroke.
5. Take 100  $\mu$ L “whole-cell” sample for purity test. Distribute homogenized cells in  $3 \times 2$  mL Eppendorf tubes, and sediment unbroken cells and nuclei by centrifugation ( $600 \times g$  for 5 min at 4 °C).
6. Transfer supernatant to a Falcon tube carefully. Resuspend the pellet in 5 mL 1× buffer M in total and treat it 15 strokes by glass-Teflon homogenizer again.
7. Distribute homogenized cells in  $3 \times 2$  mL Eppendorf tubes, and sediment unbroken cells and nuclei by centrifugation ( $600 \times g$  for 5 min at 4 °C).
8. Transfer supernatant to a Falcon tube carefully, and mix it with the supernatant from the first homogenization.
9. Spin again to sediment unbroken cells and nuclei by centrifugation ( $600 \times g$  for 5 min at 4 °C). Transfer supernatant

- carefully to clean centrifuge tubes. Take 100  $\mu\text{L}$  “post-nuclear supernatant” (PNS) sample for purity test.
10. Spin the tube with supernatant to sediment crude mitochondria fraction ( $8000 \times g$  for 10 min at 4  $^{\circ}\text{C}$ ). Remove the supernatant carefully.
  11. Resuspend the pellet in 2 mL cold 1 $\times$  M buffer by gentle pipetting using a tip with wide opening (or a tip whose top is chopped off). Take 50  $\mu\text{L}$  “crude 1” (“ $8000 \times g$ ”) for purity test.
  12. Spin the suspension to sediment mitochondria again ( $6000 \times g$  for 10 min at 4  $^{\circ}\text{C}$ ). Carefully remove the supernatant.
  13. Resuspend pellets gently in 2 mL cold 1 $\times$  M buffer. Take 50  $\mu\text{L}$  “crude 2” (“ $6000 \times g$ ”) for purity test. Quantify protein concentration by Bradford assay. If the protein concentration of the crude mitochondrial suspension is above 5 mg/mL, dilute it to a concentration of 5 mg/mL protein with cold 1 $\times$  M buffer. Normally, the concentration of the suspension is lower, around 2 mg/mL when  $4 \times 10^7$  HEK cells are used.
  14. Prepare Percoll solutions (for two samples as an example): 40% Percoll, 8 mL Percoll + 10 mL 2 $\times$  buffer M + 2 mL  $\text{H}_2\text{O}$  (Total 20 mL); 24% Percoll, 4.8 mL 40% + 3.2 mL 1 $\times$  buffer M (Total 8 mL); 19% Percoll, 5 mL 40% + 5.5 mL 1 $\times$  buffer M (Total 10.5 mL).
  15. Mix 2 mL crude mitochondria suspension ( $\sim 10$  mg mitochondrial protein) with the same volume of 24% Percoll to make a 12% Percoll solution (total 4 mL) (*see Note 10*).
  16. Set Percoll step gradient in a 13.5 mL ultracentrifuge tube: place 2 mL 40% Percoll solution at the bottom of the tube, and overlay it with 4 mL 19% Percoll solution carefully by a glass pipette and then put the mitochondria suspension in 12% Percoll on the top of 19% Percoll carefully. If you have odd numbers of samples, set up a blank sample as a balance.
  17. Run sedimentation centrifugation ( $42,000 \times g$ , 30 min at 4  $^{\circ}\text{C}$ , slow deceleration).
  18. Pure mitochondria will be concentrated at the 19%/40% interface (fraction 3, Fig. 1b, right panel).
  19. Recover three bands (fraction 1, 2, 3, Fig. 1b) separately by a pipette ( $\sim 1$  ml each). Dilute 1:5 with buffer M in a centrifuge tube.
  20. Spin the tube to harvest mitochondria ( $13,200 \times g$ , 5 min at 4  $^{\circ}\text{C}$ ).
  21. Resuspend the mitochondrial pellet with 1 mL 1 $\times$  M buffer carefully by gentle pipetting, and transfer it to an Eppendorf-type tube. Spin it to harvest mitochondria ( $13,200 \times g$ , 5 min

at 4 °C). Remove the supernatant carefully. Repeat the wash to remove Percoll two more times.

22. Resuspend the final pellet in 100  $\mu$ L 1 $\times$  M buffer. Determine protein concentration in all fractions by Bradford assay. Normally, the concentration of the pure mitochondrial sample (from fraction 3) is around 2 mg/mL (~200  $\mu$ g in total) when  $4 \times 10^7$  HEK cells are used. Transfer 20  $\mu$ g protein of pure mitochondria to a clean tube for lipid extraction (Subheading 3.3.1). Transfer 50  $\mu$ g protein from each fraction to Eppendorf tubes for SDS-PAGE. Freeze the rest and the sample for lipid extraction in liquid nitrogen, and store them at  $-80$  °C.
23. Analyze equal amounts (50  $\mu$ g) of protein samples from every fraction by SDS-PAGE and immunoblotting to verify the purity of mitochondria (Fig. 1b, left panel).

### 3.3 Extraction of Lipids

#### 3.3.1 One-Step Lipid Extraction

The following protocol is used for extraction of lipids from gradient-purified yeast or mammalian mitochondria. With a minor modification, described below, it can also be used for lipid extraction from whole yeast cells. To avoid inhalation of organic solvents, whole procedure shall be done in a fume hood.

1. Rinse twice as many 10 mL glass tubes as samples to be analyzed with 1 ml methanol each. Dry them up.
2. Infuse internal standards (IS) to 10 mL glass tubes by gas-tight Hamilton syringes. The amount of IS used for each sample type is listed in Table 1. Add 1 mL SBD to each tube.
3. For lipid extraction from whole yeast cells, proceed to **step 4**. For lipid extraction from gradient-purified mitochondria, proceed to **step 5**.
4. Treatment by glass beads (for whole yeast cells): put 0.5 OD unit of yeast culture (equivalent to 0.5 mL of culture with OD at 600 nm = 1) in an Eppendorf-type tube, and harvest cells by centrifugation (10,000  $\times g$ , 2 min). Wash the cells twice with 500  $\mu$ L Milli-Q water. Resuspend the washed cells in 250  $\mu$ L MS-grade pure water, and transfer the cell suspension to the glass tube with ISs and SBD. Add 300  $\mu$ L glass beads to the tube. Mix it vigorously for 30 min at RT on a shaker. Proceed to **step 6**.
5. Extraction (for pure mitochondria): collect 20  $\mu$ g (protein content) of pure mitochondria in an Eppendorf-type tube by centrifugation (16,100  $\times g$ , 5 min, 4 °C). Resuspend the mitochondria in 250  $\mu$ L pure water, and transfer them to the glass tube with ISs and SBD. Mix the suspension vigorously for 10 min at RT on a shaker.
6. Add 250  $\mu$ L chloroform to the tube and mix the sample for 20 s by vortexing. Add 250  $\mu$ L MS-grade pure water and mix the tube for ~1 min by vortexing.

7. Induce phase separation by centrifugation ( $800 \times g$ , 2 min,  $4\text{ }^{\circ}\text{C}$ ). Transfer lower chloroform phase carefully to a new tube (this is the second tube), and add  $400\text{ }\mu\text{L}$  pure water to it (washing step). Mix the second tube for 20 s by vortexing. Keep the first tube with the upper water phase; it will be needed in **step 9**.
8. Induce phase separation in the second tube by centrifugation ( $800 \times g$ , 2 min,  $4\text{ }^{\circ}\text{C}$ ). Transfer lower chloroform phase carefully to a small (1 mL) glass vial. Keep the water phase in the tube; it will be needed in **step 10**.
9. Re-extraction: add  $300\text{ }\mu\text{L}$  chloroform to the first tube with upper water phase. Mix the tube for 1 min by vortex.
10. After phase separation, transfer lower chloroform phase from the first tube to the second tube with the upper water phase from the washing step. After mixing for 20 s by vortex, induce phase separation by centrifugation, and transfer the lower chloroform phase to the small glass vial with the chloroform phase from the first extraction. Check water drops floating on the chloroform phase in the tube and remove them by a pipette.
11. Place the glass vials on a heat block equipped with gas nozzles connected to an inert gas line (nitrogen or argon). Evaporate the solvent under a gentle stream of inert gas at  $37\text{ }^{\circ}\text{C}$ . Seal the tube by a screw cap. The tubes can be stored for several weeks at  $-20\text{ }^{\circ}\text{C}$ .

### 3.3.2 Neutral-Acidic Lipid Extraction

This protocol is used for lipid extraction from whole mammalian cells for CL analysis. To avoid inhalation of organic solvents, whole procedure shall be done in a fume hood.

1. Rinse as many 10 mL glass tubes as samples to be analyzed with 1 mL methanol each. Dry them up.
2. Infuse internal standards (IS) to 10 mL glass tubes. See Table 1 for the amount of ISs infused. Add 1 mL chloroform/methanol 17:1 (v/v) to each tube.
3. Treatment of cells by ceramic balls: put cell suspension containing a million HEK cells (after cell counting) in an Eppendorf-type tube, and harvest cells by centrifugation ( $2000 \times g$ , 5 min). Wash the cells twice with  $500\text{ }\mu\text{L}$  PBS. Dissolve the washed cells in  $40\text{ }\mu\text{L}$  MS-grade pure water, and transfer the cell suspension to a 2 mL reinforced tube with  $250\text{ }\mu\text{L}$  ceramic balls. Add  $360\text{ }\mu\text{L}$  155 mM ammonium carbonate and seal the tube with a screw cap. Cool the tubes on ice for 5 min. Treat the tube in a bead mill cell disruptor for 30 s. Cool the tube on ice for 5 min and repeat the treatment. Measure the protein concentration of cell suspension by

Bradford assay. Typically, the concentration of protein is between 0.3 and 1 mg/ml.

4. Neutral extraction: take 200  $\mu\text{L}$  cell suspension to the tube with ISs and chloroform/methanol 17:1 (v/v). Mix it vigorously for 30 min at room temp on a tabletop shaker. Induce phase separation by centrifugation ( $2000 \times g$ , 5 min, RT). Transfer lower chloroform phase carefully to a small glass vial. This is neutral extract (N). Keep the water phase; it will be needed in the next step.
5. Acidic extraction: add 10  $\mu\text{L}$  2N HCl to the water phase. Mix the tube vigorously by vortexing for 30 s. Add 375  $\mu\text{L}$  SBD to the tube. Mix it vigorously by vortexing for 30 s. Incubate the tube on ice for 15 min. Mix it vigorously by vortexing for 30 s every 3 min during the incubation. Induce phase separation by centrifugation ( $2000 \times g$ , 5 min, 4 °C). Transfer lower chloroform phase carefully to a small glass vial. This is acidic extract (A).
6. Check water drops floating on the chloroform phase in the tube and remove them by a pipette. Place the glass vials of both N and A on a heat block equipped with gas nozzles connected to an inert gas line (nitrogen or argon). Evaporate the solvent under a gentle stream of inert gas at 37 °C. Seal the tubes by screw caps. The tubes can be stored for several weeks at  $-20$  °C.

### 3.4 Nano-electrospray Ionization Mass Spectrometry

The TriVersa NanoMate is a robotic device which works with nano-ESI chips consisting of an array of 400 nano-ESI nozzles. It allows direct sample infusion into the mass spectrometer at extremely low flow rate (down to 20 nL/min). Therefore, the sample must be free of any particles or air bubbles which can cause clogging of the nozzles on the chip. Moreover, settings of the device should be optimized for each sample type to cope with the difference in viscosity and surface tension of the solvent. The optimal lipid concentration in samples depends on the sensitivity of the system and the content of the target lipid. In general, for highly sensitive new-generation mass spectrometers, further dilution of sample is often beneficial. Here, I describe our settings that are optimized for the analysis of major mitochondrial glycerophospholipid classes using TriVersa NanoMate and QTRAP 6500. Modifications for the detection of phosphatidylglycerolphosphate (PGP) and cytidine diphosphate diacylglycerol (CDP-DAG) are found in **Note 12**. For the assessment of lipids of the other classes (neutral lipids, sphingolipids, or sterols) using nano-infusion technique, please refer to the excellent protocol published recently [12].

1. Dissolve the lipid film, prepared in Subheading 3.2 or 3.3, in 100  $\mu\text{L}$  10 mM ammonium acetate in methanol. Vortex the vial vigorously for 20 s.
2. Treat the vial in an ultrasonic bath at room temperature for 5 min to dissolve the lipid completely and to remove air.

3. Take 10  $\mu\text{L}$  lipid sample to an Eppendorf-type tube. Add 70  $\mu\text{L}$  degassed 10 mM ammonium acetate in methanol.
4. Spin the tube to remove particles ( $12,000 \times g$ , 5 min,  $10^\circ\text{C}$ ).
5. Transfer 20  $\mu\text{L}$  supernatant carefully to two wells, one for CL analysis and the other for analysis of other phospholipids, in a clean 96-well plate. Seal the wells by sealing foil and set the plate into the TriVersa NanoMate.
6. The settings of TriVersa NanoMate are listed in Table 2. In our normal quantification workflow for all major mitochondrial glycerophospholipid classes, one sample is injected twice, once for separate analysis of CLs and once for all other glycerophospholipids. Each injection takes ca. 15 min (30 min per sample). For the analysis of lipid extracts from whole mammalian cells, neutral and acidic extracts are analyzed separately.
7. To analyze high molecular weight CL species ( $>1250$  Da) and other glycerophospholipids simultaneously, the QTRAP 6500 is set to “high mass” mode. Pairing of the mass spectrometer

**Table 2**  
**Parameters of TriVersa NanoMate**

<b>Sample infusion volume</b>	12 $\mu\text{l}$
<b>Volume of air to aspirate after sample</b>	1 $\mu\text{l}$
<b>Air gap before chip</b>	Enabled
<b>Aspiration delay</b>	0 s
<b>Pre-piercing</b>	With Mandrel
<b>Spray sensing</b>	Enabled
<b>Temperature</b>	$12^\circ\text{C}$
<b>Gas pressure</b>	0.4 psi
<b>Ionization voltage</b>	1.15 kV
<b>Polarity</b>	Positive
<b>Vent headspace</b>	Enabled
<b>Pre-wetting</b>	1 $\times$
<b>Volume after delivery</b>	0.5 $\mu\text{l}$
<b>Contact closure delay</b>	1 s
<b>Volume timing delay</b>	0 s
<b>Aspiration depth</b>	1 mm
<b>Pre-piercing depth</b>	9 mm
<b>Output contact closure</b>	Rel 1, 2.5 s duration

and the infusion device is established according to the manufacturer's instructions. Scan settings of the QTRAP 6500 for each glycerophospholipid classes are listed in Table 3 (except CL) and Table 4 (CL).

### 3.4.1 Data Processing

Practical workflow for the processing of mass spectra and quantification of lipid species will be very divergent depending on the software integrated in the mass spectrometer used. In general, to obtain the amount of a lipid species, its peak intensity is normalized to the intensity of the peak of the internal standard (with known amount). However, simple quantification by this procedure is often inaccurate because of (1) mass-dependent response difference between lipid species even within a single lipid class and (2) isotope overlaps, including product overlap (especially in CL).

**Table 3**  
**Setting of QTRAP 6500 (for glycerophospholipids other than CL)**

Common parameters												
<b>Mode</b>	High mass	<b>EP</b>	10	<b>Scan rate</b>	200 Da/s	<b>Sync</b>	LC sync					
<b>CUR</b>	20	<b>Step size</b>	0.1 Da	<b>Pause</b>	5 ms	<b>Resolution</b>	Unit					
<b>CAD</b>	Mid	<b>Settling time</b>	0 ms	<b>CEM</b>	2000	<b>Scan mode</b>	Profile					
<b>IHT</b>	90											
Lipid class	Polarity	Ion format	Scan type	Q3 m/z	Q1 scan range (mammalian)		Q1 scan range (Yeast)		DP	CE	CXP	Cycles
					Start	Stop	Start	Stop				
PC	Positive	[M + H] <sup>+</sup>	Prec	184	670	870	618	818	100	50	35	100
PE	Positive	[M + H] <sup>+</sup>	NL	141	660	860	576	776	100	25	35	100
PI	Positive	[M + NH <sub>4</sub> ] <sup>+</sup>	NL	277	780	980	712	912	30	30	35	100
PS	Positive	[M + H] <sup>+</sup>	NL	185	675	875	620	820	100	20	35	100
PA	Positive	[M + NH <sub>4</sub> ] <sup>+</sup>	NL	115	620	820	550	750	60	25	35	100
PG	Positive	[M + NH <sub>4</sub> ] <sup>+</sup>	NL	189	690	890	624	824	100	30	35	100
CDPDAG	Positive	[M + NH <sub>4</sub> ] <sup>+</sup>	NL	403			860	1060	60	40	35	200
PGP	Positive	[M + NH <sub>4</sub> ] <sup>+</sup>	NL	269			704	904	100	25	15	200

**Table 4**  
**Setting of QTRAP6500 (for CL)**

Common parameters							
Mode	High mass	EP	10	Scan rate	200 Da/s	Sync	LC sync
CUR	20	Step size	0.1 Da	Pause	5 ms	Resolution	Unit
CAD	Mid	Settling time	0 ms	CEM	2000	Scan mode	Profile
IHT	90	CXP	7	DP	140	Cycles	100
Q1 scan range [M + NH <sub>4</sub> ] <sup>+</sup>							
Scan type	Q3 m/z (Da)	[DAG- H <sub>2</sub> O+H] <sup>+</sup>	Start	Stop	CE	IS	
Prec	465.4	26:1	1150	1350	40		
Prec	467.4	26:0	1150	1350	40		
Prec	491.4	28:2	1230	1280	40	*	
Prec	493.4	28:1	1200	1400	40		
Prec	495.4	28:0	1200	1400	40		
Prec	505.5	29:2	1230	1280	40	*	
Prec	519.5	30:2	1250	1400	40		
Prec	521.5	30:1	1250	1400	40		
Prec	523.5	30:0	1250	1400	40	*	
Prec	535.5	31:1	1300	1350	40	*	
Prec	547.5	32:2	1250	1450	40		
Prec	549.5	32:1	1250	1450	40		
Prec	551.5	32:0	1300	1450	40		
Prec	573.5	34:3	1350	1500	45		
Prec	575.5	34:2	1300	1500	45		
Prec	577.5	34:1	1300	1500	45		
Prec	579.5	34:0	1350	1500	45		
Prec	601.5	36:3	1380	1530	50		
Prec	603.5	36:2	1330	1600	50	*	
Prec	605.5	36:1	1330	1530	50		
Prec	607.5	36:0	1380	1530	50		
Prec	631.5	38:2	1650	1700	50	*	
Prec	715.5	44:2	1550	1600	50	*	
Prec	771.5	48:2	1650	1700	50	*	

\*These scans detect internal standards

Below I explain how to correct for these two most common problems.

1. The ionization efficiency and thus the ion yield (ion counts) of a molecule decreases with increasing molecular weight of the molecule in a mass spectrometer (so-called mass dependency) [18]. In general, peaks from lipids with high molecular weight appear less intense than those from lipids with low molecular weight, resulting in underestimation of lipid species carrying longer acyl chains. This effect is severe in high mass range (>1250 Da), practically at the range of CLs (*see* Fig. 2 as an example). The LipidView software package (version 1.2, SCIEX) offers a database of a wide variety of lipid species with “correction factors” that can be used for correction of the mass-dependent response differences. If lipid spectra are processed in LipidView by using a “target method” with the correction factors provided by the software, corrected intensities of individual lipids are obtained in “Advanced Data View” by one mouse click (*see* Note 13). However, this (semi-)automatic correction of response difference by LipidView 1.2 is not compatible with our new method for the detection and quantification of the various CL species. We obtain correction factors by drawing a response curve from the analysis of nonnatural CLs in “CL mix I” from Avanti Polar Lipids (Fig. 2). Using the response curve, correction factors for each CL species are calculated according to their molecular weight and used to normalize the response differences among CLs.

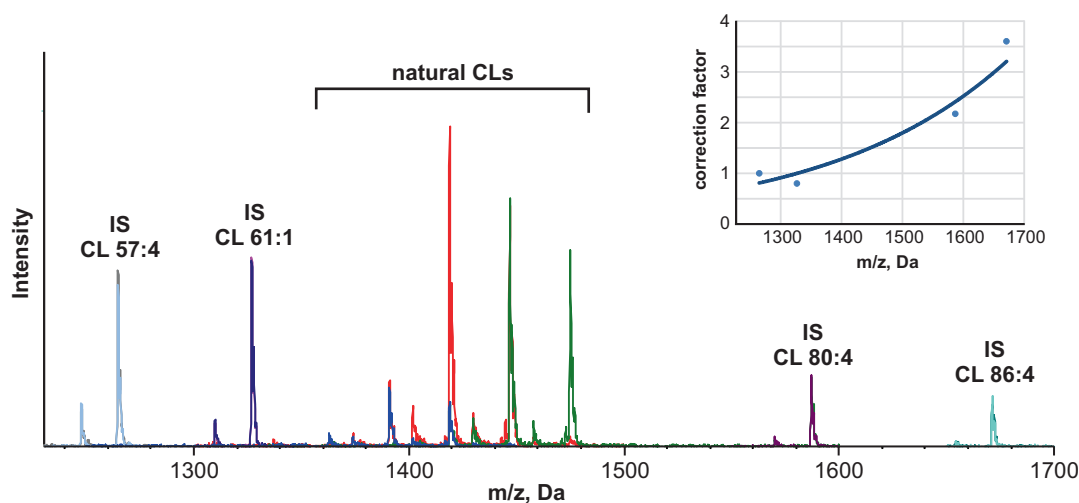


**Fig. 2** Typical spectrum from Prec analysis of CL in isolated mitochondria from wild-type yeast cells. Identical amounts of four ISs (50 pmol) appear as peaks with different heights. Intensities of these peaks are normalized to the intensity of CL 57:4 and plotted according to their  $m/z$  (inlet)

2. Due to the existence of natural isotopes, in the case of organic compounds particularly due to heavy carbon atoms ( $C^{13}$ ), a characteristic isotope pattern can be observed in mass spectra of lipids (*see* Fig. 3c as an example). The proportion of a lipid molecule containing heavy carbon atom(s) increases proportionally to the number of C atoms in the lipid. Often, considerable proportion of the [M+2] isotope (containing two  $C^{13}$  atoms in most cases) are detected when the lipid carries long acyl chains. The problem is that such ions are isobaric with the lipid species carrying one double bond less in an acyl chain (e.g., [M+2] of CL 68:4 is isobaric to monoisotopic CL 68:3; *see* Fig. 3a, b). This overlap (so-called precursor overlap) should be corrected. This is especially necessary if lipid species with saturated or monounsaturated fatty acyl chains, which are often less abundant, have to be accurately quantified. In the case of neutral loss (NL) or of the precursor ion scan (Prec) by a small fragment ion (e.g., Prec  $m/z$  184 for PC), isotopes of product ion do not need to be taken into account, since these lost moiety or small product ions contain only a small number of C atoms. In contrast, the isotope overlap of the product ion (so-called product overlap) should also be corrected in the case of our new CL detection procedure, because CLs are scanned by Prec of large DAG fragments containing many C atoms. Figure 3 illustrates the correction of isotope overlaps in a set of CL species as an example. The  $[M+NH_4]^+$  ion of CL 68:4 (34:2/34:2, monoisotopic  $m/z$  1419 Da) generates a DAG- $H_2O+H$  fragment  $m/z$  575.5 Da upon CID (Fig. 3a). By Prec 575.5 scan, a typical isotope pattern of CL 68:4 is seen (Fig. 3c, left panel). The signal of the [M+2] isotope overlaps with the signal of monoisotopic CL 68:3 (34:2/34:1,  $m/z$  1421 Da). Moreover, a fraction of CL 68:4 (34:2/34:2) generates a fragment  $m/z$  577.5 when two heavy carbon atoms exist in the product ion (DAG fragment) that is detected as a peak at 1421 by Prec 577.5. This overlaps with the signal of monoisotopic CL 68:3 (34:1/34:2). These overlaps need to be subtracted to obtain a correct amount of CL 68:3 (34:2/34:1) (Fig. 3c, right panel).
3. The LipidView software is able to calculate isotope overlaps and provide corrected intensities automatically when the “deisotope” function is activated in the processing methods. As mentioned above, this automatic correction of isotope overlap is not compatible with our new CL detection method in the current version of LipidView. We calculated theoretical occurrences of [M+2] isotopes in both precursors and products (for very abundant species, [M+4] isotopes are also considered) according to previous publications [14, 19] and integrated them into a Microsoft Excel spreadsheet which we used for the correction of isotope overlaps.

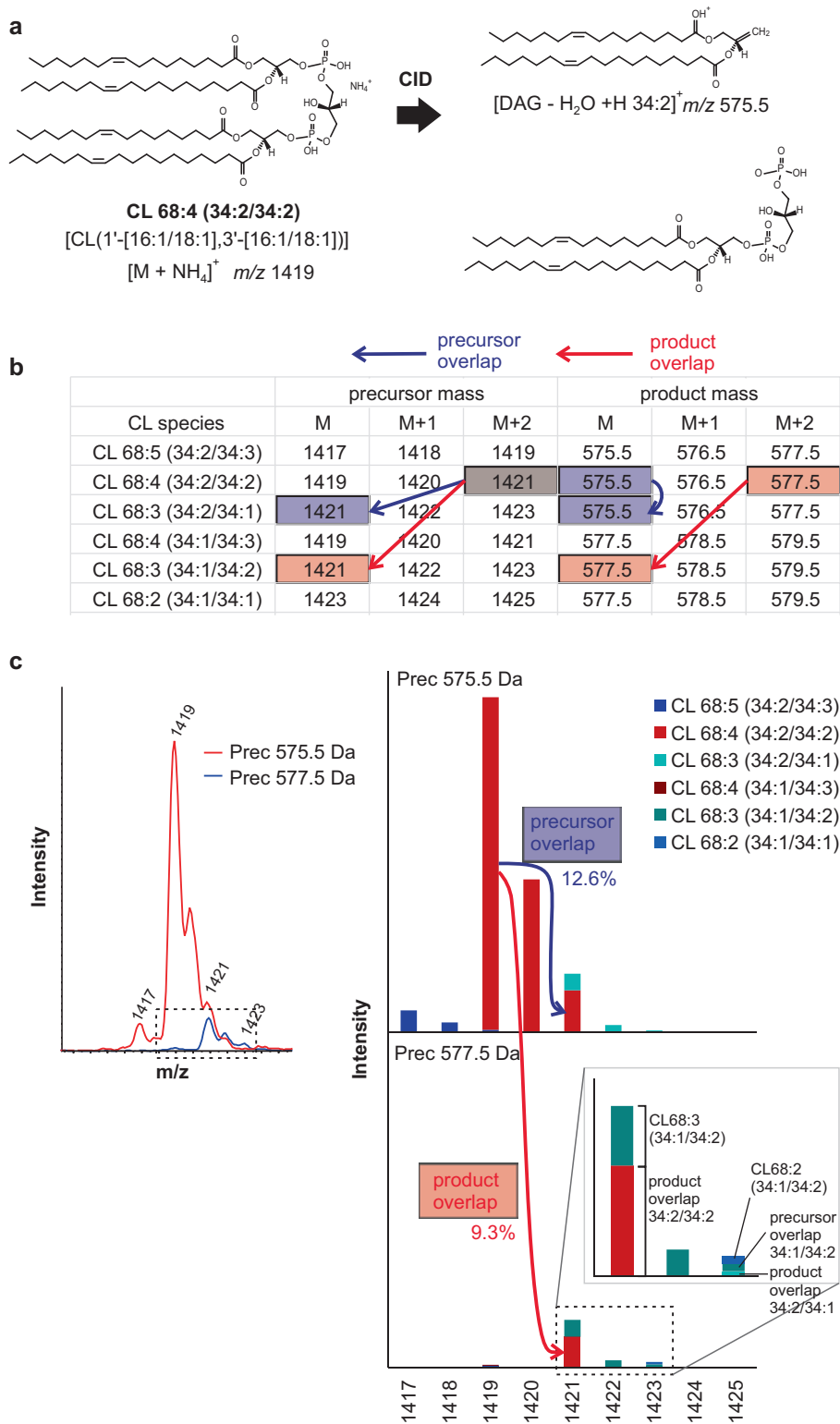


**Fig. 3** Example of correction of isotope overlap. **(a)** Collision-induced dissociation (CID) of a CL (CL 68:4 [34:2/34:2]). **(b)** Masses of CL species and their isotopes seen in Fig. 3c. Mass of [M+2] isotope of CL 68:4 [34:2/34:2] and its overlap with CL 68:3 are highlighted. **(c)** Typical isotope overlap in CL analysis. *Left panel:*

### 3.4.2 Evaluation of Data

Usually, normalized and corrected amounts of glycerophospholipid classes are represented as percentage of the total glycerophospholipid amount in the sample [11] (Fig. 4). The distribution of acyl-chain subspecies within a lipid class is also represented as percentage. The amount of a lipid species can also be represented as an absolute value that is normalized to the amount of sample used for extraction; however, in this case quantitative accuracy will be affected by the recovery during lipid extraction and by the accuracy of the quantification of the sample amount (protein content or cell number).

After obtaining final results from lipid analysis of isolated mitochondria, PS content should be checked first. Because mitochondria harbor PS decarboxylase (PSD) that converts PS to PE efficiently, their PS content is usually very low (around 2% of total glycerophospholipids). In contrast, all other membrane compartments contain much more PS (Fig. 4). Thus, if the amount of PS detected in the mitochondria prep is higher than ~4% of the total glycerophospholipid content, a contamination of the prep by considerable amount of membranes from other cell organelles is very likely. When multiple samples are analyzed simultaneously to see an effect of, for example, a specific treatment, purity of mitochondria among samples should be comparable. If counter-correlations between PS and CL content are observed, it is possible that there is a variation in purity of mitochondria among samples. In this case, contamination of microsomal membrane by immunodetection of an abundant ER-resident protein (in our laboratory Sec61 in yeast or PDI in mammalian cells are analyzed routinely; *see* Fig. 1b) should be checked first. If variation in microsomal contamination is evident, isolation of mitochondria should be done again (*see* Note 14).

---

## 4 Notes

1. Any enzyme which digests  $\beta$ -glucan in the cell wall of yeast can be used, but the specific activity as well as the purity of the enzyme is critical. Different batches of the enzyme from the same source can have different activities. The activity for the lysis of yeast cells shall be determined by a titration experiment

---

**Fig. 3** (continued) representative CL spectra of a lipid extract from mitochondria from HEK293 cells by Prec 575.5 (corresponding to DAG-OH 34:2) and that by Prec 577.5 (corresponding to DAG-OH 34:1) are overlaid. *Right panel:* isotope precursor (*upper panel*) and product (*lower panel*) overlaps. M+2 isotopes of CL 68:5 (34:2/34:3), CL68:4 (34:2/34:2), and CL68:3 (34:2/34:1) overlap with monoisotopic CL 68:4 (34:1/34:3), CL68:3 (34:1/34:2), and CL68:2 (34:1/34:1), respectively. For clarity, [M+3] and [M+4] isotopes as well as other overlaps are not depicted

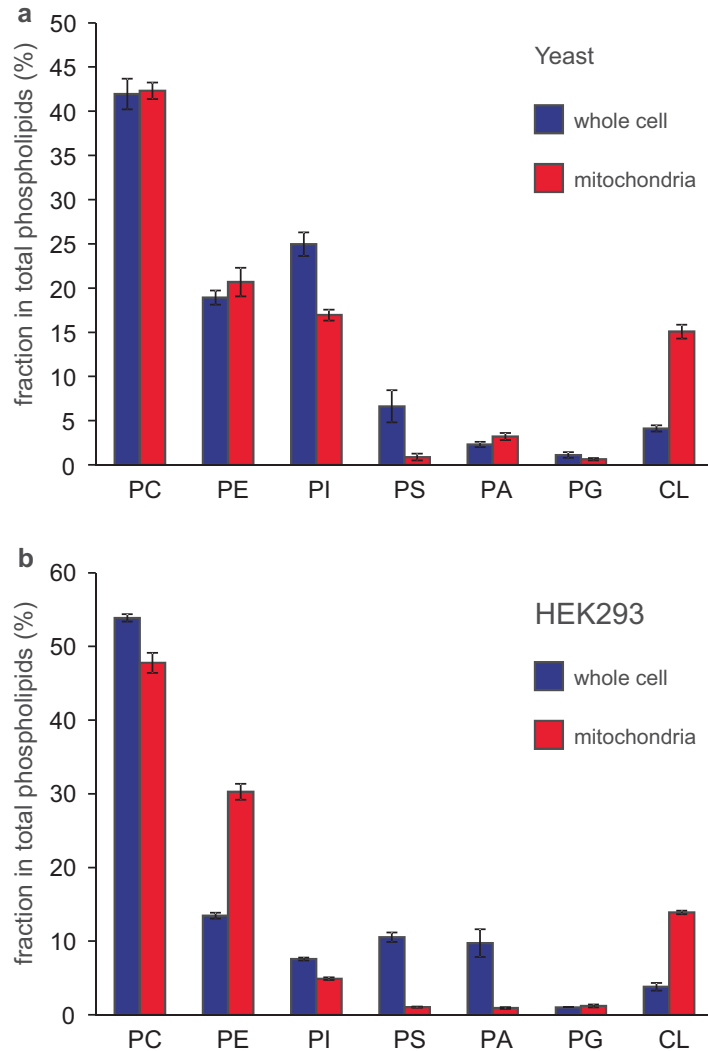


**Fig. 4** Typical representation of the glycerophospholipid composition in whole cell and isolated mitochondria of wild-type yeast cells grown in YP-gal (a) and of HEK 293 cells grown in standard culture conditions (DMEM high glucose GlutaMax, supplemented with 10% FCS and 100  $\mu\text{g}/\text{ml}$  of each sodium pyruvate and nonessential amino acids) (b). Data represents the mean of three biological replicates with SEM

when batch of the enzyme is changed. We are currently using lyticase from *Arthrobacter luteus* (Sigma L2524).

2. We are using Optima L-80 XP ultracentrifuge with SW-41Ti rotor and thinwall Ultra-Clear™, 13.2 mL tubes, all from Beckman Coulter.
3. In the homogenizer, optimal spacing between glass cylinder and plunger is critical to avoid disruption of nucleus that causes

undesirable release of nuclear DNA and contamination of the mitochondrial fraction by nuclear membranes. For homogenization of yeast spheroplasts, we are currently using the hand homogenizer from Sartorius. We ordered several sets of borosilicate glass cylinder and glass plunger (with “S” clearance) and chose a set having appropriate clearance (ca. 0.03 mm) by comparing the yield and the intactness of isolated mitochondria. The best set brings high yield and the majority of isolated mitochondria remain intact. The intactness of mitochondria can be verified by checking the protection of a protease-sensitive protein residing at the intermembrane space (e.g., Yme1) against externally added protease. For homogenization of mammalian cells, we utilize motor-driven homogenizer (Potter S from Sartorius) with 5 ml cylinder and plunger made of PTFE.

4. HEK293 cells bring the best yield and purity of mitochondria by this procedure, but from other cell types (mouse embryonic fibroblast (MEF), HeLa cells, primary immortalized fibroblast), mitochondria have successfully been isolated in our hands, although the yield is lower.
5. The best way to check the cleanness of the material used is running whole lipid extraction and the MS procedure without biological sample (blank run). If undesired peaks overlapping with the peaks of target lipids appear in MS scan, the source of contamination should be identified. It is highly recommended to routinely do blank runs.
6. Although tubes and tips made of plastic should be avoided, some high-quality tubes and tips (e.g., Eppendorf Safe-Lock tubes and e.p.TIPS from Eppendorf, ART tips from Thermo Fisher Scientific) do not cause problems when prolonged contact with chloroform is avoided.
7. We are currently using the following materials specifically: chloroform (Roth 7331.2), methanol (Fisher A456-1), water (Merck 1.15333.1000), 25% HCl (w/v, 7.75 N, VWR 20257.296), ammonium carbonate (Fluka 74,415), ammonium acetate (Fluka 73,594), twin.tec PCR plate skirted colorless (0030 128.648, Eppendorf), and Thermowell sealing tape (6570, Corning).
8. Cells can be grown in synthetic complete (SC) medium if necessary (e.g., to keep plasmids with auxotrophic markers). Please note that the concentration of *myo*-inositol in the media will affect the lipid profile in this case.
9. Keeping cells in log phase at least for four doubling times before harvesting is necessary. Once the OD600 becomes over 4.0 during the upscaling phase, start cultivation of cells from the overnight culture again.

10. The amount of mitochondria loaded on a gradient is critical for the proper sedimentation of mitochondria in a gradient. Overloading causes impurity of mitochondria. I recommend setting up multiple tubes when >10 mg crude mitochondrial fraction is obtained. When the amount of crude mitochondria is less than 10 mg, resuspend all in 2 ml buffer, and proceed to sedimentation centrifugation. However, we often observe low yield when less than 2 mg crude mitochondria are used.
11. MAM fraction can be isolated by collecting the low density fraction, diluting it with 5× volume of buffer A and harvesting by ultracentrifugation (1 h, 100,000 × *g*).
12. CDP-DAG and PGP are the intermediate lipid species which are produced during the synthesis of CL, and their accumulations in mitochondria are hallmarks of CL synthesis defect. They are highly water soluble and not efficiently dissolved into methanol from the lipid film after evaporation of solvent. Thus, we take 20 μL chloroform phase before the water-wash step in one-step lipid extraction protocol (**step 7** in Subheading 3.3.1), mix it with 40 μL 37.5 mM ammonium acetate in methanol/chloroform/water=1:1:0.05 (v/v/v), and inject it directly into the mass spectrometer. Because an IS for PGP is not available, the peak intensity from PG 17:0/14:1 is used for normalization.
13. The procedure to integrate correction factors into a “target method” has been described in Özbalci et al. [12].
14. There are many possible reasons for the impurity of mitochondria. The first thing that should be carefully controlled is the growth conditions. Try to avoid overgrowing or stress during the cultivation of cells. One annoying situation (which is unfortunately not rare) is that the experimental setting of interest imposes a change in the behavior of mitochondria during the sedimentation centrifugation. In this case, optimization of the gradient sedimentation step will be necessary to obtain pure mitochondria.

---

## Acknowledgments

I thank Shotaro Saita and Kavia Bakka for providing protocols and example results, Susanne Brodesser and Mari Aaltonen for critical reading of the manuscript, and Thomas Langer for continuous support. I also acknowledge S. B. and Matthias Haag for technical advices in lipidomics. This work is supported by a grant of the Deutsche Forschungsgemeinschaft (TA 1132/2-1).

## References

1. Ren M, Phoon CK, Schlame M (2014) Metabolism and function of mitochondrial cardiolipin. *Prog Lipid Res* 55:1–16. doi:[10.1016/j.plipres.2014.04.001](https://doi.org/10.1016/j.plipres.2014.04.001)
2. Scharwey M, Tatsuta T, Langer T (2013) Mitochondrial lipid transport at a glance. *J Cell Sci* 126(Pt 23):5317–5323. doi:[10.1242/jcs.134130](https://doi.org/10.1242/jcs.134130)
3. Horvath SE, Daum G (2013) Lipids of mitochondria. *Prog Lipid Res* 52(4):590–614. doi:[10.1016/j.plipres.2013.07.002](https://doi.org/10.1016/j.plipres.2013.07.002)
4. Frohman MA (2015) Role of mitochondrial lipids in guiding fission and fusion. *J Mol Med (Berl)* 93(3):263–269. doi:[10.1007/s00109-014-1237-z](https://doi.org/10.1007/s00109-014-1237-z)
5. Claypool SM, Koehler CM (2012) The complexity of cardiolipin in health and disease. *Trends Biochem Sci* 37(1):32–41. doi:[10.1016/j.tibs.2011.09.003](https://doi.org/10.1016/j.tibs.2011.09.003)
6. Richter-Dennerlein R, Korwitz A, Haag M, Tatsuta T, Dargazanli S, Baker M, Decker T, Lamkemeyer T, Rugarli EI, Langer T (2014) DNAJC19, a mitochondrial cochaperone associated with cardiomyopathy, forms a complex with prohibitins to regulate cardiolipin remodeling. *Cell Metab* 20(1):158–171. doi:[10.1016/j.cmet.2014.04.016](https://doi.org/10.1016/j.cmet.2014.04.016)
7. Monteiro JP, Oliveira PJ, Jurado AS (2013) Mitochondrial membrane lipid remodeling in pathophysiology: a new target for diet and therapeutic interventions. *Prog Lipid Res* 52(4):513–528. doi:[10.1016/j.plipres.2013.06.002](https://doi.org/10.1016/j.plipres.2013.06.002)
8. Shevchenko A, Simons K (2010) Lipidomics: coming to grips with lipid diversity. *Nat Rev Mol Cell Biol* 11(8):593–598. doi:[10.1038/nrm2934](https://doi.org/10.1038/nrm2934)
9. Wang M, Han X (2014) Multidimensional mass spectrometry-based shotgun lipidomics. *Methods Mol Biol* 1198:203–220. doi:[10.1007/978-1-4939-1258-2\\_13](https://doi.org/10.1007/978-1-4939-1258-2_13)
10. Almeida R, Pauling JK, Sokol E, Hannibal-Bach HK, Ejsing CS (2015) Comprehensive lipidome analysis by shotgun lipidomics on a hybrid quadrupole-orbitrap-linear ion trap mass spectrometer. *J Am Soc Mass Spectrom* 26(1):133–148. doi:[10.1007/s13361-014-1013-x](https://doi.org/10.1007/s13361-014-1013-x)
11. Shevchenko A, Surendranath V, Ejsing CS, Klemm RW, Simons K, Sampaio JL, Ekroos K, Duchoslav E (2009) Global analysis of the yeast lipidome by quantitative shotgun mass spectrometry. *Proc Natl Acad Sci U S A* 106(7):2136–2141. doi:[10.1073/pnas.0811700106](https://doi.org/10.1073/pnas.0811700106)
12. Ozbalci C, Sachsenheimer T, Brügger B (2013) Quantitative analysis of cellular lipids by nano-electrospray ionization mass spectrometry. *Methods Mol Biol* 1033:3–20. doi:[10.1007/978-1-62703-487-6\\_1](https://doi.org/10.1007/978-1-62703-487-6_1)
13. Brügger B (2014) Lipidomics: analysis of the lipid composition of cells and subcellular organelles by electrospray ionization mass spectrometry. *Annu Rev Biochem* 83:79–98. doi:[10.1146/annurev-biochem-060713-035324](https://doi.org/10.1146/annurev-biochem-060713-035324)
14. Scherer M, Schmitz G, Liebisch G (2010) Simultaneous quantification of cardiolipin, bis(monoacylglycerol)phosphate and their precursors by hydrophilic interaction LC-MS/MS including correction of isotopic overlap. *Anal Chem* 82(21):8794–8799. doi:[10.1021/ac1021826](https://doi.org/10.1021/ac1021826)
15. Vance JE (2014) MAM (mitochondria-associated membranes) in mammalian cells: lipids and beyond. *Biochim Biophys Acta* 1841(4):595–609. doi:[10.1016/j.bbali.2013.11.014](https://doi.org/10.1016/j.bbali.2013.11.014)
16. Bligh EG, Dyer WJ (1959) A rapid method of total lipid extraction and purification. *Can J Biochem Physiol* 37(8):911–917
17. Gray A, Olsson H, Batty IH, Priganica L, Peter Downes C (2003) Nonradioactive methods for the assay of phosphoinositide 3-kinases and phosphoinositide phosphatases and selective detection of signaling lipids in cell and tissue extracts. *Anal Biochem* 313(2):234–245
18. Koivusalo M, Haimi P, Heikinheimo L, Kostianen R, Somerharju P (2001) Quantitative determination of phospholipid compositions by ESI-MS: effects of acyl chain length, unsaturation, and lipid concentration on instrument response. *J Lipid Res* 42(4):663–672
19. Ejsing CS, Duchoslav E, Sampaio J, Simons K, Bonner R, Thiele C, Ekroos K, Shevchenko A (2006) Automated identification and quantification of glycerophospholipid molecular species by multiple precursor ion scanning. *Anal Chem* 78(17):6202–6214. doi:[10.1021/ac060545x](https://doi.org/10.1021/ac060545x)

## Detection of Cysteine Redox States in Mitochondrial Proteins in Intact Mammalian Cells

Markus Habich and Jan Riemer

### Abstract

Import, folding, and activity regulation of mitochondrial proteins are important for mitochondrial function. Cysteine residues play crucial roles in these processes as their thiol groups can undergo (reversible) oxidation reactions. For example, during import of many intermembrane space (IMS) proteins, cysteine oxidation drives protein folding and translocation over the outer membrane. Mature mitochondrial proteins can undergo changes in the redox state of specific cysteine residues, for example, as part of their enzymatic reaction cycle or as adaptations to changes of the local redox environment which might influence their activity. Here we describe methods to study changes in cysteine residue redox states in intact cells. These approaches allow to monitor oxidation-driven protein import as well as changes of cysteine redox states in mature proteins during oxidative stress or during the reaction cycle of thiol-dependent enzymes like oxidoreductases.

**Key words** Cysteine, Intermembrane space (IMS), Mia40, Oxidative folding, Redox state, Thiol modification

---

### 1 Introduction

Of the 20 proteinaceous amino acids, cysteines are least abundant in proteins [1]. However, when present, cysteines are often conserved and fulfill important functions, for example, in active centers of enzymes (e.g., aldehyde dehydrogenases [2, 3], thiolases [4–6], and oxidoreductases [7, 8]), during the (oxidative) folding of proteins and the formation of multiprotein complexes [9, 10], and in the regulation of enzyme activities, localizations, and stabilities (*for review, see* [11]) [12–14] (Fig. 1a). The functionality of a cysteine residue is based on its thiol group which, in its deprotonated thiolate form, exhibits high reactivity toward electrophilic groups and can thereby undergo various modifications (Fig. 1b). These modifications include the oxidation of thiol groups to the oxygen-containing species sulfenic, sulfinic, and sulfonic acid, but also the formation of disulfide-linked forms like glutathionylated cysteine residues. Moreover, cysteine residues can become nitrosylated [15].

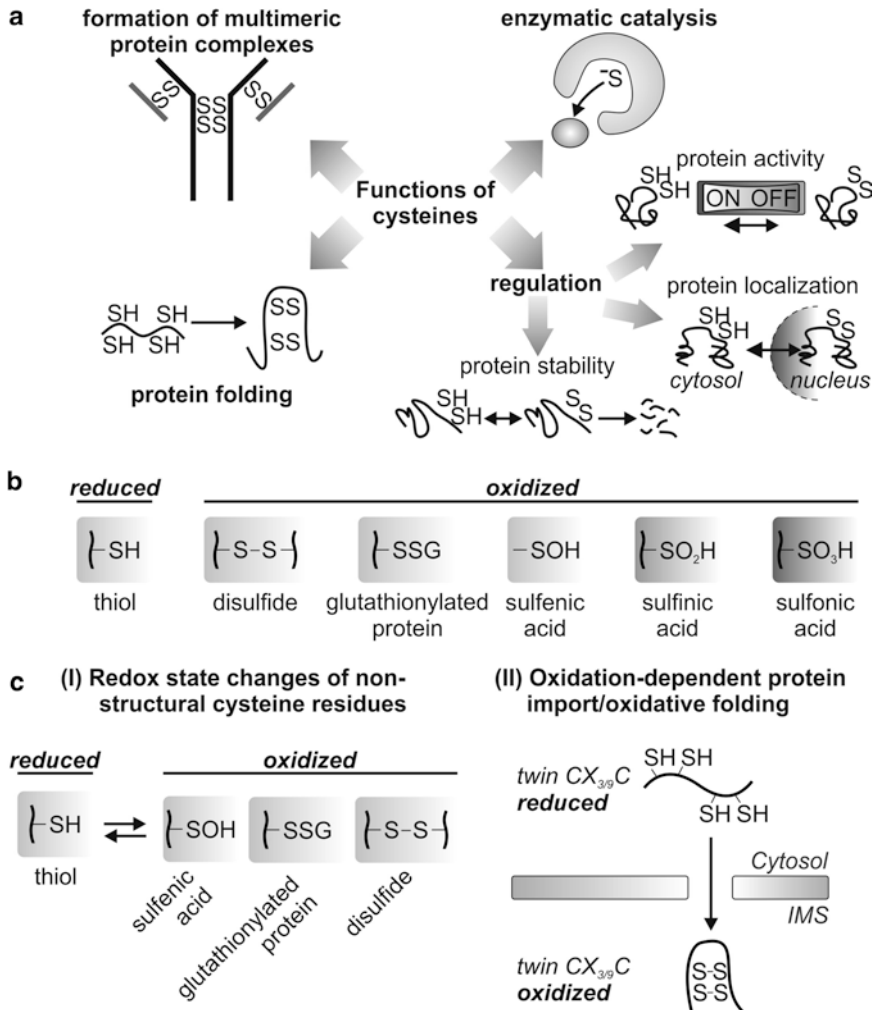


**Fig. 1** Functions and different forms of cysteines in intact cells. **(a)** Cysteines fulfill numerous functions in proteins. Cysteines are important for the formation of disulfide-linked multiprotein complexes as in immunoglobulins (Ig) in which disulfide bonds connect individual Ig chains [9]. In active centers of enzymes, cysteines often have essential functions in enzymatic catalysis such as in aldehyde dehydrogenases [2, 3] or thiolases [4–6] in which the reactive cysteine was found to covalently react with  $NADP^+$  or to form an acyl-thioester intermediate with the substrates, respectively. Also oxidoreductases such as DsbA and DsbB in the bacterial periplasm or Mia40 in the IMS functionally rely on reactive cysteines [7, 8]. Regulatory functions of cysteines can influence protein activity, localization, and stability. Protein activity can be influenced in a thiol switch manner as in the endoplasmic reticulum (ER)-sulfhydryl oxidase Ero1 which can be reversibly inactivated by disulfide bond formation between regulatory cysteines [14]. Influences on protein localization were, for example, reported for the cytosolic transcription factor Yap1 which translocates into the nucleus upon oxidation [12]. Protein stability can be regulated by cysteines as reported for Cdc25C—a protein which is involved in cell cycle progression and which was suggested to be degraded upon oxidation upon oxidative stress conditions [13]. In protein folding cysteines play important roles as disulfide bonds are essential for many ER, IMS, and periplasmic proteins to acquire their native fold [10]. **(b)** Cysteine modifications. Cysteines can be present in a reduced or oxidized state. In their reduced form cysteines are present as thiols. In their oxidized state, they can, for example, be present as intra- or intermolecular disulfide bonds, glutathionylated proteins,

In this chapter we will present approaches to analyze changes in cysteine redox states: (I) in the course of redox regulation and activity of mitochondrial enzymes (nonstructural disulfide bonds) and (II) during oxidation-dependent protein import into mitochondria (formation of structural disulfide bonds; Fig. 1c).

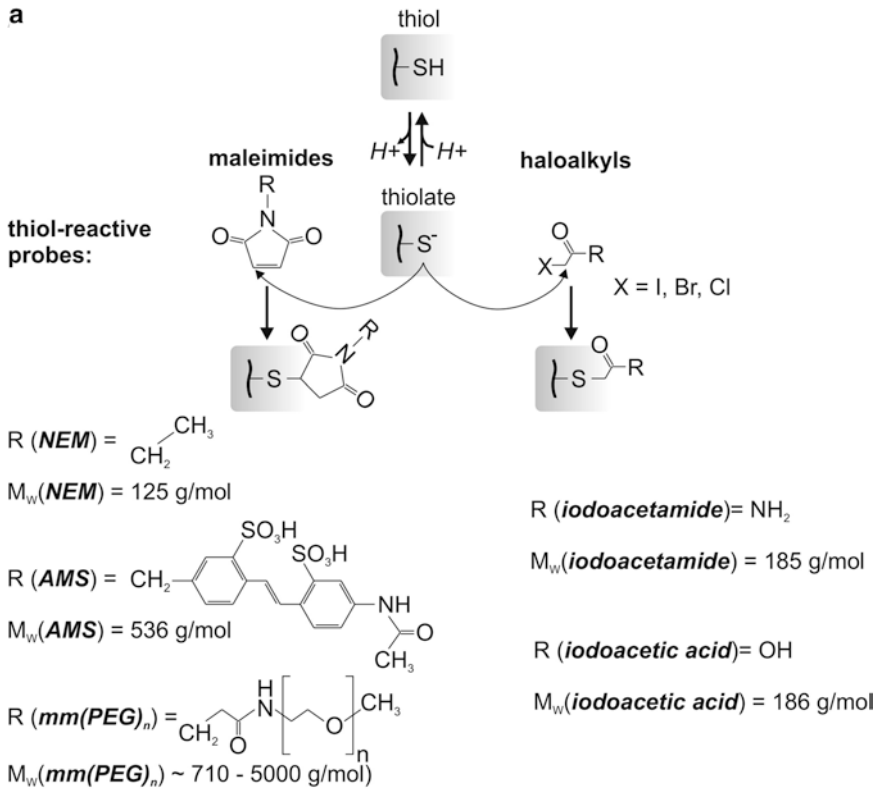
### 1.1 Redox State Changes of Nonstructural Cysteine Residues

Nonstructural cysteine residues in mitochondrial proteins can exhibit different redox states. For example, cysteine residues in oxidoreductases undergo reversible redox state changes during the catalytic cycles of the enzymes, or mitochondrial enzymes can be modulated in their activity by specific cysteine modifications (“thiol switch”; *for review, see [7]*).

For both oxidative folding and redox state changes in mature proteins, a tight control by multiple often redundant redox systems is required. During experimental analyses, these redox systems are often perturbed or destroyed (e.g., during cell lysis). Therefore, great care has to be taken to preserve the respective redox situation found in intact cells. To this end, two different approaches exist: rapid acidification (and lysis) of cells using, for example, trichloroacetic acid (TCA), and blockage of reduced thiols by the membrane-permeable thiol-reactive compound *N*-ethylmaleimide (NEM). With the former approach, otherwise reactive thiols are reversibly protonated and thus nucleophilic attacks on targets are prevented. NEM covalently modifies reduced thiols and thus likewise prevents further reactions. To subsequently identify the redox state of specific thiols, their reactivity in the thiolate state is used to modify them with thiol-reactive probes (Fig. 2a). There are several thiol-reactive probes which differ in the nature of their reactive group, but all have in common that they add a certain molecular mass to each free thiol of a protein. This additional mass leads to a slower migration in SDS-PAGE (i.e., a shift) compared to a non-modified protein (Fig. 2b). Among the thiol-reactive probes, the most commonly used are haloalkyls (iodoacetamide, iodoacetic acid) and maleimides (NEM, AMS, mm(PEG)<sub>n</sub>).

---

**Fig. 1** (continued) or oxygen-containing forms sulfenic, sulfinic, and sulfonic acid. **(c)** Redox state changes in mitochondrial proteins. **(I)** Redox state changes of nonstructural cysteine residues. Nonstructural cysteines can change their redox state reversibly from a reduced state to various oxidized species and vice versa. These changes occur during the catalytic cycle of mitochondrial enzymes or during the modulation of mitochondrial enzyme activity. **(II)** Oxidation-dependent protein import/oxidative folding. Many proteins of the IMS contain highly conserved cysteines (e.g., twin CX<sub>3/9</sub>C proteins). After their synthesis in the cytosol, they are present as reduced and unfolded precursors. During the import over the OM via the Mia40/ALR system, they become oxidized, thereby reaching their native fold containing stable disulfide bonds



**b** SHIFT ASSAY TO DETERMINE SUITABLE THIOL-REACTIVE PROBES

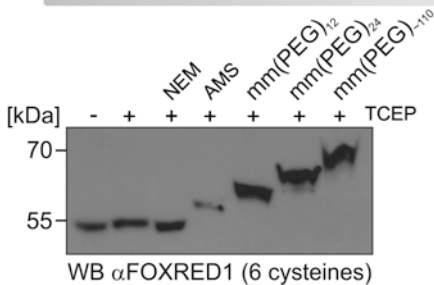


**Fig. 2** Approaches to monitor protein redox states. **(a)** Protein thiol modification. Maleimides and haloalkyls are the most commonly used thiol-reactive probes and differ in the length of their nonreactive rest (R) and thus in molecular weight (MW). After deprotonation of a thiol, the thiolate anion performs a nucleophilic attack on the thiol-reactive probe resulting in a thioether-linked product. **(b)** Shift assay to determine suitable thiol-reactive probe for the 6-cysteine-containing protein FOXRED1. The addition of thiol-reactive probes to a protein increases its mass which leads to a slower migration on SDS-PAGE compared to an unmodified protein (i.e., “shift”). Here, cellular proteins were precipitated using TCA and dissolved in Laemmli buffer in presence or absence of the reductant TCEP (–/+ TCEP). Samples were treated with the thiol-reactive probes NEM, AMS, mm(PEG)<sub>12</sub>, mm(PEG)<sub>24</sub>, and mm(PEG)<sub>110</sub> which are indicated to modify reduced thiols. Subsequently, the samples were analyzed by SDS-PAGE and immunoblotting. In TCEP-treated samples, all cysteines of the protein became reduced and modified by the thiol-reactive probes. Note the different shift heights obtained by different probes. For FOXRED1 mm(PEG)<sub>24</sub> was determined as a suitable thiol-reactive probe because it resulted in a high shift (compared to NEM, AMS, or mm(PEG)<sub>12</sub>) with a high signal intensity (compared to AMS) and normal migration behavior (compared to mm(PEG)<sub>110</sub>)

## 1.2 Oxidation-Dependent Protein Import/Oxidative Folding

Mitochondrial proteins become imported into mitochondria via different pathways. Many IMS proteins rely on an oxidation-dependent import pathway (e.g., twin CX<sub>3/9</sub>C proteins) [10, 16–19, 20]. These proteins contain conserved cysteines and are synthesized in the cytosol as reduced and unfolded precursors. During translocation over the outer membrane (OM) of mitochondria, they undergo thiol oxidation by the mitochondrial oxidoreductase Mia40 (Fig. 1c). They thereby acquire stable structural disulfide bonds. Defects in mitochondrial oxidation-dependent import can manifest in human disease like the Mohr–Tranebjaerg syndrome/deafness–dystonia syndrome where a cysteine of the twin CX<sub>3</sub>C protein Timm8a is mutated, leading to decreased mitochondrial Timm8a levels [21, 22].

The methods described in the following allow analyzing the redox state of mitochondrial proteins and dissecting mitochondrial translocation events in intact mammalian cells. First we describe the shift assay that allows to determine the optimal thiol-reactive probe for modifying the protein of interest. Then we describe two methods to analyze the redox states of cysteine residues in the protein of interest. Finally, we describe a method that allows to follow oxidative folding of Mia40/ALR substrates during their import into the IMS. This approach employs multiple sequential steps: a radioactive pulse-chase approach followed by thiol modification and immunoprecipitation (IP).

---

## 2 Materials

### 2.1 Cell Culture

1. HEK293 cells (*see Note 1*).
2. Complete medium: Dulbecco's modified Eagle medium (DMEM) with 4500 mg/L D-glucose, sodium bicarbonate, and L-glutamine (Sigma-Aldrich). Add 10 % (v/v) fetal calf serum (FCS, Sigma-Aldrich) and dilute a 100× penicillin/streptomycin stock solution (GE Healthcare) 1:100. Store at 4 °C. Prewarm to 37 °C before use.
3. Cell culture dishes: 100 mm, 35 mm dishes and 12-well plates.
4. CO<sub>2</sub> incubator set at 37 °C and 5 % CO<sub>2</sub>.
5. Laminar Flow Hood Class II.
6. Vacuum suction pump. For removal of medium using sterile glass Pasteur pipets.
7. Autoclaved glass Pasteur pipets.
8. Pipetboy: electrical pipetting aid to transfer liquids using serological pipettes.
9. Serological pipettes: sterile individually packed 2, 5, 10, and 25 ml pipettes (Sarstedt).

10. Phosphate-buffered saline (PBS): purchased as powder without  $Mg^{2+}$  and  $Ca^{2+}$  (Merck Millipore) and dissolved in double-distilled water. Sterilize by autoclaving before use in cell culture. Store at 4 °C. Prewarm to 37 °C before use.
11. Trypsin–EDTA: dilute a 10× Trypsin–EDTA stock solution (GE Healthcare) 1:10 with PBS. Store at 4 °C. Prewarm to 37 °C before use.
12. Poly-L-lysine: purchased as 0.01 % solution in water and sterile-filtered. Store at 4 °C.
13. Sterile 50 ml “Falcon” tube.
14. Trypan blue. Trypan blue is a cell stain which stains dead cells dark blue while live cells appear white. Solve trypan blue powder in PBS to a final concentration of 0.01 % (w/v). Store at RT.
15. Hemocytometer.
16. Inverse cell culture microscope.
17. Rubber policeman.

## 2.2 Shift Assay

1. One 12-well plate with HEK293 cells at 50 % confluency.
2. Phosphate-buffered saline (PBS): purchased as powder without  $Mg^{2+}$  and  $Ca^{2+}$  (Merck Millipore) and solved in double-distilled water. Store at 4 °C. Keep on ice during experiment.
3. Metal plate with the approximate dimensions of a 12-well plate.
4. 8 % (w/v) Trichloroacetic acid (TCA) in water. Store at 4 °C.
5. 5 % (w/v) TCA in water. Store at 4 °C.
6. Nonreducing 1× Laemmli buffer: 2 % (w/v) SDS, 60 mM Tris–HCl pH 6.8, 10 % (v/v) glycerol, 0.0025 % (w/v) bromophenol blue. Store at RT.
7. 1× Laemmli buffer + TCEP: 2 % (w/v) SDS, 60 mM Tris–HCl pH 6.8, 10 % (v/v) glycerol, 0.0025 % (w/v) bromophenol blue, 10 mM Tris(2-chlorethyl)phosphate (TCEP). Store at RT.
8. Thiol-reactive probes (*see Note 2*): stock solutions are prepared in DMSO (*see Note 3*). 250 mM mm(PEG)<sub>12</sub> (Thermo Fisher); 250 mM mm(PEG)<sub>24</sub> (Thermo Fisher); 150 mM mm(PEG)<sub>110</sub> (mPEG-MAL MW5000, Laysan Bio Inc.); 250 mM NEM (Sigma-Aldrich); 75 mM 4-acetamido-4'-maleimidylstilbene-2,2'-disulfonic acid (AMS; Molecular Probes). Thiol-reactive probes are not stable in solution and should be protected from light. Store as single-use aliquots at –20 °C.
9. 1 M Tris–HCl, pH 8. Store at 4 °C.
10. Tip sonifier (e.g., UP50H, Hielscher) (*see Note 4*).
11. Antibodies for Western blot detection of protein of interest (*see Note 5*).

### 2.3 Direct Redox State Determination

1. One 12-well plate with HEK293 cells at 50 % confluency.
2. PBS: purchased as powder without  $Mg^{2+}$  and  $Ca^{2+}$  (Merck Millipore) and dissolved in double-distilled water. Store at 4 °C. Keep on ice during experiment.
3. Metal plate with the approximate dimensions of a 12-well plate.
4. 8 % (w/v) TCA in water. Store at 4 °C.
5. 5 % (w/v) TCA in water. Store at 4 °C.
6. Thiol-reactive probe as determined in Subheading 3.2 Shift assay.
7. Nonreducing 1× Laemmli buffer: 2 % (w/v) SDS, 60 mM Tris-HCl pH 6.8, 10 % (v/v) glycerol, 0.0025 % (w/v) bromophenol blue. Store at RT.
8. 1× Laemmli buffer + TCEP: 2 % (w/v) SDS, 60 mM Tris-HCl pH 6.8, 10 % (v/v) glycerol, 0.0025 % (w/v) bromophenol blue, 10 mM TCEP. Store at RT.
9. 1 M Tris-HCl, pH 8. Store at 4 °C.
10. Antibodies for Western blot detection of protein of interest (*see Note 5*).

### 2.4 Inverse Redox State Determination

1. One 12-well plate with HEK293 cells at 50 % confluency.
2. PBS: purchased as powder without  $Mg^{2+}$  and  $Ca^{2+}$  (Merck Millipore) and dissolved in double-distilled water. Store at 4 °C. Keep on ice during experiment.
3. Metal plate with the approximate dimensions of a 12-well plate.
4. 500 mM diamide in water. Store at -20 °C.
5. PBS-diamide: 1 mM diamide in PBS. Use 500 mM stock of diamide and dilute it in PBS. Prepare freshly and store at 37 °C for experiment.
6. 9.8 M  $H_2O_2$  in water. Store at 4 °C.
7. PBS- $H_2O_2$ : 1 mM  $H_2O_2$  in PBS. Use 9.8 M stock of  $H_2O_2$  and dilute it in PBS. Prepare freshly and store at 37 °C for experiment.
8. 250 mM NEM in DMSO (*see Note 3*). Note that thiol-reactive probes are not stable in solution and should be protected from light. Store aliquots at -20 °C.
9. PBS-NEM: 20 mM NEM in PBS. Use 250 mM NEM stock and dilute it in PBS. Prepare freshly and store on ice for experiment.
10. 8 % (w/v) TCA in water. Store at 4 °C.
11. 5 % (w/v) TCA in water. Store at 4 °C.

12. Thiol-reactive probe as determined in Subheading 3.2 Shift assay.
13. Nonreducing 1× Laemmli buffer: 2 % (w/v) SDS, 60 mM Tris-HCl pH 6.8, 10 % (v/v) glycerol, 0.0025 % (w/v) bromophenol blue. Store at RT.
14. 1× Laemmli buffer + TCEP: 2 % (w/v) SDS, 60 mM Tris-HCl pH 6.8, 10 % (v/v) glycerol, 0.0025 % (w/v) bromophenol blue, 10 mM TCEP. Store at RT.
15. Antibodies for Western blot detection of protein of interest (*see Note 5*).

## 2.5 Oxidative Folding of Mitochondrial IMS Proteins

### 2.5.1 Radioactive Pulse Chase

1. Starve medium: DMEM with 4500 mg/L D-glucose and sodium bicarbonate, without L-methionine, without L-cysteine, and without L-glutamine (Sigma-Aldrich). Add 1 M HEPES-KOH pH 7.4 to a final concentration of 100 mM. Prewarm to 37 °C for experiment.
2. Pulse medium: use starve medium and add [<sup>35</sup>S]-L-methionine/[<sup>35</sup>S]-L-cysteine to a final concentration of 100 μCi/ml (*see Notes 6–8*). Prewarm to 37 °C for experiment.
3. 1 M HEPES-KOH pH 7.4. Sterile filter before use and store at 4 °C.
4. Chase medium: use DMEM with 4500 mg/D-glucose, sodium bicarbonate, and L-glutamine (Sigma-Aldrich) and add 10 mM L-methionine (prepare a 100 mM methionine stock solution in 50 ml medium; sterilize by filtration and add it to 400 ml medium). Add 1 M HEPES-KOH pH 7.4 to a final concentration of 100 mM (50 ml; *see Note 9*).
5. Metal plate with the approximate dimensions of a 12-well plate.
6. 8 % (w/v) TCA in water. Store at 4 °C.
7. 5 % (w/v) TCA in water. Store at 4 °C.
8. Vacuum suction pump (*see Note 10*).

### 2.5.2 Thiol Modification

1. Buffer A: 6 M urea, 0.2 M Tris-HCl pH 7.5, 10 mM EDTA, 2 % SDS. Store at RT. (*see Note 11*).
2. 20 mM Tris(2-chlorethyl)phosphate (TCEP) in water. Adjust pH 7 using 1 M pH-unadjusted Tris (*see Note 12*). Store aliquots at –20 °C.
3. Thiol-reactive probe as determined in Subheading 3.2 Shift assay.

### 2.5.3 Denaturing Immunoprecipitation

1. Protein A Sepharose beads: usually supplied as 50 % slurry. If purchased as lyophilized powder, activate the beads as described by the manufacturer. Aliquots of activated beads can be stored for several months at 4 °C.

2. Antibodies against the protein of interest which are suited for immunoprecipitation (IP; *see* **Notes 5** and **13**).
3. IP buffer: 30 mM Tris-HCl pH 8.1, 100 mM NaCl, 5 mM EDTA. Store at 4 °C.
4. IP buffer + Triton X-100: prepare a 20 % (v/v) solution of Triton X-100 in water, and use it to prepare a 1 % solution and a 2.5 % solution in IP buffer (*see* **Note 14**). Store at 4 °C.
5. Buffer A: 6 M urea, 0.2 M Tris-HCl pH 7.5, 10 mM EDTA, 2 % SDS. Store at RT (*see* **Note 11**).
6. 1× Laemmli buffer: 2 % (w/v) SDS, 60 mM Tris-HCl pH 6.8, 10 % (v/v) glycerol, 0.0025 % (w/v) bromophenol blue (*see* **Note 15**). Store at RT.

## 2.6 Translocation of Mitochondrial Proteins

### 2.6.1 Radioactive Pulse Chase

1. Starve medium: DMEM with 4500 mg/L D-glucose and sodium bicarbonate, without L-methionine, without L-cysteine, and without L-glutamine (Sigma-Aldrich). Add 1 M HEPES-KOH pH 7.4 to a final concentration of 100 mM. Prewarm to 37 °C for experiment.
2. Pulse medium: use starve medium and add [<sup>35</sup>S]-L-methionine/ [<sup>35</sup>S]-L-cysteine to a final concentration of 100 μCi/ml (*see* **Notes 6–8**). Prewarm to 37 °C for experiment.
3. 1 M HEPES-KOH pH 7.4. Sterile filter before use and store at 4 °C.
4. Chase medium: use DMEM with 4500 mg/D-glucose, sodium bicarbonate, and L-glutamine (Sigma-Aldrich) and add 10 mM L-methionine (prepare a 100 mM methionine solution in 50 ml medium; sterilize by filtration and add to 400 ml medium). Add 1 M HEPES-KOH pH 7.4 to a final concentration of 100 mM (50 ml; *see* **Note 16**).
5. Metal plate with the approximate dimensions of a 12-well plate.
6. Vacuum suction pump (*see* **Note 10**).

### 2.6.2 Cell Fractionation

1. Metal plate with the approximate dimensions of a 12-well plate.
2. Fractionation buffer: 20 mM HEPES-KOH pH 7.4, 250 mM Sucrose, 50 mM KCl, 2.5 mM MgCl<sub>2</sub>, 1 mM DTT. Prepare freshly and store on ice for experiment.
3. Digitonin: prepare a 2 % (w/v) stock solution in water (*see* **Note 17**). Store aliquots at -20 °C.
4. Fractionation buffer + 0.005 % digitonin: add 2 % digitonin stock to fractionation buffer to a final digitonin concentration of 0.005 %. Prepare freshly and store on ice for experiment.
5. TCA: prepare a 50 % (w/v) solution in water. Store at 4 °C.

### 2.6.3 Denaturing Immunoprecipitation

1. Protein A Sepharose beads: usually supplied as 50 % slurry. If purchased as lyophilized powder, activate the beads as described by the manufacturer. Aliquots of activated beads can be stored for several months at 4 °C.
2. Antibodies against the protein of interest which are suited for immunoprecipitation (IP; *see* **Notes 5** and **13**).
3. IP buffer: 30 mM Tris-HCl pH 8.1, 100 mM NaCl, 5 mM EDTA. Store at 4 °C.
4. IP buffer + Triton X-100: prepare a 20 % (v/v) solution of Triton X-100 in water, and use it to prepare a 1 % solution and a 2.5 % solution in IP buffer (*see* **Note 14**). Store at 4 °C.
5. Buffer A: 6 M urea, 0.2 M Tris-HCl pH 7.5, 10 mM EDTA, 2 % SDS. Store at RT (*see* **Note 5**).
6. 1× Laemmli buffer: 2 % (w/v) SDS, 60 mM Tris-HCl pH 6.8, 10 % (v/v) glycerol, 0.0025 % (w/v) bromophenol blue (*see* **Note 15**). Store at RT.

---

## 3 Methods

### 3.1 Cell Culture

In our lab we routinely use HEK293 cells for redox experiments. Their fast growth and ease of cultivation make them a good model to study fundamental biochemical questions in human cells. We culture HEK293 cells in high glucose medium supplemented with 10 % fetal calf serum and a penicillin/streptomycin antibiotic mix. For passaging purposes we use 100 mm cell culture dishes and dilute them when they reach a confluency of circa 90 % into a fresh 100 mm dish. For experiments we use 12-well plates or 35 mm dishes which we coat with poly-L-lysine to ensure that cells adhere tightly to the dish surface.

Our cultivation protocol is as follows:

1. Cultivate HEK293 on 100 mm cell culture dishes in 10 ml complete medium in an incubator at 37 °C and 5 % CO<sub>2</sub> until they reach a confluency of 90 %.
2. Transfer the dish and all the necessary material into a laminar flow hood (*see* **Note 18**).
3. Remove the medium with the vacuum suction pump.
4. Rinse the cells with 10 ml PBS by carefully releasing the PBS from a serological pipette at the edge of the dish.
5. Remove PBS and add 1 ml Trypsin-EDTA dropwise onto the cells.
6. Incubate the dish 5 min at 37 °C and 5 % CO<sub>2</sub> until cells detach from the dish. Check this by tilting the plate and flicking it with your hand.

7. Transfer the plate back into the laminar flow hood and add 9 ml complete medium.
8. Resuspend and singularize the cells by sucking the cell suspension into a 10 ml serological pipette and releasing it with the motor of the Pipetboy, while the pipette tip is pressed softly onto the dish bottom.
9. Transfer 1 ml cell suspension into a fresh 100 mm dish containing 9 ml fresh complete medium.
10. Move the dish with the diluted cell suspension in the shape of an “8” to distribute the cells on the plate.
11. Transfer the 10 cm dish into the incubator and cultivate at 37 °C and 5 % CO<sub>2</sub>.
12. Observe cell growth under a microscope daily.

To seed cells for experiments onto 12-well plates or 35 mm dishes proceed as follows:

1. Coat 35 mm dishes with 750 µl poly-L-lysine (500 µl per well of a 12-well plate) and incubate them for 10 min at RT.
2. Remove poly-L-lysine (can be reused) and let the dishes dry for 1 h at RT.
3. Wash coated dishes 2× with 1 ml PBS.
4. Use a 100 % confluent HEK293 10 cm dish and follow the cultivation protocol above beginning from **step 2** until **step 8** to obtain a cell suspension.
5. Transfer the cell suspension into a sterile 50 ml Falcon tube.
6. Transfer 50 µl cell suspension into a 1.5 ml tube. Add 50 µl trypan blue and mix by pipetting.
7. Pipet a few µl of the trypan blue-cell suspension into the counting chamber of a hemocytometer, and determine cell concentration using a microscope.
8. Dilute the cells in a fresh 50 ml Falcon tube and seed 250,000 cells in 2 ml (35 mm dish) or 100,000 cells in 1 ml (per well of 12-well dish) (*see Note 19*).
9. After 2 days continue with the experiment.

### 3.2 Shift Assay

Numerous thiol-reactive probes are available to examine the redox state of a protein (Fig. 2a). The main differences between different thiol-reactive probes are the lengths of the nonreactive part of the probe as well as the charge and hydrophobicity of this part. This leads to altered protein properties after modification and thus during sample processing. Due to these changes the modified proteins might show unexpected behavior in SDS-PAGE, Western blotting, and antibody detection (immunoblotting or immunoprecipitation (IP); *see Note 20*). Often, the use of high molecular mass probes

leads to large shifts but at the cost of signal intensity as the transfer efficiency from SDS-PAGE onto membranes decreases. Therefore, it is necessary to determine the best thiol-reactive probe for each individual protein. To examine which probe is best suited for the protein of interest, a shift assay is performed in which proteins are completely reduced, subsequently modified with various probes, and detected via immunoblotting (Fig. 2b).

1. For each sample, use one well of cells from a 12-well plate. For the method described here, seven wells are required: **untreated, unmodified, NEM-modified, AMS-modified, mm(PEG)<sub>12</sub>-modified, mm(PEG)<sub>24</sub>-modified, and mm(PEG)<sub>110</sub>-modified samples**. HEK293 cells should not exceed 50 % confluency at the day of the experiment (*see Note 21*).
2. Put the 12-well plate on an ice-cold metal plate—from now on work on ice until **step 12**.
3. Remove the growth medium and wash cells with 1 ml ice-cold PBS per well. To not detach the cells, let the PBS carefully flow from the edge into the well. Do so well per well.
4. After PBS was added to all wells, remove PBS from each well and add 500  $\mu$ l 8 % ice-cold TCA. Do this with all wells.
5. Scratch the cells off from the plate using a rubber policeman (*see Note 22*). Transfer the cells in 1.5 ml reaction tubes. Label the tubes with the seven sample names (see above).
6. Incubate the samples at  $-20$  °C for at least 1 h or overnight (*see Note 23*).
7. Thaw the samples at RT and precipitate denatured proteins at 4 °C for 15 min at  $13,000 \times g$ .
8. Remove the supernatant and add 900  $\mu$ l ice-cold 5 % TCA to each tube. Vortex briefly to wash the TCA pellet in the 5 % TCA.
9. Centrifuge the samples at 4 °C for 15 min at  $13,000 \times g$ .
10. Remove the supernatant and centrifuge the samples at 4 °C for 1 min at  $13,000 \times g$ .
11. Remove the remaining TCA completely (*see Note 24*).
12. From now on work at RT (*see Note 25*).
13. Add 30  $\mu$ l 1 $\times$  nonreducing Laemmli buffer to **untreated sample**.
14. Add 30  $\mu$ l 1 $\times$  Laemmli buffer + TCEP to **unmodified sample**.
15. Add 28.2  $\mu$ l 1 $\times$  Laemmli buffer + TCEP to **NEM-modified sample** (*see Note 26*).
16. Add 24  $\mu$ l 1 $\times$  Laemmli buffer + TCEP to **AMS-modified sample** (*see Note 26*).

17. Add 28.2  $\mu\text{l}$  1 $\times$  Laemmli buffer + TCEP to **mm(PEG)<sub>12</sub>-modified sample** (*see Note 26*).
18. Add 28.2  $\mu\text{l}$  1 $\times$  Laemmli buffer + TCEP to **mm(PEG)<sub>24</sub>-modified sample** (*see Note 26*).
19. Add 27  $\mu\text{l}$  1 $\times$  Laemmli buffer + TCEP to **mm(PEG)<sub>110</sub>-modified sample** (*see Note 26*).
20. Usually TCA-precipitated samples are still acidic at this step (i.e., yellow-colored Laemmli). Adjust pH by adding 1–2  $\mu\text{l}$  1 M Tris pH 8 stepwise until the sample becomes blue (*see Note 24*).
21. Sonicate all samples at RT with ten strokes using a tip sonifier to dissolve precipitated proteins (*see Notes 4, 27 and 28*).
22. Incubate samples for 15 min at 45 °C (*see Note 29*).
23. Incubate samples for 5 min at RT to cool down and add thiol-reactive probe to a final concentration of 15 mM, as described in the following steps.
24. **Untreated sample:** leave untreated.
25. **Unmodified sample:** leave untreated.
26. **NEM-modified sample:** add 1.8  $\mu\text{l}$  250 mM NEM (*see Note 26*).
27. **AMS-modified sample:** add 6  $\mu\text{l}$  75 mM AMS (*see Note 26*).
28. **mm(PEG)<sub>12</sub>-modified sample:** add 1.8  $\mu\text{l}$  250 mM mm (PEG)<sub>12</sub> (*see Note 26*).
29. **mm(PEG)<sub>24</sub>-modified sample:** add 1.8  $\mu\text{l}$  250 mM mm (PEG)<sub>24</sub> (*see Note 26*).
30. **mm(PEG)<sub>110</sub>-modified sample:** add 3  $\mu\text{l}$  150 mM mm (PEG)<sub>110</sub> (*see Note 26*).
31. Incubate all samples for 1 h at RT in the dark (*see Note 30*).
32. Analyze the samples by SDS-PAGE (*see Note 31*) and immunoblotting against the protein of interest. An example of such an experiment is shown in Fig. 2b.

### 3.3 Direct Redox State Determination

With this experiment the redox state of a protein can be determined at steady state in intact cells. It can be used to show that a protein is completely reduced, completely oxidized, and semi-oxidized or that the protein is present as populations of either redox state (*see Note 32*, Fig. 3a). In a direct redox state determination experiment, a thiol-reactive probe is used to modify reduced but not oxidized thiols (Fig. 3b). This adds molecular mass to the reduced cysteine residues of a protein which can be analyzed by SDS-PAGE and subsequent immunoblotting (Fig. 3c).

To determine the redox state of a protein, always take along reduced (maximum shift) and unmodified (no shift) control samples. In addition, in situ controls in which intact cells are incubated with cell-permeable reductants (e.g., 10 mM DTT) or oxidants

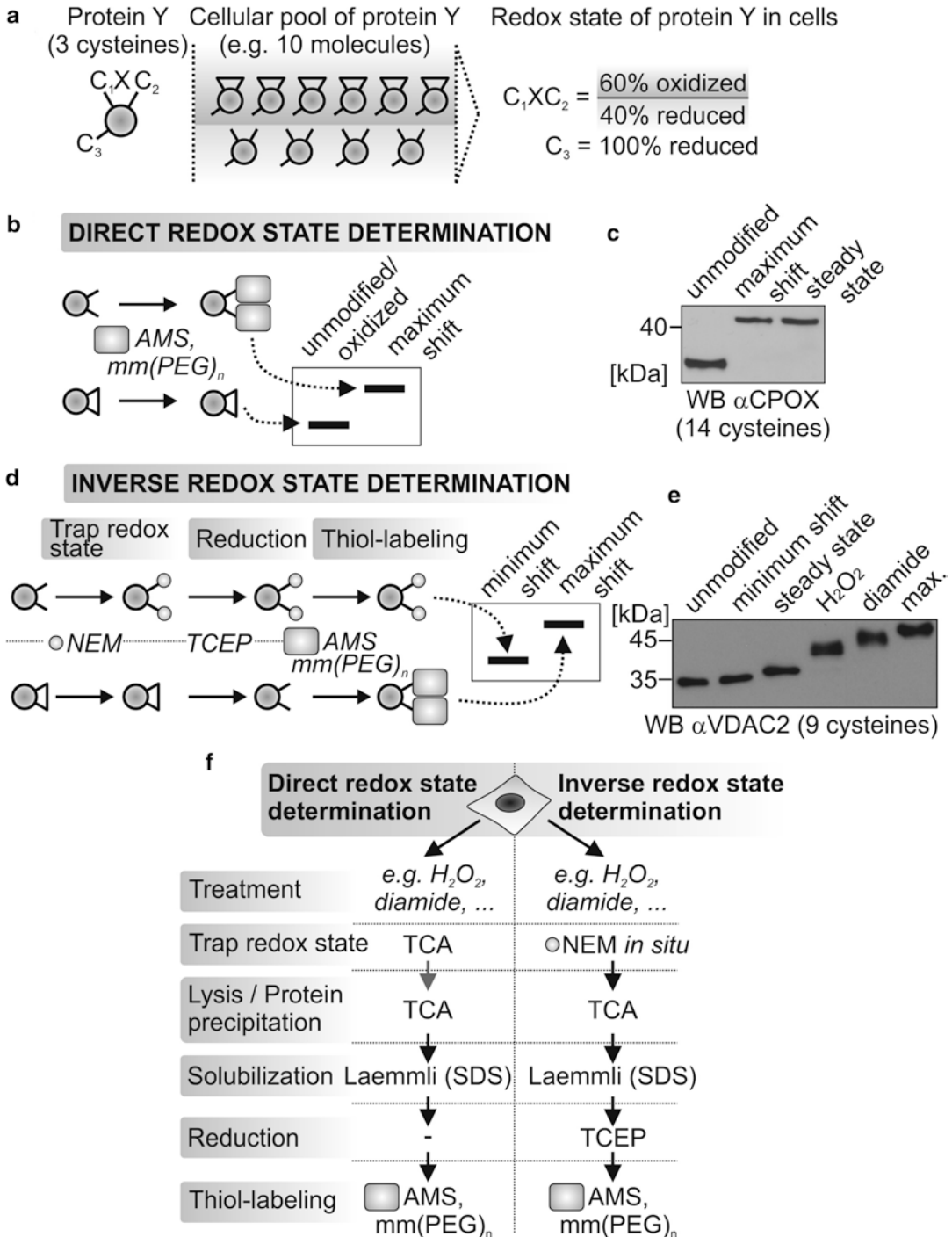


**Fig. 3** Determination of protein redox states at steady state in intact cells. (a) Example of a protein redox state. A protein redox state can be either fully reduced, i.e., all cysteines are reduced; fully oxidized, i.e., all cysteines are oxidized; or partially oxidized/reduced. An example for a partially oxidized redox state of an exemplary protein Y is shown. Protein Y contains the three cysteines C1, C2, and C3. C1 and C2 occur in a CXC motif (X=arbitrary amino acid). The cellular pool of protein Y consists of ten molecules where six out of ten molecules contain a disulfide bond between C1 and C2 (i.e., C1 and C2 are oxidized), while four are completely reduced.

(e.g., 1 mM diamide or 1 mM  $\text{H}_2\text{O}_2$ ) can be performed. Before performing a thiol modification experiment, the best thiol-reactive probe should be determined for the protein of interest in a shift assay as explained in Subheading 3.2.

1. For each sample, use one well of a 12-well plate. For the method described here, three wells are required: **unmodified**, **maximum shift**, and **steady-state samples**. HEK293 cells should not exceed 50 % confluency at the day of the experiment (*see Note 21*).

**Fig. 3** (continued) Thus the protein is to 60 % partially oxidized as 60 % of the C1XC2 motif is oxidized and 40 % reduced. C3 is reduced in all molecules. **(b)** Direct redox state determination. In a direct redox state determination, reduced thiols but not oxidized thiols become modified by thiol-reactive probes (AMS, mm(PEG)<sub>n</sub>, etc.). This additional mass leads to a slower migration in SDS-PAGE (i.e., a shift; see maximum shift) compared to an unmodified protein (see unmodified/oxidized). **(c)** Direct redox state determination for CPOX, a 14 cysteine-containing protein. Cellular proteins were precipitated using TCA and dissolved in Laemmli buffer in the presence (maximum shift) or absence (unmod, steady state) of the reductant TCEP. After protein solubilization the thiol-reactive probe AMS was added to modify reduced thiols (maximum shift, steady state). Subsequently, the samples were analyzed by SDS-PAGE and immunoblotting. The distance between the unmodified sample and the maximum shift sample shows the “highest” shift which can be obtained using the combination of this protein and this thiol-reactive probe. In the unmodified sample no cysteine was modified, while in the maximum shift sample 14 cysteines were modified with AMS. Since the protein signal in the steady-state sample migrates at the height of the maximum shift sample, it can be concluded that CPOX is completely reduced at steady state. Please note that the most suitable thiol-reactive probe should be determined for each protein individually, as explained in Subheading 3.2. **(d)** Inverse redox state determination. In comparison to a direct redox state determination, this experiment is based on the shift of formerly oxidized thiols and not of reduced thiols. First, reduced thiols of a protein are blocked with NEM after treatment of cells (e.g., with  $\text{H}_2\text{O}_2$ , diamide, etc.). After blocking all reduced thiols with NEM, oxidized thiols become reduced by the treatment with TCEP. The formerly oxidized thiols are modified by addition of a larger thiol-reactive probe such as mm(PEG)<sub>24</sub> leading to a slower migration on SDS-PAGE (*see* maximum shift) compared to reduced thiols which become modified with rather small NEM (*see* minimum shift). **(e)** Inverse redox state determination for VDAC2, a 9-cysteine-containing protein. HEK293 cells were treated for 5 min with 1 mM  $\text{H}_2\text{O}_2$  ( $\text{H}_2\text{O}_2$ ) and 1 mM diamide (diamide) or were left untreated. Afterward reduced thiols of steady-state sample,  $\text{H}_2\text{O}_2$  sample, and diamide sample were blocked with NEM and then subjected to TCA precipitation, while the other three were directly subjected to TCA precipitation without NEM treatment. Precipitated proteins were solubilized in Laemmli buffer in presence of the reductant TCEP. Thiol modification was performed using NEM (minimum shift) or mm(PEG)<sub>24</sub> (maximum shift, steady state,  $\text{H}_2\text{O}_2$ , diamide). Subsequently, the samples were analyzed by SDS-PAGE and immunoblotting. The steady-state sample reveals that the protein is partially oxidized at steady state. Treatment with the oxidants  $\text{H}_2\text{O}_2$  and diamide reveals that most but not all thiols are susceptible to oxidation. Please note that mm(PEG)<sub>24</sub> was previously found to be the most suitable thiol-reactive probe for VDAC2. The most suitable thiol-reactive probe should be determined for each protein individually, as explained in Subheading 3.2. **(f)** Experimental steps of a direct and inverse redox determination. In both experiments intact cells can be treated with chemicals such as oxidants ( $\text{H}_2\text{O}_2$ , diamide) or reductants (dithiothreitol, DTT, not shown) to observe their effect in intact cells. By trapping the redox state either with rapid acidification using TCA or blocking thiols using NEM, further disulfide exchange reactions are prevented. After protein precipitation using TCA and further solubilization in Laemmli buffer, formerly oxidized proteins are reduced by TCEP in an inverse redox determination (but not in a direct redox determination). Finally, reduced cysteines are modified with a thiol-reactive probe such as AMS, mm(PEG)<sub>n</sub>, etc

2. Put the 12-well plate on an ice-cold metal plate—from now on work on ice until **step 12**.
3. Remove the growth medium and wash cells with 1 ml ice-cold PBS per well. To not detach the cells, let the PBS carefully flow from the edge into the well. Do so well per well.
4. After PBS was added to all wells, remove PBS of each well and add 500  $\mu$ l 8 % ice-cold TCA. Do this with all wells.
5. Scratch the cells off from the plate using a rubber policeman (*see Note 22*). Transfer the cells in 1.5 ml reaction tubes. Label the tubes with the respective sample name.
6. Incubate the samples at  $-20\text{ }^{\circ}\text{C}$  for at least 1 hour or overnight (*see Note 23*).
7. Thaw the samples at RT and precipitate denatured proteins at  $4\text{ }^{\circ}\text{C}$  for 15 min at  $13,000 \times g$ .
8. Remove the supernatant and add 900  $\mu$ l ice-cold 5 % TCA. Vortex briefly to wash the TCA pellet in the 5 % TCA.
9. Centrifuge the samples at  $4\text{ }^{\circ}\text{C}$  for 15 min at  $13,000 \times g$ .
10. Remove the supernatant and centrifuge the samples at  $4\text{ }^{\circ}\text{C}$  for 1 min at  $13,000 \times g$ .
11. Remove the remaining TCA (*see Note 24*).
12. From now on work at RT (*see Note 25*).
13. Add 30  $\mu$ l nonreducing  $1\times$  Laemmli buffer to **unmodified sample**.
14. Add 28.2  $\mu$ l  $1\times$  Laemmli buffer + TCEP to **maximum shift sample** (*see Note 26*).
15. Add 28.2  $\mu$ l nonreducing  $1\times$  Laemmli buffer to **steady-state sample** (*see Note 26*).
16. Usually TCA-precipitated samples are still acidic at this step (i.e., yellow-colored Laemmli). Adjust pH by adding 1–2  $\mu$ l 1 M Tris pH 8 stepwise until the sample becomes blue (*see Note 24*).
17. Sonicate all samples at RT with ten strokes using a tip sonifier to dissolve precipitated proteins (*see Notes 4, 27, and 28*).
18. After dissolving the pellet incubate **Maximum shift sample** for 15 min at  $45\text{ }^{\circ}\text{C}$  (*see Note 29*). Keep the other samples at RT during this time.
19. Incubate samples for 5 min at RT to cool down and add thiol-reactive probe, as described in the following steps.
20. Add 1.8  $\mu$ l 250 mM mm(PEG)<sub>12</sub> (*see Note 26*) to **maximum shift** and **steady-state** samples and mix by pipetting. **Unmodified sample** remains as is.
21. Incubate all samples for 1 h at RT in the dark (*see Note 30*).

22. Analyze the samples by SDS-PAGE (*see* **Note 31**) and immunoblotting against the protein of interest. An example of such an experiment is shown in Fig. 3c.

### 3.4 Inverse Redox State Determination

The redox state at steady state can also be analyzed by an inverse redox state determination (Fig. 3d). In an inverse redox state experiment, not the reduced but the oxidized thiols result in a shift on SDS-PAGE. This is achieved by a three-step experiment. In the first step, reduced thiols are blocked in intact cells with a small membrane-permeable thiol-reactive probe such as NEM (Fig. 3d). In the second step, oxidized cysteine residues are reduced by treatment with a strong reductant such as TCEP after cell lysis. In the third step, the previously oxidized thiols are modified with a larger thiol-reactive probe such as mm(PEG)<sub>24</sub>. Consequently, previously oxidized thiols become modified with the larger probe thus leading to a shift (Fig. 3d, e).

A comparison of direct and inverse redox shift experiments highlights the respective critical steps (Fig. 3f). In the former experiment, there is the danger of modifying reactive primary amines; however also disulfide-linked dimers (intermolecular disulfide bonds) can be detected. Conversely, the inverse shift experiment does not allow the detection of disulfide-linked oligomers due to the TCEP reduction step. Instead, after thiol modification, the protein fraction which was formerly disulfide linked to an interaction partner will migrate as fast as the fraction which formerly contained an intramolecular disulfide bond. Disulfide-linked interactions should be visualized in a direct redox state determination analyzed by nonreducing SDS-PAGE (*see* **Notes 15** and **32**). However, in the inverse shift experiment, primary amines—if reactive—are blocked by the small compound NEM and thus are not susceptible to modifying by the larger thiol-reactive probe. This conveys a high confidence that only cysteine modification results in a shift. In addition, the inverse experiment can also be modified to be performed without TCA precipitation thus avoiding a potentially experimentally challenging step. In general both the direct and the inverse redox state determination should be performed for the protein of interest to obtain a comprehensive and confident picture of the protein's redox state.

We routinely prepare six samples in an inverse redox state determination: (1) **unmodified sample** will show the migration behavior of an unmodified, reduced protein of interest. The (2) **minimum shift sample** will be reduced *in vitro*, and all cysteines will be modified with the small thiol-reactive probe NEM only indicating the migration behavior of a completely reduced protein of interest. The (3) **steady-state sample** reflects the redox state in intact cells, i.e., shows the different pools of a protein of interest with different cysteine oxidation statuses. The (4) **H<sub>2</sub>O<sub>2</sub> sample** and (5) **diamide sample** are two samples with which one can test

the susceptibility of a protein of interest to oxidation *in situ*, i.e., in intact cells (*see Note 33*). Finally, the (6) **maximum shift sample** will be reduced *in vitro* and modified with the larger thiol-reactive probe, e.g., mm(PEG)<sub>24</sub> only to indicate the migration behavior of a completely modified and thus previously oxidized protein of interest. In principle, an *in situ* DTT (reductant) treatment can also be performed to test the stability of disulfide bonds. Since the treatment is performed under physiological conditions at 37 °C, only redox-active/regulatory disulfide bonds will usually become reduced, while structural disulfide bonds remain intact. Before performing a thiol modification experiment, the best thiol-reactive probe should be determined for the protein of interest in a shift assay as explained in Subheading 3.2.

1. For each sample, use one well from a 12-well plate. For the method described here, six wells are required: **unmodified, minimum shift, steady-state, H<sub>2</sub>O<sub>2</sub>, diamide, and maximum shift samples**. HEK293 cells should not exceed 50 % confluency at the day of the experiment (*see Note 21*).
2. For **H<sub>2</sub>O<sub>2</sub>** and **diamide samples** (*see Note 33*), remove medium and add 1 ml PBS-H<sub>2</sub>O<sub>2</sub> and PBS-diamide, respectively. Leave medium in the other wells and incubate the 12-well plate for 5 min at 37 °C.
3. Put the 12-well plate on an ice-cold metal plate—from now on work on ice until **step 13**.
4. Start with removing the PBS-H<sub>2</sub>O<sub>2</sub> from **H<sub>2</sub>O<sub>2</sub> sample**, the PBS-diamide from the **diamide sample**, and the medium of the **steady-state sample** and wash the cells with 1 ml ice-cold PBS-NEM. Add 1 ml ice-cold PBS-NEM and incubate cells for 10 min on ice.
5. During the 10 min incubation period, proceed with the **unmodified, minimum shift, and maximum shift samples** by removal of medium and washing of cells with 1 ml ice-cold PBS. Remove PBS and add 500 µl 8 % ice-cold TCA. Keep the samples as they are in the 12-well plate until **step 7**.
6. After the 10 min incubation of **H<sub>2</sub>O<sub>2</sub>, diamide, and steady-state sample** in PBS-NEM, remove PBS-NEM and add 500 µl 8 % ice-cold TCA.
7. Scratch off the cells of all wells from the plate using a rubber policeman and transfer them to 1.5 ml reaction tubes. Incubate the samples at -20 °C for at least 1 hour or overnight (*see Note 23*).
8. Thaw all the samples at RT and precipitate denatured proteins at 4 °C for 15 min at 13,000 × *g*.
9. Remove the supernatant and add 900 µl ice-cold 5 % TCA. Vortex briefly to wash the TCA pellet in the 5 % TCA.

10. Centrifuge the samples at 4 °C for 15 min at 13,000 × *g*.
11. Remove the supernatant and centrifuge the samples at 4 °C for 1 min at 13,000 × *g*.
12. Remove the residual TCA (*see Note 24*).
13. From now on work at RT (*see Note 25*).
14. **Unmodified sample:** add 30 μl 1× Laemmli + TCEP.
15. **Minimum shift, steady-state, H<sub>2</sub>O<sub>2</sub>, diamide, and maximum shift sample:** add 28.2 μl 1× Laemmli + TCEP (*see Note 26*).
16. Usually TCA-precipitated samples are still acidic at this step (i.e., yellow-colored Laemmli). Adjust pH by adding 1–2 μl 1 M Tris pH 8 stepwise until the sample becomes blue (*see Note 24*).
17. Sonicate all samples at RT with ten strokes using a tip sonifier to dissolve precipitated proteins (*see Notes 4, 27, and 28*).
18. Incubate all samples for 15 min at 45 °C (*see Note 29*).
19. Let the samples cool down for 5 min at RT and add thiol-reactive probes, as described in the steps below.
20. **Minimum shift sample:** add 1.8 μl 250 mM NEM (*see Note 26*).  
**16. Maximum shift sample, steady-state sample, H<sub>2</sub>O<sub>2</sub> sample, and diamide sample:** add 1.8 μl 250 mM mm(PEG)<sub>24</sub> (*see Note 26*).
21. **Unmodified sample:** leave untreated.
22. Incubate the samples for 1 h at RT in the dark (*see Note 30*).
23. Analyze the samples by SDS-PAGE (*see Note 31*) and immunoblotting against the protein of interest. An example of such an experiment is shown in Fig. 3e.

### **3.5 Oxidative Folding of Mitochondrial IMS Proteins**

The method described below is used to analyze oxidative folding of IMS proteins with twin CX<sub>3/9</sub>C motifs that become imported into mitochondria by the Mia40/ALR system. This is an advanced method that combines several individual methods (Fig. 4a). A radioactive pulse-chase experiment is performed first (**steps 1–16**), followed by thiol modification (**steps 17–23**) and immunoprecipitation under denaturing conditions (**steps 24–44**). In the last steps, the samples are analyzed by SDS-PAGE and autoradiography (**steps 45–48**).

During a pulse period, radioactive [<sup>35</sup>S]-L-methionine and [<sup>35</sup>S]-L-cysteine are incorporated into newly synthesized proteins. After the pulse, the radioactive labeling is stopped by an excess of nonradioactive (“cold”) methionine and cysteine. During this chase time, the radioactively labeled proteins undergo their normal life cycle which, in the case of IMS proteins imported via the Mia40/ALR system, includes their translocation across the outer membrane that is coupled to the oxidation of their thiol groups by Mia40 (*see Note 34*).

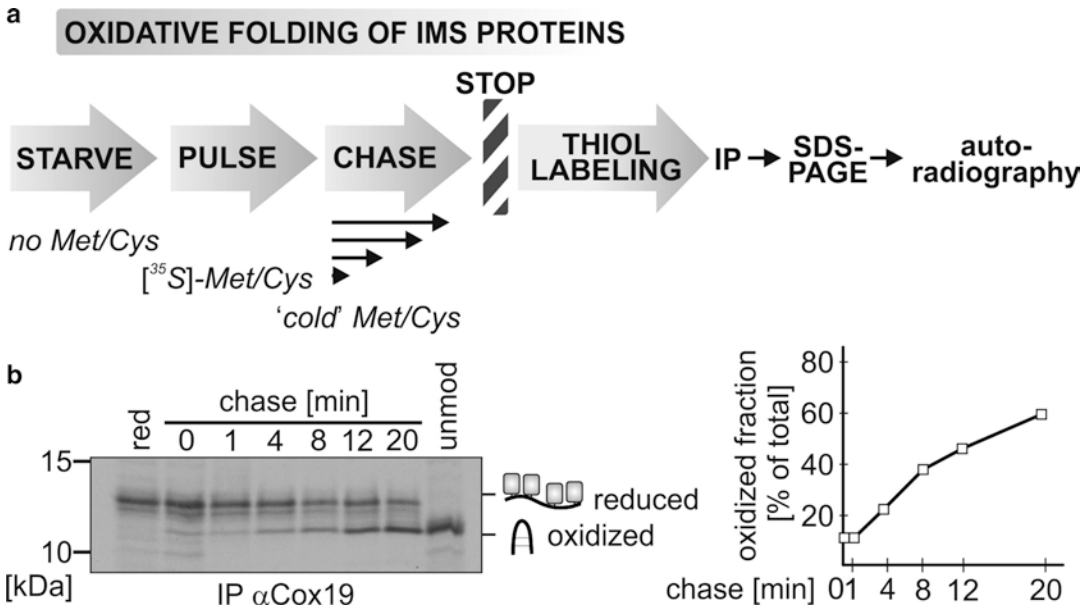


**Fig. 4** Radioactive pulse-chase experiments to monitor oxidative folding and translocation of mitochondrial proteins. **(a)** General approach to monitor oxidative folding of mitochondrial IMS proteins. The scheme shows steps used to analyze oxidative folding of IMS proteins with twin  $CX_{3/9}C$  motifs whose import into mitochondria is mediated by Mia40/ALR system. In radioactive pulse-chase experiments, proteins are labeled radioactively and followed during different times of their biogenesis. First, during the starve period, cells are treated with starve medium lacking methionine and cysteine to deplete respective cellular pools and to increase radioactive labeling in the pulse period. During the pulse period, cells are treated with medium containing radioactive  $[^{35}S]$ -methionine and  $[^{35}S]$ -cysteine which is incorporated into newly synthesized proteins, thereby labeling them radioactively. Radioactive labeling is stopped by addition of chase medium which contains an excess of nonradioactive (“cold”) methionine and cysteine. Different chase periods are used to examine the kinetics of oxidative folding. After the chase, cellular processes are stopped by the addition of ice-cold TCA. The samples are subjected to thiol modification, and the protein of interest is isolated using IP and further analyzed by SDS-PAGE and autoradiography. **(b)** Analyzing oxidative folding of Cox19, a mitochondrial twin  $CX_9C$  protein. HEK293 cells were treated with starvation medium for 15 min. After a pulse period of 5 min, chase medium was added for 0, 1, 4, 8, 12, or 20 min. Cellular processes were stopped by the addition of ice-cold TCA. After protein solubilization reduced thiols were modified using the thiol-reactive probe  $mm(PEG)_{12}$ . The reduced control sample (*red*) was treated with TCEP prior to the thiol modification. The unmodified sample (*unmod*) representing the oxidized protein was not treated with a thiol-reactive probe. After isolation of the twin  $CX_9C$  protein, samples were analyzed by SDS-PAGE and autoradiography. Directly after the pulse period, the twin  $CX_9C$  protein is completely reduced (0 min) and becomes oxidized over time

Thiol modification is then used in a second step to investigate the kinetics of protein oxidation. To preserve the redox state of cysteines during lysis of cells, the radioactive pulse-chase experiment is stopped after the chase by the addition of TCA. The sudden drop in pH leads to the protonation of reduced thiols which become less reactive. Later, the pH can be increased again, and reduced thiols can be specifically modified by a thiol-reactive probe (e.g., AMS,  $mm(PEG)_n$ ) which binds covalently to reduced but not to oxidized thiols. This thiol modification adds molecular mass

to a reduced protein of interest and can usually be easily seen as a shift in running behavior of the protein in SDS-PAGE. To determine the redox state of a protein, a reduced (maximum shift) and an unmodified (no shift) control sample have to be prepared. Before performing a radioactive pulse-chase thiol modification experiment, the thiol-reactive probe best suited for the protein of interest should be determined in a shift assay as explained in Subheading 3.2.

In the third step, the protein of interest has to be enriched by immunoprecipitation (IP), since all cellular proteins are radioactively labeled during the pulse step. The IP is performed under denaturing conditions so that only the protein of interest and its covalently linked interaction partners, but not its non-covalent interaction partners, are enriched. The samples are finally analyzed by SDS-PAGE and autoradiography.

1. For each sample, use one 35 mm dish of HEK293 cells at 50 % confluency. In the protocol described below, eight dishes are required: six for six chase time points and two for reduced and unmodified control samples.
2. Add approximately 0.2 ml 1 M HEPES-KOH pH 7.4 to the medium in the 35 mm dishes to reach a final concentration of 100 mM (*see Note 16*). Bring the dishes and the equipment to the isotope lab.
3. Remove the complete medium (*see Note 10*) and wash the cells with 0.8 ml starve medium.
4. Add 0.8 ml starve medium to the cells and incubate them for 15 min in an incubator set at 37 °C (*see Notes 3, 18, and 19*).
5. Remove the starve medium and add 0.8 ml pulse medium.
6. Incubate cells for 5 min at 37 °C (*see Notes 6, 35, and 36*).
7. Remove the pulse medium and add 0.8 ml chase medium.
8. Incubate the dishes in an incubator set at 37 °C during the chase period. For six chase time points, incubation times are 0, 1, 4, 8, 12, and 20 min (*see Notes 34 and 37*). Two control samples are incubated for 20 min.
9. Remove the chase medium and add 950  $\mu$ l ice-cold 8 % TCA. Store the dish on an ice-cold metal plate until next step.
10. Scratch off the cells by using a rubber policeman and transfer them into a chilled 1.5 ml reaction tubes (*see Note 38*).
11. Incubate the samples at -20 °C for at least 1 h or overnight (*see Note 23*).
12. Thaw the samples at RT and precipitate denatured proteins at 4 °C for 15 min at 13,000  $\times g$ .
13. Remove the supernatant and add 900  $\mu$ l ice-cold 5 % TCA. Vortex briefly to wash the TCA pellet in the 5 % TCA.

14. Centrifuge the samples at 4 °C for 15 min at 13,000 × *g*.
15. Remove the supernatant and centrifuge the samples at 4 °C for 1 min at 13,000 × *g*.
16. Remove the remaining residual TCA (*see Note 24*).
17. Add 60 µl buffer A to the TCA pellet of **unmodified control sample**. Sonicate the sample at RT with ten strokes using a tip sonifier to dissolve precipitated proteins (*see Note 4*). Boil for 5 min at 95 °C. Keep at RT until further processing.
18. Add 50 µl buffer A (*see Note 26*) to the TCA pellet of **reduced control sample** and 6 µl 20 mM TCEP. Sonicate the sample at RT with ten strokes using a tip sonifier to dissolve precipitated proteins (*see Note 4*). Boil for 5 min at 95 °C. Cool down at RT for 5 min and add 4 µl 250 mM mm(PEG)<sub>12</sub> (*see Note 26*) and mix the sample. Keep at RT until further processing.
19. Add 56 µl buffer A (*see Note 26*) and 4 µl 250 mM mm(PEG)<sub>12</sub> to the TCA pellets of **six chase time point samples**. Sonicate the sample at RT with ten strokes using a tip sonifier to dissolve precipitated proteins (*see Note 4*). Keep at RT until further processing.
20. Incubate all the samples for 1 h at RT in the dark (*see Note 30*).
21. Add 40 µl buffer A to all the samples.
22. Vortex and boil the samples for 5 min at 95 °C.
23. Let the samples cool down at RT for 5 min.
24. Add 900 µl IP buffer + 2.5 % Triton X-100 to all the samples from **step 23**.
25. Invert the samples four times and incubate them for 30 min on ice (*see Note 39*).
26. During the incubation time of **step 25**, protein A beads should be prepared to be coupled to the antibody against the protein of interest (*see Notes 40 and 41*). Therefore transfer 160 µl protein A beads with a precut pipet tip into a 1.5 ml reaction tube (*see Note 42*).
27. Wash the beads 2× with 1 ml IP buffer + 1 % Triton X-100. To do so, add the buffer, invert the tubes three times while flicking the tip of the tube, and directly centrifuge it for 2 min at 2000 × *g* and 4 °C.
28. Add 1 ml IP buffer + 1 % Triton X-100 to the beads.
29. Add 24 µl serum against the protein of interest to the beads suspension (*see Note 13*).
30. Incubate the beads–antibody suspension at 4 °C for 1 h under gentle shaking.
31. Wash the beads 3× with 1 ml IP buffer + 1 % Triton X-100 (2000 × *g*, 2 min, 4 °C) and remove the supernatant.

32. Fill the 1.5 ml reaction tube to the 1 ml line with IP buffer + 1 % Triton X-100.
33. Resuspend the beads properly in the solution.
34. Distribute 125  $\mu$ l of the bead suspension to eight 1.5 ml reaction tubes, one for each sample.
35. Store beads with coupled antibodies on ice until the samples have been centrifuged (**step 36**) (*see Note 40*). The buffer above the beads does not need to be removed.
36. Centrifuge the samples at 4 °C for 60 min at 25,000  $\times g$  (*see Note 43*).
37. Transfer 750  $\mu$ l of the supernatants each into one 1.5 ml reaction tube with the antibody–bead conjugate.
38. Incubate the tubes over night at 4 °C on an end-over-end rotator.
39. Centrifuge the beads at 4 °C for 2 min at 2000  $\times g$ .
40. Remove the supernatant carefully (*see Note 44*). Wash the beads 3 $\times$  with 1 ml IP buffer+ 1 % Triton X-100 and 1 $\times$  with 1 ml IP buffer without Triton X-100 (*see Note 45*). To do so, add the buffer, invert the tubes three times while flicking the tip of the tube, and directly centrifuge it for 2 min at 2000  $\times g$  and 4 °C.
41. Remove the supernatant of the last washing step using gel-loading tips (*see Note 46*).
42. Centrifuge the beads at 4 °C for 2 min at 2000  $\times g$  to bring down residual amounts of buffer.
43. Dry the beads completely using a 200  $\mu$ l pipette and gel-loading tips (*see Note 46*).
44. Add 40  $\mu$ l 1 $\times$  nonreducing Laemmli buffer (*see Note 15*) to the beads and boil the samples for 5 min at 95 °C.
45. Spin down the samples briefly and analyze them by SDS-PAGE (*see Note 31*).
46. Transfer proteins onto a nitrocellulose membrane and dry it.
47. Expose nitrocellulose membrane to an autoradiography film.
48. Depending on the amount of cells, pulse time, and protein expression level, develop the autoradiography film after several days up to several weeks (*see Note 47*). An example of such an experiment is shown in Fig. 4b.

### **3.6 Translocation of Mitochondrial Proteins**

The majority of mitochondrial proteins are imported from the cytosol into mitochondria via different pathways. These pathways differ, for example, in their translocation kinetics. How fast a protein of interest is imported into mitochondria can be assessed by a radioactive pulse-chase approach coupled to a cellular fractionation (Fig. 5a).

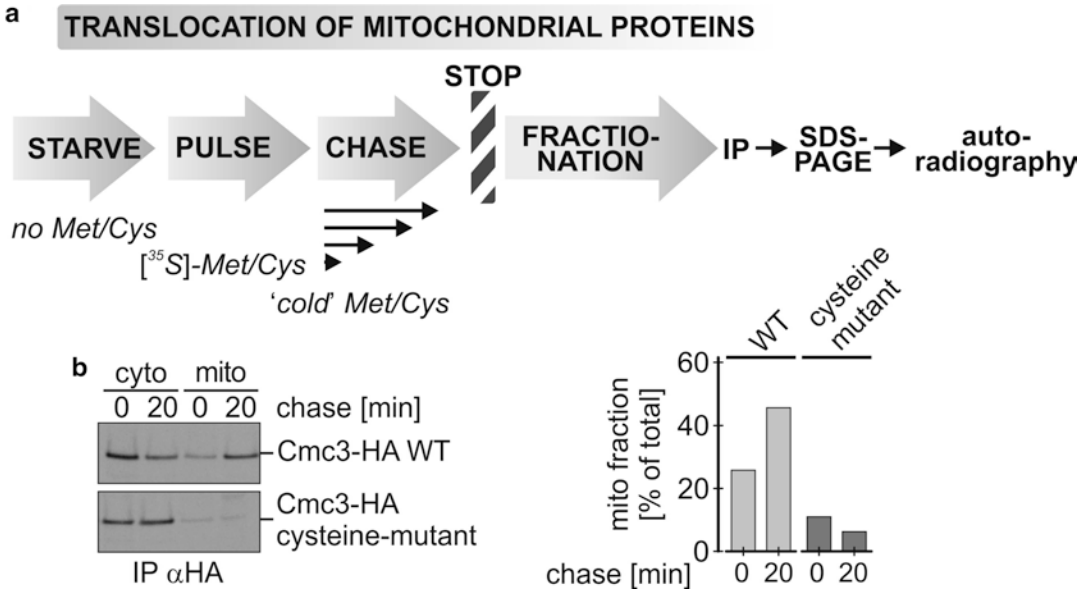


**Fig. 5** Radioactive pulse-chase experiments to monitor oxidative folding and translocation of mitochondrial proteins. **(a)** General approach to monitor mitochondrial translocation of mitochondrial proteins. The scheme shows steps used to analyze the translocation of mitochondrial proteins. After a radioactive pulse-chase experiment as described in Fig. 4, cellular processes are stopped by lowering the temperature to 4 °C, and cells are fractionated to separate different subcellular compartments. Subsequently the protein of interest is isolated using IP and further analyzed by SDS-PAGE and autoradiography. **(b)** Analyzing cellular localization of Cmc3-HA, a mitochondrial twin CX<sub>9</sub>C protein during mitochondrial protein biogenesis. HEK293 cells expressing a wild-type (WT) or a cysteine mutant of Cmc3-HA were treated with starve medium for 15 min. After a pulse period of 10 min, chase medium was added for 0 or 20 min. Cellular processes were stopped by the addition of ice-cold fractionation buffer containing 0.005 % digitonin. A low digitonin concentration permeabilizes the plasma membrane but not mitochondrial membranes. In a centrifugation step the non-cytosolic fraction (mito) was separated from the cytosolic fraction (cyto). After membrane permeabilization proteins were precipitated using TCA. Subsequently, proteins were solubilized and WT or cysteine mutant of Cmc3-HA were isolated via immunoprecipitation. Samples were analyzed by SDS-PAGE and autoradiography. Both WT and cysteine mutant are mainly detected in the cytosol after 0 min of chase. After 20 min the WT accumulates in the non-cytosolic fraction, while the cysteine mutant does not

In such an experiment the radioactive pulse-chase approach is performed as described in Subheading 3.5. The chase is stopped by adding ice-cold fractionation buffer which contains a low concentration of the mild detergent digitonin (*see Note 17*). With the appropriate digitonin concentration, only the plasma membrane of the cells and not the OM of mitochondria is permeabilized, thus leading to diffusion of cytosolic proteins into the buffer. Proteins which became imported into mitochondria do not diffuse into the buffer as they are protected by mitochondrial membranes. After solubilization of the plasma membrane, the non-cytosolic fraction (containing mitochondria) is separated from the cytosolic fraction by centrifugation. Optional washing steps or treatments with proteases like trypsin can be used to improve the quality of the results.

Subsequent immunoprecipitation of the protein of interest from both fractions and analysis by SDS-PAGE and autoradiography reveals the localization of the protein of interest at a given chase time.

1. For each sample, use one 35 mm dish of HEK293 cells at 90 % confluency (*see Note 48*). In the protocol described below, two dishes are needed. One for the 0 min chase time point and one for the 20 min chase time point.
2. Follow **steps 2–7** of Subheading **3.5**. At **step 6** incubate the cells in pulse medium for 10 min at 37 °C instead of 5 min.
3. After adding the chase medium in **step 7**, incubate the cells for 0 or 20 min at 37 °C.
4. Remove the chase medium and add 800  $\mu$ l ice-cold fractionation buffer to each dish. Immediately transfer the cells onto an ice-cold metal plate. Scratch off the cells carefully by using a rubber policeman. Transfer the cells each into a chilled 1.5 ml reaction tube.
5. Incubate the samples on ice for 20 min. Mix the samples by inverting the tubes every 5 min.
6. Centrifuge the cells at 4 °C for 2 min at  $300 \times g$  and directly afterward for 4 min at  $10,000 \times g$  (*see Note 49*).
7. Transfer the supernatants without touching the pellet each into a fresh 1.5 ml reaction tube [*S* = supernatant].
8. Add 152  $\mu$ l ice-cold 50 % TCA to the supernatant. Mix using a vortex and incubate for at least 1 h at  $-20$  °C (*see Note 23*).
9. Add 800  $\mu$ l ice-cold titration buffer + 0.005 % digitonin to the pellet (*see Note 50*).
10. Resuspend the pellet by using the pipette.
11. Add 152  $\mu$ l ice-cold 50 % TCA to the sample. Mix the samples using a vortex and incubate for at least 1 h at  $-20$  °C [*P* = pellet] (*see Note 23*).
12. Follow **steps 11–16** of the Subheading **3.5**.
13. Add 100  $\mu$ l buffer A to the TCA pellets. Sonicate the sample at RT with ten strokes using a tip sonifier to dissolve precipitated proteins (*see Note 4*). Boil for 5 min at 95 °C. Let the samples cool down for 5 min at RT and keep them at RT until further processing.
14. Transfer 10  $\mu$ l of the [*S*]-sample and 10  $\mu$ l of the [*P*]-sample into two 1.5 ml reaction tubes containing 10  $\mu$ l  $2\times$  Laemmli buffer each, respectively. These aliquots serve as control samples which need to be analyzed using SDS-PAGE and immunoblot for cytosolic (e.g., LDH) and mitochondrial (e.g., Hsp60, Smac) marker proteins in order to verify the efficiency of the cellular fractionation.

15. Use the remaining 90  $\mu\text{l}$  to perform IP against the protein of interest.
16. Add 910  $\mu\text{l}$  IP buffer + 2.5 % Triton X-100 to the samples.
17. Follow **steps 25–48** of the Subheading **3.5**.

---

## 4 Notes

1. We routinely use HEK293 and HeLa cells in our lab. For thiol modification experiments, we use twice the amount of HeLa cells compared to HEK293 cells (e.g., 100 % confluent HeLa cell plate vs. 50 % confluent HEK293 cell dishes) since the latter cells usually have a higher protein content per dish. We also employed other mammalian cells such as MEFs (mouse embryonic fibroblasts) and human fibroblasts successfully for thiol modification experiments. Note that these experiments are not limited to mammalian cells but can also be performed with other cells such as *Saccharomyces cerevisiae*. However, the disadvantage in using *S. cerevisiae* is that the cell wall complicates efficient cell lysis and protein extraction. Additionally, for different cells, times and amounts have to be adapted accordingly.
2. Haloalkyls and maleimides are the most commonly used thiol-reactive probes. We prefer maleimides as they are more specific to cysteines (and less to methionines and histidines) and less light sensitive than haloalkyls. Note that in general thiol-reactive probes are light sensitive and should be protected from light. Make sure to protect the thiol-reactive probe stocks from light by covering the tubes with aluminum foil.
3. Due to their low solubility in aqueous solutions, thiol-reactive probe stocks should be dissolved in DMSO first and diluted in aqueous solutions afterward.
4. We use a UP50H-tip sonifier (Hielscher) set to 0.5 cycle and 50 % amplitude. Sonicate the samples with ten strokes, allow them to cool down for 5 min at RT, and then check if the TCA pellet is dissolved. If the TCA pellet is not dissolved, continue with ten strokes of sonication. Keep the cooldown time of 5 min between the sonication sets to avoid extensive heating of the sample. Avoid extensive foam formation by keeping the sonication tip submerged.
5. It has to be determined for each individual protein and cell amount if an antibody is suited for Western blot and IP after a thiol modification experiment (a problem might, for example, be that the antigen contains a cysteine residue that becomes modified during thiol modification thus destroying the antigen). For Western blot perform a shift assay as explained in Subheading **3.2**. In this experiment one can compare the antibody

signal of an unmodified sample compared to signals of samples which were reduced and subsequently thiol-modified to obtain completely modified proteins. Equal signal intensities of modified vs. unmodified protein will prove that your antibody is suited to detect the protein of interest in Western blot after thiol modification. To test if an antibody is suited for IP after thiol modification, prepare a lysate of which you analyze an unmodified total sample (as a migration control of protein of interest), and compare it to one IP of an unmodified lysate to one IP of which the lysate was reduced and treated with a thiol-reactive probe prior to the IP to obtain a maximum shift. A signal for the protein of interest in the total and unmodified IP lanes will show that the antibody can be used for IP in general. Equal signal intensities in modified vs. unmodified IP samples will prove that the antibody is suited to detect the thiol-modified protein of interest in IP. We observed that antibody features such as monoclonality and polyclonality, being used as sera or affinity-purified antibodies or being from different suppliers, do not give hints whether an antibody is suited for use in thiol modification experiments (*see also Note 36*). Thus, when using an antibody the first time, we routinely test it for the use in Western blot and IP.

6. Refer to the general safety precautions when working with radioactivity.
7. *Pulse* medium can be reused several times, if it was only used for short pulse periods. This has to be tested for the respective experimental setup.
8. For short pulse durations ( $\leq 5$  min), use 200  $\mu\text{Ci}/\text{ml}$ . We use as a pulse-labeling mix the “EXPRESS [ $^{35}\text{S}$ ]-protein labeling mix” by PerkinElmer with a [ $^{35}\text{S}$ ]-L-methionine/[ $^{35}\text{S}$ ]-L-cysteine ratio of 73:22.
9. For chase periods  $>1$  h, add 10 % (v/v) fetal calf serum (FCS) to the medium.
10. Removing media with a vacuum pump facilitates the handling of a radioactive pulse-chase experiment. However, it is also possible to remove the media with a pipette although this is usually not as efficient and fast compared to using a pump system.
11. Buffer A is well suited to solubilize TCA-precipitated proteins as it, in addition to SDS, contains urea which improves protein solubilization. To maintain good protein solubilization efficiency, we prepare buffer A freshly every 2 months.
12. The phosphine TCEP is a strong reductant which in our hands is more stable and effective than DTT. In comparison to DTT and  $\beta$ -mercaptoethanol, TCEP does not react (or reacts only

very slowly) with thiol-reactive probes as it does not contain thiol groups.

13. The amount of antibody for the IP has to be determined for each individual protein and cell amount. For that, perform an antibody titration experiment (constant pulse, chase, and cell amount), and determine the amount of antibody at which the use of additional antibody does not result in additional precipitated protein of interest. Usually 1–3  $\mu$ l antibody is used for IP of one sample. We observed that IP using serum produces a higher background compared to IP using affinity-purified antibodies.
14. When preparing a 20 % (v/v) solution of Triton X-100 in water, extensively mix using a magnetic stirrer to ensure obtaining a homogenous solution. Do the same when preparing IP buffer containing 1 and 2.5 % Triton X-100.
15. Laemmli buffer can be prepared with a reductant (e.g., 50 mM DTT) to reduce disulfide-linked interactions. Consequently, proteins which were previously disulfide-linked migrate as monomeric proteins on SDS-PAGE which is beneficial if total protein levels are analyzed. However, after thiol modification, treatment with reductant can be omitted to allow detection of slower migrating disulfide-linked interactions. Note that if samples of a direct redox state determination are treated with a reductant, fractions of a protein containing intermolecular disulfide bonds cannot be distinguished from fractions containing intramolecular disulfide bonds as both proteins will migrate with the same velocities. Also note that the use of TCEP in inverse shift experiments reduced the samples. Thus, even the use of a nonreducing Laemmli buffer leaves your sample still reduced.
16. We perform pulse-chase experiments without a CO<sub>2</sub>-regulated incubator. Instead the pH of the medium can be kept constant by adding 1 M Hepes-KOH pH 7.4 to a final concentration of 100 mM. When using CO<sub>2</sub> incubators consider to put a bowl with active coal into the incubator to bind radioactive material that evaporates.
17. Use the 2 % digitonin stock solution to test the appropriate concentration of digitonin to permeabilize the plasma membrane. To this end, a titration with different digitonin concentrations has to be performed. Test by Western blotting at which concentration a signal for a cytosolic marker protein (e.g., LDH) in the cytosolic fraction can be obtained. Conversely, the use of this concentration should lead to a signal of a mitochondrial marker protein (e.g., PDH, Smac) in the non-cytosolic fraction only. Prepare a larger amount of the 2 % digitonin stock and use it to prepare fractionation buffer freshly. It is important that the digitonin stock is always completely thawed after freezing and thoroughly mixed/homogenized before dilution.

18. When working with mammalian cell culture, always work in a sterile surrounding using aseptic technique to avoid contamination of cell lines.
19. These cell numbers will approximately result in a 50 % confluent dish 2 days after cell seeding. As this might vary dependent on cell type and condition, adjust the seeded cell numbers accordingly.
20. Thiol modification might interfere with epitope recognition by the antibody. As a result thiol-modified proteins might not be detected in immunoblotting or IP (*see also Note 5*). Especially monoclonal antibodies show this problem if the respective epitope used for antibody production contained cysteine residues. For IP such a problem can be circumvented by performing the thiol modification after the elution of the protein from the beads after IP (although this results in other problems, see preservation of cellular redox states). For Western blotting the use of tagged proteins or the use of polyclonal antibodies might be a solution.
21. For a thiol modification experiment, HEK293 cells should not be confluent. Two problems usually occur when we use a confluent 35 mm dish of HEK293 cells for a thiol modification experiment: firstly, you obtain a large TCA protein pellet which can be difficult to dissolve in relatively small amounts of buffer A. Secondly, when analyzing the experiment, the amounts of thiol-reactive probe might become limiting, and thus proteins might become incompletely modified. Accordingly, reduce the cell amount or increase the amount of the thiol-reactive probe to obtain the maximum shift of the reduced control. If other cells than HEK293 are used and you obtain low intensity signals, consider increasing the cell number for the experiment.
22. Generally, thiol modification can be performed without a TCA precipitation. For this cells can be harvested in nonreducing Laemmli buffer. The thiol modification can be performed afterward as described (or the modifying agent is in the Laemmli buffer). After the thiol modification analyze the sample directly via SDS-PAGE. This method is faster and might provide data with either better quality as the protein precipitation step is omitted or worse quality as all cellular components are still present which might interfere with thiol modification. This has to be tested for the protein of interest. Importantly, consider that you might fail to preserve the cellular redox state with this approach.
23. To precipitate proteins efficiently with TCA, the samples should freeze completely. It is sufficient to incubate them for 1 h at  $-20^{\circ}\text{C}$ , but at this step the samples can also be stored for several days at  $-20^{\circ}\text{C}$  without compromising sample quality. Routinely we freeze the samples overnight.

24. In a thiol modification experiment, the pH is critical as thiol modification depends on the presence of the thiolate anion. If TCA is not removed and the pH is low, thiols are present in their protonated state which decreases modification efficiency. Note that in a solution with  $>pH$  8.5, not only cysteines but also primary amines become modified. Using 1 M Tris pH 8 to adjust the pH, we did not observe significant modification of primary amines.
25. Work at RT when Laemmli is used to avoid precipitation of SDS in the cold.
26. We use the thiol-reactive probe in a final concentration of 15 mM (although this can in principle also be titrated) and adjust the volume of Laemmli buffer (or buffer A in a pulse-chase experiment) to the volume of thiol-reactive probe accordingly. Note that before performing any thiol modification experiment, the thiol-reactive probe best suited for the protein of interest should be determined in a shift assay as explained in Subheading 3.2. As thiol-reactive probes are rather expensive, we try to keep the volume of the thiol modification reaction low (i.e., 30–60  $\mu$ l). Note that it is not possible to increase the amount of cells indefinitely in a reaction of this volume as the thiol-reactive probe will become limiting at some point resulting in incompletely modified samples.
27. Upon sonication of TCA pellets, samples may turn yellow again although they were previously pH-adjusted. Readjust the pH by addition of 1–2  $\mu$ l 1 M Tris pH 8 before further sonication to facilitate dissolving of TCA pellet.
28. We sometimes observe that TCA precipitates are difficult to solubilize in Laemmli buffer. The solubilization efficiency can be increased when Laemmli buffer is prepared with 6 M urea. We did not observe that this alters gel electrophoresis or other sample processing steps.
29. Reduction with TCEP is usually efficient at 45 °C. Obtaining a single band migrating slower than the signal of the unmodified sample hints to an effective reduction. Boiling does not significantly increase reduction efficiency but might lead to protein aggregation especially of hydrophobic membrane proteins.
30. It is not necessary to foil the tubes to incubate the samples in the dark. We put them for 1 h at RT into a drawer.
31. For thiol modification experiments, the separation on SDS-PAGE is critical as they rely on the migration difference of modified proteins compared to unmodified proteins. For small proteins ( $\sim$  10 kDa), an 18 % polyacrylamide gel is well suited. Depending on the protein size, the acrylamide concentration can be increased or decreased. To improve the separation, especially for proteins  $<$  30 kDa, Tris–Tricine PAGE can be used [23].

32. With this experiment it can be analyzed if a protein is oxidized. However, it does not permit conclusions on what kind of oxidation occurred. An oxidized protein would show the same readout no matter if it has an intramolecular disulfide bond or if it is oxidized to a sulfenic, sulfinic, or sulfonic acid. Still, glutathionylation might be observed as a protein migrating higher than the unmodified protein on a nonreducing SDS-PAGE. Also intermolecular disulfides might be determined since a disulfide-linked protein migrates slower than the monomeric protein on a nonreducing SDS-PAGE (*also see Note 15*).
33.  $\text{H}_2\text{O}_2$  and diamide both are oxidants used in redox state determination which differ in their reaction mechanism. While  $\text{H}_2\text{O}_2$  directly reacts with reduced thiols to oxidized species such as sulfenic, sulfinic, or sulfonic acid, diamide mostly induces glutathionylation of proteins.
34. Note that during this chase time, all the radioactively labeled proteins undergo their normal life cycle which includes translocation to their respective compartment, folding, posttranslational modification, and, finally, degradation. By using different chase times and subsequently different specific processing steps, the kinetics of these processes can be analyzed (*also see Note 22*). Importantly, not only mitochondrial but also redox processes in other compartments (e.g., endoplasmic reticulum) can be examined by this method.
35. Depending on the cellular process which is assessed, we usually use pulse times between 5 and 30 min.
36. Pulse times should be kept as short as possible and should be clearly shorter than the half time of the observed process. For very fast processes (e.g., mitochondrial targeting sequence (MTS) processing), this is not possible as too short pulse times lead to very weak signals. As shortest pulse time, we use 3 min.
37. The chase times depend on the cellular process which is analyzed. For fast processes such as MTS-dependent protein import, short chase times (e.g., 0, 1, and 4 min, etc.) should be used, while slower processes (e.g., protein degradation) can be analyzed using longer chase times (e.g., 0, 30 min, 1, 2, and 4 h). A 0 min chase time point is advisable to know how much protein has been radioactively labeled and to test what happened during the pulse.
38. For radioactive pulse-chase experiments, we use safe-lock tubes to avoid radioactive contaminations.
39. We observed that this step is not time-critical as incubating the samples on ice between 30 min and 2 h did not change the quality of the experiment.
40. Protein A beads can be coupled to the antibody against the protein of interest at earlier steps. We couple the antibody to

the beads freshly on the day of the IP. Make sure to keep the coupled beads on ice at all times.

41. We start the washing of protein A beads after starting the 30 min incubation in **step 25** (*also see Note 39*). When we started the coupling of antibody to the beads at **step 29**, we continue with the centrifugation of the lysates in **step 36**. During the centrifugation of the lysates, there is enough time to perform **steps 31–35**.
42. The coupling of antibody to protein A beads is performed in one tube as a stock for all samples. Per IP we use 20  $\mu$ l of the 50 % suspension in which the beads are provided in by the manufacturer.
43. This centrifugation step precipitates cell debris. Too short centrifugation (< 20 min) or pellet addition to the IP results in high background signal.
44. Accidental removal of beads at this step leads to signal loss. This can be avoided by carefully removing the supernatant while leaving 50–100  $\mu$ l buffer on the beads until the next wash.
45. Depending on the antibody, the IP can show high background signals. Increasing the number of washing steps with 1 ml IP buffer + 1 % Triton X-100 can decrease background.
46. Gel-loading tips contain a narrow opening which allows buffer removal without loss of beads. When beads are dried, they change color becoming whiter and have a more crystalline appearance.
47. How long a radioactive film has to be exposed depends on various factors such as the pulse duration, the expression rate of the protein of interest, and the quality of the antibody used for IP. However, as a rough estimation, we use for short pulse durations of 5–10 min an exposure time of 2 weeks, while for pulse durations of 30 min we expose approximately for 4 days.
48. A cell confluency of 90–100 % does not constitute a problem for experiments without modification of thiols as the buffer A amount can be increased to dissolve the TCA pellet.
49. Initial short centrifugation at low speed prevents sedimentation of cells on the side of the tube and facilitates buffer removal.
50. A broad-spectrum protease can be added to the pellet if cytosolic proteins are detected in the non-cytosolic fraction. The protease degrades proteins which attach to the mitochondrial OM after the cellular fractionation. Mitochondrial proteins will not be hydrolyzed because they are protected from the protease by the OM. We use trypsin as a broad-spectrum protease at this step and proceed from **step 7** as follows.

- (a) Add 800  $\mu\text{l}$  ice-cold titration buffer + 25  $\mu\text{g}/\text{ml}$  trypsin to the pellet.
- (b) Resuspend the pellet carefully by pipetting up and down (cut the tip).
- (c) Incubate the sample at 4  $^{\circ}\text{C}$  for 30 min. Mix the sample by inverting the tubes every 5 min.
- (d) Add 10  $\mu\text{l}$  0.2 M PMSF to the sample. Mix by inverting the tube.
- (e) Add 152  $\mu\text{l}$  ice-cold 50 % TCA to the sample. Mix the samples using a vortex and incubate for at least 1 h at  $-20^{\circ}\text{C}$  [P = pellet].
- (f) Continue with **step 12**.

---

## Acknowledgments

We would like to thank Alican Erdogan, Manuel Fischer, Alena Löschner, and Dario Wernet for providing experimental data. Research in the Riemer laboratory is supported by the Deutsche Forschungsgemeinschaft (DFG). M.H. is supported by the Carl-Zeiss Foundation.

## References

1. Poole LB (2015) The basics of thiols and cysteines in redox biology and chemistry. *Free Radic Biol Med* 80:148–157. doi:[10.1016/j.freeradbiomed.2014.11.013](https://doi.org/10.1016/j.freeradbiomed.2014.11.013)
2. Diaz-Sanchez AG, Gonzalez-Segura L, Rudino-Pinera E, Lira-Rocha A, Torres-Larios A, Munoz-Clares RA (2011) Novel NADPH-cysteine covalent adduct found in the active site of an aldehyde dehydrogenase. *Biochem J* 439(3):443–452. doi:[10.1042/BJ20110376](https://doi.org/10.1042/BJ20110376)
3. Tsybovsky Y, Malakhau Y, Strickland KC, Krupenko SA (2013) The mechanism of discrimination between oxidized and reduced coenzyme in the aldehyde dehydrogenase domain of Aldh1l1. *Chem Biol Interact* 202(1–3):62–69. doi:[10.1016/j.cbi.2012.12.015](https://doi.org/10.1016/j.cbi.2012.12.015)
4. Haapalainen AM, Merilainen G, Wierenga RK (2006) The thiolase superfamily: condensing enzymes with diverse reaction specificities. *Trends Biochem Sci* 31(1):64–71. doi:[10.1016/j.tibs.2005.11.011](https://doi.org/10.1016/j.tibs.2005.11.011)
5. Kim JJ, Battaile KP (2002) Burning fat: the structural basis of fatty acid beta-oxidation. *Curr Opin Struct Biol* 12(6):721–728
6. Modis Y, Wierenga RK (1999) A biosynthetic thiolase in complex with a reaction intermediate: the crystal structure provides new insights into the catalytic mechanism. *Structure* 7(10):1279–1290
7. Fabianek RA, Hennecke H, Thony-Meyer L (2000) Periplasmic protein thiol:disulfide oxidoreductases of *Escherichia coli*. *FEMS Microbiol Rev* 24(3):303–316
8. Terziyska N, Grumbt B, Kozany C, Hell K (2009) Structural and functional roles of the conserved cysteine residues of the redox-regulated import receptor Mia40 in the intermembrane space of mitochondria. *J Biol Chem* 284(3):1353–1363. doi:[10.1074/jbc.M805035200](https://doi.org/10.1074/jbc.M805035200)
9. Liu H, May K (2012) Disulfide bond structures of IgG molecules: structural variations, chemical modifications and possible impacts to stability and biological function. *MABS* 4(1):17–23. doi:[10.4161/mabs.4.1.18347](https://doi.org/10.4161/mabs.4.1.18347)
10. Riemer J, Bulleid N, Herrmann JM (2009) Disulfide formation in the ER and mitochondria: two solutions to a common process. *Science* 324(5932):1284–1287. doi:[10.1126/science.1170653](https://doi.org/10.1126/science.1170653)
11. Riemer J, Schwarzlander M, Conrad M, Herrmann JM (2015) Thiol switches in

- mitochondria: operation and physiological relevance. *Biol Chem* 396(5):465–482. doi:[10.1515/hsz-2014-0293](https://doi.org/10.1515/hsz-2014-0293)
12. Delaunay A, Pflieger D, Barrault MB, Vinh J, Toledano MB (2002) A thiol peroxidase is an H<sub>2</sub>O<sub>2</sub> receptor and redox-transducer in gene activation. *Cell* 111(4):471–481
  13. Savitsky PA, Finkel T (2002) Redox regulation of Cdc25C. *J Biol Chem* 277(23):20535–20540. doi:[10.1074/jbc.M201589200](https://doi.org/10.1074/jbc.M201589200)
  14. Sevier CS, Kaiser CA (2008) Ero1 and redox homeostasis in the endoplasmic reticulum. *Biochim Biophys Acta* 1783(4):549–556. doi:[10.1016/j.bbamcr.2007.12.011](https://doi.org/10.1016/j.bbamcr.2007.12.011)
  15. Hess DT, Matsumoto A, Kim SO, Marshall HE, Stamler JS (2005) Protein S-nitrosylation: purview and parameters. *Nat Rev Mol Cell Biol* 6(2):150–166. doi:[10.1038/nrm1569](https://doi.org/10.1038/nrm1569)
  16. Chacinska A, Koehler CM, Milenkovic D, Lithgow T, Pfanner N (2009) Importing mitochondrial proteins: machineries and mechanisms. *Cell* 138(4):628–644. doi:[10.1016/j.cell.2009.08.005](https://doi.org/10.1016/j.cell.2009.08.005)
  17. Endo T, Yamano K, Kawano S (2010) Structural basis for the disulfide relay system in the mitochondrial intermembrane space. *Antioxid Redox Signal* 13(9):1359–1373. doi:[10.1089/ars.2010.3099](https://doi.org/10.1089/ars.2010.3099)
  18. Fischer M, Horn S, Belkacemi A, Kojer K, Petrunger C, Habich M, Ali M, Kuttner V, Bien M, Kauff F, Dengjel J, Herrmann JM, Riemer J (2013) Protein import and oxidative folding in the mitochondrial intermembrane space of intact mammalian cells. *Mol Biol Cell* 24(14):2160–2170. doi:[10.1091/mbc.E12-12-0862](https://doi.org/10.1091/mbc.E12-12-0862)
  19. Herrmann JM, Riemer J (2010) The intermembrane space of mitochondria. *Antioxid Redox Signal* 13(9):1341–1358. doi:[10.1089/ars.2009.3063](https://doi.org/10.1089/ars.2009.3063)
  20. Sideris DP, Tokatlidis K (2010) Oxidative protein folding in the mitochondrial intermembrane space. *Antioxid Redox Signal* 13(8):1189–1204. doi:[10.1089/ars.2010.3157](https://doi.org/10.1089/ars.2010.3157)
  21. Hofmann S, Rothbauer U, Muhlenbein N, Neupert W, Gerbitz KD, Brunner M, Bauer MF (2002) The C66W mutation in the deafness dystonia peptide 1 (DDP1) affects the formation of functional DDP1.TIM13 complexes in the mitochondrial intermembrane space. *J Biol Chem* 277(26):23287–23293. doi:[10.1074/jbc.M201154200](https://doi.org/10.1074/jbc.M201154200)
  22. Koehler CM, Leuenberger D, Merchant S, Renold A, Junne T, Schatz G (1999) Human deafness dystonia syndrome is a mitochondrial disease. *Proc Natl Acad Sci U S A* 96(5):2141–2146
  23. Schagger H (2006) Tricine-SDS-PAGE. *Nat Protoc* 1(1):16–22. doi:[10.1038/nprot.2006.4](https://doi.org/10.1038/nprot.2006.4)

## Chemical Crosslinking in Intact Mitochondria

Rupa Banerjee\*, Umut Günsel\*, and Dejana Mokranjac

### Abstract

Many mitochondrial proteins perform their functions as components of large, multimeric complexes. Chemical crosslinking is a powerful method to analyze protein-protein interactions within such complexes. Using membrane-permeable crosslinkers and isolated intact mitochondria, protein-protein interactions that are secluded by two mitochondrial membranes can be readily analyzed in physiologically active, isolated organelles under a variety of physiological and pathophysiological conditions. Here, we describe two methods for chemical crosslinking in intact yeast mitochondria. The first method enables the analysis of ATP-dependent remodeling of mitochondrial protein complexes while the second one allows the identification of crosslinking partners of a protein of interest.

**Key words** Protein complex, Protein-protein interactions, Crosslinking, Mitochondria, TIM23 complex, Remodeling of protein complexes

---

### 1 Introduction

Recent proteomic analyses of isolated mitochondria demonstrate that these organelles contain about 900 different proteins in yeast and about 1200 in mammals [1, 2]. Many mitochondrial proteins perform their functions as components of large, multimeric complexes like the respiratory chain complexes, the mitochondrial protein translocases, and the mitochondrial ribosomes, to name a few. The analysis of protein-protein interactions within protein complexes in their native environment is not a trivial task. For mitochondrial protein complexes, this is further complicated by the facts that many protein-protein interactions are secluded by two membranes and that many mitochondrial protein complexes are membrane-integrated. Crosslinking has emerged as a powerful method to analyze mitochondrial protein complexes in their native environment, due to the availability of membrane-permeable

---

\* These authors contributed equally to this work.

crosslinking reagents and the possibility of isolating functionally intact mitochondria. Combined with methods to manipulate the physiological state of mitochondria, crosslinking can be used not only to analyze protein-protein interactions as such, but also to monitor dynamic conformational changes that protein complexes undergo in various states of their function.

Crosslinking is a process whereby two (or more) molecules are chemically joined by a covalent bond. Crosslinking reagents, or shortly crosslinkers, contain two (or more) reactive ends that can covalently bridge specific functional groups present in proteins or other biomolecules. Thereby, even weak and transient interactions can be stabilized, captured, and subsequently analyzed. Though crosslinking between different molecules is usually sought for, intramolecular crosslinking also takes place. When designing a crosslinking experiment, several characteristics of chemical crosslinkers should be considered. They are explained in more detail below and include their reactivity toward different functional groups, the length of their spacer arms, their membrane permeability, and the cleavability of the resulting crosslinks.

The most important feature of a chemical crosslinker is its reactivity toward different functional groups. Though many more crosslinking chemistries are available, crosslinkers containing *N*-hydroxysuccinimide esters and maleimides are particularly useful for crosslinking of mitochondrial proteins (*see Note 1*). *N*-hydroxysuccinimide esters react with primary amino groups present in side chain of lysine residues and at the N-terminus of every polypeptide chain, unless the N-terminus is blocked. Lysine residues are commonly present in proteins and are usually surface-exposed in folded proteins. Thus, they are readily available for crosslinking. Maleimides react with sulfhydryl groups present in side chain of cysteine residues. Cysteine residues occur relatively rarely in proteins and can also be buried in the hydrophobic core of proteins. In addition, they are often involved in the formation of disulfide bridges, making them inaccessible for crosslinking without previous reduction of the disulfide bond. Still, crosslinkers reactive toward cysteine residues have been successfully used with mitochondrial proteins [3]. Crosslinkers that have the same reactive groups at both ends are known as homobifunctional crosslinkers. Both amino group- and sulfhydryl group-specific homobifunctional crosslinkers are commercially available. Heterobifunctional crosslinkers react with one functional group on one end and with another functional group on the other end. Several amino- and sulfhydryl group-specific crosslinkers are available. The applicability of heterobifunctional and in particular of sulfhydryl-reactive homobifunctional crosslinkers may be limited by the occurrence of cysteine residues within the sequence of a protein of interest, which should therefore be checked beforehand.

Two reactive groups at the opposite ends of a crosslinker are separated by a spacer arm. The length of a spacer arm is usually measured in angstroms (Å) and it defines the distance between two functional groups that can be bridged by a particular crosslinker. Shorter spacer arms pose greater restrictions to crosslinking; however, such crosslinkers are usually more specific. Longer spacer arms are more flexible and reduce steric hindrance, but are therefore also more prone to capturing potentially nonspecific interactions. Spacer arm lengths range from zero length to over 100 Å. In our hands, spacer arms between 3 and 12 Å give the best results.

For crosslinking of mitochondrial proteins in intact organelles, the membrane-permeability of a crosslinker is a particularly important parameter and submitochondrial localization of the protein of interest should be carefully considered before designing a crosslinking experiment. Both membrane-permeable and membrane-impermeable crosslinkers can be used to analyze protein-protein interactions at the mitochondrial surface and, due to the presence of porins in the outer membrane, also in the intermembrane space. The inner mitochondrial membrane, however, poses a barrier for all membrane-impermeable molecules. Thus, only membrane-permeable crosslinkers can be used to capture protein-protein interactions in the mitochondrial matrix.

Crosslinkers generate a stable, covalent bond between two functional groups. Nevertheless, in some cases, it is desirable to recover individual crosslinked components. For this reason, spacer arms of some crosslinkers contain groups that are readily cleavable. The most commonly used cleavage site is a disulfide bridge present in the middle of a spacer arm that is cleaved in the presence of reducing agents such as  $\beta$ -mercaptoethanol or dithiothreitol.

In the absence of any available structural information, whether a crosslink between two proteins is observed or not is a matter of serendipitous arrangement of two reactive residues on two interacting proteins within a crosslinking distance of a chosen crosslinker. Therefore, we normally start by testing several different crosslinkers with various reactive groups and different lengths of spacer arms. The crosslinkers that we test first (*see Note 2*) are amino group-specific, homobifunctional crosslinkers 1,5-difluoro-2,4-dinitrobenzene (DFDNB, spacer arm length 3 Å), disuccinimidyl glutarate (DSG, 7.7 Å), and disuccinimidyl suberate (DSS, 11.4 Å), amino- and sulfhydryl group-specific heterobifunctional crosslinker *m*-maleimidobenzoyl-*N*-hydroxysuccinimide ester (MBS, 9.9 Å) and, if applicable, sulfhydryl group-specific, homobifunctional crosslinker 1,6-bis-maleimidohexane (BMH, 16.1 Å). They are all membrane-permeable, noncleavable crosslinkers. We have extensively applied chemical crosslinking with intact yeast mitochondria to analyze the TIM23 complex, the major protein translocase of the mitochondrial inner membrane, responsible for the transport of about 70% of all mitochondrial proteins

synthesized in the cytosol. Using the energy of membrane potential across the inner membrane and ATP in the matrix, the TIM23 complex mediates translocation of proteins across and their insertion into the inner membrane [4–8]. We have used chemical crosslinking to demonstrate the presence of an unknown component of the TIM23 complex and, in combination with a bioinformatics-based approach, identified Tim14 as the crosslinking partner of Tim44. Subsequent biochemical analysis revealed that Tim14 is an essential and highly conserved component of the TIM23 complex [9]. Furthermore, crosslinking in intact mitochondria proved to be a powerful method to follow structural rearrangements of the TIM23 complex under different physiological and pathophysiological conditions. By combining chemical crosslinking with manipulation of ATP levels in the mitochondrial matrix, we demonstrated structural rearrangements of the TIM23 complex during the ATP-hydrolysis driven cycle of mtHsp70, the ATP-consuming subunit of the complex [9–11]. When we analyzed mitochondria isolated from an mtHsp70 mutant, we observed that, under non-permissive conditions, the molecular environment of other components of the complex changed [9]. Moreover, we developed a method to *in vivo* trap the TIM23 complex at different stages of its activity and then used chemical crosslinking to demonstrate active remodeling of the TIM23 complex during translocation of proteins into mitochondria [12] and its dynamic interaction with the TOM complex, the major protein translocase of the mitochondrial outer membrane [13]. In addition, chemical crosslinking was extremely useful to analyze which subunits of the TIM23 complex are in close vicinity of translocating proteins at different stages of protein translocation into mitochondria [14].

Here, we describe two of our protocols for crosslinking in intact yeast mitochondria. In the first one, we manipulate the levels of ATP in the mitochondrial matrix prior to crosslinking. In the second one, we use crosslinking followed by an affinity purification step to identify the crosslinking partner of a protein of interest.

---

## 2 Materials

### 2.1 ATP-Dependent Crosslinking in Isolated Mitochondria

1. 2× SI buffer: 1.2 M sorbitol, 160 mM KCl, 20 mM Mg-acetate, 4 mM KH<sub>2</sub>PO<sub>4</sub>, 5 mM EDTA, 5 mM MnCl<sub>2</sub>, 100 mM HEPES-KOH, pH 7.2 (*see Note 3*). Store at –20 °C.
2. Oligomycin: make 2 mM solution in ethanol and store at –20 °C. This is a 200× stock.
3. Apyrase: make 1 U/μl solution and store in single use aliquots at –20 °C. This is a 100× stock.
4. ATP: make 0.2 M solution in water and adjust the pH with KOH to 7.0. This 50× stock is kept in aliquots at –20 °C.

5. NADH: make 0.2 M solution in water. This is a 40× stock and is kept in single use aliquots at  $-20^{\circ}\text{C}$ .
6. CP: make 1 M solution of creatine-phosphate in water. This 100× stock is kept in aliquots at  $-20^{\circ}\text{C}$ .
7. CK: make 10 mg/ml solution of creatine-kinase in water. This is 100× stock and is kept in single use aliquots at  $-20^{\circ}\text{C}$ .
8. DMSO: dimethyl sulfoxide.
9. DSS: prepare 7.5 mM disuccinimidyl suberate (DSS) in DMSO just prior to use (*see* **Notes 4–6**).
10. Glycine: make 1 M solution in water and adjust pH with KOH to 8.0. This 100× stock solution is kept in aliquots at  $-20^{\circ}\text{C}$  (*see* **Note 7**).
11. SH buffer: 0.6 M sorbitol, 20 mM HEPES-KOH, pH 7.2. Store in 50 ml aliquots at  $-20^{\circ}\text{C}$ .
12. Isolated yeast mitochondria at 10 mg/ml kept in single use aliquots at  $-80^{\circ}\text{C}$  (*see* **Note 8**).
13. Laemmli buffer: 60 mM Tris-HCl, pH 6.8, 10% (v/v) glycerol, 2% (w/v) SDS, 0.02% (w/v) bromophenol blue. Store at room temperature. Add  $\beta$ -mercaptoethanol to 3% (v/v) prior to use (*see* **Note 9**).

## **2.2 Crosslinking Followed by Affinity Purification**

1. Isolated wild-type yeast mitochondria and mitochondria containing a His-tagged version of the presumed crosslinking partner (*see* **Note 10**). Mitochondria are stored at  $-80^{\circ}\text{C}$  as single use aliquots at 10 mg/ml.
2. 2× SI buffer: 1.2 M sorbitol, 160 mM KCl, 20 mM Mg-acetate, 4 mM  $\text{KH}_2\text{PO}_4$ , 5 mM EDTA, 5 mM  $\text{MnCl}_2$ , 100 mM HEPES-KOH, pH 7.2 (*see* **Note 3**). Store at  $-20^{\circ}\text{C}$ .
3. ATP: prepare 0.2 M solution in water and adjust pH with KOH to 7.0. This is a 50× stock and is kept in aliquots at  $-20^{\circ}\text{C}$ .
4. NADH: prepare 0.2 M solution in water. This is a 40× stock and is stored in single use aliquots at  $-20^{\circ}\text{C}$ .
5. CP: prepare 1 M creatine-phosphate stock solution in water. This is a 100× stock solution that is stored in aliquots at  $-20^{\circ}\text{C}$ .
6. CK: prepare 10 mg/ml creatine-kinase solution in water. This is a 100× stock solution that is stored in single use aliquots at  $-20^{\circ}\text{C}$ .
7. DMSO.
8. DSS: prepare 7.5 mM stock solution of disuccinimidyl suberate in DMSO just prior to use (*see* **Notes 4–6**).

9. Glycine: prepare 1 M solution of glycine in water and adjust pH to 8.0 with KOH (*see Note 7*). Store in aliquots at  $-20^{\circ}\text{C}$ .
10. SH buffer: 0.6 M sorbitol, 20 mM HEPES-KOH, pH 7.2. Store in 50 ml aliquots at  $-20^{\circ}\text{C}$ .
11. Laemmli buffer: 60 mM Tris-HCl, pH 6.8, 10% (v/v) glycerol, 2% (w/v) SDS, 0.02% (w/v) bromophenol blue. Store at room temperature. Add freshly  $\beta$ -mercaptoethanol to 3% (v/v) (*see Note 9*).
12. Laemmli buffer with imidazole: Prepare 2 $\times$  Laemmli buffer (120 mM Tris-HCl, pH 6.8, 20% (v/v) glycerol, 4% (w/v) SDS, 0.04% bromophenol blue) and 1.5 M imidazole-HCl, pH 7.5. Mix 2 $\times$  Laemmli buffer, 1.5 M imidazole and water in 5:2:3 volume ratio. Store at room temperature. Add  $\beta$ -mercaptoethanol to 3% (v/v) prior to use (*see Note 9*).
13. Resuspension buffer: 50 mM Sodium phosphate buffer, 150 mM NaCl, 20 mM imidazole, pH 8.0.
14. Solubilization buffer: Add to Resuspension buffer SDS to 1% (w/v) from a 10% (w/v) stock in water (kept at  $-20^{\circ}\text{C}$ ). Just prior to use, add PMSF to 2 mM from a 0.2 M stock solution of phenylmethylsulfonyl fluoride in ethanol (stored at  $4^{\circ}\text{C}$ ).
15. Washing buffer: Add to Resuspension buffer Triton X-100 to 0.2% (v/v) from a 10% (v/v) stock solution in Resuspension buffer (stored at  $4^{\circ}\text{C}$ ). Just prior to use, add PMSF to 2 mM from a 0.2 M stock solution of phenylmethylsulfonyl fluoride in ethanol (stored at  $4^{\circ}\text{C}$ ).
16. Ni-NTA agarose.

---

### 3 Methods

#### **3.1 ATP-Dependent Crosslinking in Isolated Mitochondria**

This is a basic protocol to analyze protein-protein interactions by crosslinking in isolated mitochondria (*see Notes 11 and 12*). The ATP levels in mitochondria are manipulated prior to crosslinking to analyze the influence of the energy status of the organelle on protein-protein interactions (*see Note 13*). To assess the specificity of the observed crosslinks, a control sample is incubated in the absence of the crosslinker.

1. Mix, in tube 1, in the following order: 50  $\mu\text{l}$  of 2 $\times$  SI buffer, 38.5  $\mu\text{l}$  of water, and 5  $\mu\text{l}$  of mitochondria (*see Note 14*). This will be the tube where the control reaction without the crosslinker takes place.
2. Mix, in tube 2, in the following order: 50  $\mu\text{l}$  of 2 $\times$  SI buffer, 38.5  $\mu\text{l}$  of water, and 5  $\mu\text{l}$  of mitochondria. This will be the tube where the crosslinking reaction takes place in the presence of ATP.

3. Mix, in tube 3, in the following order: 50  $\mu\text{l}$  of 2 $\times$  SI buffer, 43.5  $\mu\text{l}$  of water, 1  $\mu\text{l}$  of apyrase, 0.5  $\mu\text{l}$  of oligomycin, and 5  $\mu\text{l}$  of mitochondria. This will be the tube where the crosslinking reaction takes place in the absence of ATP.
4. Incubate the tubes for 10 min at 25  $^{\circ}\text{C}$  (*see Note 15*).
5. Add 2  $\mu\text{l}$  of ATP, 2.5  $\mu\text{l}$  of NADH, and 1  $\mu\text{l}$  of each CP and CK, to tubes 1 and 2.
6. Incubate the tubes for 3 min at 25  $^{\circ}\text{C}$  (*see Note 16*).
7. Place all tubes on ice.
8. Add 1  $\mu\text{l}$  of DMSO to tube 1 and 1  $\mu\text{l}$  of DSS to both tubes 2 and 3.
9. Incubate the tubes for 30 min on ice (*see Note 17*).
10. Add 10  $\mu\text{l}$  of glycine to each tube and incubate for additional 10 min on ice. During this step excess of crosslinker is quenched and the reaction is stopped (*see Note 18*).
11. Add 500  $\mu\text{l}$  of SH buffer to each tube and pellet mitochondria by centrifugation at 18,000  $\times g$  for 10 min at 4  $^{\circ}\text{C}$ .
12. Remove the supernatants completely and resuspend the mitochondrial pellets in 20  $\mu\text{l}$  of Laemmli buffer.
13. Heat the samples to 95  $^{\circ}\text{C}$  for 3 min.
14. Analyze the samples by SDS-PAGE and western blotting (*see Notes 19 and 20*). One example of such an experiment is shown in Fig. 1.

### **3.2 Crosslinking Followed by Affinity Purification**

This protocol is used to confirm the identity of the crosslinking partner of the protein of interest, but it can also be used to enrich the crosslinks (*see Note 21*). Crosslinking is performed in wild type and in mitochondria containing a His-tagged version of the presumed crosslinking partner of a protein of interest. After quenching of excess crosslinker, mitochondria are solubilized in SDS-containing buffer to dissociate all noncovalent protein-protein interactions. His-tagged protein and its crosslinks are purified on Ni-NTA agarose beads.

1. Take 6 tubes and label them 1 to 6.
2. Mix, in tubes 1 and 4, in the following order: 50  $\mu\text{l}$  of 2 $\times$  SI buffer, 38.5  $\mu\text{l}$  of water, 2  $\mu\text{l}$  of ATP, 2.5  $\mu\text{l}$  of NADH, 1  $\mu\text{l}$  of CP, and 1  $\mu\text{l}$  of CK. Add 5  $\mu\text{l}$  of wild-type mitochondria to tube 1 and 5  $\mu\text{l}$  of His-tagged mitochondria to tube 4. Mix gently but thoroughly. These tubes will be used as non-crosslinked controls.
3. Mix, in tubes 3 and 6, in the following order: 300  $\mu\text{l}$  of 2 $\times$  SI buffer, 231  $\mu\text{l}$  of water, 12  $\mu\text{l}$  of ATP, 15  $\mu\text{l}$  of NADH, 6  $\mu\text{l}$  of CP, and 6  $\mu\text{l}$  of CK. Add 30  $\mu\text{l}$  of wild-type mitochondria to

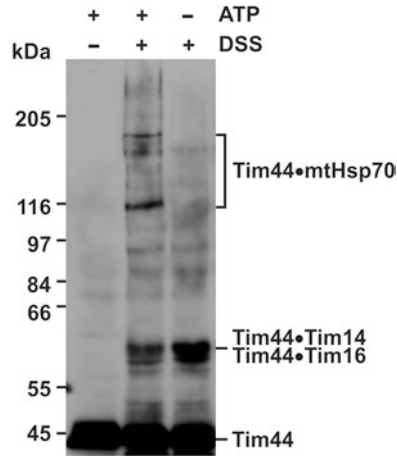


**Fig. 1** ATP-dependent crosslinking of Tim44 in isolated wild-type yeast mitochondria. Levels of ATP were manipulated in intact mitochondria prior to crosslinking with DSS. One sample was incubated in the absence of DSS as a control. After quenching of excess crosslinker, mitochondria were reisolated and samples were analyzed by SDS-PAGE and western blot using affinity purified antibodies against Tim44. In the samples incubated with DSS, multiple additional bands are visible that are absent in the control sample incubated in the absence of the crosslinker. They represent various crosslinking adducts of Tim44. The crosslinking patterns are different in the presence of high and low levels of matrix ATP showing that the molecular environment of Tim44 changes under these conditions. Known crosslinking partners of Tim44 are depicted

tube 3 and 30  $\mu$ l of His-tagged mitochondria to tube 6. Mix gently but thoroughly. These tubes will be used for crosslinking.

4. Incubate all tubes at 25  $^{\circ}$ C for 3 min.
5. Transfer all tubes on ice.
6. Add 1  $\mu$ l of DMSO to tubes 1 and 4 and 6  $\mu$ l of DSS to tubes 3 and 6.
7. Incubate all tubes on ice for 30 min.
8. Add 10  $\mu$ l of glycine to tubes 1 and 4, and 60  $\mu$ l of glycine to tubes 3 and 6.
9. Incubate all tubes on ice for 10 min.
10. Transfer 110  $\mu$ l of reaction mix from tube 3 to tube 2 and from tube 6 to tube 5. Tubes 2 and 5 will represent total crosslinking reactions.
11. Add 500  $\mu$ l of SH buffer to all tubes.
12. Centrifuge all tubes at  $18,000 \times g$  for 10 min at 4  $^{\circ}$ C.
13. Discard the supernatants carefully but completely.

14. Resuspend the pellets in tubes 1, 2, 4, and 5 in 40  $\mu\text{l}$  of Laemmli buffer each. Heat the samples for 5 min at 95  $^{\circ}\text{C}$  and keep them subsequently at -20  $^{\circ}\text{C}$  until loaded onto a SDS PA gel.
15. Resuspend the pellets in tubes 3 and 6 in 50  $\mu\text{l}$  of Solubilization buffer.
16. Mix the samples in a thermomixer for 5 min at RT.
17. Dilute the samples with 950  $\mu\text{l}$  of Washing buffer (*see Note 22*).
18. Centrifuge the samples at 125,000  $\times g$  for 20 min at 2  $^{\circ}\text{C}$ .
19. During this centrifugation step, prepare Ni-NTA agarose beads. For this, take 50  $\mu\text{l}$  of beads (volume of settled beads) to two tubes. Wash the beads three times with 1 ml of water and once with 500  $\mu\text{l}$  of Washing buffer. The step with the Washing buffer is done on an overhead mixer for 5 min in cold room and serves to equilibrate the beads.
20. Remove the Washing buffer from the beads and add the supernatants from the centrifugation step to Ni-NTA agarose beads (*see Note 23*).
21. Incubate the samples on an overhead mixer for 30 min at 4  $^{\circ}\text{C}$ . During this step His-tagged protein and its crosslinking adducts bind to Ni-NTA agarose beads.
22. Centrifuge the samples in a microfuge at max speed for 20 s at 4  $^{\circ}\text{C}$  and discard the supernatant.
23. Add 200  $\mu\text{l}$  of Washing buffer to the beads and incubate on an overhead mixer for 5 min at 4  $^{\circ}\text{C}$ . Centrifuge the samples in a microfuge at max speed for 20s at 4  $^{\circ}\text{C}$  and discard the supernatant.
24. Repeat **step 23** three times in total.
25. After the final washing step, carefully remove the entire Washing buffer from the beads (*see Note 24*).
26. Add 50  $\mu\text{l}$  of Laemmli buffer with imidazole to the beads, mix thoroughly (*see Note 25*), and heat the samples for 5 min at 95  $^{\circ}\text{C}$ .
27. Thaw the samples from **step 14** by briefly putting them at 95  $^{\circ}\text{C}$ .
28. Analyze all the samples by SDS PAGE and western blotting (*see Notes 19 and 20*). One example of such an experiment is shown in Fig. 2.

---

## 4 Notes

1. Other commonly used chemical crosslinkers are reactive toward carbohydrates and toward carboxyl groups. As mitochondrial proteins are normally not glycosylated, the former

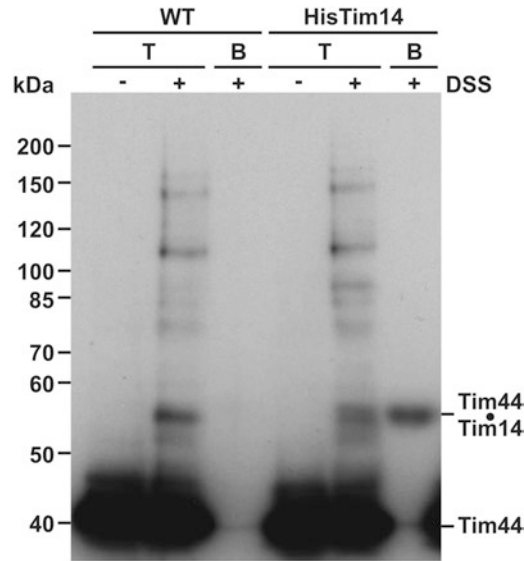


**Fig. 2** Tim44 is crosslinked to Tim14 in intact mitochondria. Wild type and mitochondria isolated from cells expressing the His-tagged version of Tim14 were subjected to crosslinking with DSS. After quenching of excess crosslinker, one aliquot was directly prepared for SDS-PAGE. The other aliquot was solubilized in SDS-containing buffer to dissociate all noncovalent interactions, and subsequently incubated with Ni-NTA agarose beads. After three washing steps, specifically bound proteins were eluted with Laemmli buffer containing 300 mM imidazole. All samples were analyzed by SDS-PAGE followed by western blot using affinity purified antibodies against Tim44. T, total mitochondria incubated in the presence or absence of DSS. B, material bound to Ni-NTA agarose beads. Total crosslinking patterns in both types of mitochondria are very similar; however, only one crosslinking adduct specifically bound to Ni-NTA agarose beads when mitochondria containing the His-tagged version of Tim14 were used for crosslinking. Since this crosslink is decorated with antibodies against Tim44 and it binds to Ni-NTA agarose beads, it represents the crosslink between Tim44 and Tim14. Note that non-crosslinked Tim44 is not recovered in the fraction bound to Ni-NTA agarose beads further demonstrating the specificity of the assay

ones are not particularly useful for the analysis of mitochondrial proteins. The applicability of the latter ones is limited due to the fact that they are only available as zero-length crosslinkers and that the crosslinking process requires acidic pH that is frequently incompatible with mitochondrial processes.

2. The most comprehensive list of commercially available crosslinkers is available from Pierce (currently a member of the Thermo Fisher Scientific group). Their crosslinking reagents technical handbook as well as crosslinker selection tool available online are excellent resources when planning crosslinking experiments.
3. The SI buffer was originally developed for studying the import of *in vitro* synthesized precursor proteins into isolated

mitochondria. We also use it for crosslinking to be able to compare different experiments. However, we have also successfully performed crosslinking in other buffers. Several points need to be considered when designing a buffer used for crosslinking. First, the buffer should keep isolated mitochondria intact. 0.6 M sorbitol or 250 mM sucrose is commonly used for this purpose. Second, primary amine buffers such as Tris are incompatible with amino group-specific crosslinkers as they compete with the crosslinking reaction. For the same reason sulfhydryl group-containing reagents such as  $\beta$ -mercaptoethanol or DTT are incompatible with sulfhydryl group-specific crosslinkers. Third, pH of the buffer should be compatible with both the crosslinking chemistry and the mitochondrial protein complex analyzed. Crosslinking with NHS esters can be done at pH between 7 and 9, though pH closer to 7 is preferred as NHS esters hydrolyze more readily at higher pH, competing with the crosslinking reactions. Crosslinking with maleimides is typically done at pH between 6.5 and 7.5. More alkaline conditions favor crosslinking with amino groups, reducing the specificity of the crosslinking reaction and they also result in increased rates of hydrolysis of maleimides.

4. Chemical crosslinkers are hygroscopic substances. We store them carefully closed and in the presence of desiccants at 4 °C. Also, we leave them at RT for at least 30 min before opening the bottles and weighing them in. We always prepare fresh solutions of crosslinkers and therefore weigh in as little as possible. Some of the crosslinkers are now commercially available as pre-weighted, single use tubes.
5. Membrane-permeable crosslinkers such as DSS are insoluble in water but are soluble in DMSO or DMF. We typically use DMSO to dissolve them but have also used DMF without any difference to the outcome of the experiment. The crosslinkers are dissolved just prior to use to minimize hydrolysis that inactivates them.
6. The optimal concentration of the crosslinker has to be experimentally determined for every protein-protein interaction. During the exploratory phase, we test several concentrations of crosslinkers, typically in the range of 2–50 mM (corresponding to 20–500  $\mu$ M final concentration in the crosslinking reactions). In our hands, 75–200  $\mu$ M final concentrations usually give the best results. Lower concentrations are usually insufficient to produce any visible crosslinks whereas the higher ones tend to give smeary gels with poorly resolved crosslinking patterns.
7. Glycine is used to quench excess amino-group-specific crosslinker at the end of the crosslinking reaction. 1 M Tris-HCl,

pH 8.0, can be used for the same purpose. For sulfhydryl group-specific crosslinkers, both homo- and heterobifunctional, we use freshly prepared 0.5 M cysteine, pH 8.0 as the quenching reagent. For quenching of sulfhydryl group-specific homobifunctional crosslinkers, free thiols can be used as well. However, note that free thiols are incompatible with some of the cleavable crosslinkers as they will reduce the disulfide bridge in the spacer arm of the crosslinker effectively destroying the crosslinks.

8. We keep mitochondria frozen at  $-80^{\circ}\text{C}$  in single use aliquots. It is advisable to thaw the needed aliquots by hand warming and place them immediately on ice. Use them as soon as possible after thawing. Keeping them for long, even on ice, strongly reduces the quality of the mitochondria.
9. Keep in mind that  $\beta$ -mercaptoethanol is incompatible with some cleavable crosslinkers.
10. Identifying the crosslinking partner of a particular protein is rarely trivial. It is sometimes possible to make educated guesses about the crosslinking partners based on the molecular masses of the obtained crosslinks and the known molecular masses of other components of the same complex. However, it is important to keep in mind that the major crosslinking partner of a protein of interest may not also always be its major interaction partner. For example, in the TIM23 complex, Tim17 and Tim23 form a stable core of the complex; however, in wild-type mitochondria so far no crosslinks of the two proteins were observed. In contrast, Tim23 is readily crosslinked to Pam17, a minor component of the complex that has almost the same molecular mass as Tim17 [12, 15].

Crosslinking can also be used to identify novel components of the complex. We have, for example, shown that Tim44 can be crosslinked to an, at that time, unidentified protein. To identify this protein, we searched yeast databases for a protein that is essential for cell viability (assumption based on the fact that all that-far known components of the TIM23 complex were essential for cell viability), is of unknown function, is known, or can be predicted, to be in mitochondria and has a molecular mass that would fit to the size of the observed crosslink. This search led to the identification of Tim14 and we used essentially the experiment described in this chapter to confirm that this protein is indeed the crosslinking partner of Tim44 [9].

It is also possible to upscale the experiment described here and subsequently identify the crosslinking partners by mass spectrometry [16].

A limited number of crosslinkers are available as mixtures of light and heavy (deuterated) versions of the crosslinker. Such

mixtures greatly facilitate identification of the crosslinked peptides in mass spectra. So far, they have only been used with purified protein complexes to provide spatial restraints for structural models and to complement structural analysis by electron microscopy and x-ray crystallography [17–20]. This approach, however, holds much promise and it is likely that in the near future it will be adapted to protein complexes embedded in their native environment.

11. This protocol has been developed for mitochondria isolated from yeast *Saccharomyces cerevisiae*. We have successfully also used it, without essentially any modification, with mitochondria isolated from *Neurospora crassa*, various mouse tissues, and human cell lines. It should be noted that mammalian mitochondria were always freshly isolated for the experiments as freezing irreversibly damages them. In case of *Neurospora* mitochondria, freezing leads to the rupture of the outer membrane but the inner membrane remains intact.
12. We describe the method using isolated wild-type mitochondria. However, mitochondria isolated from mutant strains can be used to, for example, analyze the rearrangements of complexes upon removal of one of its components [9, 10, 12, 21]. Such experiments can be very revealing to understand assembly of complexes.
13. In the protocol described, ATP levels in the matrix are manipulated prior to crosslinking. One can also easily manipulate membrane potential,  $\text{Ca}^{2+}$  levels, redox state, or translocation load in isolated organelles. Such experiments can provide important insight into remodeling of the complexes upon various stimuli.
14. Make sure that the content of the tube is mixed thoroughly after addition of every new solution. However, do not vortex vigorously as this can damage mitochondria.
15. During this incubation step, turnover of pre-existing ATP is promoted. In addition, in tube 3, oligomycin, a specific inhibitor of ATP synthase, prevents new synthesis of ATP, and apyrase hydrolyses any ATP and ADP potentially present outside of mitochondria.
16. During this incubation, mitochondria in tube 1 and tube 2 are again energized and ATP levels are kept high by the addition of an ATP-regenerating system consisting of CP and CK.
17. In our hands, crosslinking for 30 min on ice gives the best results. However, different incubation times (as short as 10 min and as long as few hours) and higher temperature (25 °C) should be tested during an exploratory phase. Crosslinking at higher temperature is usually more efficient; however, we

observed that it can lead to smeary gels with poorly resolved crosslinks.

18. Some crosslinking protocols omit a quenching step. Though this is possible when crosslinking with purified proteins is done, we think it is advisable to always include such a step when crosslinking is performed in intact mitochondria. Quenching of excess crosslinker prevents nonspecific crosslinking that would otherwise take place in subsequent steps upon solubilization of mitochondria in Laemmli buffer.
19. The percentage of acrylamide in SDS-PA gels should be chosen in such a way that the protein of interest in its non-crosslinked form runs in the lower third or quarter of the gel. In this way, the major part of the separation gel can be used to resolve the crosslinks. In order to be able to judge the molecular masses of the obtained crosslinks as precisely as possible, we usually use special molecular weight markers for these experiments. These should contain as many markers as possible and also cover higher molecular weights than usual to accommodate for increased sizes of the crosslinks as compared to non-crosslinked proteins.
20. The quality of the antibodies is essential for successful detection of crosslinks. We only use affinity purified antibodies for these experiments as nonpurified sera usually contain many nonspecific cross-reactions that severely hinder subsequent analyses. Also, it is important to keep in mind that crosslinking may destroy the epitopes recognized by the antibodies. Therefore, it is safer to use polyclonal rather than monoclonal antibodies for western blotting after crosslinking. Since the efficiency of crosslinking in intact mitochondria is usually not very high, it is sometimes helpful to use lower dilutions or prepare fresh antibodies for subsequent western blotting. We often observe that the band of the noncrosslinked protein is burnt through before any crosslink can be seen.
21. A similar protocol can be used to enrich very weak crosslinks that would otherwise not be visible at all. In such cases we use cleavable crosslinkers like DSP and follow the same protocol [13]. In the final elution step,  $\beta$ -mercaptoethanol in the Laemmli buffer with imidazole will cleave the disulfide bond in the spacer arm of DSP so that all crosslinking partners can be analyzed at their original molecular masses. With such experiments, it is advisable to do affinity purification steps also with samples without crosslinkers—only in this way it is possible to make sure that it is indeed the crosslinked protein that binds to the affinity beads.

22. Binding of proteins to Ni-NTA agarose beads is very inefficient in 1% SDS. Therefore, the samples are diluted with buffer containing 0.2% Triton X-100 that is compatible with binding.
23. All the steps from here on to the final elution from the beads are done in cold room. This significantly reduces proteolytic degradation of crosslinks.
24. It is important to remove the buffer completely at this step. We essentially dry out the beads by going in with the yellow tip all the way to the bottom of the tube and then aspirate the buffer. Care should be taken not to lose any beads in this step. If available, gel-loading tips are handy for this purpose.
25. Samples should not be pipetted up and down at this step as most of the beads will stick to the tips. Rather, the samples are placed in a thermomixer rack and mixed by brisk shaking with the hand.

---

## Acknowledgments

We would like to thank Drs Fabiana Perocchi and Walter Neupert for the comments on the manuscript. This work was supported by Deutsche Forschungsgemeinschaft (grant MO1944/1-1 to D.M.) and Deutscher Akademischer Austauschdienst (to R.B).

## References

1. Reinders J, Zahedi RP, Pfanner N, Meisinger C, Sickmann A (2006) Toward the complete yeast mitochondrial proteome: multidimensional separation techniques for mitochondrial proteomics. *J Proteome Res* 5(7):1543–1554. doi:[10.1021/pr050477f](https://doi.org/10.1021/pr050477f)
2. Pagliarini DJ, Calvo SE, Chang B, Sheth SA, Vafai SB, Ong SE, Walford GA, Sugiana C, Boneh A, Chen WK, Hill DE, Vidal M, Evans JG, Thorburn DR, Carr SA, Mootha VK (2008) A mitochondrial protein compendium elucidates complex I disease biology. *Cell* 134(1):112–123. doi:[10.1016/j.cell.2008.06.016](https://doi.org/10.1016/j.cell.2008.06.016)
3. Paschen SA, Rothbauer U, Kaldi K, Bauer MF, Neupert W, Brunner M (2000) The role of the TIM8-13 complex in the import of Tim23 into mitochondria. *EMBO J* 19(23):6392–6400
4. Endo T, Yamano K (2009) Multiple pathways for mitochondrial protein traffic. *Biol Chem* 390(8):723–730
5. Marom M, Azem A, Mokranjac D (2011) Understanding the molecular mechanism of protein translocation across the mitochondrial inner membrane: still a long way to go. *Biochim Biophys Acta* 1808(3):990–1001. doi:[10.1016/j.bbamem.2010.07.011](https://doi.org/10.1016/j.bbamem.2010.07.011)
6. Neupert W (2015) A perspective on transport of proteins into mitochondria: a myriad of open questions. *J Mol Biol* 427(6 Pt A):1135–1158. doi:[10.1016/j.jmb.2015.02.001](https://doi.org/10.1016/j.jmb.2015.02.001)
7. Schulz C, Schendzielorz A, Rehling P (2015) Unlocking the presequence import pathway. *Trends Cell Biol* 25(5):265–275. doi:[10.1016/j.tcb.2014.12.001](https://doi.org/10.1016/j.tcb.2014.12.001)
8. Stojanovski D, Bohnert M, Pfanner N, van der Laan M (2012) Mechanisms of protein sorting in mitochondria. *Cold Spring Harb Perspect Biol* 4(10). doi:[10.1101/cshperspect.a011320](https://doi.org/10.1101/cshperspect.a011320)
9. Mokranjac D, Sichtung M, Neupert W, Hell K (2003) Tim14, a novel key component of the import motor of the TIM23 protein translocase of mitochondria. *EMBO J* 22(19):4945–4956. doi:[10.1093/emboj/cdg485](https://doi.org/10.1093/emboj/cdg485)
10. Kozany C, Mokranjac D, Sichtung M, Neupert W, Hell K (2004) The J domain-related cochaperone Tim16 is a constituent of the mitochondrial TIM23 preprotein translocase. *Nat Struct Mol Biol* 11(3):234–241. doi:[10.1038/nsmb734](https://doi.org/10.1038/nsmb734)

11. Mokranjac D, Sighting M, Popov-Celeketic D, Berg A, Hell K, Neupert W (2005) The import motor of the yeast mitochondrial TIM23 preprotein translocase contains two different J proteins, Tim14 and Mdj2. *J Biol Chem* 280(36):31608–31614. doi:[10.1074/jbc.M502397200](https://doi.org/10.1074/jbc.M502397200)
12. Popov-Celeketic D, Mapa K, Neupert W, Mokranjac D (2008) Active remodelling of the TIM23 complex during translocation of pre-proteins into mitochondria. *EMBO J* 27(10):1469–1480
13. Waegemann K, Popov-Celeketic D, Neupert W, Azem A, Mokranjac D (2015) Cooperation of TOM and TIM23 complexes during translocation of proteins into mitochondria. *J Mol Biol* 427(5):1075–1084. doi:[10.1016/j.jmb.2014.07.015](https://doi.org/10.1016/j.jmb.2014.07.015)
14. Mokranjac D, Paschen SA, Kozany C, Prokisch H, Hoppins SC, Nargang FE, Neupert W, Hell K (2003) Tim50, a novel component of the TIM23 preprotein translocase of mitochondria. *EMBO J* 22(4):816–825. doi:[10.1093/emboj/cdg090](https://doi.org/10.1093/emboj/cdg090)
15. Hutu DP, Guiard B, Chacinska A, Becker D, Pfanner N, Rehling P, van der Laan M (2008) Mitochondrial protein import motor: differential role of Tim44 in the recruitment of Pam17 and J-complex to the presequence translocase. *Mol Biol Cell* 19(6):2642–2649. doi:[10.1091/mbc.E07-12-1226](https://doi.org/10.1091/mbc.E07-12-1226)
16. Gruschke S, Kehrein K, Rompler K, Grone K, Israel L, Imhof A, Herrmann JM, Ott M (2011) Cbp3-Cbp6 interacts with the yeast mitochondrial ribosomal tunnel exit and promotes cytochrome b synthesis and assembly. *J Cell Biol* 193(6):1101–1114. doi:[10.1083/jcb.201103132](https://doi.org/10.1083/jcb.201103132)
17. Bernecky C, Herzog F, Baumeister W, Plitzko JM, Cramer P (2016) Structure of transcribing mammalian RNA polymerase II. *Nature* 529(7587):551–554. doi:[10.1038/nature16482](https://doi.org/10.1038/nature16482)
18. Greber BJ, Bieri P, Leibundgut M, Leitner A, Aebersold R, Boehringer D, Ban N (2015) Ribosome. The complete structure of the 55S mammalian mitochondrial ribosome. *Science* 348(6232):303–308. doi:[10.1126/science.aaa3872](https://doi.org/10.1126/science.aaa3872)
19. Herzog F, Kahraman A, Boehringer D, Mak R, Bracher A, Walzthoeni T, Leitner A, Beck M, Hartl FU, Ban N, Malmstrom L, Aebersold R (2012) Structural probing of a protein phosphatase 2A network by chemical cross-linking and mass spectrometry. *Science* 337(6100):1348–1352. doi:[10.1126/science.1221483](https://doi.org/10.1126/science.1221483)
20. Leitner A, Faini M, Stengel F, Aebersold R (2016) Crosslinking and mass spectrometry: an integrated technology to understand the structure and function of molecular machines. *Trends Biochem Sci* 41(1):20–32. doi:[10.1016/j.tibs.2015.10.008](https://doi.org/10.1016/j.tibs.2015.10.008)
21. Banerjee R, Gladkova C, Mapa K, Witte G, Mokranjac D (2015) Protein translocation channel of mitochondrial inner membrane and matrix-exposed import motor communicate via two-domain coupling protein. *Elife* 4:e11897. doi:[10.7554/eLife.11897](https://doi.org/10.7554/eLife.11897)

## Reconstitution of Mitochondrial Membrane Proteins into Nanodiscs by Cell-Free Expression

Ketan Malhotra and Nathan N. Alder

### Abstract

The isolation and characterization of mitochondrial membrane proteins is technically challenging because they natively reside within the specialized environment of the lipid bilayer, an environment that must be recapitulated to some degree during reconstitution to ensure proper folding, stability, and function. Here we describe protocols for the assembly of a membrane protein into lipid bilayer nanodiscs in a series of cell-free reactions. Cell-free expression of membrane proteins circumvents problems attendant with *in vivo* expression such as cytotoxicity, low expression levels, and the formation of inclusion bodies. Nanodiscs are artificial membrane systems comprised of discoidal lipid bilayer particles bound by annuli of amphipathic scaffold protein that shield lipid acyl chains from water. They are therefore excellent platforms for membrane protein reconstitution and downstream solution-based biochemical and biophysical analysis. This chapter details the procedures for the reconstitution of a mitochondrial membrane protein into nanodiscs using two different types of approaches: cotranslational and posttranslational assembly. These strategies are broadly applicable for different mitochondrial membrane proteins. They are also applicable for the use of nanodiscs with distinct lipid compositions that are biomimetic for different mitochondrial membranes and that recapitulate lipid profiles associated with pathological disorders in lipid metabolism.

**Key words** Nanodisc, Mitochondria, Membrane protein, Cell-free translation

---

### 1 Introduction

Mitochondria are morphologically complex organelles that are bound by two membranes, each with a distinct lipid and protein composition. The outer membrane (OM) contains both  $\alpha$ -helical and  $\beta$ -barrel transmembrane proteins and a membrane protein content of ~50% by mass. By contrast, the highly convoluted inner membrane (IM) contains membrane proteins that are exclusively  $\alpha$ -helical, with a remarkable membrane protein content of ~75% by mass [1]. Considered another way, among the mitochondrial proteome (~1500 individual proteins in mammals or ~900 individual proteins in yeast), about 25% of mitochondria-resident proteins are associated with or embedded in the OM or IM [2, 3]. The ability to express, isolate, and functionally characterize membrane proteins

is therefore vital to our understanding of mitochondrial physiology. More generally, because membrane proteins constitute roughly one-half of pharmaceutical targets [4], their production and functional characterization is critical for drug development. But owing to their hydrophobicity, integral membrane proteins are notoriously difficult to express and purify by traditional experimental approaches, creating a major bottleneck in their biochemical, biophysical, and structural analysis. This chapter describes procedures that leverage the technical advantages of cell-free biosynthetic systems with advances in the use of nanoscale lipid bilayers for the expression and functional reconstitution of a mitochondrial membrane protein.

Cell-free protein translation systems are based on biosynthetic machinery that is isolated from metabolically active cells with relatively low amounts of endogenous messenger RNA (mRNA). The most commonly used lysates include those from rabbit reticulocytes, from bacterial cells, and from wheat germ embryos. These lysates include the components essential for translation: ribosomes, transfer RNAs (tRNAs), aminoacyl tRNA synthetases, and translation initiation, elongation, and termination factors. In cell-free translation reactions, these lysates are supplemented with mixtures that enhance protein translation, including energy generating systems and amino acids. Some systems entail programming the reaction with plasmid or linear DNA that encodes the protein of interest and from which mRNA transcripts are synthesized by endogenous RNA polymerases. In other systems, purified mRNA transcripts that are prepared during a separate *in vitro* transcription reaction are added to the cell-free translation.

Cell-free protein synthesis reactions confer several advantages over conventional expression systems (e.g., in live *Escherichia coli*, yeast, or insect cells), particularly for the expression of membrane proteins. Most notably, because living cells are not involved in the reaction, cell-free systems avoid the potential cytotoxicity of expressing hydrophobic proteins, plasmid instability, and issues associated with cellular protein trafficking and membrane integration, all of which can result in low protein yield [5, 6]. Moreover, because cell-free expression systems are open, they allow for unrestricted experimental access to the reaction for the inclusion of additives such as cofactors and probes for site-specific protein labeling (e.g., with fluorescent or EPR probes). Of course, the native milieu of a membrane protein is a lipid bilayer, and several strategies have been utilized that provide additives that mimic the nonpolar membrane environment within cell-free systems for proper folding and stability of translated proteins. By one approach, reactions contain mild nonionic detergents that are compatible with the biosynthetic machinery and allow for the cotranslational stabilization of membrane proteins in proteo-micelle complexes [5, 7]. In addition, synthetic surfactants including organic

amphipathic polymers (amphipols), fluorinated surfactants, and designed peptide surfactants have been shown to stabilize membrane proteins produced by cell-free translation [8–14].

Recent advances in model membrane systems have provided new mechanisms for the reconstitution of membrane proteins into a lipidic environment. By comparison with the above hydrophobic additives, such model membranes allow proteins to fold into physiologically relevant lamellar lipid bilayers and can satisfy requirements of specific lipid interactions for membrane protein function [15–17]. Cell-free reconstitution strategies for membrane proteins have been reported using liposomes, spherical lipid vesicles of different diameter [18–21] and bicelles, and discoidal assemblies of lipids with outer edges of short-chain lipid or detergent [22–24]. However, nanoscale lipid bilayers belted by rings of amphipathic protein or copolymers have emerged as excellent membrane mimetics for experimentation due to their small size, stability, monodispersity, and wide range of compatible lipids [25]. Most notable for cell-free translation systems, nanodiscs—discoidal nanoscale lipid bilayers that are stabilized by annuli of amphipathic polypeptides—allow for the reconstitution of membrane proteins into lamellar bilayer systems that are amenable to solution-based biochemical, biophysical, and structural analysis. Developed originally by Sligar and colleagues, nanodiscs comprise bilayers of synthetic or naturally derived lipids enclosed by engineered variants of apolipoprotein A-1, termed as membrane scaffold protein (MSP) [26–28]. Nanodiscs have most widely been used for the reconstitution of overexpressed and purified membrane proteins, as recently reviewed [29]. However, several groups have recently shown the utility of nanodiscs in the reconstitution of membrane proteins synthesized by cell-free systems [23, 30–35]. In this regard, multiple reconstitution strategies have been reported, including the cotranslational insertion of membrane proteins into preassembled nanodiscs added to the translation reaction and the simultaneous formation of nanodiscs and the target membrane protein.

In this chapter, we describe methods for the cell-free synthesis and nanodisc reconstitution of Tim23, the central subunit of the TIM23 protein transport complex of the mitochondrial inner membrane. The workflow (Fig. 1) includes all necessary steps for the setup of the cell-free system, which is based on wheat germ lysates and programmed with purified mRNA transcripts that encode Tim23. We provide procedures for cotranslational assembly of Tim23-containing nanodiscs (wherein Tim23 is synthesized in the presence of preformed nanodiscs) as well as for posttranslational assembly (wherein pre-synthesized Tim23 is added to nanodisc assembly reactions). These two distinct approaches are provided because different target proteins may be more amenable for reconstitution by one approach over the other.

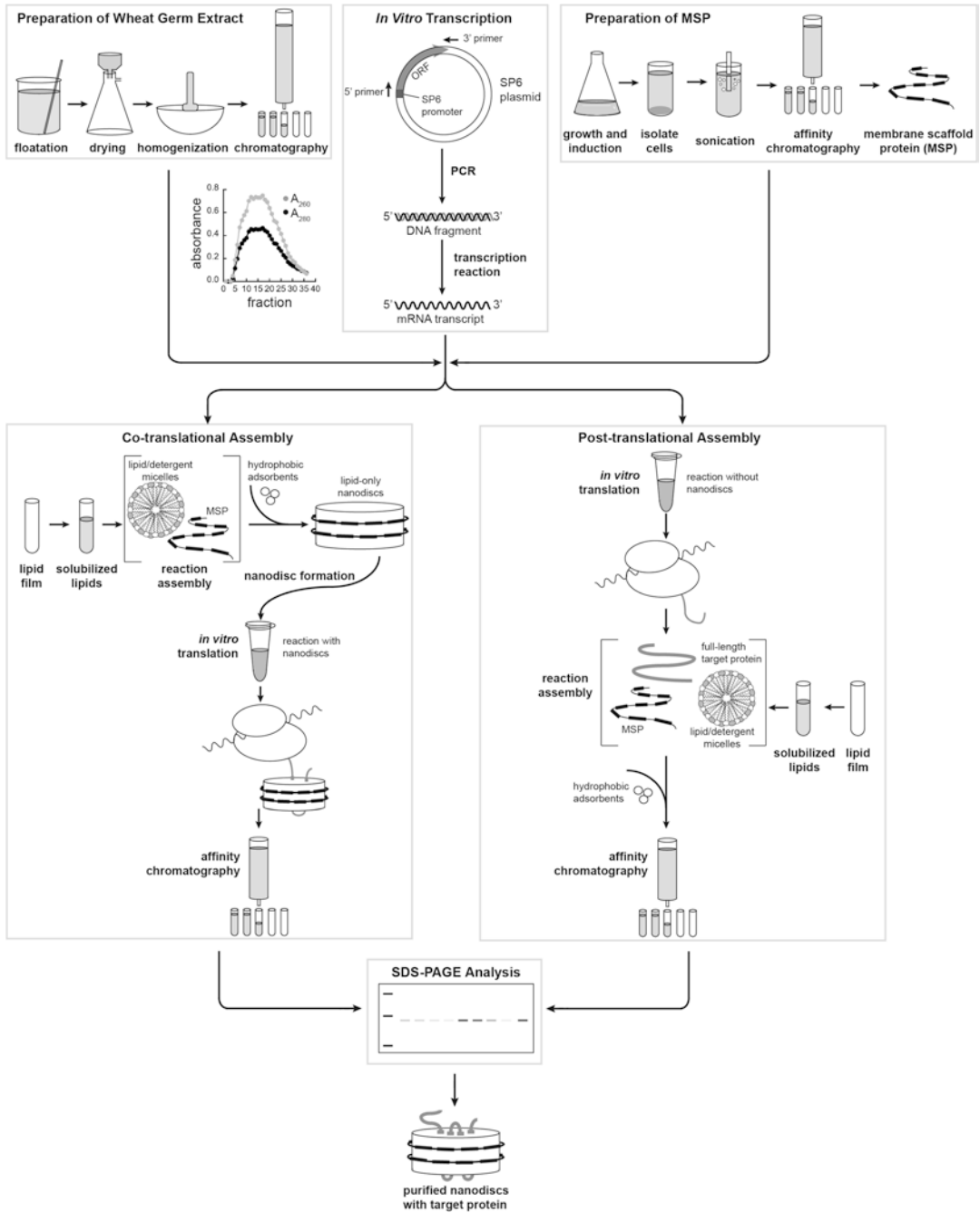


**Fig. 1** Protocol flowchart, including Preparation of Wheat Germ Extract (Subheadings 2.1 and 3.1), In Vitro Transcription (Subheadings 2.2 and 3.2), Preparation of MSP (Subheadings 2.3 and 3.3), Assembly of Nanodiscs with Target Protein (Subheadings 2.4 and 3.4), and Gel-Based Analysis of Assembly (Subheadings 2.5 and 3.5)

## 2 Materials

### 2.1 Preparation of Wheat Germ Extract (See Note 1)

1. Wheat germ, untreated (Sigma W0125) (*see Note 2*).
2. Mortar and pestle (*see Note 3*).
3. Flootation solvent: carbon tetrachloride and cyclohexane (3:1 v/v).
4. Liquid nitrogen.
5. Homogenization buffer: 40 mM HEPES-KOH, pH 7.5, 100 mM KOAc, 1 mM Mg(OAc)<sub>2</sub>, 2 mM CaCl<sub>2</sub>, and 4 mM DTT (*see Note 4*).
6. Column buffer: 40 mM HEPES-KOH, pH 7.5, 100 mM KOAc, 5 mM Mg(OAc)<sub>2</sub>, and 4 mM DTT (*see Note 4*).
7. Buchner funnel and Whatman #1 filter paper with corresponding diameter.
8. Centrifuge and 50 mL centrifuge tubes.
9. Column (approximately 2.5 cm I.D. × 28 cm length, bed volume 140 mL) packed with gel filtration medium (Sephadex G-25, fine) and equilibrated with column buffer (*see Note 5*).
10. Fraction collector
11. 1% (v/v) SDS.
12. UV-visible absorbance spectrophotometer and 1 mL quartz cuvette.

### 2.2 In Vitro Transcription (See Note 6)

1. Transcription vector containing the gene of interest under an SP6 promoter (*see Note 7*).
2. Primers for DNA amplification of the gene of interest. The upstream (5') oligonucleotide is complementary to the plasmid SP6 promoter, and the downstream (3') oligonucleotide is complementary to the gene sequence downstream of the stop codon (*see Notes 8 and 9*).
3. DNA polymerase and dNTP mix (*see Note 10*).
4. PCR cleanup kit (*see Note 11*).
5. PCR thermal cycler and thin-walled PCR tubes (*see Note 12*).
6. Refrigerated microcentrifuge.
7. Transcription buffer (10× Master Mix): 1 M HEPES-KOH, pH 7.5, 200 mM MgCl<sub>2</sub>, and 25 mM spermidine.
8. 100 mM DTT.
9. Ribonucleotide triphosphate (rNTP) solution mixture: 100 mM each of rATP, rGTP, rUTP, and rCTP in 20 mM Tris-HCl, pH 7.5.
10. 0.1 U/μL diguanosine triphosphate [G(5')ppp(5')G] (New England Biolabs #S1407).

11. 20 U/ $\mu$ L ribonuclease inhibitor (RNasin).
12. 0.5 U/ $\mu$ L pyrophosphatase.
13. SP6 RNA polymerase (*see Note 13*).
14. Thermoblock or water bath for incubation of reactions in microfuge tubes.
15. 3 M NaOAc, pH 5.2.
16. 100% Ethanol.
17. TE buffer: 10 mM Tris, pH 7.5, 1 mM EDTA, pH 7.5.
18. Rotary evaporator.

### 2.3 Preparation of MSP

1. YT culture medium: 0.5% (w/v) yeast extract, 0.8% (w/v) tryptone, 80 mM NaCl.
2. YT-agar selective medium: 0.5% (w/v) yeast extract, 0.8% (w/v) tryptone, 80 mM NaCl, 1.5% (w/v) agar, 25  $\mu$ g/mL kanamycin (*see Note 14*).
3. SOC medium: 0.5% (w/v) yeast extract, 2% (w/v) tryptone, 8.5 mM NaCl, 2.5 mM KCl, 10 mM MgCl<sub>2</sub>, 20 mM D-glucose (*see Note 15*).
4. 20% (w/v) D-glucose, filter-sterilized with 0.22  $\mu$ m filter.
5. BL21 (DE3) chemically competent *E. coli* cells (*see Note 16*).
6. pET28a:MSP1E3D1 plasmid DNA (*see Note 17*).
7. 50 mg/mL kanamycin (*see Note 18*).
8. Growth medium: YT culture medium, 0.2% (w/v) filter-sterilized glucose, 25  $\mu$ g/mL kanamycin (*see Note 19*).
9. 1M isopropyl- $\beta$ -D-thiogalactopyranoside (IPTG) in H<sub>2</sub>O.
10. 500 mM phenylmethanesulfonyl fluoride (PMSF) in 100% ethanol.
11. 10% (v/v) Triton X-100.
12. Ultrasonic liquid processor with microtip (*see Note 20*).
13. Ni-NTA agarose and chromatography column approx. 0.8 cm I.D.  $\times$  4 cm length.
14. Resuspension buffer: 20 mM Na-phosphate, pH 7.5
15. Column wash 1 buffer: 40 mM Tris-HCl, pH 8.0, 300 mM NaCl, 1% (v/v) Triton X-100.
16. Column wash 2 buffer: 40 mM Tris-HCl, pH 8.0, 300 mM NaCl, 20 mM imidazole, 50 mM Na-cholate.
17. Column wash 3 buffer: 40 mM Tris-HCl, pH 8.0, 300 mM NaCl, 50 mM imidazole.
18. Column elution buffer: 40 mM Tris-HCl, pH 8.0, 300 mM NaCl, 400 mM imidazole.

19. Dialysis buffer: 20 mM Tris-HCl, pH 7.5, 100 mM NaCl, 0.5 mM EDTA.
20. Dialysis cassette with 2000 Da molecular weight cutoff (MWCO).

#### **2.4 Assembly of Nanodiscs with Target Protein**

1. Pyrex 50 mL round-bottom centrifuge tube.
2. Rotary evaporator.
3. Source of compressed nitrogen gas.
4. Stocks of synthetic lipids in chloroform, each at a concentration of 25 mg/mL. The lipid stocks include: (a) 1-hexadecanoyl-2-(9Z-octadecenoyl)-*sn*-glycero-3-phosphocholine (POPC; Avanti #850457C), (b) 1-hexadecanoyl-2-(9Z-octadecenoyl)-*sn*-glycero-3-phosphocholine (POPE; Avanti #850757C), and (c) 1,1',2,2'-tetra-(9Z-octadecenoyl) cardiolipin (TOCL; Avanti #710335C) (*see Note 21*).
5. ND buffer A: 20 mM Tris-HCl, pH 7.5, 100 mM NaCl, 0.5 mM EDTA.
6. ND buffer B: 20 mM Tris-HCl, pH 7.5, 100 mM NaCl, 0.5 mM EDTA, 59 mM Na-cholate.
7. ND column buffer 1: 40 mM Tris-HCl, pH 8.0, 300 mM NaCl.
8. ND column buffer 2: 40 mM Tris-HCl, pH 8.0, 300 mM NaCl, 400 mM imidazole.
9. ND storage buffer: 20 mM HEPES-KOH, pH 7.5, 200 mM NaCl, 50 mM KOAc, 5 mM Mg(OAc)<sub>2</sub>, 5% (v/v) glycerol.
10. Laboratory vortex mixer.
11. Bath sonicator.
12. 15 mL conical tubes.
13. Laboratory rotisserie.
14. BioBeads SM-2 (Bio-Rad) hydrophobic adsorbents.
15. Ni-NTA agarose and chromatography column approx. 0.8 cm I.D. × 4 cm length.
16. Amicon Ultra centrifugal filter units (Millipore), 3000 Da MWCO, 5 mL capacity.
17. Translation buffer (10×): 200 mM HEPES-KOH, pH 7.5, 1 M KOAc, pH 7.5, 25 mM Mg (OAc)<sub>2</sub>, 2 mM spermidine, 0.08 mM S-adenosylmethionine.
18. Protease inhibitor mixture (200×): 50 µg/mL each of anti-pain, chymostatin, leupeptin, pepstatin A, and 5% (v/v) of aprotinin.
19. Energy generating system (EGS) and amino acid mixture: 90 mM HEPES-KOH, pH 7.5, 15 mM ATP, pH 7.5, 15 mM

GTP, pH 7.5, 120 mM creatine phosphate, 0.12 U/ $\mu$ L creatine phosphokinase, 0.38 mM each of 20 common L-amino acids, excluding methionine (*see Note 22*).

20. Wheat germ extract (prepared as in Subheading 3.1)
21. L-[<sup>35</sup>S] methionine (*see Note 23*).

## 2.5 Gel-Based Analysis of Assembly

1. Mini-PROTEAN Tetra Cell (Bio-Rad).
2. PowerPac Universal Power Supply (Bio-Rad).
3. Mini-PROTEAN TGX Precast Gel (Bio-Rad) (*see Note 24*).
4. Electrophoresis running buffer: 25 mM Sigma 7–9 buffer, 0.2 M glycine, 0.1% (w/v) sodium dodecyl sulfate
5. SDS-PAGE sample buffer: 125 mM Tris–Base, 18% (v/v) glycerol, 3.6% (w/v) sodium dodecyl sulfate, 0.045% (w/v) bromophenol blue, 0.1 M DTT.
6. Destain solution: 50% (v/v) methanol, 10% (v/v) acetic acid
7. Coomassie stain solution: 50% (v/v) methanol, 10% (v/v) acetic acid, 0.5% (w/v) Coomassie G-250.
8. Gel imaging system capable of imaging radiolabeled samples (*see Note 25*).
9. Gel drying apparatus (*see Note 26*).
10. Imaging screen-K, 20 × 25 cm phosphor imaging screen (Bio-Rad 170-7843) and exposure cassette-K (Bio-Rad 170-7861).
11. <sup>14</sup>C-methylated protein molecular weight markers (PerkinElmer #NEC81100).
12. Precision Plus All Blue Prestained Standards (Bio-Rad 161-0373).

---

## 3 Methods

### 3.1 Preparation of Wheat Germ Extract

These procedures are based on protocols modified from Erickson and Blobel [36]. Flootation enriches the wheat germ for viable, intact embryos. The extract is then prepared in three steps: homogenization of the floated germ, homogenate centrifugation, and gel filtration of the supernatant. The following protocol is optimized for 50 g of wheat germ starting material, which yields approximately 15–20 mL of active extract.

#### 3.1.1 Flootation of Wheat Germ

1. Prepare 800 mL of floatation solvent in a 1 L beaker in a well-ventilated hood. Stir with a glass rod until no Schlieren lines are visible.
2. Carefully pour 25 g of wheat germ to the top of the solution and gently stir. During the 2–3 min separation process, damaged embryos will settle, and intact, viable embryos will float.

3. Decant the floating embryos into a Buchner funnel fitted with Whatman #1 filter paper and dry the wheat germ embryos by pulling air through the funnel for 30 min (*see Note 27*).
4. Spread the dried wheat germ onto fresh aluminum foil in fume hood.
5. Repeat **steps 1–4** with another 25 g of wheat germ (*see Note 28*).
6. Combine and weigh the dried wheat germ. The target yield of the floated wheat germ is 30–40% (w/w) (*see Notes 29 and 30*).

### 3.1.2 Preparation of Wheat Germ Extract

1. All steps should be carried out in a cold room at 4 °C.
2. Place the combined dried wheat germ in a prechilled mortar, cover with liquid nitrogen, and grind wheat germ to a fine powder with a pestle. The total grinding time should be about 2 min, using reasonable force (*see Note 31*). Transfer the dried powder to a fresh sheet of foil.
3. Add homogenization buffer to the mortar at a sufficient volume to saturate the powder (*see Note 32*), slowly add powdered wheat germ, and grind until a thick homogeneous paste is obtained.
4. Transfer the homogenate into two 50 mL prechilled sterile centrifuge tubes using a sterile rubber policeman. Centrifuge at  $23,000 \times g$  at 4 °C for 10 min.
5. Transfer the supernatant to fresh 50 mL centrifuge tubes using a sterile Pasteur pipette (*see Note 33*).
6. Repeat centrifugation step ( $23,000 \times g$  at 4 °C for 10 min) and transfer the supernatants (now termed the S23 wheat germ extract) to a fresh tube. Measure the extract volume (*see Note 34*).
7. Perform gel filtration of the extract by loading the S23 wheat germ extract on the G-25 column, and elute with column buffer under gravity flow. Collect eluate in 1 mL fractions (*see Note 35*).
8. Measure the absorbance of each fraction at 260 and 280 nm ( $A_{260}$  and  $A_{280}$ , respectively) by adding 5  $\mu$ L fraction to 1 mL of 1% (v/v) SDS in a quartz cuvette with a spectrophotometer blanked with 5  $\mu$ L of column buffer and 1 mL of 1% (v/v) SDS. The profile should be similar to that shown in Fig. 1.
9. Target fractions are optimally those with  $A_{260} > 0.4$  and  $A_{260}/A_{280}$  ratios of about 1.6. Depending on the amount of S23 wheat germ extract, this will be about 15–20 fractions. Pool target fractions into a sterile 50 mL centrifuge tube, aliquot into microfuge tubes, flash-freeze in liquid nitrogen, and store at  $-80$  °C (*see Note 36*).

**Table 1**  
**PCR protocol**

Component	Volume ( $\mu\text{L}$ )	Final concentration
Nuclease-free $\text{H}_2\text{O}$	80.0	n/a
10 $\times$ PCR buffer	10.5	1 $\times$
10 mM dNTP mix	2.0	0.2 mM, each dNTP
50 mM $\text{MgCl}_2$	4.0	2 mM
50 $\mu\text{M}$ forward primer	1.0	0.5 $\mu\text{M}$
50 $\mu\text{M}$ reverse primer	1.0	0.5 $\mu\text{M}$
100 ng/ $\mu\text{L}$ DNA template	1.0	1 ng/ $\mu\text{L}$
DNA polymerase (5 U/ $\mu\text{L}$ )	0.5	0.025 U/ $\mu\text{L}$
Total	100.0	

### 3.2 *In Vitro* Transcription

The procedure outlined here uses PCR to generate DNA fragments for the transcription reaction. Alternatively, one could use plasmid linearized with appropriate restriction endonuclease(s).

#### 3.2.1 PCR Amplification of DNA Fragments

1. Assemble the PCR reaction mixture (Table 1) in a PCR tube (*see Note 37*).
2. Add the reaction to a PCR thermal cycler programmed as follows: first denature (94  $^{\circ}\text{C}$ , 4 min); 30 cycles of amplification (denature 94  $^{\circ}\text{C}$ , 20 s; anneal 54  $^{\circ}\text{C}$ , 20 s; extension 72  $^{\circ}\text{C}$ , 1 min per 1 kb); final extension (72  $^{\circ}\text{C}$ , 4 min) (*see Note 38*).
3. Purify the amplified DNA fragment using the QIAquick PCR Purification Kit and elute with 50  $\mu\text{L}$  of RNase-free  $\text{H}_2\text{O}$  (*see Note 39*).

#### 3.2.2 *In Vitro* Transcription Reaction

1. Assemble the *in vitro* transcription mixture (Table 2) in a 1.5 mL microfuge tube and incubate the reaction at 37  $^{\circ}\text{C}$  for 1.5 h (*see Note 40*).
2. Isolate and purify RNA by adding reaction to 340  $\mu\text{L}$  of 100% ethanol and 13.3  $\mu\text{L}$  of 3 M NaOAc (pH 5.2) and precipitating mRNA on ice for 2 h (*see Note 41*).
3. Pellet samples at maximum speed for 20 min in a microfuge (4  $^{\circ}\text{C}$ ) and carefully aspirate supernatant.
4. Wash pellet with 1 mL 70% (v/v) ethanol, re-centrifuge (10 min at maximum speed in a microfuge at 4  $^{\circ}\text{C}$ ) and aspirate supernatant.
5. Dry pellet in a rotary evaporator for 5 min and resuspend mRNA pellet in 100  $\mu\text{L}$  TE, pH 7.5.
6. Aliquot mRNA in volumes of 25  $\mu\text{L}$  each, flash-freeze in liquid nitrogen, and store at  $-80^{\circ}\text{C}$  (*see Note 42*).

**Table 2**  
**In vitro transcription protocol**

Component	Volume ( $\mu\text{L}$ )	Final concentration
Nuclease-free $\text{H}_2\text{O}$	43.3	n/a
10 $\times$ transcription buffer	10.0	100 mM HEPES, pH 7.5 20 mM $\text{MgCl}_2$ 2.5 mM spermidine
100 mM DTT	10.0	10 mM
100 mM rNTP mixture	4.0	4 mM, each rNTP
0.1 U/ $\mu\text{L}$ (5')ppp(5')G	13.0	0.013 U/ $\mu\text{L}$
20 U/ $\mu\text{L}$ RNasin	2.0	0.4 U/ $\mu\text{L}$
100–200 ng/ $\mu\text{L}$ PCR product DNA <sup>a</sup>	13.0	13–26 ng/ $\mu\text{L}$ <sup>b</sup>
5 $\mu\text{M}$ SP6 RNA polymerase	3.5	0.18 $\mu\text{M}$ <sup>c</sup>
0.5 U/ $\mu\text{L}$ pyrophosphatase	1.2	0.006 U/ $\mu\text{L}$
Total	100.0	

<sup>a</sup>This corresponds to the purified DNA template with an SP6 promoter

<sup>b</sup>The final DNA concentration is variable, depending on efficiency of PCR reaction and purification

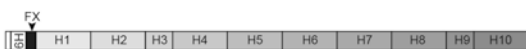
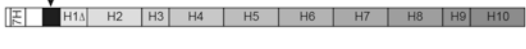
<sup>c</sup>The final SP6 polymerase concentration is variable, depending on source of polymerase

### 3.3 Preparation of MSP

Several variants of MSP have been described (*see* Fig. 2 and reviewed in [29]). Among them, plasmids comprised of the pET28a vector with different MSP coding sequence variants are available in the Addgene plasmid repository. These contain an N-terminal affinity tag followed by specific cleavage sites just upstream of the MSP (Fig. 2). This protocol describes the preparation of MSP1E3D1 construct; the expression and purification of other variants is similar (*see* Note 43).

#### 3.3.1 MSP1E3D1 Expression

1. Transform prechilled BL21 (DE3) cells with 25 ng pET28a/MSP1E3D1 plasmid DNA by incubation on ice for 30 min, heat shock at 42 °C for 45 s, incubation on ice for 2 min, and recovery at 37 °C in 0.95 mL SOC Medium for 1 h.
2. Plate 100  $\mu\text{L}$  transformed cells on kanamycin-selective plates and incubate overnight at 37 °C.
3. Prepare 100 mL growth medium, divide into several (five to ten) 5 mL aliquots in culture tubes, inoculate each with individual colonies from transformation plate, and grow overnight (37 °C, 250 rpm) (*see* Note 44).
4. Prepare 4  $\times$  500 mL growth medium each in 2 l flasks, inoculate each with 1 mL overnight culture, and grow (37 °C, 250 rpm) to  $\text{OD}_{600} = 0.8\text{--}1.0$  (*see* Note 45).

MSP type	organization	MW (kDa)	$\epsilon_{280}$ ( $M^{-1}cm^{-1}$ )	nanodisc diameter (nm)
MSP1		24.6	23,950	9.7 - 9.8
MSP1E1		27.5	32,430	10.4 - 10.6
MSP1E2		30.0	32,430	11.1 - 11.9
MSP1E3		32.5	32,430	12.1 - 12.9
MSP1D1		24.7	21,430	9.5 - 9.7
MSP1E3D1		32.6	29,910	12.1

**Fig. 2** MSP constructs available through the Addgene plasmid repository. The composition of each construct includes N-terminal hexahistidine (6H) or heptahistidine (7H) affinity tags, cleavage sites including factor X (FX) and tobacco etch virus (TEV) proteolysis sequences, and Apo-A-I derived helices comprising 11 residues (H1 $\Delta$ , H3, and H9) and 22 residues (H1, H2, H4, H5, H6, H7, H8, and H10). The molecular weights indicated are for the intact, uncleaved polypeptide. The disc diameters are published values based on gel filtration chromatography and small angle x-ray scattering [28]

- Induce expression by reducing growth temperature to 26 °C, allowing cultures to reach 26 °C, adding 1 mM IPTG, and continuing incubation for 3 h.
- Harvest cells by centrifugation ( $4000 \times g$  for 20 min), decant medium, flash-freeze pellets in liquid nitrogen, and store at  $-80$  °C.

### 3.3.2 MSP1E3D1 Purification (See Note 46)

- Thaw pellets from each 500 mL culture on ice and resuspend each pellet in 20 mL resuspension buffer with 1 mM PMSF.
- Add Triton X-100 to a final concentration of 1% (v/v).
- Disrupt cells by ultrasonication in an ice bath using a microtip, 50% amplitude, eight total times of 30 s sonication rounds with 60 s breaks in between (see Note 47).
- Clarify the lysate by centrifugation ( $30,000 \times g$  for 30 min) and combine supernatants.
- Equilibrate Ni-NTA agarose in chromatography column (matrix bed 8 mL) with a minimum of five column volumes (CV) of column wash 1 buffer (see Note 48).
- Load clarified lysate supernatant onto column, and wash the column with 5 CV column wash 1 buffer, 5 CV column wash 2 buffer, and 5 CV column wash 3 buffer.
- Elute MSP1E3D1 with column elution buffer ( $10 \times 1$  mL fractions). Pool peak protein-containing fractions, add to dialysis cassette (MWCO 2000), and dialyze at 4 °C in 3 l dialysis

buffer with two steps (dialyze for 3 h, exchange the buffer, and then dialyze overnight) (*see Note 49*).

8. Measure MSP concentration by  $A_{280}$  and known molar extinction coefficients (Fig. 2). Aliquot into 250  $\mu$ L fractions, flash-freeze in liquid nitrogen, and store in  $-80\text{ }^{\circ}\text{C}$  (*see Note 50*).

### 3.4 Assembly of Nanodiscs with Target Protein

#### 3.4.1 Preparation of Solubilized Lipids

1. Assemble the desired lipid blend by combining 25 mg/mL chloroform stocks of lipids in a 50 mL round-bottom Pyrex tube using a Hamilton syringe. To assemble a mitochondrial inner membrane biomimetic lipid combination (40 mol% POPC, 40 mol% POPE, 20 mol% TOCL), add 0.2 mL of POPC, 0.19 mL of POPE, and 0.2 mL of TOCL. This corresponds to 5.0 mg POPC, 4.8 mg POPE, and 5.0 mg TOCL.
2. Evaporate the chloroform under a gentle nitrogen stream in a fume hood (*see Note 51*).
3. Cover the tube with Parafilm with small hole on top and place in vacuum desiccator (rotary evaporator in stationary desiccator mode) for a minimum of 2 h to remove all traces of organic solvent.
4. Hydrate the lipid film by adding 0.8 mL of ND buffer B, vortexing lipids into solution, and placing in a bath sonicator for a total of  $4 \times 1$  min cycles until suspension is clear (*see Notes 52 and 53*).

#### 3.4.2 Assembly of Lipid-Only Nanodiscs (for Cotranslational Assembly Only)

1. Prepare a 2 mL lipid-only nanodisc assembly reaction in a 15 mL conical tube by assembling cholate-solubilized lipids (from Subheading 3.4.1) and MSP (from Subheading 3.3) with ND buffer A as shown in Table 3. Incubate assembly at room temperature for 30 min (*see Note 54*).
2. Prepare BioBeads by adding 1.5 g of dry beads to a 15 mL conical tube and hydrating with 1.0 mL of ND buffer A on laboratory rotisserie at room temperature for 30 min.

**Table 3**  
Lipid-only biomimetic nanodisc assembly reaction

Component	Volume ( $\mu$ L)	Final concentration
20.5 mM lipid blend	590	2.4 mM POPC 2.4 mM POPE 1.2 mM TOCL
200 $\mu$ M MSP1E3D1	500	50 $\mu$ M
ND buffer A	910	
Total	2000	

**Table 4**  
**Nanodisc affinity purification buffers**

	ND column buffer 1	ND column buffer 2
Buffer	Volume (mL)	Volume (mL)
Wash 1 (no imidazole)	25.00	0
Wash 2 (20 mM imidazole)	23.75	1.25
Wash 3 (50 mM imidazole)	21.87	3.13
Elution (400 mM imidazole)	0	25.00

Carefully remove as much buffer as possible by pipetting; it is fine if the beads retain a small amount of buffer.

3. Initiate the self-assembly reaction by adding the nanodisc assembly mixture to the conical vial containing pre-hydrated BioBeads. Incubate reaction on laboratory rotisserie at room temperature for 2 h (*see Note 55*).
4. Affinity purify assembled nanodiscs via batch purification with Ni-NTA agarose by adding 1 mL of Ni-NTA beads (equilibrated with ND buffer A) to the assembly reaction and incubating for 45 min at room temperature. Add the slurry to chromatography column. Prepare wash and elution buffers as shown in Table 4, and add 2 CV of wash 1 buffer, 2 CV of wash 2 buffer, and 2 CV of wash 3 buffer, and elute with elution buffer in  $4 \times 1$  mL fractions (*see Note 56*).
5. Perform nanodisc concentration and buffer exchange by adding elution fractions to 5 mL Amicon Ultra centrifugal filter units (3000 MWCO), pre-equilibrated with ND storage buffer. Perform the following four times: centrifuge sample at  $3500 \times g$  for 15–20 min at 4 °C, discard eluate, add 3.0 mL ND Storage Buffer to nanodisc sample in filter device, and, finally, concentrate the sample to approximately 0.5 mL (*see Note 57*).
6. Purified nanodiscs can be used immediately in translation reactions. Alternatively, they may be stored long term by flash-freezing in liquid nitrogen and store at  $-80$  °C.

### 3.4.3 Cotranslational Assembly of Target Protein in Nanodiscs

1. Assemble translation reaction with nanodiscs (Table 5) in a 1.5 mL microfuge tube, and incubate the reaction at 26 °C for 40 min (*see Note 58*).
2. Centrifuge the reaction mixture at  $20,000 \times g$  for 10 min to pellet precipitated protein, and transfer clarified supernatant containing nanodiscs with target protein to a new microfuge tube.

**Table 5**  
**Translation reaction**

Component	With nanodiscs	No nanodiscs	Final concentration
	Volume ( $\mu\text{L}$ )	Volume ( $\mu\text{L}$ )	
Nuclease-free $\text{H}_2\text{O}$	146.4	73.2	n/a
10 $\times$ translation buffer	50	25	20 mM HEPES, pH 7.5 100 mM KOAc, pH 7.5 2.5 mM $\text{Mg}(\text{OAc})_2$ 200 $\mu\text{M}$ spermidine 8 $\mu\text{M}$ S-adenosylmethionine
100 mM DTT	5	2.5	1 mM
200 $\times$ protease inhibitors	2.6	1.3	1 $\times$
20 U/ $\mu\text{L}$ RNasin	2.6	1.3	0.1 U/ $\mu\text{L}$
EGS	40	20	7.2 mM HEPES, pH 7.5 1.2 mM ATP, pH 7.5 1.2 mM GTP, pH 7.5 9.6 mM creatine phosphate 9.6 U/mL creatine phosphokinase 30 $\mu\text{M}$ amino acids (-Met)
Wheat germ extract <sup>a</sup>	100	50	20% (v/v)
10 $\mu\text{Ci}/\mu\text{L}$ [ <sup>35</sup> S]methionine	13.4	6.7	0.25 $\mu\text{Ci}/\mu\text{L}$
3–4 $\mu\text{g}/\mu\text{L}$ Tim23 mRNA <sup>b</sup>	40	20	240–320 ng/ $\mu\text{L}$ , 8% (v/v)
Purified nanodiscs <sup>c</sup>	100	n/a	20% (v/v) nanodiscs
ND storage buffer	n/a	50	20% (v/v) buffer
Total	500	250	

<sup>a</sup>Typical preparations of wheat germ extract have  $A_{260}$  values from 0.5 to 0.8 and  $A_{260}:A_{280}$  ratios of  $\sim 1.6$

<sup>b</sup>Stock concentrations of purified mRNA will vary depending on the transcript

<sup>c</sup>Typical preparations of nanodiscs will contain approximately 0.5 mg/mL protein and 3 mg/mL lipid

- To repurify and concentrate the [<sup>35</sup>S]Tim23-containing nanodiscs, the sample can be subjected to a second round of Ni-NTA-based chromatography, exactly as detailed in Subheading 3.4.2, steps 4 and 5 (see Note 59).

#### 3.4.4 Posttranslational Assembly of Target Protein in Nanodiscs

- Assemble translation reaction without nanodiscs (Table 5) in a 1.5 mL centrifuge tube and incubate the reaction at 26 °C for 40 min (see Note 58).
- Prepare a 2 mL target protein-nanodisc assembly reaction in a 15 mL conical tube by assembling cholate-solubilized lipids (from Subheading 3.4.1) and MSP (from Subheading 3.3) at optimized molar ratios and adjusting the volume with ND buffer A as shown in Table 6. Incubate assembly at room temperature for 30 min.

**Table 6**  
**Target protein-biomimetic nanodisc assembly reaction**

Component	Volume ( $\mu\text{L}$ )	Final concentration
20.5 mM lipid blend	590	2.4 mM POPC 2.4 mM POPE 1.2 mM TOCL
200 $\mu\text{M}$ MSP1E3D1	500	50 $\mu\text{M}$
[ $^{35}\text{S}$ ]Tim23 translation	250	12.5% (v/v)
200 $\times$ Protease inhibitors	20	2 $\times$
ND buffer A	640	
Total	2000	

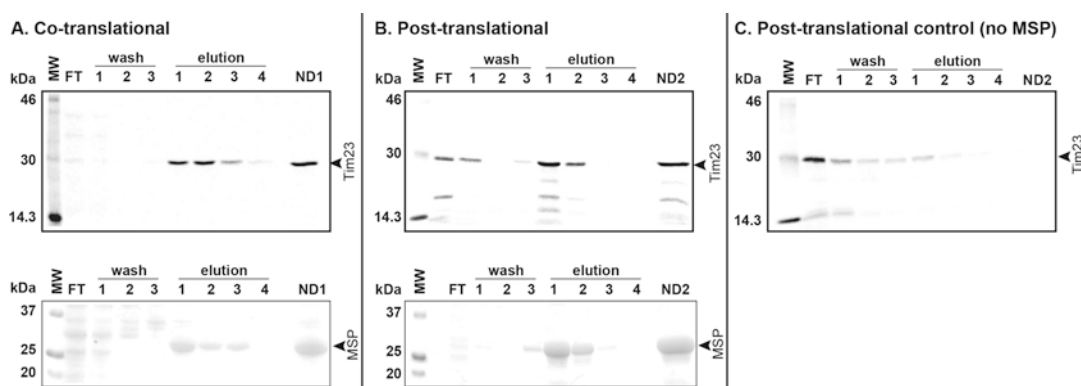


**Fig. 3** Analysis of nanodisc assembly and purification for (a) cotranslational assembly, (b) posttranslational assembly, and (c) negative control (lacking MSP). Samples were resolved by SDS-PAGE on 12.5% gels and visualized by radioisotope scanning (upper gels) to image [ $^{35}\text{S}$ ]Tim23 and by Coomassie staining (lower gels) to detect MSP. Individual flow-through, wash, and elution fractions are indicated. ND1 and ND2 denote the final combined samples for co- and posttranslational assembly reactions, respectively

3. Perform self-assembly of nanodiscs in the presence of the target protein and affinity purify the nanodiscs by following exactly **steps 3–6** of Subheading **3.4.2** above.

### 3.5 Gel-Based Analysis of Assembly

1. Set up the electrophoresis apparatus according to the manufacturer's instructions.
2. In separate microfuge tubes, premix 5  $\mu\text{L}$  nanodisc purification fractions (flow-through, wash steps, elution steps, and concentrated samples) with an equal volume of SDS-PAGE sample buffer, and heat at 65  $^{\circ}\text{C}$  for 10 min prior to gel loading. For gels in radioisotope scans, add 5  $\mu\text{L}$  of radiolabeled molecular weight markers to an equal volume of SDS-PAGE sample buffer; for Coomassie gels, add 5  $\mu\text{L}$  of all blue markers to an equal volume of SDS-PAGE sample buffer. Quantitatively load all samples onto gel. *See* Fig. 3 for a loading schematic.

3. Run gels at 125 V until the bromophenol blue dye front reaches the bottom of the separating gel.
4. Prepare gels used for radioisotope scans by washing in 100 mL of destain solution for 10 min followed by two 10 min washes in water. Dry gels for 40 min at 80 °C and place on phosphor imaging screen (*see* **Note 60**). Perform radioisotope scan on the molecular imager using the appropriate settings.
5. Stain gels used for Coomassie stain by incubating in 100 mL of Coomassie stain solution for 30 min followed by multiple 20 min washes in 100 mL destain solution. Continue destaining until signal from protein bands are sufficiently contrasted with background.

---

## 4 Notes

1. All glassware should be autoclaved and baked overnight to eliminate nucleases. Ceramic pieces (Buchner funnel, mortar, pestle) are also autoclaved. All solutions should be prepared with Milli-Q (or double-distilled) water, sterilized by filtration, and stored long term at 4 °C.
2. Wheat germ (typically from *Triticum aestivum* L.) can also be sourced from commercial mills but note that different strains of wheat will have variable activity and should be tested. Activity is best retained if wheat germ is stored in small batches in a vacuum desiccator at 4 °C.
3. We use a six inch mortar and pestle set. Any set large enough for homogenization of the wheat germ will suffice.
4. Add DTT from prepared stocks (1 M DTT) just prior to use.
5. Packed Sephadex columns can be used repeatedly if washed and stored correctly between preparations. Columns with packed gel medium should be stored with antimicrobial agents to prevent contamination (e.g., 0.02% sodium azide or 20% ethanol).
6. As an alternative to the transcription protocol described here, one may use commercially available kits to synthesize mRNA transcripts.
7. We commonly use plasmids designed for in vitro transcription/translation, such as pSP65 (Promega) with the open reading frame (ORF) of interest subcloned into the multicloning site. Plasmid stocks are stored at concentrations of about 100 ng/ $\mu$ L in TE buffer at  $-20$  °C.
8. Primer stocks are stored at concentrations of 50  $\mu$ M in TE buffer at  $-20$  °C.

9. The forward primer should allow for the inclusion of the SP6 promoter, and the reverse primer is downstream of the termination codon of the ORF. For constructs subcloned into the EcoRI/BamHI sites of the pSP65 plasmid, one can use upstream primer 5'-TGTATCATAACACATACGATTTAGGTGACACTATAG-3' and downstream primer 5'-GAATTGTGAGCGGATAACAATTTTCAC-3'.
10. For these PCR reactions, we typically use Bio-Rad iTaq DNA polymerase (Bio-Rad #170-8870) and dNTP mix (#170-8874). Comparable products from other vendors will suffice.
11. For purification of PCR products, we typically use the QIAquick PCR Purification Kit (Qiagen #28106). A comparable kit from another vendor will suffice.
12. We use a Bio-Rad C1000 thermal cycler and low tube strip individual PCR tubes.
13. SP6 polymerase is available commercially from vendors such as New England Biolabs; however, we prepare our own stocks in-house with a typical stock concentration of 5  $\mu$ M. Commercial vendors typically quantify SP6 polymerase as defined units of enzyme activity. If polymerase is obtained from a commercial vendor, the amount added for optimal transcription must be determined empirically.
14. Media, excluding antibiotic, should be sterilized by autoclave (121 °C). Kanamycin from 50 mg/mL stock can be added to medium stock once it is cooled.
15. Media, excluding glucose, should be sterilized by autoclave (121 °C). Filter-sterilized glucose can be added to medium stock once it is cooled.
16. We prepare our own competent cells for transformation. If one desired cells from a commercial source, One Shot<sup>®</sup> BL21 Star<sup>™</sup> (DE3), chemically competent *E. coli* (Thermo Fisher Scientific #C601003) is one suitable option.
17. This plasmid (the MSP1E3D1 gene in the pET28a vector backbone) is available from the Addgene plasmid repository (plasmid #20066).
18. Kanamycin is dissolved to 50 mg/mL in sterile water, filter-sterilized using a 0.22 micron filter, divided into 1 mL aliquots for convenience, and stored at -20 °C.
19. Prepare the growth medium just prior to use by adding glucose to a final concentration of 0.2% (w/v) (a 100-fold dilution of the stock of 20% (w/v) glucose) and by adding kanamycin to a final concentration of 25  $\mu$ g/mL (a 2000-fold dilution of the stock of 50 mg/mL kanamycin).
20. We use a QSonica Q700 sonicator equipped with a stepped coupler assembly that has a 1/8" tapered microtip. Comparable equipment from another manufacturer would suffice.

21. Phospholipids supplied in organic solution are stored in amber glass containers with Teflon-lined closures. The container with lipid stocks is layered with an inert gas (nitrogen or argon) and stored at  $-20^{\circ}\text{C}$ . Never store organic lipid stocks in polymer or plastic containers or expose them to plastic pipette tips or Parafilm. With proper storage, lipids stocks can be stored for up to 2 months. Alternatively, lipids can be purchased as powder stocks and resuspended in detergent-containing buffer to the desired concentration.
22. Stocks of L-amino acids can be prepared from analytical grade kits (e.g., Sigma LAA21).
23. We obtain L-[ $^{35}\text{S}$ ] methionine from PerkinElmer (product #NEG009A005MC), in shipments of 5 mCi, stored in 50 mM tricaine and 10 mM beta-mercaptoethanol. Stocks are stored at  $-80^{\circ}\text{C}$ .
24. We cast all gels for SDS-PAGE in-house using standard procedures. Bio-Rad Mini-PROTEAN precast gels, or comparable gels from another vendor, are optional if one does not want to prepare homemade gels.
25. We use a Bio-Rad Pharos FX Plus Molecular Imager with external lasers. Other imaging instrumentation (e.g., the Bio-Rad PMI system) can be used for the detection of radiolabeled samples.
26. We use a Bio-Rad Hydrotech system including Model 583 gel dryer and vacuum pump. Comparable equipment from another supplier would suffice.
27. Floated wheat germ will become much lighter in color when dry.
28. The organic solvent mixture can be reused for the second set of wheat germ.
29. If overnight storage is necessary at this step, the wheat germ can be stored in a plastic beaker covered with Parafilm and aluminum foil at  $-80^{\circ}\text{C}$ . Although longer-term storage is possible at this stage, we have not tested the activity of wheat germ lysate prepared from active embryos stored longer than overnight at this step.
30. If the yield of floated wheat germ is much less than 30–40% of the starting material, it is possible that the source contains a low fraction of intact, viable embryos. In this case, it is suggested to seek an alternate supplier.
31. Grinding the wheat germ in liquid  $\text{N}_2$  minimizes enzymatic degradation during cell disruption.
32. As a rule of thumb, the amount of extraction buffer should be 2 $\times$  weight of dried wheat germ. For example, if 20 g of floated, dried wheat germ was obtained, then 40 mL of homogenization buffer would be used. Extra buffer may be added to maintain the consistency of the paste.

33. There will be a yellowish floating layer of lipid. Take care to avoid transferring this layer into the new tube.
34. A supernatant volume of 25–30 mL should be obtained following the two centrifugation steps.
35. The opaque, brown solution eluting just after the void volume contains the target product. The slower-running yellowish lipid-rich layer is discarded.
36. If desired, the combined fractions can be normalized to a specific  $A_{260}$  by adjusting concentration with column buffer. Typical preparations of active wheat germ lysate can have  $A_{260}$  values ranging from 0.5 to 0.8. Aliquot sizes of stored wheat germ extract can vary (e.g., from 50 to 200  $\mu\text{L}$ ); however, after thawing lysate, any remaining stock should be discarded and not re-frozen. The activity of lysate stocks will remain unchanged for several months when stored at  $-80\text{ }^{\circ}\text{C}$ .
37. Reagent concentrations have been optimized for the Bio-Rad iTaq polymerase system; optimal concentrations of reagents, particularly for  $\text{MgCl}_2$ , should be tested empirically for different enzymes, plasmid templates, and primers.
38. Optimal temperatures and time lengths of the PCR reaction will vary for different constructs. Extension times will vary based on the length of the amplification product, and temperatures will vary based on factors such as polymerases and primers used. These parameters should be optimized for each construct.
39. Purification of PCR products is done in accordance with the manufacturer's protocol. We typically run PCR DNA on a 1.8% agarose gel alongside DNA standards to confirm successful amplification of the desired product.
40. To enhance the incorporation of diguanosine triphosphate, add one-tenth the concentration of GTP initially and then supplement the reaction with 4 mM GTP after 1 h.
41. Alternatively, the RNA can be isolated and purified using a commercially available kit such as the QIAgen RNeasy Mini Kit (Qiagen #74106).
42. mRNA in TE can be stored in an ultracold freezer for several months and can withstand multiple freeze/thaw cycles. Typical yields of mRNA synthesized and purified by this method range from 3 to 4  $\mu\text{g}/\mu\text{L}$ , but will vary depending on the transcript.
43. All constructs bearing a hexahistidine affinity tag will be purified using the same basic protocol outlined here. If the amount of purified scaffold protein is sub-optimal, several variables of the purification step can be modified, including detergent concentrations, ionic strengths of the buffers, and imidazole concentrations of the column steps.

44. Typical growth time for the overnight step is 12–14 h. Longer growth times could be used, but the culture should not reach an  $OD_{600} > 0.8$  at this point. We inoculate several overnight cultures at this step to ensure that there are sufficient starter cultures of approximately equal  $OD_{600}$  for each larger culture.
45. Under these conditions, growing the 500 mL cultures to  $OD_{600}$  0.8 to 1.0 takes approximately 3–3.5 h.
46. Throughout the purification, samples should be kept on ice when possible and steps should be conducted at 4 °C.
47. These sonication settings work for our sonicator and microtip used in this protocol and may need to be modified if different ultrasonic processors are used. Following sonication, the lysate should clarify slightly and appear much less viscous upon swirling.
48. This affinity chromatography step can be conducted using gravity flow. If preferred, it could also be performed using a peristaltic pump or automated liquid chromatography system.
49. For our dialysis steps, we use Slide-A-Lyzer dialysis cassettes (Thermo Fisher Scientific). Similar products from other vendors would suffice.
50. To measure the protein concentration using the  $A_{280}$  value, dilute the sample sufficiently so that the measured  $A_{280} < 1.0$ . With a 25-fold dilution of protein, an  $A_{280}$  of 0.24 corresponds to a typical MSP1E3D1 concentration of 200  $\mu$ M. For this protocol, this amounts to approximately 20 mg of purified protein per liter of culture.
51. This step can be performed by clamping the glass tube at a slight angle relative to the nitrogen stream and rotating periodically. Flush-dry the lipids until the first dry residue appears and continue drying for an additional 15 min. Overdrying the lipids at this stage, visualized by cracking of the lipid film, can make resuspension difficult.
52. During nanodisc preparation steps, make sure that the sample temperature is above the melting temperature ( $T_m$ ) of the highest melting lipid. This ensures that all lipids are in the liquid crystalline phase and is especially important for long chain, saturated lipids with high  $T_m$ . Ensure that all solutions are warmed to the proper temperature prior to exposing them to lipids. In the case of the lipid blend used here, PE has the highest  $T_m$  of 25 °C. For a comprehensive listing of  $T_m$  values for commercially available lipids, refer to the manufacturer's website (e.g., [www.avantlipids.com](http://www.avantlipids.com)).
53. During lipid hydration, the concentration of cholate should be at least twice the concentration of the lipid.

54. This lipid/MSP molar ratio (120:1) was empirically optimized for this nanodisc preparation; the optimal molar ratios of lipid and scaffolding protein will differ depending on MSP type and lipid composition. Molar ratios of other scaffolding protein and lipid compositions, and the theoretical considerations behind them, have been described (e.g., [28]).
55. Alternatively, the 2 mL self-assembly reaction can be done by extensive dialysis against a 2000× volume of ND buffer A.
56. Alternatively, assembled nanodiscs can be purified by size exclusion chromatography (e.g., by fractionation on a Superdex 200 10/300 GL column equilibrated with ND buffer A).
57. Following nanodisc concentration, it is advisable to determine the final protein concentration (e.g. using a Bradford assay [37]) and/or the final lipid concentration (e.g., using the ferrothiocyanate assay [38]) in order to normalize the amount of discs in subsequent reactions. Following concentration to 0.5 mL, a typical nanodisc sample contains approximately 0.5 mg/mL MSP protein and 3 mg/mL lipid.
58. To enhance the readout of endogenous mRNA prior to addition of the [<sup>35</sup>S]methionine label, we incubate reactions at 26 °C for 5 min prior to mRNA addition.
59. Alternatively, in order to enrich for only those nanodiscs that contain the target protein, one may perform affinity chromatography against a tag engineered onto the target protein.
60. Sufficient signal from <sup>35</sup>S-labeled protein can generally be obtained after K-screen exposure for a few hours, depending on the efficiency of translation and [<sup>35</sup>S]methionine incorporation.

---

## Acknowledgments

We thank members of the Alder Research Group for their useful input. This work is supported by grants to NNA from the National Science Foundation (MCB-1330695) and from the National Institutes of Health (1R01GM113092).

## References

1. Alder NN (2011) Biogenesis of lipids and proteins within biological membranes. In: Yeagle PL (ed) *The structure of biological membranes*. CRC, New York, pp 315–377
2. Distler AM, Kerner J, Hoppel CL (2008) Proteomics of mitochondrial inner and outer membranes. *Proteomics* 8(19):4066–4082. doi:10.1002/pmic.200800102
3. Schmidt O, Pfanner N, Meisinger C (2010) Mitochondrial protein import: from proteomics to functional mechanisms. *Nat Rev Mol Cell Biol* 11(9):655–667. doi:10.1038/nrm2959
4. Sanders CR, Myers JK (2004) Disease-related misassembly of membrane proteins. *Annu Rev Biophys Biomol Struct* 33:25–51. doi:10.1146/annurev.biophys.33.110502.140348
5. Junge F, Haberstock S, Roos C, Stefer S, Proverbio D, Dotsch V, Bernhard F (2011) Advances in cell-free protein synthesis for the

- functional and structural analysis of membrane proteins. *N Biotechnol* 28(3):262–271. doi:[10.1016/j.nbt.2010.07.002](https://doi.org/10.1016/j.nbt.2010.07.002)
6. Sachse R, Dondapati SK, Fenz SF, Schmidt T, Kubick S (2014) Membrane protein synthesis in cell-free systems: from bio-mimetic systems to bio-membranes. *FEBS Lett* 588(17):2774–2781. doi:[10.1016/j.febslet.2014.06.007](https://doi.org/10.1016/j.febslet.2014.06.007)
  7. Klammt C, Schwarz D, Fendler K, Haase W, Dotsch V, Bernhard F (2005) Evaluation of detergents for the soluble expression of alpha-helical and beta-barrel-type integral membrane proteins by a preparative scale individual cell-free expression system. *FEBS J* 272(23):6024–6038. doi:[10.1111/j.1742-4658.2005.05002.x](https://doi.org/10.1111/j.1742-4658.2005.05002.x)
  8. Bazzacco P, Billon-Denis E, Sharma KS, Catoire LJ, Mary S, Le Bon C, Point E, Baneres JL, Durand G, Zito F, Pucci B, Popot JL (2012) Nonionic homopolymeric amphipols: application to membrane protein folding, cell-free synthesis, and solution nuclear magnetic resonance. *Biochemistry* 51(7):1416–1430. doi:[10.1021/bi201862v](https://doi.org/10.1021/bi201862v)
  9. Blesneac I, Ravaud S, Juillan-Binard C, Barret LA, Zoonens M, Polidori A, Miroux B, Pucci B, Pebay-Peyroula E (2012) Production of UCP1 a membrane protein from the inner mitochondrial membrane using the cell free expression system in the presence of a fluorinated surfactant. *Biochim Biophys Acta* 1818(3):798–805. doi:[10.1016/j.bbamem.2011.12.016](https://doi.org/10.1016/j.bbamem.2011.12.016)
  10. Corin K, Baaske P, Ravel DB, Song J, Brown E, Wang X, Wienken CJ, Jerabek-Willemsen M, Duhr S, Luo Y, Braun D, Zhang S (2011) Designer lipid-like peptides: a class of detergents for studying functional olfactory receptors using commercial cell-free systems. *PLoS One* 6(11):e25067. doi:[10.1371/journal.pone.0025067](https://doi.org/10.1371/journal.pone.0025067)
  11. Park KH, Berrier C, Lebaupain F, Pucci B, Popot JL, Ghazi A, Zito F (2007) Fluorinated and hemifluorinated surfactants as alternatives to detergents for membrane protein cell-free synthesis. *Biochem J* 403(1):183–187. doi:[10.1042/BJ20061473](https://doi.org/10.1042/BJ20061473)
  12. Park KH, Billon-Denis E, Dahmane T, Lebaupain F, Pucci B, Breyton C, Zito F (2011) In the cauldron of cell-free synthesis of membrane proteins: playing with new surfactants. *N Biotechnol* 28(3):255–261. doi:[10.1016/j.nbt.2010.08.008](https://doi.org/10.1016/j.nbt.2010.08.008)
  13. Popot JL, Althoff T, Bagnard D, Baneres JL, Bazzacco P, Billon-Denis E, Catoire LJ, Champeil P, Charvolin D, Cocco MJ, Cremel G, Dahmane T, de la Maza LM, Ebel C, Gabel F, Giusti F, Gohon Y, Goormaghtigh E, Guittet E, Kleinschmidt JH, Kuhlbrandt W, Le Bon C, Martinez KL, Picard M, Pucci B, Sachs JN, Tribet C, van Heijenoort C, Wien F, Zito F, Zoonens M (2011) Amphipols from A to Z. *Annu Rev Biophys* 40:379–408. doi:[10.1146/annurev-biophys-042910-155219](https://doi.org/10.1146/annurev-biophys-042910-155219)
  14. Wang X, Corin K, Baaske P, Wienken CJ, Jerabek-Willemsen M, Duhr S, Braun D, Zhang S (2011) Peptide surfactants for cell-free production of functional G protein-coupled receptors. *Proc Natl Acad Sci U S A* 108(22):9049–9054. doi:[10.1073/pnas.1018185108](https://doi.org/10.1073/pnas.1018185108)
  15. Andersen OS, Koeppe RE II (2007) Bilayer thickness and membrane protein function: an energetic perspective. *Annu Rev Biophys Biomol Struct* 36:107–130. doi:[10.1146/annurev.biophys.36.040306.132643](https://doi.org/10.1146/annurev.biophys.36.040306.132643)
  16. Cross TA, Murray DT, Watts A (2013) Helical membrane protein conformations and their environment. *Eur Biophys J* 42(10):731–755. doi:[10.1007/s00249-013-0925-x](https://doi.org/10.1007/s00249-013-0925-x)
  17. Lee AG (2004) How lipids affect the activities of integral membrane proteins. *Biochim Biophys Acta* 1666(1–2):62–87. doi:[10.1016/j.bbamem.2004.05.012](https://doi.org/10.1016/j.bbamem.2004.05.012)
  18. Hovijitra NT, Wu JJ, Peaker B, Swartz JR (2009) Cell-free synthesis of functional aquaporin Z in synthetic liposomes. *Biotechnol Bioeng* 104(1):40–49. doi:[10.1002/bit.22385](https://doi.org/10.1002/bit.22385)
  19. Kalmbach R, Chizhov I, Schumacher MC, Friedrich T, Bamberg E, Engelhard M (2007) Functional cell-free synthesis of a seven helix membrane protein: in situ insertion of bacteriorhodopsin into liposomes. *J Mol Biol* 371(3):639–648. doi:[10.1016/j.jmb.2007.05.087](https://doi.org/10.1016/j.jmb.2007.05.087)
  20. Long AR, O'Brien CC, Alder NN (2012) The cell-free integration of a polytopic mitochondrial membrane protein into liposomes occurs cotranslationally and in a lipid-dependent manner. *PLoS One* 7(9):e46332. doi:[10.1371/journal.pone.0046332](https://doi.org/10.1371/journal.pone.0046332)
  21. Moritani Y, Nomura SM, Morita I, Akiyoshi K (2010) Direct integration of cell-free-synthesized connexin-43 into liposomes and hemichannel formation. *FEBS J* 277(16):3343–3352. doi:[10.1111/j.1742-4658.2010.07736.x](https://doi.org/10.1111/j.1742-4658.2010.07736.x)
  22. Durr UH, Gildenberg M, Ramamoorthy A (2012) The magic of bicelles lights up membrane protein structure. *Chem Rev* 112(11):6054–6074. doi:[10.1021/cr300061w](https://doi.org/10.1021/cr300061w)
  23. Lyukmanova EN, Shenkarev ZO, Khabibullina NF, Kopeina GS, Shulepko MA, Paramonov AS, Mineev KS, Tikhonov RV, Shingarova LN, Petrovskaya LE, Dolgikh DA, Arseniev AS, Kirpichnikov MP (2012) Lipid-protein nanodiscs for cell-free production of integral

- membrane proteins in a soluble and folded state: comparison with detergent micelles, bicelles and liposomes. *Biochim Biophys Acta* 1818(3):349–358. doi:[10.1016/j.bbamem.2011.10.020](https://doi.org/10.1016/j.bbamem.2011.10.020)
24. Uhlemann EM, Pierson HE, Fillingame RH, Dmitriev OY (2012) Cell-free synthesis of membrane subunits of ATP synthase in phospholipid bicelles: NMR shows subunit a fold similar to the protein in the cell membrane. *Protein Sci* 21(2):279–288. doi:[10.1002/pro.2014](https://doi.org/10.1002/pro.2014)
  25. Malhotra K, Alder NN (2014) Advances in the use of nanoscale bilayers to study membrane protein structure and function. *Biotechnol Genet Eng Rev* 30(1–2):79–93. doi:[10.1080/02648725.2014.921502](https://doi.org/10.1080/02648725.2014.921502)
  26. Bayburt TH, Grinkova YV, Sligar SG (2002) Self-assembly of discoidal phospholipid bilayer nanoparticles with membrane scaffold proteins. *Nano Lett* 2:853–856
  27. Bayburt TH, Sligar SG (2003) Self-assembly of single integral membrane proteins into soluble nanoscale phospholipid bilayers. *Protein Sci* 12(11):2476–2481. doi:[10.1110/ps.03267503](https://doi.org/10.1110/ps.03267503)
  28. Denisov IG, Grinkova YV, Lazarides AA, Sligar SG (2004) Directed self-assembly of monodisperse phospholipid bilayer Nanodiscs with controlled size. *J Am Chem Soc* 126(11):3477–3487. doi:[10.1021/ja0393574](https://doi.org/10.1021/ja0393574)
  29. Schuler MA, Denisov IG, Sligar SG (2013) Nanodiscs as a new tool to examine lipid-protein interactions. *Methods Mol Biol* 974:415–433. doi:[10.1007/978-1-62703-275-9\\_18](https://doi.org/10.1007/978-1-62703-275-9_18)
  30. Henrich E, Dotsch V, Bernhard F (2015) Screening for lipid requirements of membrane proteins by combining cell-free expression with nanodiscs. *Methods Enzymol* 556:351–369. doi:[10.1016/bs.mie.2014.12.016](https://doi.org/10.1016/bs.mie.2014.12.016)
  31. Cappuccio JA, Blanchette CD, Sulchek TA, Arroyo ES, Kralj JM, Hinz AK, Kuhn EA, Chromy BA, Segelke BW, Rothschild KJ, Fletcher JE, Katzen F, Peterson TC, Kudlicki WA, Bench G, Hoepflich PD, Coleman MA (2008) Cell-free co-expression of functional membrane proteins and apolipoprotein, forming soluble nanolipoprotein particles. *Mol Cell Proteomics* 7(11):2246–2253. doi:[10.1074/mcp.M800191-MCP200](https://doi.org/10.1074/mcp.M800191-MCP200)
  32. Katzen F, Fletcher JE, Yang JP, Kang D, Peterson TC, Cappuccio JA, Blanchette CD, Sulchek T, Chromy BA, Hoepflich PD, Coleman MA, Kudlicki W (2008) Insertion of membrane proteins into discoidal membranes using a cell-free protein expression approach. *J Proteome Res* 7(8):3535–3542. doi:[10.1021/pr800265f](https://doi.org/10.1021/pr800265f)
  33. Proverbio D, Roos C, Beyermann M, Orban E, Dotsch V, Bernhard F (2013) Functional properties of cell-free expressed human endothelin A and endothelin B receptors in artificial membrane environments. *Biochim Biophys Acta* 1828(9):2182–2192. doi:[10.1016/j.bbamem.2013.05.031](https://doi.org/10.1016/j.bbamem.2013.05.031)
  34. Roos C, Zocher M, Muller D, Munch D, Schneider T, Sahl HG, Scholz F, Wachtveitl J, Ma Y, Proverbio D, Henrich E, Dotsch V, Bernhard F (2012) Characterization of co-translationally formed nanodisc complexes with small multidrug transporters, proteorhodopsin and with the E. coli MraY translocase. *Biochim Biophys Acta* 1818(12):3098–3106. doi:[10.1016/j.bbamem.2012.08.007](https://doi.org/10.1016/j.bbamem.2012.08.007)
  35. Yang JP, Cirico T, Katzen F, Peterson TC, Kudlicki W (2011) Cell-free synthesis of a functional G protein-coupled receptor complexed with nanometer scale bilayer discs. *BMC Biotechnol* 11:57. doi:[10.1186/1472-6750-11-57](https://doi.org/10.1186/1472-6750-11-57)
  36. Erickson AH, Blobel G (1983) Cell-free translation of messenger RNA in a wheat germ system. *Methods Enzymol* 96:38–50
  37. Kruger NJ (1994) The Bradford method for protein quantitation. *Methods Mol Biol* 32:9–15. doi:[10.1385/0-89603-268-X:9](https://doi.org/10.1385/0-89603-268-X:9)
  38. Stewart JC (1980) Colorimetric determination of phospholipids with ammonium ferrothiocyanate. *Anal Biochem* 104(1):10–14

# Chapter 11

## Detection of Dual Targeting and Dual Function of Mitochondrial Proteins in Yeast

Reut Ben-Menachem and Ophry Pines

### Abstract

Eukaryotic cells are defined by the existence of subcellular compartments and organelles. The localization of a protein to a specific subcellular compartment is one of the most fundamental processes of a living cell. It is well documented that in eukaryotic cells molecules of a single protein can be located in more than one subcellular compartment, a phenomenon termed dual targeting, bimodal targeting, or dual localization. Recently, growing evidence started to accumulate for abundant dual targeting of mitochondrial proteins, which are localized to a second location in the cell, besides this specific organelle. We have termed these dual localized proteins echoforms or echoproteins (echo in Greek denotes repetition). As the research on dual targeting of proteins is developing and evidence is accumulating for high abundance of the phenomenon, there is a growing need for new methods that would allow the identification of dual localized proteins and analysis of their functions in each subcellular compartment. This is particularly critical for single translation products that are encoded by the same gene and are actually derived from the same protein but nevertheless distribute between different subcellular compartments. The above considerations have led us to develop several approaches for studying dual localized proteins and their dual function. These include an  $\alpha$ -complementation-based assay, specific depletion, and selection of the individual echoproteins.

**Key words** Dual-targeting, Dual-function, Mitochondria, *Saccharomyces-cerevisiae*, Mitochondrial targeting sequence (MTS)

---

### 1 Introduction

Eukaryotic cells are defined by the existence of subcellular compartments and organelles. This allows the partitioning of various biochemical pathways out of the cytosolic milieu into discrete organelles. Mitochondria are one such example. They are responsible for energy production and essential metabolic pathways in the cell and have also been implicated in other fundamental processes such as apoptosis, aging, and cancer. The localization of a protein to a specific subcellular compartment is one of the most fundamental processes of a living cell. Like transcription and translation, protein localization is one of the steps by which the information encoded in the DNA is expressed, and is thus a function that must

be accomplished by all life forms. Sorting of a protein to an organelle involves two main steps: targeting directed by information within the protein, that is specifically recognized by an intracellular membrane-associated apparatus, and translocation through this membrane. For example, mitochondrial precursor proteins are imported into mitochondria in a multistep process mediated by translocation systems in the outer and inner membranes [1–3]. These proteins usually harbor an amino-terminal mitochondrial targeting sequence (MTS), which is recognized by the organelle receptors and import machinery.

It is well documented that in eukaryotic cells molecules of a single protein can be located in more than one subcellular compartment, a phenomenon termed dual targeting, bimodal targeting, or dual localization [4–6]. There is growing evidence for abundant dual targeting of mitochondrial proteins. A combination of genome-wide screens and bioinformatics suggests that about a third of the yeast mitochondrial proteome is dual localized [7–9]. We have named these dual localized proteins echoforms or echo-proteins, indicating forms of the same protein that are present in the distinct compartments of the cell. This term replaces the terms “isoproteins” or “isoenzymes” that are reserved for proteins with the same activity but different amino acid sequences. Echoforms are identical or nearly identical, even though in some cases, surprisingly, they have completely different functions in different compartments. With regard to mitochondria, our operational definition of dual localized proteins refers to situations in which one echoform is translocated across or inserted into one of the two mitochondrial membranes while the other echoform is present in a different compartment.

Dual localization of mitochondrial proteins can be achieved by different mechanisms, which can be principally divided into two groups, based on whether they involve synthesis of a single or two translation products. In the latter and simpler case, one of the two translation products harbors an MTS while the other lacks it. The production of two translation products can be accomplished at the level of the DNA (two or more genes), mRNA (alternative transcription initiation or splicing), or translation initiation [10, 11]. As the research on dual targeting of proteins is developing and evidence is accumulating for high abundance of the phenomenon, there is a growing need for new methods that would allow the identification of such proteins and analysis of their functions in each cellular compartment. This is particularly critical for single translation products that distribute between two subcellular compartments. In this regard, several mechanisms of dual distribution of single translation products have been described [11, 12]. Importantly, in all these cases, both populations are encoded by the same gene and are actually derived from the same protein. Hence, traditional genetic approaches, such as knockout of the

gene of interest or knockdown of its mRNA, are not applicable for their analysis since these methods deplete all protein products of the gene.

Several methods have been developed to identify dual localization of proteins. The classical method to detect the localization of a specific protein involves subcellular fractionation followed by probing of each fraction for the presence (e.g., immunoblot) or the activity of the protein under study. However, this tedious method is limited to subcellular compartments that can be fractionated and is subject to artifacts resulting from impurities in the preparation of fractions. To this end, several methods have been developed to more easily probe protein localization. These methods are based on fusion of a reporter protein or an epitope tag to proteins, which allows them to be visualized within cells. Fusion of  $\beta$ -galactosidase may be detected by its enzymatic activity (by adding an appropriate substrate) or indirectly using immunofluorescence. Green fluorescent protein (GFP) fusions have the advantage that they can be visualized in living cells and do not need the addition of external substrates. In yeast *Saccharomyces cerevisiae*, epitope tagging and GFP fusions were used to annotate the cellular location of the majority of the proteome [13, 14].  $\beta$ -galactosidase and GFP fusions, however, involve long attachments (1024 and 238 amino acids respectively), which may perturb the function and affect the localization of the modified proteins. Epitope tagging diminishes this problem, yet it cannot be applied in living cells since it requires cell fixation and permeabilization for immunofluorescence. A limitation of both reporter fusion and epitope tagging described above is that they require the visualization of individual cells to identify proteins that are localized to a specific subcellular compartment. Another major problem is “eclipsed” distribution, when a large amount of an echoprotein in one compartment eclipses the detection of the second echoprotein in the other compartment [15, 16]. The eclipsed population of such proteins, therefore, cannot be detected using traditional methods. We predict that this phenomenon is abundant [7, 8]; however, in most genome-wide screens it is likely overlooked, due to experimental limitations.

### **1.1 Detection of Dual Targeting**

The above considerations have led us to develop an  $\alpha$ -complementation-based assay, which has proved to be a simple and sensitive method for probing dual protein localization within yeast cells [7, 17–19]. In the yeast *Saccharomyces cerevisiae*  $\alpha$ -complementation was used as a model for protein assembly mediated by molecular chaperones [20]. In our laboratory, this method was modified to specifically probe dual protein localization within yeast cells. The basis of this approach is the requirement for localization of two complementing  $\beta$ -galactosidase fragments ( $\alpha$ —77 amino acids;  $\omega$ —993 amino acids) within the same compartment to achieve enzymatic activity. In this approach, the

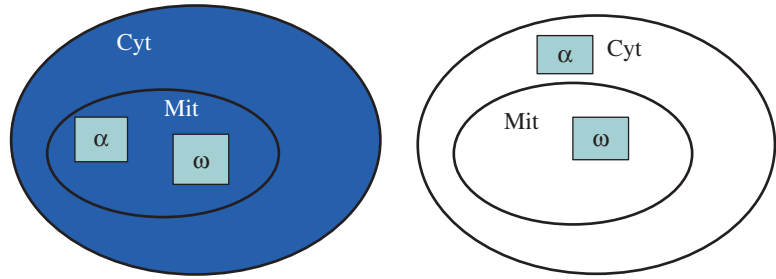


**Fig. 1** Schematic illustration of the  $\alpha$ -complementation assay. This assay is based on co-localization of  $\beta$ -galactosidase fragments,  $\alpha$  and  $\omega$ , within the same compartment. If the two fragments are localized to the same subcellular compartment, enzymatic activity should be detected by the production of blue colonies on X-gal plates (left scheme). In the case that the two fragments are in separate compartments white colonies should appear (right scheme; Cyt, cytosol; Mit, mitochondria)

$\alpha$ -fragment is attached to the C terminus of the protein of interest and co-expressed within yeast cells with a compartmentalized  $\omega$  fragment. Upon growth on plates containing X-gal, the colonies exhibit a color phenotype reflecting the localization of the  $\alpha$ -fused protein, as illustrated in Fig. 1. This method was demonstrated to be highly sensitive, as it enabled detection of eclipsed dual distribution of the proteins aconitase and Nfs1 in yeast [16, 19]. Moreover, we have used  $\alpha$ -complementation to screen the yeast mitochondrial proteome, which detected many new dual targeted proteins and supports the notion that dual targeting of mitochondrial proteins is highly abundant. In fact, as mentioned above, we estimate that a third of the mitochondrial proteome is dual targeted [7, 8].

## 1.2 Detection of Dual Function

One possible approach to prove localization is to elucidate a function of proteins in each compartment. Interestingly, such proteins can perform the same or distinct activities and functions in each location [15, 12, 21]. One way to analyze whether a protein has a function in a specific compartment is to specifically deplete the protein from one, and only one, of the compartments. While achieving mitochondrial depletion is sometimes simple (e.g., by expressing a version of the protein lacking the MTS), creating an exclusively mitochondrial targeted active protein may be a harder task. One scheme that was developed in our laboratory is based on fusing the protein of interest to a degron [22], which causes degradation of the cytosolic echoprotein in the proteasome while the mitochondrial population of the protein is protected in the organelle (and remains intact), as illustrated in Fig. 2. Thus, using this scheme, one can specifically deplete a protein from a specific subcellular location. The results of such an experiment are shown in Fig. 3 in which the yeast enzyme aconitase is analyzed; Aco1-SL17 (aconitase tagged with the degron

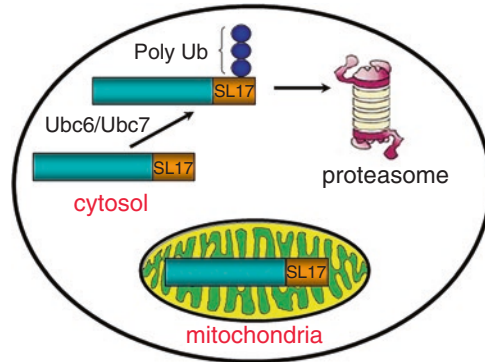


**Fig. 2** The strategy of location-specific depletion of a dual localized protein. The SL17 degradation signal is fused to the C-terminus of a dual-distributed protein. The fusion protein is recognized by the ubiquitin-proteasome system and is degraded only in the cytosol or nucleus, while its mitochondrial population remains stable

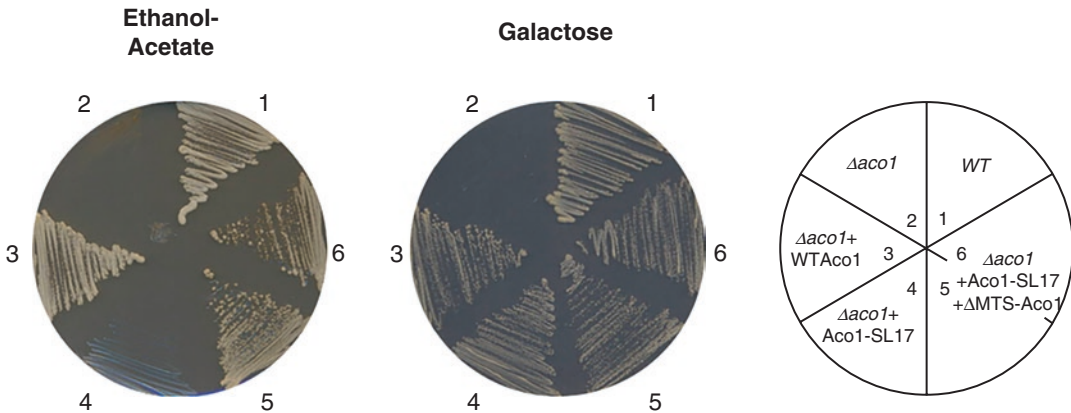


**Fig. 3** Aco1-SL17 fusion protein can complement the mitochondrial but not the cytosolic function of aconitase. Wild-type and  $\Delta aco1$  strains harboring the indicated plasmids were grown on galactose or ethanol-acetate plates. Strains lacking cytosolic aconitase ( $\Delta aco1 + Aco1-SL17$ , panels 4) cannot grow on ethanol-acetate (*left panel*) indicating a defect in the glyoxylate shunt. Accordingly, introduction of cytosolic aconitase into such a strain ( $\Delta aco1 + Aco1-SL17 + \Delta MTS-Aco1$ , panels 5, 6) restores its ability to grow on ethanol-acetate plates (compare *left panels* 5, 6 to *left panel* 4)

SL17) can complement the mitochondrial but not the cytosolic function of aconitase in  $\Delta aco1$  yeast strain background.

Another way to deplete an echoprotein from one of its subcellular compartments is to use a genetic selection. For this, we fused the protein of interest to the yeast Ura3 protein. If such a fusion protein is even partially localized to the cytoplasm, the respective yeast strain will be sensitive to 5-fluoroorotic acid (5-FOA). However, if mutations in the gene of interest or elsewhere in the yeast genome cause the Ura3 fusion protein to be targeted

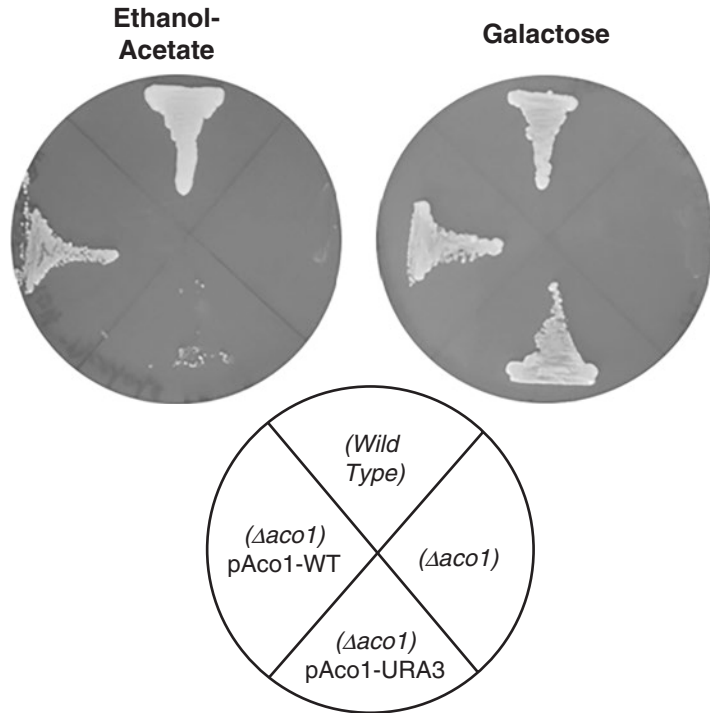


**Fig. 4** Loss of cytosolic aconitase causes a glyoxylate shunt defect. Yeast strains expressing pAco1-Ura3 (which is exclusively mitochondrial) in a  $\Delta aco1$  background show a glyoxylate shunt defect as indicated by the yeast mutant's inability to grow on ethanol-acetate plates, in contrast to the wild-type strain or  $\Delta aco1$  strain expressing the wild-type protein

exclusively to mitochondria, the strain will be resistant to 5-FOA. This allowed us to select for strains in which the fusion protein is exclusively targeted to mitochondria, as illustrated in Fig. 4 [16]. We have used the “degron” and “genetic selection” approaches to demonstrate that the enzyme aconitase in yeast is eclipsed distributed between the mitochondria, containing the vast majority of the protein, and the cytosol with a very low level [16, 22]. Typical experimental setups for the three methods, we refer to above, are described in the next section. While the approaches above work for most proteins that we have looked at, they do not apply for all (*see Note 1*).

## 2 Materials

### 2.1 Yeast Transformation

Transformation Mix. PEG 3350 (50% W/V): 50 g PEG 3350 dissolved in 100 mL DDW, Stirred and autoclaved. 1 M LiAc: 66.59 g/mol, dissolved in DDW and filter sterilized. SS-DNA (Testes DNA, Sigma cat # D-7656): 1 mL of 2 mg/mL of testes DNA in Sterile DDW, mixed and divided into aliquots in Eppendorf tubes, boiled for 5' and put on ice before adding to the transformation mix.

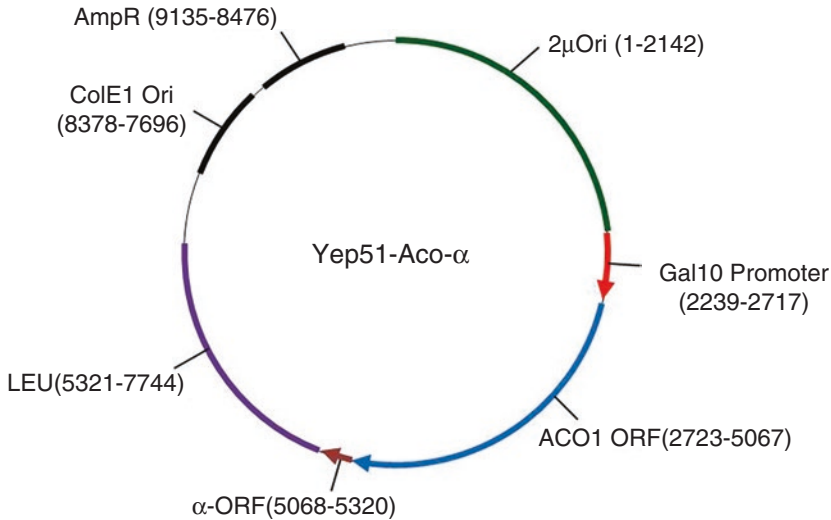


**Fig. 5** Illustration of Yep51-Aco1- $\alpha$  tagged expression plasmid. LEU2, *S. cerevisiae* gene; AmpR, *E. coli* ampicillin resistance gene; ORF, Open Reading Frame of the indicated genes. Ori, origin of replication of the indicated episomes; GAL10 Promoter, promoter of the *S. cerevisiae* gene GAL10

## 2.2 Detection of Dual Localization by the $\alpha$ Complementation Assay

1. *Plasmids*: The open reading frames of the genes of interest are C terminally tagged with the  $\alpha$  fragment sequence and cloned into yeast episomal plasmids under the GAL promoter (as illustrated in Fig. 5) such as pYEp51 or p425Gal which are commercially available, or specifically into pYEp51-Aco- $\alpha$  which we can provide (*see Note 2*). For controls, one must choose an exclusive mitochondrial protein such as KGD2- $\alpha$  and an exclusive cytosolic protein such as HXK1- $\alpha$ , both accordingly cloned in pYEp51 or p425Gal. In order to detect the localization of your chosen gene product, you must separately co-express it with cytosolic and mitochondrial omega ( $\omega_c$  and  $\omega_m$  respectively) which can be obtained from our lab [19]. Purify all plasmids (50–300 ng/ $\mu$ L) to transform them into wild-type yeast strains such as BY4741 or W303 (EUROSCARF).
2. *Synthetic depleted (SD) medium*: 0.67% (w/v) yeast nitrogen base without amino acids (Difco Laboratories), 2% glucose/2% galactose (w/v), 630 mg/liter CSM dropout mix (Qbiogene) (Adenine-10 mg/mL; L-Arginine-50 mg/mL; L-Aspartic Acid-80 mg/mL; L-Isoleucine-50 mg/mL; L-Lysine-50 mg/mL; L-Phenylalanine-50 mg/mL; L-Threonine-100 mg/mL; L-Serine-50 mg/mL; L-Tyrosine-50 mg/mL; Valine-140 mg/mL). Sterilize by autoclave. For agar plates, add 2% agar before autoclaving and pour plates after letting the liquid cool to 50 °C.
3. *X-gal (5-bromo-4-chloro-3-indolyl- $\beta$ -D-galactopyranoside) plates*: SD medium containing, 2% galactose, CSM dropout mix (Qbiogene) supplemented with the appropriate amino acids (630  $\mu$ g/mL) and 2% agar. After autoclaving, cool to

50 °C, add raffinose to 1% (stock 10% raffinose (w/v), filter sterilized), X-gal (4 mL of 20 mg/mL dissolved in 100% *N,N*-dimethylformamide in a glass tube covered with aluminum foil) to 0.008% and BU salts to a 1× concentration (25 mM) (10× stock; 250 mM Sodium Phosphate buffer titrated to pH 7), mix thoroughly and pour plates. Cover plates with aluminum foil to prevent X-gal from decomposing.

### 2.3 Detection of Dual Function

#### 2.3.1 Location-Specific Depletion of Dual-Localized Proteins

1. *Plasmids*: The open reading frames of the genes of interest are C terminally tagged with the sequence encoding the SL17 degradation signal from plasmid pBRR88-SL17, which can be obtained from our lab or from RG Kulka [23]. This tagged gene sequence is cloned into a yeast episomal plasmid (pYEp51 or p425Gal) under the *GAL* promoter (*see Note 2*) and as a control without the Mitochondrial Targeting Sequence (MTS). Additional controls are the wild-type gene with and without the MTS, cloned into the same vectors without adding the SL17 degradation signal. Purify plasmids (50–300 ng/μL) to transform them into chromosomal knockout yeast strains of your gene of interest. In some cases, to obtain chromosomal knockout strains expressing the cloned tagged gene of interest, plasmid shuffling is performed; transform the knockout strain harboring a vector expressing wild-type gene of interest with a plasmid encoding the tagged form of the genes. Subsequently cure the resultant strain of the wild-type plasmid. If your selected gene is essential, use TetO7-Promoter Strains that are promoter-shutoff strains and those can overcome the problem of deleting your gene [24].
2. *Ethanol-Acetate Plates*: 0.67% (w/v) yeast nitrogen base without amino acids (Difco Laboratories), 3% Ethanol (v/v), 2% K acetate (w/v), 630 mg/liter CSM dropout mix (Adenine-10 mg/mL; L-Arginine-50 mg/mL; L-Aspartic Acid-80 mg/mL; L-Isoleucine-50 mg/mL; L-Lysine-50 mg/mL; L-Phenylalanine-50 mg/mL; L-Threonine-100 mg/mL; L-Serine-50 mg/mL; L-Tyrosine-50 mg/mL; Valine-140 mg/mL), 2% agar. Sterilize by autoclaving and pour after letting the liquid cool down to 50 °C.
3. *TE buffer*: 0.1 M Tris-HCl, pH 7.5, 1 mM EDTA, pH 8.0.
4. *4×TENN*: 50 mM Tris-HCl, pH 8.5, 5 mM EDTA, NonidetP-40 (NP 40) 0.5% (v/v), 150 mM NaCl.
5. *1×TENNS*: 50 mM Tris-HCl, pH 7.5, 5 mM EDTA, 1.0% (v/v) NP-40, 500 mM NaCl, 5% (w/v) Sucrose.
6. *Metabolic labeling*: [<sup>35</sup>S] L-Methionine, Cysteine (Perkin Elmer, catalog number-NEG772007MC).
7. *4× sample buffer*: 200 mM Tris-HCl, pH 6.8, 40% (w/v) Glycerol, 8% (w/v) SDS, 0.04% (w/v) bromophenol blue, 400 mM DTT.

8. *10× cold methionine and cysteine*: Methionine-0.03% (w/v), Cysteine-0.04% (w/v).
9. *100 mM PMSE*: 17.42 g in 1 L DDW.
10. *Protein A magnetic Dynabeads*: (Novex Life Technologies).
11. *Glass beads*: 0.5 μm in diameter.

### 2.3.2 Genetic Selection Using the Fusion with URA3 Gene

1. *Plasmids*: Clone your gene of interest into a high copy plasmid with a *GAL* promoter, (YEp51, p425GAL, *see Note 2*). Purified plasmids (50–300 ng/μL) containing the gene of interest are transformed into a yeast strain harboring a chromosomal knockout of that gene. In some cases, to obtain chromosomal knockout strains expressing the cloned tagged gene of interest, plasmid shuffling is performed. Transform the knockout strain harboring a vector expressing wild-type gene of interest with a plasmid encoding the tagged form of the genes. Subsequently, cure the resultant strain of the wild-type plasmid. If your selected gene is essential, use TetO7-Promoter Strains that are promoter-shutoff strains and those can overcome the problem of deleting your gene [24].
2. *5-FOA plates*: For a 1-L medium, prepare a 5-FOA solution by mixing 1 g 5-FOA in 495 mL of water and 5 mL of a 2.4 mg/mL uracil solution. Stir with low heat until completely dissolved and filter sterilize (5-FOA is sensitive to light so one should keep plates and solutions in the dark).

To a separate flask add: 0.17% (w/v) yeast nitrogen base without amino acids and ammonium sulfate, 0.5% (w/v) (NH<sub>4</sub>)<sub>2</sub>SO<sub>4</sub>, 2% galactose (w/v), 630 mg/L CSM dropout mix (Adenine-10 mg/mL; L-Arginine-50 mg/mL; L-Aspartic Acid-80 mg/mL; L-Isoleucine-50 mg/mL; L-Lysine-50 mg/mL; L-Phenylalanine-50 mg/mL; l-Threonine-100 mg/mL; L-Serine-50 mg/mL; L-Tyrosine-50 mg/mL; Valine-140 mg/mL), add the appropriate amino acids for the selection of the specific vector (L-Histidine-20 mg/mL; L-Leucine-100 mg/mL; L-methionine-20 mg/mL; L-Tyrosine-50 mg/mL and no uracil), 2% agar and 500 mL of water. After autoclaving and cooling down to 50 °C, add the 5-FOA solution and pour plates. Plates should be kept in the dark.

---

## 3 Methods

### 3.1 Yeast Transformation Protocol

1. Grow a 2 mL culture overnight in YPD or SD at 30 °C.
2. Next day dilute the cells to an OD<sub>600</sub> = 0.5 in 10 mL fresh YPD. Grow until OD<sub>600</sub> = 0.9–1.2 (approximately 2 h).

3. Spin cells (5', 4500 × *g* at room temperature). Resuspend pellet in 5 mL sterile DDW. Spin under the same conditions, resuspend in 1 mL of 0.1 M LiAc, transfer to an Eppendorf tube, and spin (1 min, 4000 × *g* at room temperature).
4. Resuspend in 25 μL of Sterile DDW for each reaction (maximum 150 μL).
5. Prepare Eppendorf tubes with a transformation mix: 240 μL PEG (50% W/V PEG 3350 in DDW, autoclaved), 36 μL of 1 M LiAc, 25 μL SS-DNA (Testes DNA, 2 mg/mL; Sigma cat # D-7656. Boiled for 5' and put on ice before adding to the transformation tube) and 5 μL plasmid DNA (100–300 ng/μL).
6. Add 25 μL of cells to the transformation mix, vortex, and incubate tubes in 30 °C for 30' with shaking (1000 rpm).
7. Heat shock (15', 42 °C).
8. Spin (1', 4000 × *g*) and remove the supernatant.
9. Resuspend the pellet in 100 μL Sterile DDW and plate on a selective plate.

### 3.2 Detection of Dual Localization by the $\alpha$ Complementation Assay

1. Amplify by PCR the corresponding ORFs, using yeast genomic DNA as a template with the following primers: **Fw-primer**-cgcgtcgacATG-[16–18 base pairs following the first methionine] **Rev-primer**-ctcccgggt-[last 18–20 base pairs without the stop codon]. SalI and SmaI are within the Fw and Rev primers respectively. Cut the amplified PCR fragments with SalI and SmaI and clone into pAco1- $\alpha$  cut with SalI and SmaI which fuses the amplified sequences to the N'-terminus of the  $\alpha$ -peptide (the  $\alpha$ -peptide coding sequence corresponds to the first 81 amino acids of wild-type *Escherichia coli*  $\beta$ -galactosidase) (see **Notes 3** and **4**).
2. Transformation into yeast strains: Follow **steps 1–10** in Subheading **3.1** to produce required yeast strains. For transformation, the following combination of plasmids is used to produce the strains required for the assay:  $\omega$ c+KGD2- $\alpha$ ,  $\omega$ m+KGD2- $\alpha$ ,  $\omega$ c+H XK1- $\alpha$ ,  $\omega$ m+H XK1- $\alpha$ ,  $\omega$ c+gene of interest- $\alpha$ ,  $\omega$ m+ gene of interest- $\alpha$ .
3. Plate transformants on SD-glucose plates without uracil or leucine, choose individual transformants, and plate them on fresh SD plates without uracil and leucine. One should take into consideration that if using different wild-type strains or different plasmids, different selective markers may be required.
4. Grow the transformed strains overnight with shaking at 30 °C in 2 mL of liquid SD-glucose medium without uracil and leucine.
5. Dilute the cultures to an optical density (OD) of OD<sub>600</sub> = 0.6 in 2 mL of fresh SD medium without uracil and leucine and

incubate them with shaking at 30 °C for 1–2 h to let the strains recover (there is no change in OD). Spin 1 mL of each culture in a table top centrifuge for 3 min, 4500 × *g* at room temperature, and resuspend cell pellets in 100 μL of sterile water.

6. Plate 7 μL of each culture on X-gal plates and incubate at 30 °C for 72 h. Plate the appropriate controls for cytosolic and mitochondrial localization. If a color does not appear after 3 days, you can incubate the plates for an additional 24–48 h. The results should appear as blue or white colonies as illustrated in Fig. 6 (see Note 5).

### 3.3 Location-Specific Depletion of Dual-Localized Proteins

In order to eliminate a specific echoprotein from the yeast cytosol, we fused a previously defined degradation signal that is termed “SL17” to the C-terminus of aconitase, a protein that we have shown is distributed between mitochondria and cytosol [16]. This degradation signal is 50 amino acids long (SISFVIRSHASIRMGASNDDFFHKLYFTKCLTSVILSKFLIHLLLRSTPRV) and is recognized by the ubiquitin/proteasome system. The cytosolic and nuclear populations of the fusion protein are eliminated following degradation by the proteasome system, while the mitochondrial population of the protein remains stable [22].

#### 3.3.1 Attachment of Ubiquitin/Proteasome Degradation Signal and Preparation of Yeast Strains

1. Amplify SL17 degradation signal from a pBRR88-SL17 plasmid [kindly provided by [23]], using primers Fw: 5-TCCCCCGGGATCGATTAGTTTCGTAATACG-3 and Rev: 5-CCGGGCCCTTAAACTCTTGGCGTACTCC-3. Add your favorite restriction sites to both primers.
2. Clone your favorite gene into a yeast expression vector such as p425Gal or YEp51 (see the previous sections).

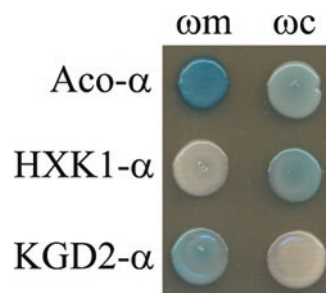


**Fig. 6** α-complementation assay for aconitase mutants. Yeast wild-type cells co-expressing cytosolic ω (ωc) or mitochondrial ω (ωm), together with the indicated fused-α proteins, were grown on galactose medium containing X-gal. Blue colonies detect alpha fragments that are associated with the indicated ω fragments. Kgd2-α, mitochondrial marker, shows a blue phenotype exclusively in mitochondria; HXK1-α, cytosolic marker, shows a blue phenotype exclusively in cytosol

3. Cut the SL17-PCR product and clone it downstream to the C-terminus of your favorite gene (Other gene cloning methods can be applied, e.g., Gibson assembly [25]).
4. As controls, clone your favorite gene without the Mitochondrial Targeting Sequence (MTS) into a yeast expression vector such as p425Gal or YEp51, and add the SL17 degradation signal. In addition, clone the wild-type gene with and without the MTS into the same vectors without adding the SL17 degradation signal. These controls will allow you to evaluate the efficiency of the degradation of your protein due to the degenon signal.
5. Transform your plasmids harboring the cloned hybrid SL17 tagged protein and the respective control into a yeast strain harboring a chromosomal knockout of its endogenous gene as described in Subheading 3.1, steps 1–10. Select for transformants (using the appropriate selection). If your selected gene is essential, use TetO7-Promoter strains that are promoter-shutoff strains and which can overcome the problem of deleting an essential gene [24].

### 3.3.2 Examination of the Stability of the Tagged Protein by Pulse-Chase

In order to show that the elimination of the protein of interest from the cytosol results from its degradation, one can examine its stability employing pulse-chase labeling experiments.

1. Grow yeast cultures in SD-galactose (as described in Subheading 2.2, item 3) to  $OD_{600} = 1.5$  (5 mL culture for each sample) to activate the promoter. Harvest the cells (5', 4500 × *g*, at room temperature), resuspend pellet in sterile DDW (1 mL for each 5 mL culture), wash and resuspend the pellet in fresh galactose synthetic depleted medium lacking methionine (5 mL for each 5 mL original culture). Incubate at 30 °C for 1 h, shaking at 200 rpm to eliminate methionine pools from the cells.
2. Harvest the starved cultures (5', 4500 × *g*), resuspend in galactose SD medium lacking methionine (400 μL for each 5 mL starved cells), and add 6.5 μCi of [<sup>35</sup>S]methionine/cysteine. Incubate for 15 min at 30 °C while gently shaking, in order to label newly synthesized proteins (*see Note 6*).
3. Stop labeling by the addition of excess “cold” methionine and cysteine to a final concentration of 0.003 and 0.004% respectively (40 μL of a 10× solution to each 400 μL of labeled cells). Incubate cultures at 30 °C with gentle shaking.
4. Aliquots are taken as a function of time (e.g., every 5 min, 400 μL at each time point), 100 mM sodium azide is added to a final concentration of 10 mM (40 μL for 400 μL time point) and the cells are placed on ice (*see Note 7*).
5. Labeled cells are collected by centrifugation (1', 4500 × *g*), and washed twice with ice cold 10 mM sodium azide.

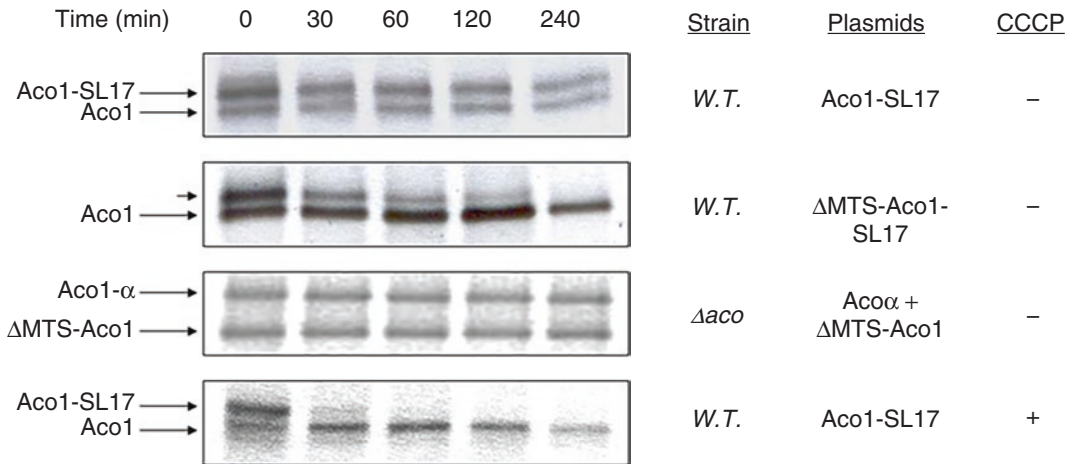


**Fig. 7** Cytosolic Aco1-SL17 is degraded in the cell. Yeast strains harboring the indicated plasmids were induced in galactose medium and pulse labeled with [<sup>35</sup>S] methionine–cysteine for 15 min in the presence or absence of CCCP that blocks import, followed by a chase (addition of cold methionine–cysteine and cycloheximide) for the times indicated. Total cell extracts were prepared, immunoprecipitated with aconitase antiserum, and analyzed by SDS-PAGE and autoradiography. Aco1-SL17 retained in the cytosol is rapidly degraded (*second* and *fourth panels*, upper bands) while the endogenous protein remains stable, (*panels 1, 2, and 4*, lower bands). Aco1-SL17 in mitochondria (*panel 1* upper band) and Aco1 without the SL17 degradation signal (*panel 3*, upper band) are stable

6. Resuspend the pellet in 350 μL ice cold TE buffer, pH 8.0, containing 1 mM phenylmethylsulfonyl fluoride (PMSF).
7. Brake with glass beads for 20 min of vigorous shaking at 4 °C, and centrifuge (5' 4500 × *g* at 4 °C) to obtain the supernatant fraction.
8. Denature protein in the supernatants by boiling for 5 min in the presence of 1% SDS.
9. Immunoprecipitate overnight at 4 °C in the presence of one-fourth of the total volume of 4× TENN buffer, with the appropriate antiserum and protein A magnetic Dynabeads (Novex by Life technologies).
10. Wash three times with ice cold 1× TENNS buffer and resuspend the pellet in 50 μL of 1× sample buffer.
11. Analyze by SDS-PAGE followed by autoradiography as illustrated in Fig. 7.

### 3.3.3 Examination of the Compartment-Specific Deletion Phenotype

After establishing a subcellular knockout of the protein of interest from the cytosol, one can assess a specific phenotype resulting from the absence of the cytosolic population of the protein. Such a phenotype would provide further evidence for the presence of the protein in the cytosol and for its specific cytosolic function.

In order to examine the effect of compartment-specific deletion, the SL17-tagged version of the protein is expressed in the deletion background and a phenotype of such a strain is analyzed under conditions that presumably require the cytosolic echoprotein (e.g., ethanol-acetate medium that requires cytosolic aconitase). The controls are plasmids encoding the wild-type protein without the MTS and tagged with SL17, and plasmids encoding the wild-type protein without the MTS and without the SL17 tag. Both controls are transformed into the specific gene deletion strain. These controls will allow you to examine the effect of the compartment specific depletion. One example of such an analysis, performed for aconitase, is shown in Fig. 3 (*see Note 8*).

1. Transform plasmids encoding the wild-type protein and the SL17-tagged wild-type protein, each into the deletion background strain. Also co-transform the  $\Delta$ MTS protein with the SL17-tagged wild-type protein.
2. Streak out the transformed strains and examine the growth phenotype on appropriate agar plates (e.g., ethanol-acetate medium that requires cytosolic aconitase).

### **3.4 Genetic Selection Using the URA3 Gene**

An alternative approach to deplete a dual-localized protein from the cytosol is to use a genetic selection. We have used the hybrid Ura3 gene product, which even when it is partially localized to the cytoplasm, such yeast strains are sensitive to 5-FOA. However, if mutations in the protein of interest or mutations elsewhere in the yeast genome cause the Ura3 fusion protein to be targeted exclusively to mitochondria, the strain will be resistant to 5-FOA. This can be exploited to select for strains that express the fusion protein exclusively in mitochondria, thereby producing a functional cytosolic knock-out strain. A specific phenotype of such a strain can then be analyzed as described below.

#### **3.4.1 Attachment of URA3 Gene to the Protein of Interest**

1. Amplify URA3 (orotidine-5'-phosphate decarboxylase) gene open reading frame (ORF) from any URA3 containing vector, using primers 5'-CCCCCGGGGATCCCAAGATCCAAGC-3' and 5'-CCCTCGAGTTAGTTTTGCTGGCCGCATC-3'. Use a two-step PCR procedure to fuse the N' terminus of URA3 gene to the C' terminus of the chosen gene lacking the stop codon (other gene cloning methods can be applied, e.g., Gibson assembly [25]). Add your favorite restriction sites to both primers.
2. Cut this PCR fragment with the appropriate restriction enzymes and clone into p425Gal or any high copy number plasmid with a GAL promoter, cut with the same restriction enzymes. Do not use Ura3 as a plasmid selective marker since it is used for our genetic selection.

### 3.4.2 Identification of a Phenotype

- 1 Transform your plasmid encoding the hybrid Ura3 protein into a yeast strain harboring a chromosomal knockout of the specific chromosomal gene and select for transformants (using an appropriate plasmid marker selection, e.g., plates lacking leucine for p425GAL).
- 2 Grow the transformants on SD-galactose agar plates containing 5-FOA (0.1%) (*see* **Note 9**).
- 3 Isolate 5-FOA resistant strains that were presumably selected for misdistribution of the hybrid protein and express it exclusively in mitochondria. The frequency of *ura3* gene reverse mutations is negligible.
- 4 Examine for a specific phenotype associated with the loss of a cytosolic function of the protein (*see*, for example, Subheading 3.4.2 and **Note 8**).

---

## 4 Notes

1. While the approaches above work for most proteins that we have looked at, they do not apply for all. For example, addition of the  $\alpha$  tag or the SL17 degradation signal to the C terminus of a protein may obscure a C-terminal targeting signal or may affect the structure and function of the protein. Thus, in certain cases, more laborious approaches are required. An illustration of such a situation was our attempt to specifically deplete the enzyme fumarase from the cytosol. We were unsuccessful using all the approaches above. To achieve specific subcellular location-depletion of this protein, the *Fum1* gene was chromosomally deleted and an adjusted *Fum1* gene was transformed into the mitochondrial genome. The result was exclusive mitochondrial localization of the gene product [26].
2. In all the above approaches, we initially recommend inducible overexpression by using plasmids with the *GAL10* promoter such as pYEp51 or p425GAL. The reasons for this are: (i) Using this strong promoter enables detection of low abundant proteins, which would be missed for many proteins under normal levels of expression. (ii) The inducible *GAL10* promoter enables expression at much lower levels on other carbon sources such as raffinose or glycerol.
3. For the  $\alpha$  complementation screen, all ORF DNAs are cloned under the *GAL10* promoter. Proteins whose distribution is achieved by alternative transcription initiation, alternative splicing, or alternative translation initiation may be missed if they require the authentic promoter and/or upstream untranslated sequences. Fusion of the  $\alpha$  fragment, by homologous recombination, to the chromosomal copy of such genes may

solve some of these problems as well as problems arising from overexpression. This approach will obviously be at the expense of reduced sensitivity, due to lower expression levels.

4. When cloning the  $\alpha$  tagged proteins, one should remember to exclude the stop codon from the reverse primer. In addition, add a linker such as glycine or alanine between the gene ORF and the  $\alpha$  tag. This linker improves separation of domains, that the chosen protein and that of  $\alpha$  tag, which in turn improves the  $\alpha$  complementation activity. After cloning and sequencing the vectors, we recommend examining fusion protein expression by Western blot using  $\alpha$ -antiserum.
5. The  $\alpha$  complementation method can also be used to screen for mutations that affect dual localization of a specific protein of interest. Using this approach, we discovered that the C-terminal domain of aconitase is necessary and sufficient for dual targeting, constituting an independent dual targeting signal [27].
6. For pulse-chase experiments, cells are labeled with  $L$ -[ $^{35}\text{S}$ ] Methionine, Cysteine (Perkin Elmer, catalog number-NEG772007MC). The total concentration is 0.83 mCi/mL and we recommend using between 5 and 8  $\mu\text{L}$  for each labeling reaction. Refer to general and specific safety precautions when dealing with radioactivity.
7. When planning the timing of taking aliquots in pulse chase experiments, we recommend initially trying 5 min intervals including time 0 (immediately after adding cold cysteine-methionine). According to the results obtained changes in the intervals should be reconsidered.
8. To detect a phenotype upon subcellular “compartment-specific depletion” or in the case of genetic selection for subcellular “compartment-specific depletion,” one must choose a specific functional assay for each protein based on previous unpublished research or published data.
9. For agar plates containing 5-FOA, it is better to use YNB-AA/AS (yeast nitrogen base without amino acids and ammonium sulfate). From our experimental experience, we get better results when adding ammonium sulfate (AS) separately.

## References

1. Lister R, Hulett JM, Lithgow T, Whelan J (2005) Protein import into mitochondria: origins and functions today (review). *Mol Membr Biol* 22(1–2):87–100
2. Mokranjac D, Neupert W (2005) Protein import into mitochondria. *Biochem Soc Trans* 33(Pt 5):1019–1023. doi:10.1042/BST20051019
3. Wiedemann N, Frazier AE, Pfanner N (2004) The protein import machinery of mitochondria. *J Biol Chem* 279(15):14473–14476. doi:10.1074/jbc.R400003200
4. Avadhani NG, Sangar MC, Bansal S, Bajpai P (2011) Bimodal targeting of cytochrome P450s to endoplasmic reticulum and mitochondria: the concept of chimeric signals. *FEBS J* 278(22):4218–4229. doi:10.1111/j.1742-4658.2011.08356.x
5. Knockaert L, Fromenty B, Robin MA (2011) Mechanisms of mitochondrial targeting of cyto-

- chrome P450 2E1: physiopathological role in liver injury and obesity. *FEBS J* 278(22):4252–4260. doi:[10.1111/j.1742-4658.2011.08357.x](https://doi.org/10.1111/j.1742-4658.2011.08357.x)
6. Raza H (2011) Dual localization of glutathione S-transferase in the cytosol and mitochondria: implications in oxidative stress, toxicity and disease. *FEBS J* 278(22):4243–4251. doi:[10.1111/j.1742-4658.2011.08358.x](https://doi.org/10.1111/j.1742-4658.2011.08358.x)
  7. Ben-Menachem R, Tal M, Shadur T, Pines O (2011) A third of the yeast mitochondrial proteome is dual localized: a question of evolution. *Proteomics* 11(23):4468–4476. doi:[10.1002/pmic.201100199](https://doi.org/10.1002/pmic.201100199)
  8. Kisslov I, Naamati A, Shakarchy N, Pines O (2014) Dual-targeted proteins tend to be more evolutionarily conserved. *Mol Biol Evol* 31(10):2770–2779. doi:[10.1093/molbev/msu221](https://doi.org/10.1093/molbev/msu221)
  9. Dinur-Mills M, Tal M, Pines O (2008) Dual targeted mitochondrial proteins are characterized by lower MTS parameters and total net charge. *PLoS One* 3(5):e2161. doi:[10.1371/journal.pone.0002161](https://doi.org/10.1371/journal.pone.0002161)
  10. Kalderon B, Kogan G, Bubis E, Pines O (2015) Cytosolic Hsp60 can modulate proteasome activity in yeast. *J Biol Chem* 290(6):3542–3551. doi:[10.1074/jbc.M114.626622](https://doi.org/10.1074/jbc.M114.626622)
  11. Yogev O, Naamati A, Pines O (2011) Fumarase: a paradigm of dual targeting and dual localized functions. *FEBS J* 278(22):4230–4242. doi:[10.1111/j.1742-4658.2011.08359.x](https://doi.org/10.1111/j.1742-4658.2011.08359.x)
  12. Karniely S, Pines O (2005) Single translation--dual destination: mechanisms of dual protein targeting in eukaryotes. *EMBO Rep* 6(5):420–425. doi:[10.1038/sj.embor.7400394](https://doi.org/10.1038/sj.embor.7400394)
  13. Huh WK, Falvo JV, Gerke LC, Carroll AS, Howson RW, Weissman JS, O'Shea EK (2003) Global analysis of protein localization in budding yeast. *Nature* 425(6959):686–691. doi:[10.1038/nature02026](https://doi.org/10.1038/nature02026)
  14. Kumar A, Agarwal S, Heyman JA, Matson S, Heidtman M, Piccirillo S, Umansky L, Drawid A, Jansen R, Liu Y, Cheung KH, Miller P, Gerstein M, Roeder GS, Snyder M (2002) Subcellular localization of the yeast proteome. *Genes Dev* 16(6):707–719. doi:[10.1101/gad.970902](https://doi.org/10.1101/gad.970902)
  15. Regev-Rudzki N, Pines O (2007) Eclipsed distribution: a phenomenon of dual targeting of protein and its significance. *Bioessays* 29(8):772–782. doi:[10.1002/bies.20609](https://doi.org/10.1002/bies.20609)
  16. Regev-Rudzki N, Karniely S, Ben-Haim NN, Pines O (2005) Yeast aconitase in two locations and two metabolic pathways: seeing small amounts is believing. *Mol Biol Cell* 16(9):4163–4171. doi:[10.1091/mbc.E04-11-1028](https://doi.org/10.1091/mbc.E04-11-1028)
  17. Burak E, Yogev O, Sheffer S, Schueler-Furman O, Pines O (2013) Evolving dual targeting of a prokaryotic protein in yeast. *Mol Biol Evol* 30(7):1563–1573. doi:[10.1093/molbev/mst039](https://doi.org/10.1093/molbev/mst039)
  18. Naamati A, Regev-Rudzki N, Galperin S, Lill R, Pines O (2009) Dual targeting of Nfs1 and discovery of its novel processing enzyme, Icp55. *J Biol Chem* 284(44):30200–30208. doi:[10.1074/jbc.M109.034694](https://doi.org/10.1074/jbc.M109.034694)
  19. Karniely S, Rayzner A, Sass E, Pines O (2006) Alpha-complementation as a probe for dual localization of mitochondrial proteins. *Exp Cell Res* 312(19):3835–3846. doi:[10.1016/j.yexcr.2006.08.021](https://doi.org/10.1016/j.yexcr.2006.08.021)
  20. Abbas-Terki T, Picard D (1999) Alpha-complemented beta-galactosidase. An in vivo model substrate for the molecular chaperone heat-shock protein 90 in yeast. *Eur J Biochem* 266(2):517–523
  21. Mueller JC, Andreoli C, Prokisch H, Meitinger T (2004) Mechanisms for multiple intracellular localization of human mitochondrial proteins. *Mitochondrion* 3(6):315–325. doi:[10.1016/j.mito.2004.02.002](https://doi.org/10.1016/j.mito.2004.02.002)
  22. Shlevin L, Regev-Rudzki N, Karniely S, Pines O (2007) Location-specific depletion of a dual-localized protein. *Traffic* 8(2):169–176. doi:[10.1111/j.1600-0854.2006.00518.x](https://doi.org/10.1111/j.1600-0854.2006.00518.x)
  23. Gilon T, Chomsky O, Kulka RG (1998) Degradation signals for ubiquitin system proteolysis in *Saccharomyces cerevisiae*. *EMBO J* 17(10):2759–2766. doi:[10.1093/emboj/17.10.2759](https://doi.org/10.1093/emboj/17.10.2759)
  24. Mnaimneh S, Davierwala AP, Haynes J, Moffat J, Peng WT, Zhang W, Yang X, Pootoolal J, Chua G, Lopez A, Trochesset M, Morse D, Krogan NJ, Hiley SL, Li Z, Morris Q, Grigull J, Mitsakakis N, Roberts CJ, Greenblatt JF, Boone C, Kaiser CA, Andrews BJ, Hughes TR (2004) Exploration of essential gene functions via titratable promoter alleles. *Cell* 118(1):31–44. doi:[10.1016/j.cell.2004.06.013](https://doi.org/10.1016/j.cell.2004.06.013)
  25. Gibson DG, Smith HO, Hutchison CA III, Venter JC, Merryman C (2010) Chemical synthesis of the mouse mitochondrial genome. *Nat Methods* 7(11):901–903. doi:[10.1038/nmeth.1515](https://doi.org/10.1038/nmeth.1515)
  26. Yogev O, Singer E, Shaulian E, Goldberg M, Fox TD, Pines O (2010) Fumarase: a mitochondrial metabolic enzyme and a cytosolic/nuclear component of the DNA damage response. *PLoS Biol* 8(3):e1000328. doi:[10.1371/journal.pbio.1000328](https://doi.org/10.1371/journal.pbio.1000328)
  27. Ben-Menachem R, Regev-Rudzki N, Pines O (2011) The aconitase C-terminal domain is an independent dual targeting element. *J Mol Biol* 409(2):113–123. doi:[10.1016/j.jmb.2011.03.045](https://doi.org/10.1016/j.jmb.2011.03.045)

# Chapter 12

## Localizing mRNAs Encoding Mitochondrial Proteins in Yeast by Fluorescence Microscopy and Subcellular Fractionation

Dmitry Zabezhinsky, Hannah Sperber, and Jeffrey E. Gerst

### Abstract

Mitochondria are thought to have evolved from ancestral proteobacteria and, as a result of symbiosis, became an indispensable organelle in all eukaryotic cells. Mitochondria perform essential functions that provide the cell with ATP, amino acids, phospholipids, and both heme and iron-sulfur clusters. However, only 1% of mitochondrial proteins are encoded by the mitochondrial genome, while the remaining 99% are encoded in the nucleus. This raises a logistical challenge to the cell, as these nuclear-encoded proteins have to be translated, delivered to the mitochondrial surface, and translocated to its various compartments. Over the past decade, it was shown that subsets of mRNAs encoding mitochondrial proteins (mMPs) are localized to the mitochondrial surface in both yeast and mammalian cells. Moreover, factors (e.g., RNA-binding proteins) have been discovered that facilitate mMP targeting, and their loss leads to RNA mislocalization and defects in mitochondrial function (e.g., deficient respiration). Therefore, there is a demand in the field of mitochondrial biology to accurately measure mMP localization to the mitochondrial surface. In this chapter, we describe two techniques that allow for the visualization of mMPs using single-molecule fluorescent in situ hybridization and preparation of a highly enriched mitochondrial fraction followed by quantitative real-time PCR. Together, these techniques constitute powerful tools to link changes in mMP trafficking to defects in mitochondrial physiology.

**Key words** RNA trafficking, Mitochondria, Real-time PCR, MS2, Single-molecule fluorescence in situ hybridization, Subcellular fractionation

---

## 1 Introduction

### 1.1 mRNA Trafficking

In recent years, increasing evidence has shown the importance of intracellular mRNA targeting and localized protein synthesis—a mechanism widely used across the eukaryotic kingdoms to localize proteins [1–6]. Targeted mRNA transport restricts the localization of proteins to specific subcellular sites (e.g., organelles, domains), thus allowing for the temporal and spatial regulation of protein synthesis and function. RNA targeting is determined by intrinsic *cis*-acting sequence elements (also called “zipcodes”) and *trans*-acting

factors, such as RNA-binding proteins (RBPs), which recognize and bind to the different *cis* elements [7–9]. Together, the RNA and protein factors assemble to ribonucleoprotein complexes (RNPs) that are transported to their final destination within the cell either directly via the cytoskeleton [10, 11] or in association with cellular membranes [12–16], the latter possibly necessitating the involvement of endomembrane transport factors [17, 18]. Since mRNA localization contributes to the intracellular distribution of proteins to specific assembly sites, membrane domains, or organelles (as shown for mRNAs encoding peroxisomal [16], secreted/membrane [19], or mitochondrial proteins [20]), regulated RNA trafficking defines protein sorting at an early step of gene expression. Importantly, RNA trafficking was shown to be relevant for many cellular processes, including cell division [21], polarity [22], and differentiation [23].

For mitochondria, in particular, the correct targeting and import of mitochondrial proteins (MPs) is essential for organellar and, ultimately, cellular physiology. Mitochondria originally developed from a proteobacterial ancestor that was engulfed and co-opted by eukaryotic predecessors. Subsequently, it became indispensable for cellular energy production, amino acid and lipid synthesis, and other processes that are crucial for cell viability. Although mitochondria harbor their own inherited genome, about 99% of MPs are encoded in the nucleus [24]. Thus, proper mitochondrial function and biogenesis rely heavily on the correct expression and translocation of MPs at the appropriate mitochondrial target sites. Defects in MP sorting and localization lead to mitochondrial dysfunction and may cause severe diseases, in particular neurodegenerative diseases [25–27].

Previous studies focused mainly on posttranslational mechanisms to unravel protein import into mitochondria [28, 29]. In this context, N-terminal or internal protein targeting motifs, which are exposed during translation, were found to be responsible for the import of many MPs [28], as also shown for proteins targeted to the endoplasmic reticulum (ER). In contrast, co-translational mechanisms for protein import into mitochondria and the influence of mRNA localization are still poorly understood. The presence of transcriptionally active membrane-bound ribosomes at the mitochondrial surface was shown many years ago [30, 31], and recent studies reveal that mRNAs encoding mitochondrial proteins (mMPs) indeed associate with mitochondria-bound ribosomes [32–34]. In support of this idea, numerous mMPs were found to be enriched in the vicinity of mitochondria, rather than being distributed randomly within cells [13, 14, 33].

Different experimental approaches have been used to explore mMP trafficking and its impact upon restricted translation at the mitochondrial surface. We describe here the combination of two commonly used techniques: single-molecule fluorescence in situ

hybridization (smFISH) and mitochondrial fractionation followed by biochemical analysis that can be used to help broaden our understanding of mMP localization and its involvement in MP import. Together, these methods provide a useful toolset to comprehensively evaluate mMP quantity and localization at the mitochondrial surface.

## **1.2 Visualization of Endogenous mRNAs Using smFISH**

In situ hybridization is the most commonly used method to simultaneously localize and quantify specific mRNAs. In the single-molecule approach, multiple short and nonoverlapping oligonucleotides (about 20 nts long) are labeled with a fluorophore and used to collectively hybridize with the target transcript to produce a bright, dot-like fluorescence signal. Here we detail the use of smFISH in yeast to detect mMPs, quantify their expression levels, and analyze their subcellular distribution with respect to mitochondria and other compartments.

In general, smFISH can be easily applied to any sufficiently accessible target transcript using a unique, but not inexpensive, synthetic probe set designed against the native gene. We also use smFISH probes targeted against an RNA aptamer sequence (e.g., bacteriophage MS2 stem loops, MS2L) that has been integrated between the open reading frame (ORF) and 3'UTR of the gene of interest in the yeast genome. The genomic insertion of a multiple RNA aptamer cassette is performed using m-TAG, a genome-tagging procedure that enables aptamer integration by homologous recombination while leaving the 3'UTR intact in the expressed mRNA [35]. Thus, a single probe set can be used to target any coding RNA in the yeast genome that has been tagged with MS2 aptamers. In addition, aptamer tagging further enables the application of other MS2-based techniques, like live-cell imaging of endogenously tagged mRNAs [36, 37] or aptamer-based mRNA affinity purification [38], which facilitates the purification of specific target RNAs and allows for the identification of coprecipitated RBPs, as well as cohort RNAs.

The decision of which approach to employ is individual—while conventional smFISH using a unique probe set might be carried out quicker and yield basic RNA localization information, smFISH based on detection of the aptamer tag allows for more opportunities to address other questions and to strengthen results obtained in situ. Here we describe the use of smFISH probes that are targeted against the MS2 aptamer sequence and allow for the visualization of the MS2-tagged RNAs.

The main successive steps of the procedure (described in detail under Subheading 3.1) are depicted in Fig. 1. Briefly, yeast cells expressing the MS2-tagged target RNA are fixed and permeabilized. Next, fluorescent-labeled antisense oligonucleotides designed to recognize the MS2 aptamer are added and hybridized to the MS2-labeled target RNA. Stringent washing thereafter removes

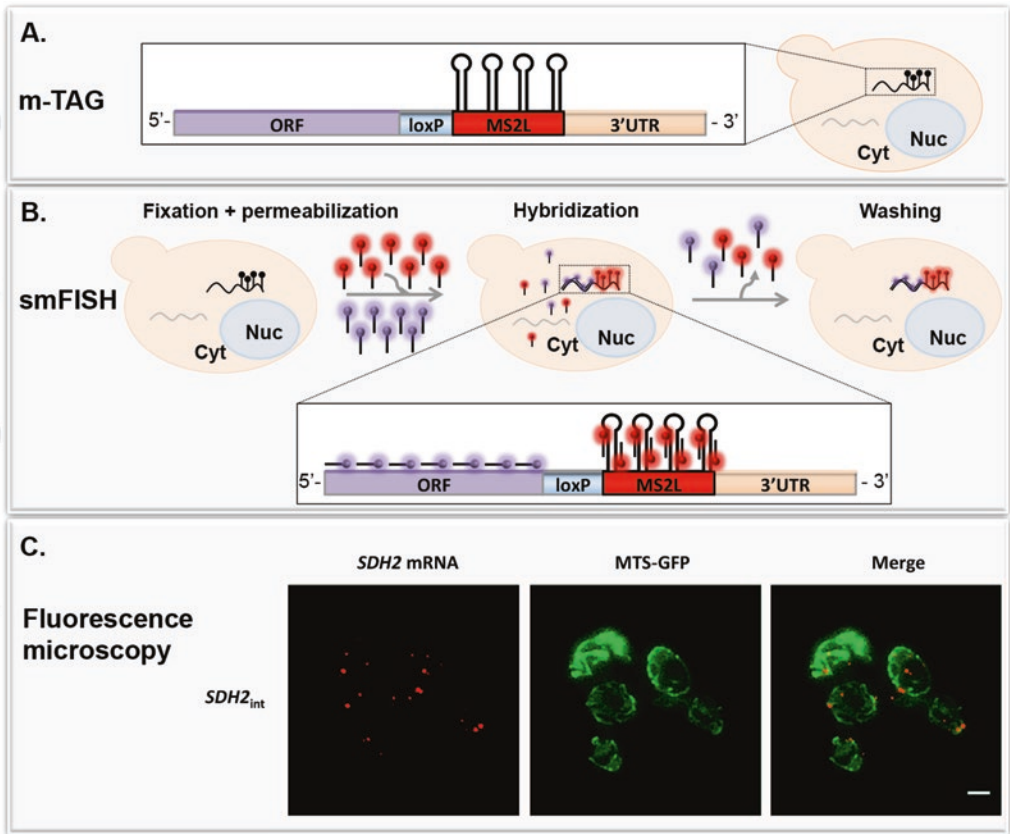


**Fig. 1** A schematic illustration of the smFISH procedure used to localize endogenously expressed MS2 aptamer-tagged RNAs in yeast. (a) m-TAG procedure. Initially, the RNA of interest is endogenously tagged with MS2 aptamer (MS2L) repeats via genomic integration, as described in [35, 36]. If desired, yeast strains expressing the tagged RNA can be transformed with other cellular (e.g., organellar) fluorescent-tagged markers to subsequently investigate RNA localization. *ORF* open reading frame, *Nuc* nucleus, *Cyt* cytoplasm. (b) Main steps of the smFISH protocol. See Subheading 2.2 for details. (c) Detection of *SDH2* mRNA in yeast by smFISH. A representative image of MS2 aptamer-tagged *SDH2* mRNA obtained by performing smFISH with probes targeting the MS2 aptamer (red). Cells were also transformed with a plasmid expressing the MTS-GFP mitochondrial marker (green). See Subheading 3.1 for details. Twenty-two RNA granules of varying size are noted in the z section shown, of which 15 overlap clearly with the MTS-GFP marker, indicating a relatively high level of co-localization (~70%) between the smFISH and GFP signals. Line = 2µm

unbound oligonucleotides, reduces false-positive signals, and improves the signal-to-noise ratio obtained during subsequent fluorescence microscopy. Scoring of the fluorescent puncta allows for quantitation of the amount and localization of the target RNA within the cell.

**1.3 Quantification of mRNAs at the Mitochondrial Surface**

FISH is a useful tool to investigate the intracellular localization of endogenous mRNAs on the single-cell level, but the number of different mRNA species that can be visualized is relatively limited. This is principally due to the amount of time-consuming

fluorescence microscopy and image analysis, but also considers the high cost of synthesizing multiple labeled probe sets. A complementary low-cost approach to FISH is subcellular fractionation, which yields a highly enriched mitochondrial fraction, followed by quantitative reverse transcription-PCR (qRT-PCR; qPCR; real-time PCR) that enables the simultaneous quantification of multiple RNA species.

Fractionation and detection assays have been shown to be a suitable tool for the analysis of mRNAs at different subcellular compartments. Previous studies using either RT-PCR or microarray analyses successfully revealed the enrichment of numerous mRNAs on ER membranes [19, 22], as well as the association of mMPs with mitochondria [20, 39]. The fractionation procedure described here allows for the preparation of a highly enriched mitochondrial fraction from yeast cells to identify mRNAs associated with the mitochondrial surface by either RT-PCR or qPCR. By employing this method, the localization of mRNAs assayed by smFISH can be verified and quantitated through biochemical analysis. Moreover, additional RNA species can be investigated using inexpensive pairs of detection oligonucleotides.

The basic procedure described in detail in Subheading 3.2 is outlined in Fig. 2. Briefly, yeast strains are grown overnight under the desired conditions and the following day harvested, washed, and treated with enzymes to create spheroplasts. Next, the spheroplasts are homogenized, and the lysate is subsequently centrifuged in consecutive steps to obtain a crude mitochondrial fraction. Finally, this fraction is loaded on top of a discontinuous sucrose gradient and further centrifuged to yield an enriched mitochondrial fraction that is relatively free of cytosol and other subcellular compartments. The purity of the mitochondrial fraction can be validated through protein extraction and Western blot analysis (Fig. 3), while mRNAs can be detected and measured via RT-PCR or qPCR (Fig. 4).

---

## 2 Materials

### 2.1 *Single-Molecule Fluorescent In Situ Hybridization*

1. Phosphate-buffered saline (PBS): Mix 0.1 volumes of PBSx10 with 0.9 volumes of double distilled water (DDW) and autoclave.
2. 1 M lithium acetate (LiOAc): Dissolve 6.6 g lithium acetate in 100 mL DDW and titrate to pH 7.5 with 2 M acetic acid.
3. 0.1 M LiOAc: Mix 0.1 volumes of 1 M LiOAc with 0.9 volumes of PBS buffer.
4. 50% (wt/vol) polyethylene glycol (PEG) 3350: Dissolve 250 g of PEG 3350 in 300 mL of PBS buffer while stirring and warming to 50 °C; fill to 500 mL and filter sterilize.

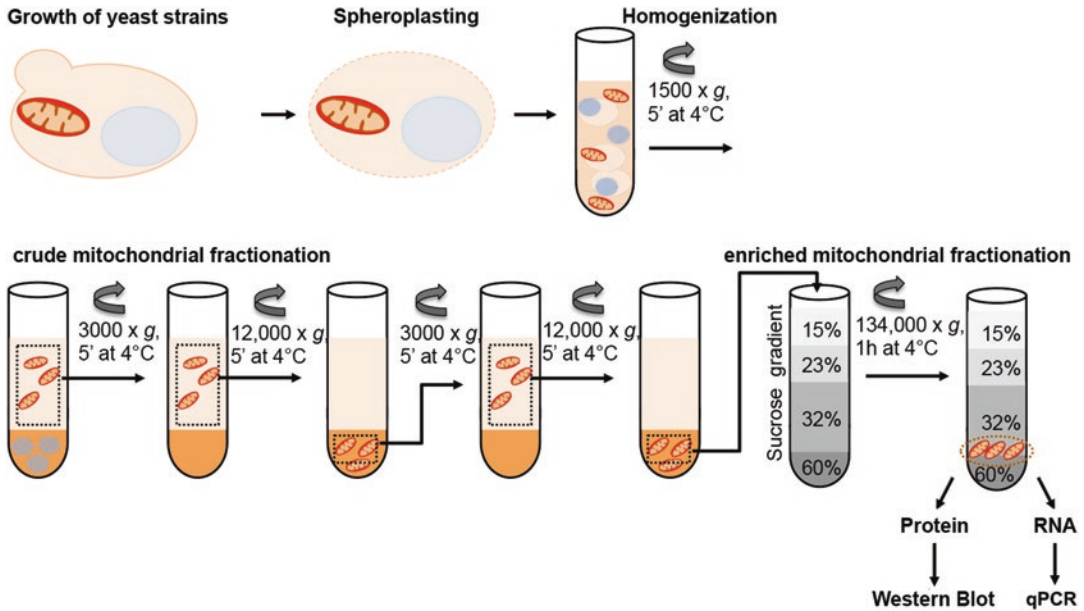


**Fig. 2** Biochemical localization of mRNAs to the mitochondrial surface. Graphical illustration of individual steps performed to isolate highly purified mitochondria and analyze copurifying mRNAs (see Subheading 3.2 for details on the growth of the yeast strains, spheroplasting, homogenization, preparation of the crude and enriched mitochondrial fractions by differential centrifugation and density gradient fractionation, and isolation of the enriched mitochondrial fraction for protein extraction and Western analysis or RNA extraction and qPCR)

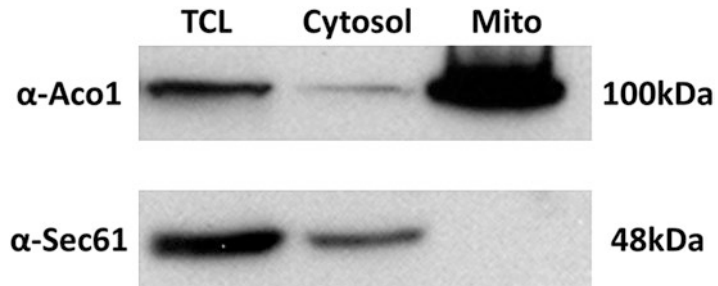


**Fig. 3** Analysis of mitochondrial purification. Western blots of samples of the total cell lysate (TCL), cytosolic fraction (cytosol), and enriched mitochondrial fraction (Mito) are shown. Samples that were electrophoresed and separated on SDS-PAGE gels and detected using polyclonal antibodies against Aco1 (1:10,000 dilution), a mitochondrial matrix protein, and Sec61 (1:5000), a marker of the endoplasmic reticulum, are shown. The molecular mass marker sizes are given

5. 45% (wt/vol) PEG in PBS buffer: Mix 0.9 volumes of 50% PEG 3350 with 0.1 volumes of 1 M LiOAc.
6. 10 mg/mL salmon sperm DNA (ssDNA): Use ssDNA (Sigma Aldrich, Cat. #D8899) sheared by sonication and boiled, as prepared using standard procedures [41].

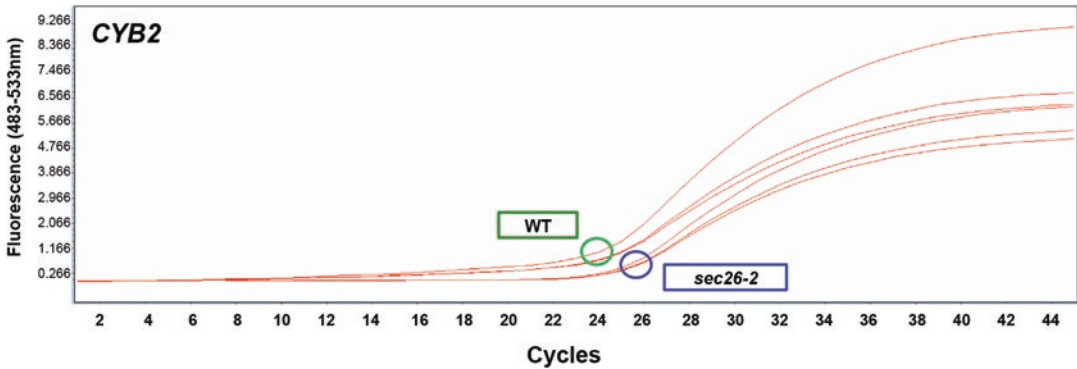


**Fig. 4** qPCR analysis of *CYB2* mRNA extracted from the enriched mitochondrial fraction derived from wild-type cells and a COPI mutant. Amplification curves of *CYB2* mRNA derived from mitochondria purified from either wild-type (WT) cells or a COPI mutant (*sec26-2*) grown on YPglycerol medium. Note the late emergence of *CYB2* mRNA during amplification of RNA derived from the *sec26-2* mutant. This shows that a lower amount of *CYB2* mRNA is present on the mitochondria under conditions where COPI is inactivated [40]

7. Plasmid DNA for yeast transformation (1  $\mu$ g/transformation), e.g., pMTS-GFP (GFP tagged with a mitochondrial targeting sequence).
8. Synthetic growth medium (SC) lacking essential amino acids and/or nucleotide bases to allow for the selective growth of yeast [41].
9. 16% (w/v) paraformaldehyde (PFA) aqueous solution (Electron Microscopy Sciences, Hatfield, PA, Cat. #15710).
10. 4.5% sucrose solution: Dissolve 4.5 g of ultrapure sucrose in DDW to reach a final volume of 100 mL.
11. Fixation buffer: Mix 2.5 mL of 16% PFA with 7.5 mL volumes of 4.5% sucrose solution.
12. 1 M  $K_2HPO_4$ : Dissolve 87 g of potassium phosphate dibasic in 500 mL of DDW and filter sterilize.
13. 1 M  $KH_2PO_4$ : Dissolve 34 g of potassium phosphate monobasic in 500 mL of DDW and filter sterilize.
14. Buffer B: Buffer B is 0.1 M potassium phosphate, pH 7.4, 1.2 M sorbitol. Mix 80.2 mL of the  $K_2HPO_4$  solution with 19.8 mL of the  $KH_2PO_4$  solution, add 218.6 g of sorbitol, and fill to 1l final volume with DDW. Filter sterilize and store at 4  $^{\circ}$ C.
15. Ribonucleoside vanadyl complexes (VRC complex) 200 mM.
16. Dithiothreitol (DTT) 1 M stock. Add 1.54 g DTT to 10 mL of DDW, filter sterilize, and store at  $-20$   $^{\circ}$ C.
17. Protease inhibitor cocktail (Roche, cat# 11836170001).
18. Spheroplast buffer: Buffer B with added (to a final concentration) 4 mM VRC complex, 40 U/mL RNasin, and 20 U/mL lyticase (Sigma Cat. #L2524; 20 units/sample). Add protease

- inhibitor cocktail (Roche Cat. #11836170001; prepared according to manufacturer's instructions; dilute 25× stock to 1:25). Use 1 mL of fresh spheroplast buffer per sample.
19. 2% sodium dodecyl sulfate (SDS): Dissolve 2 g of sodium dodecyl sulfate in DDW to reach a final volume of 100 mL.
  20. 20× SSC buffer (3 M sodium chloride, 300 mM sodium citrate): Dissolve 175.3 g of NaCl and 88.2 g sodium citrate dihydrate, titrate to pH 7 with HCl, and adjust the volume to 1 L with DDW. Autoclave and store at room temperature.
  21. 70% Ethanol.
  22. Hybridization buffer: Mix 1 mL of 20× SSC with 1 g dextran sulfate (Sigma Aldrich, Cat. #D6001), 1 mL formamide (Sigma, Cat. #F9037), and 100 μL of VRC complex, and adjust the volume to 10 mL with ultrapure (e.g., RNase-free, DNase-free) DDW. Mix, filter sterilize, aliquot to 1 mL, and store at −20 °C. Final concentrations in the buffer are 10% dextran sulfate, 2× SSC buffer, 10% formamide, and 2 mM VRC complex.
  23. TE buffer: 10 mM Tris–HCl, 1 mM EDTA, pH 8.
  24. Single-molecule fluorescent in situ hybridization (smFISH) primers labeled with Cy5: Design the primers for conjugation with the Cy5 fluorophore for either the native mRNA or the MS2 loop sequence using the Stellaris Probe Designer (<https://www.biosearchtech.com/stellarisdesigner/>). Upon arrival, dilute primers in 1× TE buffer according to manufacturer's instructions to achieve a final concentration of 25 μM, aliquot 10 μL samples, and store at −20 °C (*see Note 1*).
  25. Wash buffer: Mix 0.1 volumes of 20× SSC buffer with 0.1 volumes of formamide and add 0.8 volume of ultrapure DDW.
  26. Fluorescent microscope with filters suitable for excitation and emission of the DAPI, FITC, CY3, and CY5 fluorophores. In addition, it is highly advisable to employ a microscope with a programmable stage that allows for sampling z-stack images.

## **2.2 Quantification of mRNAs at the Mitochondrial Surface**

### **2.2.1 Preparation of a Mitochondria-Enriched Fraction**

1. YPD medium: 1% yeast extract (w/v) (Becton Dickinson, Franklin Lake, NJ; Cat. #212750), 2% peptone (w/v) (BD, Cat. #211677), and 2% d-glucose (w/v) (J.T. Baker, Cat. #50-99-7). Autoclave and store at room temperature.
2. YPglycerol medium: 1% yeast extract (w/v), 2% peptone (w/v), and 3% glycerol (v/v). Autoclave and store at room temperature.
3. Lyticase buffer: 20 mM potassium phosphate, pH 7.4, and 1.2 M sorbitol. Store at 4 °C for no longer than 1 month.
4. DTT buffer: 100 mM TRIS–H<sub>2</sub>SO<sub>4</sub>, pH 9.4, and 10 mM dithiothreitol. Prepare fresh each time.

5. Lyticase dissolved in lyticase buffer: Add 1.5 units per 1 O.D.<sub>600</sub> unit of yeast cells. Prepare fresh each time.
6. Homogenization buffer: 10 mM Tris-HCl, pH 7.4, 0.6 M sorbitol, 1 mM EDTA, and 0.2% BSA (w/v). Store at 4 °C for 1 month.
7. SEM buffer: 10 mM MOPS-KOH, pH 7.2, 250 mM sucrose, and 1 mM EDTA. Store at 4 °C for up to 1 month.
8. Ultracentrifuge with rotor for swinging buckets (e.g., Beckman Coulter Ultracentrifuge with SW41 Ti Rotor).
9. EM buffer: 10 mM MOPS-KOH, pH 7.2, and 1 mM EDTA.
10. Sucrose: The sucrose should be of the highest purity possible.
11. 60% w/v sucrose in EM buffer.
12. 32% w/v sucrose in EM buffer.
13. 23% w/v sucrose in EM buffer.
14. 15% w/v sucrose in EM buffer.
15. WT yeast strain (e.g., BY4741) and strains bearing a mutation or deletion in the gene of interest.

### 2.2.2 Protein Analysis

1. Yeast lysis buffer: 20 mM Tris-HCl, pH 7.5, 150 mM NaCl, 0.5% (v/v) Triton X-100, and 1.8 mM MgCl<sub>2</sub>.
2. Complete yeast lysis buffer: Supplement yeast lysis buffer with 1 mM phenylmethanesulfonyl fluoride, 1 mM DTT, and complete EDTA-free, protease inhibitor cocktail according to manufacturer instructions (Roche, Basel, Switzerland; Cat. #11873580001).
3. Glass beads, 0.5 mm in diameter.
4. BCA protein assay kit (Pierce, USA, Cat. #23225).
5. 5× protein sample buffer: 400 mM Tris-HCl, pH 6.8, 50% v/v glycerol, 10% (w/v) SDS, and 0.5% (w/v) bromophenol blue. Add freshly prepared 10% (v/v) β-mercaptoethanol. *Warning!* β-mercaptoethanol may be harmful upon inhalation or skin contact; use hood while preparing buffers containing this agent.
6. Standard equipment for sodium dodecyl sulfate polyacrylamide gel electrophoresis (SDS-PAGE) and Western blotting experiments.

### 2.2.3 RNA Extraction and Real-Time PCR

1. MasterPure™ Yeast RNA purification kit (Epicentre Biotechnologies, San Diego, CA; Cat. #MPY03100).
2. RQ1 RNase-free DNase (Promega, Madison, WI; Cat. #M6101).
3. M-MLV Reverse Transcriptase (Promega, Cat. #M1701).
4. 100 mM random hexamer primers.

5. 5 mM dNTP mixture: Prepare from 100 mM stocks of each dATP, dCTP, dGTP, and dTTP using ultrapure water in a 100  $\mu$ L final volume. Store at  $-20$  °C.
6. Specific qPCR primers for your gene of interest—it is highly advisable to utilize qPCR primer design software, e.g., real-time PCR tool (IDT): <https://eu.idtdna.com/scitools/Applications/RealTimePCR/> or Primer 3 Plus (<http://primer3plus.com/cgi-bin/dev/primer3plus.cgi>). First, design specific primers for *COX1*, *COX2*, or *COB* mRNAs in order to identify the most stable mitochondria-encoded transcript (whose mRNA levels should not be altered in crude cell lysate between yeast strains) for normalization of nuclear-encoded mRNAs encoding mitochondrial proteins. Second, design primers for nuclear-encoded genes of interest (e.g., *CYB2*) (*see Note 2*).
7. SYBR Green PCR Master Mix (Applied Biosystems, #43-349-73) or any other intercalating dye-based mix used in real-time PCR machines.
8. LightCycler® 480 Instrument (Roche).

---

## 3 Methods

### 3.1 *Single-Molecule Fluorescent In Situ Hybridization*

1. Transformation of yeast is performed using a standard LiOAc-based procedure [41]. Each strain should be transformed with a plasmid expressing a fluorescent mitochondrial marker (e.g., pMTS-GFP) for scoring co-localization of the mRNA of interest with the mitochondrial surface.
2. Inoculate a single colony picked from the transformation plate into a 50 mL test tube with 5 mL of selective medium and grow overnight with moderate shaking at 26 °C.
3. Measure the absorbance of the culture at O.D.<sub>600</sub>, and transfer an amount of the grown culture into 250 mL Erlenmeyer flask containing 25 mL of the selective growth medium (containing the carbon source of choice, *see Notes 3 and 4*). Yeast should reach the mid-log phase (0.5 O.D.<sub>600</sub> per mL) in about 6 h (~3 generations).
4. Centrifuge mid-log phase yeast cultures at  $1000 \times g$  for 3 min and discard the medium.
5. Wash the cells once in 10 mL of PBS, and centrifuge at  $1000 \times g$  for 3 min.
6. Discard PBS and resuspend the cell pellet in 500  $\mu$ L of fixation buffer, transfer to a 1.5 mL microfuge tube, and let stand at room temperature for 45 min for proper fixation.
7. Centrifuge at  $2500 \times g$  for 4 min at 4 °C, and remove supernatant using a pipettor.

8. Wash the pellet with 1 mL of ice-cold buffer B, and do not resuspend.
9. Repeat **steps 7 and 8**.
10. Repeat **step 7**.
11. Resuspend the pellet in 1 mL spheroplast buffer supplemented with 1.5 units lyticase/*O.D.*<sub>600</sub> units of yeast.
12. Incubate at 30 °C for 30 min.
13. Examine for the extent of spheroplast formation by taking two 2 µL samples and mixing one with 2 µL of 2% SDS and the other with 2 µL 1.2 M sorbitol on separate microscope slides. Verify the loss of intact cells (due to lysis) in the sample treated with 2% SDS using a light microscope. If <50% lysis is observed, continue incubation for another 15–30 min and recheck.
14. From now on it is advisable to use cut tips (with a widened opening) and to gently resuspend the spheroplasts, where prescribed below.
15. Centrifuge spheroplasts at 1300 × *g* for 4 min at 4 °C, and decant supernatant.
16. Wash with 1 mL of ice-cold buffer B, and do not resuspend.
17. Centrifuge spheroplasts at 1300 × *g* for 4 min at 4 °C.
18. Repeat **step 15**.
19. Gently resuspend spheroplasts with 1 mL ice-cold 70% ethanol.
20. Let stand on ice for at least 1 h for proper fixation.
21. Centrifuge at 1300 × *g* for 4 min at 4 °C.
22. Decant supernatant and wash gently with 1 mL wash buffer (do not resuspend) and let stand at room temperature for 5 min.
23. Centrifuge at 1300 × *g* for 4 min at 4 °C.
24. Gently resuspend spheroplasts with 1 mL of hybridization buffer supplemented with 0.5 µL (12.5 pmol) of labeled oligonucleotide probes per sample.
25. Incubate at 30 °C overnight in a dark lightproof chamber, box, or the like.
26. Centrifuge at 1300 × *g* for 4 min at 4 °C.
27. Pipette off the hybridization buffer and add 1 mL wash buffer (do not resuspend).
28. Incubate at 30 °C for 30 min in a dark chamber.
29. Centrifuge at 1300 × *g* for 4 min at 4 °C and pipette off supernatant.
30. Wash with 1 mL wash buffer (do not resuspend).

31. Centrifuge at  $1300 \times g$  for 4 min at 4 °C, and pipette off supernatant.
32. Add 200  $\mu$ L of wash buffer and keep the samples at 4 °C wrapped in the aluminum foil up to 2 weeks.
33. Apply 2  $\mu$ L of the sample to a clean microscope slide and cover gently with a coverslip.
34. Use a bright-field fluorescence imaging system to locate yeast cells of interest. Find the middle of the sample manually or utilizing an autofocus mode.
35. Record images in *z*-stack mode (15 focal planes with 0.2  $\mu$ m spacing per plane).
36. Record at least 15 different fields for statistical analysis afterward and score at least 100 dots (puncta) per treatment/mutant/condition.
37. Score total number of mRNA granules (i.e., fluorescent puncta) versus number of mRNA granules that overlap with the labeled mitochondria in same cells. *See Note 5.*

## **3.2 Quantification of mRNAs at the Mitochondrial Surface**

### *3.2.1 Preparation of a Mitochondria-Enriched Fraction*

1. For each strain to be examined, inoculate a single colony picked from solid medium into a 50 mL test tube containing 5 mL of YPD medium.
2. Grow at 26 °C with shaking for 6–10 h.
3. Measure absorbance of the cultures at O.D.<sub>600</sub>, and transfer an amount of the grown culture into a 2 or 3 L Erlenmeyer flask containing 500 mL of YPD or YPglycerol (*see Note 3*). It is advisable to inoculate the culture such that it will not exceed O.D.<sub>600</sub> = 1.0. For example, for overnight culture, take 1 O.D.<sub>600</sub> unit (from a mid-log phase culture) at 5 p.m., and transfer to 500 mL of growth medium.
4. Grow overnight with shaking at 26 °C. By 9 a.m. the next day, the culture will be at mid-log phase and reach a total amount of ~250 O.D.<sub>600</sub> units.
5. Measure absorbance of the culture at O.D.<sub>600</sub>, and calculate the total O.D. of the culture—the optimal O.D.<sub>600</sub> is between 0.5 and 0.8.
6. Collect the cells by centrifugation at  $3000 \times g$  for 5 min at 4 °C, and discard the growth medium.
7. Resuspend the cell pellet in 250 mL DDW.
8. Centrifuge again at  $3000 \times g$  for 5 min at 4 °C and discard supernatant.
9. Repeat **steps 7 and 8**.
10. For each strain, resuspend the cells in 8 mL DTT buffer, and transfer cells to a 50 mL conical tube.

11. Rotate the cells at 30 °C for 30 min at approximately 70 rpm.
12. Pellet the cells at 3000 × *g* for 5 min at 4 °C; discard supernatant.
13. Resuspend cells in 20 mL lyticase buffer without added lyticase.
14. Pellet the cells at 3000 × *g* for 5 min at 4 °C; discard supernatant.
15. Resuspend the cell in 20 mL lyticase buffer with added lyticase (1.5 units lyticase per 1 O.D.<sub>600</sub> unit of cells).
16. Rotate the cells at 30 °C for 45 min at approximately 70 rpm.
17. Examine extent of spheroplast formation; see Subheading 3.1, **step 13** for details.
18. Centrifuge spheroplasts at 2200 × *g* for 8 min at 4 °C.
19. Gently resuspend spheroplasts in 12 mL of ice-cold homogenization buffer using a 25 mL pipette (do not vortex).
20. Repeat **steps 18** and **19**.
21. Transfer resuspended spheroplasts to prechilled *tight-fit* homogenizer.
22. Homogenize slowly with 15 strokes and transfer the homogenate to a chilled 50 mL conical tube.
23. Add an additional 12 mL of ice-cold homogenization buffer to the homogenizer and rinse and transfer the 12 mL to the same 50 mL tube (total = 24 mL).
24. Centrifuge homogenate at 1500 × *g* for 5 min at 4 °C. The pellet contains unbroken cells, nuclei, and other cellular debris.
25. Take 1 mL of the supernatant (total cell lysate; TCL) and store at -20 °C.
26. Transfer the remainder of the supernatant to a new 50 mL conical tube.
27. Centrifuge at 3000 × *g* for 5 min at 4 °C.
28. Transfer supernatant to a new 50 mL tube.
29. Centrifuge at 12,000 × *g* for 5 min at 4 °C.
30. Take 1 mL of the supernatant (cytosolic fraction) and store at -20 °C.
31. Discard the rest of the supernatant and gently resuspend pellet in 12 mL of ice-cold homogenization buffer.
32. Centrifuge at 3000 × *g* for 5 min at 4 °C.
33. Transfer supernatant to a new 50 mL conical tube.
34. Centrifuge at 12,000 × *g* for 5 min at 4 °C.
35. Discard supernatant and resuspend the pellet containing both mitochondria and endoplasmic reticulum (i.e., the crude mitochondrial fraction) in 3 mL SEM buffer.

36. Using a glass Pasteur pipette, build a discontinuous sucrose gradient prepared using sucrose dissolved in EM buffer by layering. *See Note 6.* Layer 1.5 mL of 60% sucrose, followed by 4 mL of 32% sucrose, followed by 1.5 mL of 23% sucrose, and finish with 1.5 mL of 15% sucrose.
37. Layer 3 mL of crude mitochondrial fraction on top of the discontinuous gradient, and centrifuge at  $134,000 \times g$  for 1 h at 4 °C.
38. After centrifugation, remove successive fractions from the top and carefully collect and save the brownish cloud at the interface between the 32 and 60% layers. This contains the highly enriched mitochondrial fraction (note: the volume of the mitochondrial fraction is approximately 1–2 mL).
39. Gently add the mitochondrial fraction to 10 mL of ice-cold SEM buffer, mix slowly, and centrifuge at  $10,000 \times g$  for 30 min at 4 °C.
40. Discard supernatant and either flash-freeze mitochondrial pellet or proceed directly to protein (Subheading 3.2.2) or RNA (Subheading 3.2.3) extraction.

### 3.2.2 Protein Analysis

1. Place either the frozen or fresh mitochondrial pellet on ice, and add 1 mL of ice-cold complete yeast lysis buffer.
2. Split the resuspended mitochondrial fraction equally between two 1.5 mL microfuge tubes each containing a 500  $\mu$ L bed volume of glass beads.
3. Vortex vigorously for 10 min at 4 °C.
4. Using a hot needle, puncture the bottom of the microfuge tube and place the tube inside a 15 mL conical tube.
5. Centrifuge at  $960 \times g$  for 1 min at 4 °C.
6. Transfer the lysate from 15 mL tubes to a 1.5 mL microfuge tube and centrifuge at  $10,000 \times g$  for 10 min at 4 °C.
7. [In parallel to **steps 1–6**] Thaw on ice the samples from total cell lysate (TCL) and cytosolic fraction, and supplement with PMSF (2 mM), DTT (1 mM), and protease inhibitors cocktail (according to manufacturer's instructions).
8. Transfer the supernatant of the mitochondrial fraction to a new 1.5 mL microfuge tube.
9. Measure the protein concentration of all of three fractions (e.g., TCL, cytosol, and mitochondria) using the BCA protein assay kit.
10. Take the same amounts of protein from each of the TCL, cytosolic, and mitochondrial fraction samples. Add Laemmli sample buffer (1 $\times$  final) and DDW to reach a final volume of 40  $\mu$ L, and incubate at 100 °C for 10 min.

11. Prepare a standard SDS-PAGE mini gel (e.g., 7 × 8 cm) using a polyacrylamide concentration most suitable for the separation of the protein of interest.
12. Load the same amount of protein (e.g., 30–60 µg per lane) from TCL, cytosolic, and mitochondrial fraction samples onto the gel.
13. Electrophorese samples until sufficient protein separation is achieved; transfer proteins to nitrocellulose membranes using the voltage and time conditions recommended by the manufacturer of the transfer unit employed.
14. Block the membrane for 1 h in 5% bovine serum albumin dissolved in PBS (×1). Use standard procedures for protein detection with antibodies against the protein of interest.

### 3.2.3 RNA Extraction and Real-Time PCR

1. Extract the RNA using an Epicure MasterPure™ Yeast RNA kit. **Steps 2–12** are performed according to the manufacturer's instructions.
2. Resuspend the mitochondrial pellet in 300 µL RNA extraction buffer supplemented with 1 µL Proteinase K (50 µg/µL). Note: If using a frozen pellet, let it thaw on ice before resuspension.
3. Mix at 800 rpm in a thermomixer for 10–15 min at 70 °C.
4. Transfer to ice and let cool for 5 min.
5. Add 175 µL of MPC precipitation reagent and vortex thoroughly for 10 s.
6. Centrifuge at 10,000 × *g* for 10 min at 4 °C.
7. Transfer the supernatant to a new 1.5 mL microfuge tube.
8. Add 500 µL of isopropanol and vortex for 10 s.
9. Centrifuge at 10,000 × *g* for 10 min at 4 °C.
10. Discard supernatant and remove liquid completely using a micropipettor.
11. Dry the pellet for 10 min at 50 °C (note: leave cap open).
12. Add 30 µL of ultrapure water and let stand at 50 °C till dissolved completely (10 min). Note: using a thermomixer at 800 rpm speeds up the process.
13. Measure RNA concentration by determining the absorbance at 260 nm using a NanoDrop spectrophotometer (or the like); an absorbance of 1.0 corresponds to about 40 µg/mL. *See Note 7.*
14. Mix 1 µg RNA with 1 µL of 10× DNase buffer and 1 µL of DNase, and add ultrapure water to 10 µL final volume.
15. Incubate at 37 °C for 1 h.
16. Add 1 µL DNase stop buffer (a component of the DNase kit) and incubate for 15 min at 65 °C.

17. Add 1.3  $\mu\text{L}$  of random hexamer primers to the solution and 4.1  $\mu\text{L}$  of ultrapure water.
18. Incubate at 70 °C for 5 min and then immediately transfer to ice.
19. Add 5  $\mu\text{L}$  of 5 $\times$  RT buffer, 2.6  $\mu\text{L}$  5 mM dNTPs, and 1  $\mu\text{L}$  of reverse transcriptase enzyme.
20. Mix and incubate at 37 °C for 1 h.
21. Add 75  $\mu\text{L}$  of ultrapure water.
22. cDNA samples can be used directly in real-time PCR (steps 23–30) or can be stored at –20 °C.
23. Prepare several dilutions of the cDNA samples (e.g., 1:10, 1:20, and 1:40).
24. Design a 96-well reaction plate that includes an ultrapure water control for each primer pair used, as well as primers to at least one mitochondrial gene (e.g., *COX1*, *COX2*) for normalization.
25. The example reaction for the qPCR should include 1  $\mu\text{L}$  of the cDNA sample, 0.2  $\mu\text{L}$  of each primer (200 nM final concentration), 3.6  $\mu\text{L}$  of ultrapure water, and 5  $\mu\text{L}$  of SYBR Green  $\times 2$  Mix.
26. Load triplicate samples in the 96-well real-time PCR plate, and spin down at 1000  $\times g$  for 1 min at 4 °C.
27. Apply the plate to a real-time PCR machine, and apply a standard PCR protocol followed by melting curve measurement.
28. Analyze the data using the built-in software, check the melting curve for single amplicon occurrence, and extract the  $C_t$  values. See **Note 8**.
29. Extrapolate the  $C_t$  values to one of the following mathematical methods (e.g., see references [42] and [43]). See **Notes 8** and **9**.

---

## 4 Notes

1. We typically use single-molecule FISH primers coupled to Cy5 fluorophores from the far-red spectra. This allows for fluorophore-based sample visualization in at least three channels in the same experiment (e.g., GFP, mCherry, and Cy5). Thus, one can observe alternative sites of mRNA localization (aside from the mitochondria) in the same experiment, when employing an additional intracellular marker.
2. One should perform a preliminary real-time PCR experiment in which the levels of different mRNAs (e.g., *COX1*, *COX2*, *COB*, and *UBC6*) in the total cell lysate fraction of the WT strain and mutant strains are tested. Here, *UBC6* is used as a gene for RNA normalization [44] and allows for identification

of the most stable mitochondria-encoded mRNA (e.g., *COX1*) for later use in the normalization of mRNAs derived from the mitochondria-enriched fraction (e.g., *CYB2*).

*COX1* primers:

COX1 qPCR F: 5' gctctaattccatggtggttcaa 3'

COX1 qPCR R: 5' agctaaggcaaccaggttaa 3'

*COX2* primers:

COX2 qPCR F: 5' aggtattaaagttgatgctactct 3'

COX2 qPCR R: 5' tcagaacatgctccatagaagac 3'

*COB* primers:

COB qPCR F: 5' ggttctcagtatctaaccctctaate 3'

COB qPCR R: 5' agatgaacctgaatatgtaagcc 3'

*UBC6* primers:

UBC6 qPCR F: 5' ccatacaaaccaccggctat 3'

UBC6 qPCR R: 5' cagccaggattccaagtatca 3'

*CYB2* primers:

CYB2 qPCR F: 5' gaagcagcacctctgataaa 3'

CYB2 qPCR R: 5' ggagcatccacagtgacaaata 3'

3. Growth on different carbon sources may alter mitochondrial morphology, mitochondrial mass, and mMP localization. We recommend performing experiments using both a fermentable carbon source (e.g., glucose) and a non-fermentable carbon source (e.g., glycerol), if possible. We advise working with cultures grown to mid-log phase and not exceeding an O.D.<sub>600</sub> > 1. The use of cultures with higher O.D.<sub>600</sub> values increases the chance of starvation and the onset of phenotypes unrelated to the mutation in the gene of interest [45].
4. In our hands, we achieved best results in terms of the number of mRNA puncta visualized and best preservation of mitochondrial morphology using the following growth and fixation conditions: yeast cells were grown in a culture volume of 25 mL in a 250 mL Erlenmeyer flask with shaking at 220 rpm at 26 °C and fixed when they reached O.D.<sub>600</sub> = 0.5 (mid-log phase).
5. Co-localization is performed manually by counting the number of puncta localized (not juxtaposed) with the mitochondria marker. Typically, more than 100 yeast cells for each sample to be tested are scored. The percentage of co-localization is an absolute value and can be used to compare between different mutants without further need for normalization. In addition, one can use a freeware program (e.g., ImageJ) to facilitate analysis of the co-localization between an mRNA and a mitochondrial marker.
6. We recommend preparation of the different sucrose solutions a day before the planned mitochondrial isolation procedure and to prechill them to 4 °C. Best results are obtained when the gradient is built just before layering of the crude mitochondrial

extract. When creating the gradient by hand, we advise using a glass Pasteur pipette and an automated pipettor set to a lowest speed for layering; one should observe crisp bands between the 60%/32%, 32%/23%, and 23%/15% interphases. Employ centrifuge tubes suitable for use with a Beckman SW41 Ti ultracentrifuge rotor.

7. The  $A_{260/280}$  ratio should be  $\approx 2$  and  $A_{260/230} = \sim 2-2.2$ . High value ratios of RNA purity will ensure more reliable reverse transcription and subsequent real-time PCR measurements.
8. The  $C_t$  values of genes used for normalization (e.g., *COXI*) may be extremely low (indicating high levels of mRNA) and in the range of 10–20 cycles. We advise to first check the  $C_t$  levels of such genes and to dilute the cDNA equally between all the samples in order to achieve  $C_t$  values between 20–30 cycles.
9. An additional method to normalize mMP levels on mitochondria is to extract RNA from the total cell lysate (TCL). From the 1 mL of the TCL fraction that was saved, extract the RNA (using the same RNA extraction kit as for the mitochondrial fraction), measure the amount of RNA, and proceed to reverse transcription. The idea is to use TCL levels of a given mMP of interest for normalizing values obtained under different growth conditions or from the different mutants tested. This may eliminate the need for assaying genes transcribed from mitochondrial DNA.

---

## Acknowledgments

This work was supported by grants to J.E.G. from the Minerva Foundation (Federal German Ministry for Education and Research), Germany, the German-Israel Foundation, Germany (I-1190-96.13/2012), and the Estate of Astrachan Olga Klein. J.E.G. holds the Besen-Breder Chair in Microbiology and Parasitology, Weizmann Institute of Science.

## References

1. Vazquez-Pianzola P, Suter B (2012) Conservation of the RNA transport machineries and their coupling to translation control across eukaryotes. *Comp Funct Genomics* 2012:287852
2. Zarnack K, Feldbrügge M (2007) mRNA trafficking in fungi. *Mol Genet Genomics* 278:347–359
3. Okita TW, Choi SB (2002) mRNA localization in plants: targeting to the cell's cortical region and beyond. *Curr Opin Plant Biol* 5:553–559
4. Lécuyer E, Yoshida H, Parthasarathy N, Alm C, Babak T, Cerovina T et al (2007) Global analysis of mRNA localization reveals a prominent role in organizing cellular architecture and function. *Cell* 131:174–187
5. Chartrand P, Singer RH, Long RM (2001) RNP localization and transport in yeast. *Annu Rev Cell Dev Biol* 17:297–310

6. Rodriguez AJ, Czaplinski K, Condeelis JS, Singer RH (2008) Mechanisms and cellular roles of local protein synthesis in mammalian cells. *Curr Opin Cell Biol* 20:144–149
7. Chabanon H, Mickleburgh I, Hesketh J (2004) Zipcodes and postage stamps: mRNA localisation signals and their trans-acting binding proteins. *Brief Funct Genomic Proteomic* 3:240–256
8. Pan F, Hüttelmaier S, Singer RH, Gu W (2007) ZBP2 facilitates binding of ZBP1 to beta-actin mRNA during transcription. *Mol Cell Biol* 27:8340–8351
9. Shen Z, Paquin N, Forget A, Chartrand P (2009) Nuclear shuttling of She2p couples ASH1 mRNA localization to its translational repression by recruiting Loc1p and Puf6p. *Mol Biol Cell* 20:2265–2275
10. Böhl F, Kruse C, Frank A, Ferring D, Jansen RP (2000) She2p, a novel RNA-binding protein tethers ASH1 mRNA to the Myo4p myosin motor via She3p. *EMBO J* 19:5514–5524
11. Gagnon J, Mowry K (2011) Molecular motors: directing traffic during RNA localization. *Crit Rev Biochem Mol Biol* 46:229–239
12. Gerst JE (2008) Message on the web: mRNA and ER co-trafficking. *Trends Cell Biol* 18:68–76
13. Saint-Georges Y, Garcia M, Delaveau T, Jourdain L, Le Crom S, Lemoine S et al (2008) Yeast mitochondrial biogenesis: a role for the PUF RNA-binding protein puf3p in mRNA localization. *PLoS One* 3:e2293
14. Gadir N, Haim-Vilmovsky L, Kraut-Cohen J, Gerst JE (2011) Localization of mRNAs coding for mitochondrial proteins in the yeast *Saccharomyces cerevisiae*. *RNA* 17:1551–1565
15. Weis BL, Schleiff E, Zerges W (2013) Protein targeting to subcellular organelles via mRNA localization. *Biochim Biophys Acta* 1833:260–273
16. Zipor G, Haim-Vilmovsky L, Gelin-Licht R, Gadir N, Brocard C, Gerst JE (2009) Localization of mRNAs coding for peroxisomal proteins in the yeast, *Saccharomyces cerevisiae*. *Proc Natl Acad Sci U S A* 106:19848–19853
17. Trautwein M, Dengjel J, Schirle M, Spang A (2004) Arf1p provides an unexpected link between COPI vesicles and mRNA in *Saccharomyces cerevisiae*. *Mol Biol Cell* 15:5021–5037
18. Bi J, Tsai N-P, Lu H-Y, Loh HH, Wei L-N (2007) Copb1-facilitated axonal transport and translation of kappa opioid-receptor mRNA. *Proc Natl Acad Sci U S A* 104:13810–13815
19. Lerner RS, Seiser RM, Zheng T, Lager PJ, Reedy MC, Keene JD et al (2003) Partitioning and translation of mRNAs encoding soluble proteins on membrane-bound ribosomes. *RNA* 9:1123–1137
20. Sylvestre J, Vialette S, Corral Debrinski M, Jacq C (2003) Long mRNAs coding for yeast mitochondrial proteins of prokaryotic origin preferentially localize to the vicinity of mitochondria. *Genome Biol* 4:R44
21. Du T, Schmid M, Jansen R (2007) Why cells move messages: the biological functions of mRNA localization. *Semin Cell Dev Biol* 18:171–177
22. Aronov S, Gelin-licht R, Zipor G, Haim L, Safran E, Gerst JE (2007) mRNAs encoding polarity and exocytosis factors are cotransported with the cortical endoplasmic reticulum to the incipient bud in *Saccharomyces cerevisiae*. *Mol Cell Biol* 27:3441–3455
23. Darzacq X, Powrie E, Gu W, Singer RH, Zenklusen D (2003) RNA asymmetric distribution and daughter/mother differentiation in yeast. *Curr Opin Microbiol* 6:614–620
24. Elstner M, Andreoli C, Klopstock T, Meitinger T, Prokisch H (2009) The mitochondrial proteome database: MitoP2. *Methods Enzymol* 457:3–20
25. Ellenrieder L, Mårtensson CU, Becker T (2015) Biogenesis of mitochondrial outer membrane proteins, problems and diseases. *Biol Chem* 396:1199–1213
26. MacKenzie JA, Payne RM (2007) Mitochondrial protein import and human health and disease. *Biochim Biophys Acta* 1772:509–523
27. Rugarli EI, Langer T (2012) Mitochondrial quality control: a matter of life and death for neurons. *EMBO J* 31:1336–1349
28. Neupert W, Herrmann JM (2007) Translocation of proteins into mitochondria. *Annu Rev Biochem* 76:723–749
29. Chacinska A, Koehler CM, Milenkovic D, Lithgow T, Pfanner N (2009) Importing mitochondrial proteins: machineries and mechanisms. *Cell* 138:628–644
30. Kellems RE, Butow RA (1974) Cytoplasmic with yeast type 80 S ribosomes associated with yeast mitochondria. 3. Changes in the amount of bound ribosomes in response to changes in metabolic state. *J Biol Chem* 249:3304–3010
31. Kellems RE, Allison VF, Butow RA (1975) Ribosomes to the outer membrane of isolated mitochondria. *J Cell Biol* 65:1–14

32. Eliyahu E, Pnueli L, Melamed D, Scherrer T, Gerber AP, Pines O et al (2010) Tom20 mediates localization of mRNAs to mitochondria in a translation-dependent manner. *Mol Cell Biol* 30:284–294
33. Marc P, Margeot A, Devaux F, Blugeon C, Corral-Debrinski M, Jacq C (2002) Genome-wide analysis of mRNAs targeted to yeast mitochondria. *EMBO Rep* 3:159–164
34. Williams CC, Jan CH, Weissman JS (2014) Targeting and plasticity of mitochondrial proteins revealed by proximity-specific ribosome profiling. *Science* 346:748–751
35. Haim-Vilmovsky L, Gerst JE (2009) m-TAG: a PCR-based genomic integration method to visualize the localization of specific endogenous mRNAs in vivo in yeast. *Nat Protoc* 4:1274–1284
36. Haim L, Zipor G, Aronov S, Gerst JE (2007) A genomic integration method to visualize localization of endogenous mRNAs in living yeast. *Nat Methods* 4:409–412
37. Haim-Vilmovsky L, Gadir N, Herbst R, Gerst J (2011) A genomic integration method for the simultaneous visualization of endogenous mRNAs and their translation products in living yeast. *RNA* 17:2249–2255
38. Slobodin B, Gerst JE (2010) A novel mRNA affinity purification technique for the identification of interacting proteins and transcripts in ribonucleoprotein complexes. *RNA* 16:2277–2290
39. Garcia M, Darzacq X, Devaux F, Singer RH, Jacq C (2007) Yeast mitochondrial transcriptomics. *Methods Mol Biol* 372:505–528
40. Zabezhinsky D, Slobodin B, Rapaport D, Gerst JE (2016) An essential role for COPI in mRNA trafficking to the mitochondria and mitochondrial function. *Cell Rep* 15:540–549
41. Kaiser C, Michaelis S, Mitchell A (1994) *Methods in yeast genetics: a Cold Spring Harbor laboratory course manual*. Cold Spring Harbor Press, Cold Spring Harbor, NY
42. Pfaffl MW (2001) A new mathematical model for relative quantification in real-time RT-PCR. *Nucleic Acids Res* 29:e45
43. Livak KJ, Schmittgen TD (2001) Analysis of relative gene expression data using real-time quantitative PCR and the  $2^{-\Delta\Delta CT}$  method. *Methods* 25:402–408
44. Teste MA, Duquenne M, François JM, Parrou JL (2009) Validation of reference genes for quantitative expression analysis by real-time RT-PCR in *Saccharomyces cerevisiae*. *BMC Mol Biol* 10:99
45. Dobzinski N, Chuartzman SG, Kama R, Schuldiner M, Gerst JE (2015) Starvation-dependent regulation of golgi quality control links the TOR signaling and vacuolar protein sorting pathways. *Cell Rep* 12:1876–1886

## Assessing Mitochondrial Bioenergetics in Isolated Mitochondria from Various Mouse Tissues Using Seahorse XF96 Analyzer

Arcangela Iuso, Birgit Repp, Caroline Biagosch, Caterina Terrile, and Holger Prokisch

### Abstract

Working with isolated mitochondria is the gold standard approach to investigate the function of the electron transport chain in tissues, free from the influence of other cellular factors. In this chapter, we outline a detailed protocol to measure the rate of oxygen consumption (OCR) with the high-throughput analyzer Seahorse XF96. More importantly, this protocol wants to provide practical tips for handling many different samples at once, and take a real advantage of using a high-throughput system. As a proof of concept, we have isolated mitochondria from brain, heart, liver, muscle, kidney, and lung of a wild-type mouse, and measured basal respiration (State II), ADP-stimulated respiration (State III), non-ADP-stimulated respiration (State IV<sub>o</sub>), and FCCP-stimulated respiration (State III<sub>u</sub>) using respiratory substrates specific to the respiratory chain complex I (RCCI) and complex II (RCCII). Mitochondrial purification and Seahorse runs were performed in less than eight working hours.

**Key words** High-throughput, Seahorse XF96, Mitochondrial coupling assay, Respiratory control ratio (RCR), Mouse tissues

---

### 1 Introduction

To investigate the function of the electron transport chain in animal tissues there are two approaches. One approach is to measure the rate of oxygen consumption (OCR) directly in small biopsies permeabilized with detergents; the other is to isolate mitochondria from the tissue of interest and measure respiration in an isotonic buffer supplemented with respiratory substrates and ADP. When working with permeabilized tissues there are many variables influencing the measurement, such as the accessibility of substrates and inhibitors throughout the tissue, the limited diffusion of oxygen (O<sub>2</sub>), the coexistence of various types of cells, the variable number of mitochondria per cell, the availability of endogenous substrates,

and the rate of ATP utilization. Moreover, effective protocols to measure  $O_2$  consumption directly in permeabilized tissues are available only for a few tissues [1–3]. Instead, working with isolated mitochondria has the advantage of disconnecting the mitochondrial respiration from cellular factors. In isolated mitochondria the OCR relies only on the activity of the RCCs and on the substrates and ADP exogenously added to the system.

Measuring oxygen consumption in isolated mitochondria is not a new concept. This is carried out routinely by traditional  $O_2$  electrode-based methods [4, 5]. However, those systems require a large amount of mitochondria for each measurement, between 0.01 and 0.5 mg, depending on the tissue, and long running times, between 1 and 2 h, per replicate. Large amount of mitochondria and the challenge to perform a significant number of replicates in a timely manner to preserve mitochondrial coupling represent a major limitation when working with precious biological materials. The advance of high-throughput microplate respiratory measurements has overcome this limitation [6–8]. The protocol described in this chapter uses only 0.3–4  $\mu\text{g}$  of mitochondria per measurement (i.e., per well) and it allows performing at least 4–6 replicates for each sample in only 70 min. We will indicate how to quickly isolate mitochondria from brain, heart, liver, muscle, kidney, and lung of a wild-type mouse and how to measure OCRs for States II, III, IV<sub>o</sub>, and III<sub>i</sub>. Furthermore, we suggest how to analyze the Seahorse data to get values of respiratory control ratios (RCRs), as an indicator of mitochondrial coupling.

---

## 2 Materials

### 2.1 Equipment

Homogenizer EUROSTAR 20 digital	IKA	0004442000
Potter-Elvehjem PTFE pestle and glass tube	Sigma	P7859-1EA
Centrifuge	Sigma	4K15
Plate rotor	QIAGEN	09100
Centrifuge	Sigma	6K15
Swing-out rotor	Sigma	11150
Seahorse XF96 analyzer	Seahorse Biosciences, Inc.	
Inverted Fluorescent Microscope	Leica	DM IRE2

## 2.2 Consumables

15 mL Polypropylene Tubes	Falcon	352059
ADP	Sigma-Aldrich	A2754
Antimycin A	Sigma	A8674
d-Mannitol	Sigma-Aldrich	M9546
Dulbecco's Phosphate buffered saline	Gibco	14190-094
EGTA	Sigma-Aldrich	E3889
Fatty acid-free BSA	Sigma	A3803
FCCP	Sigma	C2920
Glutamate	Sigma-Aldrich	G8415
HEPES	Sigma-Aldrich	H3784
Hydrochloric acid 37% (HCl)	Merck	1E+09
KH <sub>2</sub> PO <sub>4</sub>	Sigma	P9791
Magnesium chloride (MgCl <sub>2</sub> )	Sigma-Aldrich	M9272
Malate	Sigma-Aldrich	M6413
Mito Tracker <sup>®</sup> Green FM	Molecular Probes	M-7514
Oligomycin	Sigma	O4876
Pasteur Pipettes	BRAND	7477-55
Petri dish 60 × 15 mm	Nunc	150288
Potassium chloride (KCl)	Sigma-Aldrich	P9541
Potassium hydroxide (KOH)	Sigma-Aldrich	221473
Protein Assay Dye Reagent Concentrate	Bio-Rad	500-0006
Rotenone	Sigma	R8875
Succinate	Sigma-Aldrich	S2378
Sucrose	Sigma	S0389
Surgical Disposable Scalpels	BRAUN	BBA215
Tween-20	Sigma	P9416
XF96 Cell Culture Microplate	Seahorse Bioscience	100850-004
XF96 Sensor Cartridge	Seahorse Bioscience	102416-100

## 2.3 Buffers

1. Prepare the mitochondrial isolation buffer (MIB1), by dissolving 210 mM of d-Mannitol, 70 mM of sucrose, 5 mM of HEPES, 1 mM of EGTA, and 0.5% (w/v) of fatty acid-free BSA in ultrapure H<sub>2</sub>O and adjust the pH to 7.2 with KOH. Prepare aliquots and store them at -20 °C (*see Note 1*).

2. Prepare the mitochondrial assay solution (MAS1) by dissolving 220 mM of d-Mannitol, 70 mM of sucrose, 10 mM of  $\text{KH}_2\text{PO}_4$ , 5 mM of  $\text{MgCl}_2$ , 2 mM of HEPES, 1 mM of EGTA, and 0.2% (w/v) of fatty acid-free BSA in ultrapure  $\text{H}_2\text{O}$  and adjust the pH to 7.2 with KOH at 37 °C. Prepare aliquots and store them at -20 °C (*see Note 1*).

#### **2.4 ADP and Respiration Reagents**

1. Prepare mitochondrial substrates by dissolving 0.5 M of succinate, 0.5 M of malate, 0.5 M of glutamate in ultrapure  $\text{H}_2\text{O}$  and adjust the pH to 7.2 at 37 °C with KOH. Prepare aliquots and store at -20 °C (*see Note 2*).
2. Prepare ADP by dissolving 40 mM of ADP in MAS1 and adjust the pH to 7.2 with KOH. Perform serial dilutions to obtain stocks of 20, 10, 5, 2.5, and 1.25 mM of ADP in MAS1 (*see Note 3*).
3. Prepare stocks of inhibitors and uncouplers by dissolving 10 mM of FCCP, 2 mM of rotenone, 5 mg/mL of oligomycin, and 40 mM of antimycin A in DMSO. Prepare aliquots and store at -20 °C. Prevent freezing and thawing of Rotenone and FCCP stocks. On the day of the experiment, dilute them with MAS1 to working concentrations of 40  $\mu\text{M}$  (*see Note 4*), 20 mM, 25  $\mu\text{g}/\text{mL}$ , and 40 mM for FCCP, rotenone, oligomycin, and antimycin A, respectively.

It is recommended to thaw all reagents on ice and keep them on ice during the whole experiment.

---

## **3 Methods**

### **3.1 Rehydrating the Cartridge (Day Before the Experiment)**

1. Hydrate the XF96 Sensor Cartridge by adding 0.2 mL of XF calibrant in each well of the utility plate (lower transparent plastic plate).
2. Carefully place the cartridge (upper green plate containing ports) back onto the utility plate (fluorophores at the bottom of the cartridge can be easily damaged).
3. Incubate the plate in a non  $\text{CO}_2$  incubator at 37 °C overnight (*see Note 5*).

### **3.2 Set Up the Experimental Protocol in the Seahorse XF96 Analyzer (Day Before the Experiment)**

1. Open the Seahorse XF96 software (*see Note 6*).
2. Select “Standard” assay.
3. Wait for the initialization of the system.
4. Go to “Assay Wizard” to fill in the project information under “General.”
5. Fill in the information concerning each mitochondrial sample under “Cell information.” Select “Cell Layout” submenu to

0.5	Brain	0.5	1	Brain	1	2	Brain	2	0.5	Kidney	0.5	1	Kidney	1	2	Kidney	2
0.5		0.5	1		1	2		2	0.5		0.5	1		1	2		2
0.5	Heart	0.5	1	Heart	1	2	Heart	2	0.5	Muscle	0.5	1	Muscle	1	2	Muscle	2
0.5		0.5	1		1	2		2	0.5		0.5	1		1	2		2
0.5	Liver	0.5	1	Liver	1	2	Liver	2	0.5	Lung	0.5	1	Lung	1	2	Lung	2
0.5		0.5	1		1	2		2	0.5		0.5	1		1	2		2
BK	BK	BK	BK	BK	BK	BK	BK	BK	BK	BK	BK	BK	BK	BK	BK	BK	BK
BK	BK	BK	BK	BK	BK	BK	BK	BK	BK	BK	BK	BK	BK	BK	BK	BK	BK

**Fig. 1** Layout of the 96-well Seahorse plate for the optimization of the mitochondrial amount. Up to three different amounts of mitochondria for a specific substrate and tissue can be tested by using this layout. Each measurement is carried out in quadruplicate. The last two rows are filled in with MAS1 and represent the background (BK)

define how mitochondrial samples will be seeded in the 96-well plate (*see* Fig. 1). Assign a different color to each group in the “Groups & Labels” submenu.

6. Fill in the information concerning the run under “Protocol.” You can adjust the parameters by selecting the commands on the display. The protocol used to test mitochondrial coupling is summarized in Table 1.
7. Save the file as template (.xls). Unless specified, the file will be automatically saved in the folder XFReader96.
8. End wizard.

### 3.3 Preparation of Mouse Organs (Day of the Experiment)

1. Mice are killed via instant cervical dislocation (*see* Note 8) without prior anesthesia such as CO<sub>2</sub>, since this influences mitochondrial respiration.
2. Subsequent organ withdrawal should be completed within max. 30 min per mouse and each organ is kept in a different Petri dish on ice upon withdrawal.
3. If necessary, carefully remove hair and fat residues from organs, as these interfere with the subsequent isolation of mitochondria.

### 3.4 Isolation of Mouse Mitochondria (Day of the Experiment)

This protocol can be applied to isolate mouse mitochondria from liver, heart, lung, brain, kidney, and hindlimb skeletal muscle tissues. Start with 30–50 mg wet-weight tissue.

1. Prepare on ice six Petri dishes with 1 mL of MIB1.
2. Place each tissue in a different Petri dish.
3. Cut tissues into very small pieces with disposable scalpels (*see* Note 9).
4. Collect pieces with a disposable 1 mL plastic Pasteur pipette and place them in 15 mL polypropylene tubes containing 5 mL of MIB1.

**Table 1**  
**Experimental outline to test mitochondrial coupling (see Notes 6–7)**

Command	Time (min)	Port
Start protocol		
Calibrate	~30	
Mix	1	
Wait	3	
Mix	1	
Wait	3	
Mix	0.5	
Measure	3	
Mix	1	
Measure	3	
Mix	0.5	
<i>Inject</i>		<i>A(ADP)</i>
Mix	0.5	
Measure	6	
Mix	1	
<i>Inject</i>		<i>B(Oligomycin)</i>
Mix	0.5	
Measure	3	
Mix	1	
<i>Inject</i>		<i>C(FCCP)</i>
Mix	0.5	
Measure	3	
Mix	1	
<i>Inject</i>		<i>D(Rotenone or Antimycin A)</i>
Mix	0.5	
Measure	3	
Mix	0.5	
Measure	6	
End Protocol		
<i>Total time</i>	72.5	

5. Transfer the suspension into the glass tube of the Potter-Elvehjem PTFE for homogenization.
6. Disrupt tissue pieces by 30 strokes at 500 rpm in the Homogenizer EUROSTAR 20 digital, except the muscle that is homogenized at 600 rpm.
7. Centrifuge the homogenate at  $800 \times g$  for 10 min at 4 °C in a swing-out rotor.
8. Collect the supernatant.
9. Centrifuge the supernatant at  $8000 \times g$  for 10 min at 4 °C in a swing-out rotor.
10. Discard the supernatant.
11. Carefully remove fat and lipids from the pellet, especially in the liver sample (*see Note 10*).
12. Wash the pellet twice with MIB1.
13. Resuspend the final pellet, which contains mitochondria, in a small volume of MASI containing the appropriate respiratory substrate. Use 10 mM of Glutamate and 5 mM Malate for complex I-driven respiration, and 10 mM Succinate for Complex II (*see Note 11*).
14. Determine the total protein amount by Bradford assay (*see Note 12*).

### **3.5 Loading the Cartridge with Compounds and Run the Calibration (Day of the Experiment)**

1. Load 10-fold concentrated compounds in the ports of the cartridge, with the help of the “loading helper” plate. Inject 20  $\mu$ L of ADP (40 mM) (*see Note 13*) into port A, 22  $\mu$ L of oligomycin (25  $\mu$ g/mL) into port B, 24  $\mu$ L of FCCP (40  $\mu$ M) into port C, and 26  $\mu$ L of antimycin A (40  $\mu$ M) or rotenone (20  $\mu$ M) into port D.
2. Open the folder XFReader96 in the Seahorse machine.
3. Select the files “XF Data & Template.xls.”
4. Select the appropriate template file and set it as “default assay” for the subsequent run.
5. Click “Run.”
6. Insert the XF96 Sensor Cartridge into the Seahorse XF96 analyzer and hit “start” to run the calibration. Calibration run takes around 30 min.

### **3.6 Testing of Optimal Mitochondrial Amounts (Day of the Experiment)**

The amount of mitochondria to use in the assay varies according to the tissue of origin, the respiratory substrate (*see Note 14*), and the purity and intactness after the isolation. Therefore, it is recommended to run an initial plate on the day of experiment to test the optimal mitochondria amount to use in the subsequent experiments. To this goal, run a mitochondrial coupling test

experiment using glutamate/malate or succinate/rotenone as respiratory substrates.

1. Dilute all mitochondria to 1  $\mu\text{g}/\mu\text{L}$  with MAS1 containing the appropriate respiratory substrate.
2. Prepare three different master mixes for each tissue, containing various amounts of mitochondria/well. Consider using larger volumes for the master mixes, to minimize pipetting errors. For example:

*Mix 0.5  $\mu\text{g}$*   $\rightarrow$  in 250  $\mu\text{L}$  of mixture, add 2.5  $\mu\text{L}$  of mitochondria (1  $\mu\text{g}/\mu\text{L}$ ) and 247.5  $\mu\text{L}$  of MAS1 with substrates.

*Mix 1  $\mu\text{g}$*   $\rightarrow$  in 250  $\mu\text{L}$  of mixture, add 5  $\mu\text{L}$  of mitochondria (1  $\mu\text{g}/\mu\text{L}$ ) and 245  $\mu\text{L}$  of MAS1 with substrates.

*Mix 2  $\mu\text{g}$*   $\rightarrow$  in 250  $\mu\text{L}$  of mixture, add 7.5  $\mu\text{L}$  of mitochondria (1  $\mu\text{g}/\mu\text{L}$ ) and 242.5  $\mu\text{L}$  of MAS1 with substrates.

Keep the mitochondrial samples and solutions on ice.

Clean the outer surface of the pipette tip after aspirating mitochondria and before adding it to the MAS1 buffer. Ensure that mitochondrial samples are well resuspended to minimize variations in the measurements.

3. Deliver mitochondria as a 50  $\mu\text{L}$  suspension to each well of the plate (*see* Fig. 1; *see* Note 15), except the wells intended for the background correction. In these wells add only MAS1 with substrates. Keep the plate on ice while pipetting. The background correction is monitoring changes in  $\text{O}_2$ , pH, and temperature due, for example, to the injection step and it is used to correct the measurement values from this noise. Therefore, different injection strategies need an independent background correction. Unfortunately, the wave program still misses the possibility to sort the background wells to specific wells in case you measure several conditions within the same plate. This should be carried out by the user during data analysis.
4. Transfer the plate to a centrifuge with a swinging bucket microplate adaptor. Spin down the mitochondria to the bottom of the plate by centrifuging the plate at  $2000 \times g$  for 20 min at 4  $^\circ\text{C}$ .
5. During the 20 min of centrifugation, start the calibration plate in the Seahorse machine (*see* Subheading 3.5).
6. After the centrifugation, inspect mitochondria briefly under the microscope to ensure consistent adherence to the bottom of the wells (*see* Note 16).
7. Add 130  $\mu\text{L}$  of pre-warmed (37  $^\circ\text{C}$ ) MAS1 with substrates (glutamate/malate or succinate/rotenone) to each well.
8. Warm up the plate at 37  $^\circ\text{C}$  in a non- $\text{CO}_2$  incubator for 5–10 min.

9. At this stage the calibration step should be ready. Remove the utility plate from the machine. The cartridge is automatically retained in the instrument.
10. Put the microplate in the analyzer and start the run at the end of the calibration (*see Note 17*).
11. At the end of the run, open the .xfd file, select Display>Group, Y1>Level, Y2>O<sub>2</sub>. The optimal mitochondrial amount is the amount that never makes the absolute O<sub>2</sub> tension decline to zero, especially in State III or State III<sub>U</sub> (*see Note 18*).

**3.7 Run  
of the Experiment  
Using the Optimal  
Mitochondria Amount  
(Day of the  
Experiment)**

Test mitochondrial coupling as described in Subheading 3.4, using the proper mitochondria amount for each tissue.

**3.8 Verification  
of Mitochondrial  
Integrity After the Run  
(Day of the  
Experiment)**

1. After the run, recover the plate from the machine.
2. Dispense ~180  $\mu$ L of MAS + BSA, 1 $\times$  buffer + 40 nM MitoTracker Green FM.
3. Incubate 15 min at 37  $^{\circ}$ C.
4. Acquire pictures with an inverted fluorescent microscope (*see Fig. 2*). Intact mitochondria are able to uptake the probe, therefore fluoresce.

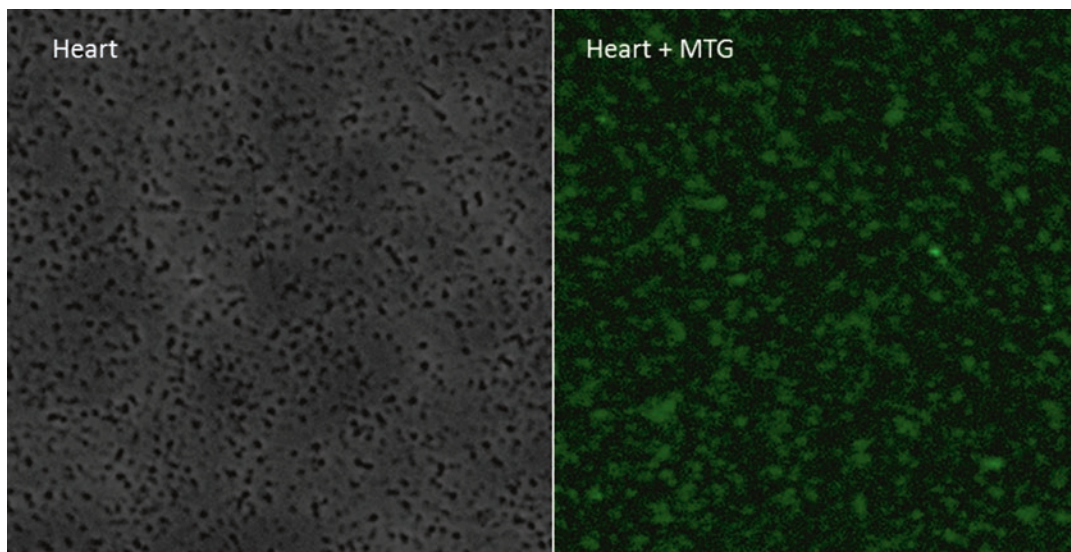


**Fig. 2** Isolated mitochondria remain attached to the plate and coupled throughout the assay. The figure shows a representative picture of mitochondria isolated from heart, plated at 1  $\mu$ g/well on the XF96 cell culture microplate and stained with 20 nM of MitoTracker Green (+MTG). The fluorescent signal in the pictures +MTG indicates that mitochondria are still able to uptake the probe, suggesting that the mitochondrial membrane potential is still intact. Pictures were acquired using an inverted microscope with 20 $\times$  magnification

### 3.9 Data Analysis (Any Day After the Experiment)

1. Open the .xfd files with the XF<sup>e</sup>Wave software.
2. Select Modify>Normalization>Apply to normalize the OCR values of each well to  $\mu\text{g}$  of mitochondria.
3. Select Display>Well, Y1>Rate, Y2>None to visualize outliers due to incorrect injection of reagents or uneven distribution of mitochondria and exclude them from the analyses by clicking on the trace.
4. Select Display>Group, Y1>Rate, Y2>None.
5. Right click on the line chart area and export graph data in an Excel sheet. You will get a list of OCR values, expressed as  $\text{pmol O}_2/\text{min}/\mu\text{g}$  mitochondrial proteins, at different time points (1, 6, 13, 20, 25, 31, and 35 min) and the S.E.M. values.
6. Calculate the basal respiration, which represents the respiration of mitochondria in the presence of substrates but without ADP, by subtracting the OCR values at minute 35 (non-mitochondrial  $\text{O}_2$  consumption) from the values at minute 1 (*see* Fig. 3).
7. Calculate State III, which represents the formation ATP from ADP and inorganic phosphate, by subtracting the OCR values at minute 35 from the values at minute 13 (*see* Fig. 5 for calculation; *see* Figs. 4 and 5 for reference values).
8. Calculate State IV<sub>o</sub>, which represents the proton leak due to the inhibition of the ATP synthase by oligomycin, by subtracting the OCR values at minute 35 from the values at minute 20 (*see* Fig. 3 for calculation; *see* Figs. 4 and 5 for reference values).
9. Calculate the State III<sub>u</sub>, which represents the status of maximal respiratory capacity, by subtracting the OCR values at

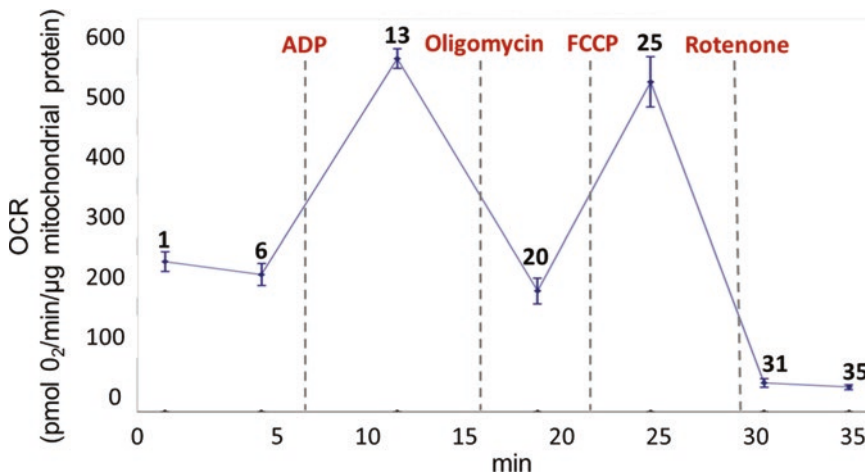


**Fig. 3** Representative trace of a coupling experiment using isolated mitochondria

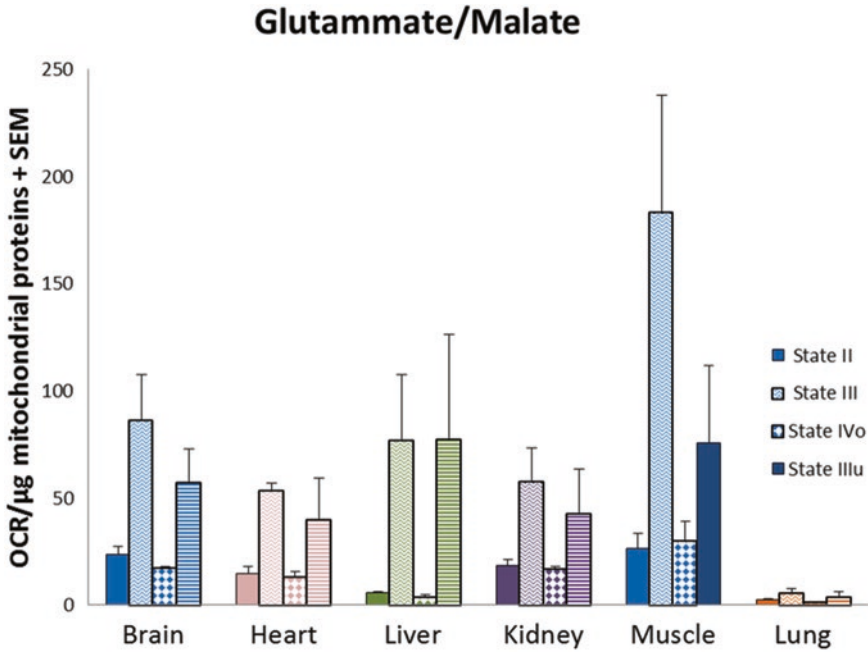


**Fig. 4** OCR and RCR for RCCI-driven respiration. Data refer to mitochondria isolated from wild-type C57Bl/6N mice, 14–19 weeks-old. Data represent the average of three independent experiments, each experiment having 4–6 replicate wells + SEM

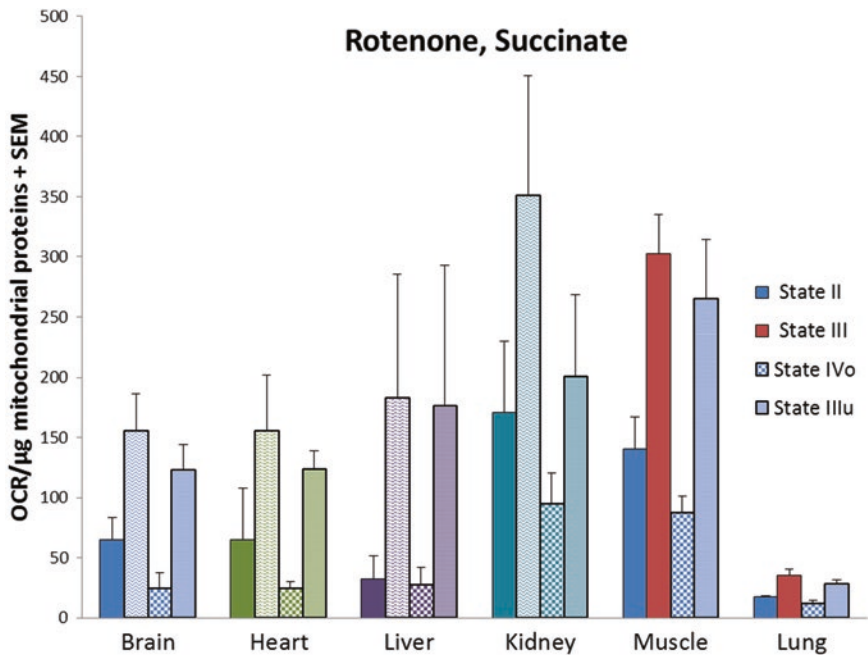


**Fig. 5** OCR and RCR for RCCII-driven respiration. Data refer to mitochondria isolated from wild-type C57Bl/6N mice, 14–19 weeks-old. Data represent the average of three independent experiments, each experiment having 4–6 replicate wells + SEM

minute 35 from the values at minute 25 (*see* Fig. 3 for calculation; *see* Figs. 4 and 5 for reference values).

10. Calculate the respiratory control ratio, RCR, which is the index of mitochondrial coupling, by dividing the corrected values of State III<sub>u</sub>/State IV<sub>o</sub> (*see* Figs. 4 and 5 for reference values).

---

## 4 Notes

1. Buffers can be prepared up to 2–3 weeks in advance and aliquots stored at  $-20\text{ }^{\circ}\text{C}$ . However, on the day of the assay, the pH has to be remeasured and eventually readjusted to 7.2 with KOH.
2. Substrates are stable for long periods ( $>1$  year) at  $-20\text{ }^{\circ}\text{C}$ .
3. 40 mM of ADP and serial dilutions should be prepared on the day of the assay or at the earliest, one the day before.
4. The concentration of FCCP depends on the BSA content in the MAS buffer, the amount of mitochondria, and the type of mitochondria. If using a different concentration of BSA in the MAS buffer, or using mitochondria isolated from tissues not described in this protocol, a preliminary FCCP titration is mandatory.
5. The hydration step is required for proper functioning of the sensors when measuring OCR. Cartridges can be used within 3–4 h of hydration, as well as up to 72 h after the addition of the calibrant solution. The incubator must be humidified if you are hydrating for longer periods of time to prevent the evaporation of the calibrant solution. Remember to hydrate as many cartridges as required for the whole experiment.
6. The protocols described here are adapted for the XF Reader version 1.4.2.3. Be aware that latest versions might have different user interfaces.
7. Extend measurement times for rotenone and antimycin A to 6 min because those measurements are going to be used as “not mitochondrial respiration,” hence background, to be subtracted from all respiratory states.
8. Attain to your local laws for animal handling. In our experiments mice are sacrificed by cervical dislocation in accordance with the German Animal Welfare Act (§7, §8, and §8a).
9. Rinse liver, heart, and kidney several times with MIB1 to remove blood.
10. Use a cotton swab to remove fat and lipids from the outer part of the mitochondrial pellet. You may recognize this fraction from the typical whitish/pale-yellow color.

18 $\mu$ l MAS + BSA	0	0	0	0	0	0	0	0	0	0	0	0
18 $\mu$ l ADP 1.25 mM	0.125	0.125	0.125	0.125	0.125	0.125	0.125	0.125	0.125	0.125	0.125	0.125
18 $\mu$ l ADP 2.5 mM	0.250	0.250	0.250	0.250	0.250	0.250	0.250	0.250	0.250	0.250	0.250	0.250
18 $\mu$ l ADP 5 mM	0.5	0.5	0.5	Tissue 1	0.5	0.5	0.5	0.5	0.5	Tissue 2	0.5	0.5
18 $\mu$ l ADP 10 mM	1	1	1	1	1	1	1	1	1	1	1	1
18 $\mu$ l ADP 20 mM	2	2	2	2	2	2	2	2	2	2	2	2
18 $\mu$ l ADP 40 mM	4	4	4	4	4	4	4	4	4	4	4	4
	BK	BK	BK	BK	BK	BK	BK	BK	BK	BK	BK	BK

**Fig. 6** Layout of the 96-well Seahorse plate for the optimization of the ADP concentration. Using the present layout you can test up to seven different concentrations of ADP for a specific substrate and tissue. Every measure is carried out in six replicates. The *last row* is filled with MAS1 and represents the background (BK)

11. Choose the volume according to the size of the pellet. Usually, 100  $\mu$ L for muscle and lung, 200  $\mu$ L for brain, 500  $\mu$ L for liver and kidney, if starting from 30 to 50 mg of tissue.
12. Prepare the reagent “blank” with MAS1 since BSA in the buffer will interfere with the Bradford measure of your samples.
13. Using an appropriate concentration of ADP is essential for determining OCR during State III. The optimal ADP concentration should not be necessarily determined on the day of the assay. It can be measured at any time before the assay, by using isolated mitochondria from a wild-type mouse. We tested ADP concentrations in the range of 0.125–4 mM, as described in (6) and we found that most of the tissues included in this chapter were stimulated by 2–4 mM of ADP. If you need to test the correct ADP amount in a different tissue, we recommend testing mitochondrial coupling using glutamate/malate or succinate/rotenone as respiratory substrates at increasing concentrations of ADP, as described here:
  - Distribute the optimal amount of mitochondria for two different tissues on the same plate.
  - Inject different amounts of ADP through port A: 0, 0.125, 0.25, 0.5, 1, 2, and 4 mM (*see* Fig. 6). Proceed by loading ports B–D as described in Subheading 3.3.
  - At the end of the run analyze the .xfd file and select the optimal ADP concentration as the concentration giving a clear increase in respiration, still responding to the oligomycin and the FCCP.
  - The molarity of ADP to be injected is 10 times higher (10 $\times$ ) than the final molarity in the well. In our hands, a final concentration between 2 and 4 mM of ADP is sufficient to induce a stable State III. Insufficient amounts of ADP will result in the exhaustion of ADP during one measurement cycle.
14. As a rule of thumb, the amount of mitochondria to use for RCCI-dependent respiration is 3–4 times higher than the amount of mitochondria to use for RCCII-stimulated

respiration. Perform pilot experiments for testing different concentrations of mitochondria for each tissue. Use a range of 0.5–2  $\mu\text{g}$  mitochondria/well for succinate-dependent respiration and of 1–5  $\mu\text{g}$  mitochondria/well for glutamate/malate-dependent respiration.

15. It is not recommended to use large suspension volumes as it will result in lower OCRs probably due to attached mitochondria at the sides of the wells.
16. Mitochondria should appear evenly distributed in each well.
17. Start the calibration run as soon as you start centrifuging the microplate with mitochondria.
18. A good indication is to keep the basal respiration between 40 and 80 pmol  $\text{O}_2/\text{min}/\text{well}$ .

## References

1. Schuh RA, Clerc P, Hwang H, Mehrabian Z, Bittman K, Chen H, Polster BM (2011) Adaptation of microplate-based respirometry for hippocampal slices and analysis of respiratory capacity. *J Neurosci Res* 89(12):1979–1988. doi:[10.1002/jnr.22650](https://doi.org/10.1002/jnr.22650)
2. Schuh RA, Jackson KC, Khairallah RJ, Ward CW, Spangenburg EE (2012) Measuring mitochondrial respiration in intact single muscle fibers. *Am J Physiol Regul Integr Comp Physiol* 302(6):R712–R719. doi:[10.1152/ajpregu.00229.2011](https://doi.org/10.1152/ajpregu.00229.2011)
3. Kraunsoe R, Boushel R, Hansen CN, Schjerling P, Qvortrup K, Stockel M, Mikines KJ, Dela F (2010) Mitochondrial respiration in subcutaneous and visceral adipose tissue from patients with morbid obesity. *J Physiol* 588(Pt 12):2023–2032. doi:[10.1113/jphysiol.2009.184754](https://doi.org/10.1113/jphysiol.2009.184754)
4. Gneiger E (2008) Polarographic oxygen sensors, the oxygraph, and high-resolution respirometry to assess mitochondrial function. John Wiley & Sons, Hoboken, NJ. doi:[10.1002/9780470372531.ch12](https://doi.org/10.1002/9780470372531.ch12)
5. Clark LC (1956) Monitoring and control blood and tissue oxygen. *Trans Am Soc Artif Intern Organs* 2:41–48
6. Rogers GW, Brand MD, Petrosyan S, Ashok D, Elorza AA, Ferrick DA, Murphy AN (2011) High throughput microplate respiratory measurements using minimal quantities of isolated mitochondria. *PLoS One* 6(7):e21746. doi:[10.1371/journal.pone.0021746](https://doi.org/10.1371/journal.pone.0021746)
7. Franko A, Baris OR, Bergschneider E, von Toerne C, Hauck SM, Aichler M, Walch AK, Wurst W, Wiesner RJ, Johnston IC, de Angelis MH (2013) Efficient isolation of pure and functional mitochondria from mouse tissues using automated tissue disruption and enrichment with anti-TOM22 magnetic beads. *PLoS One* 8(12):e82392. doi:[10.1371/journal.pone.0082392](https://doi.org/10.1371/journal.pone.0082392)
8. Bharadwaj MS, Tyrrell DJ, Lyles MF, Demons JL, Rogers GW, Molina AJ (2015) Preparation and respirometric assessment of mitochondria isolated from skeletal muscle tissue obtained by percutaneous needle biopsy. *J Vis Exp* (96):e52350. doi:[10.3791/52350](https://doi.org/10.3791/52350)

## Application of FRET-Based Biosensor “ATeam” for Visualization of ATP Levels in the Mitochondrial Matrix of Living Mammalian Cells

Tomoki Yoshida, Soaad Alfaqaan, Norio Sasaoka, and Hiromi Imamura

### Abstract

Genetically encoded biosensors utilizing the Förster resonance energy transfer (FRET) are powerful tools for live cell imaging of various cellular processes. Our group has previously developed a series of FRET-based biosensors, named “ATeam,” for visualization of ATP levels inside a single living cell. ATeam not only provides a window of insight into a single cell but also allows for visualization of ATP levels in mitochondrial matrix of a single living cell. This novel tool is able to monitor alterations in cellular ATP in response to various treatments in real time. Here we present a method for the evaluation of ATP levels in mitochondria in living cells by using ATeam. At the end of this chapter, an example of experimental results is described for a better understanding of the presented procedure.

**Key words** Fluorescent biosensor, FRET, Live imaging, ATP, ATeam

---

### 1 Introduction

Genetically encoded biosensors utilizing the Förster resonance energy transfer (FRET) principle with fluorescence proteins have been extensively applied for live cell imaging of various cellular processes. FRET is an electrodynamic phenomenon between a donor fluorophore and an acceptor molecule. An overlap between the emission spectrum of a donor and the absorption spectrum of an acceptor, and a donor and an acceptor are in close proximity, then the energy of the excited donor can be transferred to the acceptor. The efficiency of FRET depends on factors including: the extent of the spectral overlap, and the relative distance and orientation between the donor and the acceptor. A thorough description of the principle can be found in “Principles of Fluorescence Spectroscopy” textbook [1]. In general, genetically encoded FRET-based biosensors are composed of donor and acceptor fluorescent proteins, separated by a sensory protein. A conformational change of the sensory protein, induced by, for example, ligand

binding, alters the relative distance and orientation between the two fluorophores. Thus, a change in the cellular environment can be correlated to the changes in FRET efficiency between two fluorescent proteins. The detailed procedure for designing biosensors based on fluorescent fusion proteins can be found in “Live Cell Imaging; Methods and Protocols” [2] previously published by Method in Molecular Biology. One major advantage of FRET-based biosensors is their highly quantitative nature. The output signal is typically a ratio of the donor-to-acceptor emissions, or a fluorescence lifetime of the donor, which are both almost insensitive to the expression level of the biosensor itself.

Our group has previously developed a series of FRET-based biosensors for visualization of ATP levels inside a single living cell, named “ATeam” (ATP indicator based on Epsilon subunit for Analytical Measurement) [3]. The ATP imaging technique using ATeam provides an alternative method by which disadvantages in conventional ATP quantification methods can be overcome. For example, measurements of ATP by using luciferase [4] or chromatography [5] can only provide average ATP concentrations of the cell extract. In addition, they carry the risk of loss and decomposition of ATP during the extraction processes. Although valid attempts to monitor ATP levels in real-time using chemiluminescence with intracellular expression of firefly luciferase have been reported [6, 7], their applications are limited as they depend on the level of expression and activity of luciferase. Moreover, consumption of ATP by luciferase itself may disturb intracellular ATP levels.

A schematic of the mechanism of ATeam for measurement of ATP is illustrated in Fig. 1. An original ATeam (ATeam1.03) employs the  $\epsilon$  subunit of the bacterial  $F_0F_1$ -ATP synthase as an ATP sensory domain sandwiched between two fluorescence proteins—a variant of cyan fluorescent protein (mCFCP) [8] as the donor fluorophore present N-terminally to the  $\epsilon$  subunit and a circularly permuted monomeric Venus having the 173rd amino

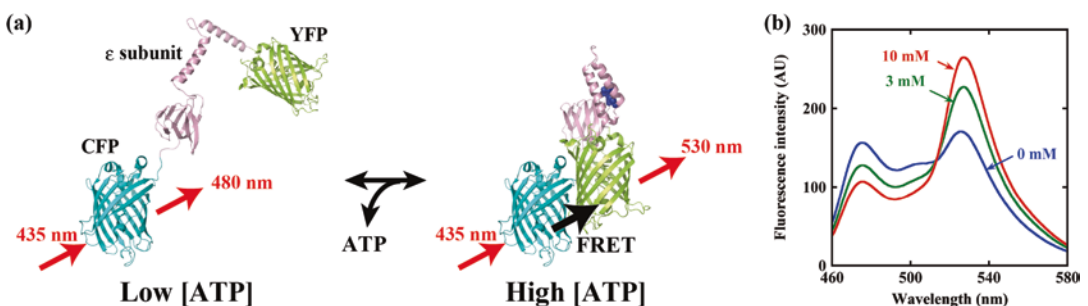


**Fig. 1** Mechanism of ATeam for measurement of ATP. (a) Schematic of ATeam. (b) ATP-dependent fluorescence spectra of purified ATeam1.03 in 50 mM MOPS–KOH (pH 7.3), 50 mM KCl, 0.5 mM MgCl<sub>2</sub>, 0.05% Triton X-100

acid as its N terminus (cp173-mVenus) [9] as the acceptor at the C-terminus of the  $\epsilon$  subunit (Fig. 1a). The bacterial  $\epsilon$  subunit is an ATP-binding protein (14 kDa) composed of an N-terminal  $\beta$ -barrel domain and two C-terminal  $\alpha$ -helices [10]. The  $\epsilon$  subunit binds to ATP by bundling  $\alpha$ -helices without hydrolysis, and greatly changes its conformation. In the absence of ATP, the  $\epsilon$  subunit extends and adopts a flexible conformation, resulting in the separation of the two fluorescence proteins. Conversely, in the presence of ATP, the  $\epsilon$  subunit binds to ATP and contorts, drawing the two fluorescence proteins closer to each other. Thus, ATP alters the fluorescent spectra of ATeam by changing the FRET efficiency between CFP and YFP (Fig. 1b). In turn, this allows the ATP levels to be quantitatively measured by calculating the emission ratios of YFP-FRET/CFP from ATeam, although it is still challenging to determine absolute intracellular ATP concentrations of living cells.

There are several variants of ATeam with different binding affinities for ATP and the fluorescent spectra. The properties of these ATeams are summarized in Table 1 [3, 11, 12]. Properties of the spectra are altered by fluorescent proteins used as the donor and the acceptor fluorophores. It should be noted that temperature highly affects the affinity of the biosensors [3]. ATP measurements using ATeam can be properly achieved by applying a suitable ATeam selected from the series with the appropriate properties for the experimental conditions. For example, AT1.03, AT1.03YEMK, GO-ATeam1, or GO-ATeam2 biosensors are suitable for mammalian cells that are maintained at 37 °C, while AT1.03NL biosensor

**Table 1**  
**Properties of ATeam series**

Name	Donor	Acceptor	$K_d$	References
ATeam1.03	mseCFP (C $\Delta$ 11)	cp173-mVenus	3.3 mM	
ATeam1.03YEMK	mseCFP (C $\Delta$ 11)	cp173-mVenus	1.2 mM	
ATeam1.03R122K/ R126K	mseCFP (C $\Delta$ 11)	cp173-mVenus	no detectable binding	Imamura et al. [3]
ATeam3.10	mseCFP (C $\Delta$ 10)	mVenus	7.4 $\mu$ M	
ATeam3.10MGK	mseCFP (C $\Delta$ 10)	mVenus	14 $\mu$ M	
GO-ATeam1	cp173-mEGFP	mKO $\kappa$	7.1 mM	
GO-ATeam2	cp173-mEGFP	mKO $\kappa$	2.3 mM	Nakano et al. [11]
GO-ATeam3	cp173-mEGFP	mKO $\kappa$	no detectable binding	
ATeam1.03NL	mseCFP (C $\Delta$ 10)	cp173-mVenus	1.8 mM (24 °C)	Tsuyama et al. [12]

The value of  $K_d$  represents apparent dissociation constants for ATP of ATeam at 37 °C. C $\Delta$ 10 and C $\Delta$ 11 represent the deletion of 10 and 11 residues of C-terminal domain, respectively

works best for organisms with much lower body temperatures, such as *C. elegans* and *D. melanogaster*.

ATeam is a useful tool for investigating the relationship between cellular functions and ATP levels in each cell. Additionally, it enables for visualization of ATP levels in subcellular compartments of a single living cell [3]. Fluorescence imaging assay with ATeam revealed that ATP levels in the mitochondrial matrix are significantly lower than those in the cytosol and nucleus [3], and positively correlate with mitochondrial membrane potential [13] in HeLa cells. A recent report using ATeam has successfully visualized a decrease in mitochondrial ATP levels after a decrease in  $\text{Ca}^{2+}$  transporting ATPase activity during activation of cellular protective machinery in the inflammatory processes [14]. Employing ATeam and an ATP production assay, another study successfully illustrated an increase in mitochondrial ATP production in response to hypoxic stress as a means to protect cells from a critical energy crisis [15]. Furthermore, our group succeeded in elucidating the role of increased cytosolic ATP on  $\text{Ca}^{2+}$  oscillation trends in glucose-stimulated pancreatic islet by using a combination of ATeam and a fluorescent  $\text{Ca}^{2+}$  dye [16].

Herein, we describe the method for the evaluation of ATP levels in the mitochondrial matrix of living mammalian cells using ATeam1.03. The procedures described below consist of three steps: (1) preparation of cells that are stably or transiently expressing ATeam in mitochondria, (2) acquisition of fluorescent images of cells expressing ATeam in mitochondria and (3) processing of fluorescent images. At the end of this chapter, an example of experimental results is described for a better understanding of the presented procedure.

---

## 2 Materials

### 2.1 Cell Culture

1. Growth Medium: Dulbecco's modified Eagle's medium (DMEM, high glucose) containing 10% fetal bovine serum (FBS) supplemented with 100  $\mu\text{g}/\text{mL}$  penicillin and streptomycin.
2. HEK293A cells are routinely cultured in growth medium in 90 mm dishes at 37 °C in 5%  $\text{CO}_2$ . At 80% confluence, cells are trypsinized and used to seed for transfection.

### 2.2 Transfection of Cells

1. D-PBS without  $\text{Ca}^{2+}$  and  $\text{Mg}^{2+}$ .
2. Trypsin-EDTA (0.25%) containing phenol red solution.
3. DMEM (high glucose).
4. 35 mm glass bottom dish: P35-1.5-14C (MatTek Corp., Ashland, MA).

5. Cellmatrix Type I-C (Nitta-Gelatin Co. Ltd, Osaka, Japan).
6. Lipofectamine® Transfection reagent (Invitrogen, San Diego, CA).
7. Lipofectamine® 2000 Transfection reagent (Invitrogen, San Diego, CA).
8. 1× Opti-MEM® medium (Gibco/BRL, Bethesda, MD).
9. PLUS™ reagent (Invitrogen, San Diego, CA).
10. pcDNA-mitAT1.03 [3]: Expression plasmid for AT1.03 with a tandem repeat of a mitochondrial targeting signal of cytochrome c oxidase subunit 8 at N-terminus. To obtain the plasmid, please contact corresponding author.
11. G418 (Geneticin®).
12. Cloning cylinders (8 mm × 8 mm).
13. Sterile silicon grease.
14. 24-well plate.
15. Fluorescence microscope.

### 2.3 Imaging

1. Microscope: Eclipse Ti-E inverted microscope with a perfect focus system (PFS), a motorized stage, a xenon light source, and filter wheels (Nikon Instrument Inc., Tokyo, Japan) (*see Note 1*).
2. Objective lens: CFI Plan Apo VC 60× oil (NA 1.40) (Nikon Instrument Inc., Tokyo, Japan).
3. Stage-top incubator: INUBG2-TIZB (Tokai Hit Co. Ltd, Fujinomiya, Japan).
4. Electric shutter: SmartShutter (Sutter Instruments, Novato, CA).
5. Camera: Zyla 4.2 sCMOS camera (Andor Technology Ltd, Belfast, UK) (*see Note 2*).
6. Optical filters for FRET imaging (Semrock, Rochester, NY): FF01-438/24 filter for excitation, FF458-Di01 dichroic mirror, FF01-483/32 filter for CFP emission and FF01-542/27 filter for YFP-FRET emission.
7. Optical filter set for YFP: YFP-A-Basic filter set (Semrock, Rochester, NY).
8. System controlling software: NIS-Elements 4.2 (Nikon Instrument Inc., Tokyo, Japan).
9. Immersion oil.

### 2.4 Processing Images

1. MetaMorph 7.6 (Molecular Devices, Sunnyvale, CA) (*see Note 3*).

### 3 Methods

#### 3.1 Preparation of Cells Expressing ATeam in Mitochondria

##### 3.1.1 Stable Transfection of Cells

1. Prepare HEK293A cells in 60 mm dish at 70% confluency in 3 mL growth medium.
2. Dilute 4  $\mu\text{L}$  PLUS<sup>TM</sup> reagent and 2  $\mu\text{g}$  pcDNA-mitAT1.03 in 250  $\mu\text{L}$  DMEM. In another tube, dilute 6  $\mu\text{L}$  Lipofectamine<sup>®</sup> in 250  $\mu\text{L}$  DMEM and incubate both mixtures for 15 min at room temperature (25 °C).
3. After incubation, combine the two reagent mixtures together and ensure blending by pipetting about 10 times. Incubate the mixed solution at room temperature (25 °C) for 15 min.
4. Add the mixed solution to the 60 mm dish (in addition to the 3 mL medium in the dish).
5. Incubate at 37 °C in 5% CO<sub>2</sub> for 3 h.
6. Change the medium to fresh growth medium and incubate at 37 °C in 5% CO<sub>2</sub> for 24 h (*see Note 4*).
7. Wash the cells with 3 mL D-PBS.
8. Add 1 mL 0.25% trypsin–EDTA and swirl the solution around the plate gently for 30 s.
9. Remove  $\approx 750$   $\mu\text{L}$  of trypsin–EDTA leaving  $\approx 250$   $\mu\text{L}$  remaining in the dish.
10. Incubate at 37 °C in 5% CO<sub>2</sub> for 1 min.
11. Suspend the cells in 1 mL growth medium.
12. Transfer the cell suspension into 10 mL of growth medium containing 0.75 mg/mL G418 onto 90 mm dish (*see Note 5*).
13. Routinely culture the transfected cells in growth medium containing 0.75 mg/mL G418 in 90 mm dishes at 37 °C in 5% CO<sub>2</sub> for 2 weeks.
14. Re-passage the cells in 10 mL of growth medium in a 90 mm dish at a density of  $1 \times 10^2$  cells/dish (Five dishes prepared as specified are adequate for making a stable transfection cell line).
15. Incubate at 37 °C in 5% CO<sub>2</sub> for 72 h.
16. Using fluorescence microscopy, individually select a single colony (about 10–20 cells/colony) expressing the fluorescent emission of ATeam in the mitochondria (*see Note 6*). To identify the location of the selected colonies, mark the bottom of the dish with a permanent marker at the selected areas.
17. Remove the medium from the dish and wash once with 3 mL D-PBS.

18. Isolate each individual colony using a cloning cylinder greased with sterile silicon grease on one end to allow the cylinder to seal to the plate.
19. Place 100  $\mu\text{L}$  0.25% trypsin–EDTA into the cloning cylinder.
20. Incubate the dish at 37 °C in 5%  $\text{CO}_2$  for 3 min.
21. Gently pipette the solution within the cloning cylinder to allow the cells to detach. Individually remove the cells in suspension and transfer them to a 24-well plate with 2 mL growth medium (*see Note 7*).
22. At this stage, the stable transfection is complete and cells can be re-passaged onto larger plates after 3 days of incubation. Routinely culture the cells permanently expressing ATeam in mitochondria in growth medium and incubate at 37 °C in 5%  $\text{CO}_2$ .
23. For imaging purposes, cells must be re-passaged onto 35 mm collagen coated glass bottom dish (*see Note 8*) in 2 mL of growth medium at desired density (*see Note 9*).

### 3.1.2 Transient Transfection of Cells

1. Wash the cells at 80% confluence in a 90 mm dish with 3 mL D-PBS.
2. Add 1 mL 0.25% trypsin–EDTA and swirl the solution around the plate gently for 30 s.
3. Remove  $\approx 750$   $\mu\text{L}$  of trypsin–EDTA leaving  $\approx 250$   $\mu\text{L}$  remaining in the dish.
4. Incubate at 37 °C in 5%  $\text{CO}_2$  for 1 min.
5. Suspend the cells in 3 mL growth medium.
6. Transfer aliquots of the cell suspension into 2 mL of growth medium onto a 35 mm collagen coated glass bottom dish at a density of  $4\text{--}6 \times 10^4$  cells/dish.
7. Gently rock the dish in a back-to-forth and side-to-side manner for 20 s at room temperature (25 °C).
8. Incubate cells at 37 °C in 5%  $\text{CO}_2$  for 24 h.
9. Individually dilute 3  $\mu\text{L}$  Lipofectamine® 2000 and 1  $\mu\text{g}$  pcDNA-mitAT1.03 in 150  $\mu\text{L}$  Opti-MEM® medium, and incubate both mixtures for 5 min at room temperature (25 °C).
10. Mix the solutions well, and incubate at room temperature (25 °C) for 5 min.
11. Add 300  $\mu\text{L}$  of the mixed solution directly into the medium and incubate cells at 37 °C in 5%  $\text{CO}_2$  for 1 h (*see Note 10*).
12. Change the medium to fresh growth medium.
13. Incubate at 37 °C in 5%  $\text{CO}_2$  for 1–3 days (*see Notes 9 and 11*).

### 3.2 Acquisition of Fluorescent Images of Cells Expressing ATeam in Mitochondria

For fluorescent live imaging in our experiments, images in CFP and YFP-FRET channels are captured from cells expressing ATeam in mitochondria by using a Nikon Ti-E-PFS inverted microscope equipped with a 60× oil-immersion objective (Nikon), a sCMOS camera (Andor), and stage-top incubator (Tokai Hit) as shown in Fig. 2. To illuminate the cells, a 75-W xenon lamp with 12.5 and 25% neutral density filters and an excitation filter (426–450 nm) was used. Excitation light was controlled by an electric shutter. To achieve dual-emission ratio imaging of ATeam, we used a motorized filter wheel to alternate between two (CFP and YFP-FRET) emission filters. The microscope system was controlled with NIS-Elements software. The detailed procedure for capturing fluorescent images is described below.

1. Stabilize the stage-top incubator at 5% CO<sub>2</sub> at 37 °C and warm the oil-immersion lens to 37 °C by wrapping it with the lens warmer (*see Note 12*).
2. Stabilize the xenon lamp for more than 30 min before starting the imaging assay.
3. Change the medium to 2 mL phenol red free DMEM (low glucose) pre-warmed at 37 °C (*see Note 13*).
4. Add a drop of immersion oil onto the warmed lens.
5. Place and fix the dish on the stage. For treatment that requires the addition of an external reagent such as oligomycin (*see Note 14*).
6. Turn on the perfect focus system.

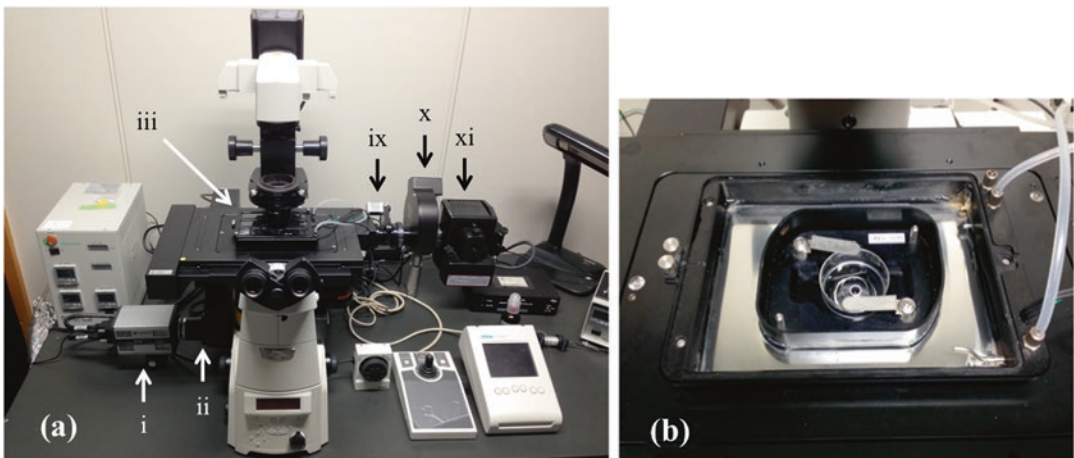


**Fig. 2** Fluorescent microscope system for imaging of ATeam. (a) General view of the fluorescence microscope system used in our experiments. The numbers represent the parts as following; (i) Zyla 4.2 sCMOS camera, (ii) filter wheel (emission), (iii) stage-top incubator, (ix) electric shutter, (x) filter wheel (excitation), (xi) xenon lamp. (b) Stage-top incubator with a sample prepared for imaging of ATeam

7. Find ATeam-expressing cells by visual detection, using a YFP-filter set. Adjust xy position and focus (*see Note 15*).
8. Readjust the xy positions and refocus using a CFP or YFP-FRET fluorescent image obtained by sCMOS camera by using NIS-Elements (*see Note 12*).
9. Input the xy positions to NIS-Elements.
10. Repeat **steps 8–10** in order to select multiple view fields. Typically, 5 or more cells should be imaged to obtain reliable results.
11. Input the time interval between each shot (*see Note 16*).
12. Set the exposure times for both CFP and YFP-FRET channels (*see Note 17*).
13. Start image acquisition.

### **3.3 Processing of Fluorescent Images**

According to the principle of ATeam described in the introduction, ATP levels in mitochondria can be evaluated by ratiometric changes of YFP-FRET per CFP emission signals from ATeam. In our experiments, MetaMorph (Molecular devices) has been used for calculation of the ratio value by processing fluorescent images in each channel as described below.

1. Open the image files of CFP and YFP-FRET channel by using processing software MetaMorph.
2. Select a region-of-interest (ROI) at the same position in CFP and YFP-FRET images within the area where no cells exist.
3. Subtract a constant background intensity value estimated from statistics of a selected ROI in CFP and YFP-FRET images, respectively, by using the “statistical model” function equipped in MetaMorph.
4. Select a ROI to surround a single mitochondria expressing ATeam in CFP and YFP-FRET images subtracted background signal, respectively.
5. Calculate integrated intensities of CFP and YFP-FRET emissions within a ROI.
6. Calculate the emission ratio of YFP-FRET/CFP by using the integrated intensity of YFP-FRET emission and CFP emission in ROI.
7. If a photographic display of the cellular ATP levels is desired, intensity modulated display (IMD) images can be obtained from background-subtracted images generated at **step 3**.

An example of the presented methods for evaluation of ATP levels in mitochondria is shown in Fig. 3. The experimental results display a mitochondrial ATP depletion as judged by a decrease in emission ratio of FRET-YFP/CFP in HEK293A cells permanently expressing ATeam1.03 in mitochondria after treatment with oligomycin A, inhibitor of oxidative phosphorylation.

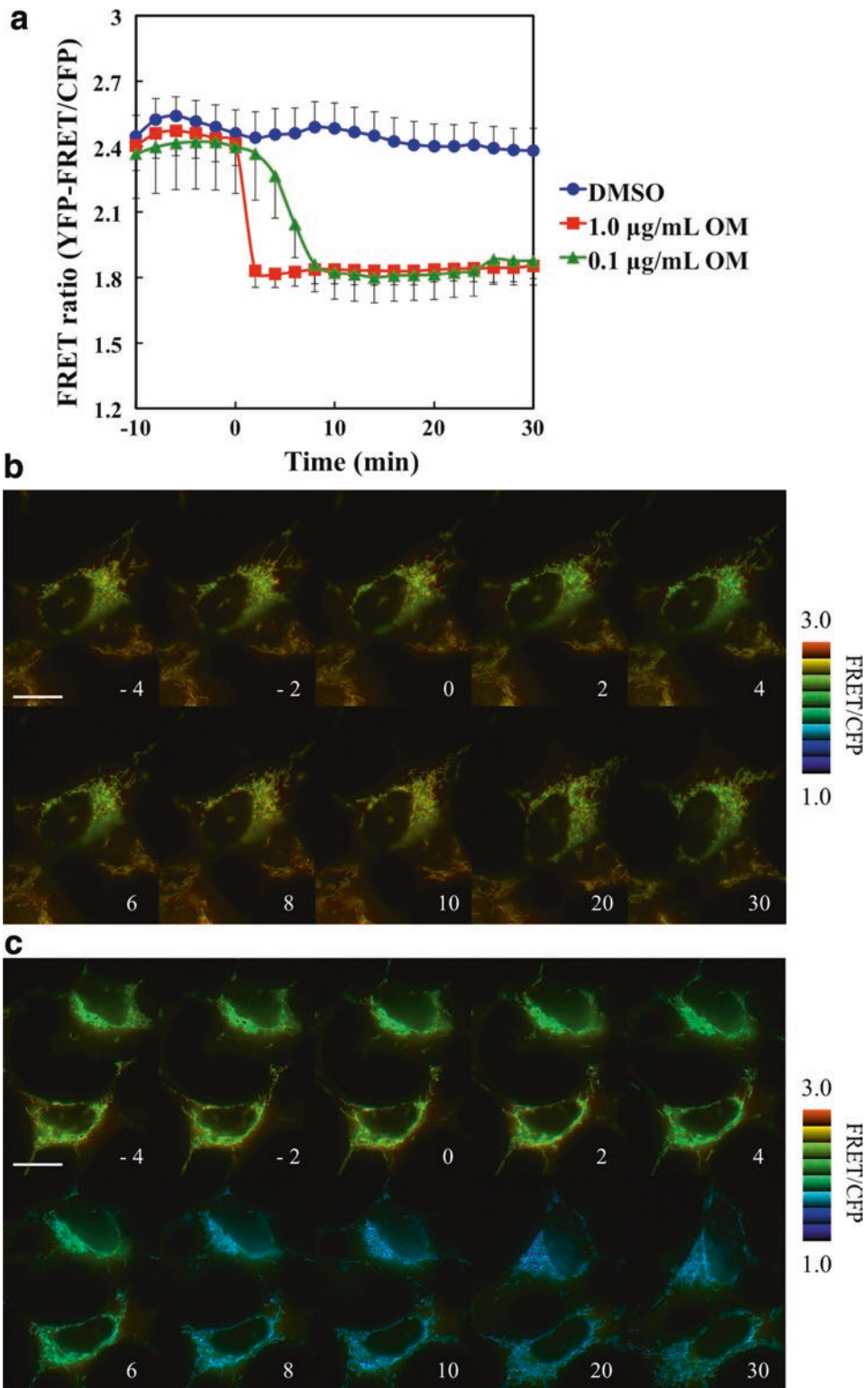


**Fig. 3** Monitoring mitochondrial ATP levels in HEK293A cells. **(a)** Time course of averaged YFP-FRET/CFP emission ratio of ATeam1.03 expressed in the mitochondrial matrix of HEK293A cells. The cells treated with 0.1% DMSO (*blue*,  $n = 6$ ) and 0.1 (*red*,  $n = 6$ ) and 1.0 (green,  $n = 5$ )  $\mu\text{g/mL}$  oligomycin for 30 min at 5%  $\text{CO}_2$  at 37  $^\circ\text{C}$ . Error bars indicate SD. **(b, c)** Sequential pseudocolored images of YFP-FRET/CFP emission ratio of the mitochondria of HEK293A cells. DMSO **(b)** or 0.1  $\mu\text{g/mL}$  oligomycin A **(c)** was added at time = 0 (min). The numbers represent time in minutes. Scale bar represents 30  $\mu\text{m}$

---

## 4 Notes

1. A PFS is quite useful if long-term imaging is required, and a motorized stage enables to obtain data from many cells in one experiment. But they are not indispensable. A xenon light source may be replaced by a mercury, metal-halide or LED light source.
2. A cooled CCD or EMCCD camera may be used. It is important to use a camera with high sensitivity, high linearity, and low noise.
3. Other image processing software, such as ImageJ, may be used.
4. When changing the medium, make sure to pre-warm the medium to 37 °C.
5. For effective selection, cells should be passaged with an antibiotic (G418) to weed out cells not expressing ATeam.
6. On average, 5 colonies of ~10–20 cells expressing ATeam in the mitochondria per plate are selected.
7. Each colony is to be plated individually in 24-well plate. For instance, if you select 5 colonies, you will have 5 wells.
8. For regular re-passaging, cells can be plated on regular non-coated plates.
9. We usually perform imaging at 50–80% confluency when the desired condition is a single cell analysis. This is due to the fact that at this confluency, cells can be captured in a single state and not crowded by other cells. On the other hand, when investigating cell communication for instance, a confluency of 90% is desirable due to the overlapping of the cells. Re-passage of cells to new glass bottom dishes may be required to adjust confluency.
10. Transfection procedure using Lipofectamine® 2000 requires an incubation of 1–3 days. However, incubation for just 1 h has proven to yield successful transfection efficiency in our laboratory. Thus, by our recommendation, exposure of 1 h is optimal and should not exceed 3 h as it might decrease cell viability.
11. The cells can be used for imaging assay between 1 and 3 days post-transfection. Prior to this time, the fluorescent protein goes through several stages until it becomes functional, termed maturation. Although the protein is already synthesized, it is not fluorescent until completion of maturation. Three days post-transfection, expression decreases, thus not allowing for accurate measurements.
12. It is critical to maintain the temperature of the culture dish during imaging via a stage-top incubator. The temperature

significantly affects the affinity of ATeam to ATP and hence the values of YFP-FRET/CFP emissions ratio.

13. Other culture media can be used for the imaging. However, culture media containing components displaying higher background signal at the imaging, such as phenol red, should be avoided.
14. When adding an external reagent to the medium during time-lapse imaging, this can be done while the dish is on the stage followed by very gentle pipetting to homogenize the mixture. Calculation of final concentration of the reagent in the medium must take into account the volume already present in the dish. Reagent solutions should be pre-warmed to 37 °C.
15. Excess exposure of the cells to excitation light causes photobleaching of fluorescent proteins, especially YFP, resulting in ATP-independent decrease in YFP-FRET/CFP emission ratio. Thus, it is important to reduce excitation light using neutral density filters and to minimize opening the excitation shutter when adjusting xy positions and focuses.
16. We usually use the time interval of 1 min or longer to avoid photobleaching of ATeam. It should be noted that a shorter interval (e.g., 10 s) can be applied for GO-ATeam, since GO-ATeam is much less subject to photobleaching than ATeam [11].
17. We typically use the same exposure time for both channels, ranging from 200 to 700 ms. In the situation where protein expression levels are low, a longer exposure time of 700 ms is recommended. Alternatively, if the expression levels are high, a shorter exposure time of 200 ms is recommended.

---

## Acknowledgments

This work was supported by a Grant-in-Aid for Scientific Research (B) to H.I. (26291027) from the Ministry of Education, Culture, Sports, Science and Technology in Japan (MEXT), and by the Platform Project for Supporting in Drug Discovery and Life Science Research (Platform for Dynamic Approaches to Living System) from MEXT and Japan Agency for Medical Research and Development (AMED).

## References

1. Lakowicz JR (ed) (2006) Principles of fluorescence spectroscopy, 3rd edn. Heidelberg, Springer
2. Pham E, Truong K (2010) Design of fluorescent fusion protein probes. In: Papkovsky DB (ed) Live cell imaging methods and protocols. Humana press, Herefordshire, pp 69–92
3. Imamura H, Nhat KP, Togawa H, Saito K, Iino R, Kato-Yamada Y, Nagai T, Noji H (2009) Visualization of ATP levels inside sin-

- gle living cells with fluorescence resonance energy transfer-based genetically encoded indicators. *Proc Natl Acad Sci U S A* 106:15651–15656
4. Ford SR, Chenault KH, Bunton LS, Hampton GJ, McCarthy J, Hall MS, Pangburn SJ, Buck LM, Leach FR (1996) Use of firefly luciferase for ATP measurement: Other nucleotides enhance turnover. *J Biol Chem* 271:149–167
  5. Smolenski RT, Lachno DR, Ledingham SJ, Yacoub MH (1990) Determination of sixteen nucleotides, nucleosides and bases using high-performance liquid chromatography and its application to the study of purine metabolism in hearts for transplantation. *J Chromatogr* 527:414–420
  6. Kennedy HJ, Pouli AE, Ainscow EK, Jouaville LS, Rizzuto R, Rutter GA (1999) Glucose generates sub-plasma membrane ATP microdomains in single islet beta-cells—Potential role for strategically located mitochondria. *J Biol Chem* 274:13281–13291
  7. Saito K, Chang YF, Horikawa K, Hatsugai N, Higuchi Y, Hashida M, Yoshida Y, Matsuda T, Arai Y, Nagai T (2012) Luminescent proteins for high-speed single-cell and whole-body imaging. *Nat Commun* 3:1262
  8. Matsuda T, Miyawaki A, Nagai T (2008) Direct measurement of protein dynamics inside cells using a rationally designed photo-convertible protein. *Nat Methods* 5:339–345
  9. Nagai T, Yamada S, Tominaga T, Ichikawa M, Miyawaki A (2004) Expanded dynamic range of fluorescent indicators for  $Ca^{2+}$  by circularly permuted yellow fluorescent proteins. *Proc Natl Acad Sci U S A* 101:10554–10559
  10. Yagi H, Kajiwara N, Tanaka H, Tsukihara T, Kato-Yamada Y, Yoshida M, Akutsu H (2007) Structures of the thermophilic  $F_1$ -ATPase  $\epsilon$  subunit suggesting ATP-regulated arm motion of its C-terminal domain in  $F_1$ . *Proc Natl Acad Sci U S A* 104:11233–11238
  11. Nakano M, Imamura H, Nagai T, Noji H (2011)  $Ca^{2+}$  regulation of mitochondrial ATP synthesis visualized at the single cell level. *ACS Chem Biol* 6:709–715
  12. Tsuyama T, Kishikawa JI, Han YW, Harada Y, Tsubouchi A, Noji H, Kakizuka A, Yokoyama K, Uemura T, Imamura H (2013) In vivo fluorescent adenosine 5'-triphosphate (ATP) imaging of *Drosophila melanogaster* and *Caenorhabditis elegans* by using a genetically encoded fluorescent ATP biosensor optimized for low temperatures. *Anal Chem* 85:7889–7896
  13. Kiyonaka S, Kajimoto T, Sakaguchi R, Shinmi D, Omatsu-Kanbe M, Matsuura H, Imamura H, Yoshizaki T, Hamachi I, Morii T, Mori Y (2013) Genetically encoded fluorescent thermosensors visualize subcellular thermoregulation in living cells. *Nat Methods* 10:1232–1240
  14. Shintani Y, Kioka H, Takashima S, Suzuki K (2014) Toll-like receptor 9 protects cardiomyocytes from stress by modulating mitochondrial ATP synthesis through the inhibition of SERCA2. *EMBO Rep* 15:438–445
  15. Kioka H, Kato H, Fujikawa M, Tsukamoto O, Suzuki T, Imamura H, Nakano A, Higo S, Yamazaki S, Matsuzaki T, Takafuji K, Asanuma H, Asakura M, Minamino T, Shintani Y, Yoshida M, Noji H, Kitakaze M, Komuro I, Asano Y, Takashima S (2014) Evaluation of intramitochondrial ATP levels identifies G0/G1 switch gene 2 as a positive regulator of oxidative phosphorylation. *Proc Natl Acad Sci U S A* 111:273–278
  16. Tanaka T, Nagashima K, Inagaki N, Kioka H, Takashima S, Fukuoka H, Noji H, Kakizuka A, Imamura H (2014) Glucose-stimulated single pancreatic islets sustain increased cytosolic ATP levels during initial  $Ca^{2+}$  influx and subsequent  $Ca^{2+}$  oscillations. *J Biol Chem* 289:2205–2216

## A Microplate-Based Bioluminescence Assay of Mitochondrial Calcium Uptake

María Teresa Alonso, Paloma Navas-Navarro, and Javier García-Sancho

### Abstract

Mitochondrial  $\text{Ca}^{2+}$  homeostasis is crucial for regulating vital functions such as respiration or apoptosis. Targeted aequorins are excellent probes to measure subcellular  $\text{Ca}^{2+}$ .  $\text{Ca}^{2+}$  concentration in mitochondria ( $[\text{Ca}^{2+}]_{\text{M}}$ ) is low at rest (about  $10^{-7}$  M) and can increase to the micromolar or even approach the millimolar range, upon cell activation. Here we describe a new quantitative luminescent protocol to directly measure mitochondrial  $\text{Ca}^{2+}$  uptake, optimized for high throughput. The sensitivity of the method allows detection of changes in either the capacity or the affinity of mitochondrial  $\text{Ca}^{2+}$  transport.

**Key words** Aequorin, Screening, Calcium uniporter, Plate-reader

---

### 1 Introduction

Dynamic changes in mitochondrial  $\text{Ca}^{2+}$  levels are essential for regulating critical cell functions such as respiration or apoptosis [1].  $\text{Ca}^{2+}$  accumulates into the mitochondrial matrix through the mitochondrial  $\text{Ca}^{2+}$  uniporter (MCU), a calcium channel located at the inner mitochondrial membrane [2, 3]. This low-affinity/high capacity transporter is driven by the mitochondrial membrane potential and is inhibited by ruthenium red. MCU activity is counteracted by mitochondrial  $\text{Ca}^{2+}$  exit through  $\text{Na}^+/\text{Ca}^{2+}$  and  $\text{H}^+/\text{Ca}^{2+}$  exchangers [4, 5], both sensitive to CGP-37157.  $[\text{Ca}^{2+}]_{\text{M}}$  is low at rest (about  $10^{-7}$  M) and can increase up to micromolar, or even millimolar levels [6], following the rise in cytosolic  $\text{Ca}^{2+}$  concentration upon cell activation.

Quantification of mitochondrial  $\text{Ca}^{2+}$  levels depends on the selective localization of the  $\text{Ca}^{2+}$  probe. In contrast to fluorescent synthetic dyes, genetically encoded  $\text{Ca}^{2+}$  indicators can be targeted to specific subcellular locations, including the mitochondrial matrix [7]. Aequorin is a calcium-sensitive photoprotein isolated from the jellyfish *Aequorea victoria*, which has been used as a calcium indicator for decades [8]. The apoprotein is reconstituted to the active

protein in the presence of molecular oxygen and coelenterazine. Binding of  $\text{Ca}^{2+}$  ions to the three highly conserved EF-hand motifs of aequorin induces a conformational change that leads to the oxidation of the cofactor coelenterazine and the emission of blue light.

Although several fluorescent assays to monitor  $\text{Ca}^{2+}$  dynamics have already been developed for high-throughput screening, the use of aequorin bioluminescence offers several advantages: (1) Unlike fluorescent probes, aequorin does not require excitation by light, thus avoiding cytotoxic effects caused by radiation. (2) Fluorescent compounds that could potentially interfere in a fluorescence-based assay, can be used in a luminescence screening. (3) Aequorin displays a high signal-to-noise ratio, typically in the range of 100–1000, in comparison with 5–10 for fluorescent sensors. This is due to the combination of a very low background—mammalian cells do not contain bioluminescent proteins—and a high dynamic range. (4) The affinity of aequorin for  $\text{Ca}^{2+}$  can be engineered to conform to the expected concentration by combining aequorin mutants of reduced affinities with different synthetic coelenterazines. These combinations permit to cover a  $\text{Ca}^{2+}$  concentration range from  $10^{-8}$  to  $5 \times 10^{-3}$  M. (5) Aequorin can be specifically targeted to a given subcellular location by fusing its gene to a minimal targeting sequence. In this protocol, GFP–aequorin is targeted to the mitochondrial matrix by fusing it to the signal peptide of the *cytochrome c oxidase*.

Here we describe a luminescent-based protocol developed for high-throughput screening of mitochondrial  $\text{Ca}^{2+}$  uptake. The novel assay offers a number of advantages: First, it is based on mitochondrial-targeted apo-aequorin reconstituted with coelenterazine *n*, a combination that allows measuring  $\text{Ca}^{2+}$  levels in the range expected in the mitochondrial matrix (1–50  $\mu\text{M}$ ) during moderate increases of  $[\text{Ca}^{2+}]_C$ . Second, selective permeabilization of the plasma membrane allows direct experimental access to the mitochondrial membrane and avoids potential false positive hits caused by chemical compounds whose targets are upstream MCU. Finally, the method provides quantitative measurements, allowing the luminescence signal to be calibrated in  $[\text{Ca}^{2+}]_M$ .

---

## 2 Materials

### 2.1 Cell Culture

1. HeLa cells stably expressing mitochondrially targeted GFP–aequorin (mitGA) [9]. The original GFP–aequorin fusion gene was obtained from Dr. Brûlet [10] and modified by PCR to fuse it in frame to the mitochondrial targeting sequence consisting of the first 31 residues of the subunit VIII of the human cytochrome c oxidase (*see Note 1*).

2. Culture media and additives: Dulbecco's Modified Eagle's Medium; HyClone fetal bovine serum; penicillin–streptomycin.
3. Trypsin–EDTA 0.05%.
4. Geneticin. Prepare 100 mg/mL stock in H<sub>2</sub>O. Store at –20 °C.

## 2.2 Equipment

1. 96-well microplates. White-walled, white-bottom plates are recommended for luminescence measurements; however, clear-bottom plates are useful for visual inspection of adherent cells under the microscope.
2. Eight-channel pipette for dispensing/washing cells in 96-well plates.
3. Genios Pro (TECAN) Plate reader. Other bioluminescence plate readers with at least two injectors would also be appropriate.

## 2.3 Bioluminescence Assay

### 2.3.1 Stock Solutions

1. KCl. Prepare 1.5 M solution.
2. Prepare 1 M KH<sub>2</sub>PO<sub>4</sub> and 1 M K<sub>2</sub>HPO<sub>4</sub>. Blend 71.7 mL of K<sub>2</sub>HPO<sub>4</sub> and 28.3 mL KH<sub>2</sub>PO<sub>4</sub> in 1 L H<sub>2</sub>O to make a solution of 0.1 M (pH 7.2 with KOH).
3. Volumetric 1 M MgCl<sub>2</sub>.
4. Na-HEPES. Prepare 1 M solution in H<sub>2</sub>O adjusted with NaOH (pH 7.2).
5. Glucose. Prepare 1 M stock in H<sub>2</sub>O. Store at –20 °C.
6. EGTA (ethylene glycol-bis(2-aminoethylether)-*N,N,N',N'*-tetraacetic acid) 0.5 M, pH 8.0.
7. Thapsigargin. Prepare 1 mM stock in anhydrous DMSO; store at –20 °C. CAUTION: tumor promoter; wear gloves.
8. Sodium succinate. Prepare 1 M solution.
9. Sodium pyruvate. Prepare 1 M solution.
10. Digitonin. Prepare 100 mM stock in anhydrous DMSO; store at –20 °C.
11. Coelenterazine *n*. Prepare 200 μM stock in methanol and aliquot in 30 μL on ice. Gas briefly with nitrogen before closing the tubes. Wrap with aluminum foil and store at –80 °C for up to 6 months.
12. Phosphate-buffered saline (PBS), without calcium or magnesium, pH 7.2.
13. Volumetric 1 M CaCl<sub>2</sub>.
14. Mg-ATP (0.1 M). Dissolve 5.51 g adenosine 5'-triphosphate disodium salt hydrate in 10 mL MgCl<sub>2</sub> of volumetric 1 M stock. Adjust pH to 7.0 with NaOH. Add H<sub>2</sub>O to 0.1 L final volume.

15. Mg-EDTA (0.25 M). Dissolve 93.1 g EDTA-Na<sub>2</sub>·2H<sub>2</sub>O and 50.8 g MgCl<sub>2</sub>·6H<sub>2</sub>O in ~800 mL H<sub>2</sub>O. EDTA will not dissolve till pH is adjusted to 8.0 by the addition of NaOH (~110 mL 5 M NaOH). Make up to 1 L final volume with H<sub>2</sub>O (*see Note 2*).
16. Ru360. Prepare 1 mM stock in H<sub>2</sub>O.

### 2.3.2 Working Solutions

The given volumes are appropriate for one full 96-well plate. Adjust according to the number of individual wells or multiwell plates.

1. Complete DMEM. DMEM containing 10% (vol/vol) FBS, 0.1 mg/mL streptomycin, 100 U/mL penicillin, and 0.2 mg/mL geneticin.
2. 2× Coelenterazine *n* medium. Prepare a 2 μM coelenterazine *n* working solution (of 200 μM stock) in *Complete DMEM*. Final well concentration: 1 μM.
3. 2× IM (Intracellular Medium). Prepare 20 mL solution in H<sub>2</sub>O by mixing 3.73 mL of 1.5 M KCl, 0.4 mL of 0.1 M KH<sub>2</sub>PO<sub>4</sub>, 0.04 mL of 1 M MgCl<sub>2</sub>, and 0.8 mL of 1 M Na-HEPES, pH 7.2.
4. 1× Thapsigargin solution. To make a final volume of 10 mL, take 5 mL of 2× IM and add 0.1 mL of 1 M glucose, 2 μL of 0.5 M EGTA and 2 μL of 1 mM thapsigargin stock. Make up to final volume with H<sub>2</sub>O. Final concentrations: 140 mM KCl, 1 mM KH<sub>2</sub>PO<sub>4</sub>, 1 mM MgCl<sub>2</sub>, 10 mM glucose, 0.1 mM EGTA, 0.2 μM thapsigargin, and 20 mM Na-HEPES, pH 7.2.
5. 4× Digitonin solution. To prepare 5 mL, take 2.5 mL of 2× IM and add 0.04 mL of 1 M Na-succinate, 0.02 mL of 1 M Na-pyruvate, 0.2 mL of 0.1 M Mg-ATP and 0.012 mL of 100 mM digitonin. Make up to final volume with H<sub>2</sub>O. Final concentrations: 8 mM Na-succinate, 4 mM Na-pyruvate, 4 mM Mg-ATP and 240 μM digitonin. Final well digitonin concentration: 60 μM.
6. 0.1 M CaCl<sub>2</sub> solution diluted of volumetric 1 M CaCl<sub>2</sub> stock in H<sub>2</sub>O.
7. 5× Calcium solutions. To make 10 mL, take 5 mL of 2× IM and add 0.02 mL of 1 M Na-succinate, 0.01 mL of 1 M Na-pyruvate, and 0.1 mL of 0.1 M Mg-ATP. Add 0.2 mL of 0.25 M Mg-EDTA stock and the corresponding volume of 0.1 M CaCl<sub>2</sub> solution given in the Table 1 to prepare each of the Calcium solutions (*see Note 3*).
8. 5× Ru360 Calcium solution. Prepare Ru360 50 μM of 1 mM stock in the 5× *Calcium solution* with the chosen final CaCl<sub>2</sub> concentration. In Fig. 1 Ru360 is added to the maximal [Ca<sup>2+</sup>] (6.4 × 10<sup>-6</sup> M). Final well concentration of Ru360: 10 μM (*see Note 4*).

**Table 1**  
**Calcium solutions used to trigger mitochondrial  $\text{Ca}^{2+}$  uptake**

Added volume of 0.1 M $\text{CaCl}_2$ ( $10^{-6}$ L)	[ $\text{CaCl}_2$ ] in 5× Calcium solution ( $10^{-4}$ M)	[ $\text{CaCl}_2$ ] <sub>total</sub> in well ( $10^{-4}$ M)	[ $\text{Ca}^{2+}$ ] <sub>free</sub> in well ( $10^{-6}$ M)
86.5	8.6	1.7	2
108.5	10.8	2.1	3
128.5	12.8	2.5	4
165	16.5	3.3	6.4

Each *Calcium solution* with the indicated [ $\text{CaCl}_2$ ] is prepared by diluting the indicated volume of 0.1 M  $\text{CaCl}_2$  solution (left-most column) to 10 mL final volume containing 5 mM EDTA as described in Subheading 2.3.2, item 7. The second column indicates the concentrations of  $\text{CaCl}_2$  in the solutions loaded in reservoir 1. The third and fourth columns indicate, respectively, the total and free final  $\text{Ca}^{2+}$  concentrations in the well, after a 1:5 dilution. Estimations of [ $\text{Ca}^{2+}$ ] were made using the *MaxChelator* software [13] with the following parameters: 7.2 pH; 25 °C; 0.15 M ionic strength;  $2 \times 10^{-3}$  M total magnesium; and,  $60 \times 10^{-6}$  M EGTA

- 6× Calibration solution: To make 10 mL add 0.93 mL of 1.5 M KCl and 0.6 mL of 1 M  $\text{CaCl}_2$ . The final well concentrations are: 140 mM KCl and 10 mM  $\text{CaCl}_2$ .

### 3 Methods

#### 3.1 Preparation of Cells for $\text{Ca}^{2+}$ Measurements

- HeLa cells stably expressing mitGA are routinely cultured in 75 cm<sup>2</sup> flasks in *Complete DMEM* in 5%  $\text{CO}_2$  at 37 °C (see **Note 5**) and sub-cultured at a splitting ratio of 1:10 when they are 70–80% confluent.
- The day of the assay, trypsinize and resuspend cells in approximately 5 mL *Complete DMEM* medium, well dispersed by thorough pipetting.
- Count cells by using a hemocytometer and adjust the density to  $10^5$  cells/mL.
- Seed 100  $\mu\text{L}$  ( $10^4$  cells) in each well of a 96-well microplate using a multichannel pipette. Culture in a 5%  $\text{CO}_2$  incubator overnight (see **Note 6**).

#### 3.2 Bioluminescent Assay

- Carefully remove 75  $\mu\text{L}$  medium from wells with a multichannel pipette.
- Add 25  $\mu\text{L}$  of 2× *Coelenterazine n medium* with a multichannel pipette. Final well volume: 50  $\mu\text{L}$ . Return plate to incubator for 2 h (see **Note 7**).
- Remove medium from wells carefully and wash twice with 100  $\mu\text{L}$  PBS using a multichannel pipette.

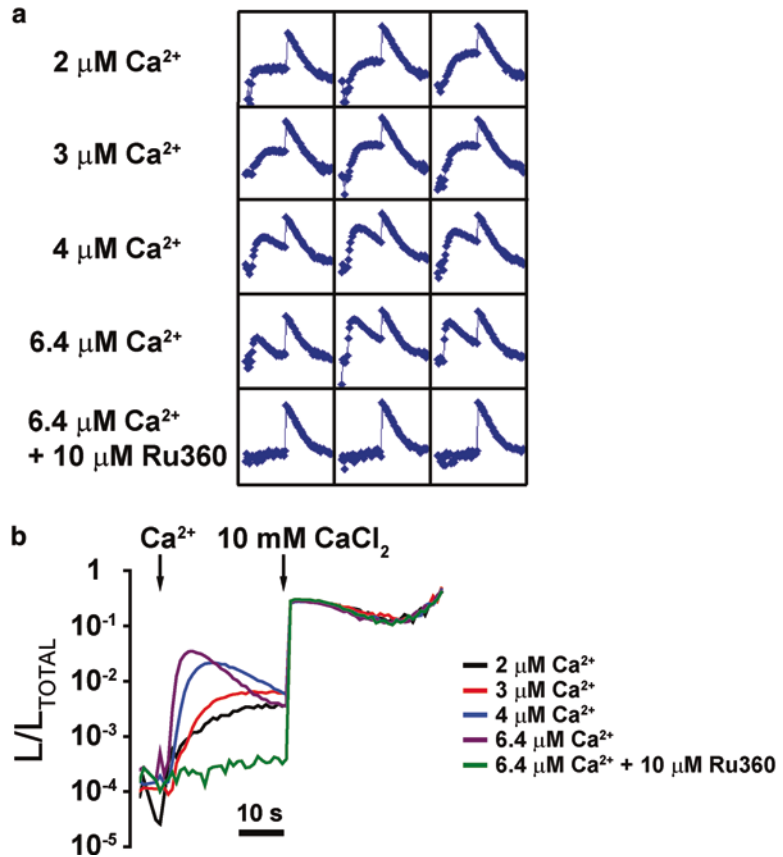


**Fig. 1** (a) Typical luminescence recordings (expressed in cps) of individual wells in a 96-well plate assay of permeabilized HeLa cells expressing mitGA. Calcium solutions with the indicated final  $[\text{Ca}^{2+}]$  were added to each well (in triplicates) to initiate mitochondrial  $\text{Ca}^{2+}$  uptake. After 30 s recording, a second addition of saturating  $\text{Ca}^{2+}$  (10 mM) evoked total luminescence, which was recorded for 40 s. (b) Dose response curve of mitochondrial  $\text{Ca}^{2+}$  uptake (expressed as  $L/L_{\text{TOTAL}}$ ) induced by different  $\text{Ca}^{2+}$  additions corresponding to the data obtained in a. Each trace is the mean of triplicates

4. Replace with 75  $\mu\text{L}$  of  $1\times$  *Thapsigargin solution* with a multi-channel pipette. Incubate at room temperature for 15 min (*see Note 8*).
5. Add 25  $\mu\text{L}$  of  $4\times$  *Digitonin solution* with a multichannel pipette. Final well volume: 100  $\mu\text{L}$ . Incubate at room temperature for 5 min. Proceed immediately to plate reader.
6. Configure the Plate reader. In the luminometer used in our lab, this is as follows: open software and set reader configuration to *Luminescence/well kinetics* mode. Select type of plate. Load one of the  $5\times$  *Calcium solutions*, and  $6\times$  *Calibration solution* in reservoirs 1 and 2, respectively. Prime the pipettor pump and connect it to the sample plate. Select the following

parameters: Integration time: 1000 ms; attenuation: none; minimum interval between wells; time between move and integration: 50 ms. Set addition volume: 25  $\mu\text{L}$  for both injectors; addition rate: 200  $\mu\text{L}/\text{s}$ ; no shaking.

7. Place sample plate into plate reader and start a previously configured protocol to read background for 5 s (*see Note 9*).
8. Add 25  $\mu\text{L}$  of each of the  $5\times$  *Calcium solutions* with injector No. 1. Read for 30 s (Fig. 1).
9. Add 25  $\mu\text{L}$  of  $6\times$  *Calibration solution* with injector No. 2. Read for 40 s (*see Note 10*).

### 3.3 Data Analysis and Quantification

1. Luminescence emission values ( $L$  at each time point ( $t$ )) are automatically stored as counts per second (cps) in a Microsoft Excel file.
2. Subtract background values determined at the beginning of the assay.
3. Calculate Total ( $L$ ) =  $\Sigma L$  values for  $t_0$  to  $t_{\text{final}}$  (including calibration).
4. Calculate Sum ( $L$ ) =  $\Sigma L$  values for  $t_0$  to  $t$ .
5. Calculate  $L_{\text{TOTAL}}$  (Total luminescence remaining at each  $t$ ) as follows:

$$L_{\text{TOTAL}} = \text{Total } (L) - \text{Sum } (L)$$

6. Calculate  $L/L_{\text{TOTAL}}$ .
7. Calibrate into  $[\text{Ca}^{2+}]_{\text{M}}$  interpolating  $L/L_{\text{TOTAL}}$  values into the calibration curve shown in Fig. 2.

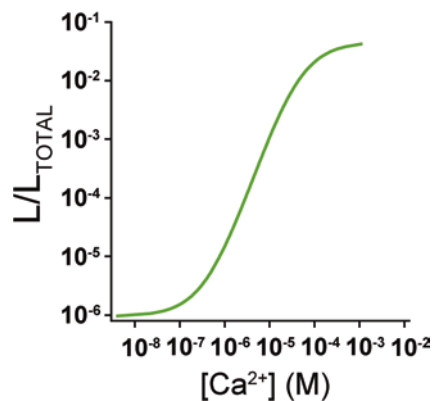


**Fig. 2** Calibration curve of wild-type aequorin reconstituted with coelenterazine *n*. Figure modified from [12]

---

## 4 Notes

1. The use of the fusion protein GFP–aequorin has several advantages over the native aequorin: it facilitates a direct visualization of the expressed GFP protein under the fluorescence microscope; aequorin protein is more stable; and, it gives a higher light yield.
2. The  $0.25\text{ M Mg-EDTA}$  stock solution and its derivative working solutions ( $5\times$  *Calcium solutions*) are critical for the described assay. It is essential that these solutions are accurately made in order to obtain the expected  $[\text{Ca}^{2+}]$  given in Table 1.
3. Users should perform a preliminary dose-response curve as shown in Fig. 1 in order to choose the optimal  $[\text{Ca}^{2+}]$  to be used in the final assay. We recommend a  $[\text{Ca}^{2+}]$  that allows measuring initial  $\text{Ca}^{2+}$  uptake rate with enough accuracy and that reaches a stable steady state. We selected the  $3\text{ }\mu\text{M}$   $[\text{Ca}^{2+}]$  solution since larger  $[\text{Ca}^{2+}]$  ( $4$  or  $6\text{ }\mu\text{M}$ ) give higher signals but the steady-state values are not stable, decaying with time.
4. Ru360 is more sensitive than ruthenium red. It is recommended to include it in the assay to confirm that the observed signal is due to MCU activity. The final volume of this solution is adjusted for the number of wells.
5. This protocol can be adapted to other adherent cell types expressing the mitGA.
6. When using a cell line other than HeLa, it is important to adjust the cell number such that all cells are well adhered to the well base; too many cells will lead to spurious luminescence peaks.
7. The combination of native aequorin and coelenterazine  $n$  allows measurements in the  $1\text{--}50\text{ }\mu\text{M}$  range. We chose coelenterazine  $n$  to reduce aequorin consumption and measure  $\text{Ca}^{2+}$  uptake initial rate more accurately.
8. Thapsigargin is used here to irreversibly empty the endoplasmic reticulum (ER) of  $\text{Ca}^{2+}$ ; this will avoid contribution of ER to the luminescence signal.
9. Background values of non-expressing cells are typically below  $50\text{ cps}$ . Total luminescence per well may range between  $2 \times 10^3$  and  $2 \times 10^5$  counts per second (cps) depending on the expression levels of mitochondrial aequorin.
10. Aequorin is consumed along the experiment and consumption rate rather than light intensity is proportional to  $\text{Ca}^{2+}$  [11]. Exposing aequorin to excess  $\text{Ca}^{2+}$  ( $10\text{ mM}$ ) with a second injection is required to discharge the remaining aequorin that was not consumed along the experiment. That allows total luminescence ( $L_{\text{TOTAL}}$ ) and fraction  $L/L_{\text{TOTAL}}$  to be calculated.

## Acknowledgments

The authors are grateful to present and past members of the laboratory. We specially thank Dr. Perocchi for her help with the assay and comments on the manuscript. This work was supported by a grant from the Spanish Ministerio de Economía y Competitividad (BFU2014-534698P) and the Instituto de Salud Carlos III (RD16/0011/0003).

## References

1. Rizzuto R, De Stefani D, Raffaello A, Mammucari C (2012) Mitochondria as sensors and regulators of calcium signalling. *Nat Rev Mol Cell Biol* 13(9):566–578. [http://www.nature.com/nrm/journal/v13/n9/suppinfo/nrm3412\\_S1.html](http://www.nature.com/nrm/journal/v13/n9/suppinfo/nrm3412_S1.html)
2. Baughman JM (2011) Integrative genomics identifies MCU as an essential component of the mitochondrial calcium uniporter. *Nature* 476:341–345
3. De Stefani D, Raffaello A, Teardo E, Szabo I, Rizzuto R (2011) A forty-kilodalton protein of the inner membrane is the mitochondrial calcium uniporter. *Nature* 476:336–340
4. Crompton M, Kunzi M, Carafoli E (1977) The calcium-induced and sodium-induced effluxes of calcium from heart mitochondria. Evidence for a sodium-calcium carrier. *Eur J Biochem* 79:549–558
5. Gunter TE, Pfeiffer DR (1990) Mechanisms by which mitochondria transport calcium. *Am J Physiol* 258:C755–C786
6. Montero M (2000) Chromaffin-cell stimulation triggers fast millimolar mitochondrial Ca<sup>2+</sup> transients that modulate secretion. *Nature Cell Biol* 2:57–61
7. Rizzuto R, Simpson AW, Brini M, Pozzan T (1992) Rapid changes of mitochondrial Ca<sup>2+</sup> revealed by specifically targeted recombinant aequorin. *Nature* 358:325–327
8. Shimomura O, Johnson FH, Saiga Y (1962) Extraction, purification and properties of aequorin, a bioluminescent protein from the luminous hydromedusa, *Aequorea*. *J Cell Comp Physiol* 59:223–239
9. Manjarres IM, Chamero P, Domingo B, Molina F, Llopis J, Alonso MT, Garcia-Sancho J (2008) Red and green aequorins for simultaneous monitoring of Ca<sup>2+</sup> signals from two different organelles. *Pflugers Arch* 455(5):961–970. doi:10.1007/s00424-007-0349-5
10. Baubet V, Le Mouellic H, Campbell AK, Lucas-Meunier E, Fossier P, Brulet P (2000) Chimeric green fluorescent protein-aequorin as bioluminescent Ca<sup>2+</sup> reporters at the single-cell level. *Proc Natl Acad Sci U S A* 97(13):7260–7265. doi: 97/13/7260 [pii]
11. Allen DG, Blinks JR, Prendergast FG (1977) Aequorin luminescence: relation of light emission to calcium concentration—a calcium-independent component. *Science* 195(4282):996–998
12. Alonso MT, Villalobos C, Chamero P, Alvarez J, Garcia-Sancho J (2006) Calcium microdomains in mitochondria and nucleus. *Cell Calcium* 40(5-6):513–525. doi:10.1016/j.ceca.2006.08.013
13. Patton C, Thompson S, Epel D (2004) Some precautions in using chelators to buffer metals in biological solutions. *Cell Calcium* 35(5):427–431. doi:10.1016/j.ceca.2003.10.006

## New Imaging Tools to Analyze Mitochondrial Morphology in *Caenorhabditis elegans*

Saroj G. Regmi and Stéphane G. Rolland

### Abstract

Mitochondria are highly dynamic organelles that constantly fuse and divide. This process is essential as several neurodegenerative diseases have been associated with defects in mitochondrial fusion or fission. Several tools have been developed over the years to visualize mitochondria in organisms such as *Caenorhabditis elegans*. Combining these tools with the powerful genetics of *C. elegans* has led to the discovery of new regulators of mitochondrial morphology. In this chapter, we present additional tools to further characterize mitochondrial morphology as well as regulators of mitochondrial morphology. Specifically, we introduce a photoactivatable mitoGFP (PAmitoGFP) that allows to investigate the connectivity of complex mitochondrial networks. In addition, we describe an immunostaining protocol that enables localization studies of these newly identified regulators of mitochondrial morphology.

**Key words** Mitochondrial dynamics, Mitochondrial morphology, *Caenorhabditis elegans*, PAmitoGFP, Immunostaining

---

## 1 Introduction

Mitochondria form a highly dynamic network, which is sculpted by fusion and fission events [1]. A proper balance of mitochondrial fusion and fission is critical as mutations in genes controlling these two processes have been associated with several neurodegenerative diseases [1]. Mitochondrial fusion and fission are regulated by a conserved family of dynamin-related GTPases. In the nematode *Caenorhabditis elegans*, FZO-1, the homologue of mammalian Mitofusins and yeast Fzo1, and EAT-3, the homologue of mammalian Opal and yeast Mgm1, are required for the fusion of the outer and inner mitochondrial membranes, respectively [2, 3]. Mitochondrial fission is controlled by DRP-1, the homologue of mammalian Drp1 and yeast Dnm1 [4]. Mitochondrial morphology in *C. elegans*, like in other multicellular animals, has been shown to vary greatly between different cell types, ranging for example from individual small organelles

trafficking in axonal processes to extremely complex mitochondrial networks in embryonic cells [5, 6]. This cell-type specificity in mitochondrial morphology has been proposed as an adaptation to particular cellular energy demands or signaling requirements, however the function and the molecular basis underlying this specificity remain to be elucidated [7].

Several “classical” tools such as mitochondrial membrane potential sensitive dyes (e.g., TMRE) or mitochondrial matrix-targeted GFP (mitoGFP) can be used to visualize mitochondria in *C. elegans*. For more details on these “classical” tools, see [6]. Using these tools along with the powerful genetics of *C. elegans*, new regulators of mitochondrial morphology have recently been identified (For an updated list of these regulators see [6]).

In this chapter, we describe new tools to further characterize these regulators such as the photoactivatable matrix-targeted GFP (PAmitoGFP) that can be employed to investigate mitochondrial network connectivity. Furthermore, we present an immunostaining approach that allows localization studies of newly identified regulators of mitochondrial morphology in *C. elegans* embryos.

---

## 2 Materials

### 2.1 Photoactivatable mitoGFP in *C. elegans* Muscle Cells

1. Worm pick.
2. 35 mm RNAi plates (“classical” NGM supplemented with 1 mM IPTG and 25 µg/mL carbenicillin [8]). To prepare RNAi plates, mix 20 g agar, 3 g NaCl, and 2.5 g Bacto peptone into 1 L H<sub>2</sub>O and autoclave. When the medium has cooled down to 55 °C, add 1 mL 1 M CaCl<sub>2</sub>, 1 mL 1 M MgSO<sub>4</sub>, 1 mL 5 mg/mL cholesterol, 0.23 g IPTG (Roth (CN08.2)), and 1 mL 25 mg/mL carbenicillin. Mix well and pour into 35 mm petri dishes. Store the plates at 4 °C and protect from light (*see Note 1*).
3. LB liquid medium supplemented with carbenicillin (25 µg/mL) and tetracycline (10 µg/mL).
4. LB liquid medium supplemented with carbenicillin (25 µg/mL).
5. RNAi feeding clones against the gene of interest (for example the LRPPRC-homolog *mma-1*) as well as negative (for example *mock*) and positive (for example *fzo-1* or *drp-1*) control RNAi feeding clones. These *E. coli* clones are commercially available from Source Bioscience (<http://www.lifesciences.sourcebioscience.com/>) (*see Note 2*).
6. *C. elegans* MD2922 strain (*bcEx856* [80 ng/mL pRF4 + 2 ng/µL *Pmyo-3PAmitoGFP* + 0.2 ng/µL *Pmyo-3mitodsRed*]) [9] (*see Note 3*).

7. Microscope glass slides, two “spacer” microscope slides covered with laboratory tape and cover glasses.
8. 2 % agarose prepared in H<sub>2</sub>O.
9. M9 liquid media: 32 mM Na<sub>2</sub>HPO<sub>4</sub>, 22 mM KH<sub>2</sub>PO<sub>4</sub>, 8.5 mM NaCl, 19 mM NH<sub>4</sub>Cl supplemented with 1 mM Levamisole (*see Note 4*) [8].
10. Confocal microscope with DIC optics and at least 60× objective (*see Note 5*), a 405 nm laser for the photoactivation of PAmitoGFP, a 488 nm laser for excitation and a 525/50 filter for emission of photoactivated GFP, a 561 nm laser for excitation and a 595/50 filter for emission of mitodsRed.

## 2.2 Immunostaining in *C. elegans* Embryos

1. Worm pick.
2. 60 mm NGM plates seeded with *E. coli* OP50 strain [8]. To prepare NGM plates, mix 20 g agar, 3 g NaCl, and 2.5 g Bacto peptone into 1 L H<sub>2</sub>O and autoclave. When the medium has cooled down to 55 °C, add 1 mL 1 M CaCl<sub>2</sub>, 1 mL 1 M MgSO<sub>4</sub>, and 1 mL 5 mg/mL cholesterol. Mix well and pour into 60 mm petri dishes. Inoculate a single colony of the OP50 *E. coli* strain in B-Broth (LB without yeast extract) and grow overnight at 37 °C. Inoculate 100 μL of the OP50 *E. coli* culture onto the 60 mm NGM plates. The plates are grown one more day at 20 °C. The plates can be used in the next 2–3 weeks. For longer storage, they can be kept at 4 °C.
3. *C. elegans* wild-type (N2) strain.
4. Microscope glass slides with frosted stripe on one side, regular cover glasses and high precision cover glass 18 × 18 (Carl Roth LH24.1) (*see Note 6*).
5. 0.25 mg/mL poly-L-lysine (Sigma P1524): prepare freshly by diluting 1 mg/mL stock solution in water. Stock solution is stored at –20 °C (*see Note 7*).
6. Rubber-wiper (for example, from Carl Roth 9552.1).
7. Glass watch (for example, from Carl Roth TK76.1).
8. 250 mL immunostaining jar.
9. Fixation solution: methanol–acetone (1:1 (v/v)) (*see Note 8*).
10. Standard PBS buffer.
11. PBS Triton: PBS with 1 % Triton X-100 (v/v).
12. PBST: PBS with 0.1 % Tween 20 (v/v).
13. PBSTB: PBS with 0.1 % Tween 20 (v/v) and 2 % BSA (w/v) (*see Note 10*).
14. PBST DAPI: PBST with 2 μg/mL DAPI (w/v). Prepare a fresh working solution from a stock solution of 1 mg/mL DAPI (dissolved in ethanol). Stock solution should be stored at –20 °C.

15. PBSFA: PBS with 3.7 % formaldehyde (v/v). Make a solution by diluting a 37 % Formaldehyde solution in PBS.
16. Vectashield (Vector Labs).
17. Transparent nail polish.
18. Primary and secondary antibodies (*see* Tables 1 and 2).

---

## 3 Methods

### 3.1 Photoactivatable mitoGFP in *C. elegans* Muscle Cells

Transgenic *C. elegans* animals expressing a mitochondrial matrix-targeted GFP (or “mitoGFP”) in a specific tissue can be used to test the effect of the inactivation or over-expression of a gene of interest on mitochondrial morphology [6]. The quantification of mitochondrial morphology is, however, hindered due to the three-dimensional structure of mitochondrial networks. For example, inactivation of the *LRPPRC*-like gene *mma-1* in *C. elegans* has been shown to cause the formation of a complex hyperfused mitochondrial network [9]. However, to determine whether *mma-1(RNAi)* causes a complete fusion of the outer and the inner mitochondrial membranes and therefore generate a mitochondrial network with a continuous mitochondrial matrix, “classical” tools such as mitoGFP are not sufficient. The recent development of a *C. elegans* photoactivatable mitoGFP (PAmitoGFP) now allows to address this question (*see* Note 11). Using *mma-1(RNAi)*-induced mitochondrial hyperfusion [9] as an example, we provide a protocol to use PAmitoGFP expressed in muscle cells to assess the connectivity of the mitochondrial network.

#### Day 1:

1. Inoculate the *mma-1* RNAi feeding clone from a  $-80\text{ }^{\circ}\text{C}$  frozen glycerol stock into 2 mL of LB supplemented with carbenicillin (25  $\mu\text{g}/\text{mL}$ ) and tetracycline (10  $\mu\text{g}/\text{mL}$ ). In parallel, inoculate the negative control (*mock(RNAi)*) and the positive controls (*fzo-1(RNAi)* and *drp-1(RNAi)*).
2. Incubate overnight with shaking (200 rpm) at 37  $^{\circ}\text{C}$ .

#### Day 2:

3. Inoculate 20  $\mu\text{L}$  of the overnight culture in 2 mL of LB supplemented with carbenicillin (25  $\mu\text{g}/\text{mL}$ ).
4. Incubate for 6 h with shaking (200 rpm) at 37  $^{\circ}\text{C}$ .
5. Use 50  $\mu\text{L}$  of the suspension to inoculate RNAi plates supplemented with IPTG (1 mM) and carbenicillin (25  $\mu\text{g}/\text{mL}$ ).
6. Incubate the plates at room temperature in the dark overnight (*see* Note 1).

#### Day 3:

It is recommended to perform the following experiments in duplicate, as variability in RNAi efficiency is often observed.

**Table 1**  
**List of the different antibodies against *C. elegans* mitochondrial proteins**

Localization	<i>C. elegans</i> proteins	Homolog in humans	Immunostaining	Methanol-acetone fixation	Dilution(v/v)	Host	Commercially available	Reference
Outer mitochondrial membrane	CEID-9	BCL2	Yes	Yes	1:150	Rabbit	No	[13, 23]
	MOMA-1	my025, CXORF33 or Apo-O-like	Yes	Not tested	*	Rabbit	No	[24]
Intermembrane space	CYC-2.1 and CYC-2.2	Cytochrome-c	Yes	Yes	1:200	Mouse	Yes (Abcam ab110325)	[13, 18, 24]
Inner mitochondrial membrane	NUO-2	NDUFS3	Not tested	Not tested	Not tested	Mouse	Yes (Abcam ab14711)	[9, 25]
	MEV-1	SDHC	Not tested	Not tested	Not tested	Mouse	No	[26]
	COX I	COX I	Yes	Yes	1:200	Mouse	Yes (Abcam ab14705)	[13]
	COX IV	COX IV	Yes	Not tested	1:30	Mouse	Yes (ThermoFisher 459600)	[19]
	H28O16.1	ATP synthase subunit $\alpha$	Yes	Yes	1:200	Mouse	Yes (Abcam ab14748)	[13]
	ATP-2	ATP synthase subunit $\beta$	Yes	Yes	1:200	Mouse	Yes (Abcam ab14730)	[13]
	IMMT-1	Mitofilin	Yes	Yes	1:50	Rat	No	[27]
	IMMT-2	Mitofilin	Yes	Yes	1:30	Rat	No	[27]
Matrix	HSP-60	HSP60	Yes	Yes	1:10	Mouse	**	[28]
	HSP-6	mtHSP70	Yes	Yes	1:200	Rabbit	No	[29]
	PDHB-1	PDHB	Yes	Not tested	1:200	Mouse	Yes (Abcam ab110334)	[13]
	SIR-2.2	SIRT4	Not tested	Not tested	Not tested	Rabbit	No	[30]

The *C. elegans* mitochondrial proteins, for which antibodies are available, are listed along with their human homologs. Recommended dilution of the antibodies, the host in which the antibodies were generated and the references of the publication are indicated. Antibodies that have been used for western-blot experiments but have not yet been tested for immunostaining (Not tested) are also shown. Finally, antibodies that we have tested using the methanol-acetone fixation protocol are indicated. (\* It was not possible to determine the concentration used by the Authors; \*\* these antibodies are available from the Developmental Studies Hybridoma Bank (<http://dshb.biology.uiowa.edu/>))

**Table 2**  
**List of the secondary antibodies that can be used for the immunostaining experiments**

Antibodies	Dilution	Purchasing reference
Alexa 488 anti-mouse	1:500	Invitrogen A11001
Alexa 488 anti-rabbit	1:500	Invitrogen A11034
Alexa 488 anti-rat	1:500	Invitrogen A11006
Alexa 594 anti-mouse	1:500	Invitrogen A21203
Alexa 594 anti-rabbit	1:500	Invitrogen A21207

The secondary antibodies and their dilutions are indicated along with the purchasing reference

7. Transfer two transgenic (i.e., roller) L4 larvae of the strain MD2922 (*Pmyo-3PAmitoGFP* + *Pmyo-3mitodsRed*) onto the RNAi plate (*see* **Notes 3** and **12**).
8. Incubate RNAi plates at 20 °C in the dark for 4 days (*see* **Note 1**).  
**Day 7:**
9. Prepare a microscope glass slide with a fresh 2 % agarose pad (as previously described [6]). Specifically, place a microscope slide between two “spacer” microscope slides covered with laboratory tape (The laboratory tape defines the thickness of the pad.). Put a drop of melted 2 % agarose onto the microscope slide and immediately cover with another microscope slide perpendicularly.
10. Using a worm pick, transfer 10 transgenic (i.e., roller) L4 larvae animals in 5 µL of M9 supplemented with 1 mM Levamisole on the agarose pad (*see* **Notes 3** and **4**).
11. Locate transgenic animals using low magnification (10×).
12. Using higher magnification (60×), identify body wall muscle cells expressing the transgene. To that end, the mitodsRed signal can be used as it is only visible in the transgene-expressing body wall muscle cells (*see* **Note 3**).
13. Select the area of the mitochondrial network, where to assess the connectivity (*see* **Note 13**).
14. Photoactivate the PAmitoGFP. The conditions of photoactivation will vary from one microscope to another (*see* **Note 14**). As an indication, using an A1 confocal microscope (Nikon) equipped with a Plan Apo VC 60× Oil DIC N2 (NA 1.4), activation of the PAmitoGFP was performed with a 405 nm laser with an ROI of 1 µm in diameter (2 % power for 2 s).
15. Image the PAmitoGFP signal every 0.25 s for 30 s (*see* Fig. 1a and *see* **Note 15**).

16. The photoactivated PAmitoGFP area can then be measured over time using an image analysis software. For example, using the software NIS element (Nikon), a threshold at the ROI of activation right after activation ( $t = 2s$ ) using a circle of 3 pixels radius (The threshold range is then adjusted automatically by the software, so the pixels in this circle fit inside this threshold). Then, using morphometric analysis tool, the photoactivated area can then be measured over time. (*see* Fig. 1b and *see* **Note 15**).

The extent of the dispersion of the PAmitoGFP can be used as a proxy for the connectivity of the mitochondrial network. While this approach can be used to quantify mitochondrial morphology, it is time consuming. Therefore, we would suggest to combine this approach with the analysis of mitochondrial morphology using a “classical” mitoGFP expressed in muscle [6]. With such a reporter and a regular epifluorescence microscope, it is possible to determine the frequency of a particular mitochondrial morphology phenotype (for example, how many animals treated with a particular RNAi show a mitochondrial hyperfusion phenotype). In a second step, the PAmitoGFP can be used to determine the connectivity of these mitochondrial networks.

### 3.2 Immunostaining in *C. elegans* Embryos

With the development of super-resolution microscopy, such as 3D-SIM, immunocytochemistry has reemerged as a tool for the visualization of sub-cellular compartments [10]. This approach is well suited to determine whether a particular protein of interest localizes to mitochondria and/or forms sub-complexes with other known mitochondrial proteins. In this section, we present a method that we have adapted from previous described protocols [11–13]. This method is particularly useful as it is compatible with regular epifluorescence microscopy, confocal microscopy as well as super-resolution 3D-SIM microscopy. One of the bottlenecks of this technique is the availability of specific antibodies. A list of the currently available antibodies against *C. elegans* mitochondrial proteins is provided in Table 1 (*see* **Note 16**). While the generation of antibodies, for example using peptides as antigens, has improved in recent years, a GFP-tagged fusion of the protein of interest can be used as an alternative (for additional information on how to perform the immunostaining using a GFP-tagged fusion, *see* **Note 17**).

#### Day 1:

1. Pick L4 larvae of the wild-type strain (N2) onto a new 60 mm NGM plate seeded with *E. coli* OP50 strain (*see* **Note 18**).
2. Incubate the plate at 20 °C overnight.

#### Day 2:

3. Ensure that the microscope slide is cleaned properly by using either 100 % ethanol or 100 % acetone and a Kimwipes tissue (*see* **Note 19**).

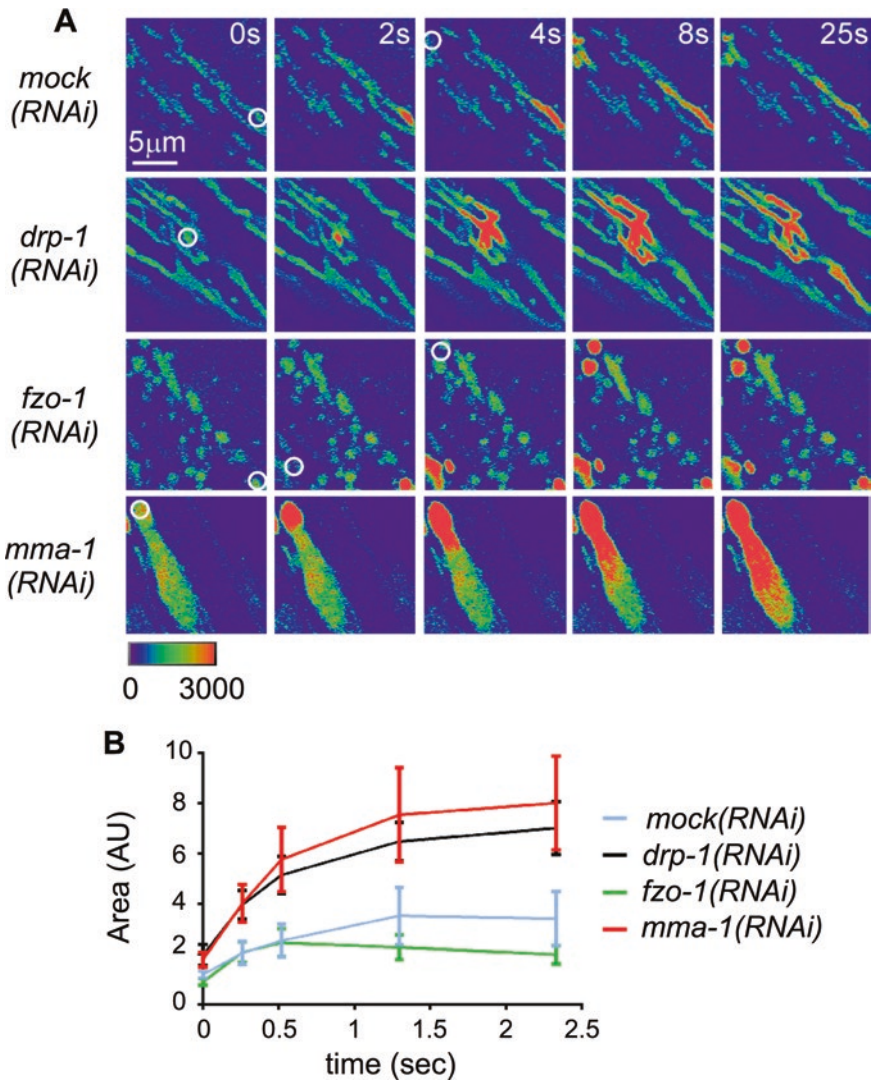


**Fig. 1** Photoactivatable mitoGFP to determine the connectivity of the mitochondrial network in *C. elegans* muscle cells. (a) *C. elegans* animals carrying the transgene *Pmyo-3:PAmiToGfp* + *Pmyo-3:mitoDsRed* treated with *mock(RNAi)*, *drp-1(RNAi)*, *fzo-1(RNAi)* or *mma-1(RNAi)* were used for a photoactivation experiment as described in the methods. PAmiToGFP was activated in the body wall muscle of an L4 larva by a 405 nm laser (white circle) and GFP signal was monitored over time. PAmiToGFP signals are shown in pseudocolor, where non-photoactivated PAmiToGFP is depicted in purple and photoactivated PAmiToGFP is depicted in red. Intensity scale is indicated. (b) A quantification of the photoactivated area over time after activation is indicated ( $n = 5-10$  ROI in 2-3 animals; SD is indicated) (adapted from [9])

4. Label the cleaned microscope slide on the frosted stripe with pencil, as any other writing will be erased by the subsequent use of solvents.
5. Dilute the stock solution of poly-L-lysine to 0.25 mg/mL (100  $\mu$ L of stock solution with 300  $\mu$ L of H<sub>2</sub>O). Transfer the dilution to an empty 60 mm plastic dish. Use a rubber-wiper

(like a paint brush) to spread evenly the poly-L-lysine solution onto the microscope slide (*see Note 7*).

6. Place the slide for 30 s on a hot plate set to 80 °C.
7. Let the slide cool down to room temperature before use.
8. Pick 20 adults into a glass watch filled with H<sub>2</sub>O.
9. Bisect animals using a scalpel blade.
10. Transfer ~50 embryos to the poly-L-lysine slide along with an adult hermaphrodite animal (*see Note 20*).
11. Gently place a cover glass onto the embryos, avoiding air bubbles and making sure that one corner of the cover glass is slightly over the edge of the microscope slide (in order to ease the flicking of the cover glass in **step 14**).
12. Remove excess H<sub>2</sub>O using a Whatman paper until the adult hermaphrodite has been crushed by the cover glass (*see Note 20*).
13. Freeze the microscope slide onto a metal block previously cooled down on dry ice or liquid nitrogen. Incubate for at least 30 min with the metal block kept on dry ice or liquid nitrogen (*see Note 21*).
14. Quickly flick the cover glass off and promptly transfer the slide to 200 mL fixation solution in a 250 mL immunostaining jar. Incubate for 10 min at room temperature (*see Notes 8 and 9*).

All the subsequent steps will be performed in a 250 mL immunostaining jar unless stated otherwise.

15. Remove the fixation solution and add 200 mL PBS Triton. Incubate for 10 min at 20 °C. Repeat the incubation 4 times in total, every time using 200 mL fresh PBS Triton. During this step, embryos are permeabilized.
16. Wash the slide 3 times for 10 min with 200 mL PBS at 20 °C.
17. Block with 200 mL PBSTB for 30 min at 20 °C (*see Note 22*).
18. Dilute primary antibody in PBSTB (*see Table 1* for concentration). Minimize the volume of the antibody dilution (for example, 0.5 µL of antibody in 100 µL for 1:200 dilution antibody). Reusing the dilution is not recommended.
19. With a Kimwipes, remove most of the liquid while avoiding the immediate area surrounding the embryos.
20. Add 5 µL of the antibody diluted in PBSTB onto the microscope slide in the immediate area surrounding the embryos.
21. Gently place a cover glass onto the embryos, taking care to avoid air bubbles (*see Note 23*).
22. Incubate overnight (typically 15 h) at 4 °C in a humid chamber (*see Notes 24*).

**Day 3:**

23. Wash 3 times for 10 min with 200 mL of PBST at 20 °C. In the first washing step, the cover glass will detach from the microscope slide.
24. Dilute secondary antibody in PBSTB (*see* Table 2 for concentration). From this point on, protect the slide from the light.
25. With a Kimwipes, remove most of the liquid while avoiding the immediate area surrounding the embryos.
26. Add 5 µL of the antibody diluted in PBSTB on the microscope slide in the immediate area surrounding the embryos.
27. Gently place a cover glass onto the embryos, taking care to avoid air bubbles (*see* Note 23).
28. Incubate the slide for 2 h at 20 °C in a humid chamber (*see* Note 24).
29. Wash 3 times for 10 min with 200 mL PBST at 20 °C. In the first washing step, the cover glass will detach from the microscope slide.
30. Wash for 10 min with 200 mL PBS at 20 °C.
31. Incubate the slide for 10 min in 200 mL of PBSFA at 20 °C.
32. Wash for 10 min with 200 mL of PBS at 20 °C.
33. Wash for 10 min with 200 mL of PBST at 20 °C.
34. With a Kimwipes, remove most of the liquid while avoiding the immediate area surrounding the embryos.
35. Add 10 µL PBST DAPI on the microscope slide in the immediate area surrounding the embryos. During this step, nuclei are stained (*see* Note 25).
36. Gently place a cover glass onto the embryos, taking care to avoid air bubbles (*see* Note 23).
37. Incubate for 15 min at 20 °C in a humid chamber (*see* Note 24).
38. Wash the slide for 10 min with 200 mL PBST at 20 °C. In this washing step, the cover glass will detach from the microscope slide.
39. Wash the slide for 10 min with 200 mL PBS at 20 °C.
40. With a Kimwipes, remove most of the liquid while avoiding the immediate area surrounding the embryos.
41. Add 5 µL of Vectashield (which inhibits photo-bleaching of fluorescent dyes) on the microscope slide in the immediate area surrounding the embryos.
42. Gently place a high precision cover glass onto the embryos, taking care to avoid air bubbles (*see* Note 23).
43. Seal the edges with transparent nail polish.
44. The slide is now ready for analysis. If not analyzed immediately, it can be stored at 4 °C for a week. For long-term storage

(several months), the slides can be kept frozen at  $-20\text{ }^{\circ}\text{C}$  (*see Note 26*).

The microscope slides can be imaged using an epifluorescence microscope and further processed by deconvolution of a Z-stack (as shown in Fig. 2). Alternatively, imaging can be performed using confocal microscopy. The protocol is also fully compatible with further analysis of the samples by high-resolution 3D-SIM microscopy. The images are then analyzed to determine whether the protein of interest localizes to mitochondria and/or forms sub-complexes with other known mitochondrial proteins (*see Note 27*). Although the results from such an experiment usually need to be supported using independent biochemical approaches, such as cell fractionation or co-immunoprecipitation, subcellular localization of a protein determined by immunohistochemistry represents a significant step towards understanding of its function.

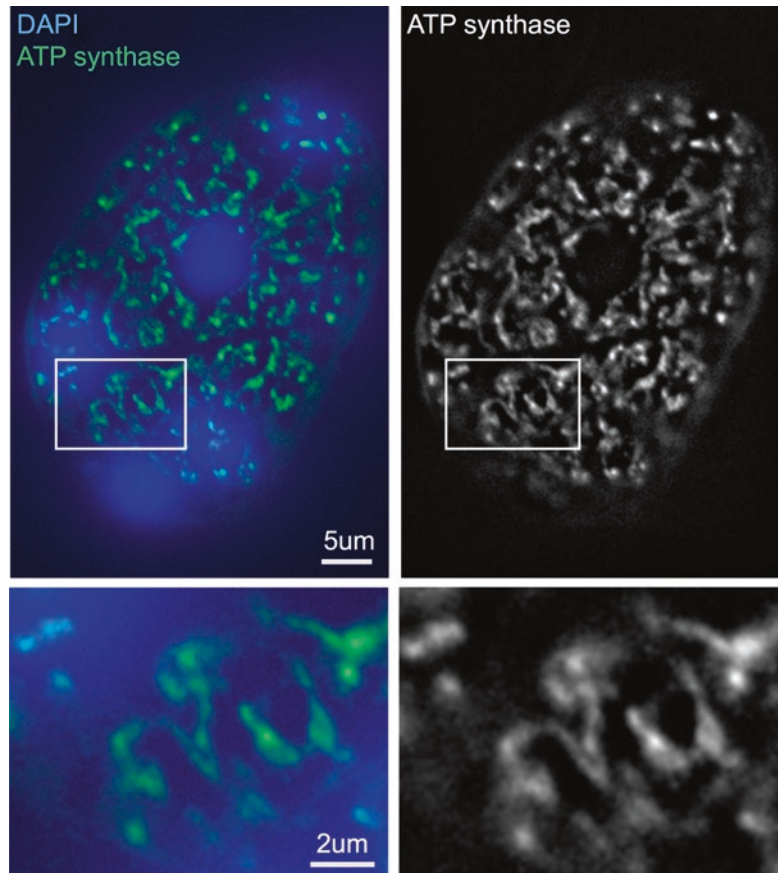


**Fig. 2** Immunostaining of wild-type *C. elegans* embryos with antibodies raised against the  $\alpha$  subunit of the ATP synthase. Eight-cell *C. elegans* wild-type embryo immunostained with mouse monoclonal anti-ATP synthase subunit  $\alpha$  antibodies and counterstained with DAPI using the protocol described in the methods

---

## 4 Notes

1. The RNAi plates contain IPTG, which is light-sensitive, and carbenicillin, which is temperature-sensitive. Therefore, it is crucial to supplement the medium with carbenicillin once the medium has cooled down to 55 °C after autoclaving. Furthermore, once poured, the plates should be kept in the dark at 4 °C. To ensure reproducibility, it is recommended to use fresh plates that are not more than 1 month old. In addition, once the plates have been seeded with the RNAi clones, they should be incubated at room temperature but still be protected from light (for example in a black plastic box). While IPTG can be added to the medium by using a 1 M IPTG stock solution, our experience shows that supplementing the medium with 0.23 g/L of IPTG gives a more reproducible result. This could be due to the higher stability of IPTG in powder compared to IPTG in solution. In addition, in our hands, ≥99 % biochemistry grade IPTG (for example, from Carl Roth (CN08.2)) gives the most reproducible results. Finally, depending on the efficiency of the RNAi, it is possible to increase the concentration of IPTG up to 6 mM (1.38 g/L).
2. RNA interference (RNAi) by feeding is a powerful tool to inactivate a gene of interest in *C. elegans*. Specifically, *C. elegans* animals are grown in the presence of an *Escherichia coli* strain expressing double-strand RNA (dsRNA) against a particular gene to inactivate this gene in the animal's progeny [14]. A commercially available RNAi feeding library that contains ~87 % of the *C. elegans* genes has been generated by Ahringer and coworkers [15]. A bacterial strain containing an empty RNAi vector (*mock*(RNAi)) is often used as a negative control. Furthermore, in order to test the efficiency of the RNAi, it is recommended to use a positive control RNAi clone. When mitochondrial morphology is analyzed, good positive controls are *fzo-1*(RNAi) which triggers mitochondrial fragmentation and/or *drp-1*(RNAi) which triggers mitochondrial hyper-elongation. As an alternative to RNAi, a *C. elegans* strain carrying a loss-of-function mutation in the gene of interest may be available from the *Caenorhabditis* Genetics Center (CGC) (<https://www.cbs.umn.edu/research/resources/cgc>). This strain can be genetically crossed with the *PAmitoGFP* reporter strain MD2922. The resulting strain can then be used to analyze the effect of the loss-of-function mutation on the connectivity of the mitochondrial network (without the need of performing an RNAi experiment). In that case, a similar protocol starting with **step 9** should be followed.
3. The *C. elegans* strain MD2922 (which is available upon request) contains an extrachromosomal array (*bcEx856*). This

extrachromosomal array is a concatemer of multiples copies of the *Pmyo-3PAmitoGFP*, *Pmyo-3mitodsRed* and pRF4 plasmids linked in series. Because it is not integrated in the genome, it segregates in a non-Mendelian fashion. Therefore, not all progeny of MD2922 animals carry an extrachromosomal array. To identify transgenic animals, the plasmid pRF4 is used as a selection marker. pRF4 contains the *rol-6(su1006dm)* allele, which causes transgenic animals to exhibit a dominant “roller” phenotype. The strain should therefore be maintained by selecting “roller” animals. Furthermore, only animals exhibiting the “roller” phenotype should be used for imaging. It should be noted that MD2922 transgenic animals are also mosaic for the presence of the transgene and thus its expression. As a consequence, only some of the body wall muscle cells will carry the extrachromosomal array and therefore, express the *PAmitoGFP* reporter. The body wall muscle cells expressing this transgene can be selected, as they will also express the *mitodsRed* reporter.

4. Levamisole is an acetylcholine agonist that will cause muscle hyper-contraction and consequently *C. elegans* paralysis. Other drugs are often used to paralyze *C. elegans* for imaging such as sodium azide but they are of course not recommended for this experiment as they affect mitochondrial function. Alternatively, longer imaging without chemically paralyzing the animals can be achieved using a 10 % agarose pad and by adding 0.25–0.5  $\mu\text{L}$  of 0.1  $\mu\text{m}$  diameter polystyrene microspheres (e.g., Polysciences 00876-15, 2.5 % w/v suspension) onto the pad as previously described by Fang-Yen and coworkers [16]. However, in our hands, the animals are not always fully paralyzed, which can be a problem during imaging. As another alternative, immobilization of *C. elegans* animals has been successfully performed using microfluidic devices [17]. While this technique has been shown to be effective, it can be challenging to gain access to such a device and to adapt it to the microscope setup. In conclusion, while all approaches are good, we would recommend paralyzing the animals with levamisole.
5. While not absolutely necessary, DIC optics can be very helpful to visualize and identify *C. elegans* tissues.
6. Alternatively, commercial poly-L-lysine pre-coated microscope glass slides can be used (for example from Sigma; P0425).
7. Store aliquots of 1 mg/mL (in  $\text{H}_2\text{O}$ ) of poly-L-lysine stock solution at  $-20\text{ }^\circ\text{C}$ . Right before use, dilute the stock solution in  $\text{H}_2\text{O}$ –0.25 mg/mL (100  $\mu\text{L}$  stock + 300  $\mu\text{L}$   $\text{H}_2\text{O}$ ). Discard the dilution afterwards. Although commercial pre-coated

poly-L-lysine slides are available, in our hands these slides did not really represent a technical advantage compared to the home-made ones.

8. The methanol–acetone (1:1) fixation solution should be stored at  $-20^{\circ}\text{C}$  (to minimize evaporation) but needs to be taken out of the freezer 30 min prior to the experiment in order to have the solution at room temperature. As a general practice and especially for high-resolution microscopy (such as 3D-SIM microscopy), the solution should not be reused more than 4 times. For most of the antibodies indicated in Table 1, the protocol of fixation using methanol–acetone (1:1) has been successfully used. With other antibodies such as anti-Cytochrome-c or anti-COX IV antibodies, fixation for 5 min using 3.7 % FA has also been used successfully [18, 19].
9. While removing the cover glass, some of the embryos may remain on the cover glass. To confirm that enough embryos remain on the microscope slide, inspect the slide using a dissecting microscope after addition of the primary antibody.
10. As the PBSTB buffer can easily get contaminated by bacteria, it is better to prepare it fresh and discard it after use.
11. In the example described in this chapter, *PAmitoGFP* is expressed in body wall muscle cells. However, it could potentially be adapted to study mitochondrial morphology in other cell types by driving its expression under the control of suitable cell-type specific promoters (Information on cell-type specific promoters can be found at <http://gfpworm.org/>). Furthermore, using *PAmitoGFP*, it is possible to track single organelle as well as visualize fusion/fission events, as previously done in cultured mammalian cells [20].
12. For general information on how to maintain *C. elegans* strain and how to identify the different developmental stages (especially the L4 larval stage), please refer to Stiernagle et al. [8].
13. We recommended activating the *PAmitoGFP* in the middle of the presumptive network to determine how far the *PAmitoGFP* diffuses.
14. To determine the optimal condition of activation, one can measure average pixel intensity before and after activation in the ROI that was used for activation, which would define the ratio of activation. We would recommend at least a twofold activation ratio.
15. Alternatively, **step 14** can be performed by acquiring a Z-stack every 0.5 s (with 6 slices of  $0.5\ \mu\text{m}$  as the thickness of body wall muscle mitochondrial networks is not more than  $2\ \mu\text{m}$ ). In that case, the morphometric analysis of **step 15** should be performed by measuring the volume over time (instead of the area over time) of photoactivated *PAmitoGFP*.

16. As indicated in Table 1, while some antibodies are commercially available, some of the antibodies are home-made and will need to be requested directly from the authors of the respective publications.
17. In order to visualize the protein of interest using a GFP-tagged fusion, tools have been recently developed in *C. elegans*. For example, a fosmid-based transgene library, where almost 75 % of all *C. elegans* genes have been tagged with GFP [21], is available from TransgeneOme (<https://transgenome.mpi-cbg.de/transgeneomics/index.html>). Transgenic *C. elegans* animals carrying the fosmid of interest can be generated and the GFP-tagged fusion protein can be detected in immunocytochemistry experiments by using the newly developed GFP-booster (Chromotek Atto488). Specifically, an essentially identical protocol can be used for immunostaining, with one modification. At **step 24**, the GFP-booster (which recognizes the GFP tag) can be diluted at 1:500 in PBSTB and used along with the secondary antibody.
18. In order to obtain a staged population of animals on day 1, it is crucial that L4 larvae are picked 24 h before starting the experiment. To ensure that an adequate number of embryos is available for each staining, it is advisable to pick around 20–30 L4 for each staining. Additionally, to compare the staining of different strains (for example, a mutant of interest compared to a wild-type strain), it is important that the immunostaining is performed on the same day, in order to reduce variations due to the staining protocol.
19. Ensuring that microscope slides and cover glasses are properly cleaned is an essential step for immunostaining. Specifically, it is important to confirm that there are no dust particles or grease on the microscope slides and cover glasses. Dust particles will affect the efficiency of the freeze-crack as the cover glass will be unevenly positioned on the microscope slide thereby causing the volume of water between the cover glass and the embryos to be uneven. Furthermore, grease and dust particles will generate background auto-fluorescence, which will affect the quality of the imaging.
20. This step is important to control the quality of the freeze-crack technique. Although, the efficiency of freeze-crack is improved when the volume of liquid between the embryos and the cover glass is reduced, excessive reduction of the volume will result in the embryos being crushed by the cover glass. The presence of an adult hermaphrodite is used to ascertain the optimal volume. *C. elegans* adult hermaphrodites have a thickness of around 50–100  $\mu\text{m}$  while *C. elegans* embryos have a thickness of around 25  $\mu\text{m}$ . Therefore, when the adult hermaphrodite is

crushed by the cover glass, the optimal volume of liquid between the embryos and the cover glass is reached.

21. If required, the immunostaining procedure can be paused after this step by storing the slides with the cover glass at  $-80^{\circ}\text{C}$ .
22. Before blocking with PBSTB, a pre-blocking step with Image-iT FX signal enhancer (Life technology) for 30 min at  $20^{\circ}\text{C}$  has been shown to result in a better signal/background ratio in samples analyzed by 3D-SIM microscopy [13]. However, in our hands, it did not represent an advantage.
23. The presence of dirt on the microscope slide or cover glass can trap air bubbles. It is therefore essential to clean them properly (*see Note 15*). In addition, air bubbles can be generated while putting the cover glass onto the microscope slide too quickly. To solve this problem, one can put one of the edges of the cover glass on the microscope slide while holding it and then use the worm pick to bring down the opposite edge of the cover glass gently onto the microscope slide.
24. To build a humid chamber, one can use a plastic box (the size of the box will depend on how many slides one wants to analyze at the same time) with wet towel papers at the bottom. On top the wet towel papers, place a smaller plastic barrier onto which the microscope slides can be placed (so they are not in direct contact with the wet towel papers).
25. DAPI staining is useful as it allows determining the stage of the embryo analyzed by visualizing the number of nuclei. However, in case one wants to perform an immunostaining with three different antibodies, the DAPI staining will need to be skipped, while the third protein can be visualized using a secondary antibody coupled with a fluorophore that emits in the DAPI range (for example, CF405S goat anti-mouse or goat anti-rabbit (Biotium #20080 and Biotium #20082)).
26. After imaging the microscope slides with a high magnification oil objective, it is important to clean the cover glass and remove any oil, especially if reimaging of slides is to be done in the future. Any remnants of oil will make future imaging of the slide difficult (especially with 3D-SIM microscopy).
27. Mitochondrial localization of the protein of interest can be determined by observing colocalization with a known mitochondrial protein. Superresolution microscopy also permits determination of subcellular localization of the protein of interest by colocalization with a known mitochondrial protein. Software packages such as ImageJ can be easily used to determine colocalization. For further information, please refer to Dunn et al. [22].

## Acknowledgments

We thank Barbara Conratt, Nadin Memar, and Anne Kathrin Müller-Rischart for their comments on the manuscript. This work was supported by funding from the National Institutes of Health (GM076651), the Center for Integrated Protein Science Munich (EXC114) and the Deutsche Forschungsgemeinschaft (C0204/6-1) to Barbara Conratt.

## References

1. Mishra P, Chan DC (2014) Mitochondrial dynamics and inheritance during cell division, development and disease. *Nat Rev Mol Cell Biol* 15(10):634–646. doi:10.1038/nrm3877
2. Ichishita R, Tanaka K, Sugiura Y, Sayano T, Mihara K, Oka T (2008) An RNAi screen for mitochondrial proteins required to maintain the morphology of the organelle in *Caenorhabditis elegans*. *J Biochem* 143(4):449–454. doi:10.1093/jb/mvm245
3. Kanazawa T, Zappaterra MD, Hasegawa A, Wright AP, Newman-Smith ED, Buttle KF, McDonald K, Mannella CA, van der Bliek AM (2008) The *C. elegans* Opal homologue EAT-3 is essential for resistance to free radicals. *PLoS Genet* 4(2):e1000022. doi:10.1371/journal.pgen.1000022
4. Labrousse AM, Zappaterra MD, Rube DA, van der Bliek AM (1999) *C. elegans* dynamin-related protein DRP-1 controls severing of the mitochondrial outer membrane. *Mol Cell* 4(5):815–826
5. Rawson RL, Yam L, Weimer RM, Bend EG, Hartweg E, Horvitz HR, Clark SG, Jorgensen EM (2014) Axons degenerate in the absence of mitochondria in *C. elegans*. *Curr Biol*: CB 24(7):760–765. doi:10.1016/j.cub.2014.02.025
6. Rolland SG (2014) How to analyze mitochondrial morphology in healthy cells and apoptotic cells in *Caenorhabditis elegans*. *Methods Enzymol* 544:75–98. doi:10.1016/B978-0-12-417158-9.00004-2
7. Kuznetsov AV, Hermann M, Saks V, Hengster P, Margreiter R (2009) The cell-type specificity of mitochondrial dynamics. *Int J Biochem Cell Biol* 41(10):1928–1939. doi:10.1016/j.biocel.2009.03.007
8. Stiernagle T (2006) Maintenance of *C. elegans*. *WormBook*: the online review of *C. elegans* biology:1–11. doi:10.1895/wormbook.1.101.1
9. Rolland SG, Motori E, Memar N, Hench J, Frank S, Winklhofer KF, Conratt B (2013) Impaired complex IV activity in response to loss of LRPPRC function can be compensated by mitochondrial hyperfusion. *Proc Natl Acad Sci U S A* 110(32):E2967–E2976. doi:10.1073/pnas.1303872110
10. Schermelleh L, Heintzmann R, Leonhardt H (2010) A guide to super-resolution fluorescence microscopy. *J Cell Biol* 190(2):165–175. doi:10.1083/jcb.201002018
11. Duerr JS (2006) Immunohistochemistry. *WormBook*: the online review of *C. elegans* biology:1–61. doi:10.1895/wormbook.1.105.1
12. Baddeley D, Chagin VO, Schermelleh L, Martin S, Pombo A, Carlton PM, Gahl A, Domaing P, Birk U, Leonhardt H, Cremer C, Cardoso MC (2010) Measurement of replication structures at the nanometer scale using super-resolution light microscopy. *Nucleic Acids Res* 38(2):e8. doi:10.1093/nar/gkp901
13. Pourkarimi E, Greiss S, Gartner A (2012) Evidence that CED-9/Bcl2 and CED-4/Apaf-1 localization is not consistent with the current model for *C. elegans* apoptosis induction. *Cell Death Differ* 19(3):406–415. doi:10.1038/cdd.2011.104
14. Timmons L, Court DL, Fire A (2001) Ingestion of bacterially expressed dsRNAs can produce specific and potent genetic interference in *Caenorhabditis elegans*. *Gene* 263(1-2):103–112
15. Kamath RS, Ahringer J (2003) Genome-wide RNAi screening in *Caenorhabditis elegans*. *Methods* 30(4):313–321
16. Kim E, Sun L, Gabel CV, Fang-Yen C (2013) Long-term imaging of *Caenorhabditis elegans* using nanoparticle-mediated immobilization. *PLoS One* 8(1):e53419. doi:10.1371/journal.pone.0053419
17. Mondal S, Koushika SP (2014) Microfluidic devices for imaging trafficking events in vivo using genetic model organisms. *Methods Mol Biol* 1174:375–396. doi:10.1007/978-1-4939-0944-5\_26

18. Labrador L, Barroso C, Lightfoot J, Muller-Reichert T, Flibotte S, Taylor J, Moerman DG, Villeneuve AM, Martinez-Perez E (2013) Chromosome movements promoted by the mitochondrial protein SPD-3 are required for homology search during *Caenorhabditis elegans* meiosis. *PLoS Genet* 9(5):e1003497. doi:[10.1371/journal.pgen.1003497](https://doi.org/10.1371/journal.pgen.1003497)
19. Liu Y, Samuel BS, Breen PC, Ruvkun G (2014) *Caenorhabditis elegans* pathways that surveil and defend mitochondria. *Nature* 508(7496):406–410. doi:[10.1038/nature13204](https://doi.org/10.1038/nature13204)
20. Berman SB, Chen YB, Qi B, McCaffery JM, Rucker EB 3rd, Goebbels S, Nave KA, Arnold BA, Jonas EA, Pineda FJ, Hardwick JM (2009) Bcl-x L increases mitochondrial fission, fusion, and biomass in neurons. *J Cell Biol* 184(5):707–719. doi:[10.1083/jcb.200809060](https://doi.org/10.1083/jcb.200809060)
21. Sarov M, Murray JI, Schanze K, Pozniakovski A, Niu W, Angermann K, Hasse S, Rupprecht M, Vinis E, Tinney M, Preston E, Zinke A, Enst S, Teichgraber T, Janette J, Reis K, Janosch S, Schloissnig S, Ejsmont RK, Slightam C, Xu X, Kim SK, Reinke V, Stewart AF, Snyder M, Waterston RH, Hyman AA (2012) A genome-scale resource for in vivo tag-based protein function exploration in *C. elegans*. *Cell* 150(4):855–866. doi:[10.1016/j.cell.2012.08.001](https://doi.org/10.1016/j.cell.2012.08.001)
22. Dunn KW, Kamocka MM, McDonald JH (2011) A practical guide to evaluating colocalization in biological microscopy. *Am J Physiol Cell Physiol* 300(4):C723–C742. doi:[10.1152/ajpcell.00462.2010](https://doi.org/10.1152/ajpcell.00462.2010)
23. Rolland SG, Lu Y, David CN, Conradt B (2009) The BCL-2-like protein CED-9 of *C. elegans* promotes FZO-1/Mfn1,2- and EAT-3/Opal-dependent mitochondrial fusion. *J Cell Biol* 186(4):525–540. doi:[10.1083/jcb.200905070](https://doi.org/10.1083/jcb.200905070)
24. Head BP, Zulaika M, Ryazantsev S, van der Blik AM (2011) A novel mitochondrial outer membrane protein, MOMA-1, that affects cristae morphology in *Caenorhabditis elegans*. *Mol Biol Cell* 22(6):831–841. doi:[10.1091/mbc.E10-07-0600](https://doi.org/10.1091/mbc.E10-07-0600)
25. Brys K, Castelein N, Matthijssens F, Vanfleteren JR, Braeckman BP (2010) Disruption of insulin signalling preserves bioenergetic competence of mitochondria in ageing *Caenorhabditis elegans*. *BMC Biol* 8:91. doi:[10.1186/1741-7007-8-91](https://doi.org/10.1186/1741-7007-8-91)
26. Senoo-Matsuda N, Hartman PS, Akatsuka A, Yoshimura S, Ishii N (2003) A complex II defect affects mitochondrial structure, leading to *ced-3*- and *ced-4*-dependent apoptosis and aging. *J Biol Chem* 278(24):22031–22036. doi:[10.1074/jbc.M211377200](https://doi.org/10.1074/jbc.M211377200)
27. Mun JY, Lee TH, Kim JH, Yoo BH, Bahk YY, Koo HS, Han SS (2010) *Caenorhabditis elegans* mitofilin homologs control the morphology of mitochondrial cristae and influence reproduction and physiology. *J Cell Physiol* 224(3):748–756. doi:[10.1002/jcp.22177](https://doi.org/10.1002/jcp.22177)
28. Hadwiger G, Dour S, Arur S, Fox P, Nonet ML (2010) A monoclonal antibody toolkit for *C. elegans*. *PLoS One* 5(4):e10161. doi:[10.1371/journal.pone.0010161](https://doi.org/10.1371/journal.pone.0010161)
29. Yokoyama K, Fukumoto K, Murakami T, Harada S, Hosono R, Wadhwa R, Mitsui Y, Ohkuma S (2002) Extended longevity of *Caenorhabditis elegans* by knocking in extra copies of hsp70F, a homolog of *mot-2* (mortalin)/mthsp70/Grp75. *FEBS Lett* 516(1-3):53–57
30. Wirth M, Karaca S, Wenzel D, Ho L, Tishkoff D, Lombard DB, Verdin E, Urlaub H, Jedrusik-Bode M, Fischle W (2013) Mitochondrial SIRT4-type proteins in *Caenorhabditis elegans* and mammals interact with pyruvate carboxylase and other acetylated biotin-dependent carboxylases. *Mitochondrion* 13(6):705–720. doi:[10.1016/j.mito.2013.02.002](https://doi.org/10.1016/j.mito.2013.02.002)

## Single Molecule Tracking and Localization of Mitochondrial Protein Complexes in Live Cells

Timo Appelhans and Karin Busch

### Abstract

Mitochondria are the power plant of most non-green eukaryotic cells. An understanding of their function and regulation is only possible with the knowledge of the spatiotemporal dynamics of their proteins. Mitochondrial membrane proteins involved in diverse functions like protein import, cell respiration, metabolite transport, and mitochondrial morphology are mobile within membranes. Here, we provide a protocol for a superresolution fluorescence microscopy technique named tracking and localization microscopy (TALM) that allows for localization and diffusion analysis of single mitochondrial membrane proteins in situ in cell cultures. This noninvasive imaging technique is a useful tool to reveal the spatiotemporal organization of proteins in diverse mitochondrial membrane compartments in living cells. Proteins of interest are tagged with the HaloTag<sup>®</sup> and specifically labeled with functionalized rhodamine dyes. The method profits from low abundance of proteins and therefore works better with substoichiometric labeling of HaloTag<sup>®</sup>-tagged proteins. In particular, the use of photostable bright rhodamine dyes enables the specific tagging and localization of single molecules with a calculated precision below 20 nm and the recording of single trajectories.

**Key words** Superresolution microscopy, Mitochondria, Membrane protein dynamics, Single molecule localization and tracking, Live cell imaging, Tom20, ATP synthase

---

### 1 Introduction

Owing to their evolutionary origin, mitochondria possess two membranes of different structure and composition. The tubular outer mitochondrial membrane (OMM) envelopes the organelle, while the intensely folded inner mitochondrial membrane (IMM) provides two sub-compartments: the inner boundary membrane (IBM) and the cristae membranes (CM). Biochemical analysis gave insights into the composition of OMM and IMM, but already the dissection of the IBM and the CM as two sub-compartments of the one continuous membrane has been challenging. However, optimal function, metabolic adaptation, and also failure of mitochondrial performance cannot be understood without the knowledge of the composition of the proteins in the respective

sub-compartments. Furthermore, membrane proteins are mobile and thus their spatial distribution might be flexible. The diffusion of compounds is determined by the architecture of the respective membrane, its lipid composition, and possible interactions with other proteins. To reveal protein dynamics, analysis has to be done in situ and in a noninvasive manner in living cells. FRAP allows for the determination of mobile protein fractions but does not record slow or immobile fractions adequately. In recent years, superresolution microscopy provided techniques for localizing single proteins. Here, we extend this toolbox and provide a protocol that allows also for tracking of single membrane proteins, here in mitochondria in live cells [1]. We localized and tracked Tom20 in the outer mitochondrial membrane (Fig. 1) and  $F_1F_0$  ATP synthase in the inner mitochondrial membrane (Fig. 2). Since membrane proteins have a reduced mobility compared to soluble proteins individual proteins can be tracked. During recording time, mobile proteins occupy different positions at different time points, limited by their specific functional and structural microcompartment (Fig. 1b, c; Fig. 2b, d). Thus, the localization and trajectory map of a recorded protein represents the spatiotemporal dynamics of this particular protein in its membrane microcompartment. Because of this feature, the number of molecules required to pinpoint the structure of a certain microcompartment is much lower than with other techniques. This is an advantage, especially when proteins with low expression levels are analyzed. Low labeling degree also reduces the danger of phototoxic effects and allows for prolonged live cell imaging. The mobility analysis reveals different trajectory maps and diffusion coefficients for outer and inner membrane proteins (Figs. 1c and 2d), clearly related to the underlying structure of the membrane [1].

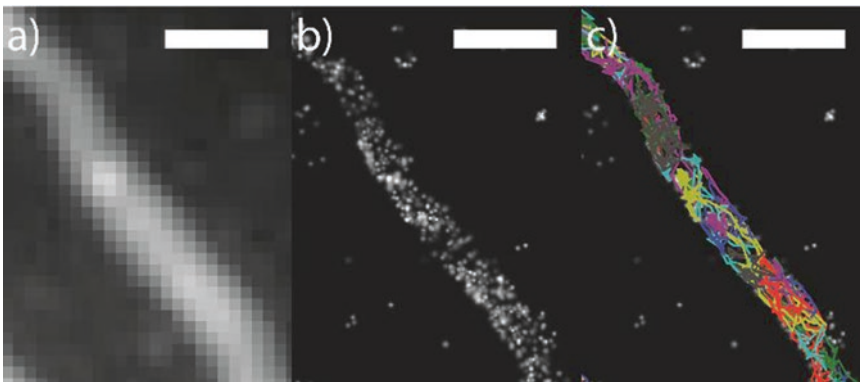


**Fig. 1** TALM analysis of single TOM20-HaloTag<sup>®</sup>/TMR<sup>HTL</sup> in a living HeLa cell. **(a)** Diffraction limited view of summed fluorescent signals from 3500 frames (frame rate 33 Hz, 32 ms exposure time/frame) showing TOM20:HaloTag<sup>®</sup>/TMR<sup>HTL</sup> signals in the outer mitochondrial membrane. **(b)** Cumulated image of localized TOM20 proteins in the OMM from 3500 frames (112 s). **(c)** Trajectories of individual TOM20 proteins with a minimum overall step number of 15 steps in sequence (single trajectories with different colors). *Scale bars: 1 μm*

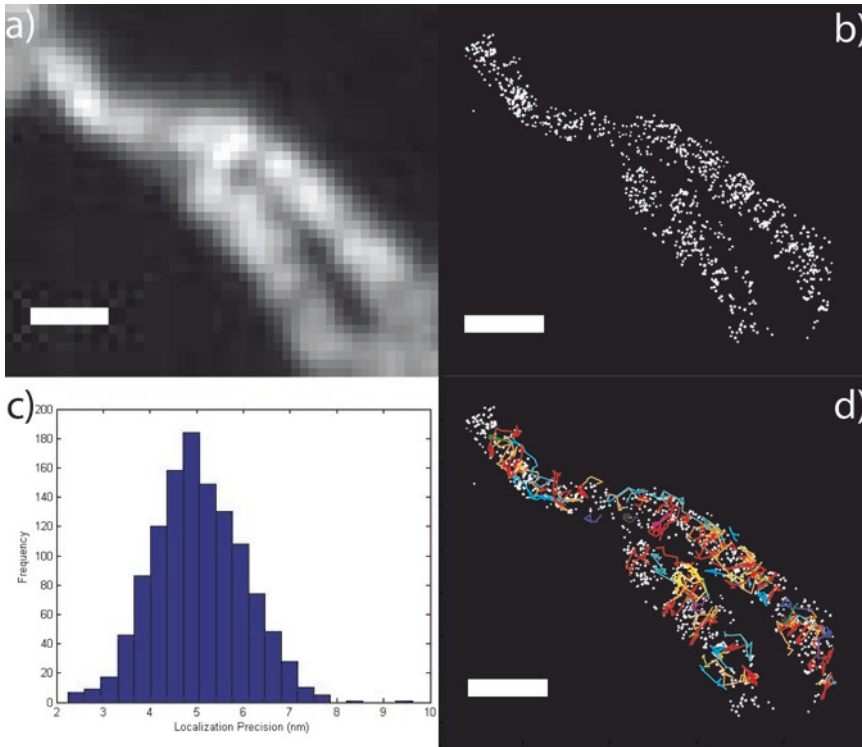


**Fig. 2** TALM analysis of single  $F_1F_0$  ATP-Synthase: HaloTag<sup>®</sup>/TMR<sup>HTL</sup>. **(a)** Diffraction limited view of summed fluorescent signals from ATP-Synthase: HaloTag<sup>®</sup>/TMR<sup>HTL</sup> in the inner mitochondrial membrane from 3500 frames (16 ms/frame). **(b)** Localization map of ATP-Synthase: HaloTag<sup>®</sup>/TMR<sup>HTL</sup> proteins. Localization patterns reflect distribution of ATP synthase in cristae microcompartments. **(c)** Calculated localization precision of the localized proteins shown in **(b)**. **(d)** Trajectory map of ATP Synthase: HaloTag<sup>®</sup>/TMR<sup>HTL</sup> proteins. Most red and orange trajectories demonstrate the diffusion of ATP-Synthases in the cristae and reveal the orthogonal cristae membrane (CM) orientation while blue trajectories demonstrate the likely diffusion of ATP-Synthase: HaloTag<sup>®</sup>/TMR<sup>HTL</sup> proteins along the inner boundary membrane (IBM). *Scale bars: 1  $\mu$ m (a, b, and d)*

In order to visualize specific proteins, these are tagged by genetic fusion to the HaloTag<sup>®</sup>. The HaloTag<sup>®</sup>-Protein [2] is a “suicide” protein that covalently reacts with its substrate, the HaloTag<sup>®</sup>-Ligand (<sup>HTL</sup>). Cells are transfected with the according plasmid and the expressed tagged protein of interest is posttranslationally labeled with a fluorescent dye linked to the HaloTag<sup>®</sup>-Ligand. Today, several suitable fluorescent dyes for labeling of HaloTag<sup>®</sup> proteins are available, however, for intracellular labeling membrane-permeable dyes are required. In this protocol, tetramethylrhodamine-HaloTag<sup>®</sup>-Ligand (TMR<sup>HTL</sup>) is used. The bright TMR fluorescence enables localization of single molecules with high precision (Fig. 2c). Correct mitochondrial localization of labeled proteins can be controlled by co-staining with MitoTracker<sup>®</sup> Deep Red FM or MitoTracker<sup>®</sup> Green.

---

## 2 Materials

### 2.1 TIRF

#### *Microscope Setup*

Single molecule tracking and localization can be performed with a commercially available inverse total internal reflection fluorescence (TIRF) microscope, equipped with a TIRF-condensor, a TIRF objective, and diode pumped solid-state lasers with sufficient power (100–200 mW). For detection, a single molecule sensitive and fast camera is necessary. In our case, a commercially available inverse total internal reflection fluorescence (TIRF) microscope (e.g., Olympus IX71), equipped with a TIRF-condensor (Olympus), a diode pumped solid-state laser (excitation 561 nm, 200 mW, [Cobolt Jive 561](#), [Cobolt](#)), and a back-illuminated electron multiplying charged coupled device (EMCCD) camera was used. The TIRF-microscope otherwise has no specific or special fabrication. In order to perform single molecule tracking and localization microscopy (TALM) with high signal to noise (S/N) ratio within living cells, a highly inclined and laminated optical sheet (HILO) is used for excitation [3]. Therefore, an incident beam angle is chosen just below the critical angle for TIRF-mode. The fluorescence-labeled specimen is excited through the objective. For excitation of tetramethylrhodamine, a diode pumped solid-state laser (excitation 561 nm, 200 mW, [Cobolt Jive 561](#), [Cobolt](#)) is coupled into a single mode fiber ([Qoptiq](#)) connected to the motorized integrated TIRF illumination combiner ([MITICO](#), cell<sup>^</sup>TIRF, Olympus) with laser light. The MITICO system enables the user to couple up to four laser lines into the microscope. For each illumination pathway an individual angle for illumination between Epi- and TIRF-illumination can be chosen. The MITICO software allows a simple and precise identification of the appropriate objective to reproducibly adjust the angle of illumination and thereby the penetration depth of the excitation light. The microscope is equipped with an apochromatic 150× oil immersion objective designed for TIRF microscopy (150× TIRF objective numerical aperture N.A. = 1.45, Olympus, UAPO). With the 150× objective, a pixel size of 107 nm is obtained fulfilling the Nyquist-Shannon theorem for diffraction limited imaging [4, 5]. The high magnification and N.A. is needed to achieve high laser power densities in the focal plane (maximum 1–2 kW/cm<sup>2</sup>). For single molecule tracking, the power density is adjusted to one-tenth (100 W/cm<sup>2</sup>) to reduce photobleaching and blinking to obtain longer trajectories. Laser light reflected from a dichroic mirror (OBS-U-M3TIR 405/488/561, Semrock) passes through the 150× objective. The fluorescence is filtered by a HC Quadband pass filter, 446/523/600/677 (F72–866 from AHF analysentechnik AG) installed in the U-MF2 filter cube. Image acquisition is performed with a back-illuminated EMCCD camera ([Andor iXon Ultra 897](#)), providing high quantum efficiency of >90% between 500 and 700 nm and a maximal frame rate of 32 frames per second (fps) at full resolution (512 × 512 pixel, each 16 μm × 16 μm in size), which can be reduced, when

**Table 1**  
**Used frame rates**

Imaging area (pixel, x,y)	Exposure time (ms)	Frame rate (Hz)
512 × 512	32	30.42
512 × 256	24	40.15
256 × 256	16	59.17
200 × < 200	8	112
125 × 125	8	112

Smaller imaging areas allow for reduction of the exposure time.

smaller areas are imaged (Table 1). The pixel to photon conversion factor (EM gain 300) was 9.2 under the settings used.

## 2.2 Buffers

1. 1 M HEPES (4-(2-Hydroxyethyl)piperazine-1-ethanesulfonic acid) buffer, pH 7.5.
2. 100 mM HEPES buffer, pH 7.5.
3. 100 mM HEPES buffer, 1 mM EDTA, pH 7.5.
4. PBS buffer, pH 7.4 without  $\text{Ca}^{2+}$  and  $\text{Mg}^{2+}$ .

## 2.3 Chemicals

1. 10 % PEG 800 (Polyethylene glycol, molar mass 800 g/mol).
2. 30 %  $\text{H}_2\text{O}_2$ .
3. 70 % v/v Ethanol.
4. 98 % sulfuric acid.
5. Acetyl-CG-RGD-S-COOH (Sigma Aldrich, Germany).
6. Dimethyl sulfoxide (anhydrous,  $\geq 99.9\%$ ) (DMSO).
7. Ethylenediaminetetraacetic acid (EDTA).
8. Isopropanol.
9. Immersion Oil-Immersoil™ 518 F ( $n_c = 1.518$ ,  $v_c = 45$ ).
10.  $\text{N}_2$  gas.
11. NHS-PEG-MAL, Rapp Polymer (Rapp Polymere GmbH Tübingen).
12. PLL-PEG-RGD-Peptide.
13. Poly-l-lysine (PLL).
14. Tris(1-chloroethyl) phosphate (TCEP).

## 2.4 Preparation of PLL-PEG-RGD for Surface Coating

PLL-PEG-RGD is a short name of Poly-l-Lysine- $\mathcal{g}$ (3)-PEG<sub>2k</sub>-RGD. “ $\mathcal{g}$ ” means graft modification on Poly-l-Lysine. “3” means 33% of side chain lysine groups ( $\text{NH}_2$ ) were coupled with PEG so that the ratio of total l-lysine to the coupled one is 3. “PEG<sub>2k</sub>-RGD” denotes that the graft PEG has an average molecule weight of 2 kDa with a terminal RGD peptide.

1. Dissolve 7.6 mg Acetyl-CG-RGD-S-COOH in 0.1 ml 100 mM HEPES buffer containing 1 mM EDTA, pH 7.5.
2. Dissolve 3 mg TCEP in 0.1 ml 1 M HEPES buffer, pH 7.5, check the pH to be 6–7.
3. Incubate for 10 min at RT.
4. Dissolve 7.5 mg Poly-L-Lysin (PLL) in 0.25 ml 1 M HEPES, pH 7.5.
5. Dissolve 36 mg M alemeid-PEG-NHS (3000 Da) in 0.05 ml 1 M HEPES, pH 7.5.
6. Mix Acetyl-CG-RGD-S solution with M alemeid-PEG-NHS solution and incubate at RT for 5 min, check the pH to be 6–7.
7. Add dissolved PLL to the mixture, adjust pH to 7–8.3.
8. Place the mixture on a shaker overnight.
9. Lyophilize the mixture the next day 12–20 h (*see Note 1*).

## 2.5 Plasmids

For tracking mitochondrial membrane proteins, we used Tom20, an outer mitochondrial membrane protein, and complex V ( $F_1F_0$  ATP synthase, CV) as an inner membrane protein, predominantly found in the cristae membranes. In principle, it is possible to use any other membrane protein as well. Please note that for most inner membrane proteins the mitochondrial targeting sequences are at the N-terminus. Mitochondrial localization can be checked by GFP constructs, before starting single molecule experiments with Halo7-fusion proteins.

1. TOM20-link-Halo7-psems [1], generated from pSNAP<sub>F</sub>-Tag<sup>®</sup> New England Biolabs<sup>®</sup> by substitution of the SNAPf-ORF with Halo7-ORF.
2. CV $\gamma$ -Halo7-psems [1].

## 2.6 Cells

Cervix Cancer Cells-HeLa Cells (Tissue Culture) (Leibniz Institute DSMZ-German, Collection of Microorganisms and Cell Cultures).<sup>1</sup>

## 2.7 Media

### 2.7.1 Growth Medium

1. Minimal Essential Medium with Earle's salts and Phenolred.
2. 10 $\times$  Fetal Bovine Serum Superior (FBS) (Biochrom AG, Cat. No. S0615, Lot. No. 0513C).
3. 1 % (v/v) HEPES.
4. 1 % (v/v) nonessential amino acids NEA.
5. 1 % (v/v) stable Alanine-L-Glutamine.
6. 2.2 g/l NaHCO<sub>3</sub>.

<sup>1</sup>PC12 cells (a pheochromocytoma of the rat adrenal medulla), 143b cells (human osteosarcoma), and MEF (mouse embryonic fibroblast cells) were also successfully used for TALM in different experiments.

**2.7.2 Selective  
Growth Medium**

1. Growth medium.
2. 0.8 mg/ml Neomycin.

**2.7.3 Imaging Medium**

1. Earle's Minimum Essential Media (MEM) (w/o Phenol red).
2. 10× Fetal Bovine Serum Superior (FBS).
3. 1 % (v/v).
4. 1 % (v/v) nonessential amino acids NEA.
5. 1 % (v/v) stable Alanine-L-Glutamine.
6. 2.2 g/l NaHCO<sub>3</sub>.

**2.7.4 Transfection  
Medium**

1. 2.5 M CaCl<sub>2</sub> solution.
2. HBS Buffer.
3. 50 mM HEPES.
4. 280 mM NaCl.
5. 1.5 mM Na<sub>2</sub>HPO<sub>4</sub>.

**2.7.5 Detaching Medium**

1. 0.025 % (w/v) Trypsin.
2. 2.5 mM EDTA.
3. 1× PBS.

**2.8 Fluorescent Dyes**

Store fluorescent dyes as stock solutions in DMSO. Later dilute with imaging medium to appropriate concentrations. Do not keep dyes diluted in medium.

1. 1 μM Tetramethylrhodamine-HaloTag®-Ligand (TMR<sup>HLL</sup>).
2. 1 mM MitoTracker® Deep Red FM.

**2.9 Software/  
Algorithms**

1. Andor IQ3 (Andor Technology).
2. ImageJ (MacBiophotonics).
3. Matlab R2013b (TheMathWorks).
4. Matlab-Algorithm: FPALM localization gui (Labor Samuel T. Hess [6–8]).
5. Matlab-Algorithm *MultiTargetTracer* (Serge et al. [11]; see Note 2).

**2.10 Specific  
Equipment**

1. Coverslips (0.15 mm, Ø 24 mm) (VWR).
2. Microscopy-Chamber (Fig. 3) Optomechanics-University of Osnabrück.
3. Plasma Cleaner, Femto-Variante A, Diener electronic GmbH & Co. KG.

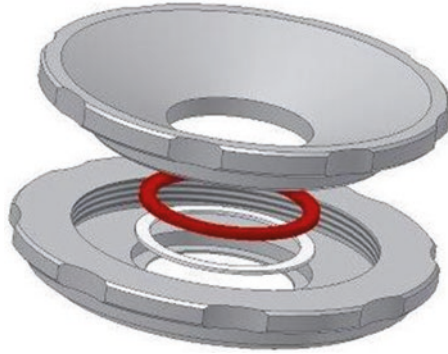


**Fig. 3** Microscopy chamber for live cell imaging. The coverslip with an appropriate cell layer is mounted between the top and bottom part of the homemade chamber (developed by J. Bereiter-Hahn©), which is connected by a screwed joint. A Teflon® ring (*white ring*) and a rubber ring (*red ring*) seal the system. The buffer reservoir is open and allows exchange of imaging medium (drawing from H. Heine©, Optomechanics-University of Osnabrück)

### 3 Methods

#### 3.1 Cell Culture

##### 3.1.1 Cultivation

Cultivate HeLa cells in T25 cell culture flasks, with 5 ml Growth medium at 37 °C and 5 % CO<sub>2</sub>. Passage cells when reaching confluence.

##### 3.1.2 Passaging (1:5)

1. Remove the old medium from confluent cells grown in T25 flasks.
2. Wash the cells thoroughly with 4 ml PBS.
3. Remove the PBS.
4. Add 1 ml Detaching medium to remove cells from the flask surface.
5. Incubate the flask at 37 °C and 5 % CO<sub>2</sub> until the cells are removed from the bottom (1–2 min).
6. Stop the reaction when all cells are solute by adding 4 ml fresh medium.
7. Pipette up and down to homogenize the cell solution.
8. Transfer 1 ml to a new T 25 flask and fill up to 5 ml with fresh culture medium.

##### 3.1.3 Cell Transfection

Mammalian HeLa cells for transient transfection and direct imaging are grown in a 35 mm Cellstar® tissue culture dish on coverslips (0.15 mm, Ø 24 mm). For transfection, the calcium phosphate method [9] is used.

1. Seed  $2 \times 10^3$  to  $5 \times 10^3$  cells into a 35 mm Cellstar® tissue culture dish containing a coverslip and 2 ml Growth medium.

2. Pipette 10  $\mu\text{l}$  plasmid solution, containing 5  $\mu\text{g}$  pure DNA in an Eppendorf Cup.
3. Add 20  $\mu\text{l}$   $\text{CaCl}_2$  solution (2.5 M).
4. Mix by carefully pipetting up and down once.
5. Wait for 30 s.
6. Add 170  $\mu\text{l}$  milliQ  $\text{H}_2\text{O}$ .
7. Pipette 200  $\mu\text{l}$  HBS Buffer (pH  $7 \pm 0.04$ ) in another Eppendorf Cup.
8. Vortex the HBS Buffer in the Eppendorf Cup.
9. Add the 200  $\mu\text{l}$  buffered DNA/ $\text{CaCl}_2$  solution by dropping it into the HBS Buffer during vortexing.
10. Replace the Growth medium of the HeLa cells in the 35 mm Cellstar<sup>®</sup> tissue culture dishes with 1 ml fresh Growth medium.
11. Pipette the DNA solution in single drops into the 35 mm Cellstar<sup>®</sup> tissue culture dishes filled with 1 ml medium. Increase the height of pipetting to avoid “dancing” of drops onto the medium surface, which can lead to inhomogeneous DNA concentration in the sample.
12. Incubate the transfected HeLa cells at 37 °C and 5 %  $\text{CO}_2$  overnight.
13. Replace the Growth medium after 12 h.
14. Let the cells grow for 24 h after replacing the Growth medium.
15. In order to have good expression levels of your protein of interest image transfected cells 36 to 48 h after transfection.

At day of imaging:

1. Wash each dish with 2 ml PBS twice.
2. Wash each dish with 2 ml Imaging medium once.
3. Keep the cells at 37 °C and 5 %  $\text{CO}_2$  in 2 ml fresh Imaging medium until mounting on stage.
4. Replace the medium before imaging with 1 ml fresh Imaging medium.

#### 3.1.4 Generation of Stable Transfected Cell Lines

For generation of a stable cell line the transfected plasmid has to be integrated into the target cell genome. The advantage is a stable, long-term expression of the protein of interest with usually uniform and moderate expression levels.

1. Seed  $5 \times 10^3$  cells into a 60 mm Cellstar<sup>®</sup> tissue culture dish.
2. Transfect cells 1 day after seeding at 60–80 % confluency as described under Subheading 3.2.
3. Wash cells with 4 ml PBS, 18 h after transfection.
4. Wash cells with 4 ml Selective growth medium.

5. Incubate cells with 5 ml Selective growth medium.
6. During a period of 10–14 days change Selective growth medium every day.
7. Colonies (visible by eye) which grow in the selective medium are from stable transfected cells and are isolated as follows.
8. Incubate cells with detaching solution until cells rounding and starting to detach.
9. Pick colonies with 200  $\mu$ l pipette and transfer into separate 35 mm Cellstar<sup>®</sup> tissue culture dish.
10. Add 2 ml Selective growth medium.
11. Incubate at 37 °C and 5 % CO<sub>2</sub>.
12. Continue proliferation in selective growth medium in T25 flask until confluency reached, then split and freeze leftovers.
13. Check stable transfection by imaging cells after staining with 500 nM TMR<sup>HTL</sup>-substrate for 20 min and subsequent washing: all stable transfected cells shall be fluorescent (*see Note 3*).

### 3.2 Surface Cleaning of Coverslips

Usually, the dirt on the surface of coverslips enhances the background in single molecule imaging. In order to get a clean coverslip, plasma cleaning or cleaning with Piranha solution is performed. During the procedures, particles on the glass surface are oxidized, which destroys the fluorescence. To avoid re-contamination, always wear gloves when performing cleaning procedures. The freshly cleaned coverslips are used for coating immediately.

#### 3.2.1 Piranha Cleaning (Alternative A)

1. Prepare Piranha solution by mixing 98 % sulfuric acid into 30 % H<sub>2</sub>O<sub>2</sub> in a 2:1 volume ratio. (Cautious!! It is very corrosive).
2. Put coverslips into freshly prepared Piranha solution for more than 1 h.
3. Afterward, the glass substrate should be extensively washed with MiliQ water.
4. Dry by steam treatment with nitrogen gas.

#### 3.2.2 Plasma Cleaning (Alternative B)

1. Wash each coverslip in pure water to remove dust from the coverslip.
2. Blow coverslips dry with nitrogen gas.
3. Scratch an achiral symbol on the topside of each coverslip.
4. Place the coverslips topside up into a shallow beaker without overlapping one another.
5. Set plasma cleaning time to 15 min.
6. Set the power to 40 W.
7. Open the plasma cleaner.

8. Place the open shallow beaker in the middle of the glass tray of the plasma cleaner.
9. Evacuate the plasma cleaner for 2 min.
10. Start the generator, plasma cleaning will stop automatically after 15 min.
11. Turn on the ventilation for approximately 30 s.
12. Switch off the pump.
13. Continue to ventilate the chamber for approximately 15 s.
14. Remove the lid with two hands and turn off the main switch.
15. Place each cleaned coverslip topside up into a 35 mm Cellstar® tissue culture dish (*see Note 4*).

### **3.3 PLL-PEG-RGD: Coverslip Coating**

To prevent unspecific binding of fluorescent molecules to the coverslip surface and to reduce background signals, coverslips are coated with Poly-L-Lysine—Polyethylene Glycol—Arginine Glycine Aspartate (PLL-PEG-RGD). PLL-PEG-RGD is a poly-L-Lysine (PLL) derivative attached with a polyethylene glycol 3000 Da and a Cysteine-Glycine-Arginine-Glycine-Aspartate--Serine (CGRGDS) peptide. The RGD motif is a signal peptide of the integrin receptor.

1. Add 15  $\mu$ l PLL-PEG-RGD (0.8 mg/ml) on a plasma cleaned coverslip.
2. Slowly place another plasma cleaned coverslip upside down on the first one.
3. The PLL-PEG-RGD gets soaked between the coverslips.
4. Avoid bubbles between the coverslips. If bubbles occur you may slightly push on the upper coverslip.
5. Incubate the coated coverslips below the hood for 1 h.
6. Wash the coverslips 3 times with milli Q water.
7. Blow coverslips dry with nitrogen gas.
8. Place a single coverslip in a 35 mm Cellstar® tissue culture dish, the coated site up (*see Notes 5 and 6*).

### **3.4 Preparation of Cells for Imaging**

1. Cells for transient transfection should be seeded on coated coverslips 1 day before transfection and 2 days before imaging. Stable transfected cells can be seeded 1 day before imaging on coated coverslips.
2. Coated coverslips are incubated at 37 °C for 5 min, if previously stored at -20 °C.
3. Add 2 ml imaging medium in a 35 mm Cellstar® tissue culture dish containing a coated coverslip.
4. Remove the Growth medium from the T25 culture flask containing the cells to be seeded.

5. Add 3 ml PBS and slightly shake the flask.
6. Remove the PBS.
7. Add 1 ml Detaching medium.
8. Incubate the flask at 37 °C and 5 % CO<sub>2</sub> until the cells are removed from the bottom (1–2 min).
9. Add 4 ml Growth medium.
10. Pipette up and down gently to avoid cell clusters.
11. Passage  $2 \times 10^3$  (for imaging after 36–49 h) to  $5 \times 10^3$  (for imaging the next day) into the provided 35 mm Cellstar® tissue culture dish, containing 2 ml Imaging medium.
12. Slightly shake the culture dish to homogenize the cell suspension.
13. Incubate the samples at 37 °C and 5 % CO<sub>2</sub>.
14. Change the Imaging medium the next day.
15. Incubate the cells before imaging with 2 ml fresh Imaging medium for 1 h at 37 °C and 5 % CO<sub>2</sub>.

### **3.5 Posttranslational Labeling**

It is necessary to adapt the right labeling concentration for every cell line and specific tagged protein of interest. Therefore, different labeling concentrations need to be tested to achieve an optimum between as much as possible but still distinct single molecules.<sup>2</sup> The correct mitochondrial localization of labeled proteins is confirmed by co-staining of mitochondria with MitoTracker®DeepRed FM.

1. Use cells grown on glass coverslips when confluency of 60–80 % is reached.
2. Warm up the imaging medium to 37 °C.
3. Pipette 1 ml pre-warmed, fresh imaging medium into an Eppendorf Cup.
4. Add 0.5–1 µl TMR<sup>HTL</sup> 1 µM stock solution for final concentration: 0.5–1 nM) and
5. Vortex gently.
6. Remove the medium from the cells in the 35 mm Cellstar® tissue culture dish. Make sure that medium is removed completely, but do not touch the coverslip in the imaging area.
7. Add the imaging solution with TMR<sup>HTL</sup> prepared in **steps 1–3**.
8. Incubate the cells at 37 °C and 5 % CO<sub>2</sub> for 20 min.
9. Wash twice with 2 ml PBS.
10. Wash once with 2 ml Imaging medium.
11. Add 1 ml fresh Imaging medium.

---

<sup>2</sup>Note: Take care that the DMSO concentration does not exceed 10 % for reasons of cell toxicity.

12. Incubate the samples at 37 °C and 5 % CO<sub>2</sub> for 1 h.
13. Replace the Imaging medium before imaging.
14. Labeled cells should be imaged on the same day (*see Note 7 and 8*).

### **3.6 Specimen Clamping**

The coverslips from the 35 mm dishes with the labeled cells, prepared as described under Subheading 3.7, are mounted on imaging chambers for inverse microscopy (Fig. 3). Prepared specimen chambers can be stored for 2 h at 37 °C and 5 % CO<sub>2</sub> but the imaging medium should be renewed 1 h before microscopy. Storage of empty chambers is in 70 % ethanol.

1. Perform a final check on the sample checking that cell confluency is ~60% and dead detached cells are removed by washing with PBS.
2. Prepare the microscopy chambers (kept in 70 % EtOH but non-sterile).
3. Use tissues to dry the chamber, the Teflon® ring, and the rubber band.
4. Place a Teflon® ring in the notch of the lower chamber part.
5. Transfer the coverslips from the 35 mm dishes on the Teflon® ring in the notch of the lower chamber part.
6. Put the rubber band above the coverslip.
7. Put the upper chamber part on to it.
8. Screw the chamber carefully and make sure the chamber is sealed and the coverslip is not broken.
9. Dry and clean the undersurface of the coverslip and the chamber with a tissue.
10. Add 800 µl imaging medium at the rim of the coverslip.
11. The samples are ready for imaging.
12. After imaging take the chamber apart and wash the individual parts with 70% ethanol solution.

### **3.7 Imaging**

1. Switch on the microscope, the Acousto Optic Tunable Filter (AOTF), and the laser(s).
2. Start the Computer.
3. Start the TIRF controller.
4. Start the Camera.
5. Launch the manufacturer software.
6. Control hardware via software.
7. Clean the objective with a KIMTECH Science Precision Wipe and Isopropanol.
8. Place a small droplet of immersion oil on the pupil of the objective.

9. Clean the undersurface of the coverslip in the microscopy chamber with a KIMTECH Science Precision Wipe soaked in isopropanol and then rub the undersurface dry with a new dry KIMTECH Science Precision Wipe.
10. Prepared specimen is placed in a microscopy chamber (Fig. 3).
11. Pre-adjust the objective position/the focal plane.
12. Set the electron multiplier gain (EM-gain) to 300.
13. Choose frame transfer.
14. Image at full frame ( $512 \times 512 \text{ px}^2$ ) with 32 ms exposure time.
15. Monitor in live mode, and find the cells through the ocular or via the camera.
16. Searching for cells is done using a laser power of  $<1 \text{ mW}$  (appropriate for TMR<sup>HTL</sup>).
17. If possible, take an image of the entire cell (Fig. 4a).
18. Adjust the focal plane, the inclination angle, and the laser power.
19. Find an area in the cell periphery with distinct, elongated mitochondria (Fig. 4a framed, Fig. 4b, c).

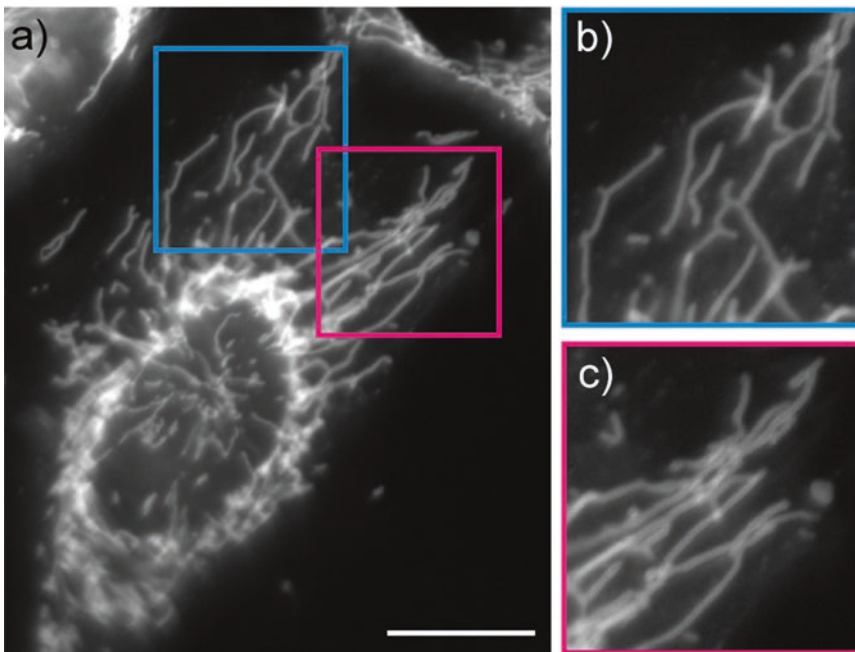


**Fig. 4** Selection of adequate regions of imaging with elongated, separated mitochondria. **(a)** Morphology of mitochondria throughout mammalian cells shows some diversity. Focus on cells with elongated, clearly separated mitochondria and select adequate regions of imaging (ROIs, *blue* and *magenta* frames) from the mitochondrial network for TALM image series. **(b)** and **(c)** ROIs with separated mitochondria as in **(b)** are preferred. Avoid recording ROIs with overlapping mitochondria as shown in **(c)**. Also, set small imaging regions for fast recording with short frame rates ( $>30 \text{ Hz}$ ) needed in single molecule tracking experiments. *Scale bar: 10  $\mu\text{m}$*  **(a)**

20. Adjust imaging area to the area of the separated, elongated mitochondria (e.g., 200 px × < 200 px) (Fig. 4b, c). A reduced imaging area allows for the increase of imaging frame rates (Hz). The higher the frame rate, the more accurate the step length determination (but in parallel the signal decreases due to reduced exposure and emission time, which lowers the localization precision) (*see* Table 1).
21. Adjust the HILO inclination angle to the specific region of interest, if necessary.
22. Adjust the laser power to 3.5–5.2 mW.
23. Start recording.
24. Image at least 3000 frames (*see* Notes 9–13).

### 3.8 Evaluation

Single molecule localization and tracking are post imaging processes that reveal a non-diffraction limited view of proteins localizations and their dynamic organization. Localization-based methods circumvent the diffraction barrier [6]. However, adjacent single fluorescent molecules still need to fulfill the Rayleigh criterion  $R$  to be seen as single signals.  $R$  is the minimum distance  $d$  between adjacent single fluorescent particles.

$$R = \frac{0.61\lambda}{NA},$$

where  $\lambda$  is the emission wavelength of the used fluorophore and NA is the numerical aperture of the used objective. For localization of single emitters, a modified 2D Gaussian mask for approximation is used [5–7] to determine the peak of single point spread functions in front of the cellular background. Localization data are rendered using Thompson blurring [10]. The localization precision  $\sigma_{xy}$  for each localized signal is given by:

$$\sigma_{xy}^2 = \frac{s^2 + q^2 / 12}{N} + \frac{8\pi s^4 b^2}{q^2 N^2}$$

where  $s$  is the standard deviation of the PSF,  $N$  is the number of recorded photons of the signal,  $q$  is the pixel size of the EMCCD camera chip divided by the total magnification, and  $b$  is the background noise per pixel of the illuminated region. For  $F_1F_0$ -ATP synthase TMR signals in the example shown (Fig. 2c), a mean localization precision of 5 nm was calculated from S/N. In order to localize fluorescent signals, a pixel conversion factor of the used setup needs to be handed over to the software. Be aware that the EM gain influences the pixel conversion factor. The positions of individual fluorescence emitters are determined with sub-pixel precision in a two-step process, which is developed for high-density single particle tracking as described previously in detail [1]. Initial emitter positions are identified using a pixel-wise statistical test

limiting the rate of false-positive detection to  $10^{-6}$  per pixel. The dimensions are fitted with a polynomial fit taking into account the microscope's PSF. In addition, TALM takes advantage that single, fluorescently labeled, mobile proteins travel along a biological structure. Therefore, the right labeling degree and exposure time are crucial. The first step for tracking is the localization of single fluorescent signals. From the localization data, single particle tracking is performed by using the multiple-target tracing (MTT) algorithm described by Serge et al. [11]. Several parameters like the exposure time, the image pixel size  $q$ , the  $NA$  of the used objective, and the emission wavelength of the imaged fluorophore have to be set before tracking algorithm can be started. Additionally parameters like the size of the detection box, the error rate, the performed deflation loops, and the particle offtime have to be selected. In order to track proteins with the MTT, a maximal diffusion coefficient has to be set. To avoid false connections of localized emitters, the maximal diffusion coefficient has to be set as small as possible. Therefore, the value has to be approximated to the lowest possible value and has to be adapted to the crowding level. This is an iterative process and needs some experience. The maximal diffusion coefficient in the MTT algorithm [11] stands for the maximal step size in all lateral directions and is not the mean diffusion coefficient of a single trajectory of a protein. Most of the mitochondrial proteins can be tracked with a maximal expected diffusion coefficient between  $0.2 \mu\text{m}^2/\text{s}$  and  $0.3 \mu\text{m}^2/\text{s}$ . Nevertheless, some small proteins may be faster and need higher  $D_{\text{max}}$  values. Step-length distributions are obtained from single molecule trajectories (five steps,  $\sim 160$  ms for exposure time of 32 ms). Average diffusion constants are finally determined by the slope in mean square displacement analysis (2–10 steps). When trajectories have been obtained, the user has to check for meaningful trajectories (no cross trajectories between adjacent mitochondria), and eventually adjust the settings<sup>3</sup> (see Notes 14–16).

---

## 4 Notes

1. Lyophilization is done according to standard protocol with a Lyophilisator Alpha 1–2 LD plus.
2. Localization and tracking procedure are described in 1, 6, 7, and 8.
3. Stable transfected cells are easier to handle and show more homogenous expression levels. Avoid fragmentation of mitochondria by any stress.

---

<sup>3</sup>The software cannot be provided due to copy right reasons. Please contact S.T. Hess laboratory.

4. Coverslips should be plasma cleaned on the day of use for cell seeding or coating.
5. Coating of coverslips improves results by increasing the signal-to-noise ratio.
6. Coated coverslips can be stored at  $-20^{\circ}\text{C}$  for a few days in cell culture dishes, sealed with parafilm.
7. Compare different fluorescent dyes functionalized with<sup>HTL</sup> and check specificity of labeling by co-staining with MitoTracker<sup>®</sup>. For co-staining, add MitoTracker<sup>®</sup>DeepRed FM in a final concentration of 500 nM.
8. Optimize labeling degree (0.5–20 nM), excitation power, and angle of incidence to obtain single molecule signals.
9. Choose a region in the periphery of a cell, where a mitochondrial network with separated, elongated mitochondria is seen.
10. Exposure time needs to be set as low as possible to avoid photon blur and as high as possible to increase the SNR.
11. Use frame transfer mode when using an EMCCD camera.
12. The given laser power refers to the used fluorescent dye TMR<sup>HTL</sup>. Adapt the laser power to the respective fluorophores.
13. Avoid phototoxic effects by not going beyond 10.000 frames per region of interest.
14. Check mitochondrial movement at any time by generating an overlay of rendered images from first 0~20 s of the time series to the following ~20 s interval until the last ~20 s. No shift of the mitochondrial shape should be seen (Fig. 5).
15. Adapt evaluation parameters, e.g., the maximal expected diffusion coefficient is dependent on the investigated membrane protein, the structure and composition of the membrane, possible supercomplex formation, etc. In general, free diffusing molecules are faster than molecules with anomalous diffusion. For outer membrane proteins a higher diffusion coefficient is expected than for inner membrane proteins. Diffusion coefficients are, in general, slower than expected from FRAP experiments that exclusively determine the diffusion coefficients from mobile molecules.
16. FPALM and MTT allow for watching the data processing. Use this feature to be sure that your chosen parameters are correct. Test different parameters on the same data sets and optimize parameters iteratively.

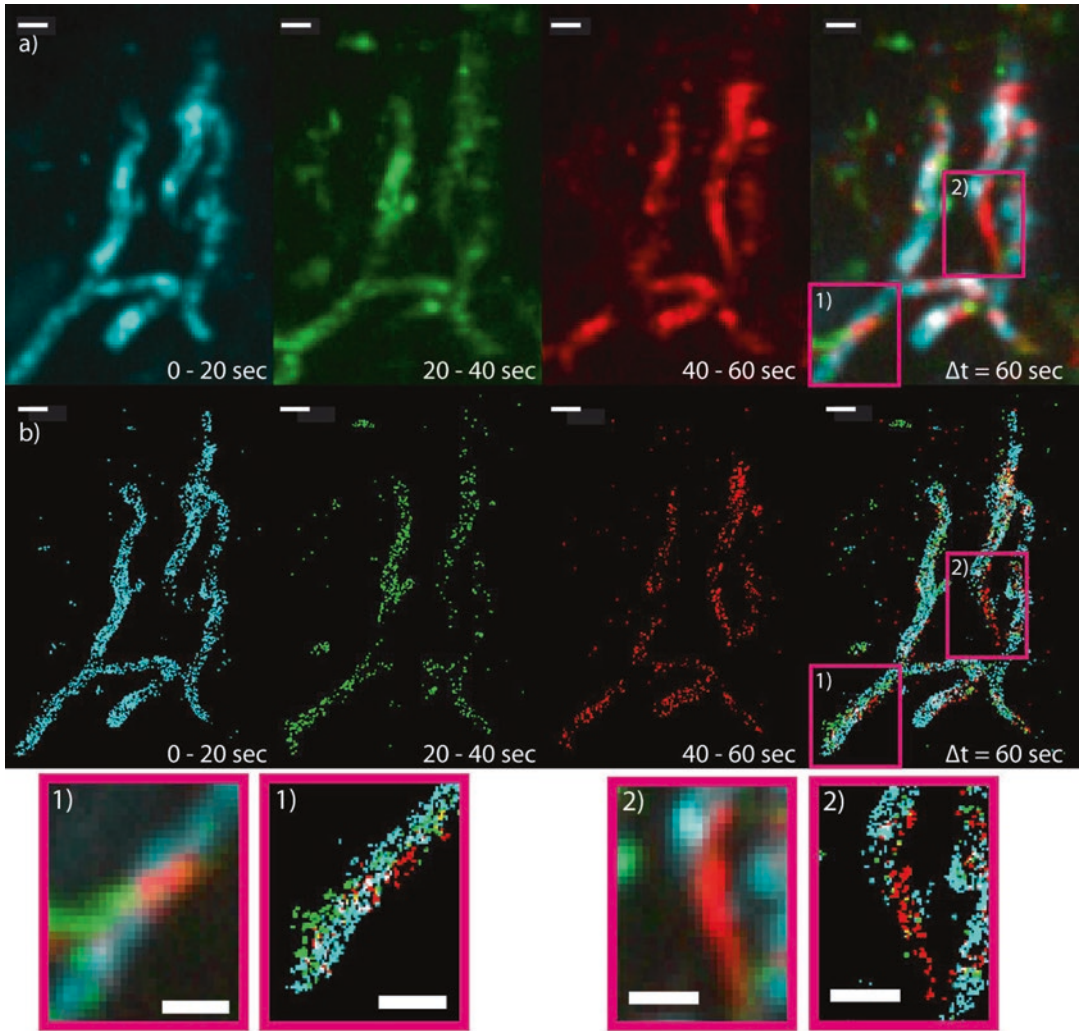


**Fig. 5** Investigation of Lateral Drift with FPALM. **(a)** Superimposed non-rendered signals from 1250 binned frames each color. Some parts of mitochondria moved (framed in superimposed image: 1, 2). Other parts of the mitochondrial network obviously did not move during recording and are suitable for single molecule localization and single molecule tracking analysis. **(b)** Same signals after localization and rendering. **(1)** and **(2)** Enlarged view of the areas where mitochondrial movement occurred. Analyses of subsequent time frames of ~20 s are generally suitable to exclude possible movement [1]. In most cases, time series of ~150 s can be used to image mitochondria without severe movement [12]. *Scale bars:* 1  $\mu\text{m}$

## References

1. Appelhans T, Richter CP, Wilkens V, Hess ST, Piehler J, Busch KB (2012) Nanoscale organization of mitochondrial microcompartments revealed by combining tracking and localization microscopy. *Nano Lett* 12: 610–616
2. Los GV, Encell LP, McDougall MG, Hartzell DD, Karassina N, Zimprich C, Wood MG, Learish R, Ohana RF, Urh M, Simpson D, Mendez J, Zimmerman K, Otto P, Vidugiris G, Zhu J, Darzins A, Klauert DH, Bulleit RF, Wood KV (2008) HaloTag: a novel protein labeling technology for cell imaging and protein analysis. *ACS Chem Biol* 3:373–382
3. Tokunaga M, Imamoto N, Sakata-Sogawa K (2008) Highly inclined thin illumination enables clear single-molecule imaging in cells. *Nat Methods* 5:159–161
4. Shannon, C. E. (1949) Communications in the presence of noise, *Proc. IRE* 37, 10–21.
5. Nyquist H (1928) Certain topics in telegraph transmission theory. *AIEE Trans* 47: 617–644
6. Gould TJ, Verkhusha VV, Hess ST (2009) Imaging biological structures with fluorescence photoactivation localization microscopy. *Nat Protoc* 4:291–308
7. Hess ST, Girirajan TPK, Mason MD (2006) Ultra-high resolution imaging by fluorescence photoactivation localization microscopy. *Biophys J* 91:4258–4272
8. Hess S. T., Gould T. J., Gunewardene M., Bewersdorf J., and Mason M. D. (2009) Ultrahigh resolution imaging of biomolecules by fluorescence photoactivation localization microscopy, micro and nano technologies in bioanalysis, Springer protocols 544 of the series: methods in molecular biology™, chapter 32, 483–522.
9. Graham FL, van der Eb AJ (1973) A new technique for the assay of infectivity of human adenovirus 5 DNA. *Virology* 52:456–467
10. Thompson RE, Larson DR, Webb WW (2002) Precise nanometer localization analysis for individual fluorescent probes. *Biophys J* 82:2775–2783
11. Serge A, Bertaux N, Rigneault H, Marguet D (2008) Dynamic multiple-target tracing to probe spatiotemporal cartography of cell membranes. *Nat Methods* 5:687–694
12. Lin SL, Peter KP, Rego EH, Gustafsson MGL (2011) Super-resolution 3D microscopy of live whole cells using structured illumination. *Nat Methods* 8:1044–1046

## Analysis of Yeast Mitochondria by Electron Microscopy

Ann-Katrin Unger, Stefan Geimer, Max Harner, Walter Neupert,  
and Benedikt Westermann

### Abstract

Budding yeast *Saccharomyces cerevisiae* represents a widely used model organism for the study of mitochondrial biogenesis and architecture. Electron microscopy is an essential tool in the analysis of cellular ultrastructure and the precise localization of proteins to organellar subcompartments. We provide here detailed protocols for the analysis of yeast mitochondria by transmission electron microscopy: (1) chemical fixation and Epon embedding of yeast cells and isolated mitochondria, and (2) cryosectioning and immunolabeling of yeast cells and isolated mitochondria according to the Tokuyasu method.

**Key words** Immunoelectron microscopy, Mitochondria, Organelle architecture, *Saccharomyces cerevisiae*, Tokuyasu cryosectioning, Transmission electron microscopy

---

## 1 Introduction

Mitochondria are double membrane-bounded organelles with a complex architecture [1–4]. They are enveloped by an outer and an inner membrane. The inner membrane is further subdivided into two compartments with different protein compositions: the inner boundary membrane, which is apposed to the outer membrane, and the cristae, which are large membrane invaginations accommodating the respiratory chain complexes. Cristae are connected to the inner boundary membrane through rather narrow junctions, called crista junctions. Thereby, the very narrow aqueous intermembrane space between the outer and the inner boundary membrane is linked to the intracrista space. The mitochondrial outer and inner membranes are physically connected by various protein complexes at contact sites. The aqueous inner compartment of mitochondria is called the matrix.

Budding yeast *Saccharomyces cerevisiae* is an important model organism to study various aspects of mitochondrial biology, including mitochondrial metabolism [5], biogenesis [6], dynamics [7], and inheritance [8]. Also, yeast turned out to be the prime organism

for the identification and mechanistic dissection of the molecular machinery that governs mitochondrial architecture. For example, the mitochondrial contact site and cristae organizing system, MICOS, is a large protein complex in the inner membrane that is crucial for the maintenance of crista junctions, inner membrane architecture, and formation of contact sites [9]. This complex was first discovered and characterized by three independent groups using yeast as a model organism [10–12] and then found to be conserved also in mammalian cells [13].

Transmission electron microscopy is an essential method to observe the ultrastructure of mitochondria and its changes upon mutation of relevant genes or perturbation of physiological conditions and to visualize mitochondrial contacts with other cellular membranes, such as the endoplasmic reticulum or the plasma membrane. Furthermore, immunoelectron microscopy is the method of choice for the localization of proteins in mitochondrial subcompartments. Our group has used electron microscopy recently to observe ultrastructural changes in mutants defective in mitochondrial inheritance [14, 15], lipid metabolism [16, 17], and cristae biogenesis [10, 18], to reconstruct the 3D structure of mitochondrial contacts with the plasma membrane by electron tomography [19], to localize the myosin motor protein Myo2 on isolated mitochondria [20], and to examine the localization of MICOS components at cristae junctions by immunoelectron microscopy [18].

A variety of different methods are available to observe mitochondrial ultrastructure by electron microscopy [21]. The choice of the appropriate method depends on the scientific question to be addressed, the available laboratory equipment, and also personal skills and preferences. This chapter is not intended to give a comprehensive overview of all available approaches and protocols. Rather, we provide detailed protocols of methods that we successfully utilized in our laboratory. We describe a standard protocol for chemical fixation of yeast cells, a protocol for chemical fixation of isolated mitochondria, and protocols for fixation and cryosectioning of yeast cells and isolated mitochondria using the Tokuyasu method [22]. Tokuyasu cryosectioning is very useful both for the visualization of mitochondrial membranes and for immunolabeling, which we also describe in this chapter. *See Fig. 1* for an overview of the methods described in this chapter. We anticipate that the protocols described here will be useful not only for the analysis of mitochondria, but can be easily adapted to the study of other cell organelles.

---

## 2 Materials

*Safety note:* many of the required chemicals are highly toxic. Make sure to take appropriate precautions to protect yourself and the environment.

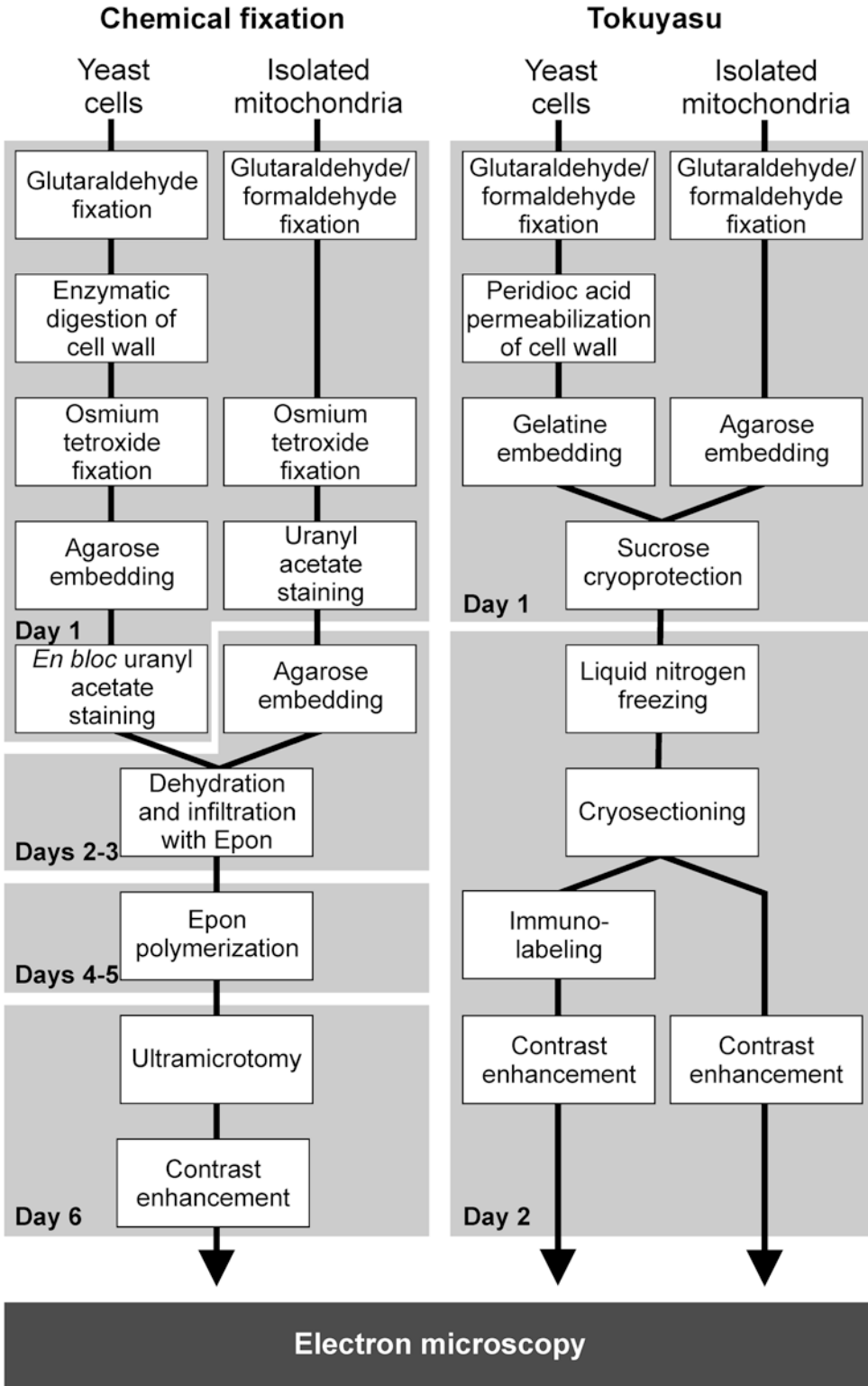


Fig. 1 Work flow of the methods described in this chapter

## 2.1 Chemical Fixation of Yeast Cells and Isolated Mitochondria

1. PBS: 8.1 mM Na<sub>2</sub>HPO<sub>4</sub>, 1.5 mM NaH<sub>2</sub>PO<sub>4</sub>, 150 mM NaCl, adjust pH with HCl to pH 7.4.
2. CaCo buffer: 0.1 M sodium cacodylate, 1 mM CaCl<sub>2</sub>, adjust pH with HCl to pH 7.2.
3. 25% glutaraldehyde stock in water: EM grade, high purity (Serva, Heidelberg, Germany; cat.no. 23114.02). Purchase as such and store at 4 °C.
4. 16% formaldehyde stock in water: EM grade, high purity (16% stock; Plano, Wetzlar, Germany, cat. no R1026). Needed only for chemical fixation of isolated mitochondria (*see* Subheading 3.2). Purchase as such and store at 4 °C.
5. 2.5% (w/v) sucrose; needed only for chemical fixation of isolated mitochondria (*see* Subheading 3.2).
6. 2% (v/v) glutaraldehyde in CaCo buffer for chemical fixation of yeast cells (*see* Subheading 3.1) or 1.5% (v/v) glutaraldehyde, 3% (v/v) formaldehyde, and 2.5% (w/v) sucrose in CaCo buffer for chemical fixation of isolated mitochondria (*see* Subheading 3.2).
7. Zymolyase 20T from *Arthro bacter luteus* (Seikagaku Biobusiness, Tokyo, Japan): 1.0–3.0 mg/ml dissolve freshly in 50 mM Tris–HCl, pH 7.5, 5 mM MgCl<sub>2</sub>, 1.4 M sorbitol, 0.5% (v/v) β-mercaptoethanol. Needed only for chemical fixation of yeast cells (*see* Subheading 3.1).
8. 2% (w/v) osmium tetroxide (OsO<sub>4</sub>) stock: carefully break glass ampule containing 500 mg crystalline OsO<sub>4</sub> (Carl Roth, Karlsruhe, Germany; cat. no. 8371.2) and dissolve overnight at 4 °C in 20 ml ddH<sub>2</sub>O in a light-tight reaction bottle. Prepare under fume hood and wear eye protection. Store at 4 °C.
9. 1.6% (w/v) potassium ferrocyanide stock: dissolve 0.32 g of K-ferrocyanide (II) in 20 ml ddH<sub>2</sub>O in a light-tight reaction bottle, stir until dissolved and store at 4 °C.
10. 2% (w/v) agarose: add 1 g of agarose Type I-A, low EEO (Sigma-Aldrich, St. Louis, MO, USA, cat. no. A0169) to 50 ml ddH<sub>2</sub>O, heat the solution until dissolved.
11. 2% (w/v) uranyl acetate stock: add 1 g uranyl acetate (Electron Microscopy Sciences, Hatfield, PA, USA; cat. no. 22,400) to 50 ml ddH<sub>2</sub>O, stir until dissolved in a light-tight bottle, store at 4 °C.
12. Graded series of ethanol, propylene oxide, and Epon (*see* Subheadings 3.1, **step 8** and Subheading 3.2, **step 7**). Use 2 ml per sample. Use ethanol p.a. kept free of residual water by a molecular sieve.
13. As embedding resin, we use an Epon-812 [23] replacement (will be termed Epon in this chapter) which consists of the following four components: 2-dodecenylsuccinic acid anhydride

(DDSA) (Serva, Heidelberg, Germany, cat. no: 20755.01), glycid ether 100 (Serva, Heidelberg, Germany, cat. no: 21045.02), methylnadic anhydride (MNA) (Serva, Heidelberg, Germany, cat. no: 29452.02), 2,4,6-tris(dimethylaminomethyl) phenol (Serva, Heidelberg, Germany, cat. no: 36975.03). For EponA mix 75.64 g glycid ether 100 with 95 g DDSA in a disposable plastic beaker. For EponB, mix 122 g glycid ether 100 and 115.7 g MNA in a separate beaker. Cover both beakers with parafilm and stir at room temperature to obtain homogenous mixtures. Then mix 150 g EponA with 220 g EponB. Again, cover the beaker with parafilm and stir at room temperature to obtain a homogenous mixture. Finally, add 6.5 ml of the catalyst EponC (2,4,6-tris(dimethylaminomethyl) phenol) while stirring. As soon as the solution adopts a homogenous yellowish to brownish color, prepare 10 ml aliquots and store at  $-20^{\circ}\text{C}$ .

14. Lead citrate solution: freshly degas ddH<sub>2</sub>O by boiling for 10 min, dissolve 1.33 g Pb(NO<sub>3</sub>)<sub>2</sub> (Merck, Darmstadt, Germany, cat. no. 1.07398.0100) in 15 ml degassed ddH<sub>2</sub>O, dissolve 1.76 g tri-sodium citrate, Na<sub>3</sub>(C<sub>6</sub>H<sub>5</sub>O<sub>7</sub>)•2H<sub>2</sub>O (Sigma-Aldrich, St. Louis, MO, USA, cat. no.W302600), in 15 ml degassed ddH<sub>2</sub>O. Mix both solutions (white precipitation occurs) and leave the mixture for 30 min at room temperature, shake the solution, add 8 ml freshly prepared 1 M NaOH (precipitation disappears), fill up with 12 ml ddH<sub>2</sub>O, aliquot in 2 ml reaction tubes, and store at 4 °C. Centrifuge before use to remove precipitates.

## **2.2 Tokuyasu Cryosectioning and Immunolabeling**

1. 0.2 M stock PHEM buffer pH 6.9 (120 mM PIPES, 50 mM HEPES, 4 mM MgCl<sub>2</sub>, 20 mM EGTA): dissolve three NaOH pellets in 75 ml ddH<sub>2</sub>O, add 3.63 g PIPES and stir at room temperature until the solution is clear, confirm that the pH is between 6.8 and 7.2, add 1.19 g HEPES, 0.08 g MgCl<sub>2</sub>, and 0.76 g EGTA while stirring, adjust to pH 6.9 with 1 M NaOH, add ddH<sub>2</sub>O to bring the volume to 100 ml, and store the buffer at 4 °C.
2. 1× fixation buffer: 2% (v/v) formaldehyde, 0.2% (v/v) glutaraldehyde (*see* Subheading 2.1, items 3 and 4) in 0.1 M PHEM buffer. Prepare 10 ml fixation buffer per sample.
3. 2× fixation buffer: 4% (v/v) formaldehyde, 0.4% (v/v) glutaraldehyde in 0.1 M PHEM buffer. Prepare 10 ml fixation buffer per sample.
4. 1% (w/v) freshly prepared periodic acid (H<sub>5</sub>IO<sub>5</sub>) in 0.1 M PHEM buffer. Prepare 1 ml per sample.
5. 12% (w/v) gelatine (powder, food quality) in 0.1 M PHEM buffer. Needed only for Tokuyasu cryosectioning of yeast cells

(see Subheading 3.3). Add 12 g of gelatine to 75 ml of 0.1 M PHEM buffer and stir for 10 min at room temperature. Incubate the solution for 4–6 h at 60 °C until the gelatine is dissolved. Cool the solution down to 37 °C and add 0.1 M PHEM buffer to a total volume of 100 ml while gently stirring. Prepare 10 ml aliquots and store at 4 °C. Warm up to 37 °C before use. Use 1 ml of gelatine per sample.

6. 2.3 M sucrose in 0.1 M PHEM buffer.
7. Uranyl oxalate pH 7.0: Add 50 ml of 4% (w/v) uranyl acetate to 50 ml of 0.15 M oxalic acid while stirring, adjust pH 7.0 with ammonium hydroxide (25% stock, NH<sub>4</sub>OH) under constant stirring; filter the solution through a filter (0.45 µm) and store at 4 °C in the dark.
8. 2% (w/v) methyl cellulose: heat 45 ml ddH<sub>2</sub>O to 90 °C, start stirring, and add 1 g of methyl cellulose 25 centipoises (Sigma Aldrich, St. Louis, MO, USA, cat. no. M-6385). Cool the solution down on ice, seal it with parafilm, and stir overnight at 4 °C. Leave the solution two more days at 4 °C without stirring. Bring the volume to 50 ml with ddH<sub>2</sub>O, centrifuge for 1.5 h at 20,000 × g, and store the supernatant at 4 °C in the dark.
9. Methyl cellulose/uranyl acetate, pH 4.0: add 9 ml of 2% methyl cellulose to 1 ml of 4% (w/v) uranyl acetate filtered through 0.45 µm, mix gently, and store at 4 °C in the dark.
10. Ruthenium red solution: add a few mg ruthenium red to 50 ml ddH<sub>2</sub>O until the color is red. Needed only for Tokuyasu cryosectioning of isolated mitochondria (see Subheading 3.4).
11. 2% (w/v) low-melting point agarose in ddH<sub>2</sub>O, needed only for Tokuyasu cryosectioning of isolated mitochondria (see Subheading 3.4). Add 1 g of low melting agarose to 50 ml ddH<sub>2</sub>O and heat the solution until the agarose is dissolved. Let the solution cool down at RT before use.

### 2.2.1 Additional Materials for Immunolabeling

1. 1% (w/v) bovine serum albumin (BSA) in PBS.
2. 0.02 M glycine in PBS (dissolve 0.075 g glycine in 50 ml PBS).
3. 2% (w/v) gelatine in 0.1 M PHEM buffer. Fill the gelatine in petri dishes with 5 cm diameter, seal with parafilm, and store at 4 °C.
4. 1% glutaraldehyde (see item 3 of Subheading 2.1) in PBS.
5. Blocking buffer (1% (w/v) BSA, 0.5% (v/v) cold-water fish skin gelatine, 0.01% (w/v) BSA-c<sup>TM</sup> (Aurion, Wageningen, The Netherlands) in PBS).
6. Specific antibodies.
7. Protein A-gold (10 nm size). Prepare the protein A-gold solution freshly. Add 2 µl of protein A-gold to 98 µl of 1% BSA in

PBS (the color should be a very faint pink). Vortex immediately and spin down aggregates by centrifugation for 30 s at full speed in a microfuge ( $12,000 \times g$ ). Place on ice until use.

### 2.3 Major Equipment

1. To prepare ultrathin sections of samples embedded in Epon (*see* Subheadings 3.1 and 3.2), we use a Leica Ultracut UCT ultra microtome equipped with a diamond knife. For cryo-ultramicrotomy after Tokuyasu fixation (*see* Subheadings 3.3 and 3.4) we use a Leica EM UC6i ultramicrotome equipped with a FC6 cryo-chamber and a diamond knife.
2. Samples can be viewed in standard transmission electron microscopes. We have two EM setups available: a Zeiss CEM 902A TEM equipped with a tungsten filament and a 1.3 megapixel camera (Gatan Erlangshen ES500W), and a JEOL JEM-2100 TEM equipped with a LaB<sub>6</sub> emitter, a 4k camera (Gatan UltraScan 4000) and a 1.3 megapixel camera (Gatan Erlangshen ES500W).

---

## 3 Methods

### 3.1 EM of Yeast Cells After Chemical Fixation

Glutaraldehyde and osmium tetroxide are well-established reagents for chemical fixation of biological samples for electron microscopy [21, 24]. We describe a method for chemical fixation that includes the removal of the rather thick yeast cell wall by enzymatic digestion to facilitate the diffusion of fixatives and contrast-enhancing reagents into the cell. This method is based on a slightly modified protocol according to Bauer et al. [25] combined with contrast enhancement according to Reynolds [26].

Overview of the method: Cells are harvested, washed, and then fixed with 2% glutaraldehyde. Glutaraldehyde efficiently immobilizes proteins by covalently cross-linking primary amino groups. In the next step, the cell wall is digested with zymolyase, an enzyme isolated from *Arthrobacter* sp. that hydrolyzes linear glucose polymers with  $\beta$ -1,3-linkages in yeast cell walls. A second fixation with potassium ferrocyanide-reduced osmium tetroxide is used for fixation of lipids and staining of membranes. Osmium tetroxide oxidizes unsaturated fatty acids and is reduced to osmium dioxide that adds contrast to the sample. Then, yeast cells are embedded in agarose to facilitate handling of the sample. En bloc staining with uranyl acetate is used to further enhance the contrast. The sample is then dehydrated with a graded ethanol series and infiltrated with Epon using propylene oxide as intermediate solvent [23]. After polymerization of Epon, ultrathin sections are prepared at room temperature. After mounting on copper grids contrast is enhanced by post-staining the sections with uranyl acetate followed by lead citrate.

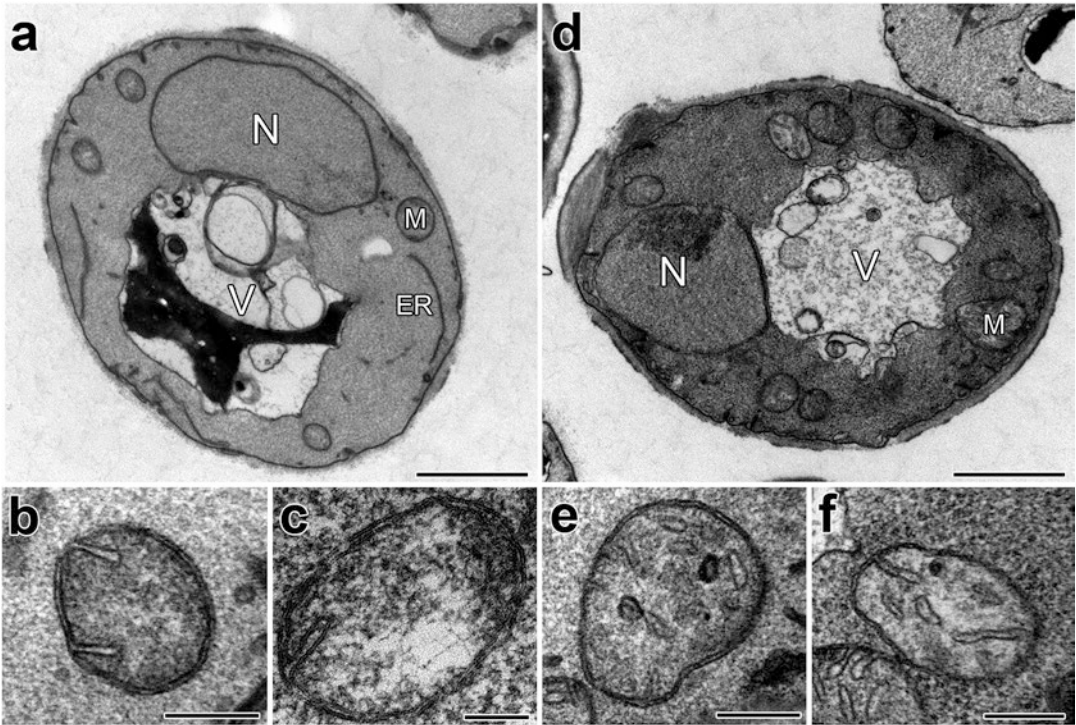


**Fig. 2** Electron microscopy of yeast cells after chemical fixation. **(a)** *Saccharomyces cerevisiae* strain YPH499 [32] grown on glucose-containing YPD medium. *ER* endoplasmic reticulum, *M* mitochondrion, *N* nucleus, *V* vacuole; bar 1  $\mu\text{m}$ . **(b, c)** Mitochondria of cells grown on YPD medium. Bars, 200 nm. **(d)** YPH499 cells grown on non-fermentable glycerol-containing YPG medium. Bar, 1  $\mu\text{m}$ . **(e, f)** Mitochondria of cells grown on YPG medium. Bars, 200 nm

The advantages of this method are that handling is relatively easy and no special equipment is needed. On the other hand, zymolyase treatment has to be optimized for each strain and growth condition and sample preparation is rather time-consuming. The protocol is not useful for immunolabeling, because most antigens are masked or destroyed by high glutaraldehyde and osmium tetroxide concentration and Epon embedding. See Fig. 2 for examples of electron microscopy of chemically fixed yeast cells.

1. Grow yeast cells in 25 ml liquid medium overnight to logarithmic growth phase ( $\text{OD}_{600}$  0.5) (see Note 1).
2. Harvest the cells by centrifugation for 10 min at  $2300 \times g$  and wash in 10 ml PBS at room temperature.
3. For glutaraldehyde fixation, add 10 ml of a solution of 2% (v/v) glutaraldehyde in CaCo buffer, gently resuspend the cells, and incubate for 30 min at 4  $^{\circ}\text{C}$ . Then resuspend and wash three times in 10 ml CaCo buffer ( $2300 \times g$ , 5 min).

4. For the digestion of the cell wall, resuspend the cells in 10 ml 50 mM Tris-HCl, pH 7.5, 5 mM MgCl<sub>2</sub>, 1.4 M sorbitol, 0.5% (v/v)  $\beta$ -mercaptoethanol and add the desired amount of zymolyase 20 T (final concentration about 1.0–3.0 mg/ml; *see Note 2*). Incubate for 10 min at room temperature. Wash two times in 10 ml CaCo buffer, transfer the cells to a 1.5 ml microfuge tube, wash again in 1 ml CaCo buffer (centrifuge for 5 min at 1700  $\times g$  in a microfuge), and discard the supernatant.
5. For potassium ferrocyanide-reduced osmium tetroxide fixation, add 250  $\mu$ l 2% OsO<sub>4</sub>, 250  $\mu$ l H<sub>2</sub>O, and 500  $\mu$ l 1.6% K-ferrocyanide (II) (*see Note 3*). Vortex the cells for at least 20 s to obtain a homogeneous suspension. Incubate for 5 min at 4 °C, spin down the cells, and repeat the fixation step. Wash three times in 1 ml ddH<sub>2</sub>O by centrifuging at 1700  $\times g$  for 5 min.
6. To start agarose embedding, freshly prepare a 2% (w/v) agarose solution and allow it to cool down to about 40–50 °C. Use a toothpick to stir the cell pellet to loosen it before adding the agarose. Add the same volume of agarose to the cell pellet and vortex immediately until the suspension is homogeneous. Put the sample on ice or into the fridge for a few minutes to allow the agarose to solidify. Carefully remove the sample from the microfuge tube (*see Note 4*). Place the sample in a drop of ddH<sub>2</sub>O on a microscope slide, cut blocks of about 1 mm<sup>3</sup> volume, and place them into a fresh 1.5 ml reaction tube (up to ten blocks of the same sample can be placed in the same reaction tube) filled with ddH<sub>2</sub>O. Wash three times for 10 min at room temperature by removing the water using a plastic Pasteur pipette tip with a narrow opening (*see Note 5*).
7. For en bloc staining, incubate the agarose block in 1.5 ml 1% (w/v) uranyl acetate overnight at 4 °C or for 90 min at room temperature.
8. Prepare 30, 50, 70, 95, and 100% ethanol solutions and store them at 4 °C (30%, 50%) or –20 °C (70–100%) until use. Prepare and pre-cool (–20 °C) ethanol/propylene oxide mixture (1:1), pure propylene oxide, and Epon/propylene oxide mixtures (1:3, 1:1, 3:1).
9. Before dehydration and Epon infiltration, remove the uranyl acetate solution and wash the sample for 5 min in H<sub>2</sub>O. Dehydrate the sample according to the following scheme (*see Note 6*). Use plastic Pasteur pipettes with a narrow opening and use 2 ml of each solution per sample.  
30% ethanol, 15 min at 4 °C.  
50% ethanol, 15 min at 4 °C.

70% ethanol, 15 min at  $-20^{\circ}\text{C}$ .

95% ethanol, 15 min at  $-20^{\circ}\text{C}$ .

Three times 100% ethanol, 20 min each at  $-20^{\circ}\text{C}$ .

Ethanol/propylene oxide (1:1), 15 min at  $-20^{\circ}\text{C}$ .

Two times pure propylene oxide, 15 min each at  $-20^{\circ}\text{C}$ .

Proceed with the infiltration according to the following scheme:

Epon/propylene oxide (1:3), 3 h at  $-20^{\circ}\text{C}$ .

Epon/propylene oxide (1:1), overnight at  $-20^{\circ}\text{C}$ .

Epon/propylene oxide (3:1), 3 h at room temperature.

Pure Epon; 3 h at room temperature (*see Note 7*).

Change Epon and incubate overnight at room temperature (*see Note 8*).

10. To prepare for Epon polymerization, fill two drops of Epon into BEEM<sup>®</sup> capsules or the cavities of an embedding mold, add a single agarose block per capsule/cavity, and fill up with fresh Epon. Polymerize for about 48 h at  $60^{\circ}\text{C}$ .
11. The sample is now ready for trimming and sectioning. Cut ultrathin sections of 50–70 nm and retrieve sections on pioloform-coated copper slot grids.
12. For contrast enhancement, place the grid with the section down on a droplet of 2% (w/v) uranyl acetate (*see Note 9*) in a petri dish, cover the petri dish (uranyl acetate is sensitive to light), and incubate the grid for 25 min at room temperature. Wash the grid with the section down in a series of drops of ddH<sub>2</sub>O (in total four drops, incubate three times for 1 min followed by one time for 2 min). Place the grid on a droplet of lead citrate in a petri dish, cover the petri dish, and incubate for 2.5 min. Wash the grid with the section down in a series of drops of ddH<sub>2</sub>O (in total six drops, four times for 1 min, two times for 2 min), pick up the grid with forceps, and carefully remove the water using a piece of filter paper. Dry the grid for at least an hour before examination in the transmission electron microscope. Grids can be stored indefinitely at room temperature.

### **3.2 EM of Isolated Mitochondria After Chemical Fixation**

Mitochondria isolated by differential centrifugation [27, 28] can be manipulated *in vitro* in various assays and analyzed by electron microscopy after chemical fixation [29]. However, possible changes of ultrastructure that might occur during isolation or manipulation of mitochondria have to be considered. For example, the mitochondrial outer membranes tend to fuse during centrifugation. This can be avoided by the addition of EDTA or another inhibitor of the GTP-dependent fusion machinery during the isolation procedure. Furthermore, if preservation of mitochondrial ultrastructure is critical, the organelles have to be always treated gently to

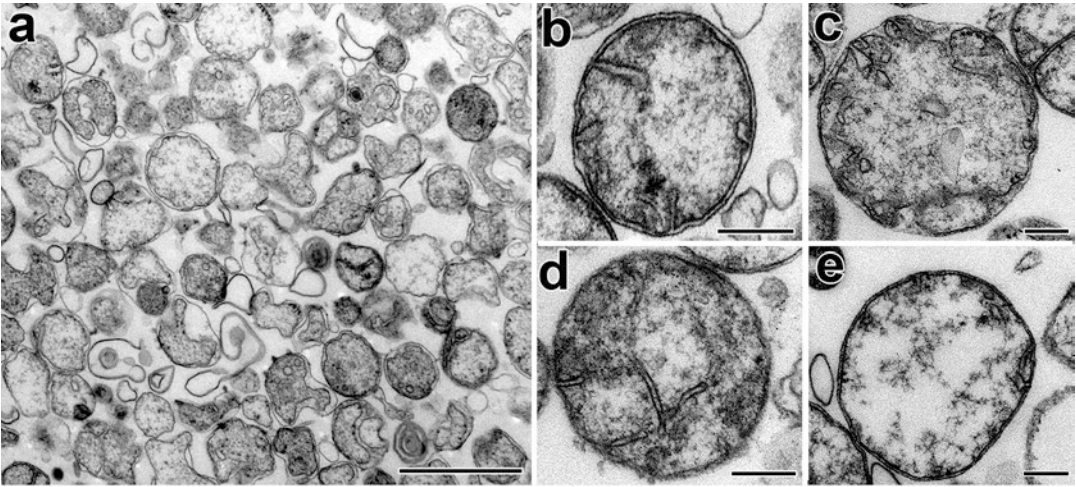


**Fig. 3** Electron microscopy of isolated mitochondria after chemical fixation. **(a)** Overview of a region of the organelle pellet containing a high portion of intact mitochondria. Bar, 1  $\mu\text{m}$ . **(b–e)** Mitochondria isolated from wild-type cells grown on respiratory media. Bars, 200 nm

avoid unnecessary physical forces. Moreover, depending on the osmotic conditions used, swelling or shrinking of the mitochondrial matrix will be observed. The general procedure for fixation is very similar to chemical fixation of yeast cells described above (*see* Subheading 3.1). As mentioned above, this protocol is not suitable for immunolabeling. *See* Fig. 3 for examples of electron microscopy of isolated mitochondria after chemical fixation.

1. Spin down the mitochondria at  $13,000 \times g$  in a 1.5 ml microfuge tube. The pellet should be compact and have a diameter of 2–4 mm.
2. For fixation, add 1 ml of a solution of 1.5% (v/v) glutaraldehyde, 3% (v/v) formaldehyde, and 2.5% (w/v) sucrose (*see* Note 10) in CaCo buffer (*see* Note 11) to the mitochondrial pellet, gently detach the pellet from the wall of the tube by carefully agitating, and incubate for 1 h at 4 °C. During the incubation time, gently agitate the tube from time to time and change the fixation buffer twice, using a plastic Pasteur pipette with a narrow opening (*see* Note 12).
3. Remove the fixation buffer carefully, but not completely, using a Pasteur pipette tip with a narrow opening (*see* Note 13). Wash the pellet by carefully adding 1 ml ddH<sub>2</sub>O and incubate for 10 min at room temperature. Repeat the washing step twice. Incubate the pellet in 1 ml 1% (v/v) OsO<sub>4</sub> for 1 h at 4 °C (*see* Note 3). Wash four times for 10 min with 1 ml ddH<sub>2</sub>O at room temperature.

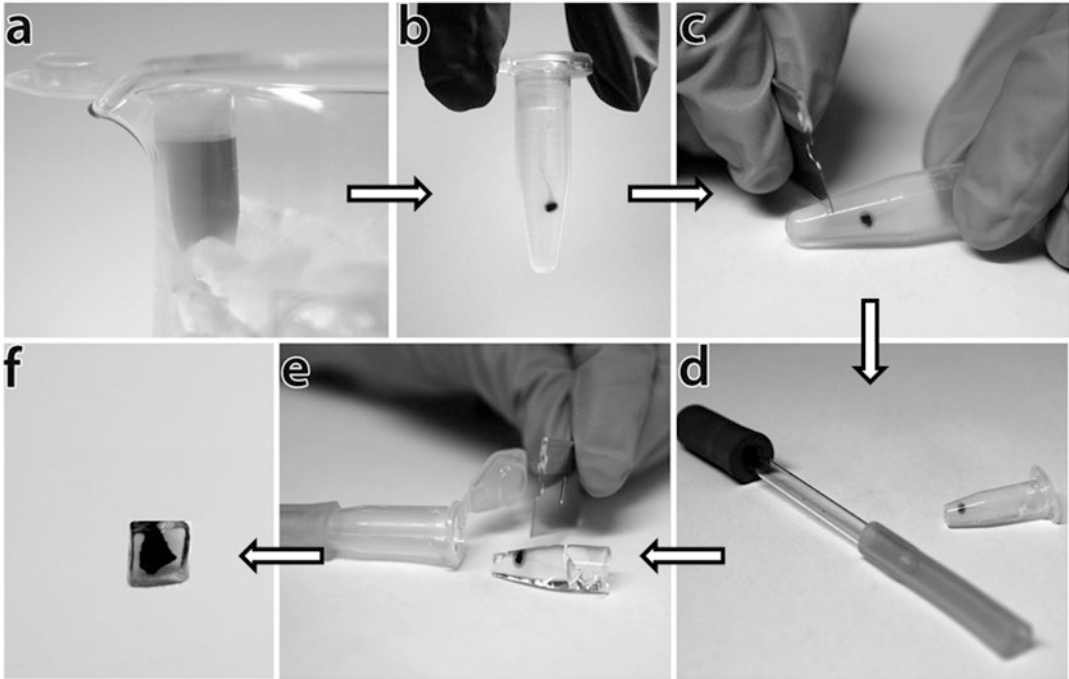


**Fig. 4** Agarose embedding of isolated mitochondria. (a) To allow the agarose to solidify first at the bottom of the tube, place the microfuge tube with its tip on ice (the agarose was stained to make it visible on the photograph). (b) The ruthenium red-stained pellet should be located somewhere in the middle of the tube after the agarose has solidified. (c) The tip of the tube is cut off using a single edge razor blade. (d) To remove the agarose from the tube we use a device assembled from a rubber bulb, a glass Pasteur pipette with a broken tip, and a rubber tube of suitable diameter. (e) This device is used to blow the agarose block out of the microfuge tube to facilitate further trimming with a razor blade. (f) The sample is ready for dehydration and Epon embedding or cryo-protection, respectively

4. Incubate the pellet overnight in 1.5 ml 0.5% uranyl acetate at 4 °C. Wash the pellet three times in 1 ml ddH<sub>2</sub>O.
5. Carefully remove the pellet from the tube and place it into a drop of water. Cut the pellet into pieces of about 1 mm<sup>3</sup> (see **Note 14**).
6. To start agarose embedding (Fig. 4), freshly prepare a 2% (w/v) agarose solution and allow it to cool down to about 40–50 °C. Fill a 1.5 ml microfuge tube with warm agarose and place its tip on ice for 2 min to allow the agarose to solidify first at the bottom of the tube. Then add the sample (only one sample per reaction tube, it should be located in the middle of the reaction tube), close the tube, and cover it completely with ice for a few minutes. Cut off the tip of the tube, remove the agarose block, and recover the sample by removing most of the agarose using a razor blade. Leave some agarose around the sample and put it into a 2 ml reaction tube filled with ddH<sub>2</sub>O.

7. Prepare 30, 50, 70, 90, and 100% ethanol solutions and store them at 4 °C (30%, 50%) or -20 °C (70–100%) until use. Prepare and pre-cool (-20 °C) ethanol/propylene oxide mixture (1:1), pure propylene oxide, and an Epon/propylene oxide mixture (1:1).
8. Wash the sample for 5 min in 2 ml ddH<sub>2</sub>O. For dehydration and Epon infiltration, add increasing concentrations of ethanol, propylene oxide, and Epon according to the following scheme and incubate at the indicated temperatures (*see Note 6*):
  - 30% ethanol, 15 min at 4 °C.
  - 50% ethanol, 15 min at 4 °C.
  - 70% ethanol, 15 min at -20 °C.
  - 90% ethanol, 15 min at -20 °C.
  - Two times 100% ethanol, 20 min each at -20 °C.
  - Ethanol/propylene oxide (1:1), 15 min at -20 °C.
  - Two times pure propylene oxide, 15 min each at -20 °C.
  - Epon/propylene oxide (1:1), over-night at -20 °C.

Warm the sample to room temperature, open the tube, and allow the propylene oxide to evaporate for 6–8 h at room temperature (*see Note 15*). Put the sample into a new tube, cover it with fresh Epon, and incubate overnight at room temperature (*see Note 16*).
9. Place the sample in the cavity of an embedding mold containing some drops of Epon, orient the sample in the desired way, fill the cavity completely with Epon, and polymerize for about 48 h at 60 °C.
10. Continue with **step 11** as described above (*see Subheading 3.1*).

### **3.3 Tokuyasu Cryosectioning and Immunolabeling of Yeast Cells**

The Tokuyasu method [22] combines chemical fixation with infiltration of sucrose as cryo-protectant and cryosectioning. The procedure preserves antigens because it avoids the use of high glutaraldehyde concentrations, osmium tetroxide, dehydration, and plastic embedding. It yields a clear negative contrast of cellular membranes and permits immunogold labeling. The protocol described here is based on the procedure published by Griffith et al. [30].

Overview of the method: Cells are fixed with formaldehyde/glutaraldehyde under relatively mild conditions that preserve epitopes for immunolabeling. In the next step, the yeast cells are treated with periodic acid to permeabilize the cell wall [31]. To facilitate handling of the sample, cells are embedded in gelatine. Infiltration with sucrose serves as a cryo-protectant to prevent ice crystal formation when the sample is frozen. The sample is then frozen in liquid nitrogen and sectioned in a frozen state. Ultrathin sections are retrieved on methyl cellulose/sucrose and warmed up to room temperature. Staining with uranyl oxalate and uranyl

acetate yields negative contrast. Sections can be either viewed directly by transmission electron microscopy or be further treated for immunogold labeling [30].

The advantages of this method are that it yields a superb contrast of organellar membranes, antigens are preserved for immunolabeling, and the procedure is relatively fast. On the other hand, the procedure depends on the availability of a cryo-ultramicrotome, large amounts of liquid nitrogen are consumed, and pickup and contrast enhancement of cryosections are rather difficult and require some practice. *See* Fig. 5 for examples of electron microscopy of yeast cells after Tokuyasu cryosectioning.

1. Grow yeast cells in 10 ml liquid medium overnight to logarithmic growth phase ( $OD_{600}$  0.8–1.2).
2. For fixation, harvest the cells by centrifugation at  $2300 \times g$ , resuspend them in 10 ml  $2\times$  fixation buffer, and incubate for 20 min at room temperature on a roller. Centrifuge again, resuspend the cells in 10 ml  $1\times$  fixation buffer, incubate for 2.5–4 h at room temperature on a roller (the longer this fixation step is, the better), pellet the cells, and resuspend them in 1.5 ml 0.1 M PHEM buffer. Wash the cells three times in 1.5 ml 0.1 M PHEM buffer (centrifuge for 30 sec at full speed in a microfuge, i.e.,  $17,000 \times g$ ).
3. To permeabilize the yeast cell wall, add 1 ml freshly prepared 1% periodic acid in 0.1 M PHEM buffer, gently resuspend the cells, and incubate for 1 h at room temperature on a roller. During the incubation time, pre-warm 12% gelatine in 0.1 M PHEM buffer to  $37^\circ\text{C}$ . Wash the cells three times in 1.5 ml 0.1 M PHEM buffer (*see* **Note 17**).
4. To embed the cells, resuspend them in 1 ml 12% (w/v) gelatine in 0.1 M PHEM buffer and incubate for 10 min at  $37^\circ\text{C}$ . Gently mix one or two times during the incubation. Centrifuge for 3 min at room temperature at full speed in a microfuge (use a swing-out rotor if available) to concentrate the cells (do not remove the supernatant). Incubate for 15 min at  $4^\circ\text{C}$ , remove the solidified sample from the tube (cut off the tip of the tube where the cells are concentrated and carefully remove the sample using a toothpick), place it in a drop of 0.1 M PHEM buffer on a microscope slide, and cut blocks of about  $1\text{ mm}^3$  volume.
5. For cryo-protection, immerse all blocks of the same sample in a 2 ml tube filled with 2.3 M sucrose in 0.1 M PHEM buffer and incubate overnight at  $4^\circ\text{C}$  under agitation.
6. Mount the sample on an ultramicrotome specimen holder (use aluminum or copper pins), remove surplus sucrose with filter paper (some sucrose should remain on the sample as glue to hold it on the pin), and freeze the sample by plunging into liquid nitrogen.

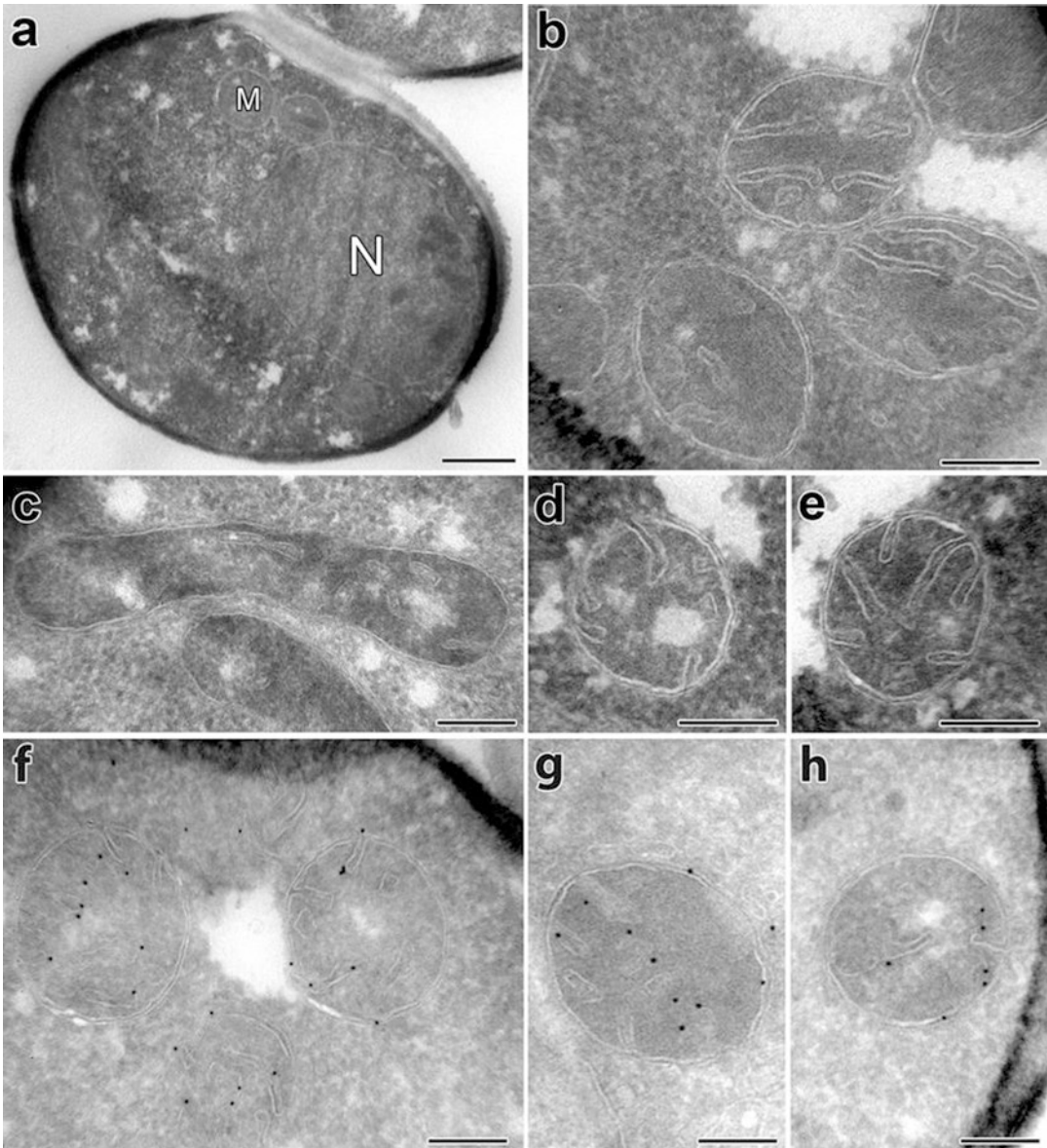


**Fig. 5** Electron microscopy of yeast cells after Tokuyasu cryosectioning. (a) *Saccharomyces cerevisiae* strain YPH499 [32] grown on non-fermentable glycerol-containing YPG medium. M mitochondrion, N nucleus; bar, 500 nm. (b–e) Mitochondria of cells grown on YPG medium. Bars, 200 nm. (f–h) Immunogold labeling of yeast cells expressing a subunit of the ATP synthase, Atp2, fused to a triple HA tag (Atp2-3xHA). Cells were grown on glycerol-containing YPG medium. Bars, 200 nm

7. Prepare the pickup solution half an hour before sectioning: mix 2% (v/v) methyl cellulose solution with the same volume of 2.3 M sucrose (in 0.1 M PHEM buffer) solution, place it on a rotator at 4 °C until it is homogeneous, and keep it together with Formvar-coated mesh grids on ice (*see Note 18*) until use.

8. After trimming the sample to a suitable size, cut 50 nm sections at  $-120^{\circ}\text{C}$ . Shift flat ribbons of sections with an eyelash from the knife-edge and pick up in a wire loop filled with a drop of pickup solution (1% methyl cellulose, 1.15 M sucrose in PHEM buffer). Thaw sections on the pickup droplet and transfer them, sections downward, onto Formvar-coated copper grids.
9. (a) If no immunolabeling is required, place the grid, section downward, on a drop of PBS, incubate for 20 min at  $37^{\circ}\text{C}$ , and then incubate on a drop of ddH<sub>2</sub>O for 20 min at  $37^{\circ}\text{C}$ . Continue with **step 11**.  
(b) If immunolabeling is required, place the grid, section downward, on 2% gelatine in 0.1 M PHEM buffer in a small petri dish (diameter 5 cm), and incubate for 40 min at  $37^{\circ}\text{C}$ .
10. For immunolabeling, prepare a long strip of parafilm with a series of drops (prepare them right before they are needed) for the following incubations: incubate six times for 2 min each on 0.02 M glycine in PBS and six times 2 min each on PBS. Incubate the grid for 1 h on blocking buffer at room temperature (*see Note 19*). Place the grid on a droplet (7  $\mu\text{l}$  per grid) containing an appropriate concentration of antibody diluted in blocking buffer (*see Note 20*) and incubate for 60 min (*see Note 19*). To wash the sample, incubate six times for 2 min on PBS drops. Then, incubate for 20 min on a protein A-gold droplet (7  $\mu\text{l}$  per grid) (*see Notes 19 and 20*). Wash six times for 2 min on PBS. To crosslink the antibody to protein A-gold, incubate for 10 min on a droplet of 1% glutaraldehyde in PBS. Wash six times for 2 min on PBS (*see Note 21*).
11. For contrast enhancement, prepare a long strip of parafilm with a series of drops (prepare them right before they are needed) for the following incubations: incubate six times for 2 min each on ddH<sub>2</sub>O at room temperature, incubate for 10 min on uranyl oxalate pH 7.0 at room temperature, rinse in a big drop of ddH<sub>2</sub>O and two drops of methyl cellulose/uranyl acetate pH 4.0 on ice, and incubate for 10 min on methyl cellulose/uranyl acetate pH 4.0 on ice. Pick up the grid with a loop with 3.5–4 mm diameter, remove excess methyl cellulose/uranyl acetate by tilting the loop, touching a filter paper with the loop carrying excess methyl cellulose/uranyl acetate and then immediately pulling it over the filter paper leaving behind a thin film of methyl cellulose/uranyl acetate on the grid (*see Note 22*).
12. Dry the grids overnight before analyzing them in a transmission electron microscope. Grids can be stored indefinitely at room temperature.

### 3.4 Tokuyasu Cryosectioning of Isolated Mitochondria

For the analysis of isolated mitochondria by Tokuyasu cryosectioning and immunolabeling, the same considerations as outlined above should be taken into account (*see* Subheading 3.2). Ruthenium red is used to stain the mitochondrial pellet and improve its visibility to facilitate handling of the sample. This chemical does not have any influence on the ultrastructure of mitochondria. Low-melting point agarose is used instead of gelatine for embedding, because sections are more stable and agarose can be removed during immunogold labeling. *See* Fig. 6 for examples of electron microscopy of isolated mitochondria after Tokuyasu cryosectioning.

1. For fixation, spin down the mitochondria at  $13,000 \times g$  in a 1.5 ml microfuge tube. The pellet should be well visible and have a diameter of 2–4 mm. Resuspend the mitochondria in 1 ml 2 $\times$  fixation buffer, and incubate for 20 min at room temperature on a roller. Then, centrifuge for 5 min at 3000 rpm ( $800 \times g$ ) at room temperature in a microfuge, resuspend in 1 ml 1 $\times$  fixation buffer, and incubate for 2.5–4 h (the longer

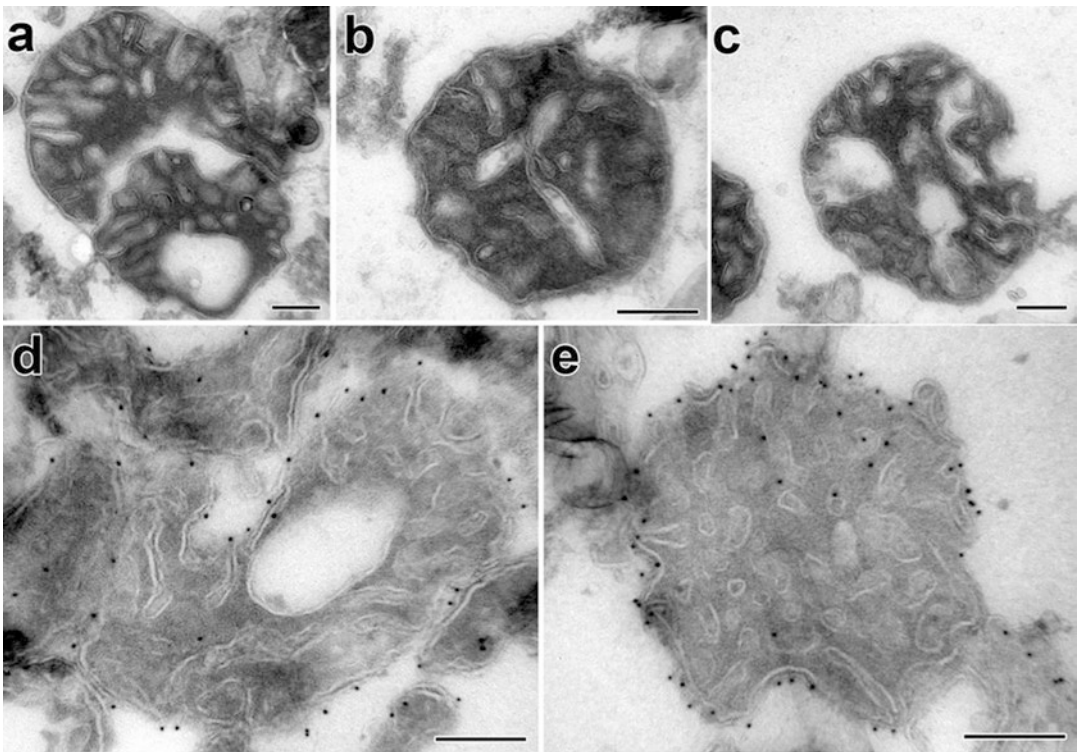


**Fig. 6** Electron microscopy of isolated mitochondria after Tokuyasu cryosectioning. (a–c) Mitochondria isolated from wild-type cells grown on glycerol-containing YPG medium. (d, e) Immunogold labeling of mitochondria isolated from a strain expressing the outer membrane porin, Por1, fused to a triple HA tag (Por1-3xHA). Bars, 200 nm

the incubation is, the better) at room temperature. Wash the mitochondria three times for 10 min in ddH<sub>2</sub>O at room temperature (*see Note 13*). Add 1 ml ruthenium red solution to the pellet and incubate for 20–30 min. The pellet should have a clearly visible red/pink color. Repeat this step once if necessary. Wash the mitochondrial pellet three times in 1 ml ddH<sub>2</sub>O without resuspension.

2. To start agarose embedding (Fig. 4), heat 2% low-melting point agarose and allow it to cool down to about 40–50 °C. Fill a 1.5 ml microfuge tube with warm low-melting point agarose and place it with its tip on ice. Remove the mitochondrial pellet carefully out of the reaction tube using a toothpick and put the mitochondrial pellet into a water drop on parafilm. Cut the pellet into pieces of a maximum size of 1 mm<sup>3</sup> using a razor blade (*see Note 14*). Then add the sample to the agarose (it should be located in the middle of the reaction tube), close the tube and cover it completely with ice for a few minutes. Cut off the tip of the tube, remove the agarose block, and recover the sample by removing most, but not all, of the agarose using a razor blade.
3. Continue with **step 5**, as described above (*see Subheading 3.3*).

---

## 4 Notes

1. The OD is very important. When cells enter the stationary growth phase the cell wall becomes very thick and it will be difficult to remove it by zymolyase treatment. If the OD is too low, over-digestion of the cell wall occurs and organellar ultrastructure will not be well preserved. When growing cells in rich YPD medium we find it convenient to inoculate 20 ml medium with an inoculation loop of cells and then prepare three serial dilutions (1:1, 1:5, 1:25) for the overnight culture. The next morning choose the culture with the best OD.
2. The zymolyase concentration is critical and has to be optimized for each strain and experimental condition. Zymolyase solutions should always be prepared freshly, and different batches of zymolyase might vary. For strains in the YPH499 or W303 genetic background grown on rich glucose-containing medium a zymolyase concentration of 1.5–2.0 mg/ml is a good starting point. When grown on non-fermentable carbon sources the concentration should be increased to at least 2.5 mg/ml. For strains in the BY4741 genetic background grown on rich glucose-containing medium a concentration of 1.0–1.8 mg/ml might suffice, whereas this strain background often requires 3.0 mg/ml or more after growth on non-fermentable carbon sources. Mutants might require different conditions.

3. The reagents have to be added in that order. Be careful!  $\text{OsO}_4$  is not only highly toxic but also volatile. Work under the fume hood and wear eye protection!
4. You may use a single edge razor blade to cut the tube to remove the agarose block more easily.
5. To prepare the pipette tip heat a plastic Pasteur pipette with a lighter. When the plastic starts to get soft pull the tip with forceps to elongate it. Let it cool down for a few seconds until it gets hard and cut it with a razor blade. Use this tip to avoid loss of agarose blocks during the washing and dehydration steps.
6. For 100% ethanol, propylene oxide, and Epon-containing mixtures, it is important to avoid absorption of moisture from the air. Always close all bottles and tubes immediately after use.
7. It is important to fully remove the previous solution before adding pure Epon.
8. The sample should sink to the bottom of the tube before polymerization is started. If it still floats change the Epon again and incubate for another few hours at room temperature until the sample does sink.
9. To avoid contamination of the sample with crystals or precipitates from the uranyl acetate and lead citrate solutions, centrifuge both solutions before use for 8 min at high speed ( $12,000 \times g$ ) in a microfuge.
10. Sucrose is added to avoid osmotic swelling of mitochondria. Depending on the experiment the sucrose concentration might be varied.
11. Glutaraldehyde lowers the pH of the solution. Check and readjust pH.
12. When collaborating with another lab, it is convenient to mail the sample in fixation buffer at this step. A 1.5 ml microfuge tube should be filled almost completely with buffer. To avoid that the sample ends up in the air bubble at the top of the tube, plug it with cotton wool thereby submerging the sample completely.
13. To keep the pellet intact do not remove the solutions completely. The pellet is very unstable at this stage. Always use a plastic pipette tip prepared according to **Note 5**. Avoid using glass pipettes as minute glass splinters easily end up in the sample that will damage the diamond knife during ultramicrotomy.
14. Always keep the pellet in water when cutting it. The center of the pellet usually contains the highest portion of intact mitochondria. Try to avoid using the outer parts of the pellet, because they may contain a high percentage of mitochondria that were damaged during their isolation or manipulation.

15. Complete evaporation of the propylene oxide should take about 6–8 h. The rate of evaporation can be regulated by closing the lid of the tube every hour or so for about 30 min or by partly closing the lid in such a way that just a small opening is left. Proceed when the propylene oxide is completely evaporated as judged by the reduction of the volume by about 50%.
16. The sample should be at the bottom of the tube the next day. If it still floats incubate for some more hours in fresh Epon until the sample does sink.
17. The cells tend to clump after periodic acid treatment. Cut a pipette tip and resuspend the cells by pipetting up and down.
18. Pioloform support film is known to attract colloidal gold and should be avoided when immunolabeling is planned.
19. To avoid water evaporation place some wet tissue next to the drop and cover it with a lid of a Petri dish or incubate in a container with wet tissue.
20. Prepare the antibody solution freshly. Add the antibodies to the blocking solution, mix thoroughly, and spin down antibody aggregates by centrifugation for 30 s at full speed in a microfuge ( $12,000 \times g$ ). Place on ice until use.
21. PBS should be removed completely by the following washing steps because phosphate buffers may precipitate with uranium salts.
22. The removal of methyl cellulose/uranyl acetate is critical and requires some practice. A too thick film causes problems to obtain sharp pictures in the TEM, whereas a too thin film causes inhomogeneous staining. Always prepare enough grids.

---

## Acknowledgments

We thank Fulvio Reggiori and Muriel Mari (University Medical Centre Utrecht, The Netherlands) for advice and excellent training in cryo-sectioning, Rita Grotjahn for technical assistance, and Anja Heublein for photography. This work was supported by the Elitenetzwerk Bayern and a Max-Planck-Fellowship to A.-K.U. and grants of the Deutsche Forschungsgemeinschaft to B.W.

## References

1. Zick M, Rabl R, Reichert AS (2009) Cristae formation-linking ultrastructure and function of mitochondria. *Biochim Biophys Acta* 1793(1):5–19. doi:[10.1016/j.bbamcr.2008.06.013](https://doi.org/10.1016/j.bbamcr.2008.06.013)
2. Frey TG, Mannella CA (2000) The internal structure of mitochondria. *Trends Biochem Sci* 25(7):319–324
3. Mannella CA (2006) Structure and dynamics of the mitochondrial inner membrane cristae. *Biochim Biophys Acta* 1763(5–6):542–548. doi:[10.1016/j.bbamcr.2006.04.006](https://doi.org/10.1016/j.bbamcr.2006.04.006)
4. Neupert W (2012) SnapShot: mitochondrial architecture. *Cell* 149(3):722–722. doi:[10.1016/j.cell.2012.04.010](https://doi.org/10.1016/j.cell.2012.04.010)e721

5. Rutter J, Hughes AL (2015) Power(2): the power of yeast genetics applied to the powerhouse of the cell. *Trends Endocrinol Metab* 26(2):59–68. doi:[10.1016/j.tem.2014.12.002](https://doi.org/10.1016/j.tem.2014.12.002)
6. Neupert W (2015) A perspective on transport of proteins into mitochondria: a myriad of open questions. *J Mol Biol* 427(6 Pt A):1135–1158. doi:[10.1016/j.jmb.2015.02.001](https://doi.org/10.1016/j.jmb.2015.02.001)
7. Westermann B (2010) Mitochondrial dynamics in model organisms: what yeasts, worms and flies have taught us about fusion and fission of mitochondria. *Semin Cell Dev Biol* 21(6):542–549. doi:[10.1016/j.semcdb.2009.12.003](https://doi.org/10.1016/j.semcdb.2009.12.003)
8. Westermann B (2014) Mitochondrial inheritance in yeast. *Biochim Biophys Acta* 1837(7):1039–1046. doi:[10.1016/j.bbabi.2013.10.005](https://doi.org/10.1016/j.bbabi.2013.10.005)
9. Pfanner N, van der Laan M, Amati P, Capaldi RA, Caudy AA, Chacinska A, Darshi M, Deckers M, Hoppins S, Icho T, Jakobs S, Ji J, Kozjak-Pavlovic V, Meisinger C, Odgren PR, Park SK, Rehling P, Reichert AS, Sheikh MS, Taylor SS, Tsuchida N, van der Blik AM, van der Klei IJ, Weissman JS, Westermann B, Zha J, Neupert W, Nunnari J (2014) Uniform nomenclature for the mitochondrial contact site and cristae organizing system. *J Cell Biol* 204(7):1083–1086. doi:[10.1083/jcb.201401006](https://doi.org/10.1083/jcb.201401006)
10. Hoppins S, Collins SR, Cassidy-Stone A, Hummel E, Devay RM, Lackner LL, Westermann B, Schuldiner M, Weissman JS, Nunnari J (2011) A mitochondrial-focused genetic interaction map reveals a scaffold-like complex required for inner membrane organization in mitochondria. *J Cell Biol* 195(2):323–340. doi:[10.1083/jcb.201107053](https://doi.org/10.1083/jcb.201107053)
11. Harner M, Körner C, Walther D, Mokranjac D, Kaesmacher J, Welsch U, Griffith J, Mann M, Reggiori F, Neupert W (2011) The mitochondrial contact site complex, a determinant of mitochondrial architecture. *EMBO J* 30(21):4356–4370. doi:[10.1038/emboj.2011.379](https://doi.org/10.1038/emboj.2011.379)
12. von der Malsburg K, Müller JM, Bohnert M, Oeljeklaus S, Kwiatkowska P, Becker T, Loniewska-Lwowska A, Wiese S, Rao S, Milenkovic D, Hutu DP, Zerbes RM, Schulze-Specking A, Meyer HE, Martinou JC, Rospert S, Rehling P, Meisinger C, Veenhuis M, Warscheid B, van der Klei IJ, Pfanner N, Chacinska A, van der Laan M (2011) Dual role of mitofilin in mitochondrial membrane organization and protein biogenesis. *Dev Cell* 21(4):694–707. doi:[10.1016/j.devcel.2011.08.026](https://doi.org/10.1016/j.devcel.2011.08.026)
13. Alkhaja AK, Jans DC, Nikolov M, Vukotic M, Lytovchenko O, Ludewig F, Schliebs W, Riedel D, Urlaub H, Jakobs S, Deckers M (2012) MINOS1 is a conserved component of mitofilin complexes and required for mitochondrial function and cristae organization. *Mol Biol Cell* 23(2):247–257. doi:[10.1091/mbc.E11-09-0774](https://doi.org/10.1091/mbc.E11-09-0774)
14. Altmann K, Frank M, Neumann D, Jakobs S, Westermann B (2008) The class V myosin motor protein, Myo2, plays a major role in mitochondrial motility in *Saccharomyces cerevisiae*. *J Cell Biol* 181(1):119–130
15. Hammermeister M, Schödel K, Westermann B (2010) Mdm36 is a mitochondrial fission-promoting protein in *Saccharomyces cerevisiae*. *Mol Biol Cell* 21(14):2443–2452
16. Osman C, Haag M, Potting C, Rodenfels J, Dip PV, Wieland FT, Brügger B, Westermann B, Langer T (2009) The genetic interactome of prohibitins links their function to cardiolipin and phosphatidylethanolamine in mitochondria. *J Cell Biol* 184:583–596
17. Connerth M, Tatsuta T, Haag M, Klecker T, Westermann B, Langer T (2012) Intramitochondrial transport of phosphatidic acid in yeast by a lipid transfer protein. *Science* 338(6108):815–818. doi:[10.1126/science.1225625](https://doi.org/10.1126/science.1225625)
18. Harner ME, Unger AK, Izawa T, Walther DM, Ozbalci C, Geimer S, Reggiori F, Brügger B, Mann M, Westermann B, Neupert W (2014) Aim24 and MICOS modulate respiratory function, tafazzin-related cardiolipin modification and mitochondrial architecture. *eLife* 3:e01684. doi:[10.7554/eLife.01684](https://doi.org/10.7554/eLife.01684)
19. Klecker T, Scholz D, Förtsch J, Westermann B (2013) The yeast cell cortical protein Num1 integrates mitochondrial dynamics into cellular architecture. *J Cell Sci* 126(Pt 13):2924–2930. doi:[10.1242/jcs.126045](https://doi.org/10.1242/jcs.126045)
20. Förtsch J, Hummel E, Krist M, Westermann B (2011) The myosin-related motor protein Myo2 is an essential mediator of bud-directed mitochondrial movement in yeast. *J Cell Biol* 194(3):473–488
21. Perkins EM, McCaffery JM (2007) Conventional and immunoelectron microscopy of mitochondria. *Methods Mol Biol* 372:467–483. doi:[10.1007/978-1-59745-365-3\\_33](https://doi.org/10.1007/978-1-59745-365-3_33)
22. Tokuyasu KT (1973) A technique for ultracryotomy of cell suspensions and tissues. *J Cell Biol* 57(2):551–565
23. Luft JH (1961) Improvements in epoxy resin embedding methods. *J Biophys Biochem Cytol* 9:409–414
24. Palade GE (1952) A study of fixation for electron microscopy. *J Exp Med* 95(3):285–298
25. Bauer C, Herzog V, Bauer MF (2001) Improved technique for electron microscope visualization of yeast membrane structure. *Microsc Microanal* 7(6):530–534

26. Reynolds ES (1963) The use of lead citrate at high pH as an electron-opaque stain in electron microscopy. *J Cell Biol* 17:208–212
27. Altmann K, Dürr M, Westermann B (2007) *Saccharomyces cerevisiae* as a model organism to study mitochondrial biology: general considerations and basic procedures. *Methods Mol Biol* 372:81–90
28. Weckbecker D, Herrmann JM (2013) Methods to study the biogenesis of membrane proteins in yeast mitochondria. *Methods Mol Biol* 1033:307–322. doi:[10.1007/978-1-62703-487-6\\_20](https://doi.org/10.1007/978-1-62703-487-6_20)
29. Meeusen S, McCaffery JM, Nunnari J (2004) Mitochondrial fusion intermediates revealed in vitro. *Science* 305(5691):1747–1752
30. Griffith J, Mari M, De Maziere A, Reggiori F (2008) A cryosectioning procedure for the ultrastructural analysis and the immunogold labelling of yeast *Saccharomyces cerevisiae*. *Traffic* 9(7):1060–1072. doi:[10.1111/j.1600-0854.2008.00753.x](https://doi.org/10.1111/j.1600-0854.2008.00753.x)
31. van Tuinen E, Riezman H (1987) Immunolocalization of glyceraldehyde-3-phosphate dehydrogenase, hexokinase, and carboxypeptidase Y in yeast cells at the ultrastructural level. *J Histochem Cytochem* 35(3):327–333
32. Sikorski RS, Hieter P (1989) A system of shuttle vectors and host strains designed for efficient manipulation of DNA in *Saccharomyces cerevisiae*. *Genetics* 122:19–27

# Chapter 19

## Analysis of Mitochondrial Membrane Protein Complexes by Electron Cryo-tomography

Vicki A.M. Gold, Tobias Brandt, Laetitia Cavellini, Mickael M. Cohen, Raffaele Ieva, and Martin van der Laan

### Abstract

The visualization of membrane protein complexes in their natural membrane environment is a major goal in an emerging area of research termed structural cell biology. Such approaches provide important information on the spatial distribution of protein complexes in their resident cellular membrane systems and on the structural organization of multi-subunit membrane protein assemblies. We have developed a method to specifically label active membrane protein complexes in their native membrane environment with electron-dense nanoparticles coupled to an activating ligand, in order to visualize them by electron cryo-tomography. As an example, we describe here the depiction of preprotein import sites of mitochondria, formed by the translocase of the outer membrane (TOM complex) and the presequence translocase of the inner membrane (TIM23 complex). Active import sites are selectively labeled via a biotinylated, quantum dot-coupled preprotein that is arrested in translocation across the outer and inner mitochondrial membranes. Additionally, a related method is described for direct labeling of mitochondrial outer membrane proteins that does not depend on binding of a ligand.

**Key words** Electron cryo-tomography, Quantum dots, Mitochondria, Protein translocation, Membrane proteins, TOM complex, Presequence translocase

---

## 1 Introduction

In most organisms, membrane proteins constitute up to 30 % of the cellular proteome [1]. They are localized to the plasma membrane or intracellular membrane-bound compartments (organelles) where they assemble into functional protein complexes that mediate the transport of ions, metabolites, or macromolecules, engage in signal transduction events, energy-converting reactions, and many other processes. Methods for the subcellular localization and biochemical characterization of membrane protein complexes are well established in many laboratories worldwide. However, the direct visualization of protein complexes and analysis of their spatial distribution in native membranes have remained

major challenges. Recent technological advances in the field of electron cryo-tomography (cryo-ET) have opened up new avenues to tackle this problem [2]. Cryo-ET involves three-dimensional imaging of flash-frozen biological material at liquid nitrogen temperature in a dedicated electron microscope, allowing information on surface exposed and internal cellular/organellar architecture to be obtained at nanometer resolution. However, only membrane protein complexes that are sufficiently large, or exhibit a characteristic shape of their soluble domains, such as the mitochondrial  $F_1F_0$  ATP-synthase, are easily identified by this technique in native membrane preparations [3]. Another challenge is the ability to discriminate between active (ligand-bound) membrane protein complexes and the inactive population. We have recently established a technology termed STAMP (Specifically TArgeted Membrane nanoParticle) that enables, for the first time, the direct visualization of active, ligand-bound membrane protein complexes in native membranes using dense quantum dots (QDs) specifically coupled to a protein ligand. The STAMP method was first used to label and localize active preprotein import sites of isolated mitochondria in situ by cryo-ET [4].

Most mitochondrial proteins are encoded by nuclear genes and are synthesized with amino-terminal, positively charged presequences in the cytosol. The presequences are recognized by receptors on the mitochondrial surface and preproteins enter mitochondria via the general preprotein translocase of the outer mitochondrial membrane (TOM complex) [5–7]. In the mitochondrial intermembrane space the preproteins are transferred to the presequence translocase of the inner membrane (TIM23 complex) [8–10]. The direct hand-over of preproteins from the TOM to the TIM23 machinery leads to the formation of two-membrane-spanning translocation intermediates that expose their presequence-containing amino terminus to the mitochondrial matrix, whereas the carboxy terminus is still accessible on the outer surface of the mitochondria. Driving forces for mitochondrial protein import are provided by the electrical potential across the inner membrane and ATP hydrolysis by mitochondrial Hsp70, the core component of the presequence translocase-associated import motor (PAM).

To develop the STAMP method, we established an experimental protocol to generate arrested, two-membrane-spanning translocation intermediates of an intensively studied model preprotein, termed  $b_2\Delta$ -DHFR [11–14]. The preprotein is composed of the presequence-containing amino-terminal domain of the mitochondrial protein cytochrome  $b_2$  fused to dihydrofolate reductase (DHFR). To obtain stable translocation intermediates, the inner membrane sorting signal of cytochrome  $b_2$  was deleted from the fusion protein [11]. We used a modified version of  $b_2\Delta$ -DHFR containing a single cysteine residue at the carboxy terminus of the DHFR moiety ( $b_2\Delta$ -DHFR<sub>cys</sub>) [4]. The preprotein was expressed

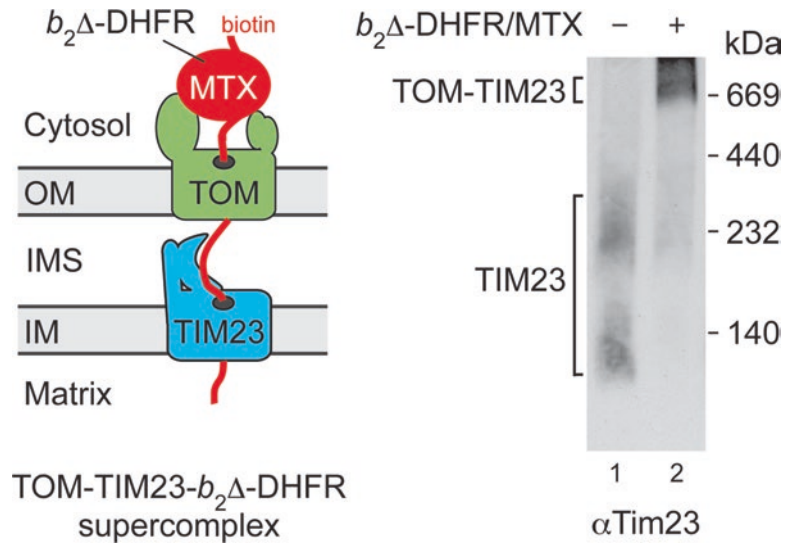


**Fig. 1** Accumulation of  $b_2\Delta$ -DHFR<sub>biotin</sub> in mitochondrial preprotein import sites. *Left:* Schematic representation of active preprotein import sites composed of the TOM and TIM23 complexes holding a translocation-arrested  $b_2\Delta$ -DHFR<sub>biotin</sub> preprotein. *OM* outer membrane, *IM* inner membrane, *IMS* intermembrane space, *MTX* methotrexate. *Right:* Blue native-PAGE analysis of mitochondrial preprotein import sites. TIM23 complexes are detected in untreated (*lane 1*) or  $b_2\Delta$ -DHFR<sub>biotin</sub>-loaded (*lane 2*) mitochondria by Western blotting using an antibody against the Tim23 subunit. Translocation arrest of  $b_2\Delta$ -DHFR<sub>biotin</sub> in a two membrane-spanning fashion tethers TOM and TIM23 into preprotein-carrying supercomplexes

in *E. coli* cells and purified. The C-terminal cysteine residue was subsequently biotinylated and the resulting modified preprotein  $b_2\Delta$ -DHFR<sub>biotin</sub> was incubated with isolated mitochondria in the presence of the DHFR-ligand methotrexate. Under these conditions, the folding of the methotrexate-bound DHFR domain is stabilized preventing its passage through the mitochondrial protein import channels [11]. Two-membrane-spanning import intermediates are formed that contain the TOM and TIM23 complexes connected by the arrested preprotein (Fig. 1, cartoon). The folded DHFR-domain of the preprotein remains on the outer surface of the mitochondria. The exposed biotin moiety is then used to specifically couple streptavidin-coated QDs to the translocation intermediate thereby labeling active preprotein import sites. The fluorescent properties of the QDs are used to determine labeling specificity of large sample sizes quickly, without the need for highly specialized equipment, whereas the dense core of these nanoparticles allows for their precise localization in cryo-tomograms of preprotein-loaded mitochondria. We also briefly describe a variation of our STAMP method that does not rely on labeling via an

activating ligand, and is therefore more generally applicable for labeling exposed membrane protein targets. In this approach, biotinylation of an outer mitochondrial membrane protein (e.g., Fzo1/mitofusin) is achieved by fusing the exposed carboxy-terminus of the protein with an Avi-tag, a 15 amino-acid peptide that is recognized and specifically biotinylated by the *E. coli* biotin ligase BirA [15, 16].

---

## 2 Materials

### 2.1 Expression and Purification of $b_2\Delta$ -DHFR<sub>cys</sub>

1. Plasmid pUHE- $b_2\Delta$ -DHFR<sub>cys</sub> [4].
2. Competent *E. coli* cells (see Note 1).
3. 10 ml ampicillin stock solution at 100 mg/ml in H<sub>2</sub>O.
4. 6 × 5 l baffled flasks.
5. 12 l LB medium: 100 g Bacto tryptone, 50 g yeast extract, and 100 g NaCl, dissolved in 10 l dH<sub>2</sub>O (adjust pH to 7.5, sterilize by autoclaving).
6. LB-Amp agar plates: 100 ml sterile LB medium with 1.5 g agar (dissolve in a microwave, add 100 µg/ml ampicillin [final concentration] and pour into sterile petri dishes to set).
7. 12 ml 1 M IPTG solution.
8. 500 ml Resuspension buffer: 20 mM Tris-HCl pH 8, 50 mM NaCl, 1 mM EDTA, 10 mM DTT.
9. Cell disruptor (Constant Systems Ltd., Northamptonshire, UK).
10. Ion exchange chromatography column packed with SP-Sepharose Fast-Flow (GE Healthcare, Chalfont, UK) to a bed volume of approximately 80 ml.
11. Protein purification system, e.g., ÄKTA pure (GE Healthcare, Chalfont, UK).
12. Buffer A: 20 mM Tris-HCl pH 8, 150 mM NaCl, 1 mM EDTA, 10 mM DTT.
13. Buffer B: 20 mM Tris-HCl pH 8, 500 mM NaCl, 1 mM EDTA, 10 mM DTT.
14. Buffer C: 20 mM Tris-HCl pH 8, 150 mM NaCl, 1 mM EDTA.
15. 2 × 10 % Tris-glycine SDS-PAGE gels and gel running apparatus.
16. Size-exclusion chromatography column, e.g., Superdex 75 16/600 (GE Healthcare, Chalfont, UK).
17. Amicon Ultra-15 ml with a molecular weight cutoff of 30 kDa (Merck Chemicals, Darmstadt, Germany).

**2.2 Biotinylation  
of Purified  
 $b_2\Delta$ -DHFR<sub>cys</sub>**

1. Purified  $b_2\Delta$ -DHFR<sub>cys</sub> (prepared according to Subheading 3.1).
2. 20 mM Maleimide-PEG<sub>2</sub>-biotin (Pierce, Rockford, USA) stock solution prepared in Buffer C described in Subheading 2.1 (*see Note 2*).
3. Size-exclusion chromatography column, e.g., Superdex 75 10/300 (GE Healthcare, Buckinghamshire, UK).
4. HABA biotin quantitation kit (Pierce, Rockford, USA).

**2.3 Generation  
of  $b_2\Delta$ -DHFR<sub>biotin</sub>  
Import Intermediates**

1. Isolated mitochondria, e.g., from the baker's yeast (*Saccharomyces cerevisiae*) wild-type strain YPH499 (*see Note 3*).
2. Biotinylated preprotein  $b_2\Delta$ -DHFR<sub>biotin</sub> (prepared according to Subheading 3.2).
3. SEM buffer: 250 mM sucrose, 1 mM EDTA, 10 mM MOPS-KOH pH 7.2.
4. Import buffer: 10 mM MOPS-KOH pH 7.2, 3 % (w/v) fatty acid-free BSA, 250 mM sucrose, 80 mM KCl, 5 mM MgCl<sub>2</sub>, 2 mM KH<sub>2</sub>PO<sub>4</sub>, 5 mM methionine, 2 mM NADH, 2 mM ATP, 5 mM creatine phosphate, 0.1 mg/ml creatine kinase.
5. Methotrexate stock solution, 10 mM dissolved in 100 mM MOPS-KOH pH 7.2 (*see Note 4*).

**2.4 Verification  
of  $b_2\Delta$ -DHFR<sub>biotin</sub>  
Import Intermediates**

1. Digitonin buffer: 20 mM Tris-HCl pH 7.4, 0.1 mM EDTA, 50 mM NaCl, 1 % (w/v) digitonin, 10 % (v/v) glycerol.
2. 10× Blue native-PAGE loading buffer: 100 mM Bis-Tris-HCl pH 7.0, 500 mM 6-aminocaproic acid, 5 % (w/v) Coomassie Brilliant Blue G-250.
3. 6–16.5 % polyacrylamide Blue native-PAGE gradient gel (*see Note 5*).
4. PVDF blotting membrane.
5. Polyclonal antibodies raised against the Tim23 protein (*see Note 6*).

**2.5 Labeling  
 $b_2\Delta$ -DHFR<sub>biotin</sub> Import  
Intermediates  
with QDs**

1. Mitochondria loaded with  $b_2\Delta$ -DHFR<sub>biotin</sub> import intermediates (prepared according to Subheading 3.3).
2. Amicon Ultra-0.5 ml with a molecular weight cutoff of 50 kDa (Merck Chemicals, Darmstadt, Germany).
3. Streptavidin-coated QD<sub>605</sub> (Invitrogen, Carlsbad, USA).
4. Sorbitol Buffer A: 30 mM Tris-Cl pH 7.4, 12.25 % sorbitol, 3 mM EDTA.
5. Sorbitol Buffer B: 10 mM Tris-Cl pH 7.4, 8.75 % sorbitol, 1 mM EDTA.
6. Working Solution (WS) of 40 % iodixanol, made by mixing 4 volumes of Optiprep density gradient medium (Sigma-Aldrich, St. Louis, USA) with 2 volumes of Sorbitol Buffer A.

7. Iodixanol gradient solutions prepared by diluting the WS with Sorbitol Buffer B to concentrations of 0–27 % iodixanol (0, 3, 6, 9, 12, 15, 18, 21, 24, 27 % [v/v]). Five hundred microliter of each solution will be sufficient for two samples (labeling experiment and control); larger volumes can be prepared and stored at 4 °C.
8. SEM buffer (*see* Subheading 2.3).
9. Ultracentrifuge with swing-out rotor, such as Optima MAX-XP with TLS-55 rotor (Beckman Coulter, Brea, USA).

## 2.6 Confocal Fluorescence Microscopy

1. MitoTracker Green dye (Invitrogen, Carlsbad, USA) stock solution, prepared in high-quality anhydrous dimethylsulfoxide (DMSO) to a concentration of 1 mM. The solution can be stored at –20 °C protected from light.
2. 8-well chamber slides (Sarstedt, Nümbrecht, Germany).
3. SeaKem low-melting point agarose (Lonza, Basel, Switzerland), dissolved in water to a final concentration of 2 %. This should be prepared immediately before use.
4. SEM buffer (*see* Subheading 2.3).
5. QD-labeled and control mitochondria, prepared according to Subheading 3.5.
6. Inverted confocal microscope, e.g., LSM 710 (Carl Zeiss, Jena, Germany).

## 2.7 Electron Cryo-tomography

1. Mitochondria subjected to import of b<sub>2</sub>Δ-DHFR<sub>biotin</sub> or to a control reaction, both incubated with QDs as described in Subheadings 3.3 and 3.5.
2. R2/2 Cu 300 mesh holey carbon-coated support grids (Quantifoil, Jena, Germany).
3. Glow discharge cleaning system, e.g., PELCO easiGlow (Ted Pella Inc., Redding, USA).
4. Suspension of 10 nm protein A-gold particles (Aurion, Wageningen, Netherlands). The volume required depends on the number of grids to prepare. For 10 grids, approximately 15 μl will be sufficient.
5. High-precision tweezers, e.g., Dumont carbon steel (Plano, Wetzlar, Germany).
6. Whatman filter paper grade 41 (GE Healthcare, Chalfont, UK).
7. Grid storage boxes.
8. Plunge-freezing device, home-made or company produced, e.g., Vitrobot (FEI, Hillsboro, USA) or EM GP (Leica, Wetzlar, Germany).
9. Tomography-capable electron microscope with cryo-transfer holder for vitrified specimens, ideally operating at 300 keV,

e.g., Titan Krios (FEI, Hillsboro, USA) or JEOL3200-FSC (JEOL, Tokyo, Japan), with a high-tilt stage, energy filter and direct electron detector camera, e.g., K2 Summit (Gatan, Pleasanton, USA).

10. Computer software capable of tomographic data collection, e.g., Digital Micrograph (Gatan, Pleasanton, USA) or SerialEM [17], plus software capable of tomographic reconstruction and visualization, e.g., IMOD [18] or AMIRA (FEI, Hillsboro, USA).

### **2.8 Variation on a Theme: Direct Labeling of Mitochondrial Outer Membrane Proteins**

1. Isolated mitochondria exposing an Avi-tag (a 15 amino-acid peptide: GLNDIFEAQKIEWHE [15]) fused to an outer mitochondrial membrane protein of interest, e.g., Fzo1/mitofusin.
2. Biotin Protein Ligase kit (GeneCopocia Inc., Rockville, USA): BirA (1  $\mu\text{g}/\mu\text{l}$  stock solution), Biomix-A, Biomix-B, d-biotin solution.
3. NMIB buffer: 20 mM Hepes-KOH pH 7.4, 0.6 M sorbitol, 5 mM  $\text{MgCl}_2$ , 50 mM KCl, 100 mM KOAc.
4. Biotinylation buffer: 700  $\mu\text{l}$  NMIB + 100  $\mu\text{l}$  Biomix-A + 100  $\mu\text{l}$  Biomix-B + 100  $\mu\text{l}$  d-biotin solution.
5. Streptavidin-coated QD<sub>525</sub> (Invitrogen, Carlsbad, USA).
6. EM buffer: 320 mM trehalose, 20 mM Tris-HCl pH 7.4, 1 mM EGTA.

---

## **3 Methods**

### **3.1 Expression and Purification of $b_2\Delta$ -DHFR<sub>cys</sub>**

The first step of the method includes expression and purification of the target protein. For the downstream application of  $b_2\Delta$ -DHFR<sub>cys</sub> in preprotein import reactions, it is important to obtain highly concentrated, fully soluble protein and to avoid oxidation of the engineered cysteine residue at the carboxy terminus (leading to dimer formation).

1. Transform plasmid pUHE- $b_2\Delta$ -DHFR<sub>cys</sub> into competent *E. coli* cells using standard bacterial transformation methods (see **Note 1**).
2. Spread cells onto an LB-Amp agar plate and incubate at 37 °C overnight.
3. Using a sterile pipette tip, select a single colony from the LB agar plate and drop into 100 ml LB medium containing 100  $\mu\text{g}/\text{ml}$  ampicillin (final concentration). Loosely cover the culture and incubate at 37 °C for 12–18 h, shaking at 200 rpm.
4. Divide the 100 ml culture into 6  $\times$  5 l baffled flasks, each containing 2 l LB medium with 100  $\mu\text{g}/\text{ml}$  ampicillin (final concentration). Loosely cover the cultures and incubate at 37 °C for 4 h, shaking at 200 rpm.

5. Lower the incubator temperature to 15 °C. After 1 h, induce expression of  $b_2\Delta$ -DHFR<sub>cys</sub> with 1 mM IPTG (final concentration) and incubate for further 12–18 h at 15 °C.
6. Harvest the cells by centrifugation at  $5000 \times g$  for 10 min at 4 °C. From this point on, all solutions should be ice-cold and the preparation should be kept on ice.
7. Wash and resuspend the cell pellet in 100 ml Resuspension buffer.
8. Break open the cells using a cell disruptor at 1800 bar.
9. Remove cell debris by centrifugation at  $20,000 \times g$  for 20 min.
10. Using a protein purification system according to the instructions of the supplier, equilibrate an SP-Sepharose column with Buffer A.
11. Load the supernatant from **step 9** onto the column and wash extensively with Buffer A (300–500 ml) until no further protein elutes from the column, monitored by reduction in absorbance at  $A_{280}$ .
12. Elute the bound  $b_2\Delta$ -DHFR<sub>cys</sub> protein from the column using a gradient of 0–100 % Buffer B over 10 column volumes, e.g., for an 80 ml column this takes 80 min at a flow rate of 10 ml/min.
13. Run an SDS-PAGE gel of eluted fractions to determine which ones contain the highest amount of pure protein.  $b_2\Delta$ -DHFR<sub>cys</sub> is identified as a clear band at ~38 kDa (*see Note 7*).
14. Using a protein purification system according to the instructions of the supplier, equilibrate a Superdex 75 16/600 column with Buffer C at a flow rate of 1.5 ml/min.
15. Pool the fractions of SP-Sepharose chromatography step that contain the highest amount of pure  $b_2\Delta$ -DHFR<sub>cys</sub> and load onto the Superdex 75 16/600 column (*see Note 8*). Perform size-exclusion chromatography using Buffer C at the same flow rate.
16. Collect protein fractions and run an SDS-PAGE gel to determine which fractions contain pure  $b_2\Delta$ -DHFR<sub>cys</sub> monomer. Oxidized dimers are clearly visible at ~76 kDa. Dimer-containing fractions should be discarded.
17. Pool the eluted fractions and concentrate the protein to a volume of < 5 ml. Determine the protein concentration and proceed immediately to the next step. In typical preparations ~4 ml of 200  $\mu$ M  $b_2\Delta$ -DHFR<sub>cys</sub> could be obtained.

### **3.2 Biotinylation of Purified $b_2\Delta$ -DHFR<sub>cys</sub>**

1. Incubate the purified  $b_2\Delta$ -DHFR<sub>cys</sub> with a tenfold molar excess of maleimide-PEG<sub>2</sub>-biotin (added from a 20 mM stock solution in Buffer C) overnight at 4 °C, while gently rotating.

From here on the labeled protein will be termed  $b_2\Delta$ -DHFR<sub>biotin</sub>. Typically, reaction volumes are ~ 1 ml of 200  $\mu$ M  $b_2\Delta$ -DHFR<sub>cys</sub> (*see Note 2*).

2. Remove unbound label and isolate pure  $b_2\Delta$ -DHFR<sub>biotin</sub> monomers by size-exclusion chromatography, e.g., using a high-resolution Superdex 75 10/300 column and Buffer C.
3. Assess protein purity by SDS-PAGE and Coomassie blue staining. In typical preparations,  $b_2\Delta$ -DHFR<sub>biotin</sub> is ~95 % pure.
4. Determine the degree of biotinylation using the HABA biotin quantitation kit according to the manufacturers' instructions. Preparations should only be used when the labeling is 1:1  $\pm$  10 %.

### 3.3 Generation of $b_2\Delta$ -DHFR<sub>biotin</sub> Import Intermediates

1. Thaw isolated mitochondria slowly on ice (*see Note 9*).
2. Prepare an import reaction master mix (800  $\mu$ l) by diluting 800  $\mu$ g mitochondria in import buffer (final concentration of 1 mg of total mitochondrial protein per ml of buffer).
3. Thaw an aliquot of 10 mM methotrexate and dilute it to a final concentration of 5  $\mu$ M into the import reaction master mix (*see Note 3*).
4. Divide the master mix into two aliquots of 400  $\mu$ l: import reaction and control reaction.
5. Supplement the import reaction with  $b_2\Delta$ -DHFR<sub>biotin</sub> in Buffer C (from the biotinylation reaction). Supplement the control reaction with an equal volume of buffer without  $b_2\Delta$ -DHFR<sub>biotin</sub>. To ensure efficient labeling of preprotein import sites (generation of import intermediates) a >100-fold molar excess of  $b_2\Delta$ -DHFR<sub>biotin</sub> over the amount of the core TIM23 complex subunit Tim23 in mitochondria is added. Yeast mitochondria contain approximately 16 pmol of Tim23 per mg of total protein amount (calculated as described in [19]). Thus, at least 1.6 nmol  $b_2\Delta$ -DHFR<sub>biotin</sub> per mg of the total mitochondrial protein content should be added. If necessary, pre-dilute  $b_2\Delta$ -DHFR<sub>biotin</sub> in Import buffer.
6. Incubate the import reactions for 15 min at 25  $^{\circ}$ C.
7. Take 70  $\mu$ l from both reactions to verify the formation of the  $b_2\Delta$ -DHFR<sub>biotin</sub> import intermediates (*see Subheading 3.4*).
8. Re-isolate the remaining mitochondria (330  $\mu$ g) by centrifugation (10 min, 20,000  $\times g$ , 4  $^{\circ}$ C).
9. Wash mitochondria twice with 400  $\mu$ l SEM buffer. Finally resuspend mitochondria in 75  $\mu$ l of SEM buffer (*see Note 10*).

### 3.4 Verification of $b_2\Delta$ -DHFR<sub>biotin</sub> Import Intermediates

For subsequent visualization of preprotein import sites on the mitochondrial surface by cryo-ET, it is important to make sure that all available preprotein import sites in the sample are stably occupied by arrested  $b_2\Delta$ -DHFR<sub>biotin</sub>. To verify the saturation of

import sites, the preprotein-carrying TOM-TIM23 supercomplexes must be carefully extracted from mitochondrial membranes using the mild detergent digitonin and subjected to Blue native-PAGE [11] (*see Note 5*). As a control, an equal amount of digitonin extract from mitochondria that were not incubated with  $b_2\Delta$ -DHFR<sub>biotin</sub> is loaded onto the gel. A western blot of this gel should be analyzed with antibodies against Tim23. TOM complexes of the outer membrane are approximately 3–4 times more abundant than inner membrane TIM23 complexes [20], because the TOM complex serves as the general entry gate for all proteins into mitochondria and also shuttles proteins without amino-terminal presequences into other downstream import pathways [5–7]. In control mitochondria, antibodies against Tim23 decorate two different forms of TIM23 complexes [14, 19] (Fig. 1, lane 1). If maximal occupancy of preprotein import sites by methotrexate-bound  $b_2\Delta$ -DHFR<sub>biotin</sub> is achieved, the entire population of TIM23 complexes is shifted into a higher molecular weight (preprotein-loaded) TOM-TIM23 supercomplex [4] (Fig. 1, lane 2).

1. Pellet 70  $\mu$ g of mitochondria (total protein amount) from both the import and the control reactions using a benchtop centrifuge (10 min, 20,000  $\times g$ , 4 °C) and remove the supernatant (*see Note 11*).
2. Solubilize the mitochondrial pellet using 70  $\mu$ l of digitonin buffer precooled on ice (*see Note 12*).
3. Incubate samples on ice for 15 min.
4. Perform a clarifying centrifugation step to remove non-solubilized material (benchtop centrifuge, 10 min, 20,000  $\times g$ , 4 °C).
5. Transfer the supernatant into a new precooled Eppendorf tube.
6. Supplement each sample with 10 $\times$  ice-cold Blue native-PAGE loading buffer.
7. Load the samples onto a 6–16.5 % polyacrylamide Blue native gradient gel for electrophoretic separation of solubilized membrane protein complexes. We use a Hoefer SE600 electrophoresis system and run the gel at 100 V for approximately 15 h (*see Notes 5 and 13*).
8. Transfer separated proteins onto a PVDF membrane.
9. Immunodecorate the membrane using  $\alpha$ -Tim23 antibodies (*see Note 14*).

### **3.5 Labeling of $b_2\Delta$ -DHFR<sub>biotin</sub> Import Intermediates with QDs**

QDs are dense fluorophores, which may be discriminated in the electron microscope by their ability to scatter electrons strongly, as well as in the light microscope by their bright fluorescence. QDs are available in different sizes and shapes leading to different fluorescent and electron-scattering properties. The choice of QD

can therefore be made according to specific requirements of the experiment. Here, the specificity of QD binding to mitochondrial membranes is assessed using the QD fluorescence and a MitoTracker fluorescent dye for mitochondrial membranes. In order to provide complementary emission spectra between the QD and the membrane dye, various options of both QD and MitoTracker are available (also *see* Subheading 3.6). For our analysis of active mitochondrial preprotein import sites shown here, we have used streptavidin-coated QD<sub>605</sub> (Fig. 2). In all cases, a control QD labeling reaction is performed in parallel with mitochondria that were not loaded with b<sub>2</sub>Δ-DHFR<sub>biotin</sub> import intermediates to assess unspecific binding of streptavidin-coated QDs to the mitochondrial surface.

1. Centrifuge 55 μl of an approximately 2 μM QD solution (the concentration of the QD<sub>605</sub> streptavidin conjugate suspension provided by the supplier is in the range of 1.8–2.2 μM) at 5000 × *g* for 3 min in a benchtop centrifuge and discard the pellet containing aggregated material.
2. Remove 50 μl of the supernatant and equilibrate QDs with SEM by buffer exchange using Amicon Ultra-0.5 ml centrifugal filters with 50 kDa molecular weight cutoff. To this end, add 450 μl of SEM buffer to 50 μl of the QD solution, place the solution into the filter and centrifuge at 10,000 × *g* until the volume is reduced to ~50 μl. Repeat this step one more time.
3. Supplement both labeling (mitochondria carrying arrested b<sub>2</sub>Δ-DHFR<sub>biotin</sub>) and control reactions as described in Subheading 3.3. with 25 μl of QD suspension prepared in **step 2** (*see Note 15*). Incubate the reactions for 4 h at 4 °C with gentle shaking.
4. Gently layer 200 μl aliquots of each iodixanol gradient solution (prepared as described in Subheading 2.5) into 2 × 2.2 ml ultra-clear centrifugation tubes.
5. Layer 100 μl (i.e., the total volume) of each mitochondrial sample (pre-loaded with arrested b<sub>2</sub>Δ-DHFR<sub>biotin</sub> and control), as prepared in **step 3**, on top of the gradients and centrifuge at 80,000 × *g* for 20 min at 4 °C with gentle braking.
6. Remove ~400 μl of the mitochondria-containing bands in the gradient, first by gently removing the upper layers by pipetting, and subsequently the mitochondrial band (Fig. 2, upper panel) and dilute into 2 ml SEM buffer.
7. Pellet the mitochondria at 20,000 × *g* for 20 min at 4 °C and resuspend in 20 μl SEM buffer. A significant amount of material will have been lost during gradient centrifugation. The final amount of mitochondria needed for electron cryo-tomography can be estimated by ensuring the total protein content is ~10 mg/ml.

### 3.6 Confocal Fluorescence Microscopy

To assess the specificity of QD binding to preprotein-containing mitochondrial import sites, samples are screened by fluorescence microscopy prior to cryo-ET. It is important to ensure that a fluorescent dye chosen for staining of mitochondria has different emission properties from those of the chosen QDs. For example, here we have used MitoTracker Green (emission 516 nm) to visualize mitochondria labeled with QD<sub>605</sub> (emission 605 nm) (Fig. 2, lower panel). Alternatively, mito-mCherry (emission 610 nm) co-expressing plasmids can be used, providing a convenient readout

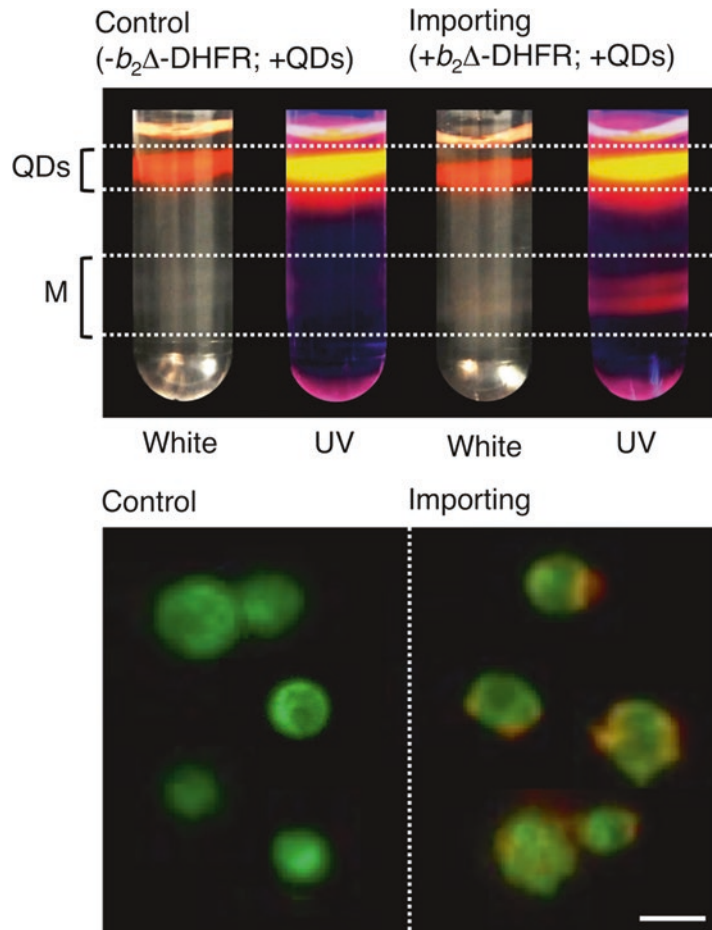


**Fig. 2** QD labeling of  $b_2\Delta$ -DHFR<sub>pilotin</sub>-loaded mitochondria. *Upper panel:* Free QDs are separated from labeled mitochondria on an iodixanol gradient. Under white light, both mitochondria (M) and QD<sub>605</sub> are visible. Under UV excitation, QDs only are detected. Co-localization of QDs with mitochondria is clearly seen in the labeling experiment (+ $b_2\Delta$ -DHFR) and not the control ( $-b_2\Delta$ -DHFR). *Lower panel:* Confocal fluorescence images of the mitochondrial fractions (M) isolated from the gradient. In this example, mitochondria are labeled with MitoTracker Green and QD<sub>605</sub> fluorescence is shown in red; scale bar = 1  $\mu$ m

to optimize labeling conditions. In this case, a QD<sub>525</sub> (emission 525 nm) would provide complementary emission properties.

1. For MitoTracker labeling, dilute control and b<sub>2</sub>Δ-DHFR<sub>biotin</sub>-loaded mitochondria from the QD labeling reactions to a concentration of ~1 mg/ml total mitochondrial protein, in a total volume of 200 μl SEM. Incubate with 50 nM MitoTracker Green (final concentration) for 15 min at 37 °C (*see Note 16*).
2. Add 100 μl of each suspension to separate wells of 8-well chamber slides and fix with 1–2 % SeaKem low-melting point agarose to prevent mitochondrial movement. This is performed by gently pouring ~ 1 ml molten agarose into the wells on top of the mitochondria.
3. Set excitation and emission wavelengths on the fluorescence microscope to correspond to the chosen type of QDs and MitoTracker, e.g., 488 nm, and emission 492–535 nm for MitoTracker Green, and 597–700 nm for QD<sub>605</sub>.
4. Screen individual fluorescent mitochondria from the labeling experiment and control samples to determine the specificity of QD binding to the b<sub>2</sub>Δ-DHFR<sub>biotin</sub>-carrying mitochondrial import sites. Statistics should be collected to determine the number of labeled mitochondria for both experiment and control. Typically, we were able to obtain 100 % labeling for b<sub>2</sub>Δ-DHFR<sub>biotin</sub>-loaded mitochondria, and only 0.3 % labeling for control mitochondria [4].

### 3.7 Electron Cryo-tomography

#### 3.7.1 Sample Preparation

Obtaining cryo-fixed samples is the first step in cryo-ET. The method involves the use of liquid nitrogen and ethane, which are extremely cold (~ -180 °C or below) and in the case of ethane also flammable. Samples must be prepared in a fume-hood and safety goggles and cryo-protection gloves worn. Optimal ice-thickness (*see Note 17*) will likely have to be determined for each sample by varying the sample concentration and the blotting time. Ice thickness of <500 nm and at least ten gold fiducials evenly distributed throughout the area of interest are ideal.

1. Glow-discharge the grids by depositing ions on the surface of the carbon to render them hydrophilic. Place grids carbon side up in a glow discharge cleaner and operate according to the manufacturer's instructions. Best results are achieved if EM grids are washed in chloroform for at least 3 h before use.
2. Mix labeled mitochondria at a total protein concentration of ~10 mg/ml 1:1 with a suspension of 10 nm protein A-gold as fiducial markers. For example, to make 10 EM grids (3 μl solution per grid), mix 15 μl mitochondria with 15 μl protein A-gold.
3. Apply 3 μl sample to a glow-discharged EM grid, held securely in tweezers, and insert into the vitrification device (*see Note 18*).

4. Blot the sample by placing the filter paper parallel to the grid surface and hold until the liquid stops spreading. This can take ~3–6 s depending on the concentration of sample. Plunge freeze the grids rapidly into liquid ethane (*see Note 17*).
5. Transfer the grid swiftly from liquid ethane into liquid nitrogen and store in a grid storage box under liquid nitrogen until analysis.

### 3.7.2 Electron Cryo-tomography

For cryo-ET, a “tilt series” is collected, which is a series of projection images taken of the same sample at different angles relative to the electron beam (Fig. 3). These 2D images are then computationally reconstructed to build a 3D volume of the original sample. Compromises must be made between a high-enough electron dose to be able to visualize the sample at the required level of detail, and a low-enough dose to ensure that the sample does not experience too much radiation damage. For studies of morphology and protein localization, mitochondria can tolerate electron doses up to  $200 \text{ e}^-/\text{\AA}^2$ . Naturally, acquisition of high quality data

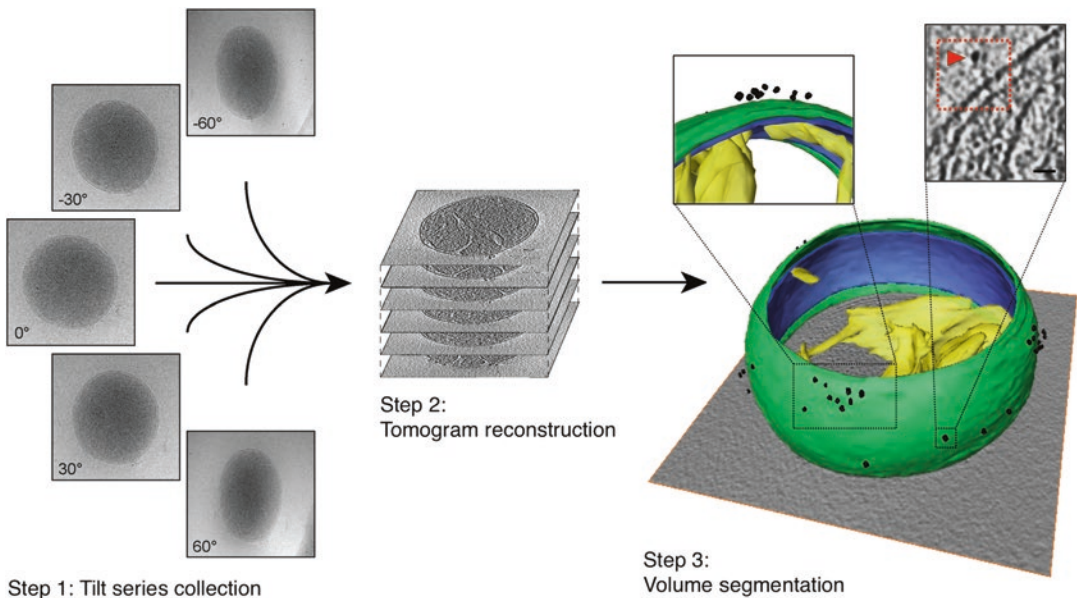


**Fig. 3** Work flow for cryo-ET. *Step 1*: After finding an appropriate area of interest, a tilt series of electron micrographs is taken at regularly spaced intervals (only five example tilt images are shown). *Step 2*: These images are used to reconstruct the tomographic volume computationally. *Step 3*: Finally, the tomogram is segmented in 3D and features of interest may be highlighted (mitochondrial outer membrane in *green*, inner boundary membrane in *blue* and crista membranes in *yellow*). The *upper left panel* shows an enlargement of a cluster of protein import sites. The *upper right panel* (adapted from [4]) shows a close up of a two-dimensional slice through a tomogram. The area around the labeled protein import machinery is indicated with a *red box*, QD<sub>605</sub> is highlighted with a *red arrow*. Scale bar, 10 nm

is dependent on a perfectly aligned microscope. For detailed information on electron microscopy setup and data recording, refer to Davies et al. [21].

1. Search the grid at a low magnification so that several ice holes are visible in one image, e.g., 3600 $\times$ , corresponding to a pixel size of 3.8 nm on a Titan Krios equipped with a K2 Summit direct detector camera. This can be performed either manually, or automatically by creation of an atlas using microscopy software such as Serial EM [17]. Locate mitochondria, which are easily identified by a fuzzy double membrane visible at this magnification if an energy filter is used (*see Note 19*).
2. Bring the sample to eucentric height by altering the z-height of the stage. This is the point whereby minimal xy movement of the sample is seen when tilting.
3. Determine the tilt range for the sample by tilting the stage  $\pm 60^\circ$  to ensure that both the area of interest and the area of focus can be viewed fully without obstruction (*see Note 20*).
4. Decide on an appropriate magnification for data collection. Mitochondria often fit within a 2  $\mu\text{m}$  hole on a Quantifoil R2/2 grid, thus choose a magnification on the microscope in which a hole can be completely visualized. For a Titan Krios equipped with a K2 Summit direct detector camera, we use a magnification of 26,000 $\times$  corresponding to a pixel size of 5.3  $\text{\AA}$ .
5. Establish the optimal beam intensity and dose distribution parameters for the tomographic tilt series. For the K2 Summit camera in counting mode, an electron dose rate of  $\sim 8$  e $^-$ /pixel/s per recorded image is optimal. As the sample is tilted, the ice thickness increases. Software can compensate for this by increasing the exposure time of samples at high tilt. Determine the thickness of the ice by recording a 1 s image of a test area with similar ice thickness at both  $0^\circ$  and  $60^\circ$  tilt. Divide the average counts for the  $0^\circ$  image with the  $60^\circ$  image to determine the  $I_0/I_{60}$  ratio and include this value in the tomographic setup parameters. Then collect a 1 s image over an ice hole and multiply the electron dose value obtained for a single image (in e $^-$ / $\text{\AA}^2$ ) by the total number of images in the series (for a series from  $-60^\circ$  to  $+60^\circ$  at tilt steps of  $2^\circ$ , this would be 61 images). Check that the total dose for the tilt series is not over the recommended limit ( $< 200$  e $^-$ / $\text{\AA}^2$ ) (*see Note 21*).
6. Set the desired defocus value in the tomographic setup. High defocus increases contrast at the loss of resolution. A defocus of 6–8  $\mu\text{m}$  is a good compromise between contrast and morphological detail for relatively thick specimens such as mitochondria.
7. Collect a tomographic tilt series using automated software, such as Latitude (Digital Micrograph, Gatan, Pleasanton, USA) or Serial EM [17]. If possible, we recommend collecting

images as movie frames, whereby beam-induced sample movement can be corrected for by aligning the individual frames during processing (*see* **Notes 22** and **23**).

### 3.7.3 Tomogram Reconstruction and Visualization

1. Align the movie frames by cross-correlating single frames, aligning and then summing them. Various software, such as IMOD [18], is able to do this (*see* **Note 23**).
2. Reconstruct a tomogram by aligning and back-projecting individual images of the tilt series to generate a 3D volume of the sample. This is carried out computationally using software such as IMOD, which is well documented (*see* <http://bio3d.colorado.edu/imod/doc/etomoTutorial.html> for a tutorial). At this step QDs should be clearly visible in the tomogram and can be identified by a white halo around a black sphere (diameter depending on the type of QDs used).
3. If necessary, increase the contrast of the tomogram by filtering, such as by nonlinear anisotropic diffusion (NAD) or low pass filtering in IMOD.
4. Segment the tomogram to enable features of interest to be highlighted and visualized in 3D. Programmes such as IMOD or AMIRA can be used. Voxels corresponding to the inner or outer membrane are assigned a label, which is then used to generate a surface. Features of interest, such as QDs, can then be located and marked in the 3D volume for statistical analysis.

### 3.8 Variation on a Theme: Direct Labeling of Mitochondrial Outer Membrane Proteins

Above, we have described the visualization of active mitochondrial preprotein import sites via QD-labeling of  $b_2\Delta$ -DHFR<sub>biotin</sub> arrested in TOM-TIM23 supercomplexes using the STAMP method. This procedure can be easily adapted for direct labeling of surface exposed outer mitochondrial membrane proteins carrying an Avi-tag instead of a bound ligand. In such cases, it is of crucial importance to verify expression of the Avi-tagged protein (*see* **Note 24**) and to test if tagging interferes with its function (*see* **Note 25**). An example for such a variation of the STAMP method is described briefly in this final section for the visualization of Fzo1 (mitofusin). Fzo1 is a mitochondrial fusion protein required for tethering and accumulates at mitochondrial contact sites prior to mixing of outer membranes [22, 23]. In order to label the outer membrane fusion protein Fzo1 in *S. cerevisiae*, we expressed Fzo1-AviTag or wild-type Fzo1 from centromeric plasmids under control of the native *FZO1* promoter (pRS314-*FZO1*-AviTag or pRS314-*FZO1*, respectively) in a strain where the chromosomal copy of the *FZO1* gene had been deleted (derived from the wild-type strain W303). With mitochondria isolated from these strains, the surface-exposed Avi-tag is biotinylated using the biotin ligase BirA. Prior to QD labeling, biotinylated mitochondria are concentrated by centrifugation and incubated on ice to promote their Fzo1-dependent attachment.

This procedure induces the accumulation and concentration of Fzo1 molecules at mitochondrial contact sites favoring the probability of biotinylated molecules being recognized by streptavidin-coupled QDs. Following QD labeling all steps for electron cryo-tomography analysis (*see* Subheading 3.7) are carried out in the same way as for the labeling of active preprotein import sites with  $b_2\Delta$ -DHFR<sub>biotin</sub>. As control samples, mitochondria that do not express an Avi-tagged version of the Fzo1 protein are used in the biotinylation and QD labeling reactions.

1. Isolate mitochondria from wild-type Fzo1- and Fzo1-AviTag-expressing yeast cells (*see* **Note 3**).
2. Perform the biotinylation reaction by resuspending isolated mitochondria (500  $\mu$ g total mitochondrial protein amount) in 200  $\mu$ l biotinylation buffer supplemented with 10  $\mu$ l of BirA at 1  $\mu$ g/ $\mu$ l. Incubate samples for 1 h at room temperature on a rotating wheel.
3. Centrifuge the samples at  $10,000 \times g$  for 10 min at 4 °C, remove the supernatant, add 40  $\mu$ l of biotinylation buffer to the pellets and leave the samples horizontally on ice for 40 min. The centrifugation step brings mitochondria in close proximity. The subsequent incubation on ice is necessary to allow for efficient accumulation of Fzo1 molecules at mitochondrial junctions and Fzo1-dependent mitochondrial attachment.
4. Add to each sample 60  $\mu$ l of a 83 nM QD<sub>525</sub> solution in NMIB buffer (~50 nM final concentration of QDs), carefully resuspend the pellet by pipetting three or four times, and incubate samples on ice for 1 h.
5. Centrifuge at  $3000 \times g$  for 10 min at 4 °C, wash mitochondria twice with 1 ml EM buffer to remove unbound QDs and resuspend pellets in 40  $\mu$ l EM buffer that is suitable for cryo-ET analysis.
6. For electron cryo-tomography, follow steps described in Subheading 3.7.

---

## 4 Notes

1. For this study, we used *E. coli* BMH 71–18 cells (Clontech, Mountain View, USA) as described by Dekker et al. [11].
2. The volume and exact concentration of maleimide-PEG<sub>2</sub>-biotin depends on the protein concentration and the volume of the labeling reaction desired. In this case, standard volumes are 1 ml of 200  $\mu$ M  $b_2\Delta$ -DHFR<sub>cys</sub> after size-exclusion chromatography (described in Subheading 3.1), requiring 2 mM (final concentration) maleimide-PEG<sub>2</sub>-biotin. The maleimide-PEG<sub>2</sub>-biotin reagent used (Pierce, Rockford, USA) comes in a “no-weigh” format, making a stock solution of 20 mM.

3. For a detailed protocol describing the isolation of intact, protein import-competent mitochondria from the yeast *Saccharomyces cerevisiae* refer to Meisinger et al. [24].
4. Ten microliter aliquots of the methotrexate stock solution are prepared and can be stored at  $-20\text{ }^{\circ}\text{C}$ . Methotrexate stock aliquots are thawed immediately before dilution into the import reaction. To achieve a dilution of 1:2000 in import buffer, the 10 mM methotrexate stock solution in MOPS buffer may be first diluted 1:20 in water to a final concentration of 500  $\mu\text{M}$  methotrexate. Finally, a 1:100 dilution of this solution in import buffer is prepared.
5. The use of Blue native-PAGE for the analysis of mitochondrial protein import has been described in detail by Vögtle et al. [25].
6. The antibodies against *S. cerevisiae* Tim23 used in our study were kindly provided by Nikolaus Pfanner (Freiburg, Germany) [4].
7. High concentrations of DTT are maintained throughout the purification until the last step. This prevents dimers of  $\text{b}_2\Delta\text{-DHFR}_{\text{cys}}$  forming through the unique carboxy-terminal cysteine. Removal of DTT in the last step and immediate labeling with maleimide-PEG<sub>2</sub>-biotin minimizes the amount of protein lost through dimerization.
8. If the total volume of pooled protein exceeds 10 % of the total bed volume of the column, concentrate the protein before loading. This can be done using Amicon Ultra-15 ml concentrators with a molecular weight cutoff of 30 kDa (Subheading 2.1).
9. Mitochondria isolated from *S. cerevisiae* cells are quickly frozen in liquid nitrogen and can be stored in SEM buffer at  $-80\text{ }^{\circ}\text{C}$  for several years without losing protein import competence.
10. Mitochondria must be carefully washed to remove the  $\text{b}_2\Delta\text{-DHFR}_{\text{biotin}}$  that is not stably engaged in import sites. This is achieved by repeating the washing step at least twice. To preserve the integrity of mitochondrial membranes, resuspension of mitochondria with a pipette during the washing steps is not recommended. Instead, Eppendorf tubes containing the mitochondrial samples are placed in the centrifuge rotor with an opposite orientation compared to the previous centrifugation round (turn the tubes by  $180^{\circ}$  around their vertical axis). This leads to the transfer of the mitochondrial pellet to the opposite side of the tube wall during centrifugation.
11. The amount of mitochondria to be subjected to Blue native-PAGE analysis depends on the relative abundance of the protein complex that is analyzed and the complex-specific antibodies used in the procedure. Approximately 70  $\mu\text{g}$  of total

mitochondrial protein content is the optimal amount for the detection of TIM23 complexes with the polyclonal antibodies raised in rabbits against the central Tim23 subunit that was used in our studies.

12. To efficiently solubilize mitochondrial membrane protein complexes while preserving their integrity, carefully and thoroughly dissolve the mitochondrial pellet in digitonin-containing buffer. The use of small tips with a 20–200  $\mu$ l pipette is preferred over the larger tips for 1000  $\mu$ l pipettes. While pipetting, avoid foam formation and prolonged handling at room temperature.
13. The choice of polyacrylamide concentrations for preparing Blue native gradient gels depends on the molecular weight of the protein complexes of interest. Concentrations of 6–16.5 % are optimal to resolve protein complexes with a molecular weight between 100 and 700 kDa.
14. Block the PVDF membrane carrying the transferred proteins by incubation for 1 h in a solution of 5 % (w/v) skimmed milk in 20 mM Tris-HCl pH 7.5, 125 mM NaCl. Subsequently, incubate the membrane for 1 h in the same solution supplemented with 0.05 % Tween 20 and the Tim23-specific antiserum (1:400 dilution) (*see Note 6*). Wash the membrane four times with 20 mM Tris-HCl pH 7.5, 125 mM NaCl for 10 min and, finally, incubate for 1 h in 20 mM Tris-HCl pH 7.5, 125 mM NaCl, 0.05 % Tween 20 supplemented with peroxidase-conjugated anti-rabbit IgG secondary antibodies (1:2000 dilution). Peroxidase activity is revealed by enhanced chemiluminescence.
15. Note that 70  $\mu$ g of mitochondria have been previously removed for verification of  $b_2\Delta$ -DHFR<sub>biotin</sub> import intermediates (Subheading 3.4). QDs are in a ~15-fold molar excess over the molar amount of Tim23 present in the remaining 330  $\mu$ g of total mitochondrial protein.
16. This step is not necessary if mitochondria with a co-expressed fluorescent protein are used.
17. If you have trouble obtaining grids with optimal ice thickness, try blotting half of the grid only. This results in an ice-thickness gradient across the grid. Also try altering the concentration of your sample and the blotting time. Ethane solidifies in liquid nitrogen and can contaminate the grid during freezing. To avoid this, dip a piece of filter paper into the liquid ethane and quickly slide the grid along the filter paper while transferring it from liquid ethane to liquid nitrogen after plunge freezing.
18. To avoid sample dehydration before freezing, try to use a device that has a humidity controlled chamber. To prevent ice contamination after freezing, a dehumidified environment is preferable (10–20% is ideal).

19. When searching the grid for mitochondria, we found that taking a single exposure image (0.5–1 s) at your chosen data collection magnification before starting the tomogram is helpful. It can be used to verify that both mitochondrial membranes are clearly intact and that QDs are present in the sample. It also helps to determine the dose rate applied to the area of interest.
20. In order to obtain the best quality tomograms, the focus area has to be as close to the area of interest as it can be without causing radiation damage. For example, if the beam diameter is 2.5  $\mu\text{m}$ , the focus spot should be 2.5–3  $\mu\text{m}$  away from the area of interest along the tilt axis.
21. If your calculated total dose for the tilt series (required to obtain a dose rate of  $\sim 8 \text{ e}^-/\text{pixel}/\text{s}$  per recorded image) is  $>200 \text{ e}^-/\text{\AA}^2$ , your ice is too thick for good quality tomograms. You can reduce the total dose by increasing the tilt step increments (therefore reducing the total number of images), but it would be best to freeze new samples.
22. When collecting a tilt series, we recommend that it is started at  $24^\circ$  and images are collected through to the tilt minimum ( $-60^\circ$ ). Subsequently, the second part of the tilt series is collected from  $24^\circ$  to the tilt maximum ( $60^\circ$ ), thus collecting the highest quality images (at low tilt where the ice is thinnest) at the beginning of the series when least radiation damage has occurred. Alternatively the series can be started from  $-24^\circ$  and collected through to  $60^\circ$ , with the second part collected from  $-24^\circ$  to  $-60^\circ$ .
23. When collecting a tilt series as movie frames, we found that frame times of 0.3–0.4 s work best for samples with relatively thick ice such as mitochondria. Shorter frame times lead to poor alignment due to weaker signal. To align movie frames, we use IMOD-based scripts: Cross-correlation and filtering using ‘tiltxcorr’, conversion of single image transforms into alignment transform using ‘xftoxg’, creating a new, aligned stack using ‘newstack’ and finally averaging the stack into a single image using ‘clip avg’. The relevant details can be found in the IMOD online manual (<http://bio3d.colorado.edu/imod/doc/etomoTutorial.html>).
24. For this study, whole cell extracts were analyzed for expression of the wild-type Fzo1 and Fzo1-AviTag proteins by western blotting using  $\alpha$ -Fzo1 antibodies (Covalab, Villeurbanne, France). After in vitro biotinylation (**step 2**), probes such as the Strep-Tactin HRP conjugate (IBA Life Sciences, Göttingen, Germany) can be employed to detect the biotinylated Avi-tagged protein by western blot.
25. We performed a spot test with yeast cells expressing Fzo1-AviTag and control cells to ensure that the Avi-Tag fused to the target protein does not interfere with its biological function.

In brief, yeast strains were cultured overnight at 30 °C in a suitable minimal medium (without tryptophan in the case of pRS314-derived plasmids that contain a *TRPI* selection marker). Cells were washed with sterile dH<sub>2</sub>O and resuspended at an OD<sub>600</sub> of 1. We made 1:10 serial dilutions (five times) in sterile dH<sub>2</sub>O for each strain and spotted 5 µl of each dilution onto minimal medium agar plates containing a fermentable (glucose) or non-fermentable (glycerol) carbon source. Plates were incubated for 3 days (glucose medium) or 5 days (glycerol medium) at 30 °C. Growth of the AviTag-expressing cells was compared to the control cells. In general, if growth of the AviTag-expressing strain is impaired, it should be considered to move the tag to different positions in the protein of interest or to include a linker peptide.

---

## Acknowledgments

We thank Werner Kühlbrandt for discussion and critical reading of the manuscript. This work was supported by the Max Planck Society (V.A.M.G., T.B.), the Deutsche Forschungsgemeinschaft (Sonderforschungsbereich 746) (M.v.d.L), the Excellence Initiative of the German Federal & State Governments (EXC 294 BIOSS) (M.v.d.L.), the CNRS-INSERM ATIP-Avenir program (M.C., R.I.), the “fondation pour la recherche médicale” (INE 20100518343) (M.C.), the labex DYNAMO (ANR-11-LABX-0011-DYNAMO) (M.C.), a Marie Curie IRG grant to M.C. (No.276912), and an EMBO Long-Term Fellowship to V.A.M.G. (ALTF 1035-2010).

## References

1. Krogh A, Larsson B, von Heijne G et al (2001) Predicting transmembrane protein topology with a hidden Markov model: applications to complete genomes. *J Mol Biol* 305:567–580
2. Irobalieva RN, Martins B, Medalia O (2016) Cellular structural biology as revealed by cryo-electron tomography. *J Cell Sci* 129:469–476
3. Davies KM, Daum B (2013) Role of cryo-ET in membrane bioenergetics research. *Biochem Soc Trans* 41:1227–1234
4. Gold VA, Ieva R, Walter A et al (2014) Visualizing active membrane protein complexes by electron cryo-tomography. *Nat Commun* 5:4129
5. Endo T, Yamano K, Kawano S (2011) Structural insight into the mitochondrial protein import system. *Biochim Biophys Acta* 1808:955–970
6. Harbauer AB, Zahedi RP, Sickmann A et al (2014) The protein import machinery of mitochondria – a regulatory hub in metabolism, stress, and disease. *Cell Metab* 19:357–372
7. Wenz LS, Opaliński Ł, Wiedemann N et al (2015) Cooperation of protein machineries in mitochondrial protein sorting. *Biochim Biophys Acta* 1853:119–1129
8. Mokranjac D, Neupert W (2010) The many faces of the mitochondrial TIM23 complex. *Biochim Biophys Acta* 1797:1045–1054
9. Schulz C, Schendzielorz A, Rehling P (2015) Unlocking the presequence import pathway. *Trends Cell Biol* 25:265–275
10. Dudek J, Rehling P, van der Laan M (2013) Mitochondrial protein import: common principles and physiological networks. *Biochim Biophys Acta* 1833:274–285

11. Dekker PJ, Martin F, Maarse AC et al (1997) The Tim core complex defines the number of mitochondrial translocation contact sites and can hold arrested preproteins in the absence of matrix Hsp70-Tim44. *EMBO J* 16:5408–5419
12. Popov-Celeketić D, Mapa K, Neupert W et al (2008) Active remodelling of the TIM23 complex during translocation of preproteins into mitochondria. *EMBO J* 27:1469–1480
13. Tamura Y, Harada Y, Shiota T et al (2009) Tim23-Tim50 pair coordinates functions of translocators and motor proteins in mitochondrial protein import. *J Cell Biol* 184:129–141
14. Ieva R, Schrempp SG, Opaliński Ł et al (2014) Mgr2 functions as lateral gatekeeper for pre-protein sorting in the mitochondrial inner membrane. *Mol Cell* 56:641–652
15. Beckett D, Kovaleva E, Schatz PJ (1999) A minimal peptide substrate in biotin holoenzyme synthetase-catalyzed biotinylation. *Protein Sci* 8:921–929
16. Howarth M, Takao K, Hayashi Y et al (2005) Targeting quantum dots to surface proteins in living cells with biotin ligase. *Proc Natl Acad Sci U S A* 102:7583–7588
17. Mastronarde DN (2005) Automated electron microscope tomography using robust prediction of specimen movements. *J Struct Biol* 152:36–51
18. Kremer JR, Mastronarde DN, McIntosh JR (1996) Computer visualization of three-dimensional image data using IMOD. *J Struct Biol* 116:71–76
19. Gebert M, Schrempp SG, Mehnert CS et al (2012) Mgr2 promotes coupling of the mitochondrial presequence translocase to partner complexes. *J Cell Biol* 197:595–604
20. Sirrenberg C, Endres M, Becker K et al (1997) Functional cooperation and stoichiometry of protein translocases of the outer and inner membranes of mitochondria. *J Biol Chem* 272:29963–29966
21. Davies KM, Daum B, Gold VA et al (2014) Visualization of ATP synthase dimers in mitochondria by electron cryo-tomography. *J Vis Exp* 91:51228
22. Meeusen S, McCaffery JM, Nunnari J (2004) Mitochondrial fusion intermediates revealed in vitro. *Science* 305:1747–1752
23. Hoppins S, Horner J, Song C et al (2009) Mitochondrial outer and inner membrane fusion requires a modified carrier protein. *J Cell Biol* 184:569–581
24. Meisinger C, Pfanner N, Truscott KN (2006) Isolation of yeast mitochondria. *Methods Mol Biol* 313:33–39
25. Vögtle FN, Schmidt O, Chacinska A et al (2010) Native techniques for analysis of mitochondrial protein import. *Methods Mol Biol* 619:425–436

## Assays for Mitophagy in Yeast

Akinori Eiyama and Koji Okamoto

### Abstract

Elimination of damaged or surplus mitochondria is crucial to maintain cellular integrity and an energy supply-demand balance. Mitophagy serves to selectively catabolize mitochondria in a manner dependent on autophagy, and contributes to mitochondrial quality and quantity control. This degradation system is highly conserved among eukaryotes including the budding yeast, *Saccharomyces cerevisiae*. Therefore, analyses of mitophagy using yeast have the potential to provide insights into the common mechanisms of mitophagy. Here, we introduce experimental approaches with fluorescence microscopy and western blotting to validate mitophagy in yeast. The former is useful to visualize transport of mitochondria to the vacuole, a lytic compartment, and formation of mitochondria-containing autophagosomes. The latter allows us to quantify mitochondria degradation.

**Key words** Mitophagy, Mitochondria degradation, Mitophagosome, Respiration, Yeast

---

### 1 Introduction

Mitochondria compartmentalize a number of metabolic processes including ATP synthesis in eukaryotic cells. Although mitochondria are highly efficient energy converters, they also generate reactive oxygen species (ROS) that cause oxidative stress, ultimately leading to mitochondrial dysfunction. Accumulation of dysfunctional mitochondria negatively affects cellular homeostasis, which often results in various pathologies. In addition, superfluous mitochondria can be unwanted sources of ATP wasting and ROS production. To overcome these problems, cells take advantage of mitochondria degradation system termed “mitophagy,” one of the selective autophagy pathways that mediate sequestration of specific proteins or organelles into double membrane-bound structures called autophagosomes, and transport of those cargoes to lysosomes. Numerous studies have recently revealed the physiological significance of mitophagy [1–3]; however, the underlying molecular mechanisms remain largely unknown.

Mitophagy is a sophisticated catabolic system conserved from lower to higher eukaryotes. Hence, the unicellular budding yeast,

*Saccharomyces cerevisiae*, is a simple yet powerful model organism to elucidate the common basic principles of mitophagy. In addition to 15 core autophagy-related (Atg) proteins essential for formation of autophagosomes [4, 5], the mitochondria-anchored protein Atg32 is required for mitophagy in yeast [6, 7]. When oxidative stress accumulates in mitochondria, Atg32 is induced, localized on the surface of mitochondria, and interacts with other Atg proteins, which mediates formation of mitochondria-containing autophagosomes (mitophagosomes) [8]. In general, mitophagy in yeast is strongly facilitated during prolonged respiratory growth, or a shift of culture conditions from respiration to starvation [6, 7].

Here, we describe two methods for monitoring mitophagy in yeast using fluorescence microscopy and western blotting. Inhibition of mitophagy results from defects in mitophagosome formation, transport of mitophagosomes to the vacuole (a lytic organelle in yeast), or degradation in the vacuole. Fluorescence imaging enables one to clarify which phase of mitophagy is impaired in mutant cells. In addition, western blotting makes it possible to identify mutants even partially and slightly defective in mitophagy, because mitochondria degradation can be quantified by this assay. Accordingly, a combination of these fast and easy assays provides a comprehensive evaluation of mitophagy.

---

## 2 Materials

### 2.1 Preparation of DNA Cassettes for Yeast Transformation

#### 1. Plasmids.

pBSII-GPD<sup>P</sup>-mito-GFP-CgHIS3 (needed in Subheading 3.3).

pBSII-GPD<sup>P</sup>-mito-mCherry-CgHIS3 (needed in Subheading 3.4).

pBSII-TEF<sup>P</sup>-mito-DHFR-mCherry-CgHIS3 (needed in Subheading 3.5).

pBSII-mCherry-kanMX4 (needed in Subheading 3.3).

The plasmids are available from the authors upon request.

#### 2. Primers.

For PCR amplification of the GPD<sup>P</sup>-mito-GFP-CgHIS3, GPD<sup>P</sup>-mito-mCherry-CgHIS3, and TEF<sup>P</sup>-mito-DHFR-mCherry-CgHIS3 cassettes

that can be integrated into the *bis3* locus: forward primer, 5'-AATGTGATTTCTTCGAAGAATATACTAA AAAATGAGCAGGCA

AGATAAACGAAGGCAAAGCGACGGTATCGA TAAGCTTG-3'; reverse primer, 5'-G

GTATACATATATACACATGTATATATATCGTATG-CTGCAGCTTTAAATAATCGGTGTCACAAGCG-CGCAATTAACCCTC-3'.

For PCR amplification of the mCherry-kanMX4 cassette that can be integrated into the downstream of the *VPHI* locus fused in frame: forward primer, 5'-CGCATT TGAGTATAA

AGACATGGAAGTCGCTGTTGCTAGTGCAAGCTCTTC CGCTTCAAGCATGGT GAGCAAGGGCGAGG-3'; reverse primer, 5'-GCATCATT TATTATTTAATGAAG TACTTA

AATGTTTTCGCTTTTTTTTAAAAGTCCTCAAATTTA-GAAAACTCATCGAGC-3'.

Long primers (>30 mers) should be purified by an oligonucleotide purification cartridge. The concentration of primers is 10  $\mu$ M.

## 2.2 Construction of Yeast Strains

1. Yeast strain: BY4741, *MATa his3 $\Delta$ 1 lue2 $\Delta$ 0 met15 $\Delta$  ura3 $\Delta$*  (see Note 1).
2. Yeast extract medium with peptone and dextrose (YPD): 1% (w/v) yeast extract, 2% (w/v) peptone, 2% (w/v) dextrose. For YP, dissolve yeast extract and peptone in water and autoclave. Dissolve dextrose in water and autoclave. Mix YP and dextrose after autoclaving. Store liquid media at room temperature.
3. Sterile water.
4. 100 mM lithium acetate: filter-sterilize and store at room temperature.
5. 60% (w/v) polyethylene glycol (PEG) (average molecular weight: 3350): filter-sterilize and store at room temperature.
6. 1 M lithium acetate: filter-sterilize and store at room temperature.
7. 10 mg/mL single-stranded salmon sperm DNA (ssDNA): boil for 5 min and store at  $-30$  °C.
8. DNA cassette as prepared in Subheading 3.1.
9. Synthetic histidine-dropout solid medium with dextrose (SD-His): 0.17 % (w/v) yeast nitrogen base without amino acids, 0.5 % (w/v) ammonium sulfate, 2 % (w/v) dextrose, amino acid/nucleoside supplements without histidine, 2 % (w/v) agar. For solid SD, dissolve yeast nitrogen base without amino acids and ammonium sulfate in water, add agar, and autoclave. Dissolve dextrose in water and autoclave. Mix SD and dextrose together with filter-sterilized amino acid/nucleoside supplements and pour plates. Agar media are stored at 4 °C.
10. YPD solid medium with geneticin (YPD+G418): YPD, 0.25 mg/mL G418, 2 % (w/v) agar. For solid YP, dissolve yeast extract and peptone in water, add agar, and autoclave. Dissolve dextrose in water and autoclave. Mix YP and dextrose, and pour plates. Agar media are stored at 4 °C.

**2.3 Fluorescence  
Microscopy  
for Visualizing  
Mitophagy in Living  
Cells**

1. Synthetic medium with dextrose and casamino acids (SDCA): 0.17 % (w/v) yeast nitrogen base without amino acids, 0.5 % (w/v) ammonium sulfate, 0.5 % (w/v) casamino acids, 2 % (w/v) dextrose, 20 µg/mL adenine sulfate, 20 µg/mL L-tryptophan, 20 µg/mL uracil.
2. Synthetic medium with dextrose, glycerol, and casamino acids (SDGlyCA): 0.17 % (w/v) yeast nitrogen base without amino acids, 0.5 % (w/v) ammonium sulfate, 0.5 % (w/v) casamino acids, 0.1 % (w/v) dextrose, 3 % (v/v) glycerol, 20 µg/mL adenine sulfate, 20 µg/mL L-tryptophan, 20 µg/mL uracil.
3. BY4741 *vph1::VPH1-mCherry::kanMX6 his3Δ1::GPDP-mito-GFP::CgHIS3* (positive control strain).
4. BY4741 *vph1::VPH1-mCherry::kanMX6 his3Δ1::GPDP-mito-GFP::CgHIS3 atg32Δ* (negative control strain).

**2.4 Fluorescence  
Microscopy  
for Detecting  
Mitophagosomes  
in Living Cells**

1. SDCA.
2. SDGlyCA.
3. BY4741 *his3Δ1::GPDP-mito-mCherry::CgHIS3 ypt7Δ* (positive control strain).
4. BY4741 *his3Δ1::GPDP-mito-mCherry::CgHIS3 ypt7Δ atg32Δ* (negative control strain).

**2.5 Western Blotting  
for Quantifying  
Mitophagy**

1. SDCA.
2. SDGlyCA.
3. BY4741 *his3Δ1::TEFP-mito-DHFR-mCherry::CgHIS3* (positive control strain).
4. BY4741 *his3Δ1::TEFP-mito-DHFR-mCherry::CgHIS3 atg32Δ* (negative control strain).
5. 0.1 M NaOH.
6. Sample buffer: 60 mM Tris-HCl, pH 6.8, 5% (v/v) glycerol, 2% (w/v) SDS, 20 mM DTT, 0.00025% (w/v) bromophenol blue.
7. Polyacrylamide gel containing 10 % (w/v) acrylamide/*bis*-acrylamide (ratio 37.5:1).
8. Polyvinylidene fluoride (PVDF) or nitrocellulose membranes (pore size: 0.45 µm). PVDF membranes should be activated in methanol before use.
9. Blocking buffer: TBS-T, 5 % (w/v) nonfat dry milk.
10. Incubation buffer A: TBS-T, 0.1 % (w/v) nonfat dry milk.
11. Incubation buffer B: TBS-T, 1 % (w/v) nonfat dry milk.
12. Washing buffer (TBS-T): 137 mM NaCl, 2.68 mM KCl, 25 mM Tris-HCl, pH 7.4, 0.1% (v/v) Tween-20.

13. Primary antibodies: rabbit polyclonal anti-RFP (kindly provided from Shuh-ichi Nishikawa in Niigata University, Japan) and mouse monoclonal anti-Pgk1 (Invitrogen).
14. Secondary antibodies: horseradish peroxidase (HRP)-conjugated goat anti-rabbit IgG (Jackson ImmunoResearch) and HRP-conjugated rabbit anti-mouse IgG (Jackson ImmunoResearch).
15. Enhanced chemiluminescence (ECL) detection reagents.

---

### 3 Methods

#### 3.1 Preparation of DNA Cassettes for Yeast Transformation

The DNA fragment cassettes, GPD<sup>P</sup>-mito-GFP-CgHIS3 (2.8 kb), GPD<sup>P</sup>-mito-mCherry-CgHIS3 (2.8 kb), TEF<sup>P</sup>-mito-DHFR-mCherry-CgHIS3 (3.2 kb), and mCherry-kanMX4 (2 kb) can be generated by PCR reactions (described below) with the template plasmids and primers described in Subheading 2.1, purified using spin columns, and eluted into sterile water. A typical working DNA solution is 0.2–0.6 mg/mL.

DNA polymerase for PCR: KOD -Plus- Neo (TOYOBO).

PCR program: 94 °C 2 min, 30× (98 °C 10 s, 55 °C 30 s, 68 °C 1 min/kb), 68 °C 10 min, 4 °C ever (extension time at 68 °C depends on the length of DNA cassettes).

#### 3.2 Construction of Yeast Strains

When strains expressing mito-GFP and Vph1-mCherry are constructed, transformation is performed in a sequential manner. The method of one transformation is described below.

1. Grow cells to mid-log phase at OD<sub>600</sub> of 1 in 3 mL of YPD.
2. Transfer 0.5 OD<sub>600</sub> units of cells to a 1.5-mL microcentrifuge tube, collect them by centrifugation at 7900 × *g* for 30 s, and discard the supernatant using a micropipette.
3. Wash the cells with 500 μL of sterile water, collect them by centrifugation at 7900 × *g* for 30 s, and discard the supernatant using a micropipette.
4. Resuspend the cells in 400 μL of 100 mM lithium acetate and incubate statically at 30 °C for 10 min.
5. Collect the cells by centrifugation at 7900 × *g* for 30 s and discard the supernatant using a micropipette.
6. Add 60.5 μL of 60% PEG, 10.2 μL of 1 M lithium acetate, 1 μL of ssDNA, 10 μL of sterile water, 10 μL of 0.4 mg/mL DNA cassette to the cell pellet and vortex thoroughly.
7. Incubate the cells statically at 30 °C for 30 min, followed by a heat shock at 42 °C for 20 min.
8. Add 400 μL of YPD to the cell suspension and incubate statically at 30 °C for 3 h.

9. Collect the cells by centrifugation at  $7900 \times g$  for 30 s, discard 300  $\mu\text{L}$  of the supernatant using a micropipette, and vortex the cell pellet thoroughly.
10. Spread the cell suspension on agar plates of SD-His and YPD+G418 for DNA cassettes containing CgHIS3 and kanMX4, respectively, and incubate them at 30 °C for 48 h.
11. Restreak the colonies on new selection plates.
12. Grow cells to mid-log phase in 3 mL of SDCA and confirm typical expression patterns of mitochondrial tubules (mito-GFP, mito-mCherry, and mito-DHFR-mCherry) and vacuolar spheres (Vph1-mCherry) using a fluorescence microscope (*see* Figs. 1 and 2).

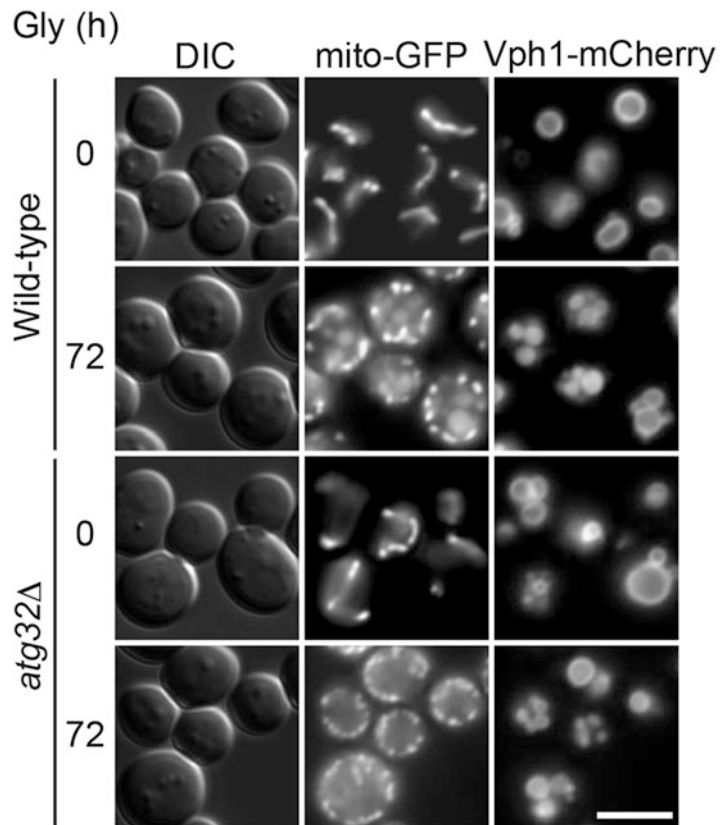


**Fig. 1** Live-cell imaging of mitophagy by fluorescence microscopy. Mitochondrial GFP- and vacuolar Vph1-mCherry-expressing wild-type and *atg32Δ* cells grown to mid-log phase in dextrose medium were transferred to respiration medium (Gly) for 72 h, and observed using a fluorescence microscope. *Scale bar*, 5  $\mu\text{m}$

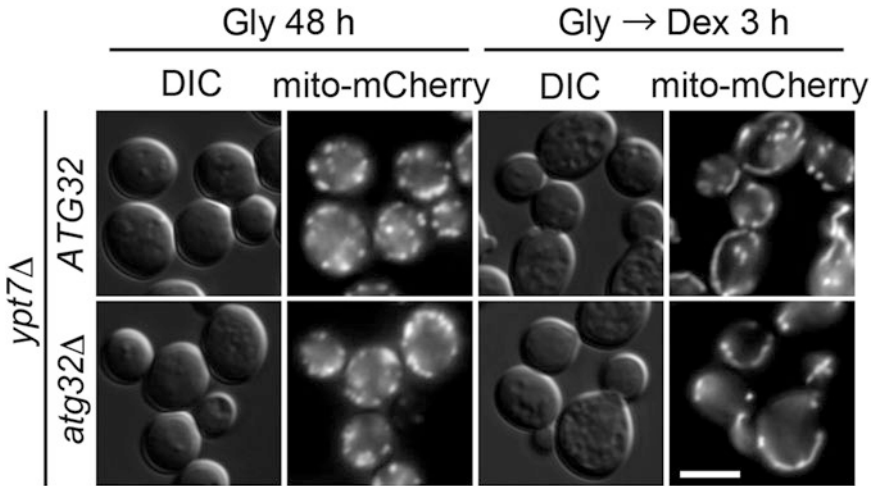


**Fig. 2** Live-cell imaging of mitophagosomes by fluorescence microscopy. Mitochondrial mCherry-expressing *ypt7Δ* and *ypt7Δ atg32Δ* cells grown to mid-log phase in dextrose medium (Dex) were transferred to respiration medium (Gly) for 48 h, shifted to Dex for 3 h, and observed using a fluorescence microscope. Scale bar, 5  $\mu$ m

### 3.3 Fluorescence Microscopy for Visualizing Mitophagy in Living Cells

Colocalization of mitochondria and vacuoles can be visualized in cells expressing GFP fused to the C-terminus of a mitochondrial targeting signals derived from *Neurospora crassa* ATP synthase subunit 9 (mito-GFP) and mCherry fused at the C-terminus of Vph1, a membrane-integrated subunit of the vacuolar ATPase (Vph1-mCherry). When mitophagy proceeds, a fraction of mitochondria is transported to the vacuole and immediately degraded by vacuolar hydrolases, while GFP is considerably resistant to degradation. Accordingly, an overlap between GFP and Vph1-mCherry signals represents mitochondria degradation ([6, 9]). Little or no overlap between the two fluorescent signals indicates that formation of mitophagosomes or transport of mitochondria to the vacuole is impaired (for live-cell imaging of mitophagosomes, see Subheading 3.4). In addition, dot-like GFP patterns colocalized with Vph1-mCherry imply that vacuolar degradation is defective.

Mitophagy extensively occurs under respiratory conditions. Here, non-fermentable glycerol medium is used for induction of mitochondria degradation.

1. Grow cells expressing mito-GFP (mitochondrial marker) and Vph1-mCherry (vacuolar marker) to mid-log phase in 3 mL of SDCA.
2. Transfer 0.07 OD<sub>600</sub> units of cells to 7 mL of SDGlyCA and incubate them at 30 °C for 72 h in a shaker (180 rpm).
3. Transfer 200  $\mu$ L of cell culture (usually OD<sub>600</sub> = 4–5) into a 1.5-mL microcentrifuge tube.

4. Collect the cells by centrifugation at  $7900 \times g$  for 30 s, discard 150  $\mu\text{L}$  of the supernatant using a micropipette, and vortex the cell pellet thoroughly.
5. Pipet 1.6–2.0  $\mu\text{L}$  of the cell suspension onto a microscope slide, and cover with a square cover slip (no sealing is necessary).
6. Observe the cells using a fluorescence microscope equipped with filter sets for GFP and mCherry (*see* **Note 2**).
7. If mitophagy occurs, the overlap between GFP and mCherry signals can be observed (*see* Fig. 1 and **Note 3**).

### 3.4 Fluorescence Microscopy for Detecting Mitophagosomes in Living Cells

Mitophagosomes can be detected in cells lacking Ypt7, a Rab family GTPase essential for homotypic vacuole fusion. Since autophagosomes do not fuse with vacuoles in *ypt7*-null cells [10], mitophagosomes remain isolated and accumulate in the cytosol during prolonged respiratory growth. Mitochondrial shape alters from tubules to fragments upon a shift of culture conditions from fermentation (SDCA) to respiration (SDGlyCA). When respiring cells are then shifted back to fermentable conditions, mitochondria reform tubular networks by their fusion, but mitophagosomes remain excluded from mitochondria. Accordingly, mitophagosomes can be observed as dot-like structures using a fluorescence microscope [6, 9, 11].

1. Grow *ypt7*-null cells expressing mCherry fused to the C-terminus of a mitochondrial targeting signals derived from *N. crassa* ATP synthase subunit 9 (mito-mCherry) to mid-log phase in 3 mL of SDCA.
2. Transfer 0.07 OD<sub>600</sub> units of cells to 7 mL of SDGlyCA and incubate them at 30 °C for 48 h in a shaker (180 rpm).
3. Collect three OD<sub>600</sub> units of cells by centrifugation at  $7900 \times g$  for 30 s and discard the supernatant using a micropipette.
4. Wash the cells with 1 mL of SDCA, collect them by centrifugation at  $7900 \times g$  for 30 s, and discard the supernatant using a micropipette.
5. Resuspend the cell pellet in 3 mL of SDCA and incubate them at 30 °C for 3 h in shaker (180 rpm) (*see* **Note 4**).
6. Transfer 200  $\mu\text{L}$  of cell culture (usually OD<sub>600</sub> = 2–3) into a 1.5-mL microcentrifuge tube.
7. Collect the cells by centrifugation at  $7900 \times g$  for 30 s, discard 175  $\mu\text{L}$  of the supernatant using a micropipette, and vortex the cell pellet thoroughly.
8. Pipet 1.6–2.0  $\mu\text{L}$  of the cell suspension onto a microscope slide, and cover with a square cover slip (no sealing is necessary).
9. Observe the cells using a fluorescence microscope equipped with a filter set for mCherry.
10. Mitophagosomes can be observed as dot-like structures (*see* Fig. 2 and **Note 5**).

### 3.5 Western Blotting for Quantifying Mitophagy

Mitochondria degradation can be quantified in cells expressing dihydrofolate reductase (DHFR)-mCherry fused to the C-terminus of a mitochondrial targeting signals derived from *N. crassa* ATP synthase subunit 9 (mito-DHFR-mCherry), a reporter localized in the matrix of mitochondria. Upon mitophagy, DHFR-mCherry is processed to generate free mCherry in the vacuole. Since free mCherry is a highly protease-resistant protein, its accumulation indicates progression of mitochondria degradation [12]. Mitophagy can thus be semiquantitatively evaluated by western blotting using an anti-RFP antibody.

1. Grow cells expressing mito-DHFR-mCherry to mid-log phase in 3 mL of SDCA.
2. Transfer 0.07 OD<sub>600</sub> units of cells to 7 mL of SDGlyCA and incubate them at 30 °C in a shaker (180 rpm).
3. Collect 1 OD<sub>600</sub> units of cells at the 0 (from SDCA), 24, 48, and 72 h time points by centrifugation at 7900 × *g* for 30 s, and discard the supernatant using a micropipette. Collected cells at the early time points are stored at –80 °C until the last time point.
4. For each sample, add 100 µL of 0.1 M NaOH to the cell pellet, vortex thoroughly, and keep at room temperature for 5 min.
5. Collect the cells by centrifugation at 17,000 × *g* for 2 min and discard the supernatant by aspirator.
6. Add 50 µL of sample buffer and vortex the pellets well.
7. Boil the cell suspension at 100 °C for 3 min and keep them on ice for 1 min.
8. Separate the supernatant by centrifugation at 17,000 × *g* for 2 min and transfer it to a 1.5-mL microcentrifuge tube.
9. Load 5 µL of each sample on the 10% polyacrylamide gel and perform electrophoresis.
10. Transfer the protein samples to a PVDF membrane by semidry blotting.
11. Block the membrane using blocking buffer at room temperature for 30 min.
12. Incubate the membrane using incubation buffer A containing an anti-RFP antibody (1:2500 dilution) at 4 °C overnight.
13. Wash the membrane three times with TBS-T for 7 min each.
14. Incubate the membrane using incubation buffer B containing HRP-conjugated goat anti-rabbit IgG (1:10,000 dilution) at room temperature for 1 h.
15. Wash the membrane three times with TBS-T for 7 min each.
16. Incubate the membrane with ECL detection reagents, and detect/quantify mCherry signals using a luminescent image analyzer (*see* Fig. 3 and Note 6).

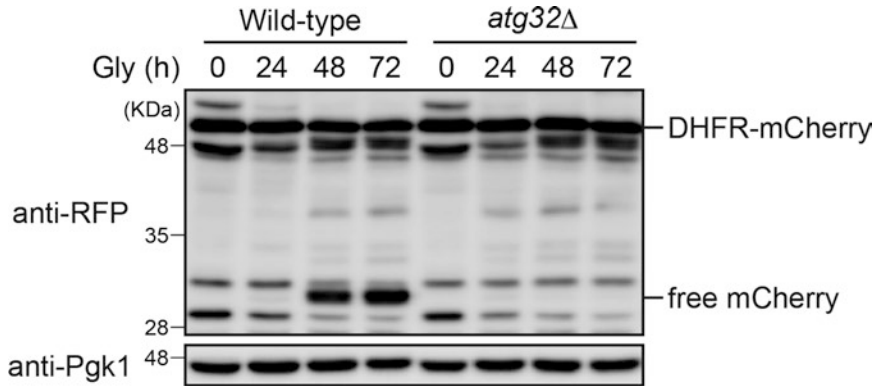


**Fig. 3** Semiquantitative analysis of mitophagy by western blotting. Mitochondria-targeted DHFR-mCherry-expressing wild-type and *atg32Δ* cells were grown in glycerol medium (Gly) for the indicated time points, and subjected to western blotting. Generation of free mCherry indicates transport of mitochondria to the vacuole. Pgk1 was monitored as a loading control

## 4 Notes

1. Although BY4741 grows better and undergoes mitophagy more extensively than other strains such as W303 and SEY6210 in non-fermentable media, W303 and SEY6210 can also be used to generate strains for mitophagy assays using the protocols described here.
2. mCherry signals should be observed first because the wavelength of excitation light for GFP is shorter than that of mCherry.
3. In vacuolar protease-deficient cells lacking Pep4 or Prb1, GFP signals colocalize with the vacuole as dot-like structures, representing mitochondria-containing autophagic bodies (mitophagic bodies) [11].
4. If cells are grown over 3 h in SDCA, mitochondria become fragmented. It is then hard to distinguish between mitophagosomes and fragmented mitochondria.
5. Cells containing mitophagosomes should be quantified by counting [11].
6. If free mCherry signals are weak, hide DHFR-mCherry signals with a paper sheet and expose the blot using a luminescent image analyzer.

## Acknowledgments

We thank Noriko Kondo-Okamoto for generating yeast strains and optimizing the original methods. This work was supported in part by Japan Society for the Promotion of Science (JSPS), and by the Ministry of Education, Culture, Sports, Science, and Technology. A.E. was supported by a JSPS Research Fellowship DC1 for Young Scientists.

## References

1. Youle RJ, Narendra DP (2011) Mechanisms of mitophagy. *Nat Rev Mol Cell Biol* 12:9–14
2. Palikaras K, Tavernarakis N (2012) Mitophagy in neurodegeneration and aging. *Front Genet* 3:1–7
3. Melser S, Lavie J, Bénard G (2015) Mitochondrial degradation and energy metabolism. *Biochim Biophys Acta* 1853:2812–2821
4. Nakatogawa H, Suzuki K, Kamada Y, Ohsumi Y (2009) Dynamics and diversity in autophagy mechanisms: lessons from yeast. *Nat Rev Mol Cell Biol* 10:458–467
5. Mizushima N, Yoshimori T, Ohsumi Y (2011) The role of Atg proteins in autophagosome formation. *Annu Rev Cell Dev Biol* 27:107–132
6. Okamoto K, Kondo-Okamoto N, Ohsumi Y (2009) Mitochondria-anchored receptor Atg32 mediates degradation of mitochondria via selective autophagy. *Dev Cell* 17:87–97
7. Kanki T, Wang K, Cao Y, Baba M, Klionsky DJ (2009) Atg32 is a mitochondrial protein that confers selectivity during mitophagy. *Dev Cell* 17:98–109
8. Liu L, Sakakibara K, Chen Q, Okamoto K (2014) Receptor-mediated mitophagy in yeast and mammalian systems. *Cell Res* 24:787–795
9. Sakakibara K, Eiyama A, Suzuki SW, Sakonakatogawa M, Okumura N, Tani M, Hashimoto A, Nagumo S, Kondo-okamoto N, Kondo-kakuta C, Asai E, Kirisako H, Nakatogawa H, Kuge O, Takao T, Ohsumi Y, Okamoto K (2015) Phospholipid methylation controls Atg 32-mediated mitophagy and Atg8 recycling. *EMBO J* 34:1–17
10. Kirisako T, Baba M, Ishihara N, Miyazawa K, Ohsumi M, Yoshimori T, Noda T, Ohsumi Y (1999) Formation process of autophagosome is traced with Apg8/Aut7p in yeast. *J Cell Biol* 147:435–446
11. Eiyama A, Okamoto K (2015) Protein N-terminal acetylation by the NatA complex is critical for selective mitochondria degradation. *J Biol Chem* 290:25034–25044
12. Kondo-Okamoto N, Noda NN, Suzuki SW, Nakatogawa H, Takahashi I, Matsunami M, Hashimoto A, Inagaki F, Ohsumi Y, Okamoto K (2012) Autophagy-related protein 32 acts as autophagic degron and directly initiates mitophagy. *J Biol Chem* 287:10631–10638

# Chapter 21

## Assessing Mitochondrial Selective Autophagy in the Nematode *Caenorhabditis elegans*

Konstantinos Palikaras and Nektarios Tavernarakis

### Abstract

Eukaryotic cells heavily depend on ATP generated by oxidative phosphorylation (OXPHOS) within mitochondria. Besides being the main suppliers of cell's energy, mitochondria also provide an additional compartment for a wide range of cellular processes and metabolic pathways. Mitochondria constantly undergo fusion/fission events and form a mitochondrial network, which is a highly dynamic, tubular structure allowing for rapid and continuous exchange of genetic material, as well as, targeting dysfunctional mitochondria for degradation through mitochondrial selective autophagy (mitophagy). Mitophagy mediates the elimination of damaged and/or superfluous organelles, maintaining mitochondrial and cellular homeostasis. In this chapter, we present two versatile, noninvasive methods, developed for monitoring in vivo mitophagy in *C. elegans*. These procedures enable the assessment of mitophagy in several cell types during development or under stress conditions. Investigating the role of mitophagy at the organismal level is essential for the development of therapeutic interventions against age-related diseases.

**Key words** Ageing, Autophagosome, Autophagy, *Caenorhabditis elegans*, DsRed, Green Fluorescent Protein (GFP), Lysosomes, Fluorescent microscopy, Mitochondria, Mitophagy, mtRosella

### Abbreviations

CCCP	Carbonyl cyanide m-chlorophenylhydrazone
DMSO	Dimethyl sulfoxide
DsRed	Red fluorescent protein
FUdR	Fluorodeoxyuridine
GFP	Green fluorescent protein
MAP1LC3/LC3	Microtubule-associated protein 1 light chain 3
mtGFP	Mitochondria-targeted green fluorescent protein
mtRosella	Mitochondria-targeted Rosella
NGM	Nematode growth medium

## 1 Introduction

Mitochondria are a distinguishing feature of eukaryotic cells and are often described as cellular powerhouses, since they are the major energy producers through oxidative phosphorylation (OXPHOS) and ATP production. In addition, these organelles play an essential role in several fundamental cellular processes including calcium homeostasis, metabolite synthesis, and apoptosis, among others [1].

Impairment of mitochondrial function is a major hallmark of many pathological conditions and ageing, highlighting the importance of proper mitochondrial activity [2]. Maintenance of cellular and organismal homeostasis necessitates a tight regulation of mitochondrial biogenesis, as well as the elimination of damaged or superfluous mitochondria [3–6]. Therefore, eukaryotic organisms have developed complex and highly specialized molecular and cellular pathways to preserve mitochondrial homeostasis [7]. Mitophagy is a selective type of autophagy mediating removal of dysfunctional and/or aged mitochondria, and the major degradation pathway by which cells regulate mitochondrial population in response to metabolic state [8].

The cytosolic E3 ubiquitin ligase Parkin and the mitochondrial phosphatase and tensin homolog (PTEN)-induced kinase 1 (PINK1), which are associated with the autosomal recessive form of parkinsonism [9, 10], have been implicated in the regulation of mitophagy. The PINK1/Parkin pathway is the best studied molecular pathway mediating selective autophagy of damaged and/or aged mitochondria. In healthy mitochondria, PINK1 translocates to the inner mitochondrial membrane and is cleaved by mitochondrial proteases [11]. Subsequently, N-terminally truncated form of PINK1 is released into the cytosol and degraded there by the proteasome [12]. Impairment of mitochondrial function inhibits import of PINK1 to the inner mitochondrial membrane and PINK1 is consequently stabilized on outer mitochondrial membrane. Accumulation of PINK1 on the mitochondrial surface stimulates mitophagy through recruitment of Parkin [8]. Following its translocation to defective mitochondria, Parkin ubiquitylates several outer mitochondrial membrane proteins, resulting in the flagging of dysfunctional organelles within the mitochondrial population [13–15]. Damaged mitochondria are so recognized and degraded by the autophagic machinery. The high conservation of PINK1 and Parkin among diverse species underlines their vital role in the maintenance of energy homeostasis [8].

Despite advances in the delineation of the molecular mechanisms that regulate mitophagy, no reliable and quantitative, *in vivo* approach for monitoring mitochondrial elimination in multicellular organisms is currently available. Aiming to fill this gap, we developed two complementary systems for monitoring mitophagy

in vivo and identified conditions that either induce or suppress mitophagy in the nematode *Caenorhabditis elegans* [4, 6]. In the first approach, we generated transgenic animals expressing the Rosella biosensor in mitochondria. Rosella is a purpose-built reporter comprising a fast-maturing pH-insensitive DsRed fused to a pH-sensitive GFP variant. The Rosella biosensor mode of function is based on the pH differences between lysosomes and other cellular compartments. GFP fluorescence becomes quenched in acidic lysosomes, whereas DsRED fluorescence remains unaffected. This biosensor has been used successfully in previous studies to monitor mitophagy in the unicellular organism *Saccharomyces cerevisiae* [16]. We adapted this versatile fluorescent microscopy assay and examined *C. elegans* animals carrying mtRosella under normal and mitophagy-inducing conditions such as oxidative stress, mitochondrial stress, and heat stress. All treatments reduce the GFP/DsRed ratio of Rosella fluorescence, indicating stimulation of mitophagy (Fig. 1). In addition to mtRosella, we generated

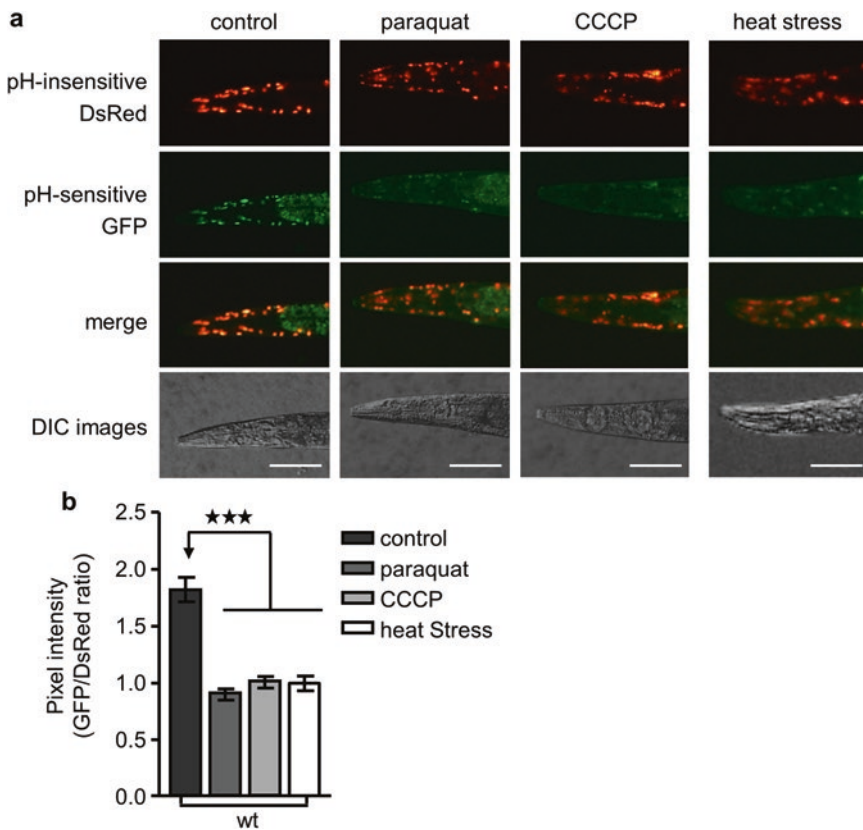


**Fig. 1** Mitophagy is induced under stress conditions. **(a)** Transgenic animals expressing the mtRosella biosensor in body wall muscle cells were treated with either paraquat or CCCP or exposed to heat stress (37 °C). **(b)** Mitophagy stimulation is described as the reduction of the ratio between pH-sensitive GFP to pH-insensitive DsRed ( $n = 120$ ;  $***P < 0.001$ ; one-way ANOVA). Acquisition information: Exposure time, 100 ms; Contrast, medium. Images were acquired using a 10 $\times$  objective lens. Size bars denote 20  $\mu\text{m}$ . Error bars denote S.E.M. values

transgenic animals expressing a mitochondria-targeted GFP (mtGFP), together with the autophagosomal marker LGG-1, the homologue of the mammalian cytosolic microtubule-associated protein 1 light chain 3 (MAP1LC3/LC3), fused with DsRed in body wall muscle cells. We examined animals carrying both the mitochondrial and autophagosomal markers, under normal and mitophagy-inducing conditions. Mitophagy stimulation induces the formation of autophagosomes that extensively co-localize with mitochondria (Fig. 2). The availability of reliable and quantitative methods for monitoring mitochondrial elimination is a prerequisite for the elucidation of the molecular mechanisms and pathophysiological implications of mitophagy in living cells and organisms and therefore for the development of therapeutic interventions to treat several human disorders including mitochondrial diseases and neurodegenerative conditions.

In the following sections, we describe detailed protocols for *in vivo* imaging of mitochondrial-selective autophagy in *C. elegans*, using two versatile imaging tools.

---

## 2 Materials

1. Wormpick or eyebrow/eyelash hair (*see Note 1a, b*).
2. Cholesterol stock solution: Prepare 5 mg/ml solution of cholesterol in absolute ethanol. Dissolve by stirring. Store at 4 °C. Do not flame or autoclave.
3. Nystatin stock solution: Prepare 10 mg/ml solution of nystatin in 70% (V/V) ethanol. Store at 4 °C and shake prior to use as this is a suspension. Do not autoclave.
4. Phosphate buffer: For 1 l, dissolve 102.2 g  $\text{KH}_2\text{PO}_4$  and 57.06 g  $\text{K}_2\text{HPO}_4$  in distilled water and fill up to 1 l. This is a 1 M solution, pH 6.0. Autoclave and keep at room temperature.
5. Prepare and autoclave 1 M  $\text{MgSO}_4$  (Sigma cat. no. M-7506) stock solution.
6. Petri dishes (60 mm × 15 mm).
7. Nematode growth medium (NGM) agar plates: Mix 3 g NaCl, 2.5 g Bactopectone, 0.2 g Streptomycin, 17 g Agar and add 900 ml distilled water. Autoclave. Let cool to 55–60 °C. Add 1 ml cholesterol stock solution (SERVA Electrophoresis GmbH, Heidelberg, Germany, cat. no. 1701), 1 ml 1 M  $\text{CaCl}_2$  (Sigma cat. no. C-5080), 1 ml 1 M  $\text{MgSO}_4$  (Sigma cat. no. M-7506), 1 ml Nystatin stock solution (Sigma cat. no. N-3503), 25 ml 1 M phosphate buffer, pH 6.0, and distilled sterile water up to 1 l. Pour about 8 ml medium per Petri dish and leave to solidify. Keep the plates at 4 °C until used (*see Note 2*).

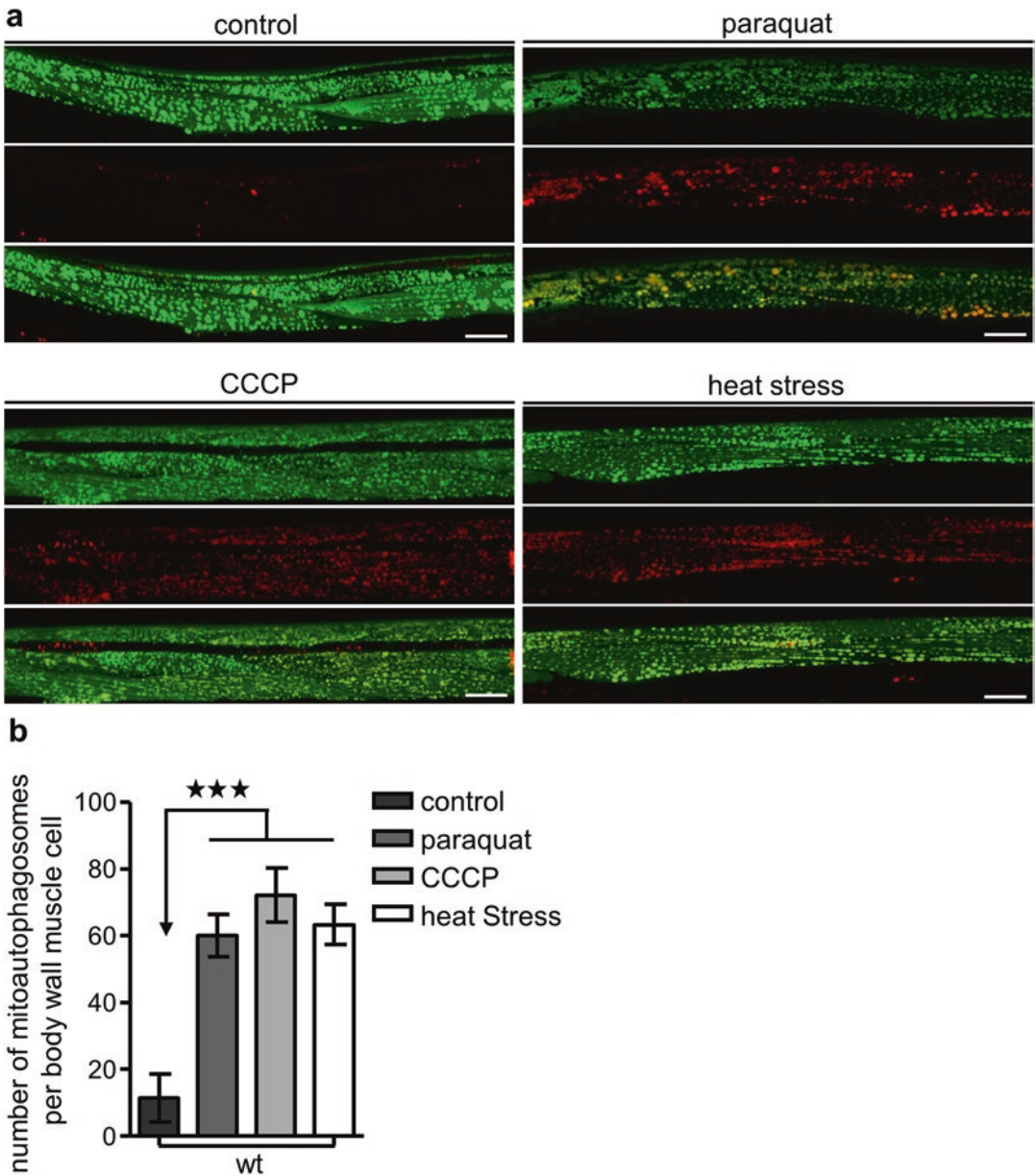


**Fig. 2** Monitoring mitophagy in vivo. **(a)** Transgenic animals co-expressing in body wall muscle cells a mitochondrially targeted GFP (mtGFP) and the autophagosomal protein LGG-1 fused with DsRed were treated with paraquat, CCCP or exposed to heat stress (37 °C) and subsequently analyzed by confocal microscopy. Z-projection images of GFP signals depicting mitochondria are shown in the *upper panels*, DsRed signals depicting autophagosomes are shown in the *middle panels*, and the merged images in the *lower panels*. Mitophagy induction is described as co-localization of GFP and DsRed signals. **(b)** Increased number of mitoautophagosomes under mitophagy-inducing conditions ( $n = 60$ ;  $***P < 0.001$ ; one-way ANOVA). Acquisition information: Resolution,  $1024 \times 1024$ ; Master gain, Track1: 775 and Track2: 510; Emission filters, Track1 Channel1: 612–671 and Track2 Channel1: 493–562; Laser intensity, Track1 (543 nm): 12% and Track2 (488 nm) 2%. Images were acquired using a 40 $\times$  objective lens. Size bars denote 20  $\mu\text{m}$ . Error bars denote S.E.M. values

8. NGM plates seeded with *Escherichia coli* (OP50 strain): OP50 strain is available at the *Caenorhabditis* Genetics Center (University of Minnesota, Minneapolis, USA; <https://www.cbs.umn.edu/research/resources/cgc>). Use a single colony of *E. coli* (OP50) and inoculate a 25 ml culture using Luria Bertani (LB) liquid medium (10 g Bacto-tryptone, 5 g Bacto-yeast extract, 5 g NaCl and distilled water up to 1 l and sterilize by autoclaving). Allow inoculated culture to grow for 8–10 h at 37 °C with shaking. Seed NGM plates with 150 µl *E. coli* (OP50) solution and incubate the plates at room temperature overnight to allow the growth of the bacterial lawn. Store the *E. coli* (OP50) solution at 4 °C. Prepare freshly new *E. coli* (OP50) solution every 4 days.
9. M9 buffer: Dissolve 3 g KH<sub>2</sub>PO<sub>4</sub> (Merck cat. no. 1.04873.1000), 6 g Na<sub>2</sub>HPO<sub>4</sub> (Merck cat. no. 1.06586.0500), 5 g NaCl (Merck cat. no. 1.06404.1000) in 1 l distilled water. Autoclave and add 1 ml 1 M MgSO<sub>4</sub> (sterile; Sigma cat. no. M-7506). Store M9 buffer at 4 °C.
10. Paraquat: Dissolve 1 g paraquat (Sigma-Aldrich, St. Louis, USA cat. no. 856,177) in 8 ml distilled water. This is a 0.5 M solution. Prepare aliquots of 400 µl to avoid contamination and store them at 4 °C (*see Note 3*).
11. Dimethyl sulfoxide cell culture grade BC (DMSO; Applichem, USA cat. no. A3672,0250; *see Note 4*).
12. CCCP: Dissolve 100 mg Carbonyl cyanide m-chlorophenylhydrazone (Sigma-Aldrich, St. Louis, USA cat. no. 857,815) in 10 ml of DMSO to make a 49 mM stock solution. Prepare aliquots of 1 ml and store them at –20 °C (*see Note 3*).
13. Levamisole: To make a 0.5 M solution, dissolve 1.2 g levamisole (Sigma-Aldrich, St. Louis, USA cat. no. 196,142) in 10 ml distilled water. Store levamisole solution at 4 °C.
14. Incubators for stable temperature (20 and 37 °C).
15. Agarose pads: Prepare 2% agarose in distilled water and keep it warm on a heating plate. Add 2–3 drops of boiled 2% agarose on a blank slide glass and cover it quickly with a second blank slide glass at 90° to the first one. Wait for 1–3 min until the agarose pads dry and remove the second blank slide (*see Note 5*).
16. Nematode strain expressing mtRosella biosensor; IR1631: N2; *Ex003* [p<sub>myo-3</sub>TOMM-20::Rosella] (*see Notes 6 and 7*).
17. Nematode strain expressing mtGFP together with the autophagosomal marker LGG-1 fused with DsRed; R1284: N2; *Is* [p<sub>myo-3</sub>mtGFP]; *Ex011* [p<sub>lgg-1</sub>DsRed::LGG-1] (*see Notes 6 and 7*).
18. Dissecting stereomicroscope.
19. UV irradiation chamber (356 nm).

20. Epifluorescence microscope.
21. Confocal microscope.
22. ImageJ image processing software: freely available at: <http://rsb.info.nih.gov/ij/> [17].
23. Microsoft Office 2011 Excel (Microsoft Corporation, Redmond, USA).
24. GraphPad Prism software package (GraphPad Software Inc., San Diego, USA).

---

## 3 Methods

### 3.1 Growth and Synchronization of Nematodes Population

Use both nematode strains expressing either mtRosella (IR1631) or mtGFP together with autophagosomal marker LGG-1 fused with DsRed (IR1284) to monitor mitophagy.

1. Use a dissecting stereomicroscope to select L4 larvae. Then, add 8–10 L4 larvae of transgenic animals on a freshly *E. coli* (OP50) seeded NGM plate. Use at least ten plates containing transgenic worms.
2. Incubate the worms at the standard temperature of 20 °C.
3. Four days later the plates contain mixed nematode population.
4. Synchronize worm population by picking L4 larvae of transgenic animals under a dissecting stereomicroscope. Select with a wormpick and transfer them onto separate plates to start the experiments (*see Note 1a*).
5. Add 15–20 L4 larvae of transgenic animals per plate. For each experimental condition, use at least three plates containing transgenic worms.
6. After 2 days, either use 2-days old adult worms directly or transfer them to freshly seeded NGM plates to avoid progeny and prevent starvation due to lack of food (*see Note 8*). After 2 days, the latter would represent 4-days old adult worms.

### 3.2 Induction of Mitophagy

#### 3.2.1 Induction of Mitophagy by Heat Stress

1. Incubate three freshly *E. coli* (OP50) seeded NGM plates for 30 min at 37 °C and keep three plates at 20 °C, as a control.
2. Transfer 10–15 2- or 4-days old adult transgenic animals on pre-warmed plates for each condition (*see Note 9*).
3. Incubate the animals for 2 h at 37 °C. Keep the control set at 20 °C.
4. Remove the plates from 37 °C and let worms recover for 30 min at 20 °C (*see Note 10*). Censored or dead animals are removed from the study (*see Notes 11 and 12*).
5. Animals are ready for microscopic examination.

**3.2.2 Induction  
of Mitophagy by Oxidative  
Stress  
and Mitochondrial Stress**

1. Kill *E. coli* (OP50) bacteria seeded on six NGM plates by exposing them to UV light (365 nm) for 15 min in an UV irradiation chamber (*see Note 13*).
2. Use paraquat to induce oxidative stress. Add paraquat to the top of three seeded NGM plates at 8 mM final concentration in the total agar volume. Add the same volume of water to the three remaining plates that will serve as controls. To specifically induce mitochondrial stress, add CCCP, instead of paraquat, to the top of three seeded NGM plated at 15  $\mu$ M final concentration in the total agar volume. Use DMSO for control plates, since CCCP is not dissolved in water (*see Notes 4 and 14*).
3. Gently swirl the plates and allow the liquid to spread over the entire surface.
4. Let the plates to dry at room temperature.
5. Transfer 10–15 2- or 4-days-old adult transgenic animals on paraquat- or CCCP-containing plates and on control plates using a wormpick (*see Note 15*).
6. Incubate the animals at 20 °C.
7. After 2 days of exposure to the drug, worms are ready for microscopic examination. Censored or dead animals are removed from the analysis (*see Notes 11 and 12*).

**3.3 Sample  
Preparation  
for Imaging**

1. Collect transgenic animals with an eyebrow/eyelash hair (*see Note 1b*).
2. Place and let the animals to crawl into an unseeded NGM plate to remove bacteria for 5 min.
3. Add a droplet of 10  $\mu$ l 20 mM M9-levamisole buffer on 2% agarose pad.
4. Collect transgenic animals with an eyebrow/eyelash hair and place them in M9-levamisole droplet to immobilize transgenic animals for imaging. Place 15–30 animals per droplet (*see Note 16*).
5. Gently place a coverslip on the top to press the animals in agarose.
6. Samples are ready for imaging.

**3.4 Imaging, Data,  
and Statistic Analysis**

**3.4.1 Imaging Process  
Using Nematode Strain  
(IR1631) Expressing  
mtRosella in Body Wall  
Muscles**

1. Capture images of single transgenic animals expressing mtRosella in body wall muscle cells using a camera attached to epifluorescence microscope. Acquire fluorescent images of whole transgenic animals by using 10 $\times$  objective lens (*see Note 17*).
2. Document and keep the same microscope and camera settings (lens and magnifier used, filters exposure time, resolution, laser intensity, gain, etc.) during imaging process.
3. Collect and save images from each method.

**3.4.2 Imaging and Data Analysis Using Nematode Strain (IR1631) Expressing mtRosella in Body Wall Muscles**

1. Open and process images with ImageJ software.
2. Select the “split channel” command via the “image” and “color” drop-down menu to convert images to grayscale images with a pixel depth of 8 bit (256 shades of gray).
3. Measure emission intensity. To analyze the area of interest manually (anterior, middle, and posterior body wall muscles), use the “freehand selection” tool to enclose the fluorescent area (*see Note 17*).
4. Select the “measurement” command via the “analyze” drop-down menu to perform pixel intensity analysis.
5. Copy the data from “results” window.
6. Paste and import the data by using any software package, such as the Microsoft Office 2011 Excel software package (Microsoft Corporation, Redmond, USA).
7. Normalize pixel intensity values to the selected area.
8. Calculate GFP to DsRed ratio. GFP/DsRed ratio is decreased upon mitophagy stimulation since GFP signal is quenched due to acidic environment of lysosomes, whereas DsRed signal remains stable.

**3.4.3 Imaging Process Using Nematode Strain (IR1284) Co-expressing Mitochondrial and Autophagosomal Marker in Body Wall Muscles**

1. Capture single body wall muscle cells of transgenic animals co-expressing mtGFP together with autophagosomal marker LGG-1 fused with DsRed using a confocal microscope.
2. Perform z-stack method, of an entire single body wall muscle cell by using 40× or 63× objective lens (*see Note 17*).
3. Document and keep the same microscope and camera settings (lens and magnifier used, filters exposure time, resolution, laser intensity, gain, etc.) during imaging process.
4. Collect and save images from each method.

**3.4.4 Imaging and Data Analysis Using Nematode Strain (IR1284) Co-expressing Mitochondrial and Autophagosomal Marker in Body Wall Muscles**

1. Open and process images acquired in Subheading 3.4.3 with the confocal software.
2. Analyze the number of mitoautophagosomes, autophagosomes containing dysfunctional or superfluous mitochondria, by manually counting the mitophagy/co-localization events between mitochondrial (mtGFP) and autophagosomal marker (DsRed::LGG-1) in each stack of body wall muscle cell (*see Note 18*).
3. Document and import the data by using the Microsoft Office 2011 Excel (Microsoft Corporation, Redmond, USA).

**3.4.5 Statistic Analysis**

1. Use any statistic analysis software, such as GraphPad Prism software package (GraphPad Software Inc., San Diego, USA), to report the significance of the study.
2. Open the desired statistic analysis software.

3. Create a new “table and graph.”
4. Select a graph (e.g., Scatter plot, column graph bar, etc.).
5. Import and analyze data obtained in Subheading 3.4.2 or 3.4.4.
6. Increase sample size to obtain more accurate results. For each experiment, at least 50–60 transgenic animals or 50 body wall muscle cells should be examined for each strain and condition. Each assay should be repeated at least three times.
7. Use the Student’s *t* test with a significance cut-off level of  $P < 0.05$  for comparisons between two groups. Use the one-factor (ANOVA) variance analysis and correct by the post hoc Bonferroni test for multiple comparisons.

Examples of such experiments are given in Figs. 1 and 2.

---

## 4 Notes

1. (a) Cut 2–3 cm of platinum wire (90% platinum, 10% iridium wire, 0.010 in. diameter, e.g., Trittech Research, Los Angeles, CA). Break off the thin part of a glass Pasteur pipette and melt the glass at the site of breakage on a Bunsen burner. Attach the end of the platinum wire. Make flat one end using pincers or a light hammer. Before using the wormpick always sterilize the tip over a flame.  
(b) Take a toothpick and glue an eyebrow/eyelash hair to the tip of it. Let it dry at room temperature. Then, use this tool to pick and place transgenic animals on agarose pads for imaging. Before using the eyebrow/eyelash hair always sterilize it by using 70% of EtOH.
2. 1 l of NGM agar medium is sufficient for 125 plates (60 mm × 15 mm). At least 30 NGM plates are needed for the described method.
3. Paraquat and CCCP are photosensitive chemicals. Cover the stock solutions, the aliquots, and plates with foil or keep them in a dark place.
4. The universal solvent DMSO could influence animal’s physiology. Use less than 1% of DMSO to avoid possible side effects and/or toxicity [18, 19].
5. Agarose pads have to be freshly made every time.
6. For basic *C. elegans* culture, maintenance, and manipulation techniques, see WormBook, <http://www.wormbook.org/>. Follow standard procedures for *C. elegans* strain maintenance. Nematode rearing temperature was kept at 20 °C, unless noted otherwise.
7. The nematode strains are available upon request to Professor Tavernarakis N (tavernarakis@imbb.forth.gr).

8. It is reported that autophagy and mitophagy are stimulated upon caloric restriction and starvation [4, 20]. Therefore, well-fed and non-starved animals should be used.
9. It is well known that autophagy efficiency diminished over ageing [21]. Therefore, young adult individuals should be used to monitor mitophagy.
10. The appropriate duration of heat stress and the recovery time should be experimentally determined each time, especially when animals of different genetic backgrounds that are likely to be sensitive to high temperatures are used.
11. Animals are characterized as censored when they display defects that interfere with normal physiology or have been compromised by experimental mishandling. Censored and dead animals are excluded from analysis. To avoid increased censoring and lethality due to excessive internal egg hatching (bag-of-worms phenotype or worm bagging), under mitophagy inducing conditions:
  - (a) Incubate specimens for shorter period in the presence of each drug or at 37 °C.
  - (b) Decrease the concentration of paraquat or CCCP.
  - (c) Use NGM plates containing fluorodeoxyuridine (FUdR), an inhibitor of DNA synthesis that blocks egg hatching.
  - (d) Use older adult hermaphrodites (e.g., 4-day-old worms) that display reduced egg production.
12. Contaminations may appear during the experimental procedure. Contamination of NGM plates with bacteria not intended for feeding or with fungi may have a detrimental impact on animal survival and mitophagy stimulation. Contaminated plates and animals should be removed from the study.
13. Drug efficiency could be affected by bacterial metabolism and therefore bacteria are killed by UV irradiation in this step.
14. Use drug-free plates containing identical solutions of distilled water or DMSO for control conditions.
15. The appropriate developmental stage, age, drug concentration, and duration of oxidative and mitochondrial stress should be experimentally determine each time, when animals of different genetic backgrounds that might be sensitive to stress are used. L1–L4 larvae are hypersensitive to paraquat and CCCP leading to severe lethality.
16. M9-levamisole buffer (final concentration 20 mM). Use M9 buffer instead of water to ensure a favorable osmotic environment. Protect the animals from drying out during the imaging process.
17. In *C. elegans*, intestinal autofluorescence increases with age. Therefore, body wall muscle cells close to the intestine should be

avoided during the imaging process. Focus on body wall muscle cells in the pharynx to avoid intestinal autofluorescence.

18. Mitophagy/co-localization event is defined by the overlap between GFP and DsRed signals, which correspond to mitochondria (mtGFP) and autophagosomes (DsRed::LGG-1) respectively.

---

## Acknowledgments

We thank A. Pasparki for expert technical support. We thank R. Devenish for providing the pASINB-CS-Rosella plasmid. Some nematode strains used in this work were provided by the *Caenorhabditis* Genetics Center, which is funded by the National Center for Research Resources (NCRR) of the National Institutes of Health (NIH). We thank A. Fire for plasmid vectors. This work was funded by grants from the European Research Council (ERC) and the European Commission 7th Framework Programme.

## References

1. Vafai SB, Mootha VK (2012) Mitochondrial disorders as windows into an ancient organelle. *Nature* 491(7424):374–383. doi:[10.1038/nature11707](https://doi.org/10.1038/nature11707)
2. Lopez-Otin C, Blasco MA, Partridge L, Serrano M, Kroemer G (2013) The hallmarks of aging. *Cell* 153(6):1194–1217. doi:[10.1016/j.cell.2013.05.039](https://doi.org/10.1016/j.cell.2013.05.039)
3. Manil-Segalen M, Lefebvre C, Jenzer C, Trichet M, Boulogne C, Satiat-Jeunemaitre B, Legouis R (2014) The *C. elegans* LC3 acts downstream of GABARAP to degrade autophagosomes by interacting with the HOPS subunit VPS39. *Dev Cell* 28(1):43–55. doi:[10.1016/j.devcel.2013.11.022](https://doi.org/10.1016/j.devcel.2013.11.022)
4. Palikaras K, Lionaki E, Tavernarakis N (2015) Coordination of mitophagy and mitochondrial biogenesis during ageing in *C. elegans*. *Nature* 521(7553):525–528. doi:[10.1038/nature14300](https://doi.org/10.1038/nature14300)
5. Palikaras K, Tavernarakis N (2014) Mitochondrial homeostasis: the interplay between mitophagy and mitochondrial biogenesis. *Exp Gerontol* 56:182–188. doi:[10.1016/j.exger.2014.01.021](https://doi.org/10.1016/j.exger.2014.01.021)
6. Schiavi A, Maglioni S, Palikaras K, Shaik A, Strappazon F, Brinkmann V, Torgovnick A, Castelein N, De Henau S, Braeckman BP, Cecconi F, Tavernarakis N, Ventura N (2015) Iron-starvation-induced mitophagy mediates lifespan extension upon mitochondrial stress in *C. elegans*. *Curr Biol* 25(14):1810–1822. doi:[10.1016/j.cub.2015.05.059](https://doi.org/10.1016/j.cub.2015.05.059)
7. Scheibye-Knudsen M, Fang EF, Croteau DL, Wilson DM III, Bohr VA (2015) Protecting the mitochondrial powerhouse. *Trends Cell Biol* 25(3):158–170. doi:[10.1016/j.tcb.2014.11.002](https://doi.org/10.1016/j.tcb.2014.11.002)
8. Pickrell AM, Youle RJ (2015) The roles of PINK1, parkin, and mitochondrial fidelity in Parkinson's disease. *Neuron* 85(2):257–273. doi:[10.1016/j.neuron.2014.12.007](https://doi.org/10.1016/j.neuron.2014.12.007)
9. Kitada T, Asakawa S, Hattori N, Matsumine H, Yamamura Y, Minoshima S, Yokochi M, Mizuno Y, Shimizu N (1998) Mutations in the parkin gene cause autosomal recessive juvenile parkinsonism. *Nature* 392(6676):605–608. doi:[10.1038/33416](https://doi.org/10.1038/33416)
10. Valente EM, Abou-Sleiman PM, Caputo V, Muqit MM, Harvey K, Gispert S, Ali Z, Del Turco D, Bentivoglio AR, Healy DG, Albanese A, Nussbaum R, Gonzalez-Maldonado R, Deller T, Salvi S, Cortelli P, Gilks WP, Latchman DS, Harvey RJ, Dallapiccola B, Auburger G, Wood NW (2004) Hereditary early-onset Parkinson's disease caused by mutations in PINK1. *Science* 304(5674):1158–1160. doi:[10.1126/science.1096284](https://doi.org/10.1126/science.1096284)
11. Jin SM, Lazarou M, Wang C, Kane LA, Narendra DP, Youle RJ (2010) Mitochondrial membrane potential regulates PINK1 import and proteolytic destabilization by PARL. *J Cell*

- Biol 191(5):933–942. doi:[10.1083/jcb.201008084](https://doi.org/10.1083/jcb.201008084)
12. Yamano K, Youle RJ (2013) PINK1 is degraded through the N-end rule pathway. *Autophagy* 9(11):1758–1769. doi:[10.4161/auto.24633](https://doi.org/10.4161/auto.24633)
  13. Chan NC, Salazar AM, Pham AH, Sweredoski MJ, Kolawa NJ, Graham RL, Hess S, Chan DC (2011) Broad activation of the ubiquitin-proteasome system by Parkin is critical for mitophagy. *Hum Mol Genet* 20(9):1726–1737. doi:[10.1093/hmg/ddr048](https://doi.org/10.1093/hmg/ddr048)
  14. Gegg ME, Cooper JM, Chau KY, Rojo M, Schapira AH, Taanman JW (2010) Mitofusin 1 and mitofusin 2 are ubiquitinated in a PINK1/parkin-dependent manner upon induction of mitophagy. *Hum Mol Genet* 19(24):4861–4870. doi:[10.1093/hmg/ddq419](https://doi.org/10.1093/hmg/ddq419)
  15. Yoshii SR, Kishi C, Ishihara N, Mizushima N (2011) Parkin mediates proteasome-dependent protein degradation and rupture of the outer mitochondrial membrane. *J Biol Chem* 286(22):19630–19640. doi:[10.1074/jbc.M110.209338](https://doi.org/10.1074/jbc.M110.209338)
  16. Rosado CJ, Mijaljica D, Hatzinisiriou I, Prescott M, Devenish RJ (2008) Rosella: a fluorescent pH-biosensor for reporting vacuolar turnover of cytosol and organelles in yeast. *Autophagy* 4(2):205–213
  17. Schneider CA, Rasband WS, Eliceiri KW (2012) NIH Image to ImageJ: 25 years of image analysis. *Nat Methods* 9(7):671–675
  18. Frankowski H, Alavez S, Spilman P, Mark KA, Nelson JD, Mollahan P, Rao RV, Chen SF, Lithgow GJ, Ellerby HM (2013) Dimethyl sulfoxide and dimethyl formamide increase lifespan of *C. elegans* in liquid. *Mech Ageing Dev* 134(3–4):69–78. doi:[10.1016/j.mad.2012.10.002](https://doi.org/10.1016/j.mad.2012.10.002)
  19. Wang X, Wang X, Li L, Wang D (2010) Lifespan extension in *Caenorhabditis elegans* by DMSO is dependent on sir-2.1 and daf-16. *Biochem Biophys Res Commun* 400(4):613–618. doi:[10.1016/j.bbrc.2010.08.113](https://doi.org/10.1016/j.bbrc.2010.08.113)
  20. Rambold AS, Kostecky B, Elia N, Lippincott-Schwartz J (2011) Tubular network formation protects mitochondria from autophagosomal degradation during nutrient starvation. *Proc Natl Acad Sci U S A* 108(25):10190–10195. doi:[10.1073/pnas.1107402108](https://doi.org/10.1073/pnas.1107402108)
  21. Rubinsztein DC, Marino G, Kroemer G (2011) Autophagy and aging. *Cell* 146(5):682–695. doi:[10.1016/j.cell.2011.07.030](https://doi.org/10.1016/j.cell.2011.07.030)

## Assessing Mitochondrial Unfolded Protein Response in Mammalian Cells

Fiona Durand and Nicholas Hoogenraad

### Abstract

Mitochondria serve a key role in the supply of energy to cells in the form of ATP, the supply of essential cellular components such as phospholipids and heme, in apoptosis and as a mediator of cellular signaling pathways. Mitochondria have their own DNA, consisting of a small number of genes, but the majority of the total protein complement is encoded in the nucleus, synthesized in the cytosol, and is imported into the mitochondria in a largely, if not completely unfolded form. These proteins need to be folded into their functional form within the organelle with the concomitant requirement that the organelle has its own suite of molecular chaperones and complexes to degrade damaged proteins to avoid stress arising from accumulation of unfolded proteins. This mitochondrial unfolded protein response can also be induced in cells and protein regulation can be determined using western blot, luciferase reporter assay, and sensitive mass spectrometry techniques. In this chapter, we describe a method to induce mtUPR in mammalian cells and the three methods to analyze components involved in it.

**Key words** Mitochondria, Unfolded protein response (UPR), Cell stress, Organelle, Mass spectrometry

---

### 1 Introduction

The evolution of complexity in cells has brought with it the problem that cells operate at the limits of their solvent capacity. The cell has a myriad of solutes that need to remain in solution for the cell to function properly. Thus, the protein levels in cells are extraordinarily high. The *E. coli* cell has a protein concentration of around 150 mg/mL [1] and in eukaryotic cells these concentrations are even higher, reaching close to 500 mg/mL in the matrix of mitochondria from hepatocytes [2]. To cope with the constant threat of loss of function due to protein aggregation, cells have evolved proteostatic mechanisms to either rescue unfolded proteins with the aid of molecular chaperones or degrade these using proteolytic systems [3].

The heat shock response is one such mechanism and a large number of proteins are inducible under conditions where proteins

unfold, such as heat stress, through the binding of heat shock elements in the promoters of genes that form part of this response mechanism [4, 5]. However, separate mechanisms acting at the level of subcellular organelles also exist. The endoplasmic unfolded protein response (erUPR) was the first organelle-specific UPR discovered [6] and has been extensively characterized [7, 8]. It consists of several elements: inhibition of protein translation to reduce the pressure of protein unfolding in the organelle, transcription of genes encoding organelle-specific molecular chaperones to refold unfolded proteins, activation of an organelle-specific proteolytic mechanism called ERAD [9], and, if all else fails, induction of an apoptotic mechanism to remove the cell [10, 11]. In essence, the heat shock response can be viewed as a whole cell UPR and many of the genes encoding organelle-localized proteostasis components have both heat shock elements and organelle-specific UPR elements.

In many ways, one might have expected an even more pressing need for a mitochondrial UPR (mtUPR) since protein concentrations in the mitochondrial matrix are even higher than in the ER. Indeed, that is what turned out to be the case. Deletion of mtDNA in rho zero cells in culture resulted in the accumulation of unfolded nuclear encoded proteins of the oxidative phosphorylation complexes, resulting in the selective increased transcription of the matrix chaperonins, chaperonins 60 and 10 and the matrix protease, ClpP, but not the heat shock inducible cytosolic chaperone, Hsp70 [12]. A more detailed analysis of the mtUPR in a cell model where a mutant form of the matrix protein, ornithine transcarbamylase, was expressed, the genes of the mtUPR-inducible chaperonins and protease were found to contain a CHOP/CEBP transcription factor binding element responsible for the mtUPR [13]. The activation of the CHOP promoter elements mirrored the levels of unfolded proteins in the matrix and deletion of the element or mutation of the CHOP transcription factor blocked the mtUPR [13].

The CHOP and CEBP $\beta$  genes are themselves induced by the mtUPR and contain mtUPR response elements in their promoters [14]. The CHOP gene itself has both erUPR (ERSE) and mtUPR elements, enabling it to be selectively responsible for both erUPR and mtUPR processes. A more detailed analysis of the mtUPR showed that the mtUPR elements in CHOP and CEBP $\beta$  are API-binding sites, which bind transcription factors cJun/API. cJun is activated by phosphorylation by JNK2, which in turn is activated by phosphorylation by MEK kinases, MKK4 and MKK7 [14, 15]. A bioinformatics analysis of a collection of mtUPR responsive genes further revealed that the promoters of these genes contained two additional elements on either side of the CHOP/CEBP $\beta$  element and were called Mitochondrial Response Elements (MURE) 1 and 2 [16]. Mutational analysis showed the requirement for both

of these elements, but so far the identity of the transcription factors that bind these elements has not been clarified. In the fullness of time, it is highly likely that there will be a large complex of DNA binding and nonbinding proteins involved in the regulation of the mtUPR.

Like the erUPR, the mtUPR has a mechanism to inhibit translation in response to the accumulation of unfolded proteins in the matrix. The mechanism in both cases is via phosphorylation and inactivation of the translation initiation factor eIF2 via two different protein kinases. Whereas PERK, an ER-membrane-located kinase that is proteolytically released upon erUPR, inhibits translation in response to erUPR, in mtUPR the enzyme is the dsRNA activatable PKR [15]. This kinase is activated through the action of the mitochondrial matrix protease ClpP, although the connection between the action of ClpP and PKR is still unknown. Once activated, PKR both inhibits translation and activates the kinase cascade that leads to the activation of JNK2. Subsequent phosphorylation of cJUN then induces the transcription factors CHOP and CEBP $\beta$ , with the consequent activation of the mtUPR responsive genes [15].

Although there are many parallels between erUPR and mtUPR, the latter response mechanism does not appear to be present in the same form in lower eukaryotes such as yeast. However, mtUPR has been well characterized in *C. elegans*, which also appears to have a quite different mechanism for solving the unfolded protein problem as compared with mammalian cells. Activation of the mtUPR in *C. elegans* correlates temporally and spatially with nuclear redistribution of the transcription factor DVE-1 with enhanced binding to the promoters of mitochondrial chaperone genes such as ubiquitin-like protein UBL-5. These events are dependent on *C. elegans* clpp-1 proteolytic activity, a homologue of the mammalian mitochondrial matrix protease, ClpP [17].

More recently, an intermembrane space (IMS) UPR (imsUPR) has been identified in mammalian cells. Accumulation of unfolded proteins in the IMS leads to an activation of the cytoplasmic kinase AKT which activates proteosomal activity. It also leads to the activation of the nuclear estrogen receptor ER $\alpha$ -P, which binds to the promoter of genes encoding IMS proteins Htra2 and Nrf1 [18].

Ornithine Transcarbamylase (OTC) is one of the urea-cycle enzymes targeted to the mitochondrial matrix and is expressed only in the liver and small intestine [19, 20]. Mutant OTC, OTC- $\Delta$ , is used to induce the mtUPR and the wild-type protein is used as a negative control. This mutant protein is still imported into mitochondria, but its folding is impeded and aggregates are formed, causing a mitochondrial stress response [13]. This approach to inducing a mtUPR has been extensively used by many researchers in many different cell lines [21]. Cells are first transfected with vectors containing the OTC or OTC- $\Delta$  DNA, and then western blot can be

performed on whole cell lysates or isolated mitochondria to assess upregulation of proteins involved in mtUPR. Alternatively, mass spectrometry analysis can be used to determine the changed levels of proteins involved in mtUPR. In a third approach, mtUPR can be assessed using a luciferase reporter assay in which luciferase expression is under the control of promoter regions containing the CHOP and/or MURE 1 and 2 binding motifs from mitochondrial genes involved in mtUPR. Genes responsive to stress caused by aggregation of OTC- $\Delta$  show up-regulation of the luciferase enzyme [16]. In the following, we describe the methods to induce mtUPR and the three methods to assess it in mammalian cells.

---

## 2 Materials

### 2.1 Induction of mtUPR

1. pCAGGS vectors containing wild-type (pCAGGS-OTC) and mutant (pCAGGS-OTC $\Delta$ ) forms of ornithine-transcarbamylase (*see Note 1*). Empty vector is used as an additional control.
2. COS-7 cells (*see Note 2*).
3. Complete Medium: Dulbecco's modified Eagle medium (DMEM) containing 45 g/L D-glucose, 4 mM L-glutamine, 110 mg/L sodium pyruvate, 5% (v/v) heat inactivated fetal calf serum, 1% (v/v) penicillin (added from 10,000 U/mL stock), and 1% (v/v) streptomycin (added from 10,000  $\mu$ g/mL stock).
4. Serum free medium: Complete medium without the addition of fetal calf serum.
5. Fetal calf serum.
6. Lipofectamine reagent.
7. 1 mM EDTA, pH 7.5.
8. Cell lysis buffer for Immunoblot assay: 50 mM Tris-HCl, pH 8.0, 100 mM NaCl, 1% (v/v) Triton X-100, 0.1% (w/v) SDS, and 0.5% (w/v) sodium deoxycholate.

### 2.2 Isolation of Mitochondria

1. PBS (Phosphate Buffered Saline): Dissolve the following in 800 mL distilled H<sub>2</sub>O, 0.8 g of NaCl (137 mM), 0.2 g of KCl (27 mM), 1.44 g of Na<sub>2</sub>HPO<sub>4</sub> (10 mM), 0.24 g of KH<sub>2</sub>PO<sub>4</sub> (18 mM). Adjust pH to 7.4 with HCl. Adjust volume to 1 L with additional distilled H<sub>2</sub>O. Sterilize by autoclaving.
2. HSDE: 20 mM HEPES-NaOH, pH 7.4, 250 mM sucrose, 1 mM DTT, 1 mM EDTA, 0.5 mM PMSF.
3. Cell lysis buffer for Immunoblot assay: 50 mM Tris-HCl, pH 8.0, 100 mM NaCl, 1% (v/v) Triton X-100, 0.1% (w/v) SDS, 0.5% (w/v) sodium deoxycholate.
4. Mass spectrometry lysis buffer: 7 M urea, 2 M thiourea, 30 mM Tris-HCl, pH 8.6 (*see Note 3*).

### 2.3 Luciferase Reporter Assay

1. Complete medium: Dulbecco's modified Eagle medium (DMEM) containing 45 g/L D-glucose, 4 nM L-glutamine, 110 mg/L sodium pyruvate, 5% (v/v) heat-inactivated fetal calf serum, 1% (v/v) penicillin (added from 10,000 U/mL stock), and 1% (v/v) streptomycin (added from 10,000 µg/mL stock).
2. COS-7 cells.
3. pCAGGS-OTCΔ: pCAGGS vector containing mutant form of ornithine-transcarbamylase (*see Note 1*).
4. Luciferase reporter plasmid: pGL3 luciferase expression plasmid in which the expression of luciferase is under the control of the promoter of one of the genes involved in mtUPR. For this purpose, promoter regions of the genes of the following mitochondrial proteins can be used -YME1L, MPPβ, Trx2, Tim17A, End G, NDUFB2, and ClpP. A promoter-less luciferase construct is used as a negative control.
5. *Renilla* luciferase plasmid, pRL-SV40.
6. Lipofectamine reagent.
7. Dual-Luciferase Reporter Assay system (Promega): the kit consists of Passive Lysis Buffer, "Stop and Glo" reagent and Luciferase Assay Reagent II.
8. Glomax luminometer (Promega) (*see Note 4*).
9. White 96-well plate.

### 2.4 Determination of Optimal SILAC Labeling Medium (*see Note 5*)

1. Labeling Medium: DMEM medium for SILAC (Thermo Fisher, 88420), containing 45 g/L D-glucose, 4 nM L-glutamine, 110 mg/L sodium pyruvate, 10% dialyzed FCS (Life Technologies, 26400-044), 1% (v/v) penicillin (added from 10,000 U/mL stock), and 1% (v/v) streptomycin (added from 10,000 µg/mL stock).
2. R<sup>0</sup>: L-Arginine reagent grade, ≥98%.
3. K<sup>0</sup>: L-Lysine monohydrochloride reagent grade, ≥98% (TLC).
4. P<sup>0</sup>: L-Proline ReagentPlus®, ≥99% (TLC).
5. K<sup>8</sup>: L-Lysine.2HCl (U-13C6, 99%; U-15N2, 99%).
6. R<sup>10</sup>: L-Arginine HCL (U-13C6, U-15N4) (*see Note 6*).
7. Light medium × 1: Labeling Medium supplemented with 146 mg/L K<sup>0</sup> and 84 mg/L R<sup>0</sup>.
8. Light medium × 2: Labeling Medium supplemented with 146 mg/L K<sup>0</sup>, 42 mg/L R<sup>0</sup>, and 600 mg/L P<sup>0</sup>.
9. Light medium × 3: Labeling Medium supplemented with 146 mg/L K<sup>0</sup>, 21 mg/L R<sup>0</sup>, 1200 mg/L P<sup>0</sup>.
10. Heavy medium × 1: Labeling Medium supplemented with 180 mg/L K<sup>8</sup> and 88 mg/L R<sup>10</sup>.

11. Heavy medium × 2: Labeling Medium supplemented with 180 mg/L K<sup>8</sup>, 44 mg/L R<sup>10</sup>, and 600 mg/L P<sup>0</sup>.
12. Heavy medium × 3: Labeling Medium supplemented with 180 mg/L K<sup>8</sup>, 23 mg/L R<sup>10</sup>, and 1200 mg/L P<sup>0</sup>.
13. Mass spectrometry lysis buffer: 7 M urea, 2 M thiourea, 30 mM Tris-HCl, pH 8.6 (*see Note 3*).
14. Freezing medium for labeled cells: 20% dialyzed FCS, 10% DMSO and respective heavy or light medium.
15. Nontransfected COS-7 cells.
16. Mass spectrometry lysis buffer: 7 M urea, 2 M thiourea, 30 mM Tris-HCl, pH 8.6 (*see Note 3*).
17. Bradford assay reagent.
18. Trypsin made up to 0.5 µg/µL in 0.1 mM HCl.
19. 2% acetonitrile/0.1%TFA (v/v) in dH<sub>2</sub>O.
20. C18 zip tip (*see Note 7*).
21. Activation buffer: 85% acetonitrile/0.1% TFA (v/v) in dH<sub>2</sub>O.
22. Wash buffer: 2% acetonitrile, 0.1% TFA (v/v) in dH<sub>2</sub>O.
23. Elution buffer: 85% acetonitrile, 0.1% TFA (v/v) in dH<sub>2</sub>O.
24. Resuspension buffer: 2% acetonitrile, 0.1% TFA (v/v) in dH<sub>2</sub>O.

## **2.5 Analysis of mtUPR by Mass Spectrometry**

1. Optimal Light and Heavy media, as determined in Subheading 3.4.
2. COS-7 cells.
3. pCAGGS vectors containing wild-type (pCAGGS-OTC) and mutant (pCAGGS-OTCΔ) forms of ornithine-transcarbamylase (*see Note 1*).
4. Lipofectamine.
5. Phosphate Buffered Saline (PBS), as in Subheading 2.1.
6. Mass spectrometry lysis buffer: 7 M urea (Sigma), 2 M thiourea (Sigma), 30 mM Tris-HCl (Invitrogen), pH 8.6.
7. 100 mM Tris-HCl, pH 7.4.
8. ABC: 50 mM ammonium bicarbonate.
9. Trypsin: made up to 0.5 µg/µL in 0.1 mM HCl.
10. 2% acetonitrile 0.1% TFA (v/v) in dH<sub>2</sub>O.
11. 10% TFA. (v/v) in dH<sub>2</sub>O.
12. TCEP: 50 mM Tris-HCl (2-carboxyethyl) phosphine.
13. IAA: 500 mM Iodoacetamide.
14. pH strips.
15. C18 zip tips (*see Note 7*).
16. Activation buffer: 85% acetonitrile/0.1% TFA (v/v) in dH<sub>2</sub>O.

17. Wash buffer: 2% acetonitrile, 0.1% TFA (v/v) in dH<sub>2</sub>O.

18. Elution buffer: 85% acetonitrile, 0.1% TFA (v/v) in dH<sub>2</sub>O.

19. Resuspension buffer: 2% acetonitrile, 0.1% TFA (v/v) in dH<sub>2</sub>O.

### 3 Methods

For successful transfection into cells, negatively charged nucleic acids are complexed with a cationic liposome formulation. This creates a net positive charge to overcome the electrostatic repulsion of the negatively charged cell membrane and allows the DNA to be taken up by the cell [22].

pCAGGS vectors contain wild-type OTC, OTC $\Delta$  sequences that contain an SV40 origin of replication and the chicken  $\beta$ -actin promoter [23]. The OTC and OTC- $\Delta$  DNA contained in the plasmids is translated into protein containing an N-terminal targeting sequence that targets this protein from the cytosol to the mitochondrial matrix. The aggregated protein of the truncated OTC- $\Delta$  causes a mitochondrial stress response and up-regulation of mitochondrial protein folding chaperones and proteases (Fig. 1).

The pGL3 luciferase reporter vectors contain promoters of some of the genes from these regulated proteins. Thus, the levels of luciferase will increase after mitochondrial stress, condition in which transcription of these genes is increased (Fig. 2).

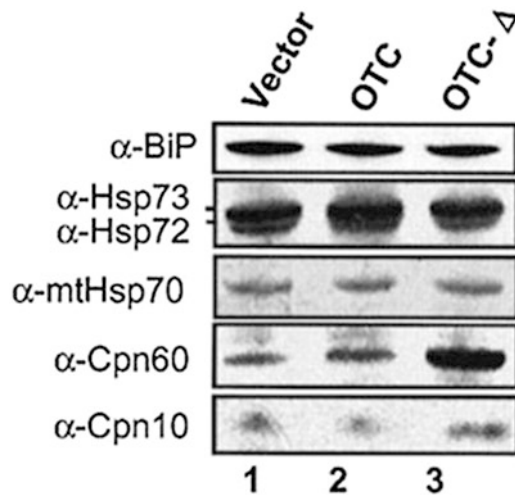


**Fig. 1** Induction of mtUPR analyzed by western blot. Cells expressing OTC or OTC- $\Delta$  were harvested 36 h posttransfection. Cells transfected with the empty plasmid were used as a control. Total cell lysates were prepared subjected to SDS-PAGE followed by western blot analysis using depicted antibodies [13]. Note the increased levels of mitochondrial chaperones Hsp60 and 10 upon expression of OTC- $\Delta$  but no difference in levels of ER chaperone BiP or cytosolic chaperones Hsp73 and Hsp72. Levels of mitochondrial Hsp70 were also unchanged

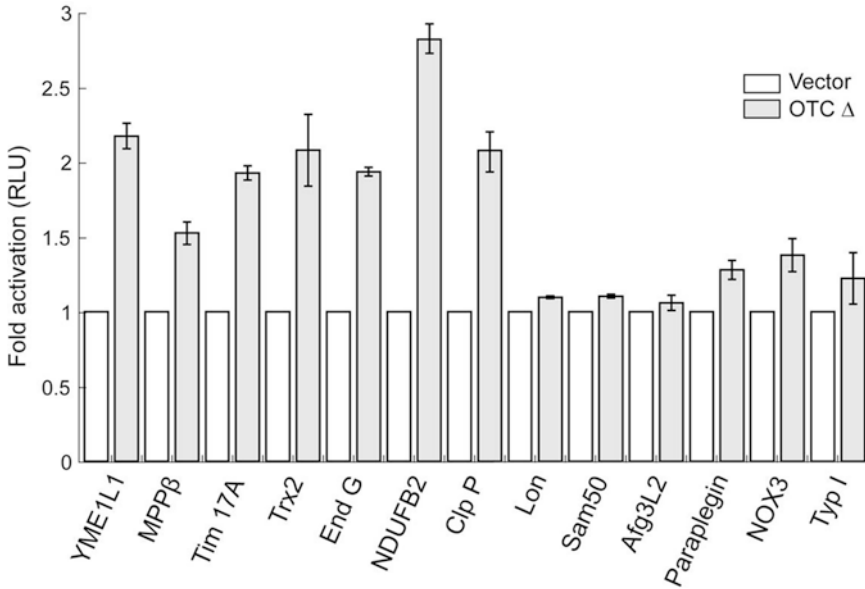


**Fig. 2** Survey of promoters responsive to mtUPR. Reporter construct for mitochondrial proteins YME1L1, MPPB (mitochondrial processing peptidase B subunit), Trx2 (mitochondrial thioredoxin), Tim17A, End G (Endonuclease G), NDUF2 (a component of complex 1), and ClpP, which all have CHOP consensus sequences, Lon, Sam50, Afg3L2 and Paraplegin, without CHOP consensus sequences, and NOX3 (NADPH oxidase 3) and Typ I (Type I iodothyronine deiodinase), which are non-mitochondrial proteins but have CHOP consensus sequences in their promoter regions, were tested. Cos-7 cells were co-transfected with vector or vector containing OTC- $\Delta$  and promoter-luciferase constructs were used for luciferase assays 32 h after transfection. Data represents the mean  $\pm$  SEM from experiments performed in triplicate [16]

### 3.1 Induction of mtUPR

1. Grow COS-7 cells in Complete Medium in an atmosphere of 5% CO<sub>2</sub> at 37 °C. Set the cells up in 10 cm plates the day before transfections so the cells are 70–80% confluent on the day of transfection. For each transfection, one such plate is needed.
2. For each transfection, prepare solution A by mixing 10  $\mu$ g of DNA (pCAGGS vectors containing OTC or OTCD DNA sequences) in 800  $\mu$ L serum-free medium.
3. For each transfection, prepare solution B by mixing 25  $\mu$ L of Lipofectamine reagent with 800  $\mu$ L serum-free medium. Incubate for 30 min at room temperature.
4. Mix gently solutions A and B and leave to stand at room temperature for 45 min (*see Note 8*).
5. Rinse the cells with 8 mL of serum-free medium twice before adding 6.4 mL of serum-free medium to the tube containing the DNA-liposome complexes.
6. Overlay the mixture onto rinsed cells and leave to incubate at 37 °C for 5 h.
7. Add 8 mL DMEM containing 20% foetal calf serum to the plate without removing the transfection mixture.

8. Replace the medium with fresh complete medium 18–24 h following the transfection.
9. Harvest the cells 36 h after transfection (*see Note 9*).
10. Whole cells are harvested by adding 1 mL 37 °C 1 mM EDTA and return to incubator ~3 min.
11. Collect cells by washing twice with 5 mL PBS and take 20  $\mu$ L for cell counts.
12. Centrifuge cells at 500  $\times g$  for 3 min and remove PBS.
13. Lyse  $\sim 1 \times 10^6$  cells in 100  $\mu$ L of Cell Lysis buffer. A 10 cm plate of COS-7 cells grown to confluence will yield  $\sim 5 \times 10^6$  cells and a concentration of  $\sim 500 \mu\text{g}/\text{mL}$ . Check using BCA assay (*see Note 10*).
14. Load 5  $\mu\text{g}$  per lane or  $\sim 10 \mu\text{L}$  of the lysate onto SDS-PAGE gel for immunoblot analysis. Probe for appropriate proteins. A typical example of such an experiment is shown in Fig. 1.

### 3.2 Isolation of Mitochondria

The following method can be used for isolation of mitochondria from all cells described in this chapter and grown on any kind of medium used here.

1. Wash 2  $\times 10$  cm plates of confluent cells twice with 10 mL PBS.
2. Harvest the cells with a rubber policeman in 1.5 mL HSDE, incubate on ice for 15 min, and centrifuge at 500  $\times g$  for 3 min.
3. Resuspend the cells in 1.5 mL HSDE and incubate on ice for 15 min.
4. Break cells with 20 strokes of a Dounce homogenizer, remove unbroken by centrifugation at 750  $\times g$  for 10 min.
5. Centrifuge the now lysed cells at 8700  $\times g$  for 10 min to collect a mitochondrial pellet fraction (*see Note 10*).
6. At this stage the mitochondrial pellet can be prepared for immunoblot analysis in 100  $\mu$ L of Cell lysis buffer. Vortex and incubate on ice for 10 min Alternatively, mitochondria isolated from SILAC labeled cells can be lysed in 100  $\mu$ L of mass spectrometry lysis buffer, vortex and incubated on ice 10 min. Centrifuge lysates at 2000  $\times g$  to remove debris (*see Note 10*).

### 3.3 Luciferase Reporter Assay

1. Transfect COS-7 cells as in Subheading 3.1. One batch of COS-7 cells is transfected with the luciferase expression plasmid, 100 ng *Renilla* luciferase plasmid, pRL-SV40, and the OTC- $\Delta$  vector and one batch with the promoterless versions of luciferase expression plasmid 100 ng *Renilla* luciferase plasmid, pRL-SV40, and the OTC- $\Delta$  vector 32 h before assaying for luciferase expression (*see Note 11*).
2. Wash cells twice with 10 mL PBS and add 1 mL of Passive Lysis Buffer to each 10 cm plate while cells are still attached to

the plate (~1 mL for a confluent 10 cm plate of COS-7 cells) 32 h after transfection.

3. Rock plate back and forth, for 5 min at room temperature and then scrape cells off plate into centrifuge tube on ice. Pipette lysate up and down to homogenize sample.
4. Freeze/thaw sample to complete lysis step.
5. Vortex the tube for 15 s.
6. Centrifuge thawed lysates at  $12,000 \times g$  for 2 min at 4 °C and transfer supernatant to clean tube.
7. Analyze the supernatant as a neat sample and diluted in Cell Culture lysis buffer (Promega), containing 1 mg BSA, to ratios of 1 in 10 and 1 in 100. Dilution of the samples ensures the luminometer readout is in the linear scale.
8. Place aliquots of 10  $\mu$ L each of neat and diluted samples in a white 96-well plate and, using a Glomax luminometer (Promega), dispense 50  $\mu$ L of Luciferase Assay Reagent II to each well and read for 10 s after a 2 s delay.
9. Add 50  $\mu$ L of “Stop and Glo” reagent to determine the background fluorescence and enable a ratio to be determined between the two signals (*see Note 12*). A typical result of such an experiment is shown in Fig. 2.

### **3.4 Determination of Optimal SILAC Labeling Medium**

Arginine can be metabolized by cells to proline, which can subsequently be incorporated into proteins [24]. Thus, it is important to obtain an estimate of the conversion of arginine to proline under the experimental conditions used in the SILAC experiments. This protocol uses nontransfected COS-7 heavy labeled cells, but growing cells in both heavy and light media can save time in the next step as labeled cell stocks can be frozen for future use.

1. Two six-well plates one containing both the three light and heavy labeled cells and one with heavy labeled cells only are split five times over 2 weeks using fresh appropriate media (*see Note 13*).
2. Collect cells grown in heavy media  $\times 1$ ,  $\times 2$ , and  $\times 3$ , wash twice with PBS, snap freeze in liquid N<sub>2</sub>, and store at  $-80$  °C.
3. Cells in all light and heavy medium from one plate can be collected as above and resuspended in 1 mL of appropriate freezing medium, placed in a freezing cell at  $-80$  °C short term or liquid N<sub>2</sub> for long-term storage of labeled cell stock.
4. Resuspend cells in 100  $\mu$ L mass spectrometry lysis buffer.
5. Perform Bradford protein concentration assay on the lysate (*see Note 14*). A typical protein concentration obtained is in the range of 400–500  $\mu$ g/mL, so 8–10  $\mu$ L will make up 4  $\mu$ g.

6. Dilute the volume of lysate corresponding to 4  $\mu\text{g}$  protein to 60  $\mu\text{L}$  with 50 mM ammonium bicarbonate. Adjust pH to 7.8 with 0.1 M HCl.
7. Add 100 ng of trypsin to the samples and leave to digest at 37 °C overnight (*see Note 15*).
8. Dry the samples in a SpeedVac.
9. Reconstitute the samples in 50  $\mu\text{L}$  2% acetonitrile, 0.1% TFA, adjusted to pH ~2 with 10% TFA.
10. Desalt the samples by passing them through a C18 zip tip.
11. Activate the C18 STAGE tips with 50  $\mu\text{L}$  of activation buffer.
12. Centrifuge at  $\sim 300 \times g$  until all liquid had passed through the tip.
13. Wash tip with 50  $\mu\text{L}$  of wash buffer and centrifuge at  $300 \times g$ .
14. Place the acidified sample in the tip and centrifuge at  $300 \times g$ .
15. Wash the tip with 50  $\mu\text{L}$  of wash buffer and transfer tip to a fresh microfuge tube.
16. Elute sample with 50  $\mu\text{L}$  of elution buffer and dry down in a speedy vac  $\sim 10$  min.
17. Resuspend tryptic peptides in 20  $\mu\text{L}$  of resuspension buffer, vortex and sonicate in a water bath for 2 min.
18. Analyze the samples labeled with heavy amino acids on an Orbitrap Elite mass spectrometer. The results are analyzed using the MaxQuant program [25, 26] (*see Note 16*).

### **3.5 Analysis of mtUPR by Mass Spectrometry**

After determining the optimal SILAC labeling medium, as described in Subheading 3.4, cells are transfected to produce a mitochondrial stress response that can be analyzed against control cells in the same mass spectrometry run.

1. Grow COS-7 cells (use frozen cells from stock) to 80 % confluence in appropriate heavy and light media.
2. Transiently transfect COS-7 cells with pCAGGS-OTC and pCAGGS-OTC- $\Delta$  vectors so that cells grown in both heavy and light media are transfected with both plasmids. For this, follow the method described in Subheading 3.1 with the difference that the cells are grown in either light or heavy medium rather than in complete medium.
3. 36 hours after transfection, lyse whole cells or isolated mitochondria in mass spectrometry lysis buffer, vortex and incubate on ice for 10 min. Centrifuge lysates at  $2000 \times g$  to remove debris.
4. Perform a Bradford protein concentration assay on the lysate (*see Note 14*).  $1 \times 10^6$  cells in 100  $\mu\text{L}$  of Cell Lysis buffer.

A 10 cm plate of COS-7 cells grown to confluence will yield  $\sim 5 \times 10^6$  cells and a concentration of  $\sim 500 \mu\text{g}/\text{mL}$ .

5. Mix together equal aliquots ( $\sim 50 \mu\text{g}$  each) of heavy labeled OTC and light labeled OTC $\Delta$  fractions and vice versa (light labeled OTC and heavy labeled OTC $\Delta$  fractions) at this early stage of sample preparation. Vortex and centrifuge to pool samples (*see Note 17*).
6. Double the volume of each sample with 100 mM Tris-HCl, pH 7.4, vortex and centrifuge to recover the samples from the tube wall.
7. Add TCEP to a final concentration of 1 mM to each sample and leave overnight at 22 °C in a Thermomixer at 700 rpm (*see Note 18*).
8. The next day, add IAA to a final concentration of 20 mM, vortex and leave at 22 °C in the dark for 40 min by covering with aluminum foil in a Thermomixer at 700 rpm (*see Note 19*).
9. Add TCEP to a final concentration of 3 mM and incubate for 1 h at 22 °C at 700 rpm to quench the alkylation reaction.
10. Add 1  $\mu\text{g}$  trypsin diluted in 100 mM ammonium bicarbonate. Add enough of the diluted trypsin mixture to each sample to bring the urea concentration down to  $\sim 1.0 \text{ M}$  (*see Note 20*).
11. Leave overnight at 37 °C in a Thermomixer at 700 rpm.
12. Place samples in a Speed-Vac and concentrate until the volume is reduced to 50–100  $\mu\text{L}$ , then centrifuge to recover the sample.
13. Acidify the samples to pH  $\sim 2$  with  $\sim 10 \mu\text{L}$  10% TFA. Check pH using 0.5  $\mu\text{L}$  on a pH strip.
14. Desalt the samples using a C18 zip tip as in Subheading 3.4, steps 11–17.
15. Transfer the samples to mass spectrometry injection vials.
16. Run each sample in duplicate using an extended HPLC acetonitrile gradient on an Orbitrap mass spectrometer (*see Note 21*).

---

## 4 Notes

1. Ornithine Transcarbamylase (OTC) is a mitochondrial protein expressed only in the liver and small intestine [19]. Mutant OTC, OTC $\Delta$ , is used to induce the mtUPR and the wild-type protein is used as a negative control. OTC $\Delta$  is a deletion mutant where an internal 255 base pair fragment, corresponding to amino acid residues 30–114, from the carbamyl phosphate binding domain was removed from the wild-type OTC DNA. This protein is still imported into mitochondria, but its folding is impeded and it aggregates, causing a mitochondrial

stress response [13]. This is the approach used here to create a cell model of organelle stress for in vitro protein and gene regulation analysis. We have widely distributed the vectors to other labs around the world and this method has been used to create an mtUPR in many different cell types and species. Thus, it is a universal method for accumulation unfolded proteins in the mitochondrial matrix and the induction of an mtUPR.

2. pCAGGS vector contains an SV40 origin of replication and the chicken  $\beta$ -actin promoter [23]. Transient transfection of these pCAGGS vectors is into COS-7 cells as these cells do not contain endogenous OTC. COS-7 cells are derived from simian monkey kidney cells. They contain a genetically integrated viral T antigen and, as such, these cells can support runaway replication of an exogenously introduced recombinant molecule carrying an SV40 origin of replication [27]. Transfection of pCAGGS-OTC into COS cells causes expression levels of OTC to be so high that it can be visualized directly from a Coomassie blue stained gel [13].
3. This buffer needs to be diluted to 1 M urea content to allow protein digestion by trypsin.
4. For luciferase assays we typically use Promega kits along with the Glomax luminometer, but other companies have similar systems. The Promega luminometer utilizes a 96-well plate sample format and has two injectors. The volume of injected reagents and the times between injections and readings of the signals can be custom set.
5. SILAC labeling of cells: This system involves metabolic labeling designed to incorporate amino acids containing different isotopes into proteins in living cells [28]. One sample is grown in the presence of natural (light) amino acids and the other in the presence of amino acids containing nonradioactive, heavy isotopes. Usually, one sample is treated in some way and the other is kept as a control. The two types of cells are mixed before sample preparation. Thus, in this approach, using mass spectrometry analysis, each peptide appears as a pair in the mass spectra; the peptide with lower mass contains the light amino acid and originates from the control population A, and the peptide with higher mass contains the heavy amino acid and originates from the population B, for example from cells in which mtUPR was induced. The ratios of these peptides are then compared to give a relative quantity between the two conditions as the expected mass differences between the labeled and unlabeled peptides are known before preparation [28].
6. The heavy amino acids include the following heavy isotope elements and the increased mass of incorporation of one of these into a protein is given in parenthesis:  $^{13}\text{C}_6^{15}\text{N}_2$  lysine (Lys8) and  $^{13}\text{C}_6^{15}\text{N}_4$  arginine (Arg10).

7. This is a desalting step to clean and concentrate peptides before mass spectrometry analysis. Peptides will bind to resin containing C18 chains and will elute using acetonitrile according to their hydrophobicity. There are a number of products available for this step.
8. Lipofectamine™ Reagent is suitable for the transfection of DNA into eukaryotic cells, and is a 3:1 (w/w) liposome formulation of the polycationic lipid 2,3-dioleoyloxy-N-[2(sperminecarboxamido)ethyl]-N,Ndimethyl-1-propanaminium trifluoroacetate (DOSPA) and the neutral lipid dioleoyl phosphatidylethanolamine (DOPE) in membrane-filtered water. Lipofectamine and vectors are left to stand at room temperature for 45 min to allow DNA-liposome complexes to form.
9. This amount of time allows for import of OTC and OTCΔ into the mitochondria, stress to take place and protein levels to accumulate. This time can be tested empirically with cells to determine optimum stress conditions.
10. Lysates can be stored at  $-80^{\circ}\text{C}$  until analysis.
11. Firefly luciferase is used in the gene reporter plasmids and *Renilla* luciferase is an internal control reporter plasmid to ensure normalization across sample batches. Because of their distinct evolutionary origins they have dissimilar enzyme structures and substrate requirements. These differences make it possible to selectively discriminate between their respective bioluminescent reactions. Use of the Dual Luciferase Reporter Assay System allows the luminescence from the firefly luciferase reaction to be quenched while simultaneously activating the luminescent reaction of *Renilla* luciferase. Promoters used in reporter constructs are based on the human genome sequence information of NCBI. Promoter regions were amplified by PCR using human genomic DNA as template and consisted of 1000 bp region upstream of the transcription start site. Promoter DNA was cloned into the pGL3-Basic vector (Promega) [16]. Empty plasmid, containing the promoter-less luciferase, is used as a negative control.
12. The Stop and Glo reagent allows the firefly and *Renilla* luciferases to be measured in succession. Dilution of the samples ensures the luminometer readout is in the linear scale.
13. The cells are split five times over 2 weeks to allow maximum incorporation of heavy labeled amino acids.
14. Bradford protein concentration assay is performed on the lysate as this assay is compatible with the lysis buffer.
15. The sample does not need to be reduced and alkylated at this stage, as this is a qualitative assay to determine the conversion of arginine to proline. Trypsin cleaves on the C terminal side of lysine and arginine, so it is expected that all peptides will contain

one of these heavy amino acids and there will be enough peptides containing proline to determine the conversion rate without the reduction and alkylation steps.

16. The MaxQuant program is able to define the expected mass of peptides after they have been fragmented into individual amino acids by the mass spectrometer. The program allows for the change in mass of heavy labeled peptides such as Pro6, inferring arginine to proline conversion.
17. Mixing equal amounts of light and heavy labeled samples at this early stage of the sample preparation workflow reduces errors related to discrepancies in reagent use and loss of sample. All steps taken from this point affect both the control and test samples in the same manner for that particular biological replicate. Care must be taken to ensure all samples are treated with the same reagents using a similar time course for sample preparation to reduce preparation effects. Many biological and technical replicates increase the statistical relevance of the results and reduce the effects of preparative and biological variations. Reversing the light and heavy stressed or control cells also verifies the power of the SILAC labeling method and can be accounted for when analyzing the data.
18. TCEP is a thiol-free reducing agent that reduces protein disulfide bonds.
19. IAA alkylates sulfhydryl groups on reduced proteins, which increases the mass by 57 Da [29].
20. The urea concentration is reduced to 1 M during digestion by dilution with 25 mM ABC to maintain the activity of the trypsin [30].
21. MaxQuant detects SILAC peptide pairs as three-dimensional objects in  $m/z$ , elution time, and signal intensity. The assembly of isotope patterns into SILAC pairs and quantitation is done prior to the submission of data to an MS/MS search engine where fragmented peptides are matched to the full length proteins from which they originate. After mitochondrial stress proteins such as HSP60 are expected to have 1.2–1.5 higher fold changes than the same protein from unstressed mitochondria.

## References

1. Ishihama Y et al (2008) Protein abundance profiling of the *Escherichia coli* cytosol. BMC Genomics 9:102
2. Srere PA, Sumegi B (1986) Organization of the mitochondrial matrix. Adv Exp Med Biol 194:13–25
3. Hartl FU, Bracher A, Hayer-Hartl M (2011) Molecular chaperones in protein folding and proteostasis. Nature 475(7356):324–332
4. Trinklein ND et al (2004) The role of heat shock transcription factor 1 in the genome-wide regulation of the mammalian heat shock response. Mol Biol Cell 15(3):1254–1261
5. Abravaya K, Phillips B, Morimoto RI (1991) Heat shock-induced interactions of heat shock transcription factor and the human hsp70 promoter examined by in vivo footprinting. Mol Cell Biol 11(1):586–592

6. Kim YK, Kim KS, Lee AS (1987) Regulation of the glucose-regulated protein genes by beta-mercaptoethanol requires de novo protein synthesis and correlates with inhibition of protein glycosylation. *J Cell Physiol* 133(3):553–559
7. Gardner BM et al (2013) Endoplasmic reticulum stress sensing in the unfolded protein response. *Cold Spring Harb Perspect Biol* 5(3):a013169
8. Schroder M, Kaufman RJ (2005) The mammalian unfolded protein response. *Annu Rev Biochem* 74:739–789
9. Meusser B et al (2005) ERAD: the long road to destruction. *Nat Cell Biol* 7(8):766–772
10. Puthalakath H et al (2007) ER stress triggers apoptosis by activating BH3-only protein Bim. *Cell* 129(7):1337–1349
11. Lin JH et al (2007) IRE1 signaling affects cell fate during the unfolded protein response. *Science* 318(5852):944–949
12. Martinus RD et al (1996) Selective induction of mitochondrial chaperones in response to loss of the mitochondrial genome. *Eur J Biochem/FEBS* 240(1):98–103
13. Zhao Q et al (2002) A mitochondrial specific stress response in mammalian cells. *EMBO J* 21(17):4411–4419
14. Horibe T, Hoogenraad NJ (2007) The chop gene contains an element for the positive regulation of the mitochondrial unfolded protein response. *PLoS One* 2(9):e835
15. Rath E et al (2012) Induction of dsRNA-activated protein kinase links mitochondrial unfolded protein response to the pathogenesis of intestinal inflammation. *Gut* 61(9):1269–1278
16. Aldridge JE, Horibe T, Hoogenraad NJ (2007) Discovery of genes activated by the mitochondrial unfolded protein response (mtUPR) and cognate promoter elements. *PLoS One* 2(9):e874
17. Haynes CM et al (2007) ClpP mediates activation of a mitochondrial unfolded protein response in *C. elegans*. *Dev Cell* 13(4):467–480
18. Papa L, Germain D (2011) Estrogen receptor mediates a distinct mitochondrial unfolded protein response. *J Cell Sci* 124(Pt 9):1396–1402
19. Tsuji S, Kanazawa S (1987) Chicken ornithine transcarbamylase: its unexpected expression. *Biochem Genet* 25(3–4):259–266
20. Horwich AL et al (1986) Targeting of pre-ornithine transcarbamylase to mitochondria: definition of critical regions and residues in the leader peptide. *Cell* 44(3):451–459
21. Jovaisaite V, Mouchiroud L, Auwerx J (2014) The mitochondrial unfolded protein response, a conserved stress response pathway with implications in health and disease. *J Exp Biol* 217(Pt 1):137–143
22. Dalby B et al (2004) Advanced transfection with Lipofectamine 2000 reagent: primary neurons, siRNA, and high-throughput applications. *Methods* 33(2):95–103
23. Niwa H, Yamamura K, Miyazaki J (1991) Efficient selection for high-expression transfectants with a novel eukaryotic vector. *Gene* 108(2):193–199
24. Lossner C et al (2011) Preventing arginine-to-proline conversion in a cell-line-independent manner during cell cultivation under stable isotope labeling by amino acids in cell culture (SILAC) conditions. *Anal Biochem* 412(1):123–125
25. Cox J, Mann M (2008) MaxQuant enables high peptide identification rates, individualized p.p.b.-range mass accuracies and proteome-wide protein quantification. *Nat Biotechnol* 26(12):1367–1372
26. Cox J et al (2009) A practical guide to the MaxQuant computational platform for SILAC-based quantitative proteomics. *Nat Protoc* 4(5):698–705
27. de Chasseval R, de Villartay JP (1992) High level transient gene expression in human lymphoid cells by SV40 large T antigen boost. *Nucleic Acids Res* 20(2):245–250
28. Mann M (2006) Functional and quantitative proteomics using SILAC. *Nat Rev Mol Cell Biol* 7(12):952–958
29. Yang Z, Attygalle AB (2007) LC/MS characterization of undesired products formed during iodoacetamide derivatization of sulfhydryl groups of peptides. *J Mass Spectrom* 42(2):233–243
30. Proc JL et al (2010) A quantitative study of the effects of chaotropic agents, surfactants, and solvents on the digestion efficiency of human plasma proteins by trypsin. *J Proteome Res* 9(10):5422–5437

## Analysis of Mitochondrial RNA-Processing Defects in Patient-Derived Tissues by qRT-PCR and RNAseq

Robert Kopajtich, Johannes A. Mayr, and Holger Prokisch

### Abstract

Transcription of the mitochondrial genome yields three large polycistronic transcripts that undergo multiple endonucleolytic processing steps, before resulting in functional mRNAs, tRNAs, and rRNAs. Cleavage of the large precursor transcripts is mainly performed by the RNase P complex and RNase Z that cleave mitochondrial pre-tRNAs at their 5' and 3' ends respectively. Most likely there are additional enzymes involved that still await identification and characterization. Defects in mitochondrial RNA processing have been associated with human disease. There are published cases of patients carrying mutations in either *HSD17B10/MRPP2* (encoding a subunit of RNase P complex) or *ELAC2* (coding for RNase Z). In addition, several mtDNA mutations within tRNA genes have been shown to affect RNA processing. Here, we describe detailed protocols for analyzing RNA processing of mitochondrial tRNAs, in particular their 3'-ends that are processed by RNase Z. These protocols should serve as a guide to extract RNA for quantitative real-time PCR and RNAseq analysis.

**Key words** Mitochondrial RNA Processing, RNase Z, RNase P, *ELAC2*, *MRPP2*, mtDNA, qRT-PCR, RNAseq

---

## 1 Introduction

Human mitochondria harbor their own small genome containing 37 genes, 13 of which encode subunits of respiratory chain complexes I, III, and IV and the ATP synthase (Fig. 1a). Translation of these genes is accomplished by the mitochondria's own transcription and translation machinery that comprises both nuclear encoded protein factors and mitochondrially encoded RNA components. Transcription initiates from different promoters and yields large polycistronic transcripts spanning both strands of almost the entire mitochondrial genome. These precursor molecules

---

<sup>s</sup>These authors contributed equally to this work.

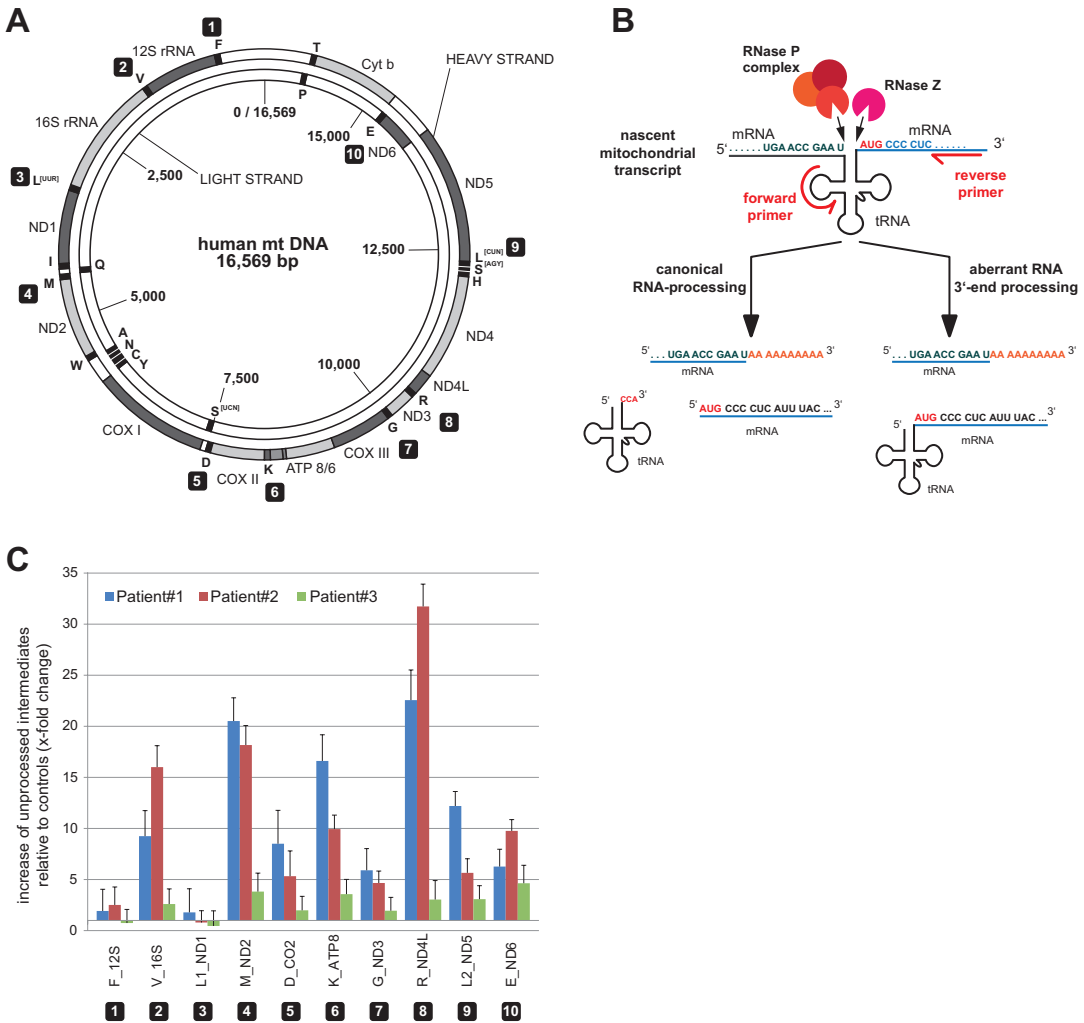


**Fig. 1** Mitochondrial genome, RNA-processing, and qRT-PCR. **(a)** Circular map of the human mitochondrial genome with annotated rRNA, mRNA, and tRNA genes among the heavy and light strands. Numbering 1–10 indicates RNA-processing sites located directly upstream of rRNAs and mRNAs. **(b)** The nascent mitochondrial transcripts are processed by RNase P-complex and RNase Z to yield individual RNA species. A defect in RNA 3'-end processing leads to an increase in intermediates that consist of tRNAs with their downstream RNAs that are identified in the real-time PCR analysis. As an example for the primer design used in the qRT-PCR analysis, the tRNA<sup>Arg</sup>-ND4L junction is given. **(c)** Quantification of ten unprocessed mitochondrial tRNA-rRNA or tRNA-mRNA junctions analyzed by qRT-PCR in fibroblasts from three patients with *ELAC2*-deficiency. Values are given as fold change to the average of three different controls. Error bars indicate ±1 standard deviation of at least three technical replicates. ND1-6, coding for complex I subunits; cytb, coding for complex III subunit, COX I-III, coding for complex IV subunits, ATP8/6, coding for ATP-synthase subunits. tRNA-genes are indicated using the single letter code for their cognate amino acids

are then further processed by endonucleases to yield the different mRNAs, tRNAs, and rRNAs. Human mitochondrial DNA is intronless and contains scarcely intergenic regions, thus individual genes are either directly adjacent to each other or only separated by single noncoding nucleotides. Consequently, processing events have

to occur with great accuracy to ensure functionality of the resulting separate transcripts. As proposed by the “tRNA punctuation model” excision of the 22 intervening tRNAs concomitantly produces all individual mature RNA species [1, 2].

Defects in tRNA 3'-end processing due to mutations in *ELAC2* have been associated with a reduced mitochondrial translation rate [3]. Eleven of the 13 organelle's mRNAs do either contain 5'-UTRs as short as 1, 2, or 3 nucleotides in length or completely lack any sequence upstream of the initiation codon. The remaining two mRNAs (ND4 and ATP6) are both part of bicistronic transcripts with overlapping open reading frames, ND4L/ND4 and ATP8/6 respectively; thus, their 5'-UTRs are the corresponding upstream ORFs [4]. A defect in tRNA 3'-end cleavage results in processing intermediates that consist of a tRNA joined to the 5'-end of an mRNA or rRNA (*see Notes 1 and 2*). It has been hypothesized that in case of mRNAs these abnormal 5'-extensions may interfere with the mitochondrial ribosome and consequently result in a translation defect in mutant or knock down cells [3, 5].

In this protocol, analysis of tRNA 3'-end processing is performed via qRT-PCR using primer pairs flanking potential RNase Z cleavage sites. Detection and visualization of tRNA 3'-end processing defects is also possible from RNAseq whole transcriptome data as obtained in gene expression studies. Accumulation of aberrantly processed transcripts was even detectable in significant amounts in RNA extracted from whole blood qualifying this method as a diagnostic tool for mitochondrial disorders.

## 2 Materials

### 2.1 Equipment, Reagents, and Consumables

#### 2.1.1 Equipment and Manufacturer

1. Benchtop centrifuge, Hettich Mikro 22-R	Hettich (Hareaus)
2. PCR cycler, Peqstar	Peqlab
3. Nanodrop 1000 spectrophotometer	NanoDrop Instruments
4. Real Time PCR Cycler (96-well format), iCycler iQ5	BioRad
5. Real Time PCR Cycler (384-well format), HT7900	Applied Biosystems
6. 2100 Bioanalyzer	Agilent Technologies

#### 2.1.2 Reagents and Consumables

1. QIAshredder	Qiagen
2. RNeasy Mini Kit	Qiagen
3. Buffer RLT Plus	Qiagen
4. Buffer RPE	Qiagen

5. Ethanol, absolute	Merck
6. PAXgene blood RNA tubes and isolation kit	PreAnalytix
7. TRIzol	Life Technologies
8. TRI reagent	Sigma-Aldrich
9. Chloroform	Merck
10. Turbo DNase	Ambion
11. Maxima reverse transcriptase	Thermo Fisher Scientific
12. RNase inhibitor	Thermo Fisher Scientific
13. RiboLock	Thermo Fisher Scientific
14. Random hexamer primers	Thermo Fisher Scientific
15. dNTPs	Thermo Fisher Scientific
16. PerfeCta® SYBR® Green FastMix® ROX™	Quanta Bioscience
17. mtDNA specific oligonucleotides	Metabion
18. RNA 6000 Nano Kit	Agilent

### 2.1.3 Oligonucleotides

Oligonucleotides (*see* Table 1) were purchased (from Metabion) in standard (“desalted”) purity, dissolved in H<sub>2</sub>O at a final concentration of 100 μM.

## 3 Methods

When working with RNA, special precautions should be taken to avoid contamination with RNases and to prevent autohydrolysis of RNA due to inappropriate storage. Consumables and reagents should be certified as “RNase-free” and gloves should be worn at all times. A separate working area including pipettes should be established to minimize the risk of contamination and carry-over or RNases from other lab areas. RNA should always be cooled on ice for shorter periods and be kept at –80 °C for long-term storage in H<sub>2</sub>O or a buffer without bivalent metal ions such as Mg<sup>2+</sup>, Ca<sup>2+</sup>, Zn<sup>2+</sup>, Mn<sup>2+</sup> to prevent autohydrolysis.

### 3.1 RNA Isolation

#### 3.1.1 RNA from PAXgene Whole Blood

The content of a PAXgene blood RNA tube (consisting of 2.5 mL whole blood and 6.9 mL additive) is processed using the PAXgene blood RNA Kit according to the manufacturer’s instructions.

#### 3.1.2 RNA from Cultured Fibroblasts

1. A fresh or frozen cell pellet from a 70–80% confluent 75 cm<sup>2</sup> flask (corresponding to 2–5 × 10<sup>6</sup> cells) is resuspended and

**Table 1**  
**Oligonucleotides used for qRT-PCR**

#	Junction/amplicon	Primer ID	mtDNA position	Sequence 5' to 3'
1	tRNA <sup>Phe</sup> —12S rRNA	MT-TF-F MT-RNR1-R1	582 708	TGTAGCTTACCTCCTCAAAGCA AGGGTGAACCTCACTGGAACG
2	tRNA <sup>Val</sup> —16S rRNA	MT-TV-F 5R	1,611 1,930	GCTTAACACAAAGCACCCAAC ACGGGTGTGCTCTTTTAGCTG
3	tRNA <sup>Leu(UUR)</sup> —ND1	MT-TL1-F 9R	3,245 3,486	CCCGGTAATCGCATAAACT TAGATGTGGCGGGTTTTAGG
4	tRNA <sup>Met</sup> —ND2	MT-TM-F GluMet4-R	4,405 4,532	AAGGTCAGCTAAATAAGCTATCG AAAAATCAGTGCGAGCTTAGC
5	tRNA <sup>Asp</sup> —COII	MT-TD-F 20R	7,527 7,663	GAAAAACCATTTTCATAACTTTGTCA GGAAAATGATTATGAGGGCG
6	tRNA <sup>Lys</sup> —ATP8/6	MT-TK-F 22R	8,336 8,539	TTAAGAGAACCAACACCTCTTTACA GGGCAATGAATGAAGCGAACAG
7	tRNA <sup>Gly</sup> —ND3	MT-TG-F 26R	10,012 10,128	CCGTAACTTCCAATTAAGTATTTG TGTAGCCGTTGAGTTGTGGTAG
8	tRNA <sup>Arg</sup> —ND4L/ ND4	MT-TR-F 28R	10,410 10,613	AACAAAACGAATGATTTTCGACTC TAAGAGGGAGTGGGTGTTGAGG
9	tRNA <sup>Leu(CUN)</sup> —ND5	MT-TLcun-F2 33R	12,281 12,443	CAGCTATCCATTGGTCTTAGGC GGATGCGACAATGGATTTTA
10	tRNA <sup>Glu</sup> —ND6	40F MT-TE-R	14,548 14,795	AATAACACACCCGACCACAC ACAACGATGGTTTTTCATATCATT
	HPRT1 nuclear encoded reference gene	HPRT1-F HPRT1-R	N/A N/A	TTCCTTGGTGAGGCAGTATAATC GGGCATATCCTACAACAAACTTG
	RPL27 nuclear encoded reference gene	RPL27-F RPL27-R	N/A N/A	GCTGGAATTGACCGCTACC TCTCTGAAGACATCCTTATTGACG

lysed in 350  $\mu$ L of buffer RLT Plus. At this step, the lysate can either be stored at  $-80^{\circ}\text{C}$  or processed immediately.

2. The lysate is further homogenized by centrifugation through a QIAshredder spin column for 2 min at full speed.
3. RNA isolation is performed using the RNeasy Mini Kit, or the AllPrep DNA/RNA Mini Kit, if also DNA has to be isolated from the same sample.

All the steps are carried out according to the manufacturer's instructions.

3.1.3 RNA  
from Muscle Tissue

1. Prior to RNA extraction, 5–20 mg of deep frozen ( $-80\text{ }^{\circ}\text{C}$ ) muscle tissue is wrapped in aluminum foil and placed on a metal block pre-cooled with dry ice or liquid nitrogen.
2. Tissue is mechanically disrupted using a hammer or similar (*see Note 3*).
3. The frozen tissue powder is scraped off using a scalpel blade and transferred to a clean micro-centrifuge tube.
4. After the addition of 500  $\mu\text{L}$  TRIZOL or TRI reagent, the sample is completely dissolved by repeatedly pipetting up and down (*see Note 4*).
5. Incubate the homogenate for 5 min at room temperature.
6. Add 200  $\mu\text{L}$  of chloroform and mix well for 15 s by vigorously shaking or vortexing.
7. Incubate the emulsion for 5 min at room temperature.
8. Centrifuge at  $12,000 \times g$  for 15 min at  $4\text{ }^{\circ}\text{C}$  to allow the phases to separate.
9. Transfer the upper (RNA-containing) aqueous phase to a clean tube.

From this solution, RNA can either be isolated by performing a 2-propanol precipitation (according to the TRIZOL/TRI reagent manuals) or purified via spin columns from the RNeasy Mini kit using a modified version of the manufacturer's protocol, described below.

10. Combine 200  $\mu\text{L}$  of the aqueous phase with 700  $\mu\text{L}$  buffer RLT (component of the RNeasy Mini kit) and 500  $\mu\text{L}$  100% ethanol (*see Note 5*).
11. Mix well by vortexing.
12. Apply half of the sample ( $\sim 700\text{ }\mu\text{L}$ ) to an RNeasy spin column placed in a 2 mL collection tube.
13. Spin for 15 s at  $9,500 \times g$ . Discard the flow through and repeat for the second half of the sample.
14. Transfer the spin column to a new collection tube and wash by adding 500  $\mu\text{L}$  of buffer RPE and centrifugation (15 s at  $9,500 \times g$ ).
15. Discard the flow through and wash the column twice, first with 80%, then with 75% ethanol (centrifugations as above).
16. Transfer the spin column to a new 2 mL collection tube and spin for 5 min at top speed ( $16,000 \times g$ ) to remove any residual ethanol that might interfere with subsequent applications.
17. Elute RNA by centrifugation ( $7,000 \times g$  for 1 min) with 30  $\mu\text{L}$  RNase-free water into a new tube (*see Note 6*).

After any of the above isolation procedures RNA concentrations should be measured using a spectrophotometer (e.g., NanoDrop). Using the procedures described above, we usually obtain high-quality RNA. Nevertheless, we recommend validating the RNA integrity by electrophoretic separation and RNA staining, e.g., using a 2100 Bioanalyzer and the RNA 6000 Nano Kit, according to the manufacturer's instructions (*see Note 7*).

### 3.2 DNase Digest

Since the mitochondrial genome does not contain any introns, even traces of co-purified DNA can compromise the qPCR analysis. Therefore, it is necessary to remove any remaining DNA contaminants prior to cDNA synthesis by DNase digestion (*see Note 8*).

1. From each sample treat equal amounts of RNA (100 ng to 1 µg) are treated with Turbo DNase in the presence of RNase inhibitor (e.g., RNaseOUT or RiboLock) in a total volume of 10 µL:

Turbo DNase (2 U/µL)	1.0 µL
Reaction buffer (10×)	1.0 µL
RNase inhibitor	1.0 µL
RNA (0.1–1.0 µg)	× µL
RNase-free H <sub>2</sub> O	ad 10.0 µL

2. Incubate reactions for 30 min at 37 °C.
3. Inactivate DNase by incubation for 10 min at 85 °C and immediately place reactions on ice.

### 3.3 cDNA Synthesis

cDNA synthesis is performed using Maxima reverse transcriptase, which has been modified by in vitro evolution from M-MuLV RT and possesses a higher thermostability and increased synthesis rate. Due to the high proportion of secondary and tertiary structural elements of tRNAs and rRNAs, the RT reaction is performed at increasing temperatures, starting at 25 °C, increasing the temperature step-wise to allow RNAs to unfold during first strand synthesis.

1. For primer annealing, add 1 µL of random hexamer primers (0.2 µg/µL) to the DNase-treated RNA, heat for 3 min at 70 °C, then immediately place on ice.
2. Set up reactions with a total volume of 20 µL as follows:

RNA, primer-annealed	11.0 µL
dNTPs (10 mM)	1.0 µL
RNase inhibitor	1.0 µL
RT buffer (5×)	4.0 µL
Maxima-RT (200 U/µL)	1.0 µL
RNase-free H <sub>2</sub> O	2.0 µL

3. Incubate RT reactions in a PCR cycler with the following parameters (10 min at 25 °C, 30 min at 50 °C, 10 min at 55 °C, 10 min at 60 °C, 10 min at 65 °C, 10 min at 65 °C, 5 min at 85 °C, 1 min at 25 °C).
4. All cDNA preparations should be stored at -20 °C until needed.

### 3.4 qPCR

For qPCR amplification, primers to ten RNase Z processing sites in the human transcriptome have been designed (see Table 1) with the forward primer being located within the tRNA and the reverse primer downstream of the tRNA's 3'-end (Fig. 1a, b). In order to adapt this protocol for the analysis of tRNA 5'-end processing, primers have to be designed to flank RNase P processing sites, accordingly (see [6] for details). For normalization, the expression of two reference genes (*HPRT1* and *RPL27*) is analyzed.

1. For each PCR amplicon, mix forward and reverse primer stocks (usually 100 μM) to obtain working dilutions with a final concentration of 1 μM of each primer (e.g., 1 μL forward primer + 1 μL reverse primer + 98 μL H<sub>2</sub>O).
2. Dilute cDNA preparation 1:25 in H<sub>2</sub>O (see Note 9).
3. Set up reactions in a total volume of 10 μL as follows:

SYBR Green Master Mix	5.0 μL
Template cDNA (1:25 dilution)	1.0 μL
Primer-Mix F+R (1 μM)	4.0 μL

4. Cycle parameters on the iCycler iQ5 are (initial denaturation: 1 min/95 °C; 40 cycles: 2 s/96 °C; 40 s/63 °C; 20 s/72 °C; final step: 10 s/25 °C). Using the HT7900 cycler, the following parameters are used (initial denaturation: 1 min/95 °C; 40 cycles: 30 s/95 °C, 30 s/60 °C; final step: 30 s/25 °C) (see Note 10).
5. For each target to be amplified, set up several technical replicates (at least in triplicate). Ct values between these replicates should not differ by more than 0.2 cycles (see Note 11).

### 3.5 Data Analysis

For technical replicates, mean Ct values from each individual sample are normalized to the mean Ct of the two reference genes to obtain delta Ct values (dCt). Next, the normalized individual dCt values of the patients are subtracted from the mean of the control Ct values to yield delta delta Ct (ddCt) values. For biological replicates first ddCt values have to be determined, which can then be used to calculate the mean ddCt. The resulting deviations (ddCt) are taken as exponents to the base 2 to obtain the x-fold change of unprocessed RNA intermediates in a given sample compared to one or several controls.

Example:

The processing intermediates of the tRNA<sup>Arg</sup> and the downstream transcript ND4L were found to be 32-fold increased in fibroblasts (derived from a patient with mutations in *ELAC2*) compared to a healthy control.

In details:

1. Mean Ct value for this amplicon was 19.9 in patient fibroblast cDNA and 25.0 in control fibroblasts.
2. The mean Ct values for the reference genes were 24.5 and 24.6 respectively.
3. dCt values (deviation of reference gene to region of interest) were:
  - for the patient:  $24.5 - 19.9 = 4.6$ .
  - in the controls:  $24.6 - 25.0 = -0.4$ .
4. Deviation of normalized dCt values yields the ddCt of this particular processing intermediate for this given patient sample:  $4.6 - (-0.4) = 5.0$ .
5. Real-Time PCR amplification exceeds the threshold level 5.0 PCR cycles earlier for this tRNA-mRNA boundary in the patient compared to the control sample.
6. This processing intermediate is therefore theoretically  $2^5 = 32$ -fold increased (Fig. 1c) (sample #2, R\_ND4L).

### 3.6 RNAseq

Detection of tRNA 3'-processing defect from standard RNAseq whole transcriptome data made use of the fact that by poly(A)-capturing, size selection and due to their complex structure, tRNAs are eliminated during library preparation and therefore not covered in the sequencing data. In the presence of unprocessed tRNA 3'-ends, the sequence reads for the downstream mRNAs and rRNAs will extend into the upstream tRNA regions leading to an increased number of sequence reads (*see Note 12*).

1. For comparison the relative coverage is calculated for each sample, by normalizing the coverage at each position to the number of reads mapped to the mtDNA, multiplied by the average number of reads mapped to mtDNA over all samples (in our case  $10^6$ ).
2. For graphic representation, the normalized coverage for each position is plotted over the mitochondrial genome to obtain a coverage histogram (Fig. 2a).
3. Detailed view of the tRNA-coding regions reveals higher number of sequence reads for the samples derived from patients carrying mutations in *ELAC2* (RNA from fibroblasts and whole blood), indicating accumulation of tRNA-mRNA intermediates (Fig. 2b).

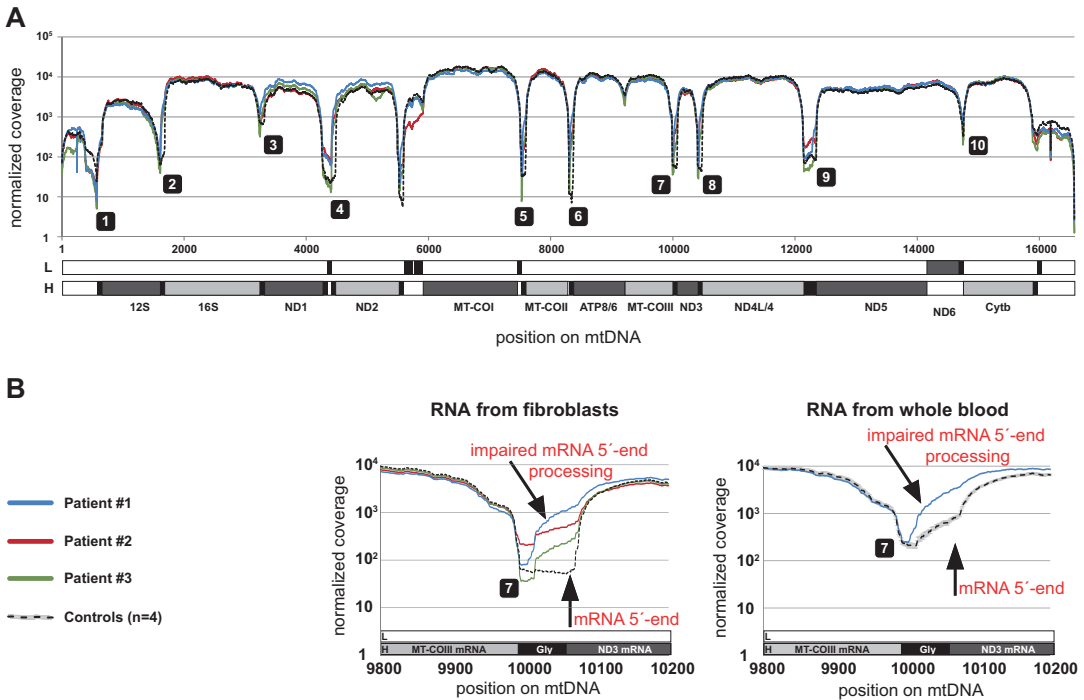


**Fig. 2** Mitochondrial transcriptome analysis. **(a)** Mitochondrial transcriptome analysis by next-generation sequencing (RNAseq) of RNA isolated from three fibroblast cell lines from patients with *ELAC2*-deficiency. Relative coverage is plotted over the mitochondrial genome (number according to RefSeq accession number J01415). *Colored lines* represent affected individuals; *black dotted line* indicates the average of four controls. **(b)** Processing site between tRNA<sup>Gly</sup> and ND3 is shown with higher magnification for RNA from three fibroblast cell lines and for RNA from one blood sample

## 4 Notes

1. Within the human mitochondrial genome, several tRNA 3'-ends are located adjacent to each other on opposite strands (the 3' ends of tRNAs for Ile and Glu, Trp and Ala, Thr and Pro respectively; Fig. 1a). Consequently, their 3'-processing sites would be located within one PCR product and cannot be analyzed individually and distinguished from each other using this protocol.
2. Junctions between neighboring tRNAs (e.g., tRNAs Tyr, Cys, Asn, Ala and His, Ser<sup>[AGY]</sup>, Leu<sup>[CUN]</sup>) were also found to be difficult targets for analyzing RNA-processing. This might be due to highly structured regions in these potentially very short RNA species that are only very inefficiently reverse transcribed using random hexamer primers.
3. Special care should be taken not to damage the aluminum foil used to wrap the frozen tissue to prevent loss and contamination of sample.

4. Depending on the amount of input material and the type of tissue used, resuspending and dissolving can take up to 5 min.
5. Excess RNA-containing aqueous phase should be frozen at  $-20^{\circ}\text{C}$  to serve as a backup in case more RNA is needed at a later time.
6. The total yield of RNA can be increased by repeating the elution with an additional 30  $\mu\text{L}$  of water from the same column. At the same time, this will decrease the final concentration of the eluate.
7. RNA Integrity Number (RIN) determined using the Bioanalyzer expresses a ratio of the two most abundant RNAs (28S and 18S rRNAs) in total RNA preparations. RIN values can range from 0 to 10 and are a measure for intactness of the RNA, where a RIN of 10 would represent intact RNA and lower RINs indicate partial degradation of the preparation. In our experience, RNA extracted from fibroblast cell pellets usually yielded RIN numbers between 9.9 and 10.0. RNA preparations from whole blood were found to have RIN values between 7.0 and 9.0 and RNA from various tissues (such as muscle, heart, and liver) resulted in RINs between 7.0 and 8.0. Whereas even a RIN of 5 or 6 is still tolerable for cDNA synthesis and subsequent qPCR analysis, samples with RIN lower than 7 should be excluded from RNAseq analysis.
8. Primer annealing, DNase digest, and cDNA synthesis should be performed in thin-walled PCR tubes to ensure a quicker temperature distribution between PCR-cycler/heating block and the sample.
9. Template cDNA concentrations can vary depending on the amount and integrity of the input RNA, as well as the efficiency during reverse transcription. Dilute cDNA to obtain Ct-values ranging from 15 to 25 during the subsequent qPCR reaction. If Ct values are too low, higher dilutions of cDNA have to be prepared, if Ct values are too high, cDNA should be used more concentrated.
10. Cycling parameters during qPCR strongly depend on the instrument used and have to be determined experimentally (e.g., denaturing time on the iCycler vs. HT7900 was 2 s vs 30 s, respectively). The necessity for including an elongation temperature step into the PCR cycle program is another factor that needs to be evaluated for every instrument and qPCR reagent used. In case of the HT7900 cycler, slightly increasing the length of the annealing step allowed for elimination of the elongation step from the cycler program.
11. If possible also biological replicates should be performed. In the case of cultured cells these correspond to RNA preparations carried out from individual cell pellets, whereas in the

case of limited biopsy material this may not be possible. Alternatively, several batches of cDNA can be reverse transcribed instead.

12. Importantly, the data for samples and controls must be processed in parallel and acquired in one sequencing run. When comparing data from individual RNA-seq experiments, batch-to-batch effects due to differences in library preparation might lead to inconclusive results.

## References

1. Ojala D, Montoya J, Attardi G (1981) tRNA punctuation model of RNA processing in human mitochondria. *Nature* 290:470–474
2. Anderson S, Bankier AT, Barrell BG et al (1981) Sequence and organization of the human mitochondrial genome. *Nature* 290:457–465
3. Haack TB, Kopajtich R, Freisinger P et al (2013) ELAC2 mutations cause a mitochondrial RNA processing defect associated with hypertrophic cardiomyopathy. *Am J Hum Genet* 93:211–223. doi:[10.1016/j.ajhg.2013.06.006](https://doi.org/10.1016/j.ajhg.2013.06.006)
4. Temperley RJ, Wydro M, Lightowlers RN, Chrzanowska-Lightowlers ZM (2010) Human mitochondrial mRNAs-like members of all families, similar but different. *Biochim Biophys Acta* 1797:1081–1085. doi:[10.1016/j.bbabi.2010.02.036](https://doi.org/10.1016/j.bbabi.2010.02.036)
5. Christian BE, Spremulli LL (2010) Preferential selection of the 5'-terminal start codon on leaderless mRNAs by mammalian mitochondrial ribosomes. *J Biol Chem* 285:28379–28386. doi:[10.1074/jbc.M110.149054](https://doi.org/10.1074/jbc.M110.149054)
6. Deutschmann AJ, Amberger A, Zavadil C et al (2014) Mutation or knock-down of 17 $\beta$ -hydroxysteroid dehydrogenase type 10 cause loss of MRPP1 and impaired processing of mitochondrial heavy strand transcripts. *Hum Mol Genet* 23:3618–3628. doi:[10.1093/hmg/ddu072](https://doi.org/10.1093/hmg/ddu072)

## Identification of Disease-Causing Mutations by Functional Complementation of Patient-Derived Fibroblast Cell Lines

Laura S. Kremer and Holger Prokisch

### Abstract

Diagnosis of mitochondrial disorders is still hampered by their phenotypic and genotypic heterogeneity. In many cases, exome sequencing, the state-of-the-art method for genetically diagnosing mitochondrial disease patients, does not allow direct identification of the disease-associated gene but rather results in a list of variants in candidate genes. Here, we present a method to validate the disease-causing variant based on functional complementation assays. First, cell lines expressing a wild-type cDNA of the candidate genes are generated by lentiviral infection of patient-derived fibroblasts. Next, oxidative phosphorylation is measured by the Seahorse XF analyzer to assess rescue efficiency.

**Key words** Mitochondrial disorders, Exome sequencing, Disease-associated gene, Functional complementation, Oxygen consumption rate

---

### 1 Introduction

Mitochondrial disorders are a heterogeneous group of diseases characterized by impaired oxidative phosphorylation [1]. Despite good progress in the field, most disease-associated mutations still have to be identified. In recent years, exome sequencing has emerged as a reliable tool to not only detect known disease-causing mutations but also to identify mutations in new disease-associated genes [2]. However, it should be noted that exome sequencing analysis rarely results in a direct identification of the disease-causing variants but rather in a list of variants in candidate genes. The most likely candidate gene for the observed disease is selected based on the type of mutation, known or predicted subcellular localization, function of the protein, biochemical data, and the clinical presentation of the patient. For a final diagnosis, the candidate gene needs to be validated using functional studies.

Fibroblast cell lines have proven to be a suitable tool to investigate the pathomechanism of a plethora of disease-causing variants in various genes, even though not necessarily being directly affected.

They are established upon taking a muscle biopsy for the measurement of the respiratory chain complexes (RCCs) activities, the standard diagnostic procedure for mitochondrial disorders. To secure the genetic diagnosis, wild-type cDNA of the respective candidate gene is expressed in the patient-derived fibroblasts and the rescue potential of the observed cellular phenotypes is assessed [2–4].

The complementation assay described is based on the widely used ViraPower™ HiPerform™ Lentiviral Expression System and we routinely transduce a control fibroblast cell line and the patient cell line with the wild-type cDNA of the respective disease-associated gene. Depending on your specific need, consider also including constructs containing cDNA carrying patient mutations, control genes (e.g., GFP), or empty constructs in your study.

The overall activity of the RCCI-IV can be determined by measuring the oxygen consumption, the respiration, of mitochondria. Here, we look for defects in the maximal oxygen consumption rate (OCR), which is frequently altered in patient-derived fibroblasts [5–8]. We measure the OCR using the Seahorse XF analyzer and derive the maximal OCR, also referred to as maximal respiration rate, by applying the XF Cell Mito Stress Test. First, ATPase is blocked by oligomycin, which leads to a complete inhibition of the respiratory chain since the proton gradient built up by RCCI-IV cannot be exploited anymore. Second, addition of FCCP, an ionophore, dismantles the proton gradient resulting in uncoupling of RCCI-IV from ATPase, thereby achieving overall maximal respiration. Third, rotenone, a RCCI inhibitor, and antimycin A, a RCCIII inhibitor, are added to stop mitochondrial respiration, whereafter only a small OCR contributed to non-mitochondrial respiration can be measured. The mitochondrial maximal respiration rate is the difference between FCCP-induced overall maximal OCR and the non-mitochondrial OCR derived upon addition of rotenone and antimycin A. The experimental setup is outlined in Fig. 1.

---

## 2 Materials

### 2.1 Generation of the Rescue Plasmid

1. Ampicillin (Sigma): prepare 100 mg/mL ampicillin in H<sub>2</sub>O and store as 1 mL aliquots at –20 °C. Aliquots can be refrozen but should be thawed on ice.
2. LB-Medium: Dissolve 10 g NaCl, 10 g Trypton, and 5 g yeast extract in 900 mL deionized H<sub>2</sub>O, adjust pH to 7.0 with 5 M NaOH, and fill up to 1 L with deionized H<sub>2</sub>O. Autoclave and store at RT.
3. LB-Amp plates: Dissolve 10 g NaCl, 10 g Trypton, and 5 g yeast extract, in 900 mL deionized H<sub>2</sub>O, adjust to pH 7.0 with 5 M NaOH. Add 20 g agar, fill up to 1 L with H<sub>2</sub>O, and autoclave. Let cool to 40 °C before adding 1 mL of ampicillin (100 mg/mL stock in H<sub>2</sub>O). Pour 25 mL in 10 cm petri dishes and let it solidify. Store at 4 °C.

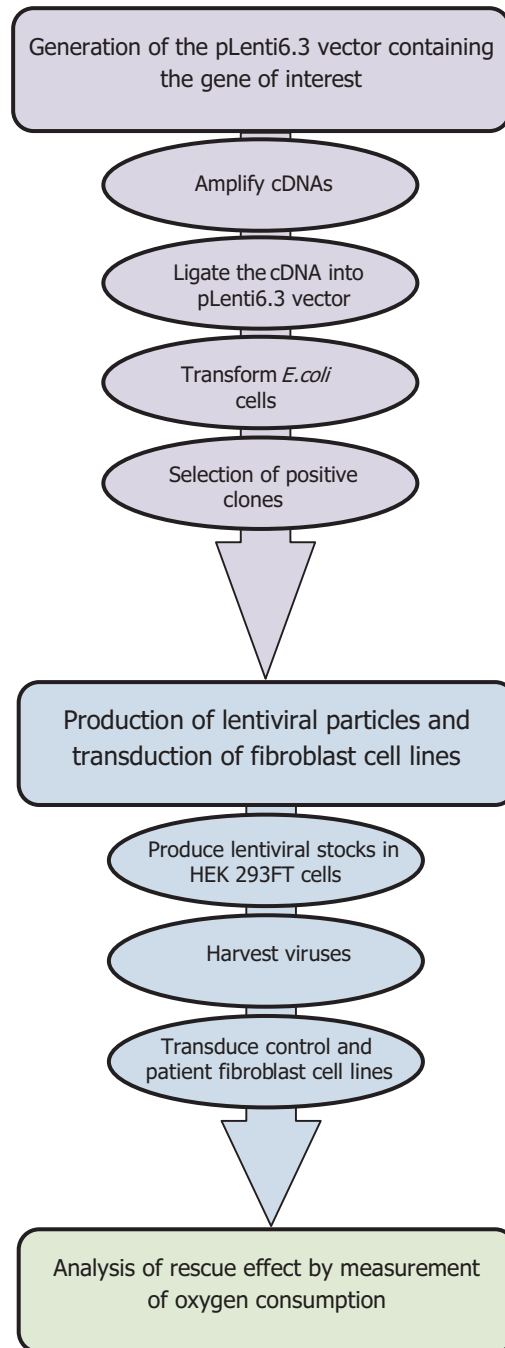


**Fig. 1** Experimental setup for target gene expression and evaluation of rescue effect in control and patient fibroblast cell lines

4. DNA Agarose, Biozym.
5. 6× DNA Loading Dye.
6. Filtration system Stericup-GP, 0.22  $\mu\text{m}$ , Merck Millipore.
7. QIAGEN Plasmid Midi Kit, Qiagen.

8. QIAprep Spin Miniprep Kit, Qiagen.
9. QIAshredder™, Qiagen.
10. Platinum® Taq DNA Polymerase High Fidelity, Thermo Fisher Scientific.
11. SERVA DNA Stain G, SERVA.
12. ViraPower™ HiPerform™ Lentiviral TOPO® Expression Kit (K531000), Thermo Fisher Scientific.

## **2.2 Production of Lentiviral Particles and Transduction of Patient Cell Lines**

1. Blasticidin S HCL, Thermo Fisher Scientific.
2. Dulbecco's Phosphate buffered saline (PBS), Gibco.
3. Geneticin-disulfate (G418) (50 mg/mL), Carl Roth.
4. Normal Human Dermal Fibroblasts from Neonatal Tissue (NHDF-neo), Lonza.
5. Penicillin-Streptomycin (5000 U/mL), Gibco.
6. 0.05%-Trypsin-EDTA, Gibco.
7. Prepare a 100 mM Uridine (Sigma) stock solution in ultrapure H<sub>2</sub>O and filter through a 45 µm filter. Store as 1 mL aliquots at -20 °C.
8. Fibroblast growth medium: High glucose Dulbecco's Modified Eagle's Medium (DMEM, Gibco) supplemented with 10% (v/v) fetal bovine serum (FBS, Gibco), 1% (v/v) penicillin-streptomycin, and 200 µM Uridine. The medium may be stored at 4 °C for 1 month.
9. 293FT growth medium: High glucose DMEM supplemented with 10% (v/v) FBS, 1% (v/v) penicillin-streptomycin, and 300 µg/mL G418. The medium may be stored at 4 °C for 1 month.
10. Medium 1: High glucose DMEM supplemented with 10% (v/v) FBS.
11. Medium 2: High glucose DMEM supplemented with 10% (v/v) FBS, 1% (v/v) penicillin-streptomycin, and 200 µM Uridine.
12. Medium 3: High glucose DMEM.
13. Medium 4: High glucose DMEM supplemented with 2% (v/v) FBS.
14. Medium 5: Nonfiltered fibroblast growth medium.

## **2.3 Measurement of Oxygen Consumption**

1. CyQUANT® Cell Proliferation Assay Kit, Life Technologies.
2. DMEM (without glucose, L-glutamine, phenol red, sodium pyruvate and sodium bicarbonate, powder, Sigma).
3. Fluorescence plate reader.
4. Glucose (20% sterile solution), B. Braun.
5. Hydrochloric acid 37% (HCl), Sigma.
6. Non-carbon dioxide incubator.

7. Cell Counter.
8. Seahorse XF96 analyzer, Seahorse Bioscience.
9. Sodium pyruvate (100 mM solution), Sigma.
10. XF96 Cell Culture Microplate, Seahorse Bioscience.
11. XF96 Sensor Cartridge, Seahorse Bioscience.
12. Seahorse medium (SH medium): dissolve one vial of sodium bicarbonate free DMEM powder in 900 mL of ultrapure H<sub>2</sub>O, add 10 mL sodium pyruvate (10 mM) and 22.5 mL 20% glucose. Adjust the pH to 7.2 with potassium hydroxide and fill up to 1 L with H<sub>2</sub>O. Prepare 50 mL aliquots and store at -20 °C.
13. FCCP (Sigma): prepare 10 mM FCCP in DMSO and store as 4 µL aliquots at -20 °C. On the day of assay, prepare a 4 µM FCCP working solution in SH medium.
14. Rotenone (Sigma): prepare 5 mM rotenone in DMSO and store as 15 µL aliquots at -20 °C. On the day of assay, prepare a 20 µM rotenone working solution in SH medium.
15. Oligomycin (Sigma): prepare 5 mM oligomycin in DMSO and store as 9 µL aliquots at -20 °C. On the day of assay, prepare a 10 µM oligomycin working solution in SH medium.
16. Antimycin A (Sigma): prepare 25 mM antimycin A in DMSO and store as 5 µL aliquots at -20 °C. On the day of assay, prepare a 25 µM antimycin A working solution in SH medium.

### 3 Methods

#### 3.1 Generation of the Rescue Plasmid

Clone the cDNA of the gene of interest into the pLenti6.3 vector using appropriate primers (*see* **Notes 1–3**) according to the ViraPower™ HiPerform™ Lentiviral TOPO® Expression Kit protocol. A brief outline is given below.

1. PCR reaction:

Component	For 10 µL reaction	Final concentration
10× High Fidelity PCR Buffer	1 µL	1×
2 mM dNTP mixture	1 µL	0.2 mM each
50 mM MgSO <sub>4</sub>	0.4 µL	2.0 mM
10 µM forward primer	0.4 µL	0.2 µM
10 µM reverse primer	0.4 µL	0.2 µM
Template DNA	1 µL	<5 ng
Platinum® Taq DNA Polymerase High Fidelity (5 U/µL)	0.04 µL	0.2 U/rxn
Ultrapure H <sub>2</sub> O	5.76 µL	–

## 2. PCR program:

	Temperature (°C)	Time
Heat Lid	110	
Denature	95	2 min
Start Cycle (30×)		
Denature	95	30 s
Anneal	primer T <sub>m</sub> - 5	30 s
Extend	68	1 min/kb
End Cycle		
Extend	68	10 min

3. Check the PCR product by agarose gel electrophoresis (*see Note 4*).
4. Warm up the water bath to 42 °C, the LB-Amp plate (1 per construct) to 37 °C and the S.O.C. medium (provided with ViraPower™ HiPerform™ Lentiviral TOPO® Expression Kit) to RT and set the shaker temperature to 37 °C.
5. Mix 1 µL fresh PCR product, 1 µL salt solution, 2 µL ultrapure H<sub>2</sub>O, and 1 µL pLenti-TOPO vector.
6. Incubate the reaction at RT for 5 min.
7. Place the mixture on ice and thaw one stock of One ShotR Stbl3™ Competent *E. coli* cells (provided with ViraPower™ HiPerform™ Lentiviral TOPO® Expression Kit).
8. Add the whole reaction volume to the cells and incubate on ice for 30 min.
9. Heat-shock the cells at 42 °C for 30 s in the water bath.
10. Place the cells on ice for 2 min.
11. Add 225 µL S.O.C. medium and shake the cells at 37 °C for 1 h in a shaker.
12. Plate the complete mix on the pre-warmed LB-Amp agar plates and incubate overnight at 37 °C.
13. On the following day, warm a LB-Amp plate to 37 °C and mark the plate with as many sections as the number of colonies you pick for follow-up analysis (*see Notes 5 and 6*).
14. Fill as many wells of a 96-well PCR plate as the number of colonies you pick with 40 µL sterile ultrapure H<sub>2</sub>O. Pick a colony with a pipette tip, dip it into the well, and spread the rest on the respective section of the LB-Amp plate. Incubate the LB-Amp plate overnight at 37 °C for subsequent inoculation of liquid cultures on the following day.

15. Place the 96-well PCR plate in a PCR cycler for 20 min at 95 °C to denature bacterial cells.
16. Use 5  $\mu\text{L}$  of denatured bacterial suspension as template for colony PCR:

Component	For 20 $\mu\text{L}$ reaction	Final concentration
DNA	5 $\mu\text{L}$	
10 $\times$ PCR-buffer	2 $\mu\text{L}$	1x
dNTPmix (2 mM)	2 $\mu\text{L}$	0.2 mM each
Forward primer (10 pmol/ $\mu\text{L}$ ) ( <i>see Note 6</i> )	0.8 $\mu\text{L}$	0.2 $\mu\text{M}$
Reverse primer (10 pmol/ $\mu\text{L}$ ) ( <i>see Note 6</i> )	0.8 $\mu\text{L}$	0.2 $\mu\text{M}$
Taq-polymerase (5 U/ $\mu\text{L}$ )	0.1 $\mu\text{L}$	0.5 U/rxn
Ultrapure H <sub>2</sub> O	9.3 $\mu\text{L}$	

	Temperature (°C)	Time
Heat Lid	110	
Denature	95	5 min
Start Cycle (25 $\times$ )		
Denature	95	1 min
Anneal	primer T <sub>m</sub> - 5	30 s
Extend	72	4 min
End Cycle		
Extend	72	5 min

17. Check the PCR product by agarose gel electrophoresis for expected product size and correct orientation (*see Note 7*).
18. Pick the respective colony from the overnight LB plate and inoculate 5 mL LB medium containing 100  $\mu\text{g}/\text{mL}$  ampicillin and incubate overnight at 37 °C (*see Note 8*).
19. Isolate the plasmid DNA using the QIAprep Spin Miniprep Kit according to the manufacturer's protocol.
20. Sequence the plasmid for sequence validation.
21. Pick the validated clone from the sectioned LB agar plate and inoculate 100 mL LB medium containing 100  $\mu\text{g}/\text{mL}$  ampicillin. Incubate overnight at 37 °C (*see Note 9*).
22. Isolate the plasmid DNA using the QIAGEN Plasmid Midi Kit according to the manufacturer's protocol.
23. Measure the DNA concentration of your pLenti expression plasmid.

### **3.2 Production of Lentiviral Particles and Transduction of Patient Cell Lines**

*Lentiviruses must be handled with care and in accordance with national and institutional guidelines and might require permission. Always consult the person in charge of health and safety before working with the lentiviral system!*

The procedure below is adapted from the ViraPower™ HiPerform™ Lentiviral TOPO® Expression Kit protocol. It is designed for one transfection experiment corresponding to one 10 cm dish of 293FT cells yielding enough virii to transduce two 10 cm dishes of fibroblast cell lines with the respective construct. For transduction of more than two fibroblast cell lines or the usage of several constructs scale up the protocol accordingly (*see Note 10*). In addition to the patient cell line a control cell line that is not derived from a mitochondrial disease patient (e.g., NHDF-neo) should be transduced to exclude unspecific rescue. The control cell line also serves as a reference for the respiration experiment described below.

#### *Day 1*

Thaw 293FT cells and maintain them in medium 1 at 37 °C and 5% CO<sub>2</sub>. On the same day, thaw patient and control cell lines and culture them in fibroblast growth medium at 37 °C and 5% CO<sub>2</sub>.

#### *Day 3*

Split the 293FT cells and seed them on a 10 cm dish in approximately 8 mL of medium 1. The 293FT cells should be 70–80% confluent on the next evening (*see Note 11*).

#### *Day 4*

1. Warm up medium 1 and 3 and thaw the Packaging Mix on ice.
2. Calculate the required vector quantity corresponding to 3 µg pLenti expression vector.
3. Mix 1.5 mL medium 3 and 36 µL Lipofectamine in a 15 mL Falcon tube.
4. Incubate for 5 min at room temperature.
5. Mix 1.5 mL medium 3.9 µL Packaging Mix, and 3 µg pLenti vector in a 15 mL Falcon tube and add this solution dropwise to the Lipofectamine solution. Gently mix by inverting the tube.
6. Incubate for 20 min at RT.
7. Aspirate the medium of the 293FT cells and add 5 mL of fresh medium 1 (*see Note 12*).
8. Add the transfection solution to 293FT cells dropwise.
9. Incubate the 293FT cells overnight at 37 °C and 5% CO<sub>2</sub>.

*Day 5*

1. Seed patient and control cells on a 10 cm dish in medium 2 to reach 70–80% confluency on the day of viral transduction.
2. Aspirate the medium from 293FT cells and replace it very carefully with 7 mL of medium 4 (add the medium dropwise) (*see Note 13*). Incubate for 72 h at 37 °C and 5% CO<sub>2</sub>.

*Day 8*

1. Cool down centrifuge to 4 °C, warm up medium 2, prepare and label 15 and 50 mL Falcon tubes, prepare syringes and filters, label cryotubes if necessary.
2. Collect the supernatant of the 293FT cells (approximately 7 mL) into a 15 mL Falcon. This supernatant contains lentiviral particles.
3. Centrifuge supernatant at 2000 × *g* for 15 min at 4 °C.
4. Transfer 7 mL of medium 2 in a 50 mL Falcon tube.
5. Filter the supernatant with a 45 µm filter into the 50 mL Falcon tube containing medium 2 and mix gently (*see Note 14*).
6. Aspirate the medium from the fibroblast cell lines and gently add 7 mL of the mixture of viral supernatant and medium to each dish of fibroblast cell lines.
7. Incubate the cells at 37 °C and 5% CO<sub>2</sub> for 24 h. During this step, the virii infect the cells.

*Day 9*

Aspirate the medium of the transduced fibroblast cell lines and replace with medium 5.

*Day 10*

Begin the selection by adding blasticidin to a final concentration of 5 µg/mL. Only infected fibroblasts expressing your gene of interest will survive the selection.

For further cultivation of transduced cell lines, change medium every 2 or 3 days (always use selection medium). Split cells if necessary (*see Note 15*). Before performing experiments with the cells assess the biosafety level (*see Note 16*).

### **3.3 Measurement of Oxygen Consumption**

We recommend measuring at least 14 replicates per cell line on the XF96 to account for outliers and variability in the assay. Therefore, a maximum of six cell lines can be investigated on one XF96 Cell Culture Microplate. The corner wells of the microplate are used for background correction. On each plate, include at least one control cell line (e.g., NHDF-neo), the patient cell line and the patient cell line transduced with the respective wild-type cDNA to be tested (*see Note 17*). The control cell line, which should be derived

from a healthy person or alternatively from a non-mitochondrial patient, serves as an indicator for normal respiratory chain activity.

1. Detach the cells from the flask by trypsinization.
2. Collect the cells by centrifugation at  $500 \times g$  for 3 min 30 s at RT.
3. Aspirate the medium and resuspend in 2 mL fresh fibroblast growth medium.
4. Determine the cell concentration using a cell counter.
5. Plates 20,000 cells/well in 80  $\mu\text{L}$  of growth medium onto the XF96 Cell Culture Microplate and incubate at 5%  $\text{CO}_2$  and 37 °C overnight.
6. Rehydrate the cartridge (green part) by lifting it off the XF96 utility plate and adding 200  $\mu\text{L}$  of XF calibrant solution per well. Place the cartridge back onto the utility plate and incubate at 37 °C overnight.
7. Set up the experimental procedure

Command	Time (min)	Port
Calibrate	30	
Equilibrate	15	
Mix	2	
Wait	2	
Measure	3	
Mix	2	
Measure	3	
Mix	2	
Measure	3	
Inject		A
Mix	2	
Wait	2	
Measure	3	
Mix	2	
Measure	3	
Mix	2	
Measure	3	
Inject		B
Mix	2	

Command	Time (min)	Port
Wait	2	
Measure	3	
Mix	2	
Measure	3	
Mix	2	
Measure	3	
Inject		C
Mix	2	
Wait	2	
Measure	3	
Mix	2	
Measure	3	
Mix	2	
Measure	3	

8. On the following day replace growth medium with SH medium (*see Note 18*) by aspirating 60  $\mu\text{L}$  growth medium.
9. Wash by adding and aspirating 150  $\mu\text{L}$  of pre-warmed SH medium.
10. Add 160  $\mu\text{L}$  of pre-warmed SH medium.
11. Place the Cell Culture Microplate into a  $\text{CO}_2$ -free incubator at 37  $^\circ\text{C}$  for 30 min to allow equilibration of the  $\text{CO}_2$  levels.
12. Load 20  $\mu\text{L}$  of 10  $\mu\text{M}$  oligomycin into port A, 22  $\mu\text{L}$  of 4  $\mu\text{M}$  FCCP into port B, and 24  $\mu\text{L}$  of 20  $\mu\text{M}$  rotenone and 25  $\mu\text{M}$  antimycin A into port C.
13. Start the experiment and insert the XF cartridge into the XF analyzer to start the calibration, which takes approximately 20 min.
14. Replace the utility plate with the Cell culture Microplate.
15. After the measurement is completed, remove the SH medium from the Cell Culture Microplate, wash once with 200  $\mu\text{L}$  PBS, and freeze the Microplate at  $-80^\circ\text{C}$  for further determination of cell number (*see Note 19*). A representative measurement is depicted in Fig. 2.

### 3.4 Determination of Cell Number/Well Using CyQuant

Growth rates of control, patient, and transduced cell lines may differ. Therefore, OCR values/well need to be normalized to the total number of cells in each well. One method employs the quantification of DNA by CyQuant Cell Proliferation Kit.

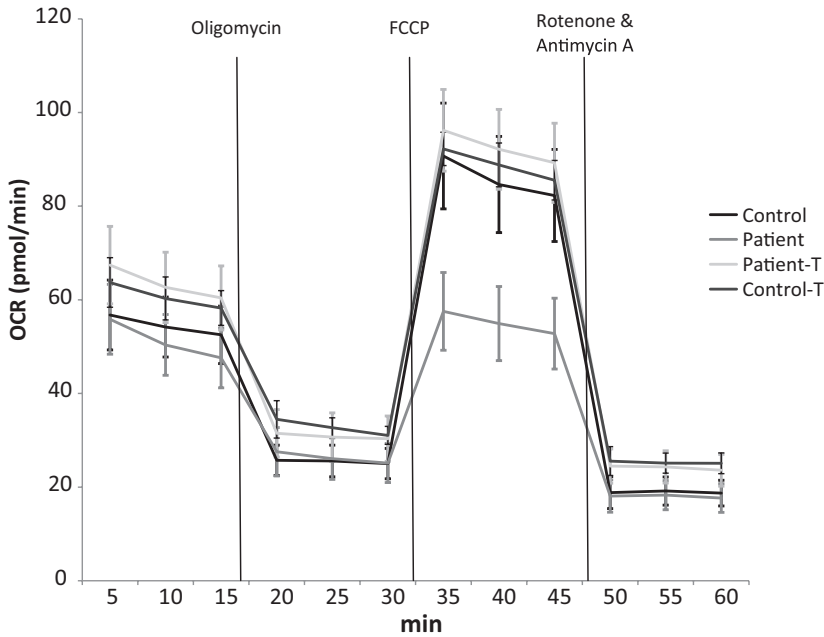


**Fig. 2** Representative result of a XF Cell Mito Stress Test seahorse measurement. OCR is monitored under basal conditions and after addition of oligomycin, of FCCP, and of rotenone and antimycin A

1. Generate a standard curve according to the manufacturer's instructions.
2. Per XF Cell Culture Microplate, dilute in a 50 mL Falcon 1 mL of the 20× cell-lysis buffer stock solution in 19 mL distilled H<sub>2</sub>O and add 50 μL of the CyQUANT® GR stock solution. Protect from light.
3. Unfreeze the measured XF Cell Culture microplate and add 200 μL of the solution to each well by vigorously pipetting up and down three times to ensure proper cell lysis.
4. Incubate the plate in the dark for 5 min.
5. Measure the fluorescence with a fluorescence microplate reader (excitation: 480 nm, emission: 520 nm).

### 3.5 Analyzing the Seahorse XF Data

The seahorse XF machine generates two files, the .xfd file that can be analyzed with the seahorse software and the .xls file that can be analyzed in excel. Here, we outline the strategy using excel.

1. Derive the OCR values of the whole plate from the excel sheet and normalize each well for the cell number calculated using the CyQuant data.
2. For each well, calculate the maximal respiration by subtracting the value of time point 12 (lowest value after the addition of rotenone and antimycin A) from its respective value at time point 7 (maximal value after FCCP addition) (*see Note 20*).

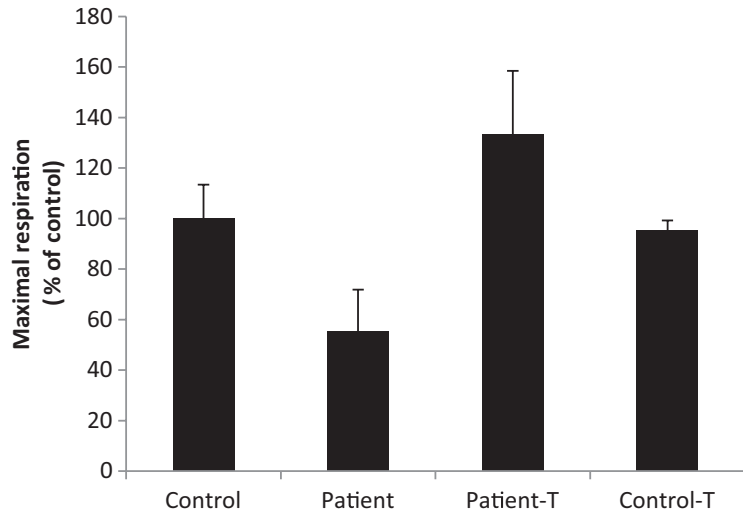


**Fig. 3** Representative result of an analyzed seahorse measurement. The maximal respiration of the patient cell line, the patient cell line transduced with the gene of interest (Patient-T), and the control cell line transduced with the gene of interest (Control-T) are normalized to the maximal respiration of the control cell line (Control)

3. For each cell line, remove outliers of the maximal respiration by excluding data points that are 50% off the median (*see Note 21*).
4. For each cell line, calculate the average maximal respiration and the respective standard deviation.
5. Express the average maximal respiration of the patient cell line and the transduced cell lines as % of the control cell line.

### 3.6 Interpretation of the Results

The disease-causing gene variant is likely identified when the defect in respiration of the patient fibroblast cell line is rescued upon lentiviral transduction with the wild-type cDNA. The maximal respiration of the complemented patient cell line should be close to normal when compared to the control cell line. This effect should not be observed for the patient cell line transduced with an empty vector. A positive example is illustrated in Fig. 3. In many instances we observed clear-cut results. In some cases, we saw improved activity but intermediary between patient and control levels. To draw final conclusions and calculate significance, replicated investigations on several plates are necessary.

---

## 4 Notes

1. Thaw all reagents on ice and keep them on ice during the whole experiment. After use, discard buffers, substrates, inhibitors, and uncouplers.

2. Human wild-type cDNA can be produced or commercially obtained (e.g., DNASU Plasmid Repository). In the latter case perform a plasmid mini-preparation and dilute the eluted DNA 1:1000.
3. pLenti6.3 does neither contain an ATG start codon nor a Kozak sequence for translation start, include both in your forward primer design if not already present in the DNA template (CGCCATG...). Depending on the template either include a stop codon in your reverse primer or clone in frame for tagging the construct with a V5 epitope.
4. Proceed to the transformation step if you see a discrete band with the expected product size. If you observe several bands gel-purify the appropriate fragment and proceed.
5. If you do not see distinctive single colonies repeat the transformation. You might try diluting the input mini-preparation DNA 1:500 and 1:1000 to produce fresh PCR products for further ligation and transformation.
6. Pick at least ten colonies if possible. Mutations might have occurred during PCR amplification and stochastically it is expected that 50% of the inserts ligated in the wrong direction.
7. Use the forward primer of the cDNA insert and the reverse primer of the vector (V5) to check for the right orientation of the insert into the vector. It is recommended to also use the forward and reverse primer of the cDNA insert to confirm proper ligation and presence of the insert.
8. If you did not obtain any bands in neither the insertion nor orientation setting, there might be a technical problem with the colony PCR. In this case, perform Mini culture of ten random colonies and sequence verify.
9. If the single colonies on the sectioned plate began to grow into each other or if the plate was contaminated, retransform One ShotR Stbl3™ Competent *E. coli* cells with mini-preparation DNA from the validated clone.
10. This protocol was designed to transduce patient fibroblast cell lines and the multiplicity of infection (MOI) of the virus was chosen to likely result in overexpression of the protein. A reduction of MOI (1:10) resulted in our hands in lower expression level [3]. If you desire other levels of protein expression or want to transduce a different cell type, you should determine the MOI as described in the Manufacturer's protocol. It is mandatory to use only patient cell lines that are free of HIV, HBV, HCV, and mycoplasma contamination.
11. If the 293FT cells are allowed to grow into a closed monolayer, they are more likely to detach from the dish during further procedures.

12. Be careful, 293FT cells detach very easily.
13. Attention: The transfected 293FT cells have now biosafety level 2. For working with biosafety level 2 organisms, refer to your local regulations.
14. Filtered viral supernatant may be used immediately or aliquoted for later transduction experiments in 1.5 mL portions in cryotubes and stored at  $-80^{\circ}\text{C}$ , biosafety level 2.
15. Do not over-split the cells during the first few days of selection.
16. Depending on the guidelines at your institution a selection of methods might be necessary to verify the biosafety level 1 of the transduced cell line for further experiments. We recommend using the HIV-1 p24 ELISA Pair Set (Sino Biological Inc.).
17. The following steps must be performed cautiously to prevent scratching off cells from the surface. Always add and aspirate the same amount of liquid from each well to eliminate differences in the total volume and consequent concentration differences in the later on added substrates or inhibitors between the wells. After the procedure each well should contain a total volume of 180  $\mu\text{L}$ .
18. Prior plating the cells on the XF96 Cell Culture Microplate the cells should not exceed 80% confluency; otherwise, the cells bioenergetic state might be affected. One 75  $\text{cm}^2$  cell culture flask is sufficient for one measurement.
19. The plate must be frozen for at least 2 h at  $-80^{\circ}\text{C}$  to guarantee sufficient cell lysis required for cell number determination by the method described.
20. The values for measurements 10, 11, and 12 (after the addition of rotenone and antimycin A) should be constant; therefore, you can use measurement 12 or the average of 10, 11, and 12 for further calculations.
21. Outlier removal is very crucial for the proper analysis and evaluation of the results of the seahorse measurement and might be adjusted to your special needs. If you have to remove too many data points, the seahorse measurement must be optimized.

## References

1. Munnich A, Rustin P (2001) Clinical spectrum and diagnosis of mitochondrial disorders. *Am J Med Genet* 106(1):4–17. doi:[10.1002/ajmg.1391](https://doi.org/10.1002/ajmg.1391)
2. Haack TB, Haberberger B, Frisch EM, Wieland T, Iuso A, Gorza M, Strecker V, Graf E, Mayr JA, Herberg U, Hennermann JB, Klopstock T, Kuhn KA, Ahting U, Sperl W, Wilichowski E, Hoffmann GF, Tesarova M, Hansikova H, Zeman J, Plecko B, Zeviani M, Wittig I, Strom TM, Schuelke M, Freisinger P, Meitinger T, Prokisch H (2012) Molecular diagnosis in mitochondrial complex I deficiency using exome sequencing. *J Med Genet* 49(4):277–283. doi:[10.1136/jmedgenet-2012-100846](https://doi.org/10.1136/jmedgenet-2012-100846)
3. Kornblum C, Nicholls TJ, Haack TB, Scholer S, Peeva V, Danhauser K, Hallmann K, Zsurka

- G, Rorbach J, Iuso A, Wieland T, Sciacco M, Ronchi D, Comi GP, Moggio M, Quinzii CM, DiMauro S, Calvo SE, Mootha VK, Klopstock T, Strom TM, Meitinger T, Minczuk M, Kunz WS, Prokisch H (2013) Loss-of-function mutations in MGME1 impair mtDNA replication and cause multisystemic mitochondrial disease. *Nat Genet* 45(2):214–219
4. Hildick-Smith GJ, Cooney JD, Garone C, Kremer LS, Haack TB, Thon JN, Miyata N, Lieber DS, Calvo SE, Akman HO, Yien YY, Huston NC, Branco DS, Shah DI, Freedman ML, Koehler CM, Italiano JE Jr, Merkenschlager A, Beblo S, Strom TM, Meitinger T, Freisinger P, Donati MA, Prokisch H, Mootha VK, DiMauro S, Paw BH (2013) Macrocytic anemia and mitochondriopathy resulting from a defect in sideroflexin 4. *Am J Hum Genet* 93(5):906–914. doi:[10.1016/j.ajhg.2013.09.011](https://doi.org/10.1016/j.ajhg.2013.09.011)
  5. Wu M, Neilson A, Swift AL, Moran R, Tamagnine J, Parslow D, Armistead S, Lemire K, Orrell J, Teich J, Chomicz S, Ferrick DA (2007) Multiparameter metabolic analysis reveals a close link between attenuated mitochondrial bioenergetic function and enhanced glycolysis dependency in human tumor cells. *Am J Physiol Cell Physiol* 292(1):C125–C136. doi:[10.1152/ajpcell.00247.2006](https://doi.org/10.1152/ajpcell.00247.2006)
  6. Moran M, Rivera H, Sanchez-Arago M, Blazquez A, Merinero B, Ugalde C, Arenas J, Cuezva JM, Martin MA (2010) Mitochondrial bioenergetics and dynamics interplay in complex I-deficient fibroblasts. *Biochim Biophys Acta* 1802(5):443–453. doi:[10.1016/j.bbadis.2010.02.001](https://doi.org/10.1016/j.bbadis.2010.02.001)
  7. Brand MD, Nicholls DG (2011) Assessing mitochondrial dysfunction in cells. *Biochem J* 435(2):297–312. doi:[10.1042/BJ20110162](https://doi.org/10.1042/BJ20110162)
  8. Invernizzi F, D’Amato I, Jensen PB, Ravaglia S, Zeviani M, Tiranti V (2012) Microscale oxygraphy reveals OXPHOS impairment in MRC mutant cells. *Mitochondrion* 12(2):328–335. doi:[10.1016/j.mito.2012.01.001](https://doi.org/10.1016/j.mito.2012.01.001)

# INDEX

## A

- Absolute protein quantitation.....71, 73  
 Adenosine 5'-triphosphate (ATP)..... 15, 34,  
 43, 55, 142, 161, 218, 232, 247, 259, 274, 307, 316,  
 337, 350, 379  
 ADP-stimulated respiration .....217  
*Aequorea victoria*.....245  
 Aequorin..... 245, 246, 251, 252  
 Ageing.....350, 359  
 Apoptosis..... 1, 33, 54, 55,  
 179, 245, 350  
 ATeam .....231–242  
 ATP synthase ..... 151, 226, 232, 259, 265, 274,  
 275, 278, 287, 307, 316, 343–345, 379  
 Autophagosomes .....55, 56, 337, 338, 344,  
 352, 353, 357, 360  
 Autophagy..... 56, 337, 338, 350, 352, 359

## B

- Basal respiration .....226, 230  
 Bioluminescence.....245–252  
 Biosensor ..... 231, 351, 354

## C

- Caenorhabditis elegans*.....255–264, 266–270, 350–360  
 Calcium .....1, 17, 21, 22, 28–30, 32, 54, 245–252,  
 280, 350  
 Carbonyl cyanide m-chlorophenylhydrazone ..... 191, 351,  
 353, 354, 356, 358, 359  
 Cardiolipin ..... 79, 161  
 Cell-free translation..... 156, 157  
 CELLO ..... 3, 4, 9, 10, 12  
 Cellular fractionation..... 127, 129, 136, 181  
 Chaperones..... 181, 363–365, 369  
 Chemical fixation ..... 294, 296–297, 299–305  
 Chromatography .....69, 70, 72, 73, 82, 160, 161, 166, 168,  
 169, 175, 176, 232, 318, 319, 322, 323, 331  
 Coelenterazine.....246–249, 252  
 Contact sites.....43–50, 53–57, 293, 294, 330  
 Crosslinking .....139–153  
 Crude mitochondria .....22–27, 30, 36–39, 41,  
 59, 61, 63, 87, 89, 102, 201, 209, 210, 213  
 Cysteines .....2, 35, 70, 105–109, 112, 113,  
 117–119, 121, 123, 124, 128, 130, 131, 133, 134, 140,  
 150, 186, 187, 190, 191, 194, 283, 316, 321, 332

## D

- Detergents .....70, 76, 128, 156, 157, 173, 174, 217, 324  
 Digitonin .....113, 128, 129, 132, 247, 248, 319, 324, 333  
 Disease-associated gene.....392  
 Dual targeting .....179–191

## E

- EF-hand .....246  
 Electron cryo-tomography ..... 315–317, 319–334  
 Electron transport chain .....55, 217  
 Endoplasmic reticulum..... 27, 106–107, 135,  
 198, 202, 209, 252, 294, 300  
 Exome sequencing.....391

## F

- Fermentation ..... 33, 34, 344  
 Fibroblasts ..... 17, 101, 130,  
 382–383, 387, 391  
 Fluorescence .....17, 28, 30, 55, 72, 73, 76, 197, 231–233,  
 236, 238, 246, 252, 269, 275, 276, 282, 287, 320, 324,  
 326–327, 338, 340, 342–344, 351, 372, 394  
 Fluorescence microscopy .....197, 236, 320, 326,  
 327, 338, 340, 342–344  
 Fluorodeoxyuridine (FUdR) .....359  
 Förster resonance energy transfer (FRET).....231  
 Functional complementation .....391–405

## G

- Glycerophospholipids.....79–102

## H

- Heat shock .....55, 165, 188, 341,  
 363, 364, 396  
 High-throughput..... 2, 80, 218, 246  
 Homeostasis .....337, 350  
 Homogenization..... 16, 26, 31, 34, 36–39, 49,  
 58, 63, 81, 85, 87, 88, 101, 159, 162, 163, 171, 173,  
 202, 205, 209, 223

## I

- Immunolectron microscopy .....294  
 Immunostaining ..... 256–266, 269, 270  
 Import ..... 1, 15, 34, 44, 61, 107, 148,  
 180, 198, 316, 350, 365

- Inner mitochondrial membranes ..... 28, 55, 56,  
245, 255, 258, 259, 273–275, 350
- In situ* hybridization.....198–199, 201–204, 206–208
- Intermembrane space (IMS) .....2, 31, 101, 106–107,  
109, 112–113, 123–127, 259, 293, 316, 317, 365
- Ions..... 15, 71, 80, 86, 96, 97, 246, 315, 318, 327, 382
- iPSORT ..... 3, 4, 7, 13
- L**
- Lentiviruses* .....398
- Lipidomics.....80
- Liquid chromatography tandem mass spectrometry  
(LC/MS/MS)..... 69–73, 75, 76
- Live-cell imaging.....199, 231, 274, 280, 342, 343
- Luciferase reporter assay.....366, 367, 371–372, 376
- Lysosomes .....27, 56, 59, 337, 351, 357
- M**
- Matrix..... 2, 8, 31, 43, 44, 56, 142, 146,  
151, 166, 231, 245, 246, 256, 258, 259, 293, 303, 316,  
363–365, 369, 375
- Membrane ..... 1, 15, 34, 43, 53, 70, 79,  
107, 139, 155, 180, 198, 225, 234, 245, 255, 273, 293,  
315, 337, 350, 365
- Membrane proteins ..... 2, 134, 155, 274, 278, 289,  
315–334, 350
- Membrane vesicles ..... 44, 47–48
- MICOS .....44, 45, 49, 50, 294
- Microscopy .....236
- Mitochondria
- inner membrane..... 79, 141, 157, 167
- intermembrane space (IMS)..... 112–113, 141, 316
- matrix..... 2, 43, 56, 141, 142, 202,  
231–242, 245, 246, 256, 258, 293, 303, 316, 345,  
363–365, 369, 375
- outer membrane.....47, 56, 63, 142, 302,  
321, 328, 330–331
- Mitochondria-associated-membranes (MAM) .....53,  
85, 88, 102
- Mitochondrial disorders ..... 381, 391
- Mitochondrial DNA ..... 15, 40, 214, 380
- Mitochondrial dynamics..... 55, 57
- Mitochondrial fission .....57, 255
- Mitochondrial fusion..... 54, 57, 255, 330
- Mitochondrial integrity..... 16, 30, 225–226
- Mitochondrial matrix .....2, 56, 141, 142, 231
- Mitochondrial morphology ..... 213, 255–264, 266–270
- Mitochondrial Response Elements (MURE).....364, 366
- Mitochondrial RNA-processing.....379
- Mitochondrial subfractionation .....41
- Mitochondrial targeting peptides ..... 2, 7–9, 12
- Mitochondrial targeting sequence (MTS)..... 135, 180,  
182, 186, 190, 192, 203, 246, 278
- Mitochondrial unfolded protein response .....363
- MitoFates ..... 4, 8, 12
- Mitophagosomes .....338, 340, 343, 344, 346
- Mitophagy..... 43, 337–346,  
350–353, 355–357, 359, 360
- MitoProt II..... 4, 5, 12
- Mouse.....15–32, 53, 57–59, 62, 96,  
101, 130, 151, 217, 218, 221–223, 229, 259, 260, 265,  
270, 341
- Multienzyme Digestion-Filter Aided Sample Preparation  
(MED-FASP) .....69–77
- N**
- Nanodiscs ..... 155–176
- Nano-electrospray ionization mass  
spectrometry ..... 80, 84, 86, 92–99
- Nematode growth medium (NGM)..... 256, 257,  
261, 352, 354–356, 358, 359
- Nitrogen cavitation..... 16, 22, 29–31
- O**
- Organelle isolation .....85
- Organelles ..... 1, 15, 16, 27, 33, 34, 54–57, 69, 71, 80,  
85, 99, 139, 141, 144, 151, 155, 179, 180, 182, 197,  
198, 255, 268, 273, 293, 294, 302, 315, 337, 350, 364,  
381
- Ornithine-transcarbamylase .....366–368
- Orthologs ..... 3, 11–13
- Orthology..... 10, 12
- Oxidative folding..... 105–107, 109, 112–113, 123–128
- Oxidative phosphorylation .....15, 28, 33, 34,  
239, 350, 364, 391, 403
- Oxidative stress.....106–107, 337, 338, 351, 356
- Oxygen consumption rate (OCR)..... 392, 401, 402
- P**
- PA-SUB ..... 3, 4, 9
- Photoactivatable mitoGFP .....256–262
- Plate reader.....30, 72, 73, 247, 250
- Polymerase chain reaction (PCR)..... 101, 159,  
164, 165, 172, 174, 188, 190, 192, 201, 205–206,  
211–212, 246, 338, 339, 341, 376, 379–381, 383,  
386–389, 395–397, 404
- PProwler ..... 3, 4, 6–7
- PredAlgo ..... 4, 8, 10
- Predictions.....2–13
- Predotar..... 3, 5, 6, 8, 13
- Preprotein.....316, 317, 319, 321, 323, 325, 326, 330, 331
- Presequence..... 2, 5–8, 10, 12, 316, 324
- Protease ..... 21, 27, 31, 46, 70, 82, 101, 128,  
136, 161, 170, 203, 205, 210, 346, 350, 364, 365, 369
- Protein complexes.....45, 139, 140, 151,  
273–290, 293, 294, 315–317, 319–334
- Protein localization..... 3, 9, 106–107, 179, 181, 328
- Protein purification .....318, 322

Protein-protein interactions .....139–141, 144, 145, 149  
 Proteolysis ..... 62, 166, 363–365  
 Proteomics .....16, 17, 30, 71, 77  
 Proteostasis .....364  
 Pure mitochondria .....17, 27–28, 58, 62, 80,  
 83, 85, 89, 90, 102

**Q**

Quantitative real-time PCR .....201  
 Quantum dots .....316

**R**

Reactive oxygen species (ROS).....337  
 Real time PCR .....201, 206, 211–212, 214, 381  
 Reciprocal best hits .....10  
 Redox states ..... 105–137, 151  
 Respiration ..... 17, 20, 22, 28, 33, 34, 217, 218, 220, 221,  
 223, 226–230, 245, 338, 342–344, 392, 398, 402, 403  
 Respiratory chain complexes (RCCs) ..... 139, 218,  
 229, 293, 379, 392  
 Respiratory control ratios (RCRs) ..... 218, 228  
 Respiratory substrates ..... 217, 223, 224, 229  
 RNA sequencing .....390  
 RNA trafficking .....197–199  
 RNase P .....380, 386  
 RNase Z ..... 380, 381, 386

**S**

*Saccharomyces cerevisiae* .....33–41, 130, 151, 181,  
 293, 300, 307, 319, 332, 338, 351  
 Seahorse XF96 ..... 217–229, 395  
 SherLoc .....3, 9  
 Single molecule fluorescence in situ hybridization  
 (smFISH) ..... 199–201, 204  
 Sonication ..... 44, 46–50, 130, 134, 166, 175, 202  
 Spheroplasts .....35–39, 41, 87, 101, 201,  
 203, 204, 207, 209

Stable isotope labeling with amino acids in cell culture  
 (SILAC) .....367–368, 371–373, 375, 377  
 Superresolution microscopy .....270, 274

**T**

Targeting peptides ..... 3, 5–9, 12  
 TargetP ..... 3–8, 12  
 Thiol modification .....108, 109, 112, 119,  
 121–125, 130–134  
 TIM23 complex .....50, 141, 142, 150,  
 316, 317, 323, 324, 333  
 Tissues ..... 2, 16, 17, 21, 22, 24–27,  
 29–31, 53–63, 258, 261, 267, 278, 280–285, 312,  
 379–390, 394  
 Tokuyasu cryosectioning ..... 294, 297–299, 305–310  
 TOM complex .....44, 50, 142, 316, 324  
 Tppred2 ..... 4, 7–8  
 Transduction .....33, 43, 315, 394,  
 398–399, 403, 405  
 Translocase .....44, 139, 141, 142, 316  
 Transmission electron microscopy .....294, 306

**U**

Uncouplers .....220, 403  
 Unfolded protein response .....363–377  
 Uniporter .....245

**W**

Western blotting .....30, 49, 110–112, 115,  
 130, 132, 133, 145, 147, 152, 194, 201, 205, 259, 317,  
 324, 334, 338, 340–341, 345–346, 365, 369

**Y**

Yeast. *See Saccharomyces cerevisiae*  
 Yeast transformation .....184, 187–188, 203,  
 338–339, 341